PB85-238046

Numerical Modeling Study of Gain and Downward Radiation for Selected FM and VHF-TV Broadcast Antenna Systems

AGL, Inc., Pacific Grove, CA

Prepared for

Office of Radiation Programs
Las Vegas Facility, NV

Jun 85

U.S. Department of Commerce
National Technical Information Service
NTIS

50272-101

REPORT DOCUMENTATION PAGE

1. REPORT NO. EPA 520/6-85-018

2.

3. Recipient's Accession No. PB85 238046/AS

4. Title and Subtitle
Numerical Modeling Study of Gain and Downward Radiation for Selected FM and VHF-TV Broadcast Antenna Systems

5. Report Date

6.

7. Author(s) Richard W. Adler and Stephan Lamont

8. Performing Organization Rept. No.

9. Performing Organization Name and Address
AGL, Inc.
P.O. Box 253
Pacific Grove, CA 93950

10. Project/Task/Work Unit No.

11. Contract(C) or Grant(G) No.
(C)
(G)

12. Sponsoring Organization Name and Address
U.S. Environmental Protection Agency
Office of Radiation Programs, Nonionizing Radiation Branch
P.O. Box 18416
Las Vegas, NV 89114-8416

13. Type of Report & Period Covered

14.

15. Supplementary Notes

16. Abstract (Limit: 200 words)

A modeling study was conducted for the purpose of examining RF radiation exposure levels caused by downward pointing radiation from commercial FM and TV broadcast antenna arrays. The Numerical Electromagnetic Code was used for radiation pattern calculations. Manufacturers' data and measurements were used to provide dimensional information for the computer models.

Generic types of FM antennas were identified and their radiation characteristics were presented with emphasis on the reconfiguration of array geometries for purposes of reducing downward directed radiation fields. The popular super-turnstile VHF TV element was also modeled. Gain curves for various interelement spacings were developed for arrays containing 2 through 16 elements.

Results demonstrate that downward radiation may not be insignificant. Variations occur with different antenna element types and for different array sizes. Reconfiguring arrays can be used to reduce downward directed energy but only an associated lower gain for a given number of elements. Substantial variation from the ideal circularly polarized omnidirectionl radiation is shown for most antennas currently in use.

17. Document Analysis a. Descriptors

b. Identifiers/Open-Ended Terms

c. COSATI Field/Group

18. Availability Statement
from NTIS

19. Security Class (This Report)

20. Security Class (This Page)

21. No. of Pages

22. Price

(See ANSI-Z39.18)

See Instructions on Reverse

OPTIONAL FORM 272 (4-77)
(Formerly NTIS-35)
Department of Commerce

United States
Environmental Protection
Agency

Office of Radiation Programs
Nonionizing Radiation Branch
P.O. Box 18416
Las Vegas NV 89114-8416

EPA-520/6-85-018
June 1985

PB85-238046

Radiation

EPA

Numerical Modeling Study of Gain and Downward Radiation For Selected FM and VHF-TV Broadcast Antenna Systems

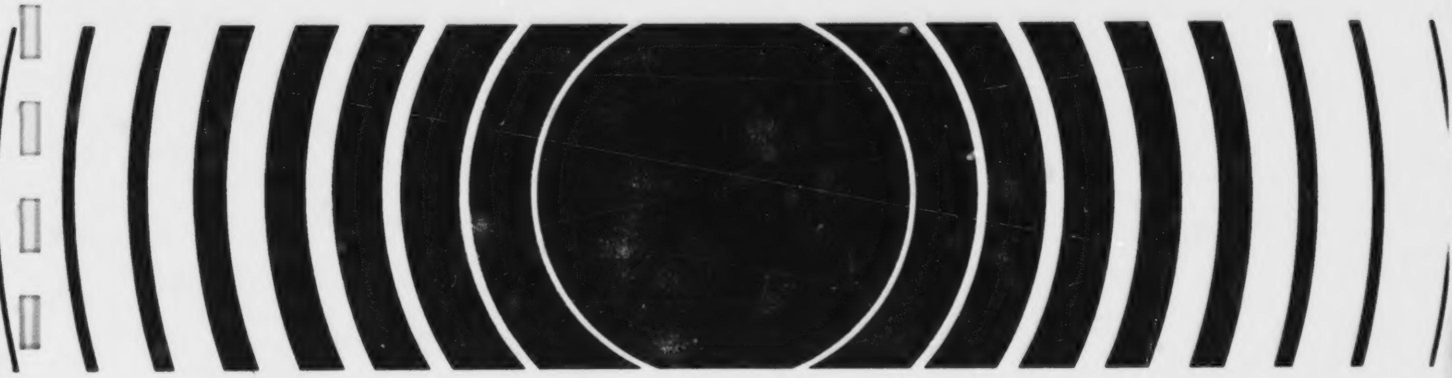

REPRODUCED BY
NATIONAL TECHNICAL
INFORMATION SERVICE
U.S. DEPARTMENT OF COMMERCE
SPRINGFIELD, VA. 22161

NUMERICAL MODELING STUDY
OF GAIN AND DOWNWARD RADIATION
FOR SELECTED FM AND VHF-TV
BROADCAST ANTENNA SYSTEMS

15 MARCH 1984

Richard W. Adler

Stephan Lamont

This report was prepared for the Environmental Protection Agency
Non-Ionizing Radiation Branch

by AGL, Inc., PO Box 253, Pacific Grove, CA 93950.

DISCLAIMER

Although the work described in this document has been funded wholly by the United States Environmental Protection Agency it has not been subjected to the Agency's required peer and policy review and therefore does not necessarily reflect the views of the Agency. No official endorsement should be inferred.

3<

TABLE OF CONTENTS

ABSTRACT 1

EXECUTIVE SUMMARY 2

A. Purpose of the Study 4

B. Historical Background 6

C. Scope and Limitations 9

D. Numerical Antenna Modeling 11

E. Description of Models 15

F. Assumed Parameters and the Real World 19

G. Modeling Studies 23

H. FM Array Gain Study 25

I. FM Array Bay Spacing Study 27

J. TV Array Bay Spacing Study 29

K. FM Element Gain/Spacing Curves 31

L. Conclusions and Recommendations 33

4<

Abstract

A modeling study was conducted for the purpose of examining RF radiation exposure levels caused by downward pointing radiation from commercial FM and TV broadcast antenna arrays. The Numerical Electromagnetic Code was used for radiation pattern calculations. Manufacturers' data and measurements were used to provide dimensional information for the computer models.

Generic types of FM antennas were identified and their radiation characteristics were presented with emphasis on the reconfiguration of array geometries for purposes of reducing downward directed radiation fields. The popular super-turnstile VHF TV element was also modeled. Gain curves for various interelement spacings were developed for arrays containing 2 through 16 elements.

Results demonstrate that downward radiation may not be insignificant. Variations occur with different antenna element types and for different array sizes. Reconfiguring arrays can be used to reduce downward directed energy but only an associated lower gain for a given number of elements. Substantial variation from the ideal circularly polarized omnidirectional radiation is shown for most antennas currently in use.

5<

EXECUTIVE SUMMARY

Objective of the Study

Representative FM broadcast transmitting antennas were modeled using the Method of Moments for the purpose of predicting downward radiation for the EPA. Additional calculations predicted the amount of downward radiation reduction that could be achieved by several mitigation techniques applied to the arrays. Attendant loss of main beam gain was also determined.

The popular VHF TV "super-turnstile" antenna was also subject to similiar analysis. These studies will assist the EPA in assessing the level of RF radiation field intensities that may exist at many broadcasters' installations and in estimating the cost of mitigation approaches.

Summary of Models and Results

Four FM element types identified (cycloid, skewed vee dipole, twisted loop and segmented twisted loop) were the subject of three modeling exercises:

1. Gain and pattern shape vs. full (normal) and half-wave (reduced) element spacing - to maintain main beam gain, arrays must expand

from 1.7 to 2 times in element numbers. The half-wave spacing did provide the expected reduction in downward radiation.

2. FM arrays of 4,6 and 8 elements were split into two bays, with the with the upper half (bay) of the array spaced one, 3/2 and two wavelengths from the lower bay. Only one of the four element types achieved any notable reduction in downward radiation at the wider spacing. The 3/2 wave spacing was detrimental to all models tested.
3. Standard handbook "gain vs. element spacing" curves for short dipoles were investigated and extended to half wave dipoles, cycloids and segmented twisted loops. The FM element curves show that they behave more like collinearly arrayed dipoles than like broadside arrayed dipoles.
4. The TV super-turnstile was subjected to the split-bay concept with generally favorable results (reduced downward radiation for 3/2 wave bay spacing.

Conclusions

The numerical models developed and exercised revealed noticeable discrepancies between real-world and assumed/advertised performance. Downward radiation field reduction by element spacing reduction is a feasible mitigation technique for FM arrays and holds definite promise for TV super-turnstiles. Bay spacing studies suggest that 3/2 wavelengths between bays is of little value for FM antennas but could improve the super-turnstile's downward radiation. FM antennas modeled followed the standard gain vs. element spacing curves of collinear dipole arrays.

8<

A. Purpose of the Study

The EPA is required to assess the potential for RF radiation exposure to the general civilian populace from broadcast transmitting antennas. This study supports that effort by providing predictions, based on numerical electromagnetic models, of radiation characteristics of popular FM and TV antennas. Particular emphasis is placed on energy radiated down towards the ground, near the base of the supporting tower or structure. It is in this zone where the most likely radiation to humans would exist.

In addition to assessing downward radiation potential, the EPA must address the financial impact on broadcasters of possible mitigation schemes in cases where proposed standards would be violated. One candidate technique for reduction of downward radiation which has been suggested involves changing the element numbers and spacings in FM and TV arrays. This study adds to earlier EPA calculations(which summed measured individual element patterns to establish downward radiation trends) by looking at the same configurations, but including full electromagnetic interaction between elements for more accurate pattern predictions.

If all commercially-available FM antennas are examined, 4 generic types evolve. Samples of these four are used throughout the study and as such provide a comparative look at existing radiation patterns, particularly in zones where downward radiation might occur for the FM station community.

B. Historical Background

When a study of FM and TV broadcast antenna radiation characteristics is launched, one first seeks out available manufacturers' antenna specifications and data sheets from catalogs. An interesting trend evolves. Virtually all competing antennas show the same performance:

Circular polarization

Equal Vertical(V) and Horizontal(H) polarization gains

Omnidirectional azimuth patterns

Unity gain (0 dB) with respect to a half-wave dipole
for a 2-bay model, for V and H polarizations

Zero radiation in the downward direction
(Perfect dipole or loop elevation plane patterns)

Nominally 1.0 wavelength vertical spacing between bays

Such published specs are not totally unexpected, for the Federal Communications Commission (FCC) has rules and regulations which require any V polarization not exceed the H polarization. The reason for those 2-bay unity gain figures is simply that that value is the maximum possible for idealized purely omni-directional elements. Since the FCC has no provision for "type-approval" testing of antennas, manufacturers are allowed to submit antenna descriptions and data for acceptance. Once any manufacturer has submitted a claim for theoretically maximum performance, market-place competition dictates that all others submitting for acceptance will meet those same numbers or suffer consequences in the sales arena.

Early EPA investigations into downward radiation from FM and TV arrays prompted a sponsored program of radiation pattern measurement of selected single element FM types. From these elemental patterns, array patterns were produced using the principle of Pattern Multiplication. These results neglect mutual interactions among elements in an array and are acceptable as first order predictions. If mutual effects are appreciable enough to alter the element patterns from their isolated values, then a full electromagnetic calculation, including interaction effects should be undertaken.

There has been very little work done in the area of computer modeling of FM and TV antennas, judged by the lack of published results. A poll of major manufacturers revealed that element patterns were almost always measured as carefully as possible, but that very few arrayed pattern measurements were ever made. Multiple element gains were simply calculated in the same manner as described in the EPA study. Elevation plane patterns are derived from idealized point source array equations.

Thus, from previously available information, the conclusion is drawn that FM and TV arrays do not radiate measurable downward energy. On-site measurements by EPA teams have shown that the converse is true. The results of this effort aids in quantifying that potential for radiation beneath the antennas.

C. Scope and Limitations

The accuracy of any mathematical or computer model of an antenna depends in part on the dimensional information available for all conducting pieces of the structure. This includes all feed lines, feed line supports and brackets, baluns or other matching devices and of course the structure supporting the antenna.

Antenna array performance is closely tied to the complex power distribution of the transmitters' output along the array's elements. Power distribution/division is a complex phenomena unless all ports along the line are identical and ideally matched to the feed line. Array designers for antenna manufacturers apparently make these simplifying assumptions.

In establishing a set of limitations and bounds on the models developed for this study, these assumptions and limits were in effect:

1. All models were constructed from manufacturers drawings and additional dimensional information, as needed, obtained from engineers at the factories.
2. Feedlines, mounting brackets and baluns, were included as scatterers of radiation, but not as functioning transmission lines
3. Feed points were excited directly with voltage sources of equal amplitude. This duplicates the designers' assumption about

power distribution.

4. No supporting structures were included because of the wide variation of mounting methods in use. In essence, all models can be assumed to be suspended by a sky hook.

If all antennas under investigation exhibited equal V and H radiation, a measure of downward radiation potential could be obtained from either polarization. Since equal polarizations is not the case, V, H and "total" radiation is presented. "Total" is the phasor sum of the vertical and horizontal radiation, a quantity of practical importance for studies involving RF radiation exposure to humans, since it establishes maximums of performance.

14<

D. Numerical Antenna Modeling

Antenna patterns, the most sought-after performance factor, can be obtained by both measurement and by calculation. A full-size real antenna can be placed on an outdoor antenna pattern range and its transmission characteristics measured. The quality of the range is the key to good results. A good antenna pattern range approximates free space, i.e. it produces patterns as if the test antenna were isolated from all of its surroundings (no appreciable reflections from nearby structures or the earth under the antenna are allowed.) Such ranges are expensive to establish and generally do not exist, even at most FM antenna manufacturers' facilities. Scale model measurements of an antenna also can provide radiation characteristics but generally require expensive indoor antenna ranges (anechoic chambers.)

The laws of physics dictate that in order to calculate radiation patterns one must know the amount of current flowing on all metal parts of the antenna and its supporting and nearby structures. For simple antennas (such as dipoles and loops) a method is employed whereby the current shape is assumed. If the assumption is correct, the results are good. This method is seldom applicable to commercial FM antennas because they are more complicated than dipoles and loops, containing support brackets and vertical feed line sections for which those simple assumptions are incorrect.

In recent years, the advent of high-speed digital computers have made it possible to use the Method of Moments to calculate the currents on an antenna, regardless of the structure's complexity. To apply this technique, an experienced antenna engineer who is thoroughly grounded in the theoretical limitations of the method can construct an accurate numerical (computer) model of the antenna. The results of this kind of analysis have been validated for a wide range of antenna types, which encompass structures operating in the same frequency range and environments as FM transmitting antennas, during the past 10 years.

The Numerical Electromagnetic Code (NEC) has been under development with Tri-Service sponsorship for over 10 years and is the most widely-used of all Method of Moments antenna programs. In NEC, the structure (the word "structure" connotes an antenna with all of its nearby conducting surroundings and appendages) under investigation is divided into small sections (segments), usually less than 1/10 wavelength long. The physical laws of electromagnetism are applied to all segments. This is in the form of calculating the electromagnetic interaction between each individual segment and all other segments in the structure, one at a time. The resulting mutual interaction matrix represents how the structure will react to any chosen sets of "excitations" (incoming received signals or transmitter outputs). By applying the excitation which represents a specific antenna application, NEC calculates the currents flowing on all parts of the structure.

Current represents a measureable physical quantity which is a structure's response to an excitation. With a knowledge of the current, it is a straightforward exercise to calculate the feed point impedance, radiation pattern, near fields, scattered fields, radar cross section, coupling between structure connection points, efficiency and resonances. For this study, radiation patterns are the desired output characteristic.

A numerical model of an FM or TV antenna provides the engineer with a valuable inexpensive tool for examining variations in the geometry of a particular antenna model. This allows rapid changes in antenna parameters such as spacing between elements, power distribution over an array, location of feed points, etc. Each change can produce a different response and these differences can quickly be seen from NEC runs. Thus, a NEC model can provide design information much more easily and rapidly than lashing up many new antenna configurations on a model range and running tests to determine what each change does to the pattern, etc.

The role of a measurement program is then reduced to validating the numerical model and accounting for the small but sometimes significant differences between the computer model and the physical model. Moving the measurement phase of a design program to this position is a more efficient use of resources and provides a more thorough design since a greater number of perturbations can be examined within the fixed time and cost limits usually present in antenna design projects.

18<

E. Description of Models

At the initiation of this project, decisions had to be made as to the generic types of FM antennas modeled and which particular manufacturer's model would represent each generic type. Four generic types emerged from the stages of literature collected from both antenna manufacturers and from FM broadcast equipment manufactueres who do not make the antennas they sell. Two of the largest broadcast equipment suppliers, Harris and Continental, purchase antennas from Electronics Research, Inc. (ERI). CETEC owns and distributes JAMPRO antennas, in addition to other broadcast products. Several other companies such as Phelps Dodge, Comark, Shively, Dielectric Communications and Bognar produce and sell antennas themselves and through smaller broadcast suppliers. The EPA compiled a list of FM antenna types in use by examining FM license applications. This list determined which generic types would be studied and the cooperation of manufacturers and broadcast consultants in supplying the necessary drawings dictated the specific model numbers that were used in developing the numerical models.

The four classes of FM antennas identified are:

1. A cycloid - A horizontal loop with a gap opposite the feed and support point. At the gap, two vertical stubs, one pointing up and one pointing down, act as a vertical dipole. (Figure 1) The loop is intended to provide azimuthally omnidirectional, H

polarized radiation. The vertical stubs are expected to radiate a V polarized omnidirectional signal. Pure CP depends upon equal amplitudes of V and H polarization plus a 90 degree (quarter wave) phase shift between the two polarizations. Hopefully the phase shift will occur as the current on the loop travels toward the gap at the ends. Both ERI and Shively produce versions of the cycloid.

2. Skewed Vee Dipoles - two vee shaped dipoles are mounted on opposite ends of a horizontal boom and then each dipole is twisted 30 degrees with respect to the boom axis. (Figure 2) This twist provides a vertical component to the radiation field. Feed stubs or segments extend from the boom to the top arms of each vee. CETEC and Dielectric Communications offer this antenna.

3. Twisted loops - a fat horizontal loop is opened at the far end (much like the loop in a cycloid). The inner quarter circles of the loop (nearest the feed point and support point) remain in the horizontal plane, while the outer quarter circles are rotated up and down, respectively, so the open ends are no longer in the horizontal plane but have a vertical searation. Then two straight line extensions are added to the outer loop ends to provide a vertical component to the radiation. (Figure 3) In comparison to the cycloid which has the total loop in the horizontal plane

and vertical stubs, this twisted loop uses the outer half of the loop and its extensions for additional horizontal radiating conductor as well as a controlled amount of vertical radiating element. Comark and Phelps Dodge offer versions of the twisted loop

4. Segmented Twisted Loop - characterized by two halves of a loop (polygonal rather than circular) separated by a horizontal support bar, twisted about the support axis 30 degrees to excite a vertical radiation component and then with another horizontal support bar at right angles to the separator bar. (Figure 4) ERI and CETEC manufacture these antennas.

The only TV antenna element studied was the "super-turnstile". It is the most popular one found at VHF TV stations, having been designed almost 40 years ago. It consists of four batwing radiators mounted radially around a center support mast. (Figure 5) The dominant polarization is horizontal, with fairly good pattern circularity. Because of low V polarization radiation, the central mast is transparent to the operation of the radiator.

Throughout this report, the antenna types are labeled in part by manufacturer and/or model numbers:

Cycloid FM	Cycloid
Skewed Vee Dipole FM	JSCP

Twisted Loop FM	CMK or Comark
Segmented Twisted Loop FM	FMH or ERI FMH
Super-turnstile VHF TV	JAT or CETEC JAT

F. Assumed Parameters and the Real World

There are noticeable differences between the idealized antenna patterns of the FCC regulations (and manufacturers data sheets) and those of the real world of tower mounted arrays with significant mutual interactions. These differences are important for this study:

1. NEC references gain to an isotrope (point radiator) while the broadcaster uses a half-wave dipole. The dipole is 2.1 dB with respect to an isotropic antenna, so that NEC gain values should be be dropped by 2.1 dB when comparing to publish data.
2. Industry rates V and H polarization gains equal and uniform in azimuth, but as seen from Figures 6-9, radiation from isolated elements (including feed lines) varies with azimuth by 6 to 8 dB for V polarization and 1 to 5 dB for H polarization. V/H ratio exceeds the allowed unity value (0 dB) by as much as 8 dB. If the total gain (of prime concern for this investigation) is examined it varies from 2 to 6 dB in azimuth.
3. Total gain values for single elements should average 0 dB with respect to a dipole (2.1 dB isotropic) but are observed to be shy by about 1/2 to 1 dB.
4. Circular polarization is sold to the broadcaster but from the ratios of V and H shown on Figures 6-9, 3 of 4 models investigated cannot produce CP within 3 dB for at least 120 degrees of the compass. This argument is a generous one, since CP requires a

quadrature phase relationship between V and H and we have discussed amplitude only. It is possible to have equal V and H fields and be completely linearly polarized (V in phase with H), missing CP by the same amount as if one polarization were completely absent! For example, the JSCP element meets the V/H ratio test for 165 degrees in azimuth, but is within 3 dB of CP for only 142 degrees.

5. Nominal spacing between elements in FM arrays is cited as one wavelength. Installation documents dictate that the spacing varies from 3% to 16 % short of one wavelength for the samples available in this study. One reason for this variation could be that manufacturers build several sizes of elements to cover the 88 to 108 MHz FM band of frequencies. The examples available during this investigation could have been for edges of the frequency range of a particular element size.

6. In most cases, FM arrays are assumed to be fed with equal, in-phase power through a bottom-fed series transmission line. The elements are placed in parallel with the 50 ohm line and if each element presents N x 50 ohms to the line, all N elements in parallel receive equal, in-phase power (assuming one wavelength electrical spacing between junctions of element locations.) If the elements are all identical in construction and impedance matching circuitry, this assumption can be in error for elements near the top and borrom of the array line because the mutual

coupling environment is different from that of elements "buried" within the array. (Mutual coupling modifies the feed point impedance from the idealized isolated input impedance.)

7. Azimuthally uniform (omnidirection) radiation is not achieved by any of these "side mounted" elements studied for the simple reason that even without supporting structures present, horizontal plane symmetry does not exist. This is due to the necessary evil of a metallic feed line structure nearby the elements. The predominance of V polarization field is largely due to the interaction of the vertical conductors of the feed line. Additionally, the typical tower upon which FM arrays are mounted scatters V polarization more readily than H polarization. One more factor in the deteriation of omnidirectional patterns is the fact that dual-fed elements such as the JSCP vee dipoles and the FMH segmented loop are supported by and fed from metallic conductors which are spaced closer to the "inboard" arm than to the "outboard" one. NEC calculations show up to 20% differences in feed point impedance between the inboard and outboard elements. This effect accounts for the FMH elements' lop-sided H polarization pattern in the azimuth plane. An obvious question in the case of the FMH element is "Why not run the feedline up through the center of the element where it would be equidistant from both radiating arms?" A quick NEC model reveals that this attempt does produce more symmetric results but with much poorer

radiation impedance properties and even greater differences between V and H polarization. This was confirmed by contact with a manufacturer who tried it and failed.

There are FM antenna designs which do not suffer most of the disadvantages described in this section. These elements control their radiation and scattering environment (not being subject to the feedlines and supporting towers) by incorporating their environment as an integral part of the antenna. One such element type is a "panel" radiator, named for its large flat reflecting screen. (Figure 10) The CP crossed dipoles in front of the reflector produce 120 degrees of azimuth coverage. For omnidirectional patterns, 3 such panels are wrapped around a tower. The reflectors are much larger than the tower cross section and extend vertically 1 to 2 wavelengths, completely blocking any tower effects on the pattern. Such installations are quite broadband, very heavy and expensive, thus appears only in larger cities where several stations share in their use, multiplexing their transmitters into a single broadband panel array. ERI also produces what could be described as "selected dipoles wrapped around a pole". These are intended to be top-mounted and as such contain their own radiating environment. Other manufacturers produce variations on these two ideas.

G. Modeling Studies

Four popular FM antennas and one VHF TV were modeled during this project. Numerous radiation patterns were produced and are included in Appendices for reference, with several sample patterns displayed in the discussions to follow. The modeling is logically divided into four sections:

1. FM Array Gain. During this effort, the effect of changing element-to-element spacing from the usual one wavelength to 1/2 wavelength was demonstrated. Reduced spacing held promise for lower downward radiation, hence reduction of radiation to humans.

2. FM Array Bay Spacing. Since multiple element arrays spaced at 1/2 wavelength suffer reduced gain, it was anticipated that splitting an array of M elements into two equal halves, N = M/2, would produce two "bays" of N elements each and would permit interbay spacing changes from the standard one wavelength which could prove a boon to RADHAZ reduction, without the inherent loss of gain suffered by 1/2 wavelength element spacing. Figure 11 demonstrates a 6 element cycloid (3 x 3) spaced at the standard one wavelength and an 8 element (4 x 4) spaced at two wavelengths (TW) between the two bays of 4 elements.

3. TV Bay Spacing. A similar modeling exercise was conducted for a Channel 2 and a Channel 10 CETEC JAT super-turnstile array of 4, 6 and 8 elements.

4. FM Element Gain/Spacing. The EPA, in looking for suggested mitigation techniques, observed that the curves of gain vs. element spacing in the "Antenna Engineering Handbook" by Jasik (Ch 5) imply that, at least for short dipole elements, gain does not drop sharply as spacing is reduced from one wavelength. Since broadcast antenna manufacturers use these kinds of handbook curves to drive their designs, it was decided that a full-interaction modeling effort should be done to see if the idealized "Jasik Curves" hold for a rigorous model of short dipoles, half wave dipoles and then determine if those trends apply to FM arrays.

28<

H. FM Array Gain Study

Three element types were selected for examination of array gain vs. number of elements when spaced at the industry standard of one wavelength and at a "downward radiation reducing" spacing of 1/2 wavelength. Appendix A contains radiation patterns used in the study. For the JSCP (skewed vee dipoles), reducing spacing to 1/2 wave did not reduce downward radiation appreciably, but for the FMH (segmented loop) and cycloid, the expected reduction did occur.

Figures 12-14 show a loss of from 2 to 3 dB gain with the reduced spacing. The cycloid suffers most from 1/2 wave spacing. Note that the total gains shown (V plus H polarizations) are maximums in azimuth, and as such exceed the expected ideal values for pure omnidirectional radiation by 1-2 dB. Nominal total gain for ideal arrays is:

No. of Elements	Total Gain (dBi)
2	5.1
4	8.1
8	11.1
16	14.1

In spite of the higher-than-omni gains, if an RMS gain were calculated, the value would be 1/2 to 1 dB below the nominal. This is further indication that each antenna type shows azimuthal preferences, which may or may not be desirable, depending on the stations desired coverage in azimuth. The JSCP seems to be a lower gain array but azimuth patterns of Appendix A show its pattern to be the most circular of the 3 studied.

If reduced element spacing were selected as a downward radiation mitigation approach, cycloid arrays would need to be doubled in size, while FMH and JSCP systems would be increased by 1.7 times.

30<

1. FM Array Bay Spacing Study

All four elements were subjected to a downward radiation (60 to 90 degrees below the horizon) study. The arrays were 4, 6 and 8 elements with the upper and lower half (bay) of the array spaced at 1, 3/2 and 2 wavelengths. The 1 wavelength is standard spacing and indicates the present RF radiation potential to humans for isolated, elevated arrays. Spacing increase to 3/2 wave gives some measure of cancellation of downward fields while hopefully not reducing gain as much as an element spacing change to 1/2 wave would. An increase to 2 waves spacing between bays was included also.

Appendix B contains the detailed patterns for this section. The maximum azimuthal total gain and total downward radiation results are summarized in Figures 15-18. Bay spacing increases to 3/2 and 2 wavelengths causes only minor main beam gain changes, less than 1 dB. The hoped-for reduction in downward radiation did not take place for 3/2 wave spacing; it was in fact detrimental, increasing prospects for radiation to humans beneath the arrays. The 2 wave spacing improved conditions for only the JSCP, reducing downward fields 2 to 4 dB. It worsened the CYCLOID appreciably, 2 to 9 dB for different size arrays. The FMH and COMARK arrays had down-going radiation within 1 dB of the standard spacing.

The patterns of Appendix B show that 3/2 wave bay spacing does "swing" the downward lobes more toward the horizon, but in some cases increases the value of that lobe, negating any hoped-for improvements.

J. TV Array Bay Spacing Study

CETEC JAT turnstile arrays were modeled for 4, 6 and 8 elements in an upper/lower bay arrangement identical to the FM arrays. Since the VHF TV band is split into a low (Ch. 2-6) and high (Ch. 7-13) portion, a representative channel from each portion was modeled. Channels 2 and 10 were chosen to represent the VHF station downward radiation situation. Bay spacings were limited to standard one wavelength and 3/2 wavelengths for cost considerations. The super-turnstile elements are quite massive electrically and tax computer resources heavily.

Appendix C presents azimuth (horizontal) and elevation (vertical) plane patterns and also downward radiation characteristics. Figures 19-21 show the summary of those radiation charts. Maximum gain is virtually the same for standard and extended (3/2 wave) spacings but downward radiation improves at the wider spacing. Since the geometry in units of wavelengths is different for Channel 2 JAT models than for Ch. 10 units, the differences revealed in Figures 19 and 20 are somehow tied to the different element designs. For Ch. 2 models the trend is for slightly reduced downward radiation as the number of elements increases. Figure 19 shows that at 4 elements, potential for radiation to humans is identical for both bay spacings, and for 6 and 8 elements, the wider spacing is 1.2 and 2.6 dB better respectively. Ch. 10 models show the opposite trend vs. element numbers, but with greater spread in downward radiation levels.

Figure 20 shows over 5 dB downward radiation improvement for 4 elements, dropping to 3.6 dB advantage for 3/2 wave spacing for 8 elements.

One additional exercise was conducted to see results for reduced ELEMENT spacing for these turnstile antennas. Figure 21 suggests that for small arrays (2 element Ch. 2 antennas were modeled here) an almost 10 dB reduction in downward emission without appreciable maximum gain drop is achieved at 5/6 wave spacing. A limited test for 6 elements shows similar downward radiation improvement but with the unacceptable drop in azimuth coverage of almost 4 dB. These trends are based on a limited "quick look" study and may not hold for a more in-depth modeling exercise.

VHF-TV Super-turnstile antennas respond to an increased bay spacing change to 3/2 wave in a generally favorable manner and show interesting trends for element-to-element spacing reductions.

34<

K. FM Element Gain/Spacing Curves

EPA conversations with FM and TV broadcast antenna manufacturers suggest that their design engineers relay on "standard handbook concepts", one in particular being that the arrays in question behave as collineer spaced elements. The array gain vs. spacing curves in Jasik's "Antenna Engineering Handbook" (Ch. 5) are held in high regard.

A modeling study using NEC was conducted for elemental and half wave dipoles arrays, both broadside and coaxially (collineerly) arranged, to compare with the "no mutual coupling" cases of Jasik. Two FM antenna models were also exercised at the "Jasik spacings" for comparison to the dipole cases. Appendix D contains radiation patterns for these "Jasik Studies".

Very good correlation was found for short dipole arrays calculated by NEC and by the standard antenna pattern methods of Jasik. (Figures 22 and 23) NEC includes all coupling effects and determines antenna currents, from which gain is calculated. The usual approximations for the Jasik results are no interaction effects and assumed current distributions. The excellent agreement indicates that the small antennas (<0.1 wavelengths long) do not couple appreciably and that the linear current distribution assumption is valid.

For half-wave long dipoles, the gain curves are well within 1/2 dB of the short antenna curves. (Figures 24 and 25). Thus, design engineers can use the Jasik curves if their antenna elements behave like half-wave dipoles arrayed broadside and/or collinearly.

If FM broadcast antenna elements are considered as equivalent to a combination of half wave vertical elements and loop horizontal elements, the "Jasik curves" for them should be a composite of both collinear and broadside dipole curves. Figures 26-28 show FMH and cycloid elements in 2, 4, 8 and 16 element arrays. The shape of these 8 element curves matches those for half wave dipole collinear arrays within 1 dB. The collinear arrangement of elements corresponds to the vertical dipoles of an idealized FMCP antenna. The reason for such good correlation with collinear and not with broadside arrays is because all of the FM antennas investigated had substantially stronger V polarized radiation than H polarized radiation. This correlation between Jasik collinear elemental antennas, half wave dipoles and FM antennas confirms, in part, initial EPA insights and allows a measure of prediction of gain/spacing trade offs.

36<

L. Conclusions and Recommendations

The performance calculations of this study (gain and downward radiaion) provide the EPA with information which will allow them to:

1. Assess the possibility of downward radiation for candidate FM and VHF-TV broadcast transmitting installations
2. Examine the cost in gain of mitigation schemes involving array or sub-array spacing changes.

Comparison of real-world FM antenna performance as determined by numerical models is in contrast to assumed, idealized, and often, advertised characteristics.

Full vs. half-wave spaced FM arrays show 2-3 dB gain loss for the three types modeled. The FMH and cycloid show lower downward radiation at reduced spacing but not so for the JSCP skewed vee dipoles.

When the FM arrays were split into 2 bays with 3/2 and 2 wave interbay spacing, 2 models showed little improvement in downward raadiated fields (FMH and COMARK), one was worse (CYCLOID) and only one (JSCP) improved measureably (2-4 dB drop) for 2 wave spacing. No worthwhile effects were found with 3/2 wave spacing. Apparently the bay spacing concept is of limited value and general trends cannot be established. Modeling must be done on a case-by-case basis.

For the single VHF-TV model (super-turnstile) investigation 3/2 wavelength bay spacing shows promise but differences between Ch. 2 and Ch. 10 models suggests caution in trying to formulate trends from the limited study conducted here. Element spacing changes for super-turnstiles should be investigated for a wider range of variables than in this "quick-look" study.

If reliable pattern measurements can be obtained or conducted, they would provide validation benchmarks for NEC numerical models. The models developed for this project were done using all available guidelines and recommendations amassed over the past 10 years during which numerous military antenna systems were modeled and compared to measurements. Since the investigators do not regularly design FM and TV broadcast antennas, some of the details concerning feed systems are not known and not available. The pattern shapes calculated via NEC are considered quite accurate. The absolute gain values, which depend upon a good representation of the feed mechanism, were checked by a necessary but not sufficient method of calculating radiated power from both patterns and input power. Additional confidence can be obtained only through accurate gain measurements.

Additional modeling in the areas of downward radiation for variable element spacings of less than one wavelength should reveal the range of useful spacings suggested by the Jasik curves and by the limited JAT element study. The added effects of tower mounting should be looked at for a few typical installations. All work in this study was for "sky-hook" supported arrays, and should not be continued without knowledge of the amount of influence towers have on downward radiated field levels.

Jasik curve studies reveal that uniformly spaced FM arrays perform, for gain/spacing considerations, like half-wave collinear dipole arrays, betraying the fact that they are not radiators of equal V and H polarization fields. This fact is confirmed by the modeling of single elements done early in this study.

LOOP–DIPOLE CP ANTENNA

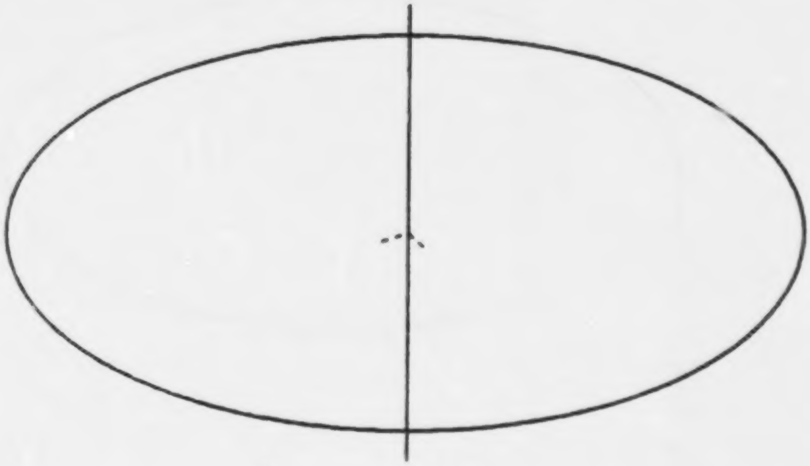

THETA = 60.00 PHI = 60.00 ETA = 90.00

FIGURE 1A

THE CYCLOID LOOP-DIPOLE ELEMENT

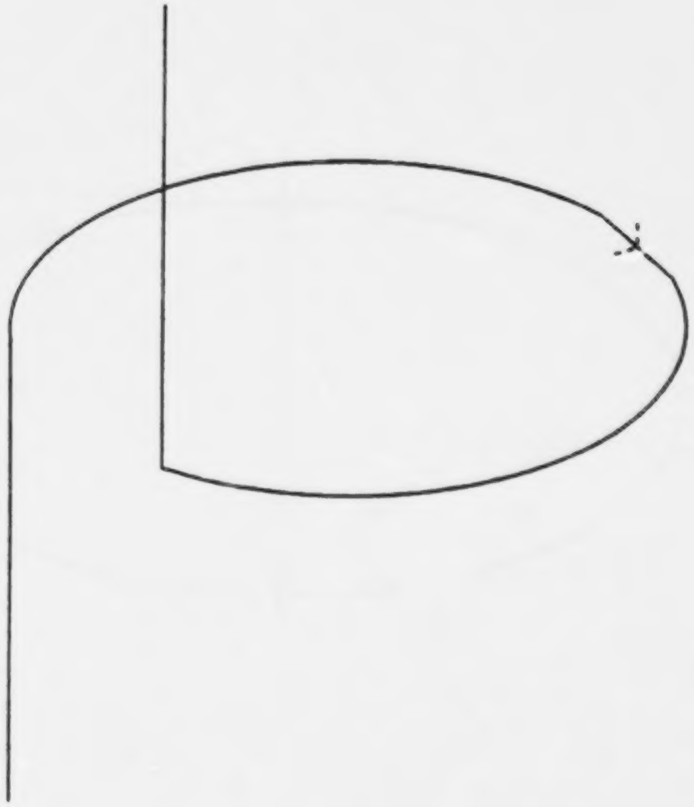

THETA = 60.00 PHI = 60.00 ETA = 90.00

FIGURE 1B

THE CYCLOID ELEMENT WITH SUPPORTING BALUN

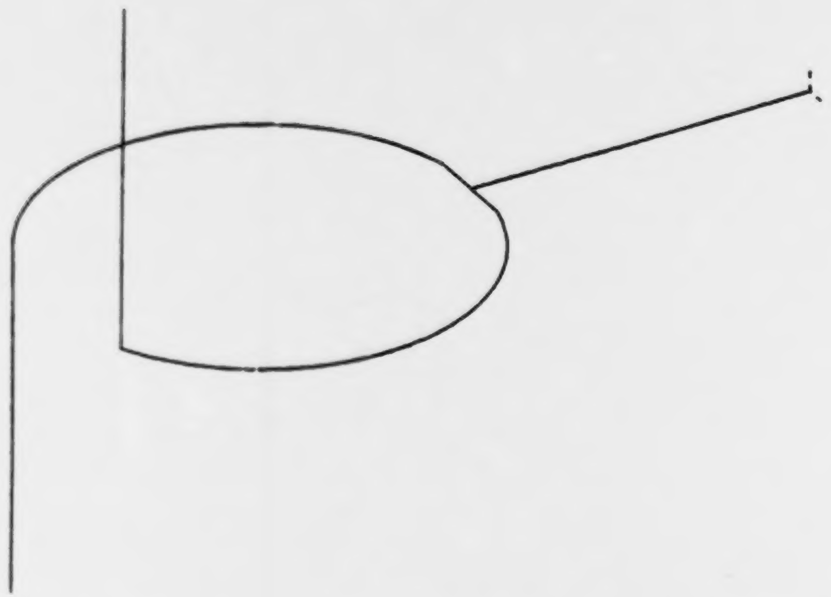

THETA = 60.00 PHI = 60.00 ETA = 90.00

FIGURE 1C

THE CYCLOID ELEMENT WITH FEEDLINE

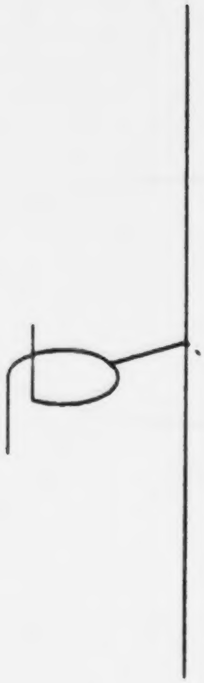

THETA = 60.00 PHI = 60.00 ETA = 90.00

FIGURE 1D

PAIR OF SKEWED VEE DIPOLES

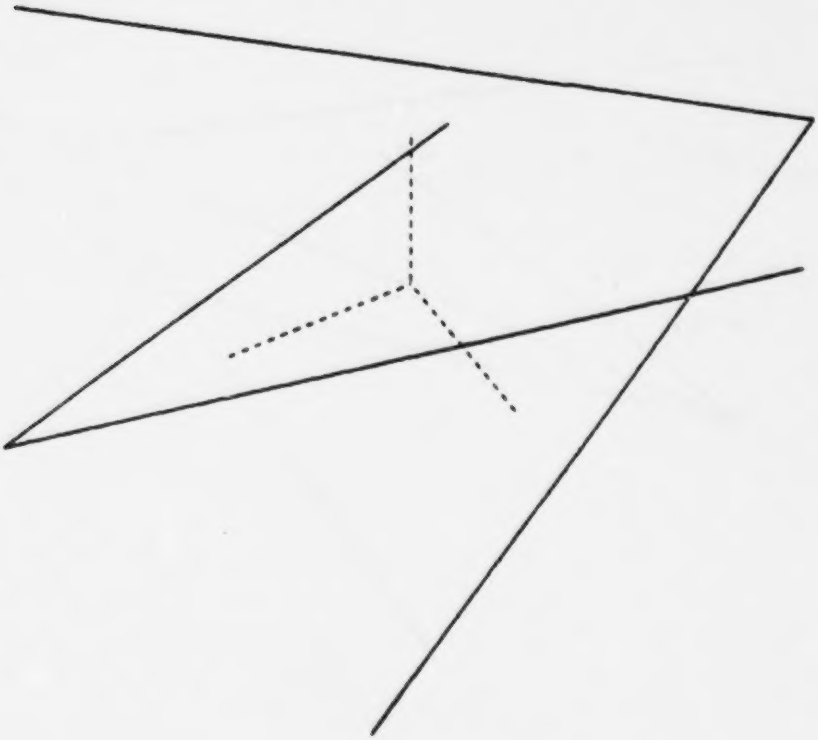

THETA = 45.00 PHI = 60.00 ETA = 90.00

FIGURE 2A

SKEWED VEE DIPOLES WITH HORIZONTAL SUPPORT

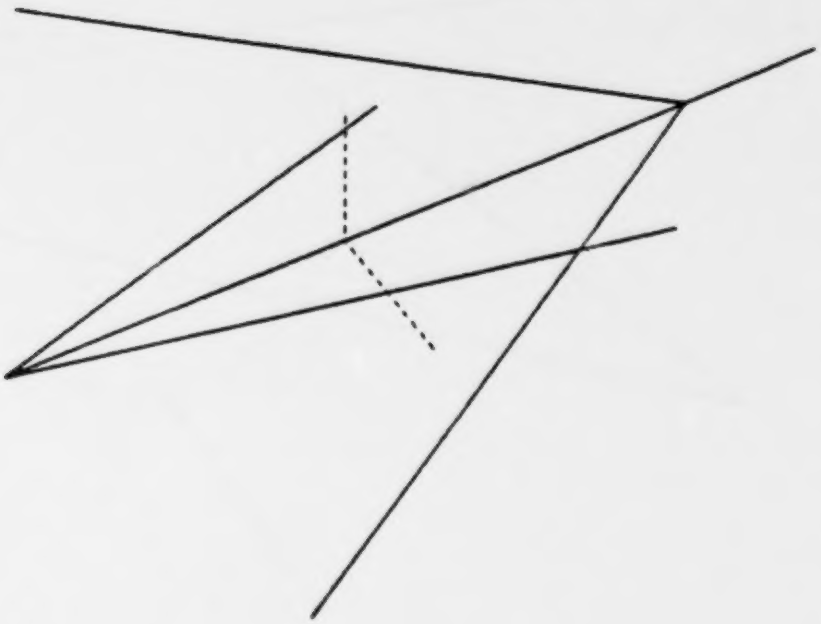

THETA = 45.00 PHI = 60.00 ETA = 90.00

FIGURE 2B

SKEWED VEE DIPOLES WITH SUPPORT AND FEEDER BARS

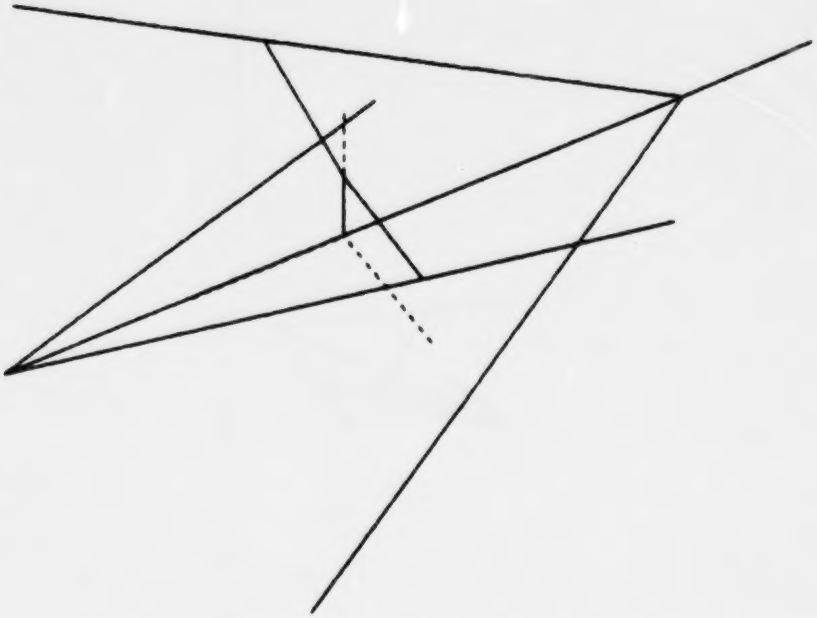

THETA = 45.00 PHI = 60.00 ETA = 90.00

FIGURE 2C

THE SKEWED VEE DIPOLE WITH FEEDLINE

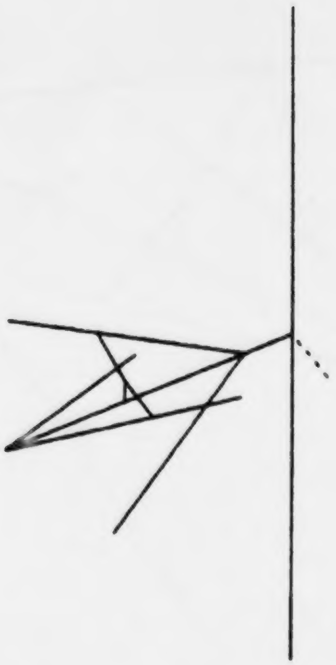

THETA = 45.00 PHI = 60.00 ETA = 90.00

47<

FIGURE 2D

TWISTED LOOP ELEMENT

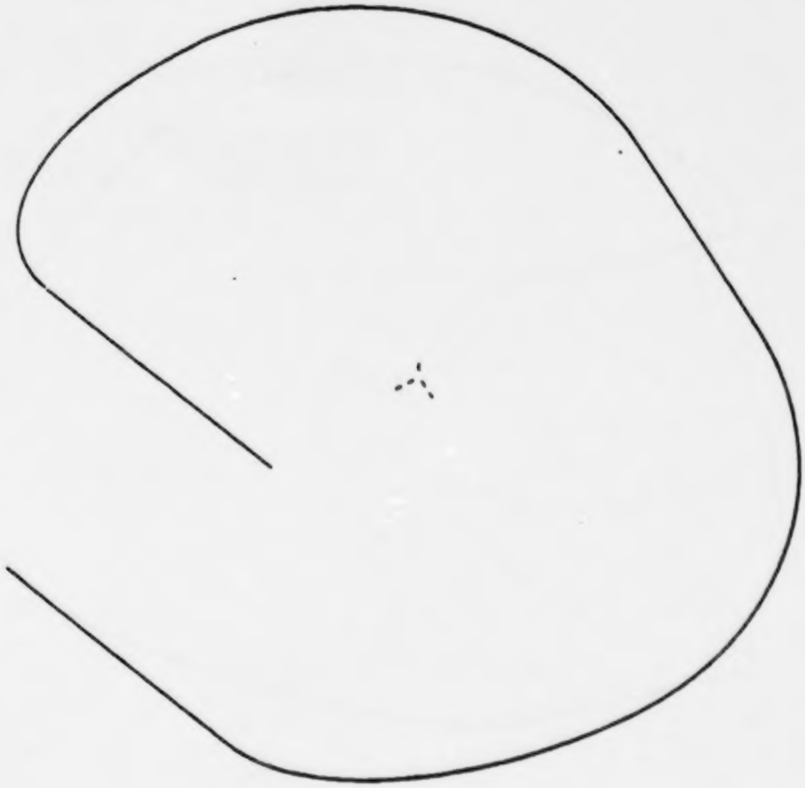

THETA = 30.00 PHI = 60.00 ETA = 90.00

FIGURE 3A

TWISTED LOOP ELEMENT

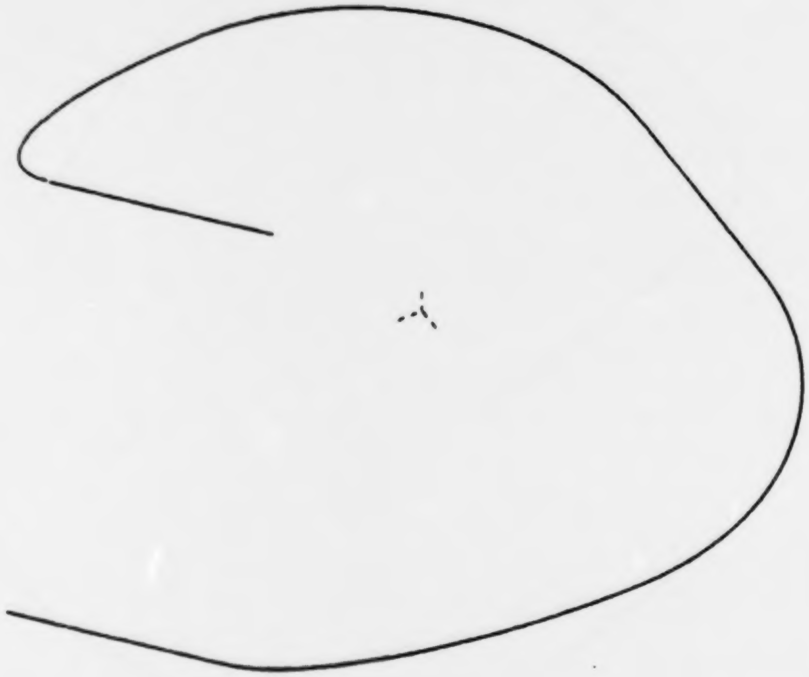

THETA = 45.00 PHI = 60.00 ETA = 90.00

FIGURE 3B

TWISTED LOOP ELEMENT

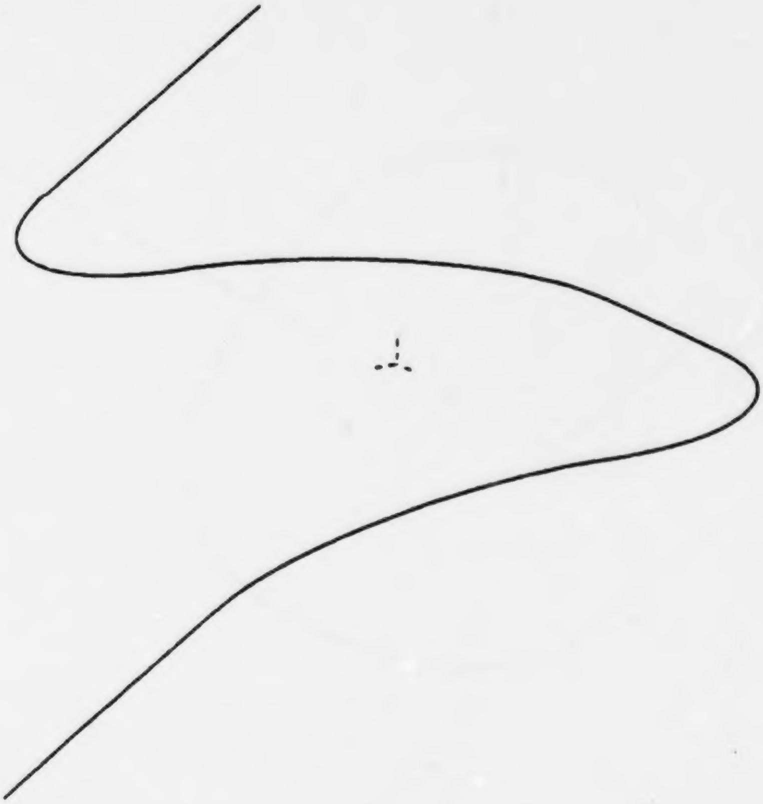

THETA = 75.00 PHI = 60.00 ETA = 90.00

FIGURE 3C

TWISTED LOOP WITH HORIZONTAL SUPPORTS

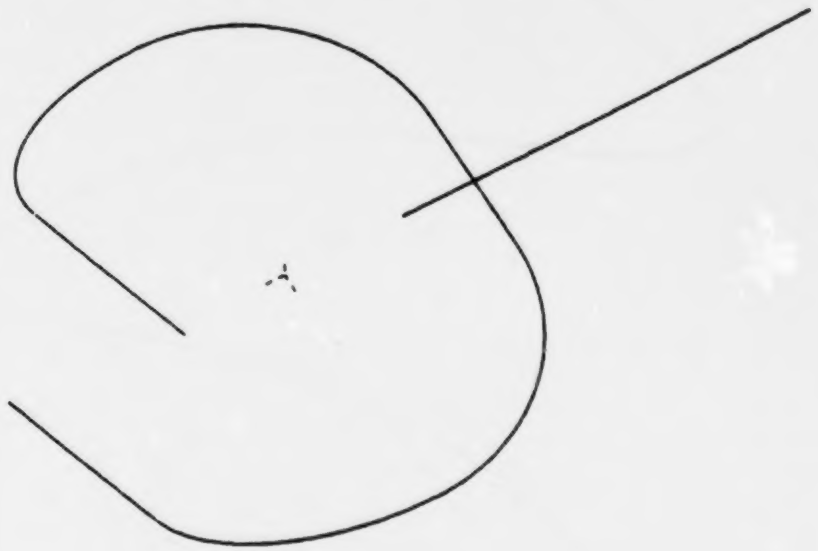

THETA = 30.00 PHI = 60.00 ETA = 90.00

FIGURE 3D

TWISTED LOOP WITH HORIZONTAL SUPPORTS

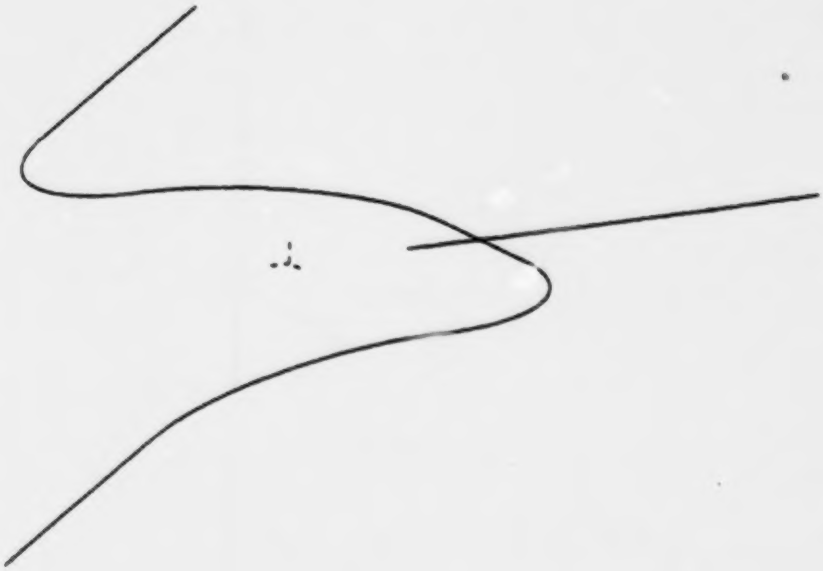

THETA = 75.00 PHI = 60.00 ETA = 90.00

FIGURE 3E

TWISTED LOOP ELEMENT WITH FEEDLINE

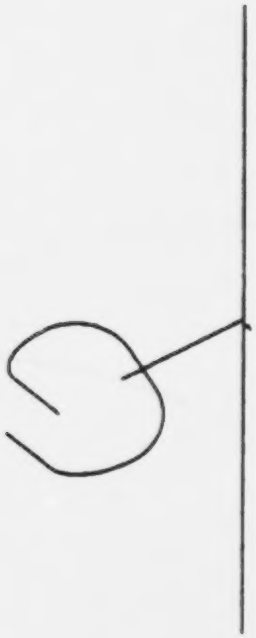

THETA = 30.00 PHI = 60.00 ETA = 90.00

FIGURE 3F

TWISTED LOOP ELEMENT WITH FEEDLINE

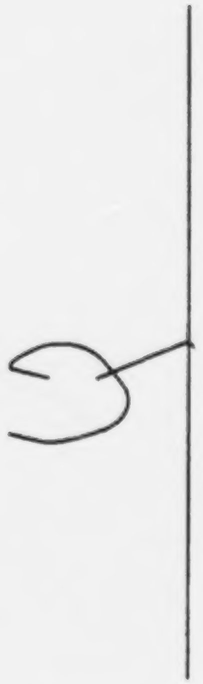

THETA = 45.00 PHI = 60.00 ETA = 90.00

FIGURE 3G

TWISTED LOOP ELEMENT WITH FEEDLINE

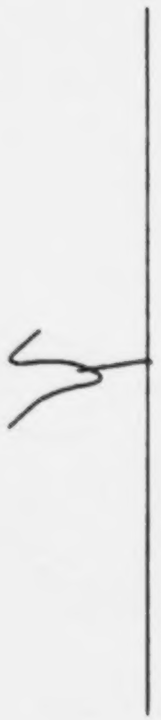

THETA = 75.00 PHI = 60.00 ETA = 90.00

FIGURE 3H

SEGMENTED TWISTED LOOP ELEMENT

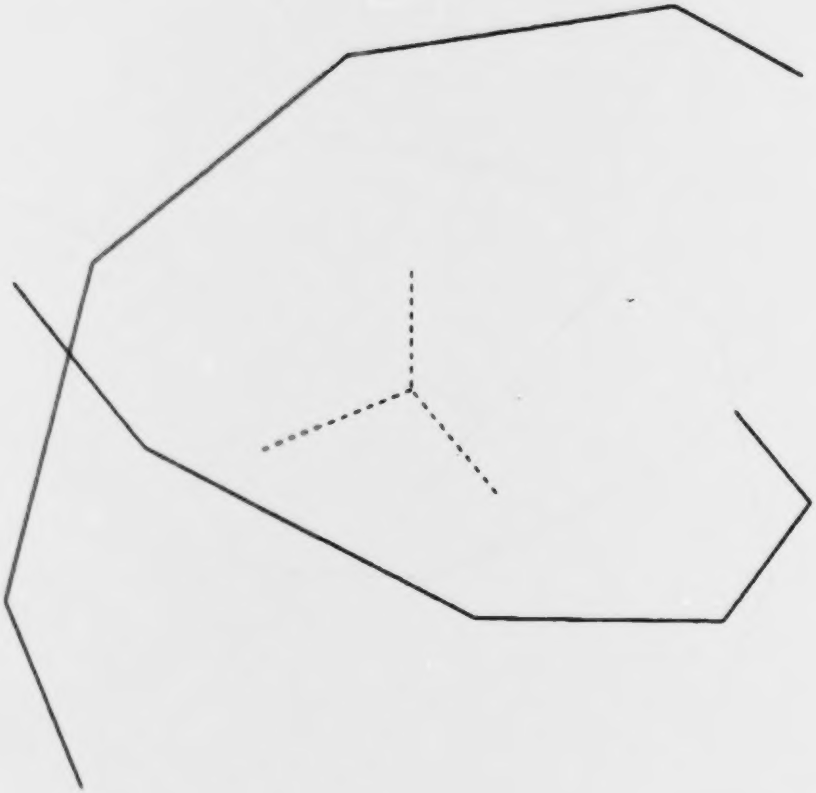

THETA = 45.00 PHI = 60.00 ETA = 90.00

FIGURE 4A

SEGMENTED TWISTED LOOP WITH HORIZONTAL SUPPORTS

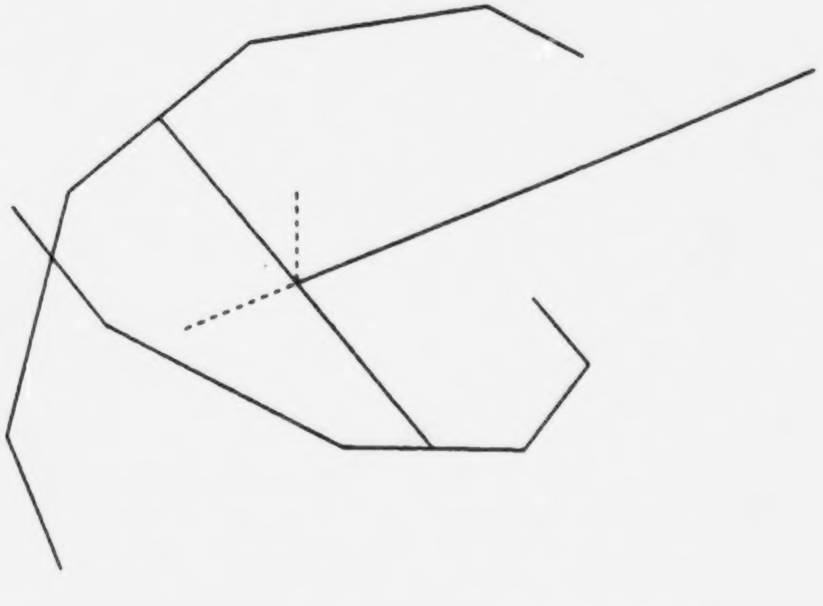

THETA = 45.00 PHI = 60.00 ETA = 90.00

FIGURE 4B

SEGMENTED TWISTED LOOP WITH FEEDLINE

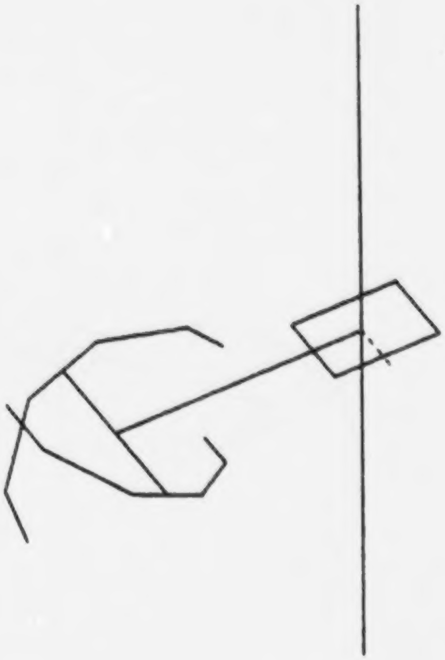

THETA = 45.00 PHI = 60.00 ETA = 90.00

FIGURE 4C

SEGMENTED TWISTED LOOP WITH FEEDLINE

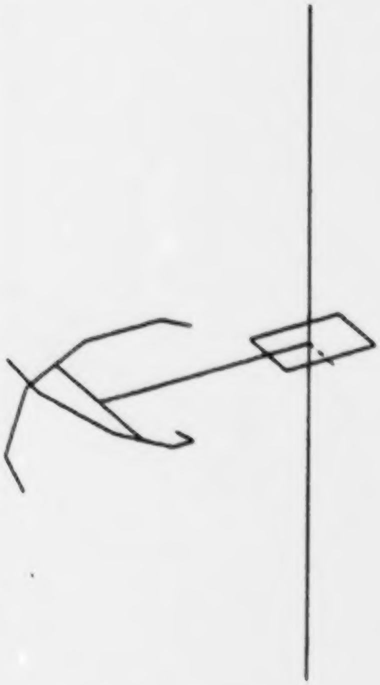

THETA = 60.00 PHI = 60.00 ETA = 90.00

FIGURE 4D

THE SUPER–TURNSTILE VHF TV ELEMENT

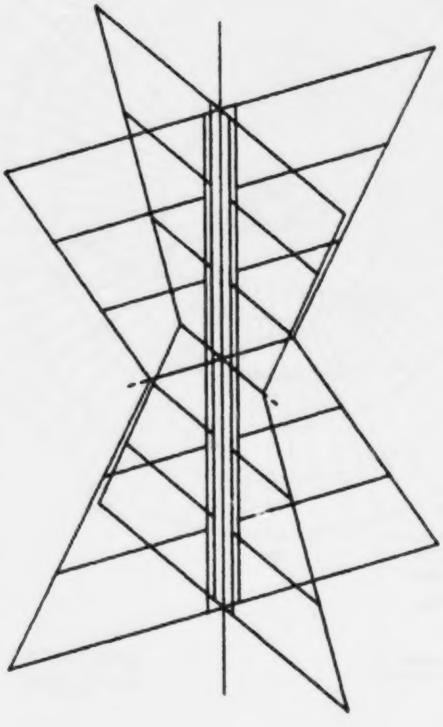

THETA = 60.00 PHI = 60.00 ETA = 90.00

FIGURE 5

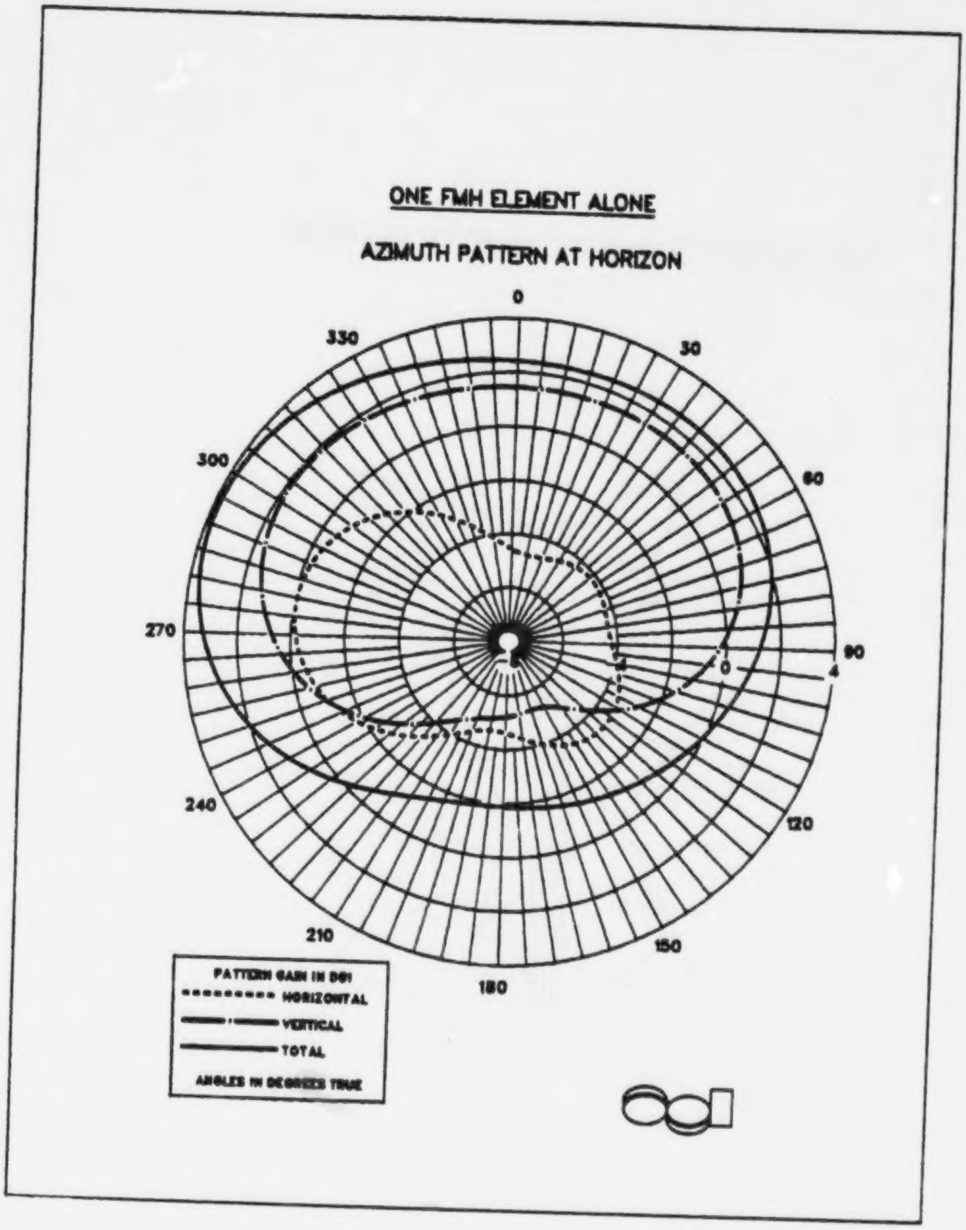
ONE FMH ELEMENT ALONE
AZIMUTH PATTERN AT HORIZON
0
30
60
90
120
150
180
210
240
270
300
330
0
4
PATTERN GAIN IN DBI
HORIZONTAL
VERTICAL
TOTAL
ANGLES IN DEGREES TRUE

FIGURE 6A

ONE FMH ELEMENT ALONE

VERTICAL PATTERN AT BORESITE

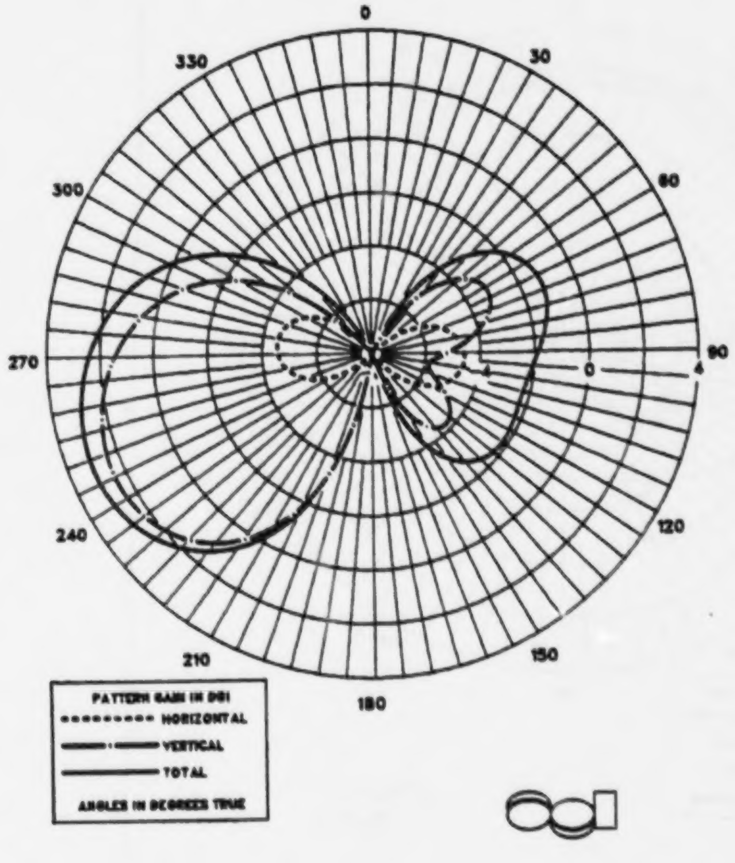

FIGURE 6B

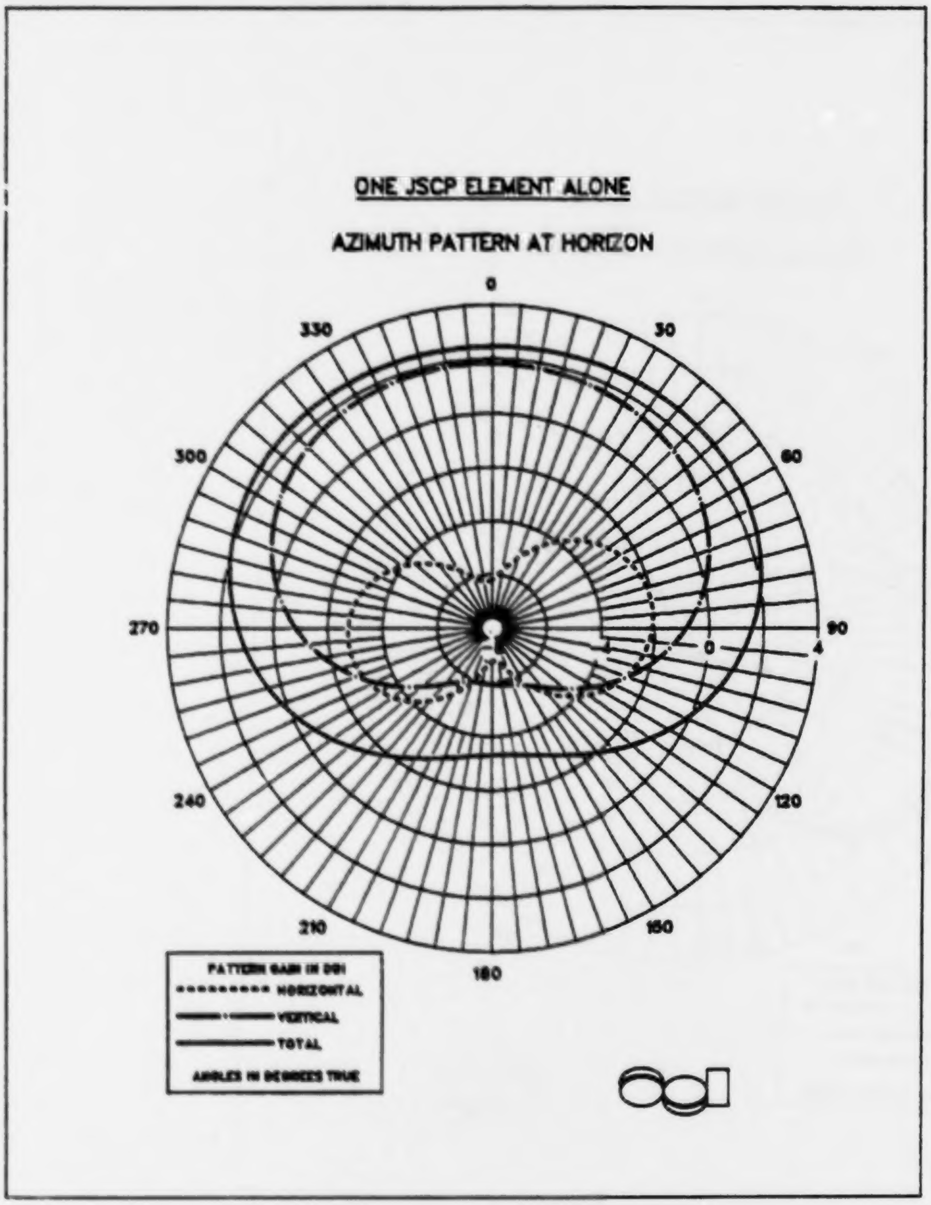

ONE JSCP ELEMENT ALONE

AZIMUTH PATTERN AT HORIZON

FIGURE 7A

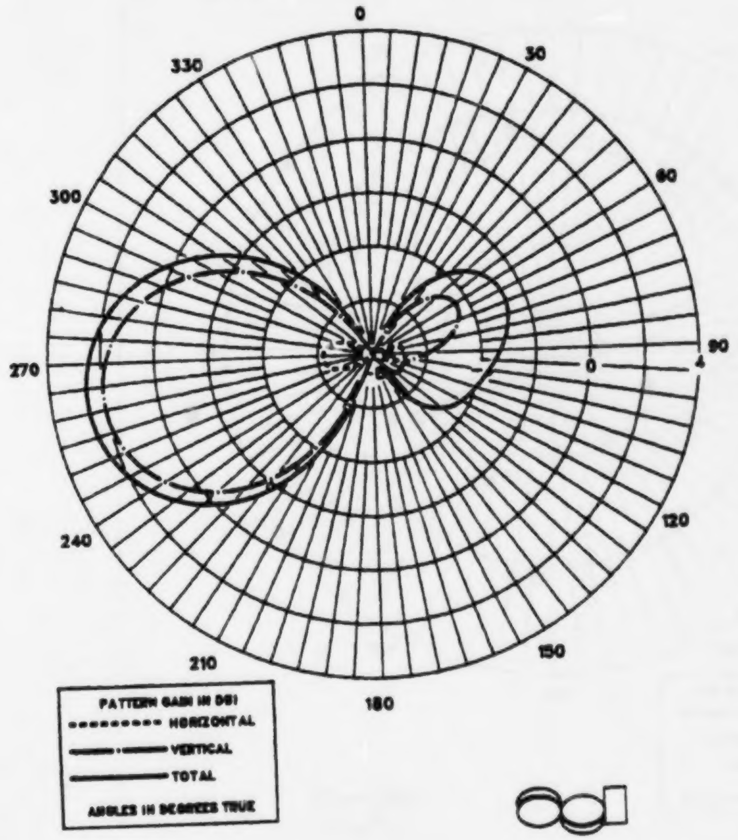

ONE JSCP ELEMENT ALONE

VERTICAL PATTERN AT BORESITE

FIGURE 7B

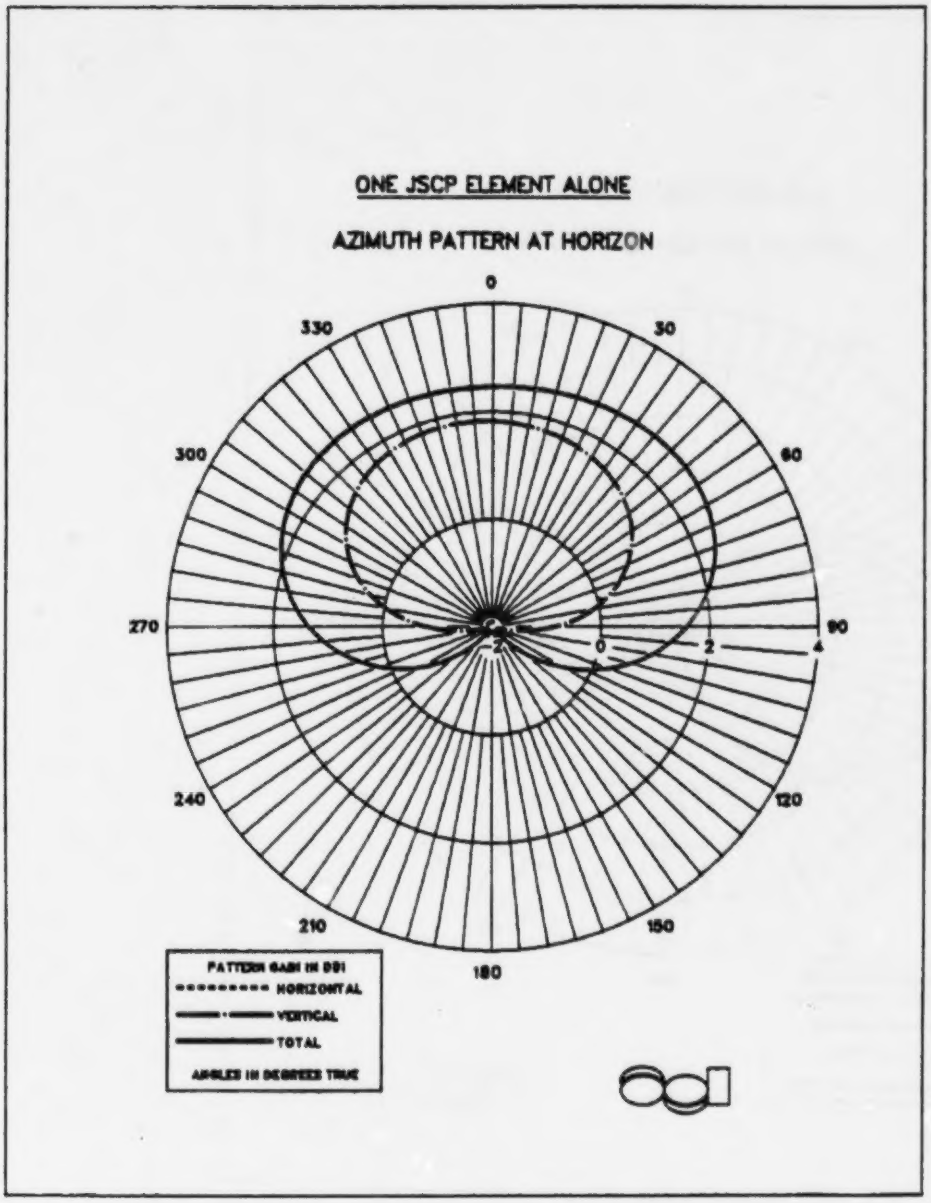
ONE JSCP ELEMENT ALONE
AZIMUTH PATTERN AT HORIZON
0
30
60
90
120
150
180
210
240
270
300
330
-2
0
2
4
PATTERN GAIN IN DBI
HORIZONTAL
VERTICAL
TOTAL
ANGLES IN DEGREES TRUE
ODI

FIGURE 7C

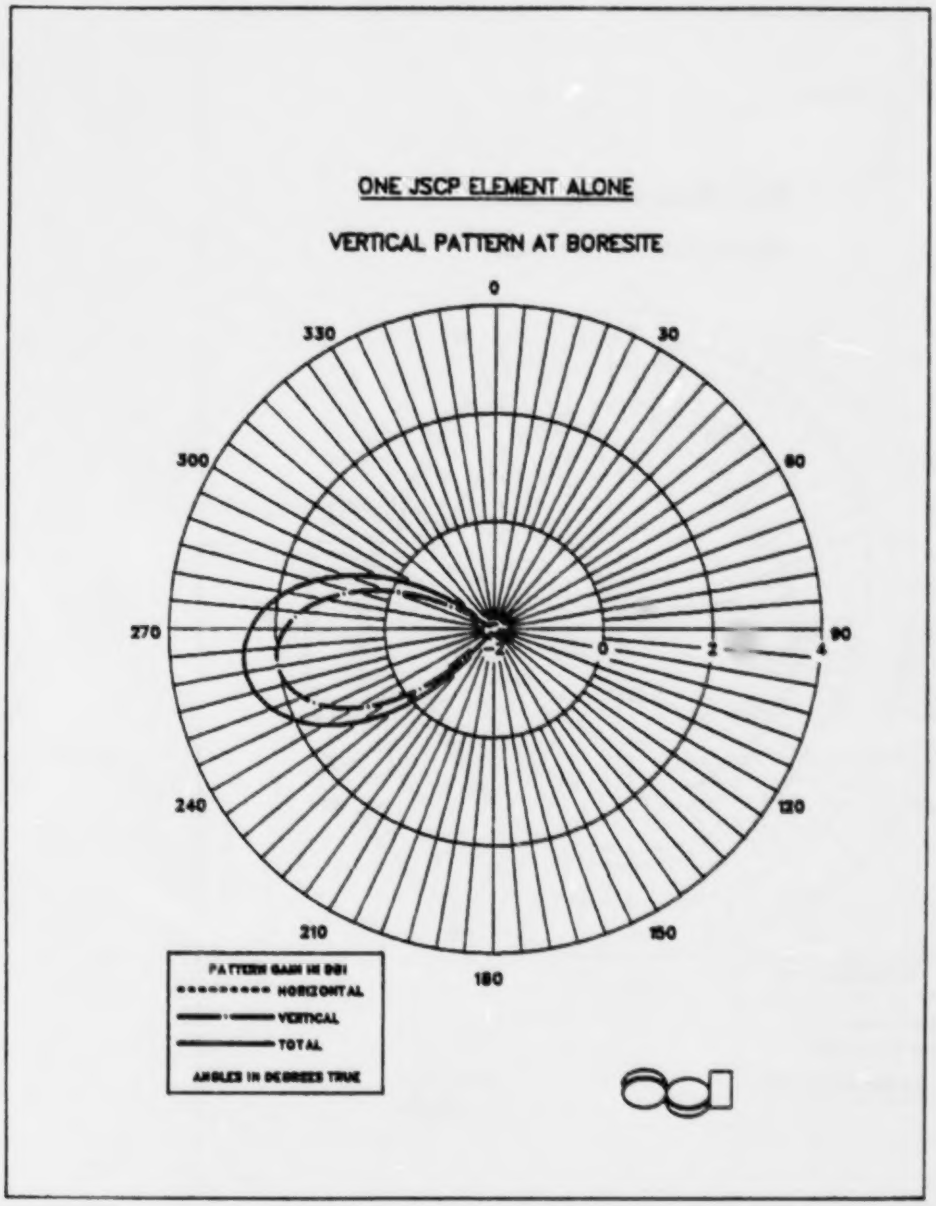
ONE JSCP ELEMENT ALONE

VERTICAL PATTERN AT BORESITE

FIGURE 7D

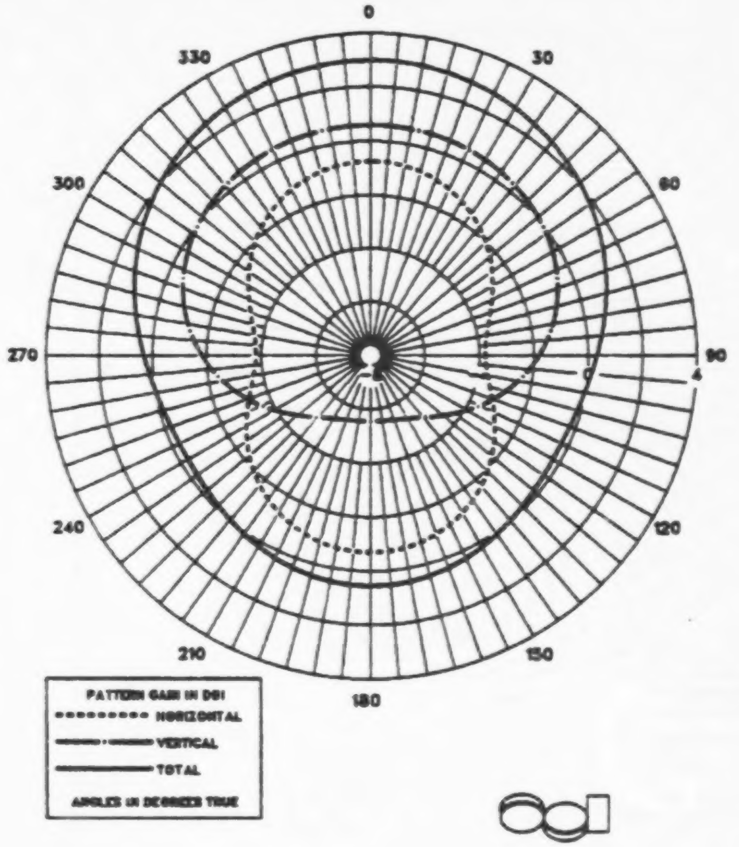

ONE CYCLOID ELEMENT ALONE

AZIMUTH PATTERN AT HORIZON

FIGURE 8A

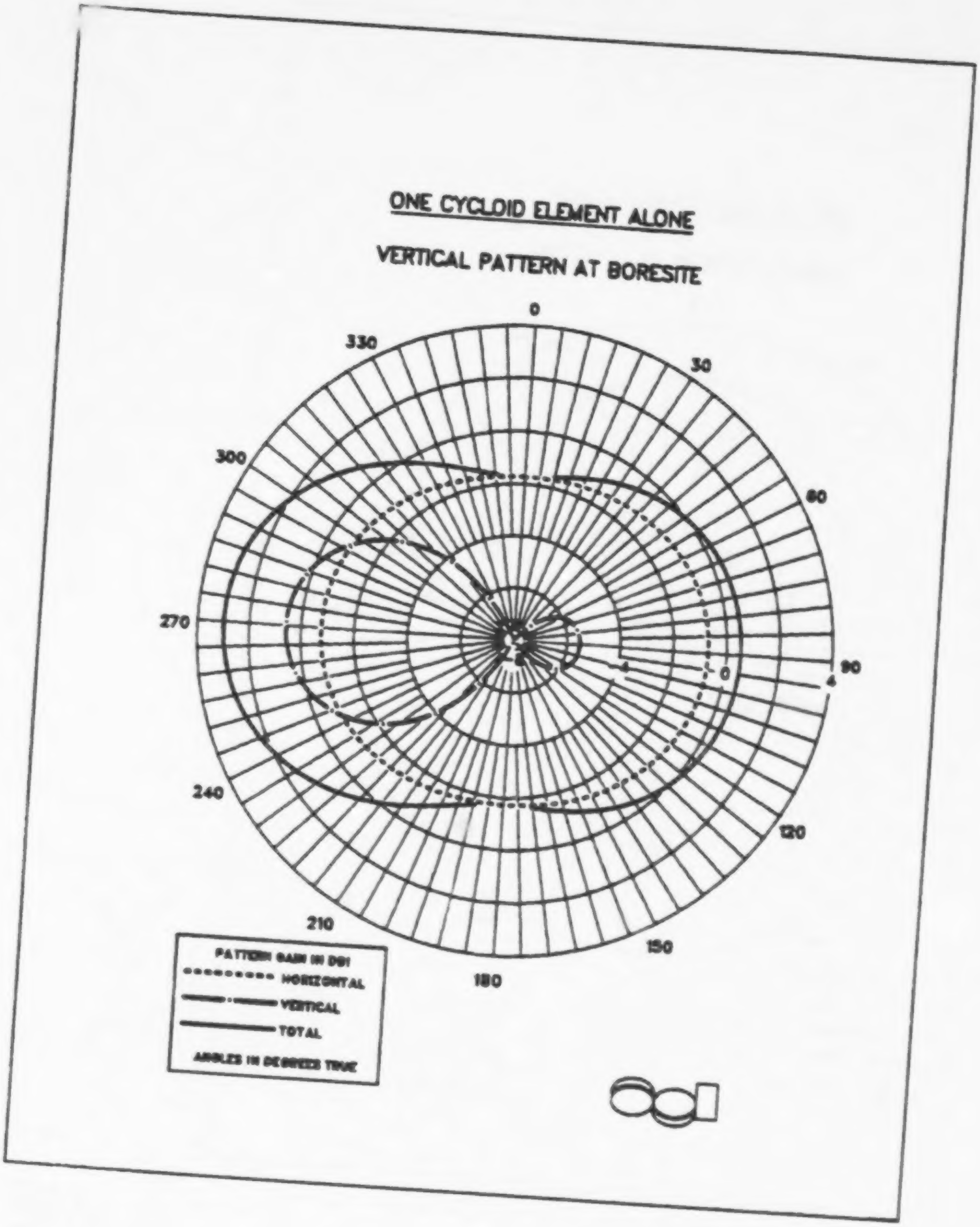
ONE CYCLOID ELEMENT ALONE

VERTICAL PATTERN AT BORESITE

FIGURE 8B

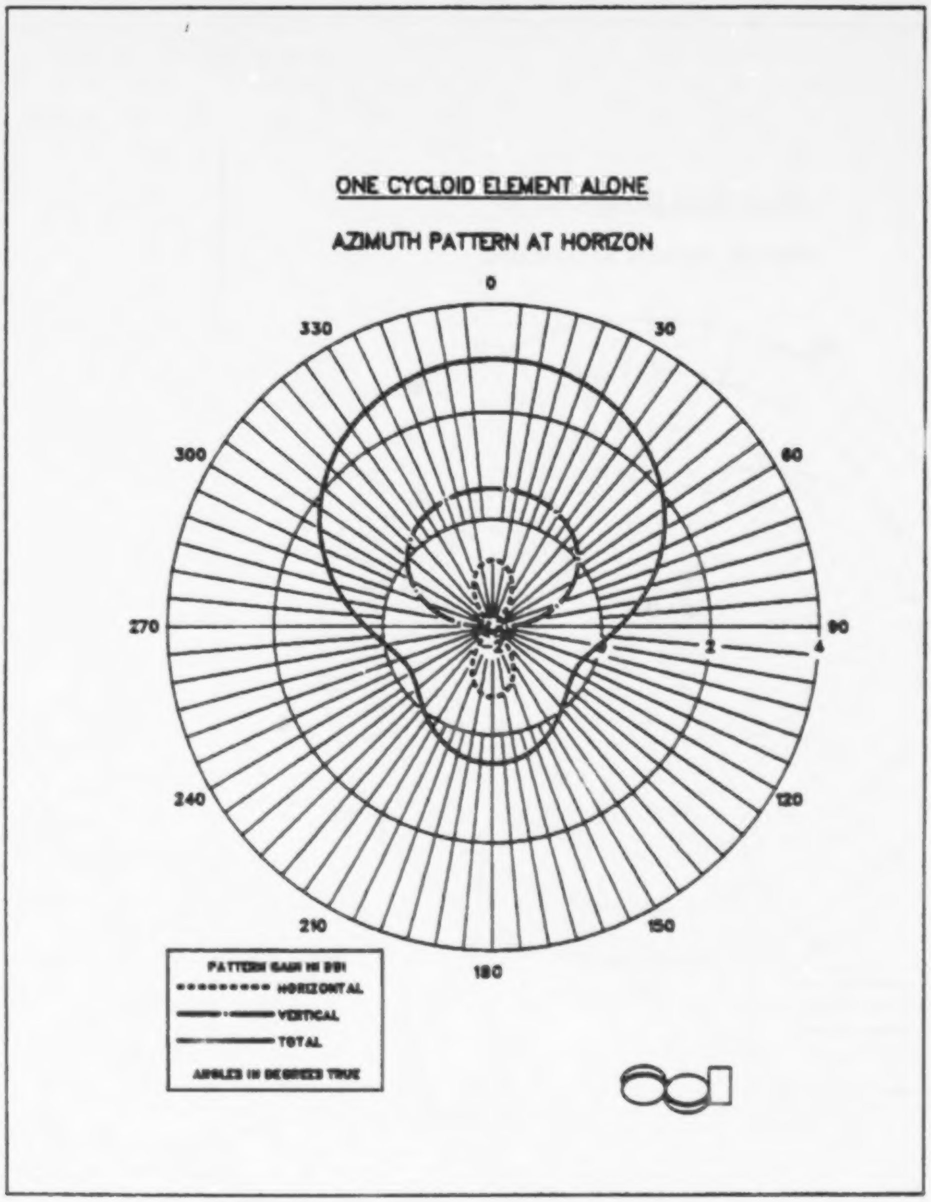
ONE CYCLOID ELEMENT ALONE

AZIMUTH PATTERN AT HORIZON

FIGURE 8C

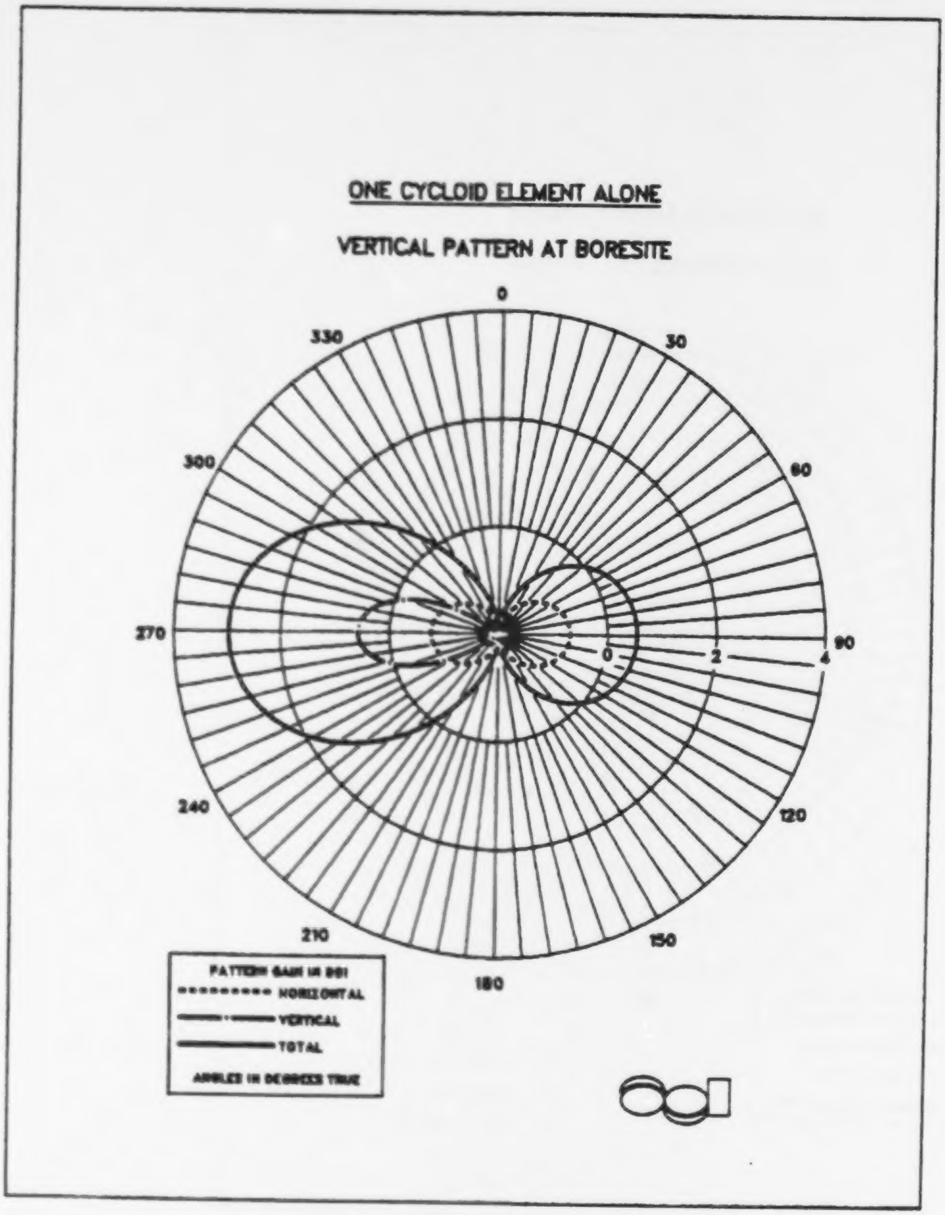

ONE CYCLOID ELEMENT ALONE

VERTICAL PATTERN AT BORESITE

FIGURE 8D

ONE COMARK ELEMENT ALONE

AZIMUTH PATTERN AT HORIZON

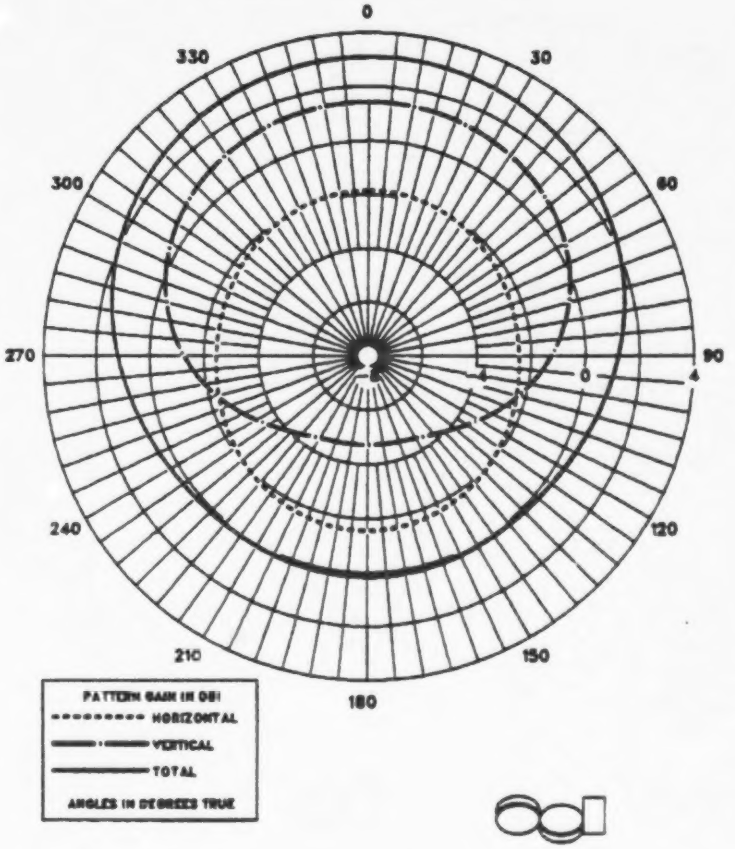

FIGURE 9A

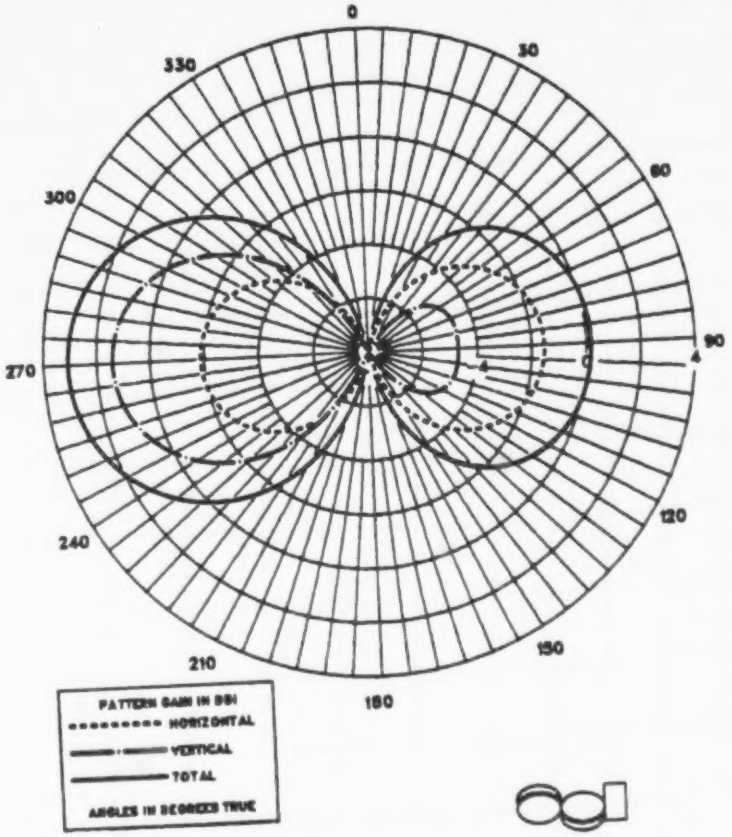

ONE COMARK ELEMENT ALONE

VERTICAL PATTERN AT BORESITE

FIGURE 9B

PANEL ANTENNA ELEMENT

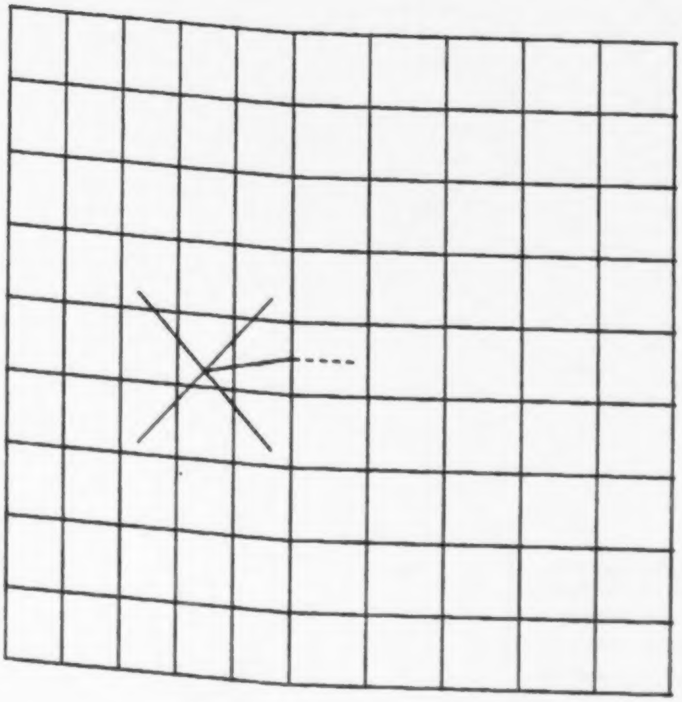

THETA = 85.00 PHI = 30.00 ETA = 90.00

FIGURE 10A

PANEL ANTENNA ELEMENT

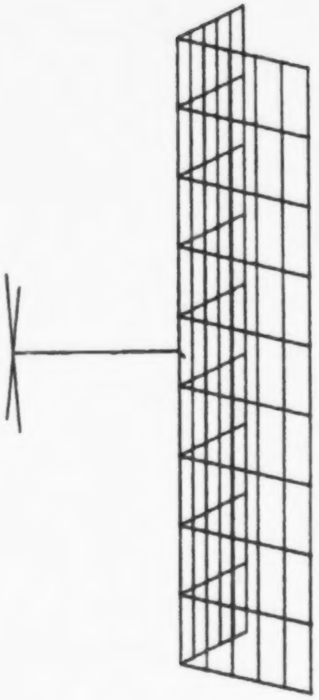

THETA = 85.00 PHI = 85.00 ETA = 90.00

FIGURE 10B

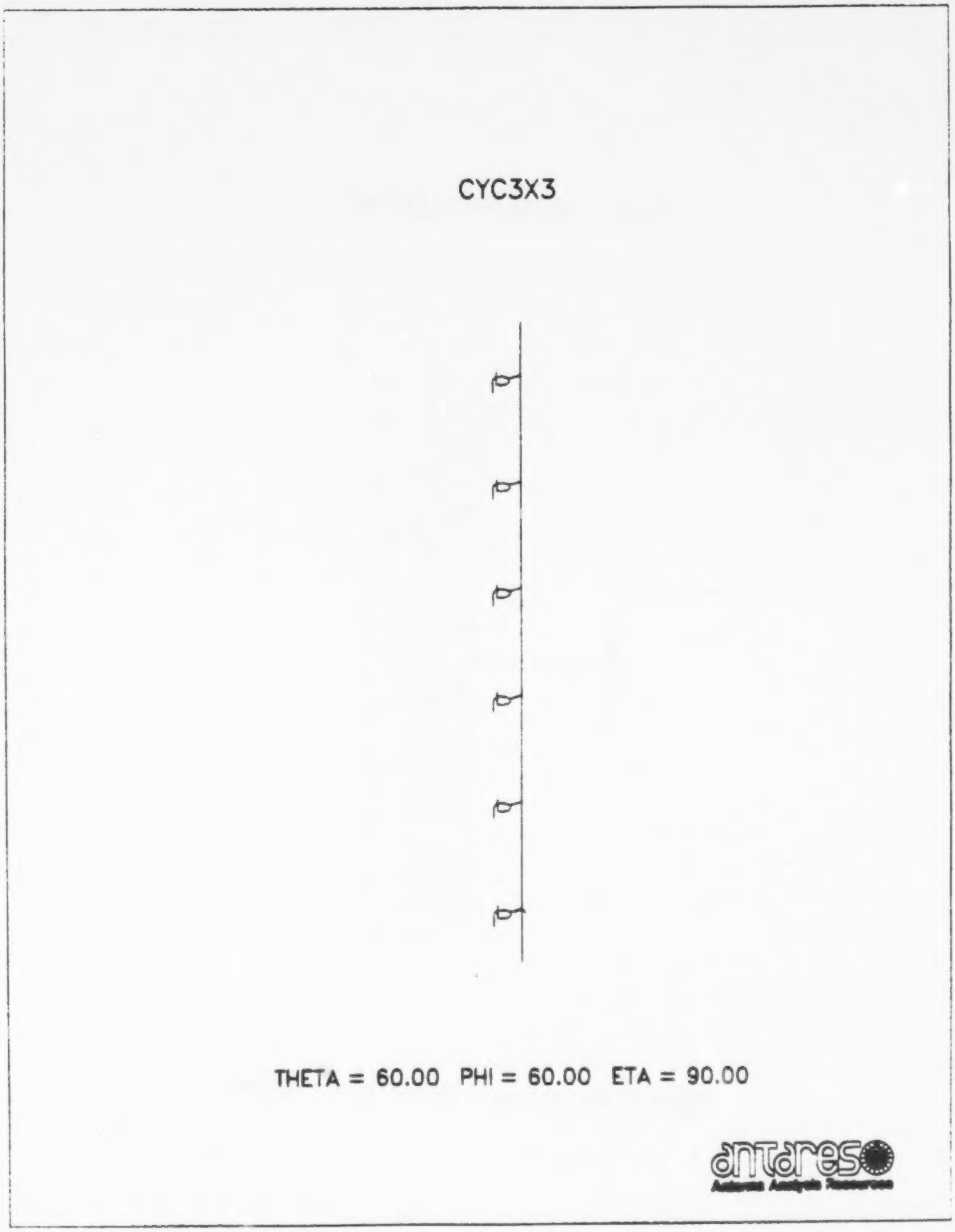
CYC3X3
THETA = 60.00 PHI = 60.00 ETA = 90.00
antares
Antares Analysis Resources

75<

FIGURE 11A

CYC4X4TW

THETA = 60.00 PHI = 60.00 ETA = 90.00

FIGURE 11B

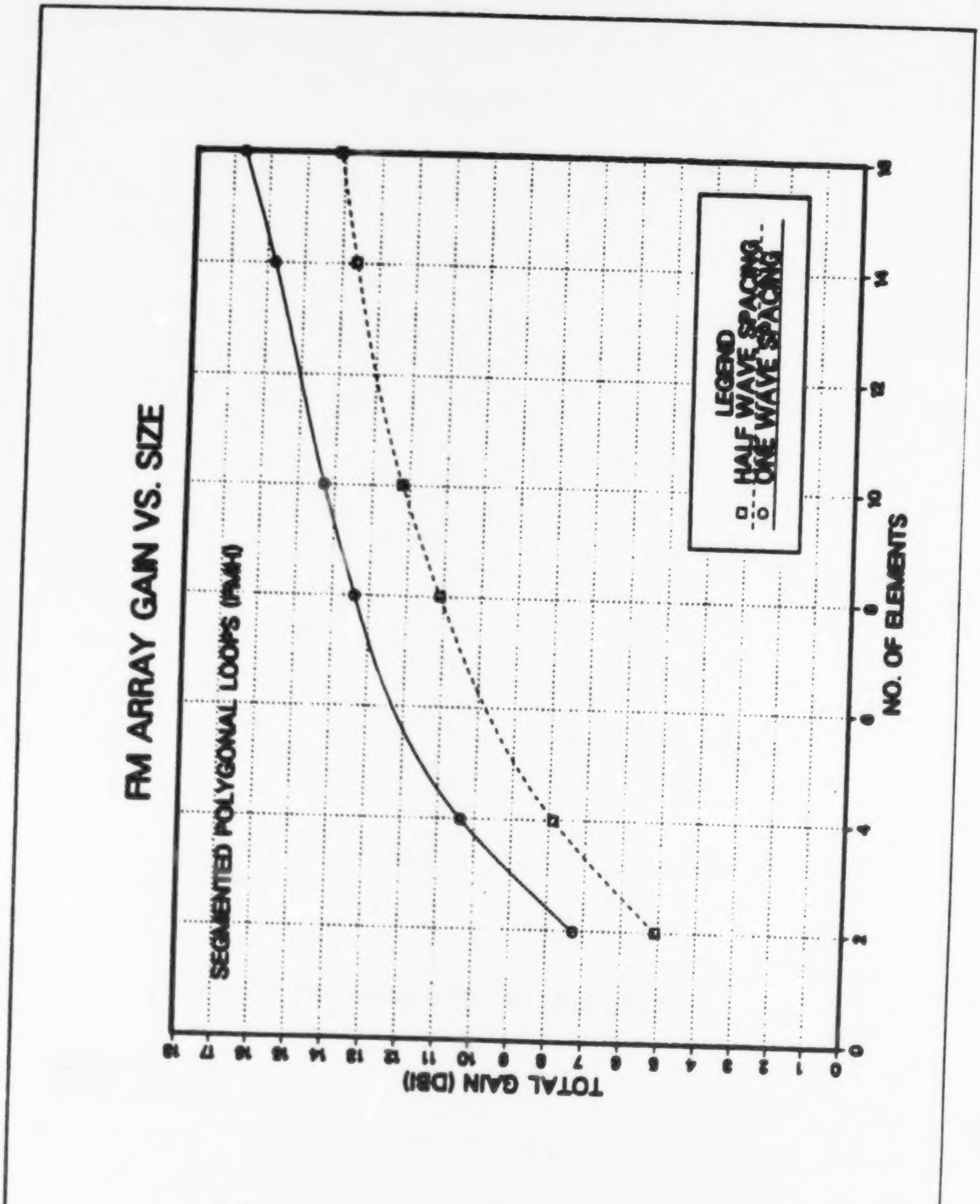
FM ARRAY GAIN VS. SIZE
SEGMENTED POLYGONAL LOOPS (FM-H)
TOTAL GAIN (DBI)
0
1
2
3
4
5
6
7
8
9
10
11
12
13
14
15
16
17
18
NO. OF ELEMENTS
0
2
4
6
8
10
12
14
16
LEGEND
□ HALF WAVE SPACING
○ ONE WAVE SPACING

FIGURE 12

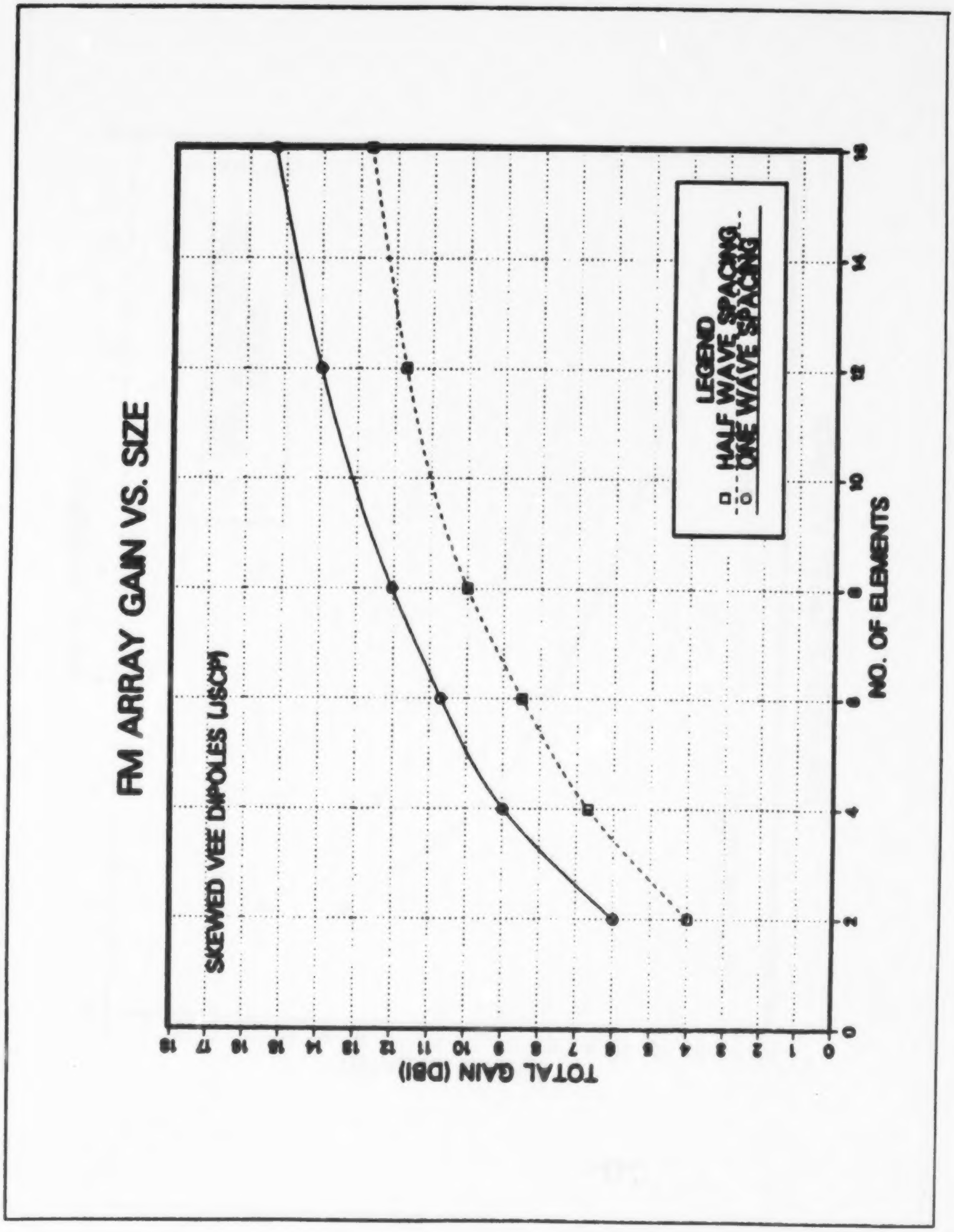
FM ARRAY GAIN VS. SIZE
SKEWED VEE DIPOLES (JSCP)
LEGEND
□ HALF WAVE SPACING
○ ONE WAVE SPACING
TOTAL GAIN (DBI)
0
1
2
3
4
5
6
7
8
9
10
11
12
13
14
15
16
17
18
NO. OF ELEMENTS
0
2
4
6
8
10
12
14
16

FIGURE 13

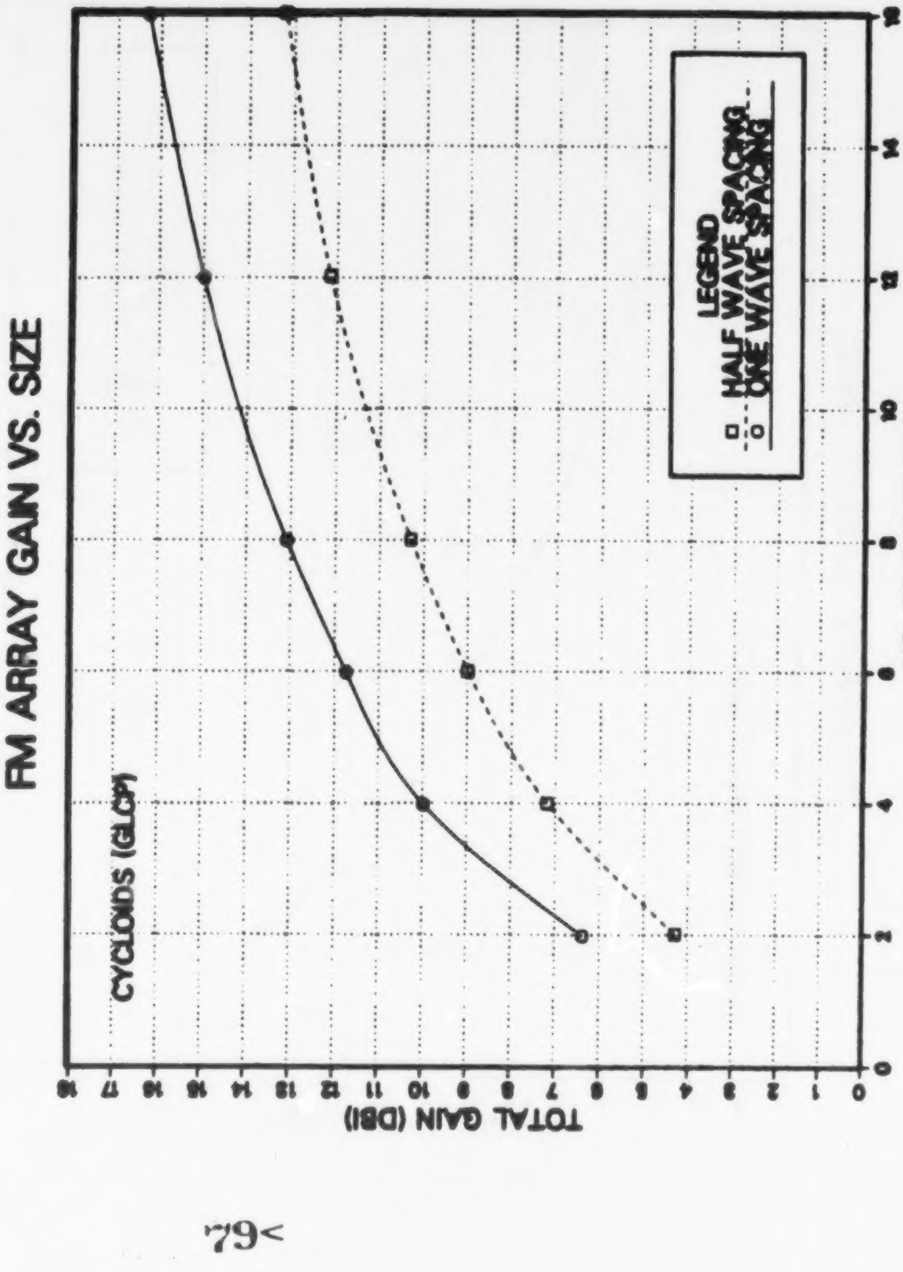
FM ARRAY GAIN VS. SIZE
CYCLOIDS (GLCP)
TOTAL GAIN (DBI)
0
1
2
3
4
5
6
7
8
9
10
11
12
13
14
15
16
17
18
NO. OF ELEMENTS
0
2
4
6
8
10
12
14
16
LEGEND
HALF WAVE SPACING
ONE WAVE SPACING

FIGURE 14

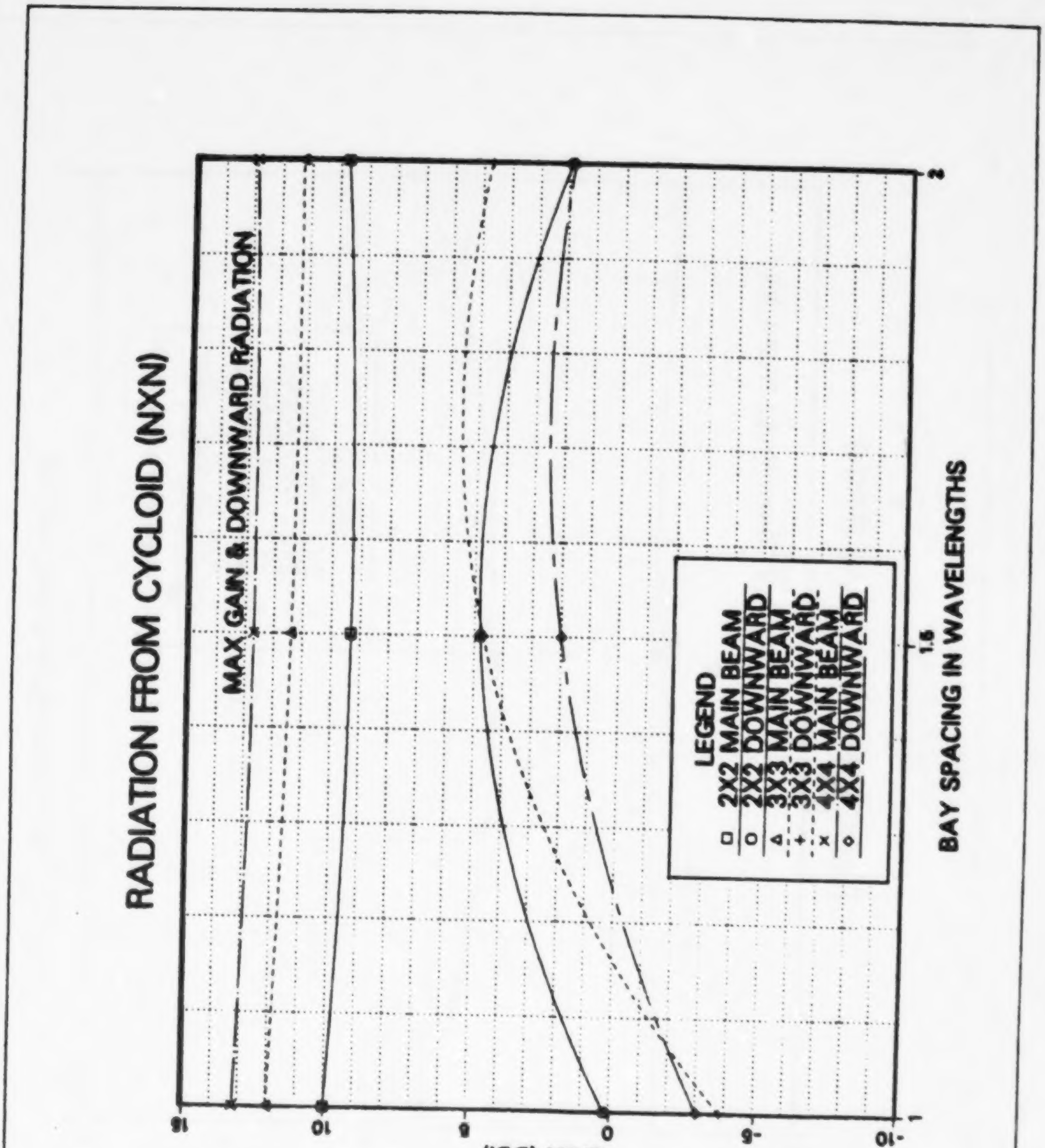
RADIATION FROM CYCLOID (NXN)
MAX GAIN & DOWNWARD RADIATION
GAIN (DBI)
15
10
5
0
-5
-10
1
1.5
2
BAY SPACING IN WAVELENGTHS
LEGEND
□ 2X2 MAIN BEAM
○ 2X2 DOWNWARD
△ 3X3 MAIN BEAM
+ 3X3 DOWNWARD
x 4X4 MAIN BEAM
◇ 4X4 DOWNWARD

FIGURE 15

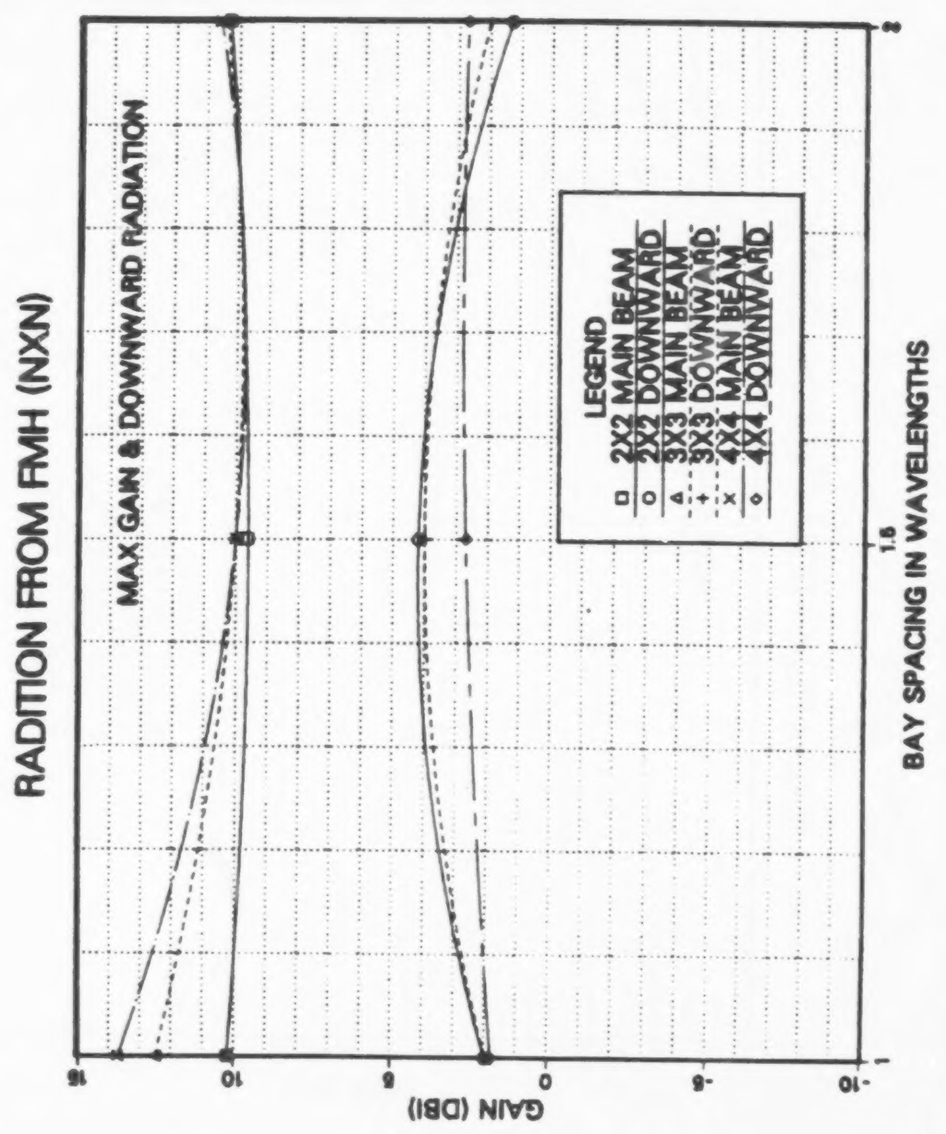
RADITION FROM FMH (NXN)
MAX GAIN & DOWNWARD RADIATION
LEGEND
□ 2X2 MAIN BEAM
○ 2X2 DOWNWARD
△ 3X3 MAIN BEAM
+ 3X3 DOWNWARD
× 4X4 MAIN BEAM
◇ 4X4 DOWNWARD
GAIN (DBI)
15
10
5
0
-5
-10
BAY SPACING IN WAVELENGTHS
1
1.5
2

FIGURE 16

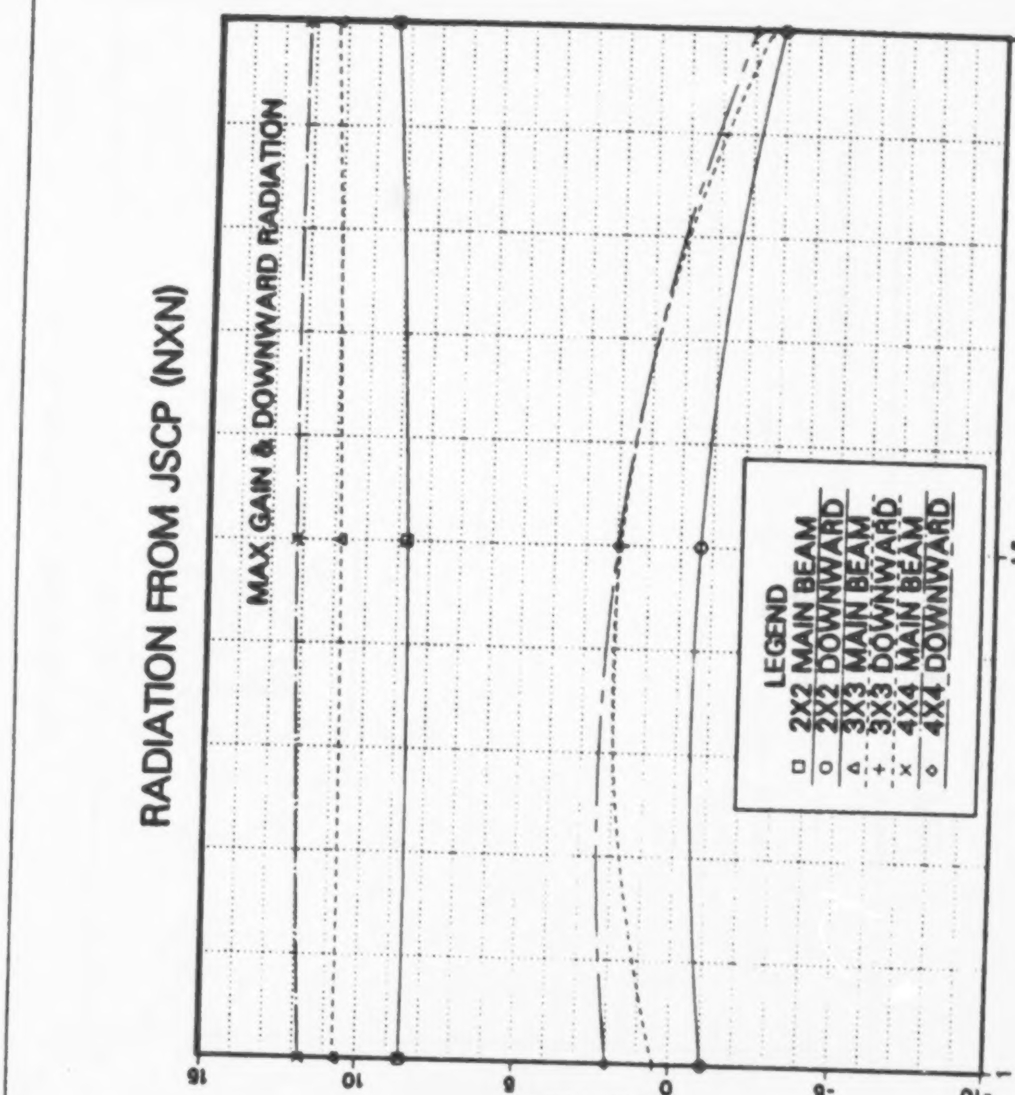
RADIATION FROM JSCP (NXN)
MAX GAIN & DOWNWARD RADIATION
GAIN (DBI)
15
10
5
0
-5
-10
1
1.5
2
BAY SPACING IN WAVELENGTHS
LEGEND
□ 2X2 MAIN BEAM
○ 2X2 DOWNWARD
△ 3X3 MAIN BEAM
+ 3X3 DOWNWARD
× 4X4 MAIN BEAM
◇ 4X4 DOWNWARD
82<

FIGURE 17

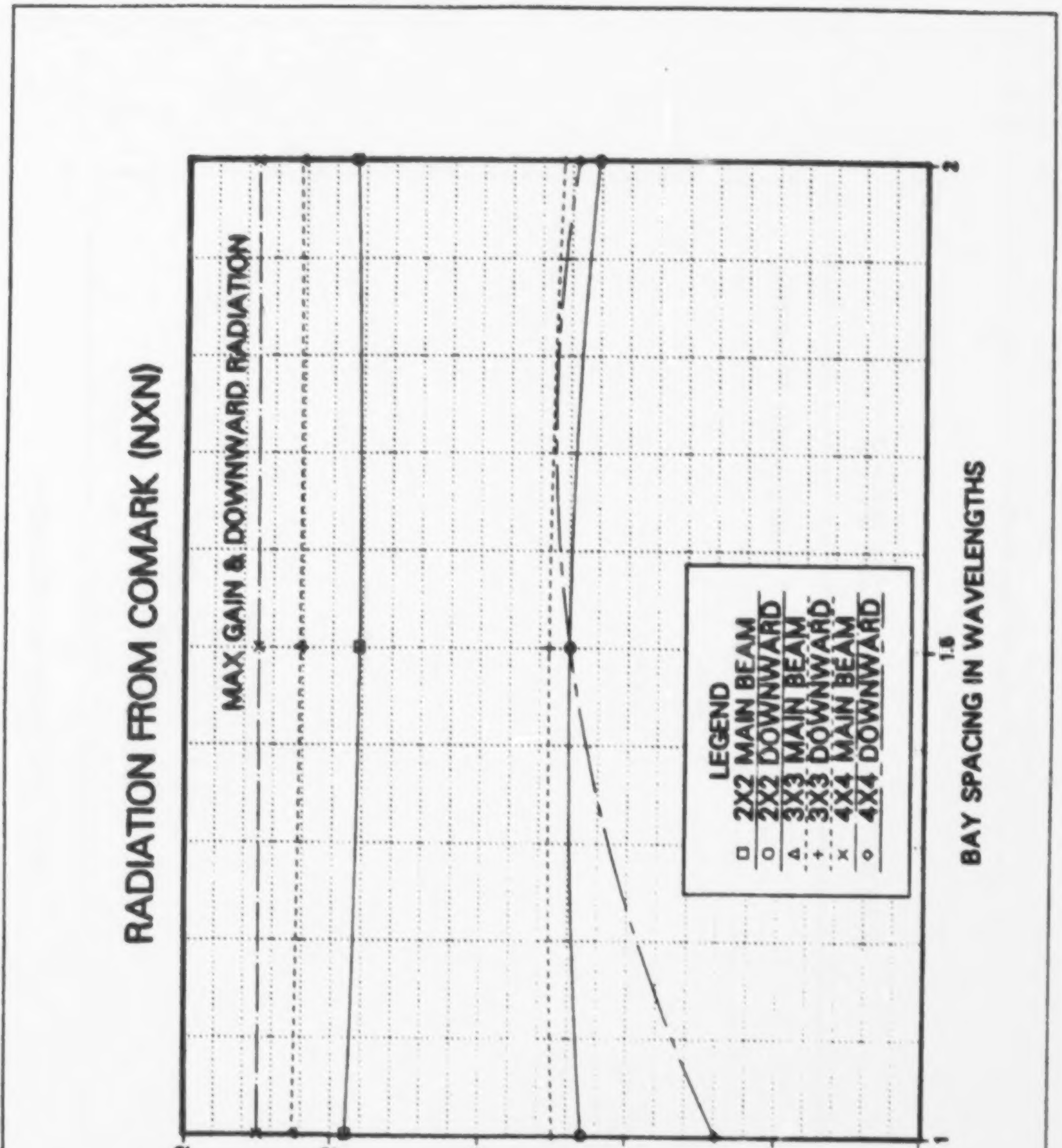
RADIATION FROM COMARK (NXN)
MAX GAIN & DOWNWARD RADIATION
GAIN (DBI)
15
10
5
0
-5
-10
BAY SPACING IN WAVELENGTHS
1
1.5
2
LEGEND
□ 2X2 MAIN BEAM
○ 2X2 DOWNWARD
△ 3X3 MAIN BEAM
+ 3X3 DOWNWARD
× 4X4 MAIN BEAM
◇ 4X4 DOWNWARD

83<

FIGURE 18

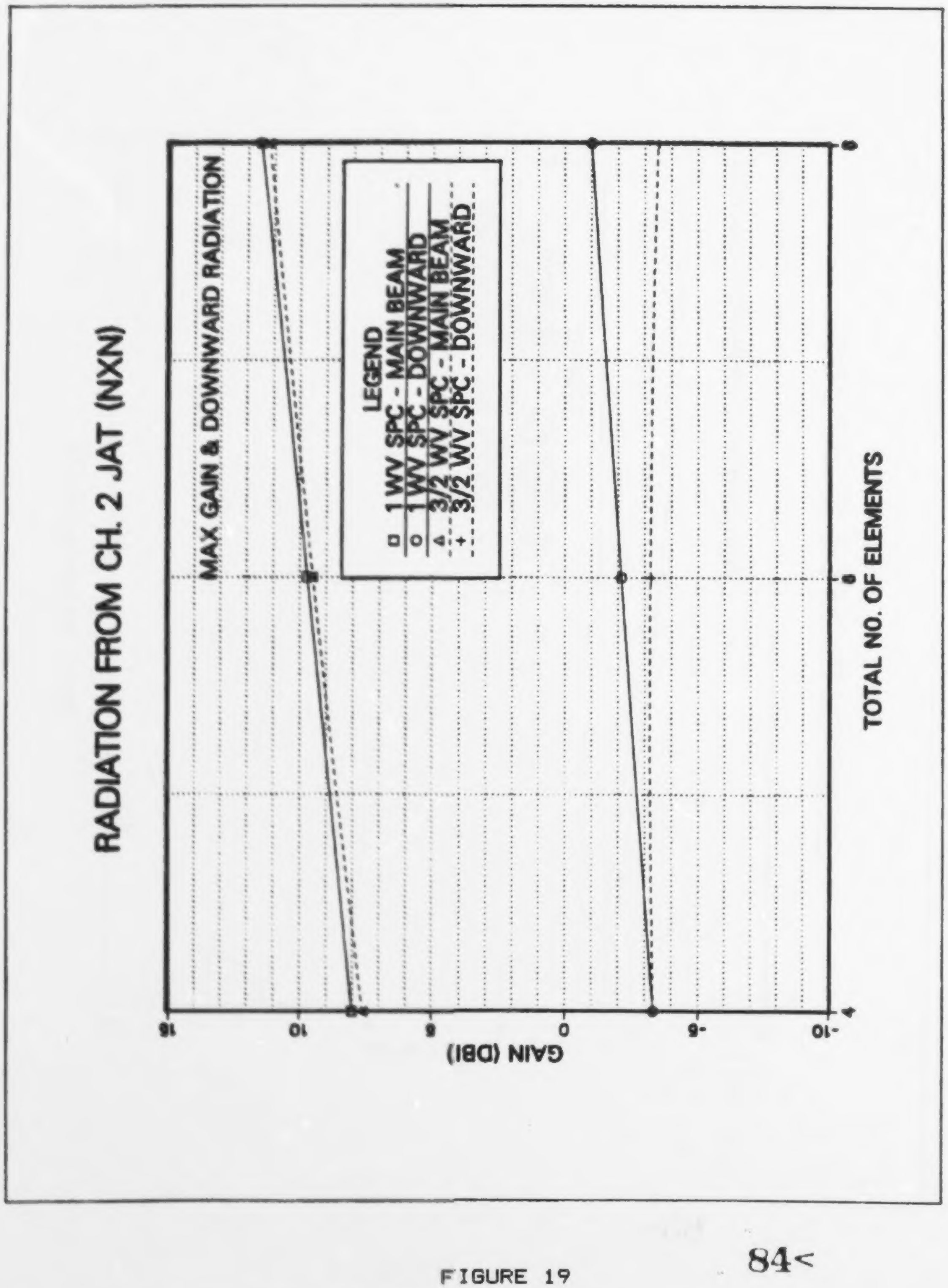
RADIATION FROM CH. 2 JAT (NXN)
MAX GAIN & DOWNWARD RADIATION
LEGEND
□ 1 WV SPC - MAIN BEAM
○ 1 WV SPC - DOWNWARD
△ 3/2 WV SPC - MAIN BEAM
+ 3/2 WV SPC - DOWNWARD
GAIN (DBI)
15
10
5
0
-5
-10
4
9
TOTAL NO. OF ELEMENTS

FIGURE 19

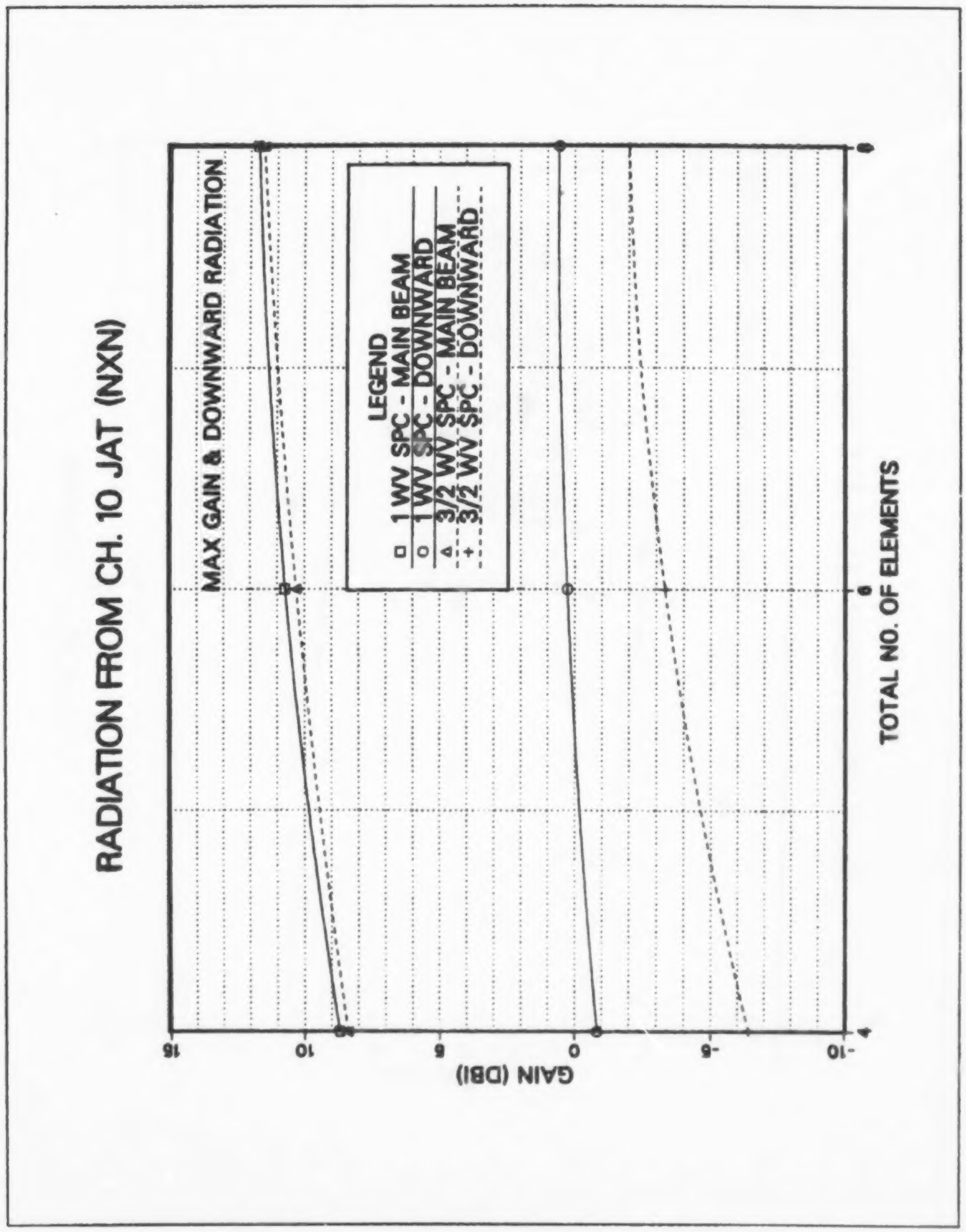
RADIATION FROM CH. 10 JAT (NXN)
MAX GAIN & DOWNWARD RADIATION
LEGEND
□ 1 WV SPC - MAIN BEAM
○ 1 WV SPC - DOWNWARD
△ 3/2 WV SPC - MAIN BEAM
+ 3/2 WV SPC - DOWNWARD
GAIN (DBI)
15
10
5
0
-5
-10
TOTAL NO. OF ELEMENTS
4
6
8

85<

FIGURE 20

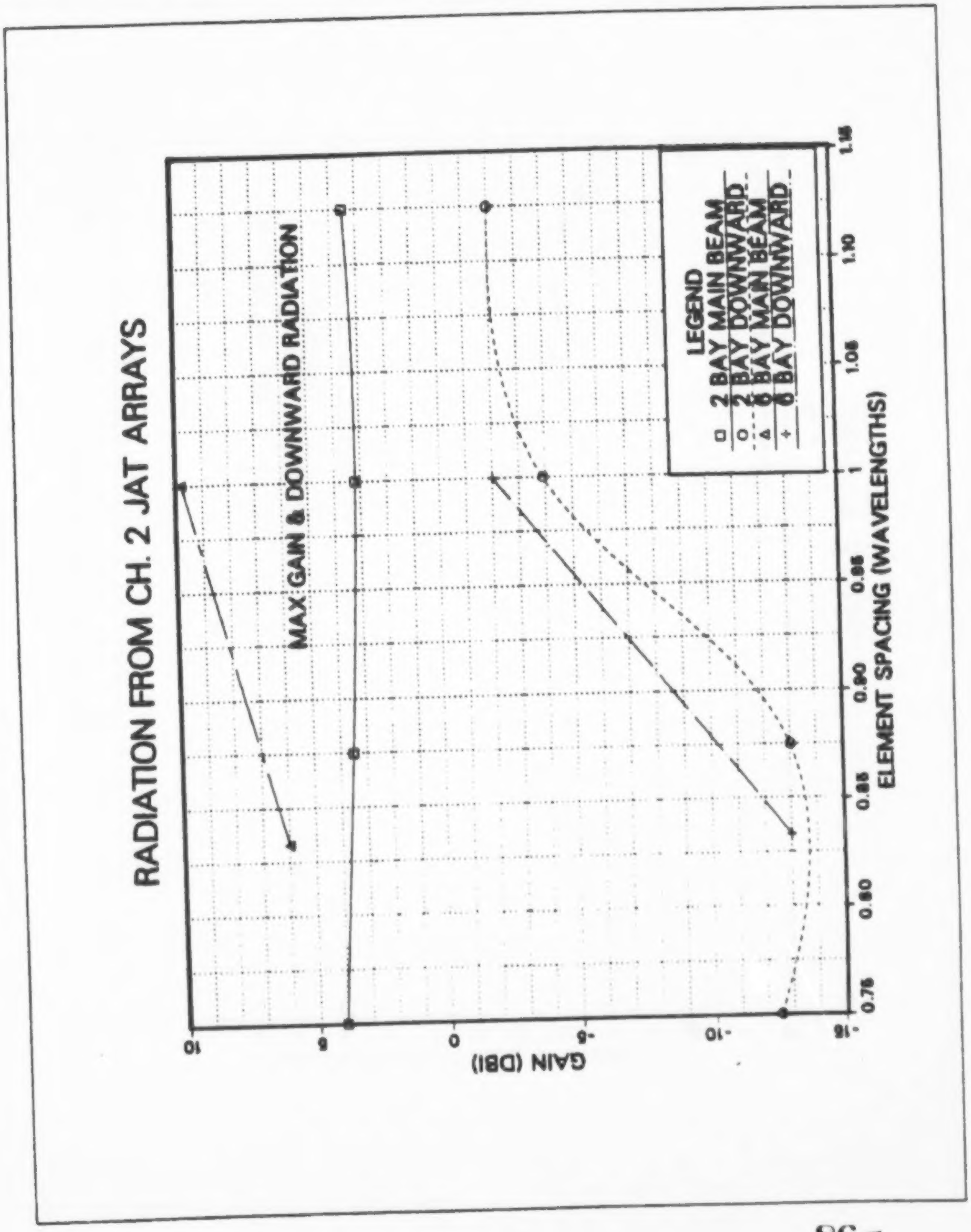
RADIATION FROM CH. 2 JAT ARRAYS
MAX GAIN & DOWNWARD RADIATION
GAIN (DBI)
10
5
0
-5
-10
-15
ELEMENT SPACING (WAVELENGTHS)
0.75
0.80
0.85
0.90
0.95
1
1.05
1.10
1.15
LEGEND
□ 2 BAY MAIN BEAM
○ 2 BAY DOWNWARD
△ 6 BAY MAIN BEAM
+ 6 BAY DOWNWARD

FIGURE 21

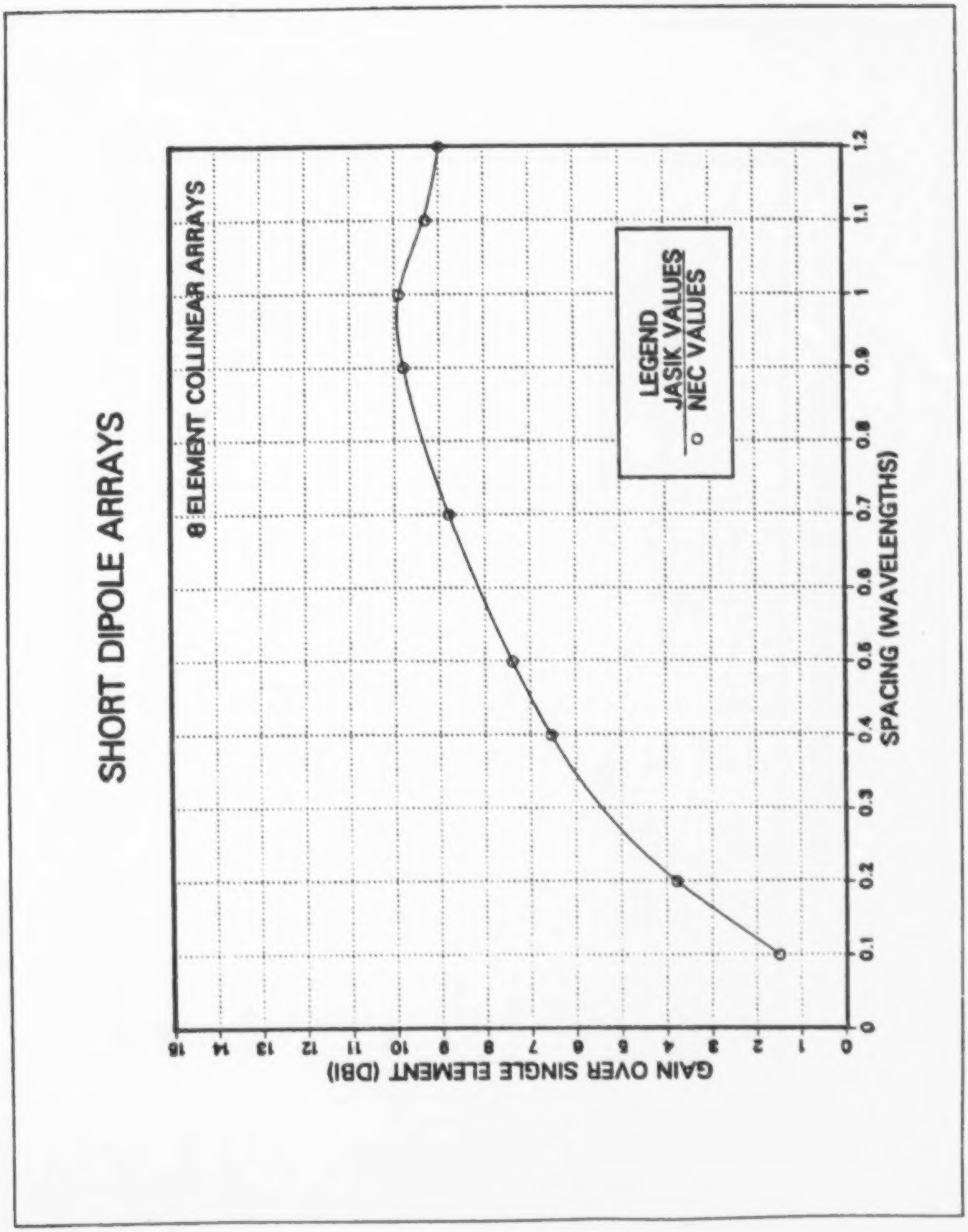
SHORT DIPOLE ARRAYS
8 ELEMENT COLLINEAR ARRAYS
GAIN OVER SINGLE ELEMENT (DBI)
0
1
2
3
4
5
6
7
8
9
10
11
12
13
14
15
SPACING (WAVELENGTHS)
0
0.1
0.2
0.3
0.4
0.5
0.6
0.7
0.8
0.9
1
1.1
1.2
LEGEND
JASIK VALUES
o NEC VALUES

FIGURE 22

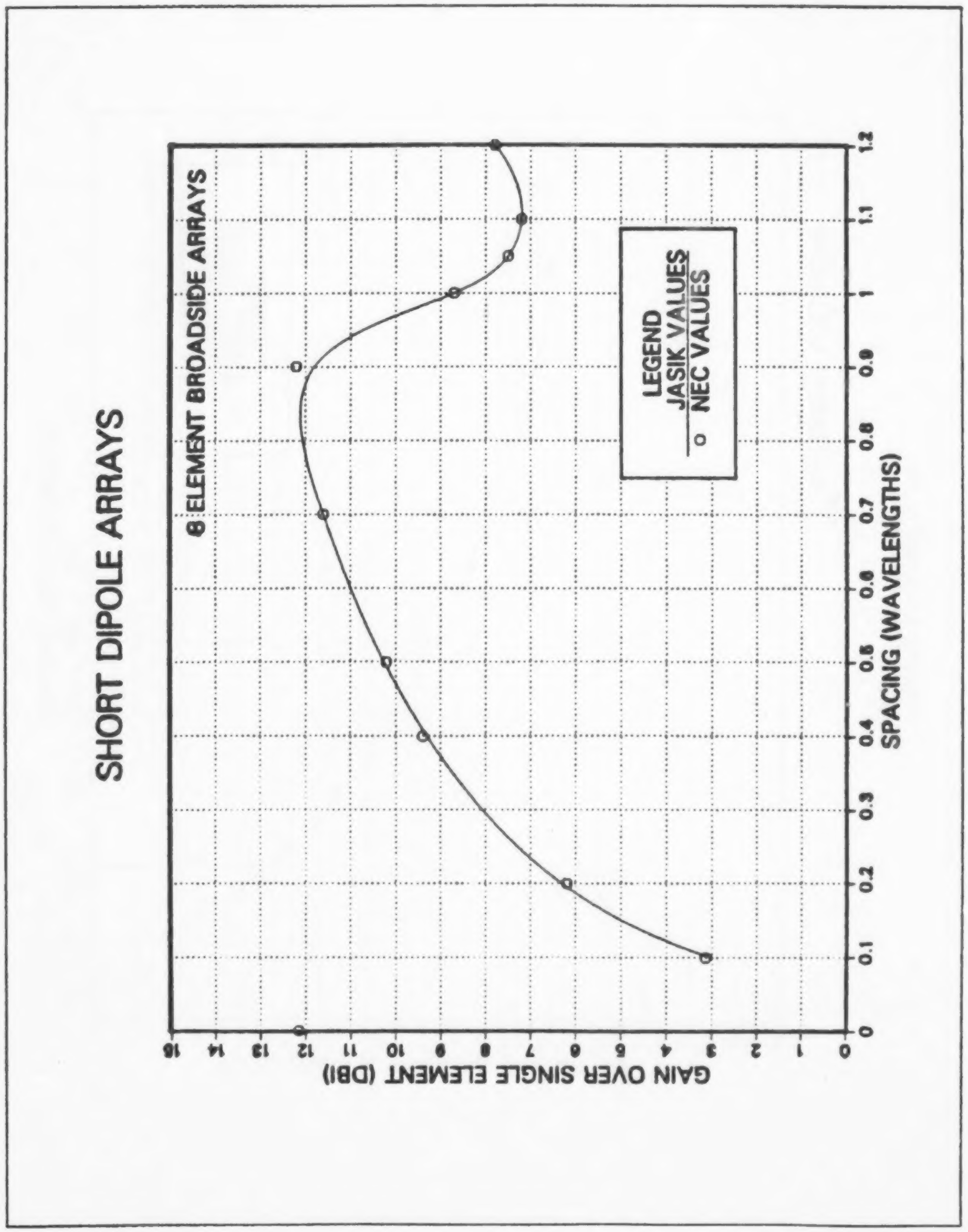
SHORT DIPOLE ARRAYS
8 ELEMENT BROADSIDE ARRAYS
LEGEND
JASIK VALUES
o NEC VALUES
GAIN OVER SINGLE ELEMENT (DBI)
0
1
2
3
4
5
6
7
8
9
10
11
12
13
14
15
SPACING (WAVELENGTHS)
0
0.1
0.2
0.3
0.4
0.5
0.6
0.7
0.8
0.9
1
1.1
1.2

FIGURE 23

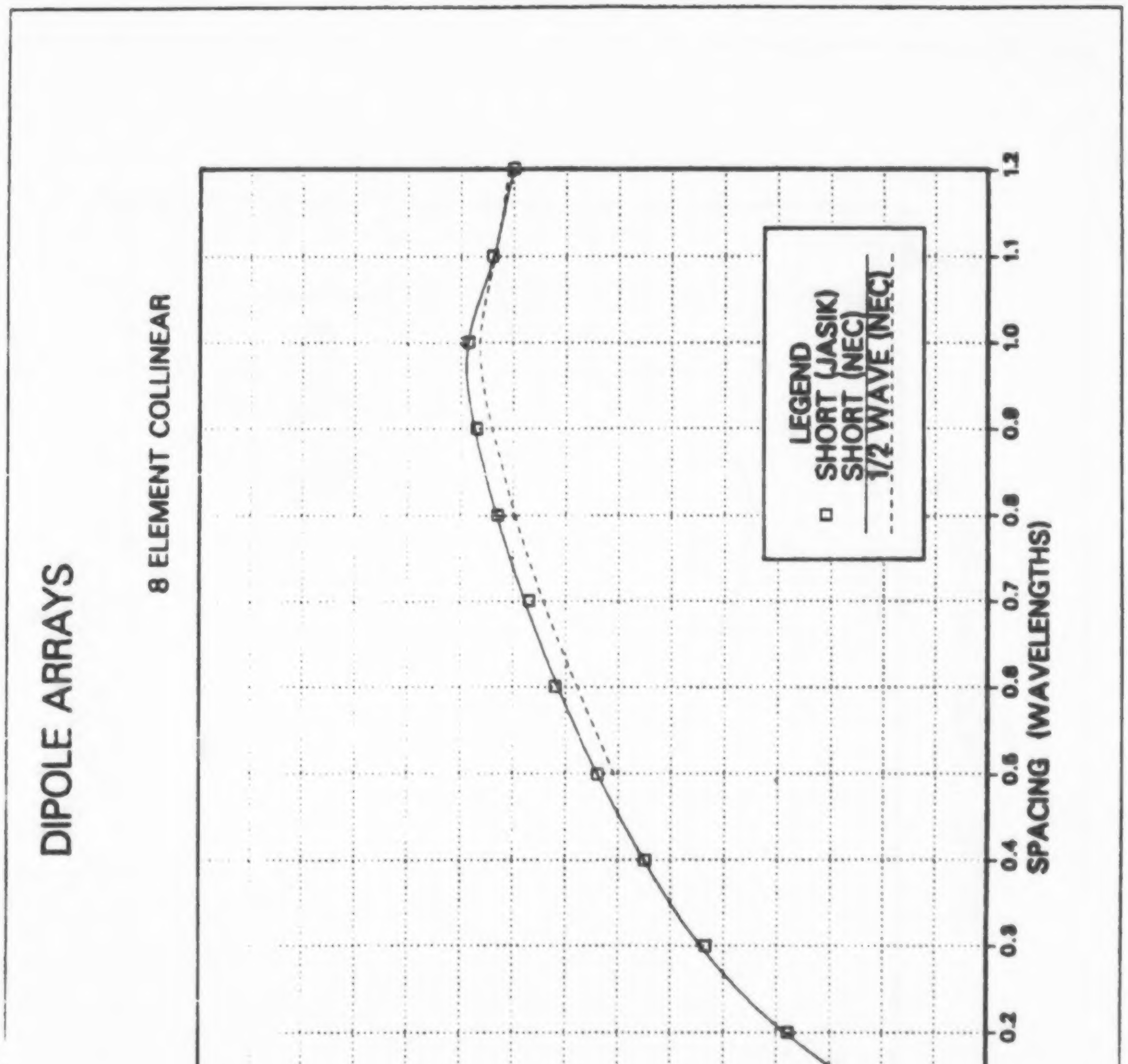
DIPOLE ARRAYS
8 ELEMENT COLLINEAR
LEGEND
□ SHORT (JASIK)
SHORT (NEC)
1/2 WAVE (NEC)
GAIN OVER A SINGLE ELEMENT (DB)
0.0
1.0
2.0
3.0
4.0
5.0
6.0
7.0
8.0
9.0
10.0
11.0
12.0
13.0
14.0
15.0
SPACING (WAVELENGTHS)
0.0
0.1
0.2
0.3
0.4
0.5
0.6
0.7
0.8
0.9
1.0
1.1
1.2

FIGURE 24

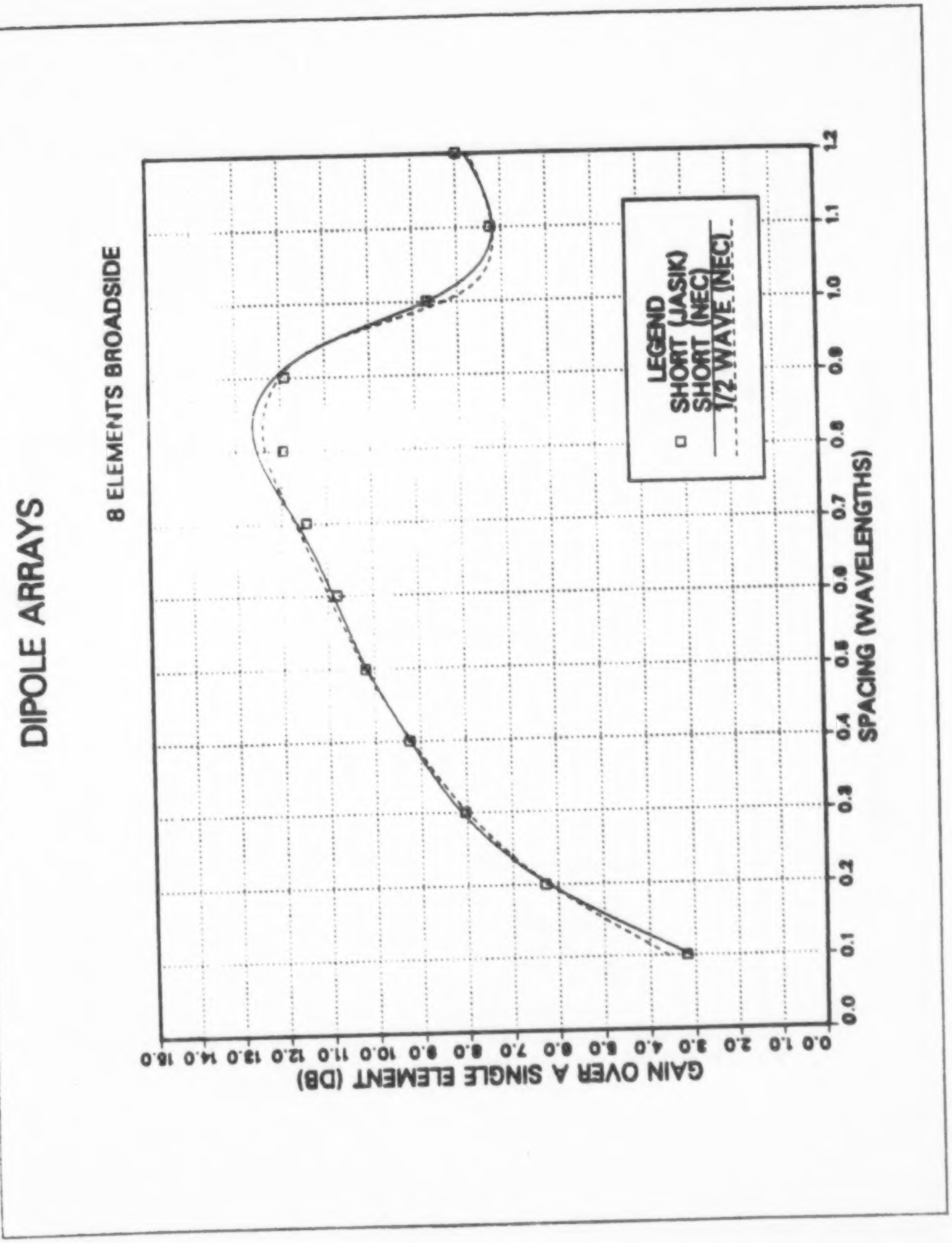
DIPOLE ARRAYS
8 ELEMENTS BROADSIDE
LEGEND
□ SHORT (JASIK)
SHORT (NEC)
1/2 WAVE (NEC)
GAIN OVER A SINGLE ELEMENT (DB)
0.0 1.0 2.0 3.0 4.0 5.0 6.0 7.0 8.0 9.0 10.0 11.0 12.0 13.0 14.0 15.0
SPACING (WAVELENGTHS)
0.0 0.1 0.2 0.3 0.4 0.5 0.6 0.7 0.8 0.9 1.0 1.1 1.2

FIGURE 25

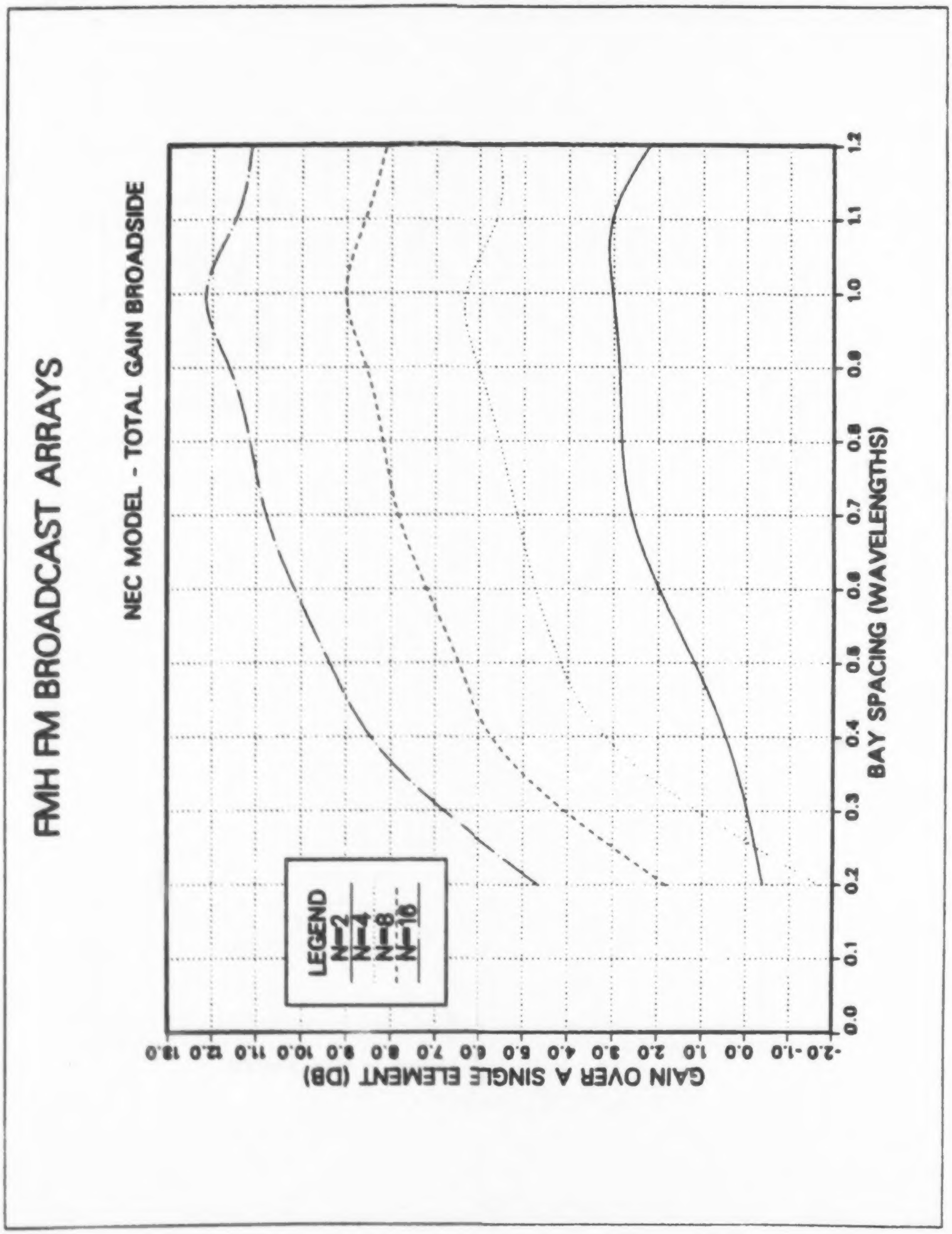
FMH FM BROADCAST ARRAYS
NEC MODEL - TOTAL GAIN BROADSIDE
LEGEND
N=2
N=4
N=8
N=16
GAIN OVER A SINGLE ELEMENT (DB)
-2.0
-1.0
0.0
1.0
2.0
3.0
4.0
5.0
6.0
7.0
8.0
9.0
10.0
11.0
12.0
13.0
BAY SPACING (WAVELENGTHS)
0.0
0.1
0.2
0.3
0.4
0.5
0.6
0.7
0.8
0.9
1.0
1.1
1.2

FIGURE 26

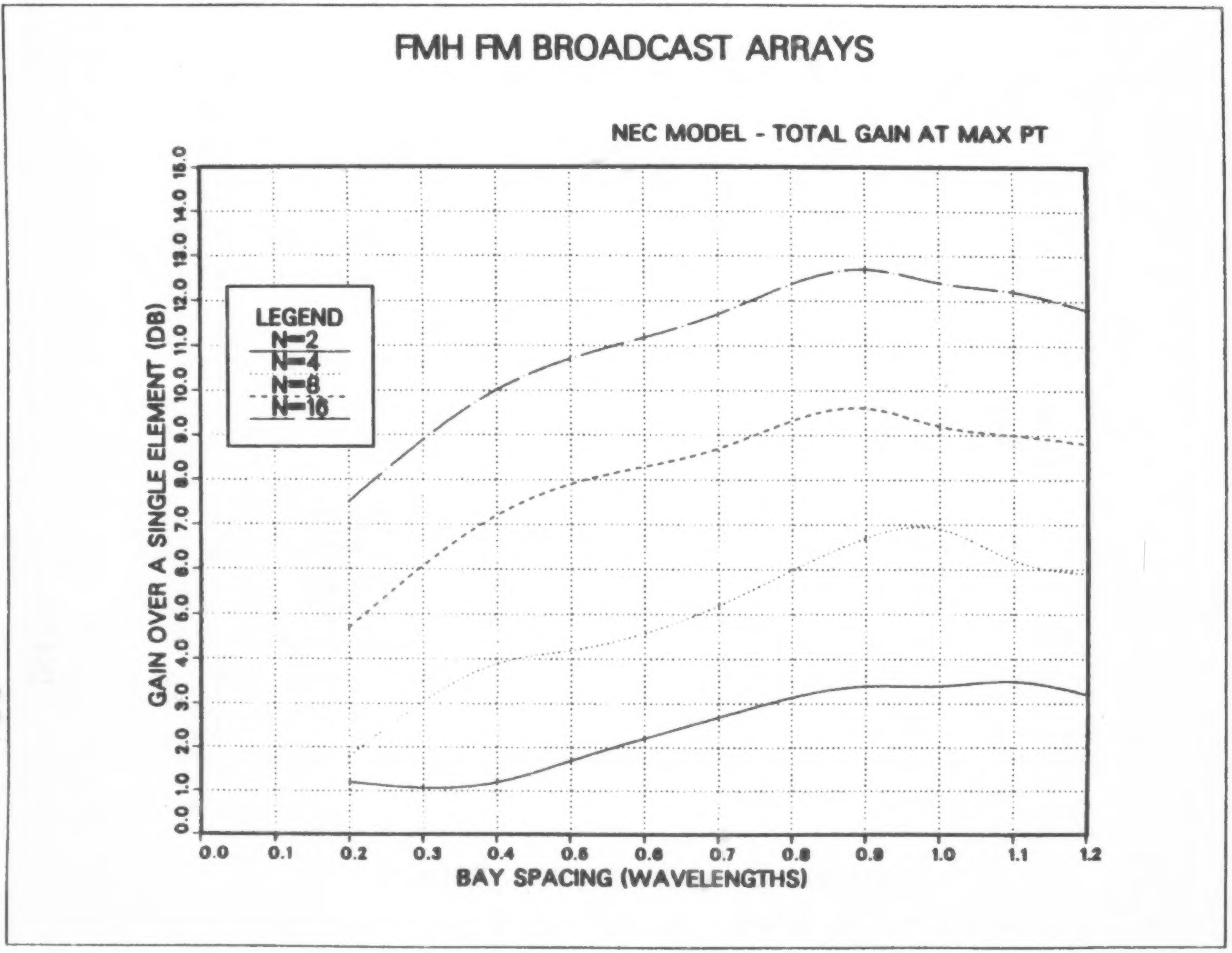
FMH FM BROADCAST ARRAYS
NEC MODEL - TOTAL GAIN AT MAX PT
GAIN OVER A SINGLE ELEMENT (DB)
0.0
1.0
2.0
3.0
4.0
5.0
6.0
7.0
8.0
9.0
10.0
11.0
12.0
13.0
14.0
15.0
BAY SPACING (WAVELENGTHS)
0.0
0.1
0.2
0.3
0.4
0.5
0.6
0.7
0.8
0.9
1.0
1.1
1.2
LEGEND
N=2
N=4
N=8
N=16

FIGURE 27

CYCLOID FM BROADCAST ARRAYS

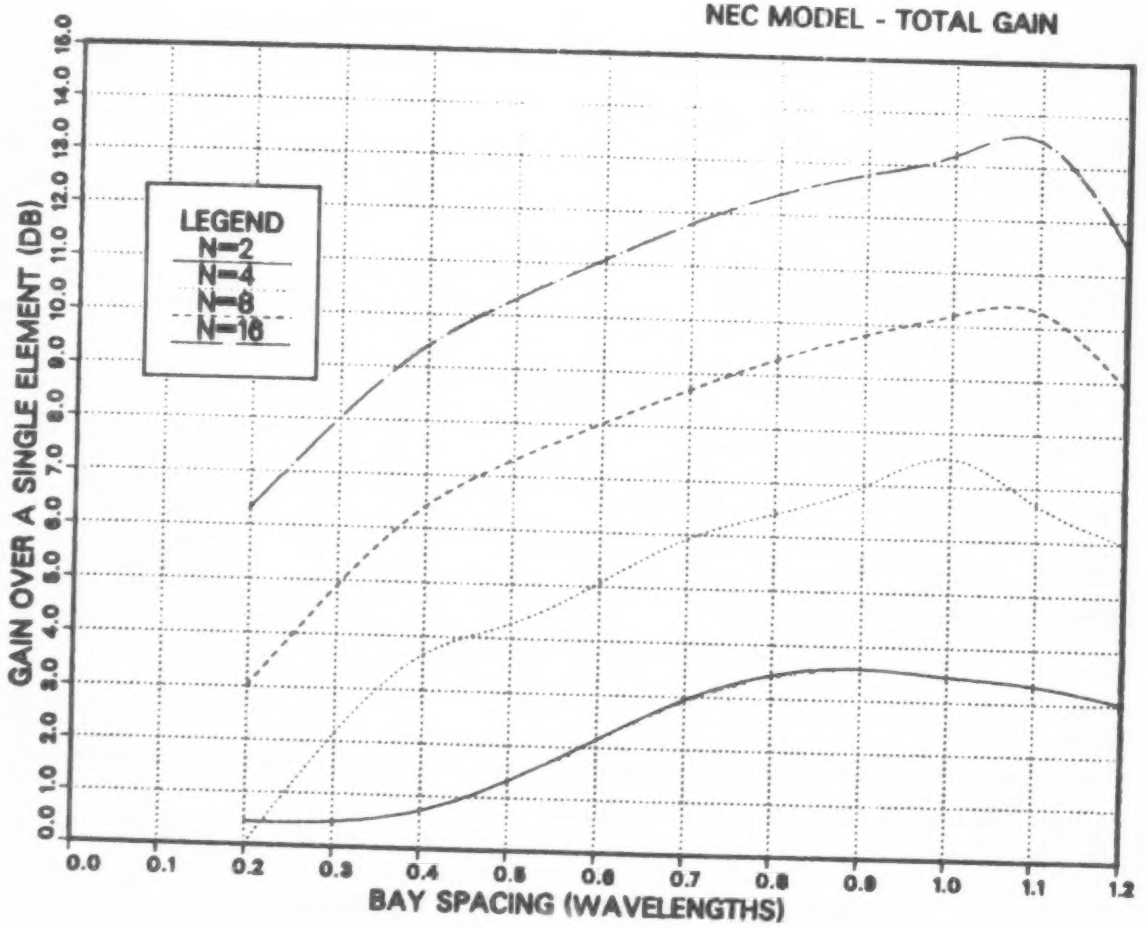

FIGURE 28

NUMERICAL MODELING STUDY
OF GAIN AND DOWNWARD RADIATION
FOR SELECTED FM AND VHF-TV
BROADCAST ANTENNA SYSTEMS

APPENDICES A - D

15 MARCH 1984

Richard W. Adler

Stephan Lamont

This report was prepared for the Environmental Protection Agency
Non-Ionizing Radiation Branch

by AGL, Inc., PO Box 253, Pacific Grove, CA 93950.

94<

APPENDIX A

FM ARRAY GAIN STUDY
RADIATION PATTERNS

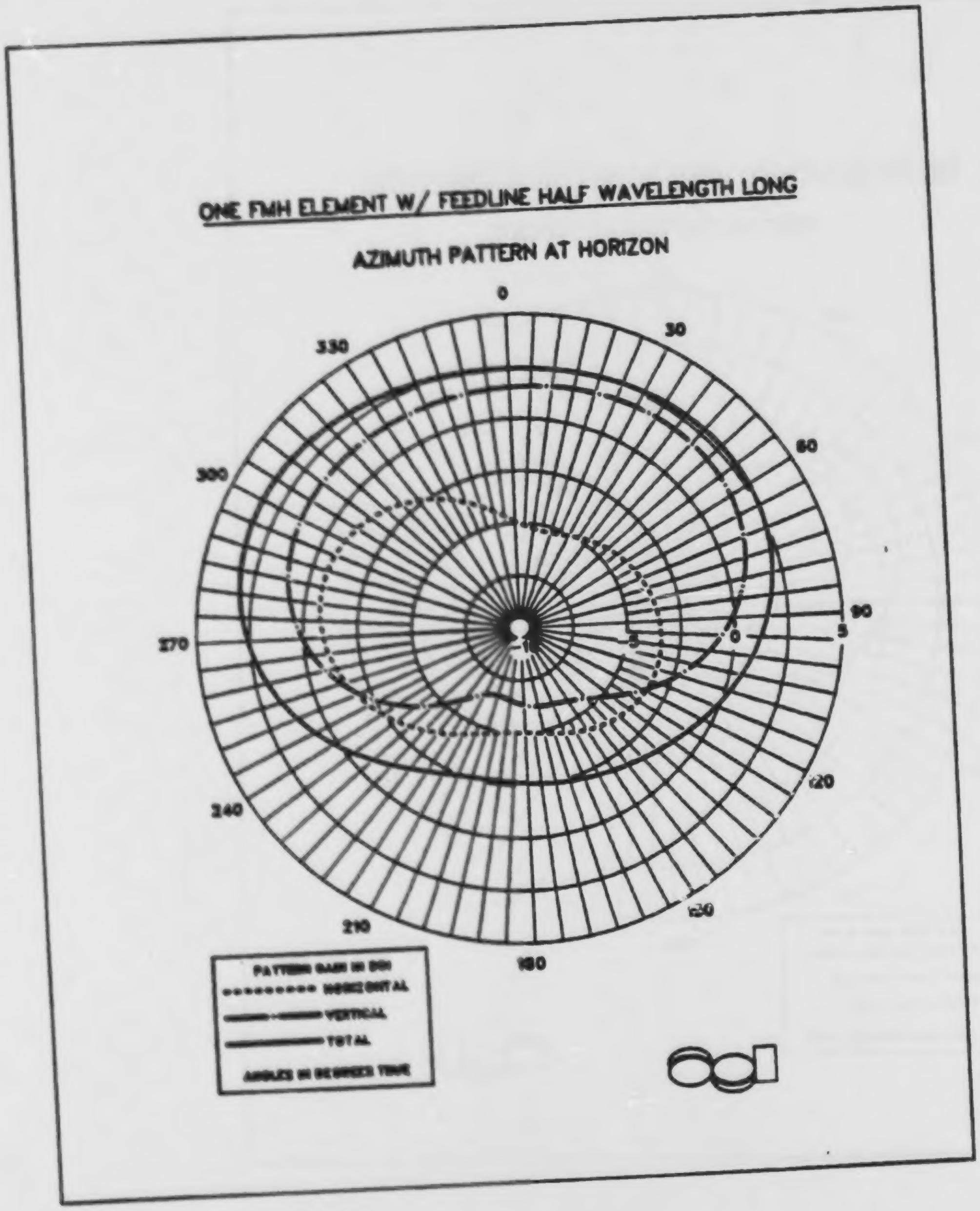

ONE FMH ELEMENT W/ FEEDLINE HALF WAVELENGTH LONG

AZIMUTH PATTERN AT HORIZON

FIGURE A 1

ONE FMH ELEMENT W/ FEEDLINE HALF WAVELENGTH LONG

VERTICAL PATTERN AT BORESITE

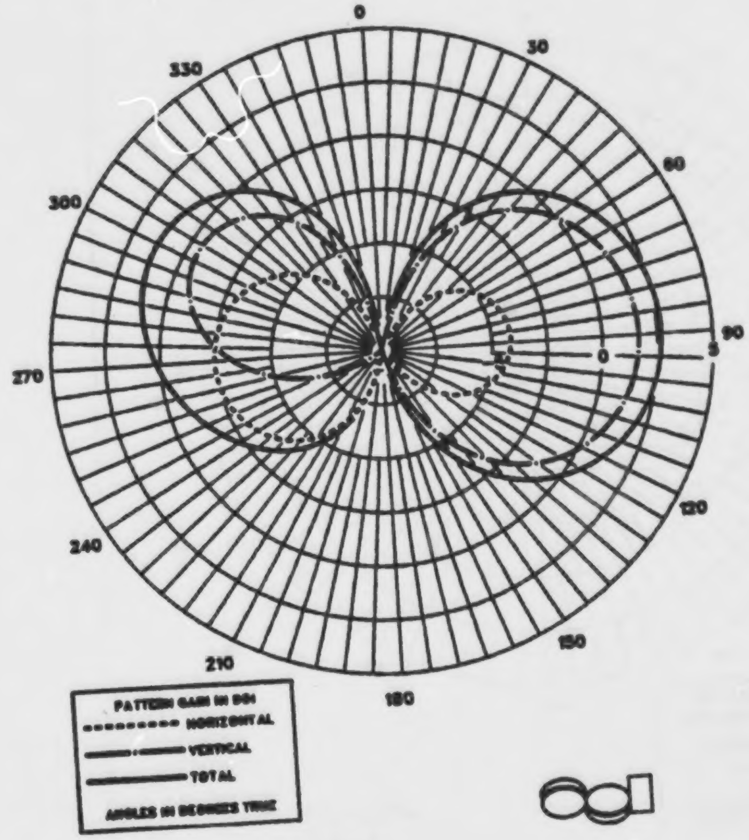

FIGURE A 2

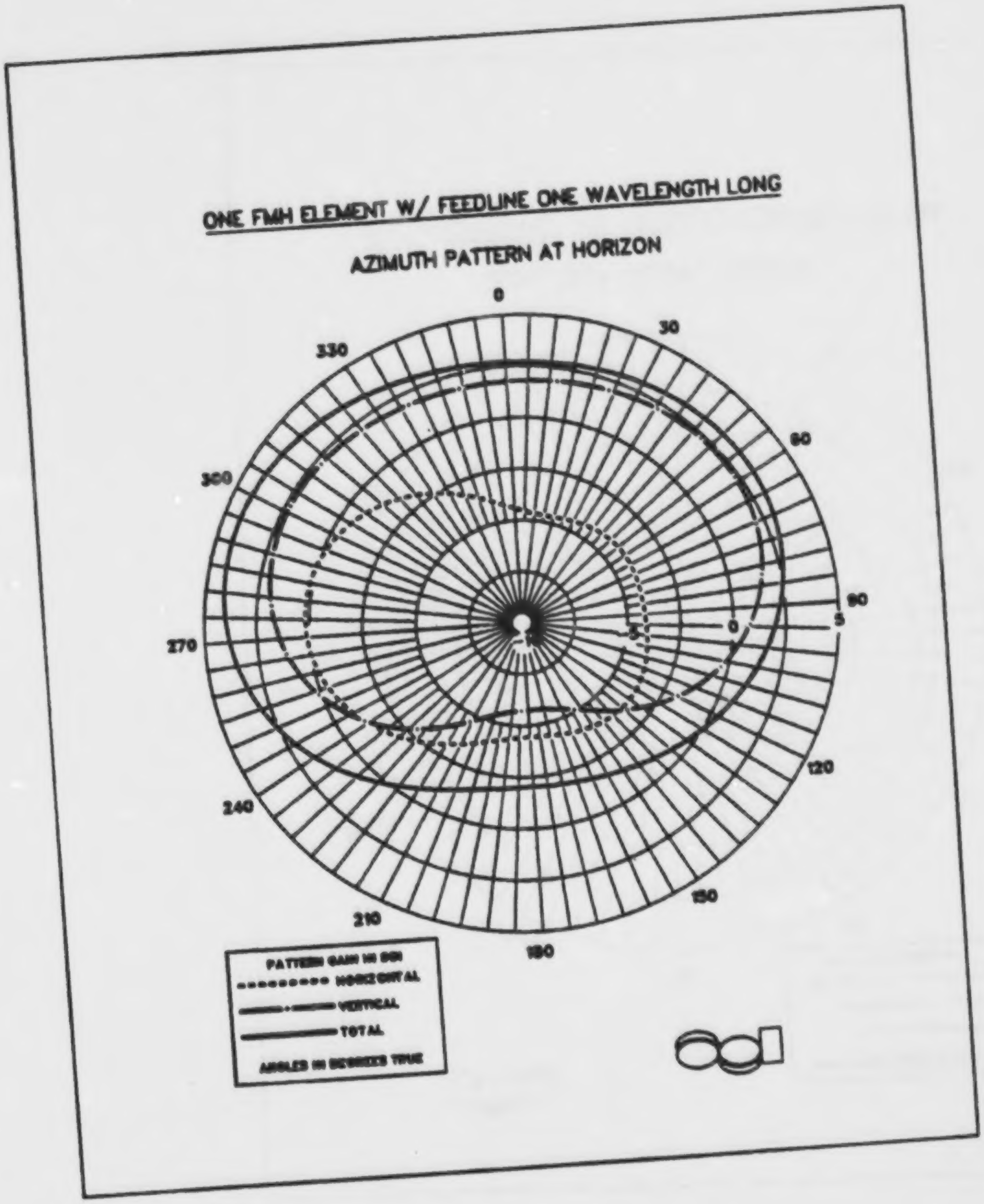

ONE FMH ELEMENT W/ FEEDLINE ONE WAVELENGTH LONG

AZIMUTH PATTERN AT HORIZON

FIGURE A 3

ONE FMH ELEMENT W/ FEEDLINE ONE WAVELENGTH LONG

VERTICAL PATTERN AT BORESITE

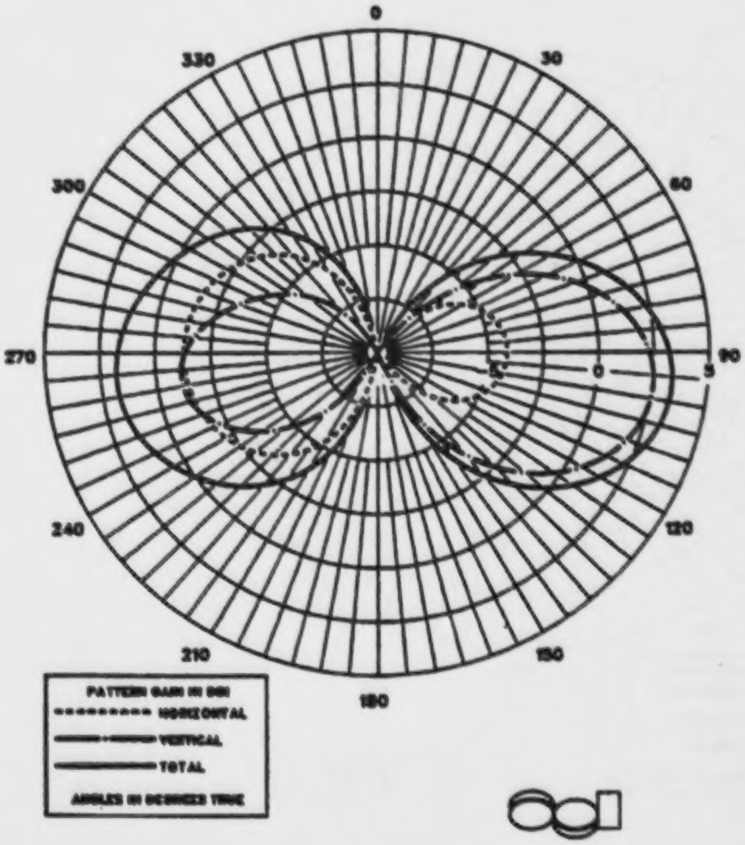

FIGURE A 4

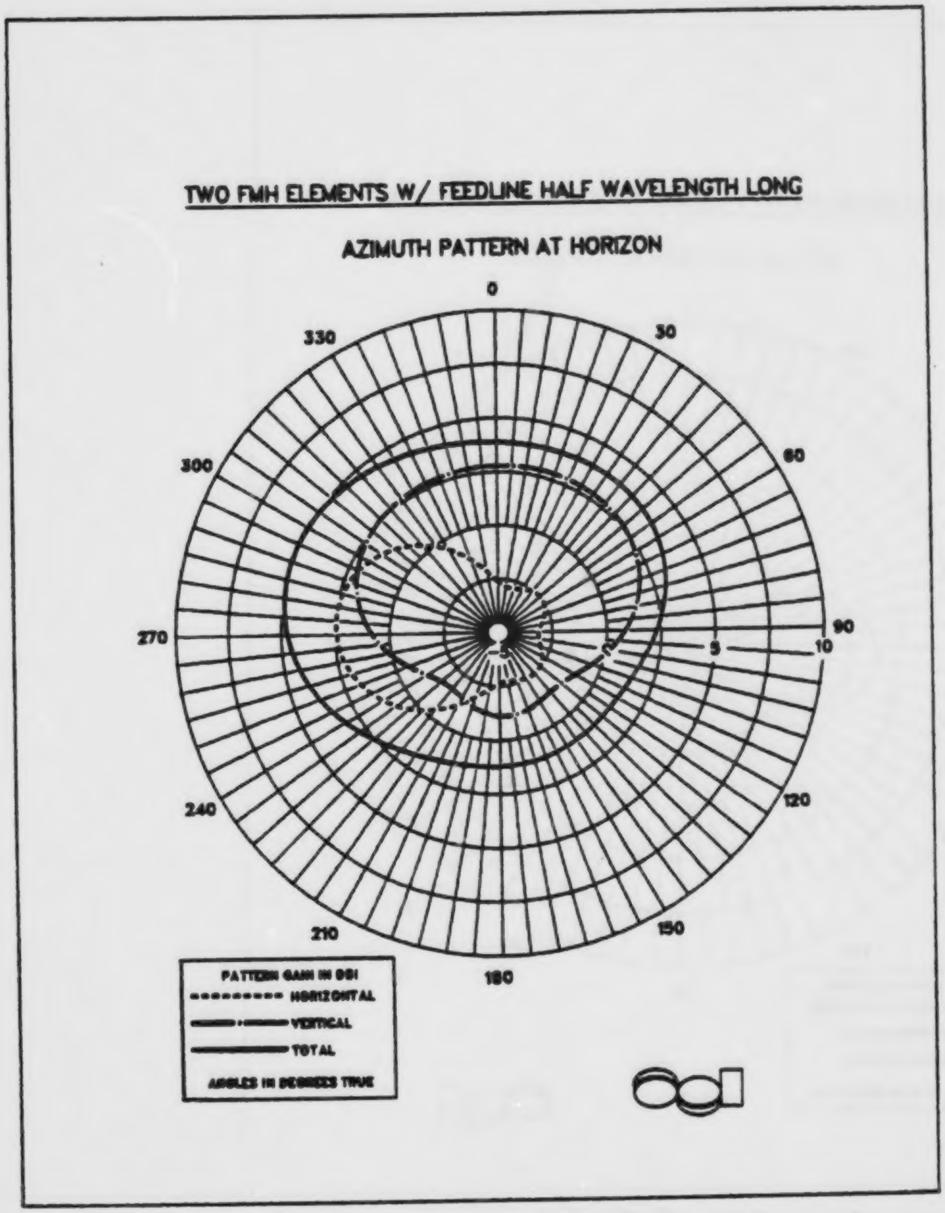
TWO FMH ELEMENTS W/ FEEDLINE HALF WAVELENGTH LONG
AZIMUTH PATTERN AT HORIZON
0
30
60
90
120
150
180
210
240
270
300
330
5
10
PATTERN GAIN IN DBI
HORIZONTAL
VERTICAL
TOTAL
ANGLES IN DEGREES TRUE

FIGURE A 5

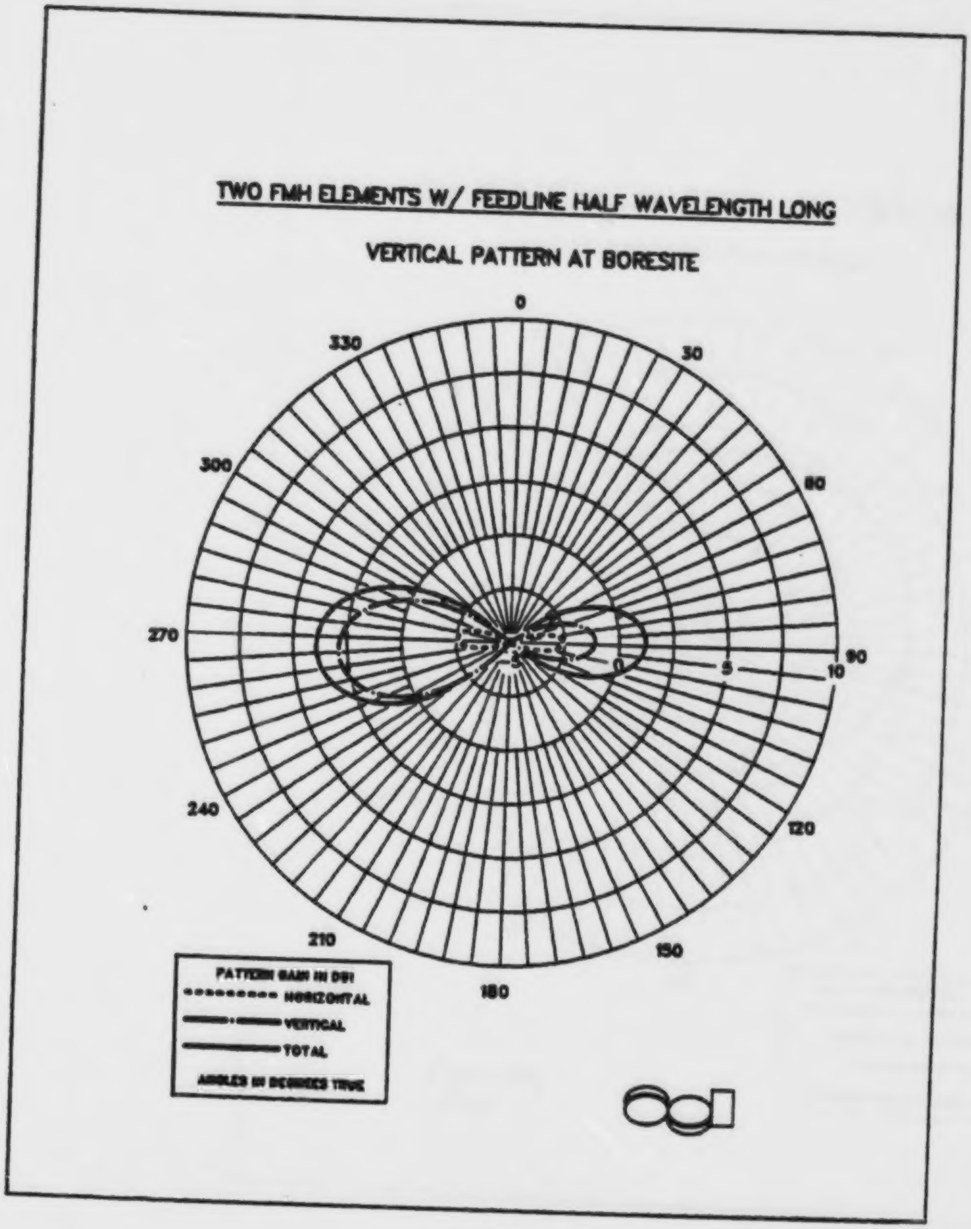
TWO FMH ELEMENTS W/ FEEDLINE HALF WAVELENGTH LONG
VERTICAL PATTERN AT BORESITE
0
30
60
90
120
150
180
210
240
270
300
330
0
5
10
PATTERN GAIN IN DBI
HORIZONTAL
VERTICAL
TOTAL
ANGLES IN DEGREES TRUE

FIGURE A 6

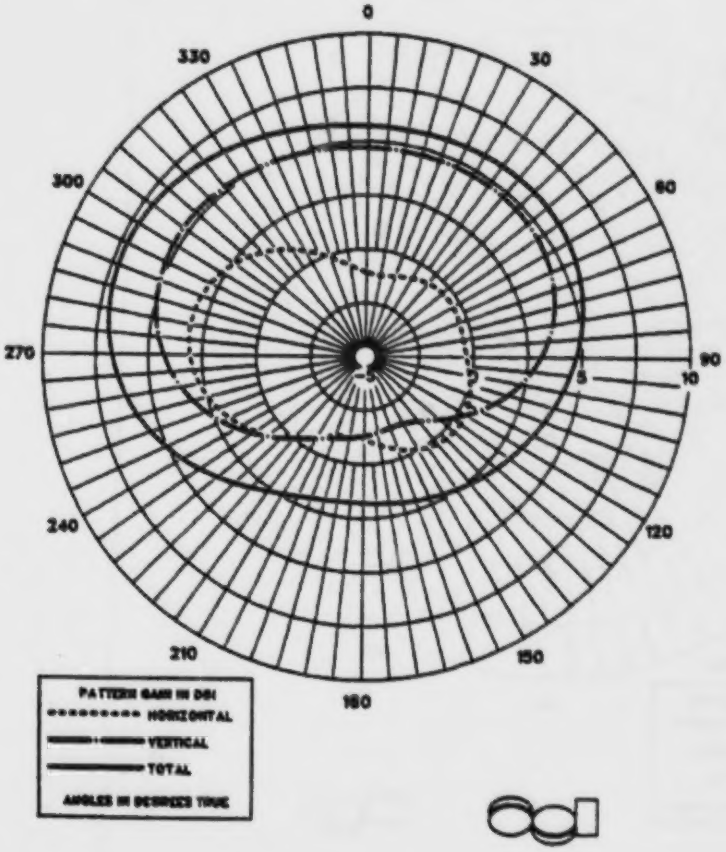

TWO FMH ELEMENTS W/ FEEDLINE ONE WAVELENGTH LONG

AZIMUTH PATTERN AT HORIZON

FIGURE A 7

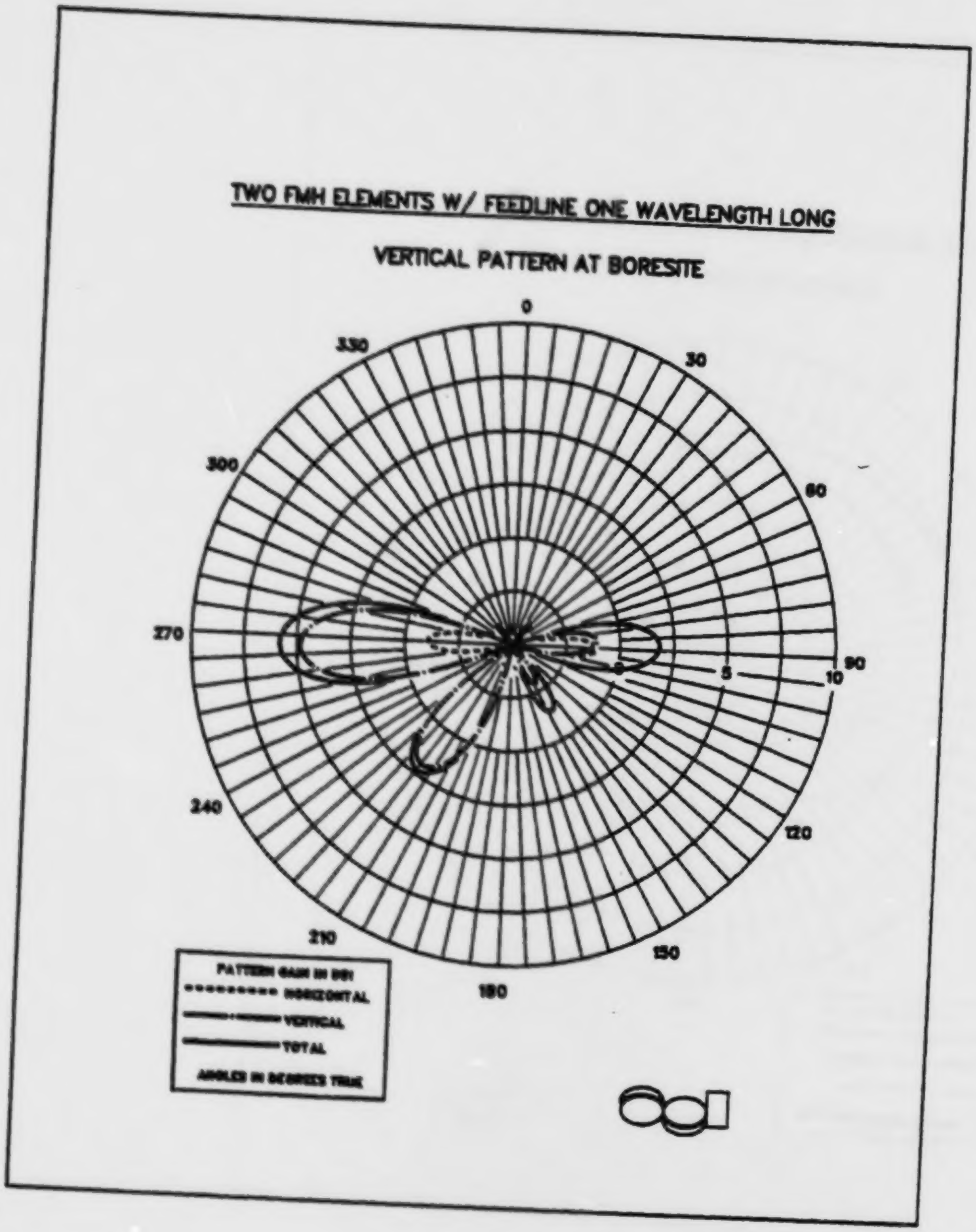
TWO FMH ELEMENTS W/ FEEDLINE ONE WAVELENGTH LONG
VERTICAL PATTERN AT BORESITE
0
30
60
90
120
150
180
210
240
270
300
330
0
5
10
PATTERN GAIN IN DBI
HORIZONTAL
VERTICAL
TOTAL
ANGLES IN DEGREES TRUE

FIGURE A 8

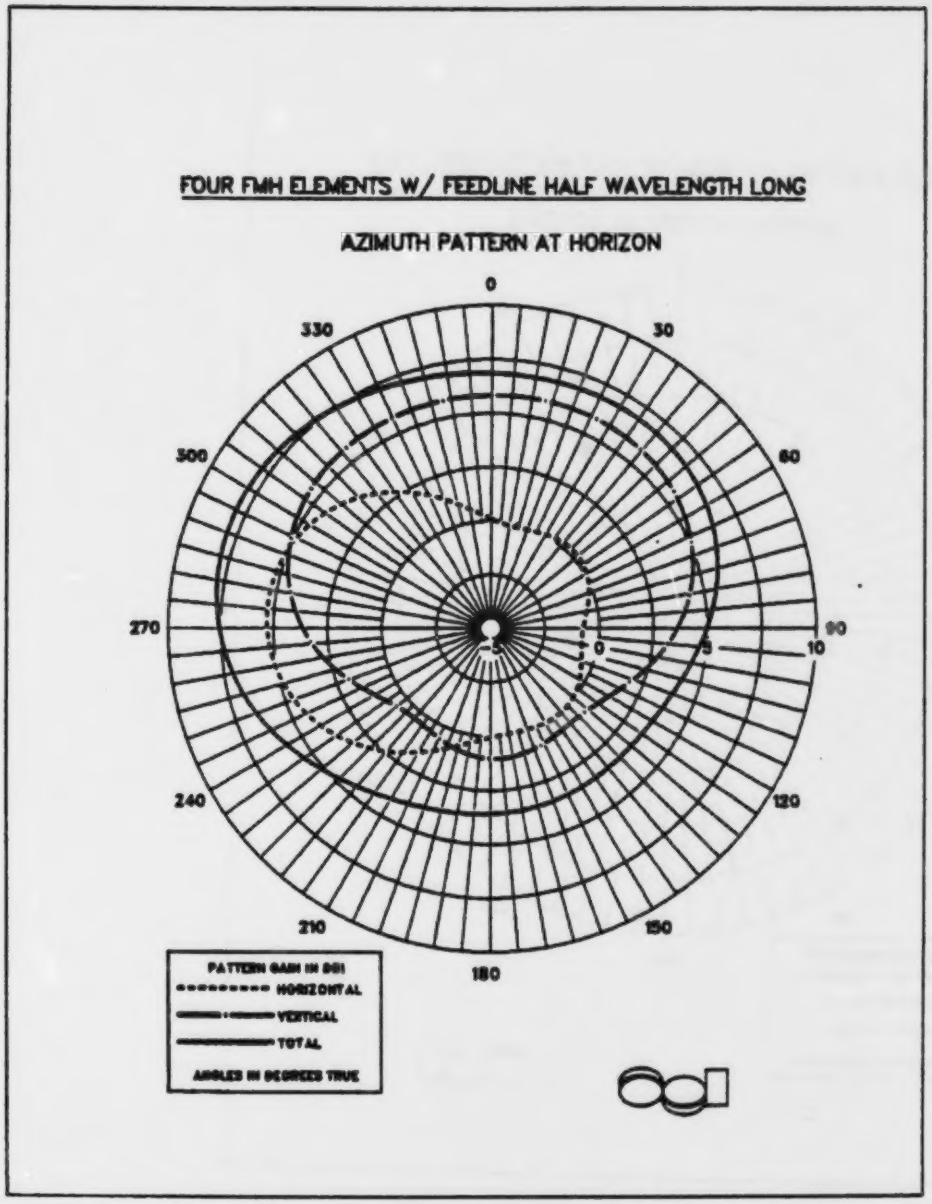
FOUR FMH ELEMENTS W/ FEEDLINE HALF WAVELENGTH LONG
AZIMUTH PATTERN AT HORIZON
0
30
60
90
120
150
180
210
240
270
300
330
-5
0
5
10
PATTERN GAIN IN DBI
HORIZONTAL
VERTICAL
TOTAL
ANGLES IN DEGREES TRUE

FIGURE A 9

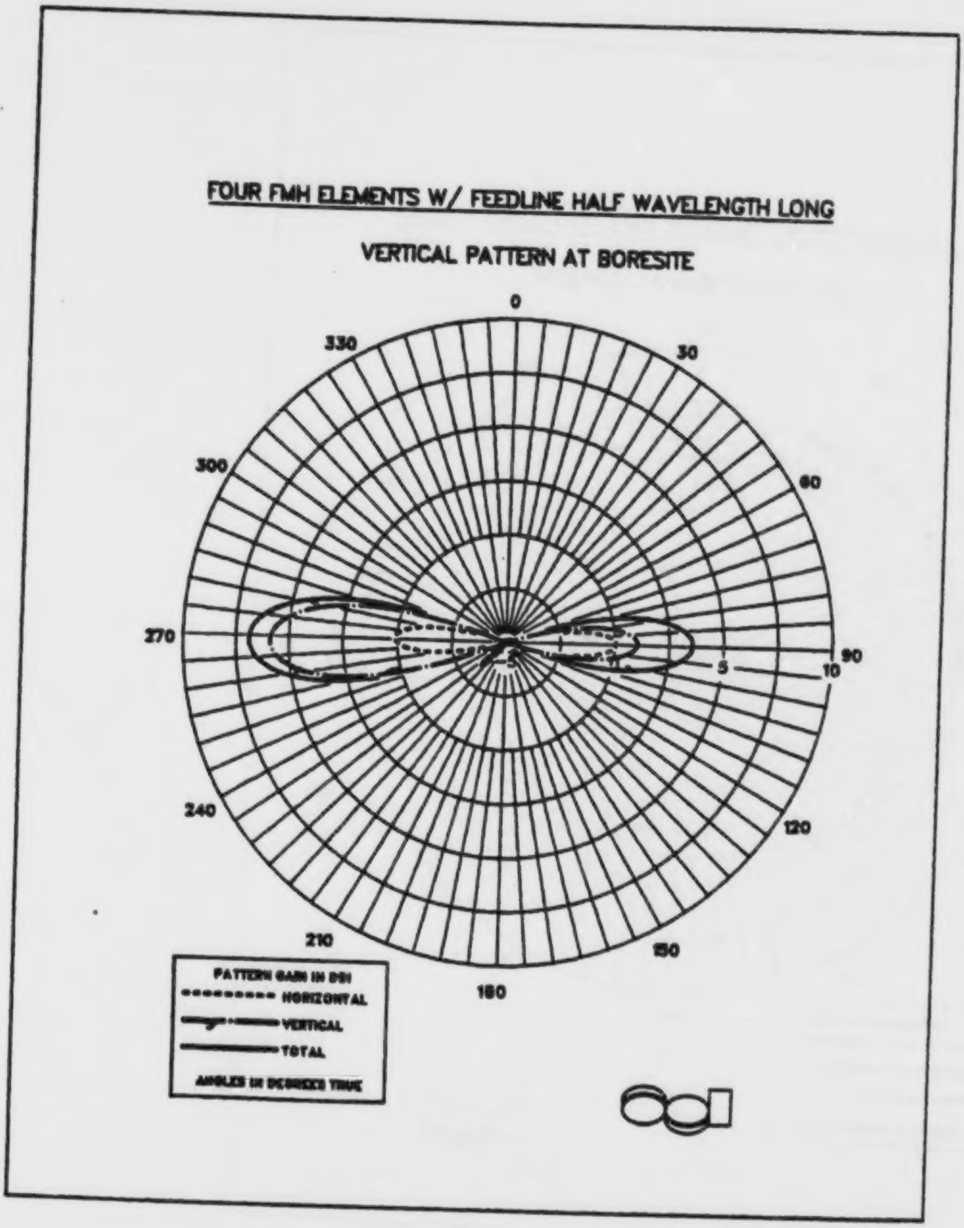
FOUR FMH ELEMENTS W/ FEEDLINE HALF WAVELENGTH LONG

VERTICAL PATTERN AT BORESITE

FIGURE A 10

FOUR FMH ELEMENTS W/ FEEDLINE ONE WAVELENGTH LONG

AZIMUTH PATTERN AT HORIZON

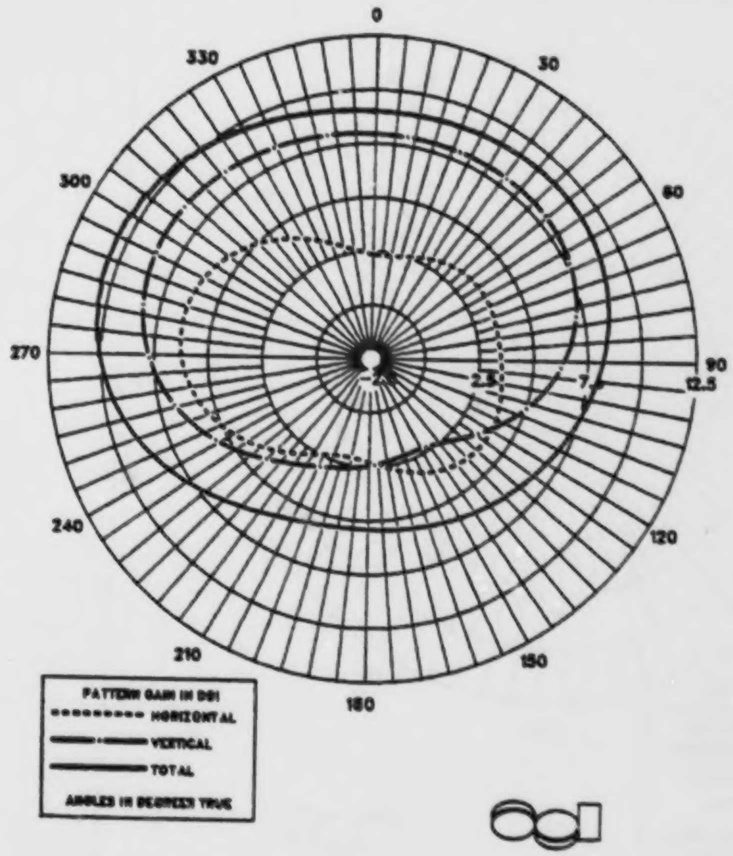

FIGURE A 11

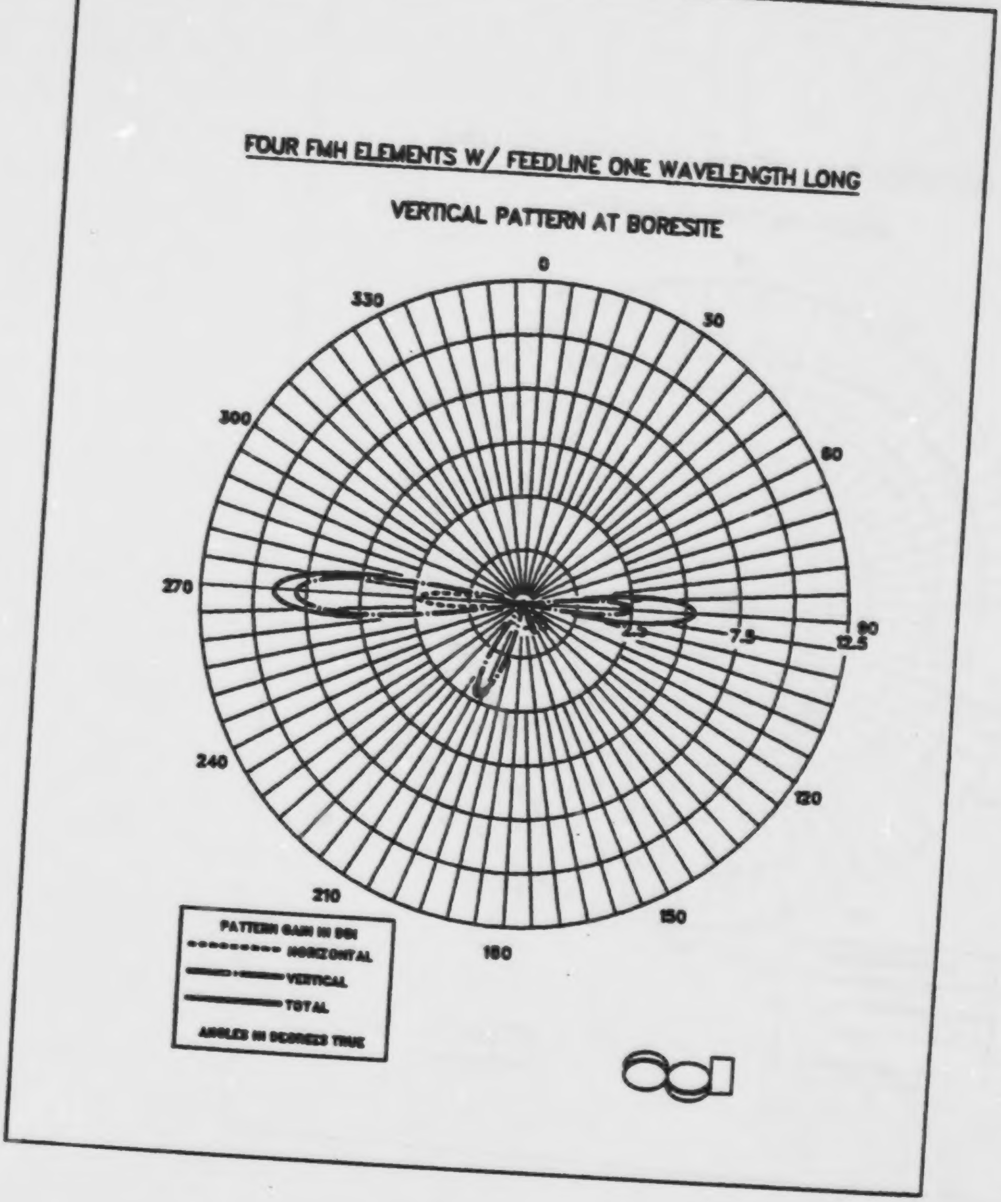
FOUR FMH ELEMENTS W/ FEEDLINE ONE WAVELENGTH LONG

VERTICAL PATTERN AT BORESITE

FIGURE A 12

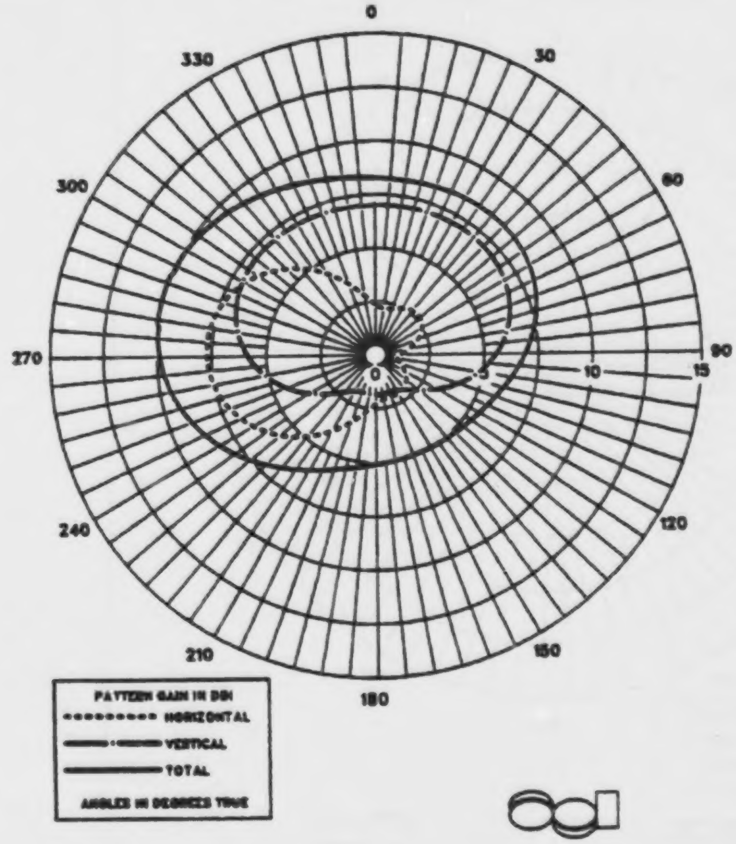

SIX FMH ELEMENTS W/ FEEDLINE HALF WAVE SPACING

AZIMUTH PATTERN AT HORIZON

FIGURE A 13

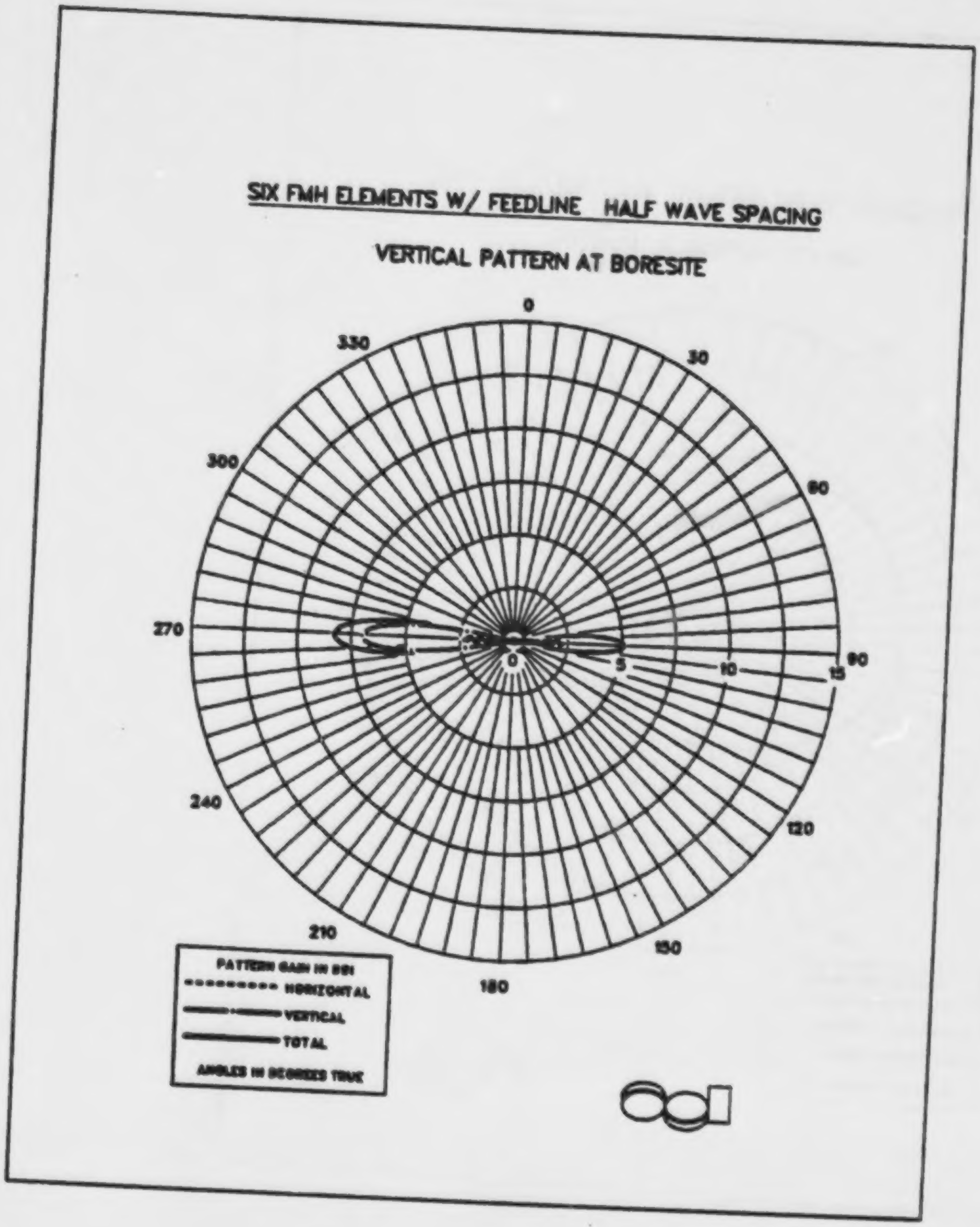

SIX FMH ELEMENTS W/ FEEDLINE HALF WAVE SPACING

VERTICAL PATTERN AT BORESITE

FIGURE A 14

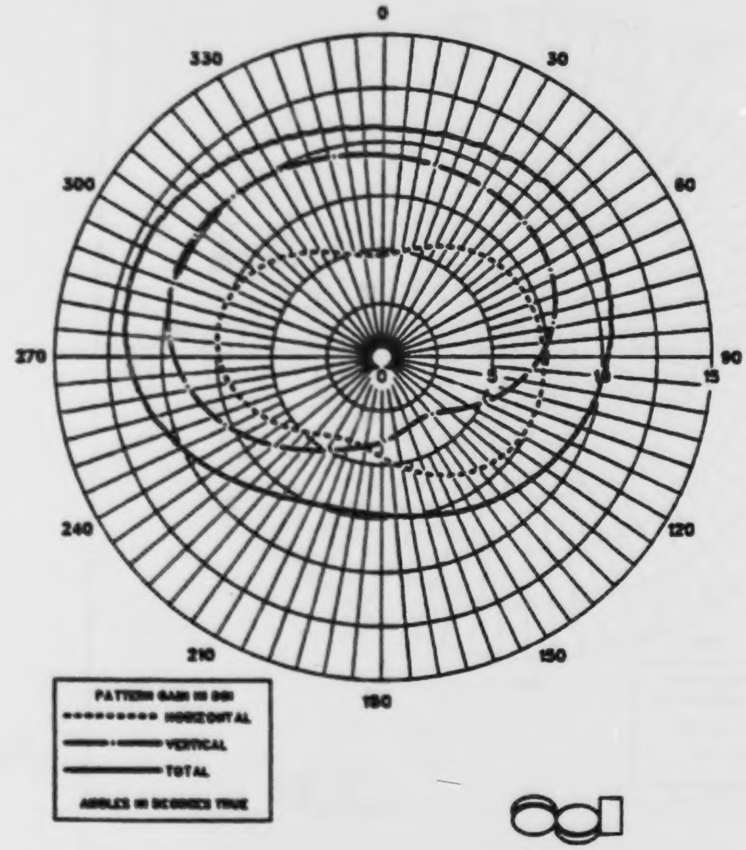

SIX FMH ELEMENTS W/ FEEDLINE ONE WAVELENGTH LONG

AZIMUTH PATTERN AT HORIZON

FIGURE A 15

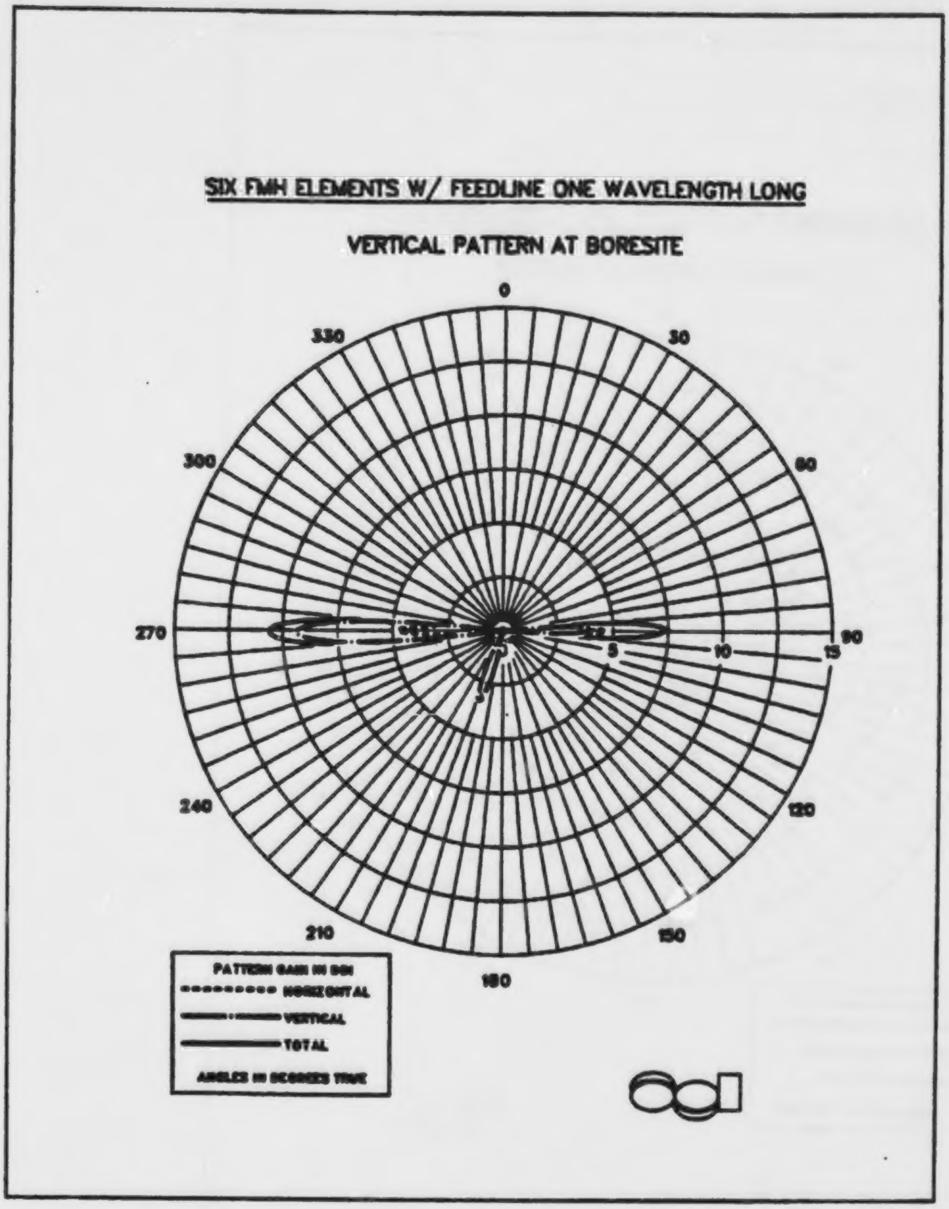
SIX FMH ELEMENTS W/ FEEDLINE ONE WAVELENGTH LONG
VERTICAL PATTERN AT BORESITE
0
30
60
90
120
150
180
210
240
270
300
330
5
10
15
PATTERN GAIN IN DBI
HORIZONTAL
VERTICAL
TOTAL
ANGLES IN DEGREES TRUE

FIGURE A 16

EIGHT FMH ELEMENTS W/ FEEDLINE HALF WAVELENGTH LONG

AZIMUTH PATTERN AT HORIZON

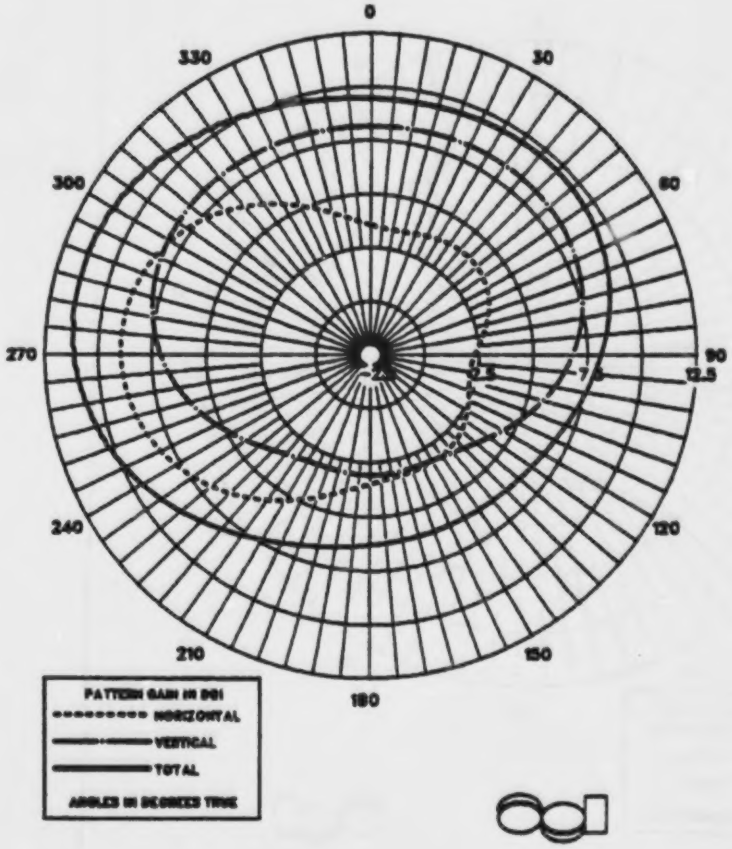

FIGURE A 17

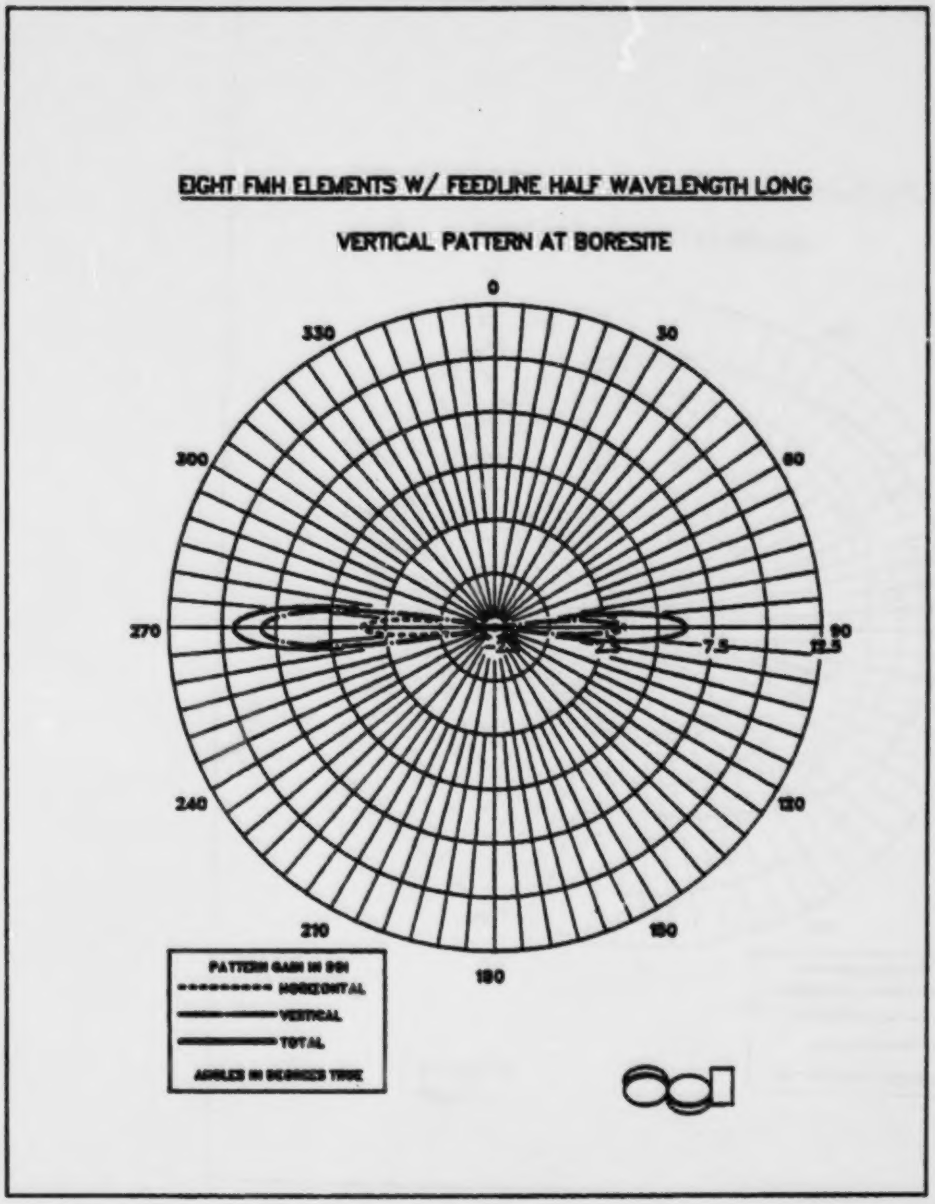
EIGHT FMH ELEMENTS W/ FEEDLINE HALF WAVELENGTH LONG
VERTICAL PATTERN AT BORESITE
0
30
60
90
120
150
180
210
240
270
300
330
-2.5
2.5
7.5
12.5
PATTERN GAIN IN DBI
HORIZONTAL
VERTICAL
TOTAL
ANGLES IN DEGREES TRUE

FIGURE A 18

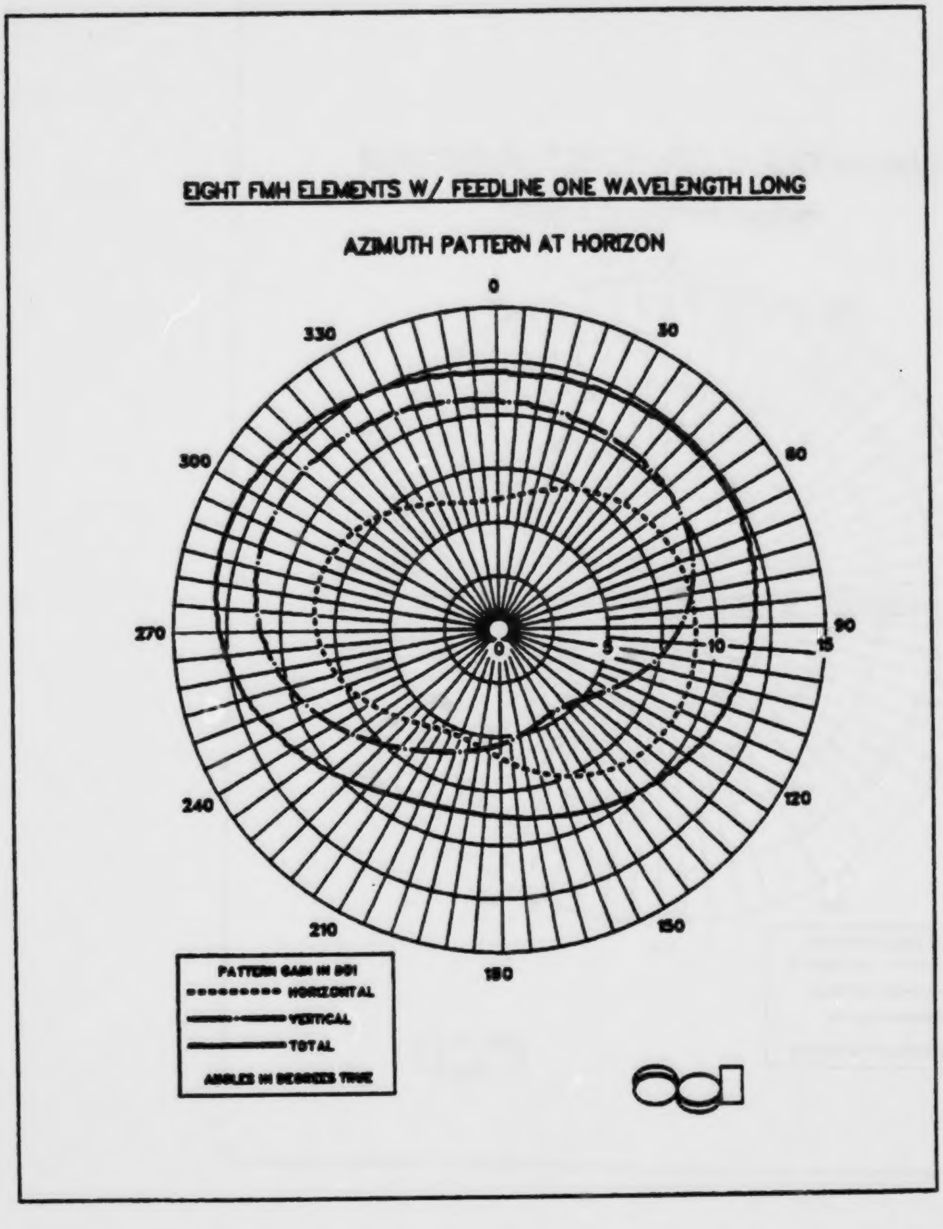
EIGHT FMH ELEMENTS W/ FEEDLINE ONE WAVELENGTH LONG
AZIMUTH PATTERN AT HORIZON
0
30
60
90
120
150
180
210
240
270
300
330
0
5
10
15
PATTERN GAIN IN DBI
HORIZONTAL
VERTICAL
TOTAL
ANGLES IN DEGREES TRUE

FIGURE A 19

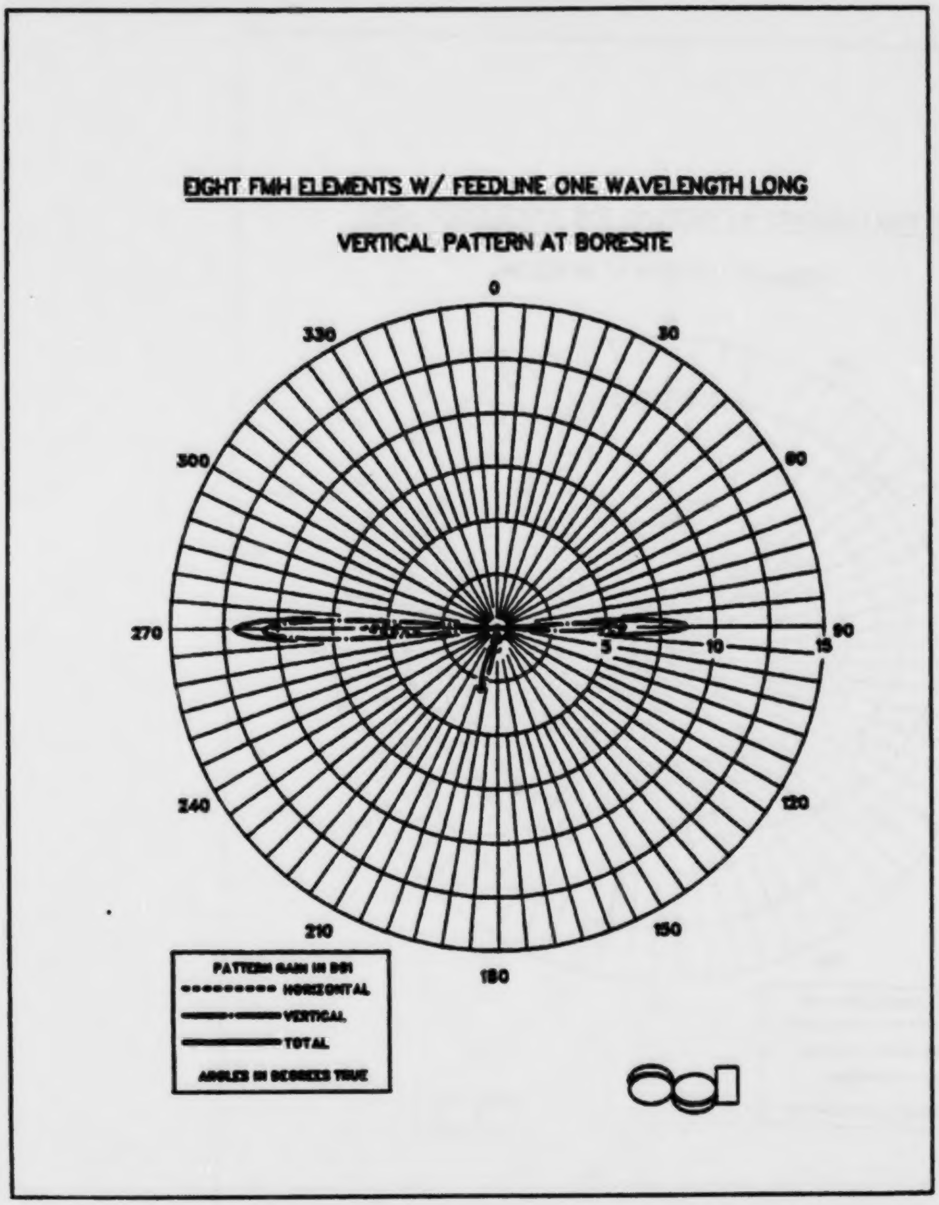
EIGHT FMH ELEMENTS W/ FEEDLINE ONE WAVELENGTH LONG
VERTICAL PATTERN AT BORESITE
0
30
60
90
120
150
180
210
240
270
300
330
5
10
15
PATTERN GAIN IN DBI
HORIZONTAL
VERTICAL
TOTAL
ANGLES IN DEGREES TRUE

FIGURE A 20

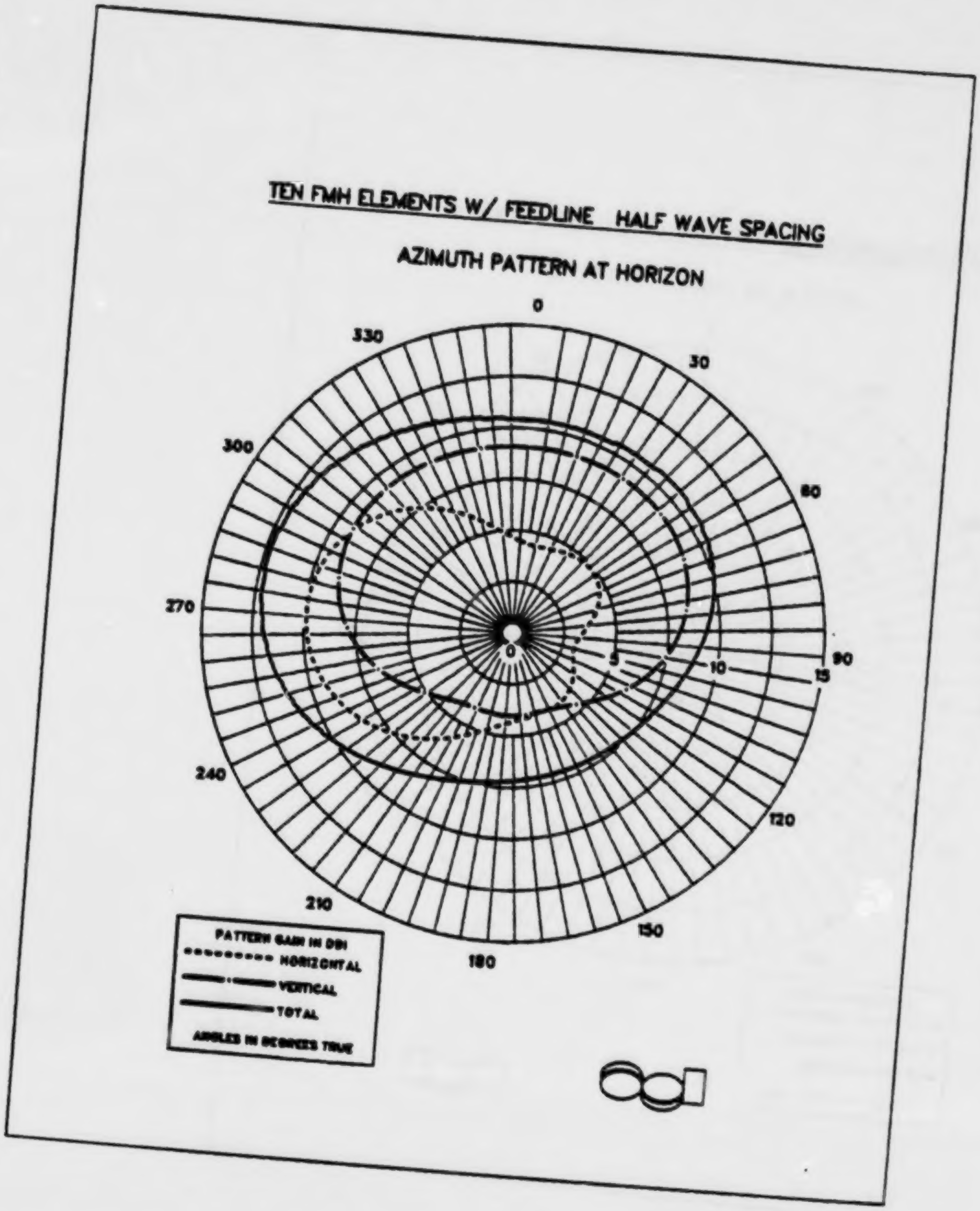

TEN FMH ELEMENTS W/ FEEDLINE HALF WAVE SPACING

AZIMUTH PATTERN AT HORIZON

FIGURE A 21

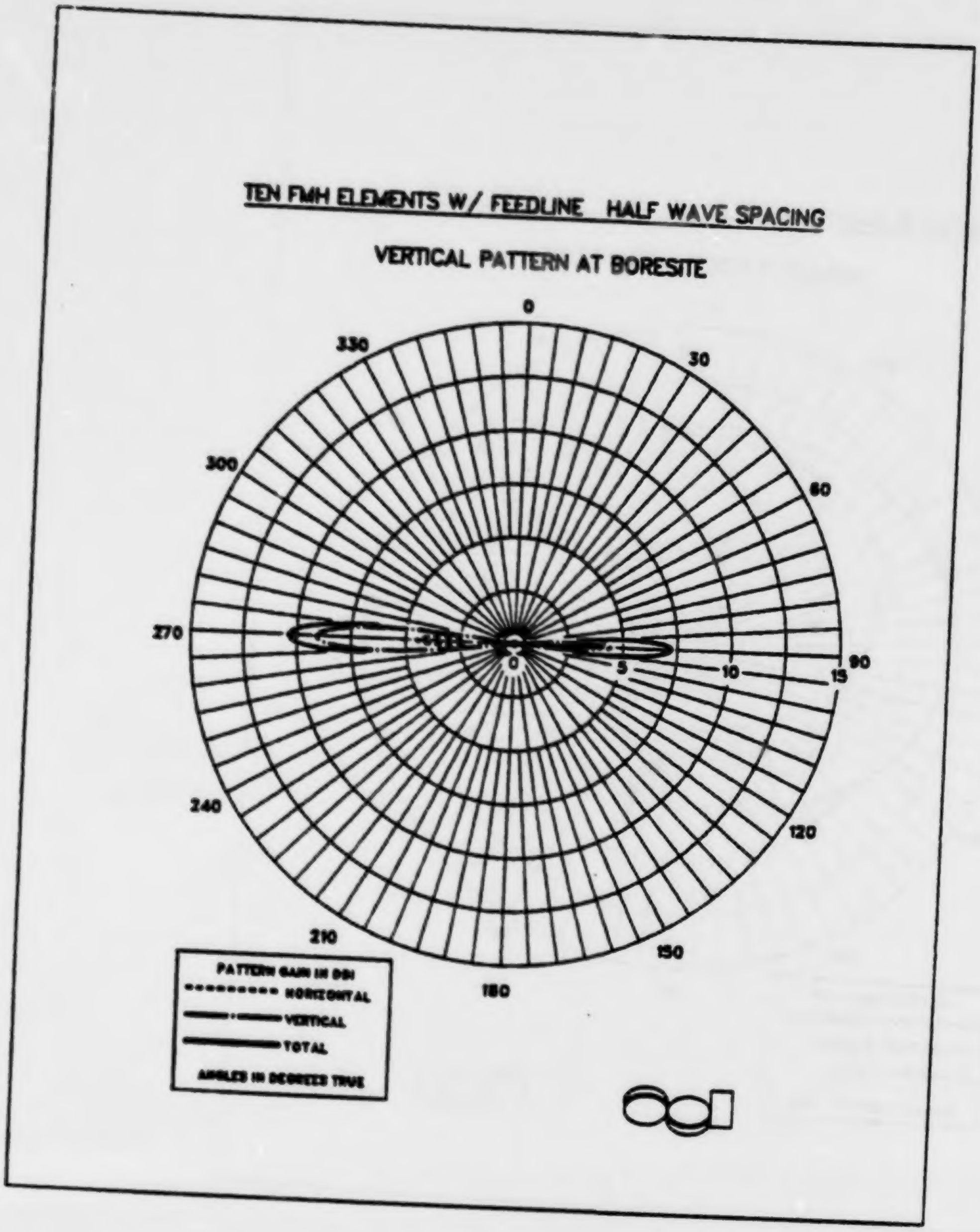
TEN FMH ELEMENTS W/ FEEDLINE HALF WAVE SPACING
VERTICAL PATTERN AT BORESITE
0
30
60
90
120
150
180
210
240
270
300
330
0
5
10
15
PATTERN GAIN IN DBI
HORIZONTAL
VERTICAL
TOTAL
ANGLES IN DEGREES TRUE

FIGURE A 22

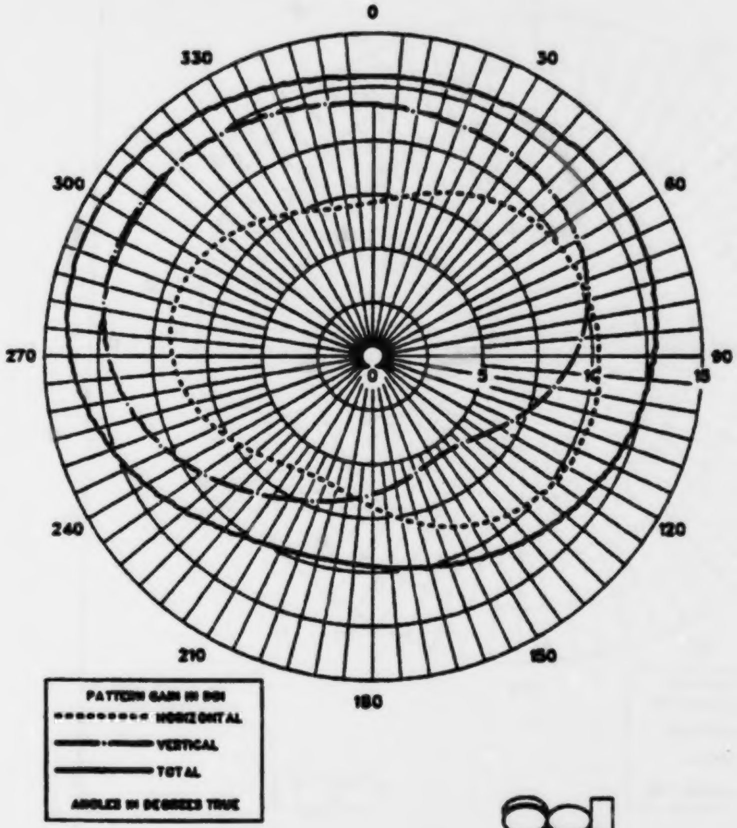

TEN FMH ELEMENTS W/ FEEDLINE ONE WAVELENGTH LONG

AZIMUTH PATTERN AT HORIZON

FIGURE A 23

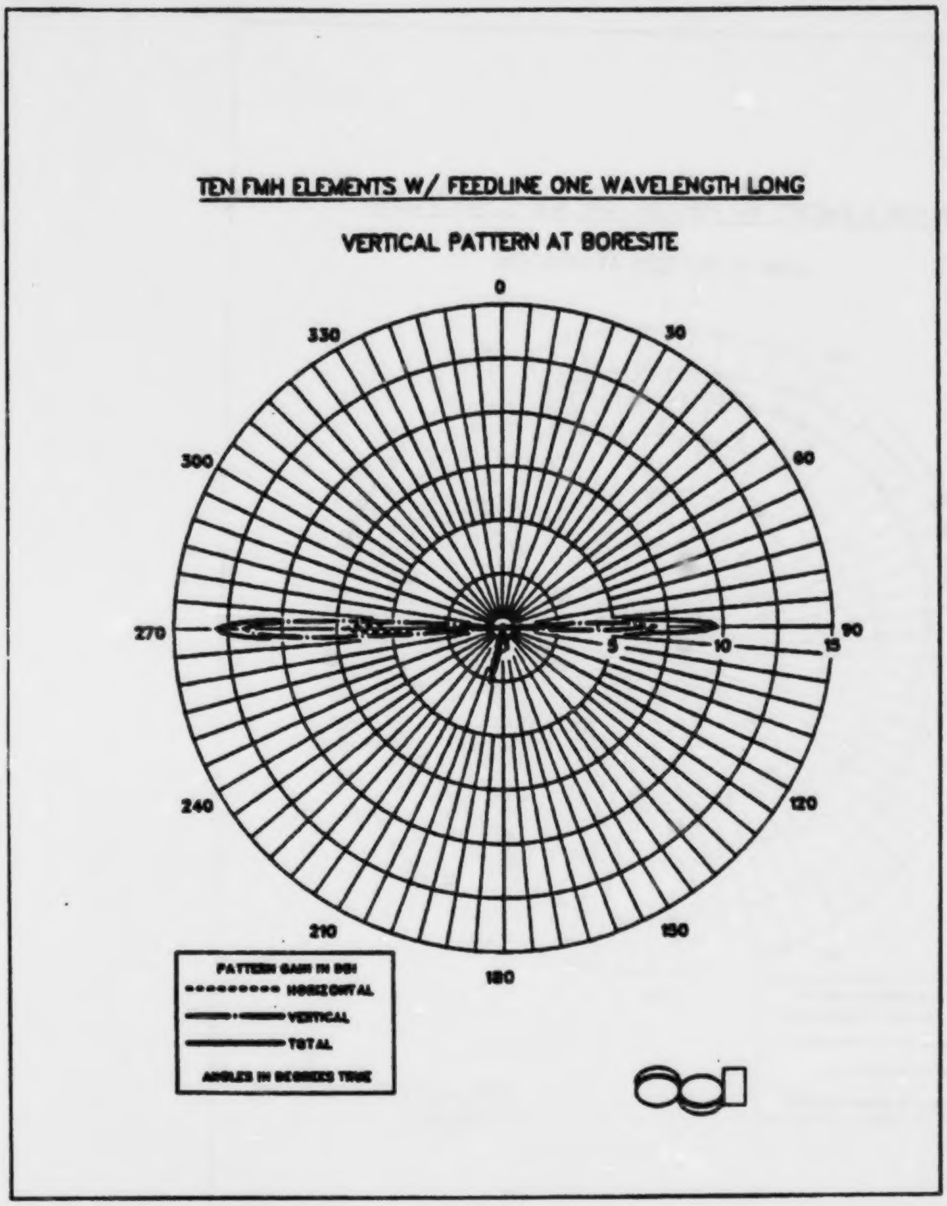

TEN FMH ELEMENTS W/ FEEDLINE ONE WAVELENGTH LONG

VERTICAL PATTERN AT BORESITE

FIGURE A 24

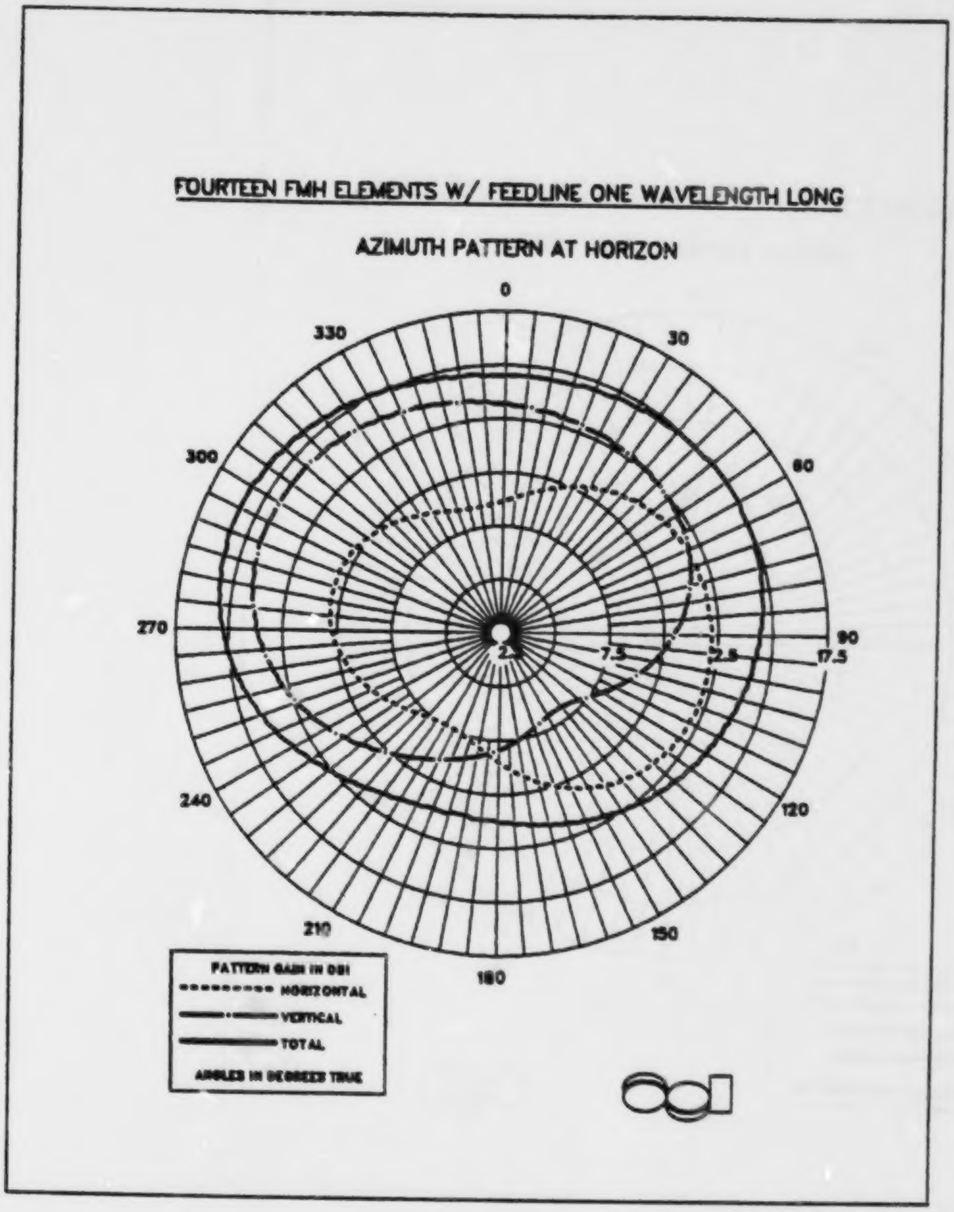
FOURTEEN FMH ELEMENTS W/ FEEDLINE ONE WAVELENGTH LONG
AZIMUTH PATTERN AT HORIZON
0
30
60
90
120
150
180
210
240
270
300
330
2.5
7.5
12.5
17.5
PATTERN GAIN IN DBI
HORIZONTAL
VERTICAL
TOTAL
ANGLES IN DEGREES TRUE

FIGURE A 25

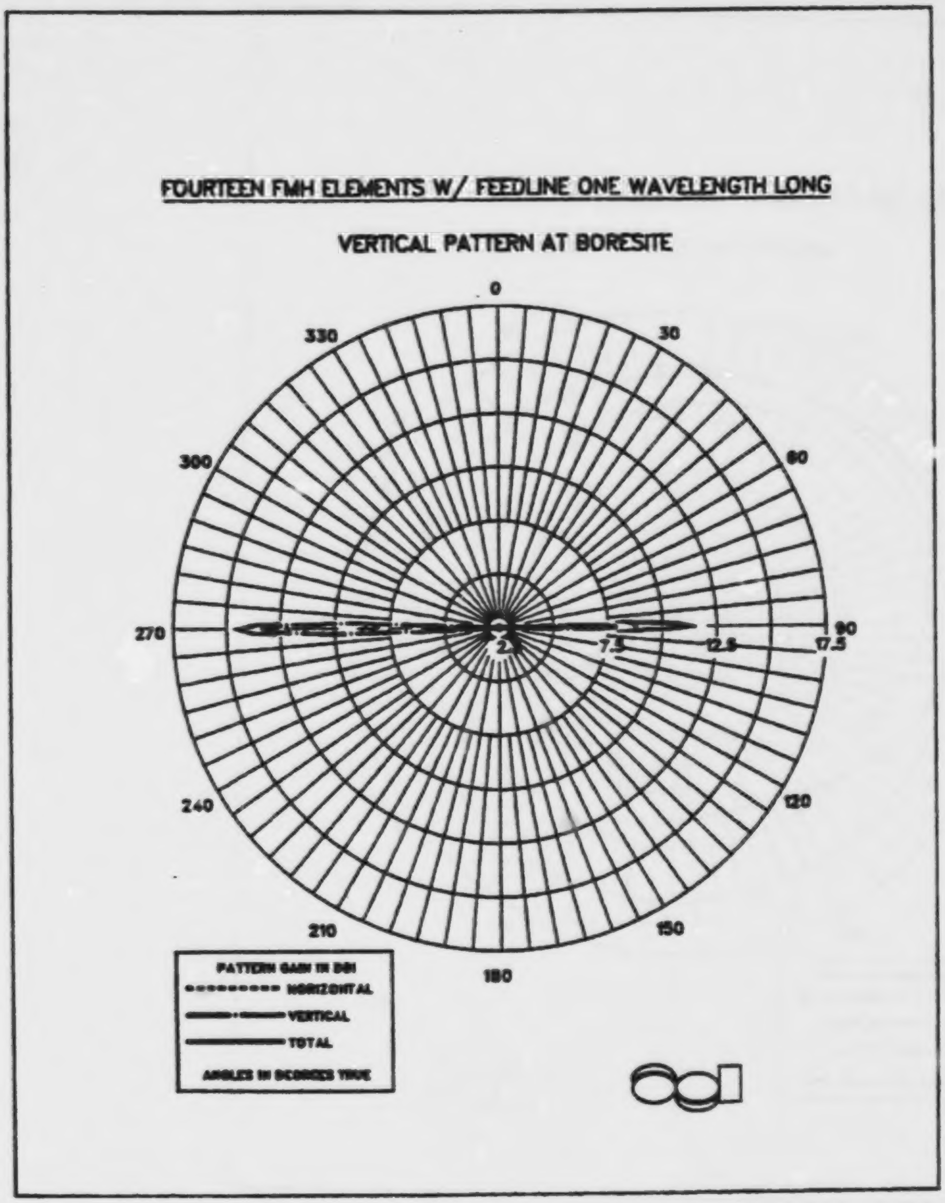

FOURTEEN FMH ELEMENTS W/ FEEDLINE ONE WAVELENGTH LONG

VERTICAL PATTERN AT BORESITE

FIGURE A 26

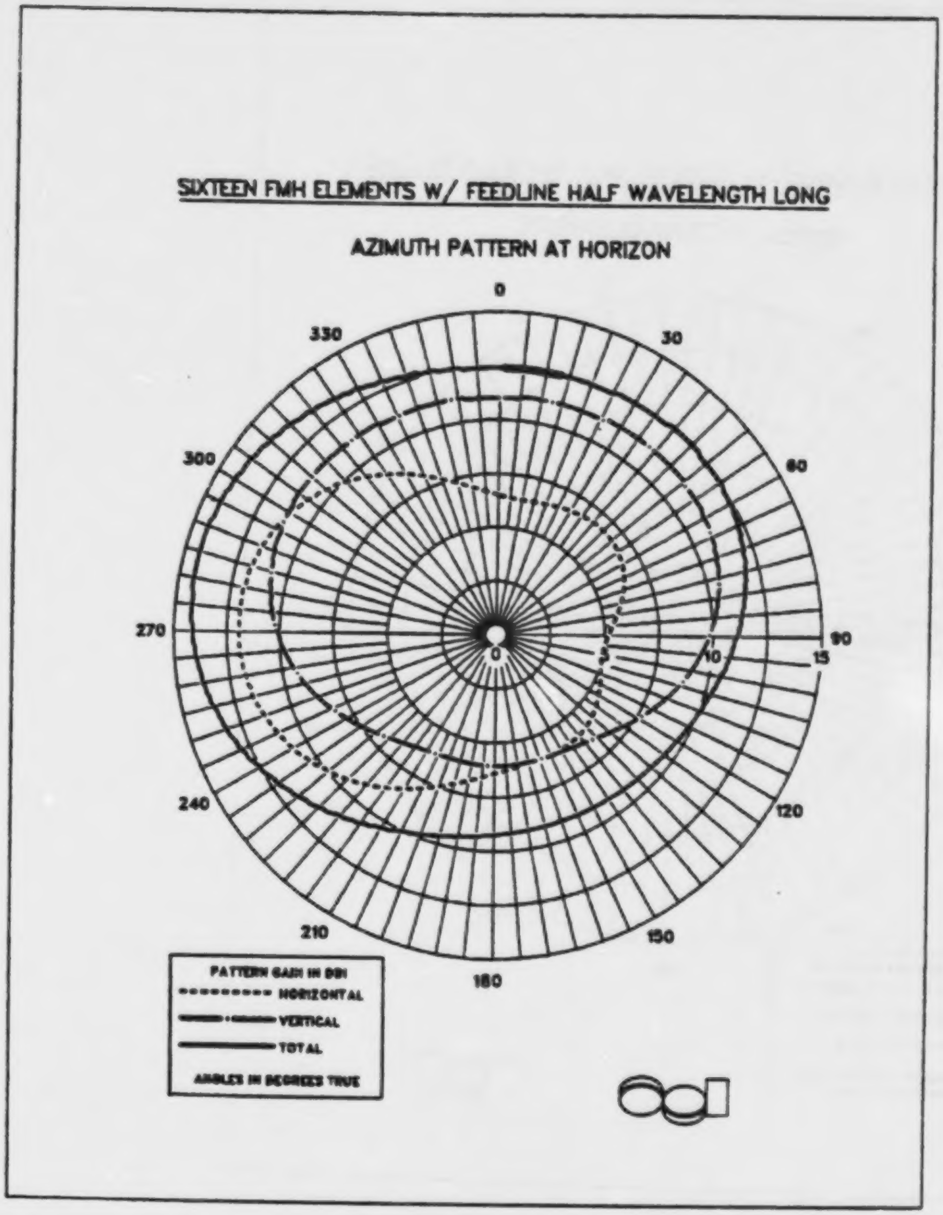
SIXTEEN FMH ELEMENTS W/ FEEDLINE HALF WAVELENGTH LONG
AZIMUTH PATTERN AT HORIZON
0
30
60
90
120
150
180
210
240
270
300
330
0
5
10
15
PATTERN GAIN IN DBI
HORIZONTAL
VERTICAL
TOTAL
ANGLES IN DEGREES TRUE

FIGURE A 27

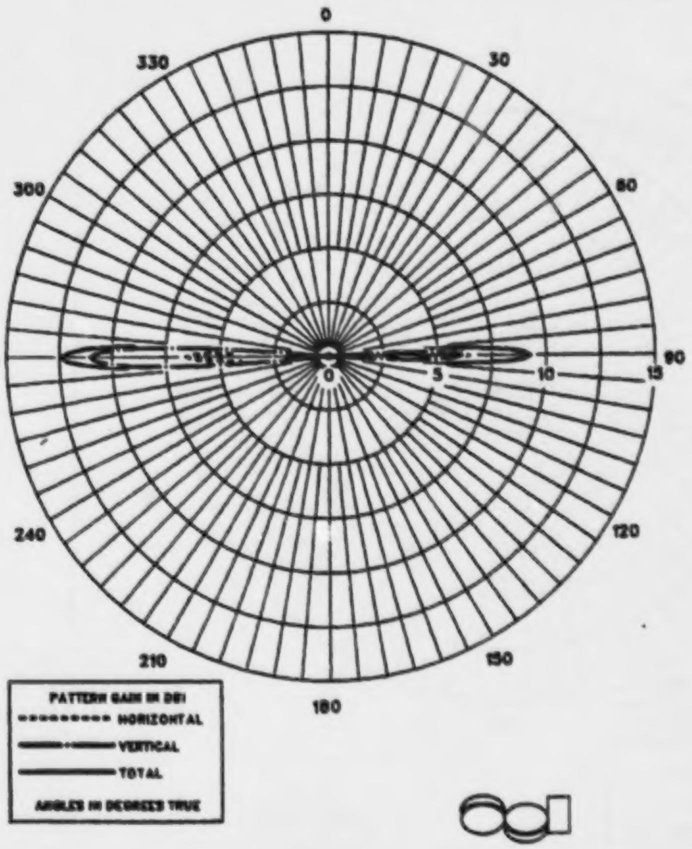

SIXTEEN FMH ELEMENTS W/ FEEDLINE HALF WAVELENGTH LONG

VERTICAL PATTERN AT BORESITE

FIGURE A 28

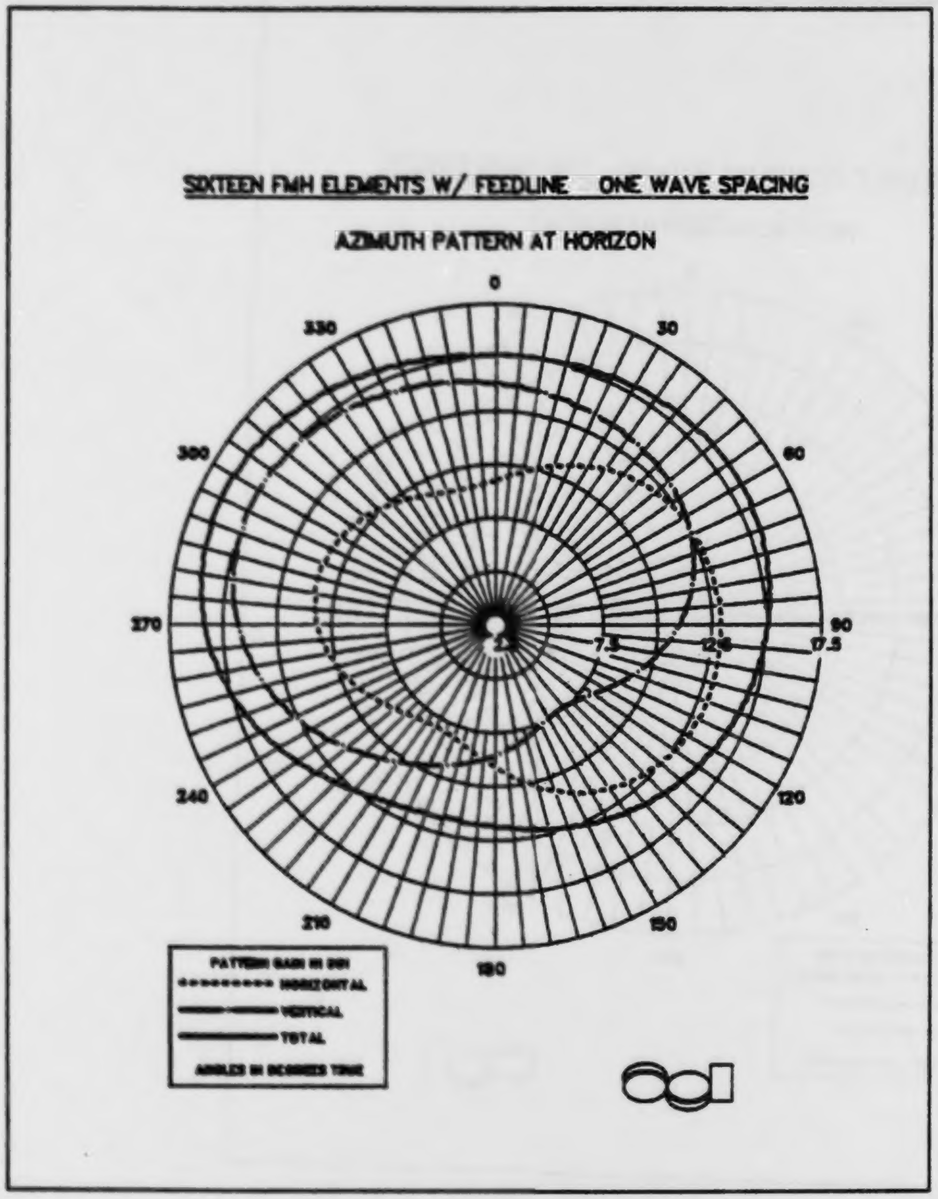
SIXTEEN FMH ELEMENTS W/ FEEDLINE ONE WAVE SPACING
AZIMUTH PATTERN AT HORIZON
0
30
60
90
120
150
180
210
240
270
300
330
2.5
7.5
12.5
17.5
PATTERN GAIN IN DBI
HORIZONTAL
VERTICAL
TOTAL
ANGLES IN DEGREES TRUE

FIGURE A 29

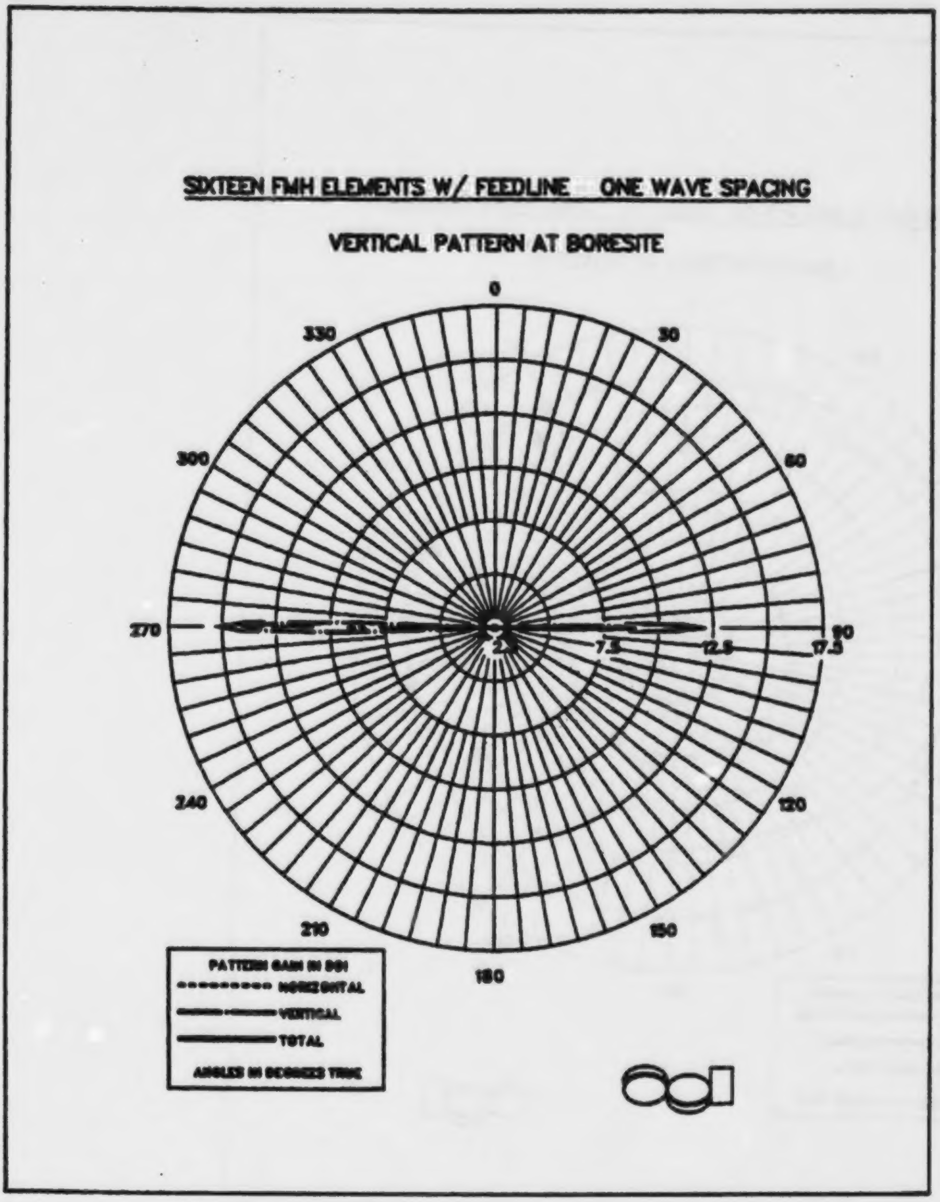

SIXTEEN FMH ELEMENTS W/ FEEDLINE ONE WAVE SPACING
VERTICAL PATTERN AT BORESITE
0
30
60
90
120
150
180
210
240
270
300
330
2.5
7.5
12.5
17.5
PATTERN GAIN IN DBI
HORIZONTAL
VERTICAL
TOTAL
ANGLES IN DEGREES TRUE

FIGURE A 30

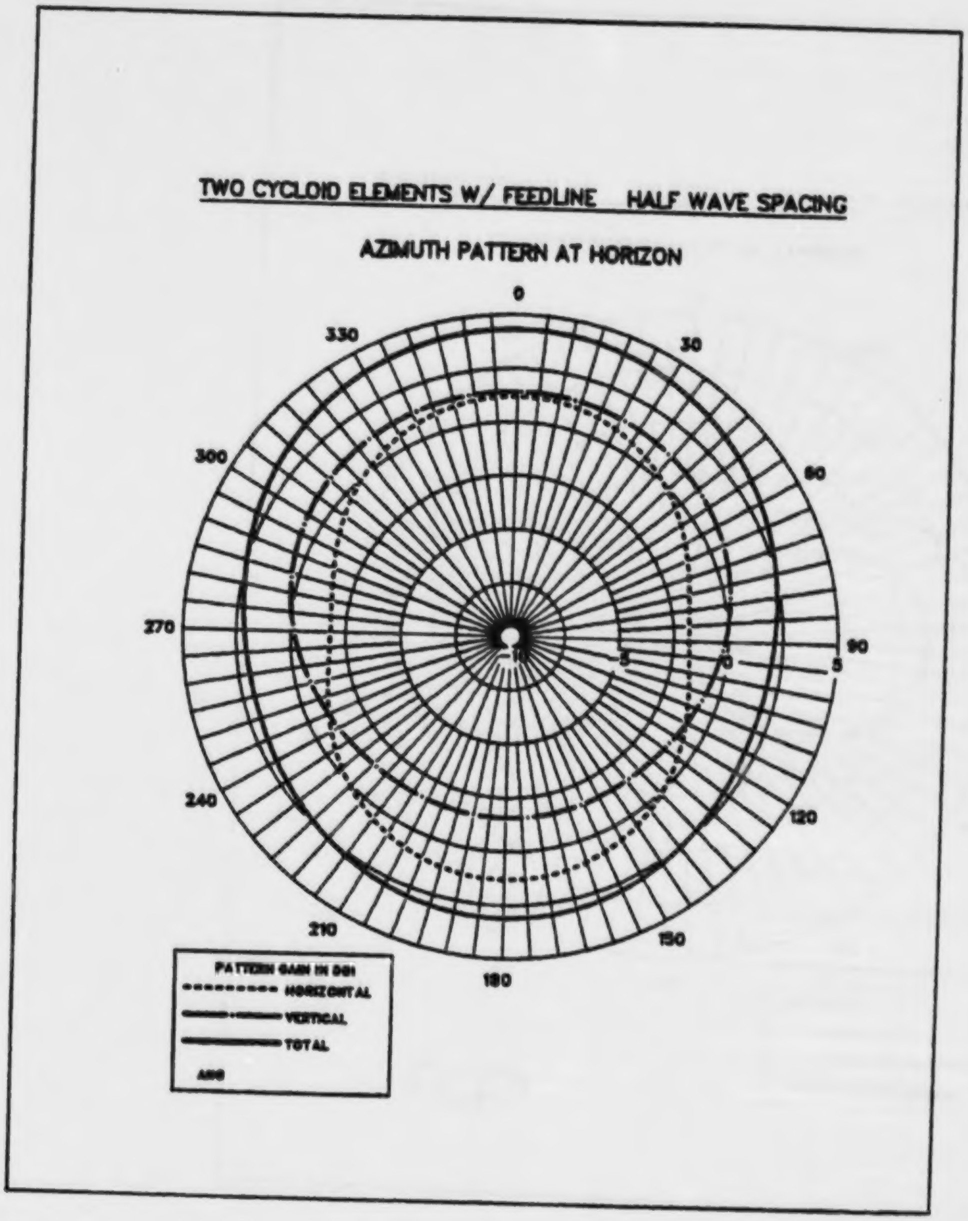

TWO CYCLOID ELEMENTS W/ FEEDLINE HALF WAVE SPACING

AZIMUTH PATTERN AT HORIZON

FIGURE A 31

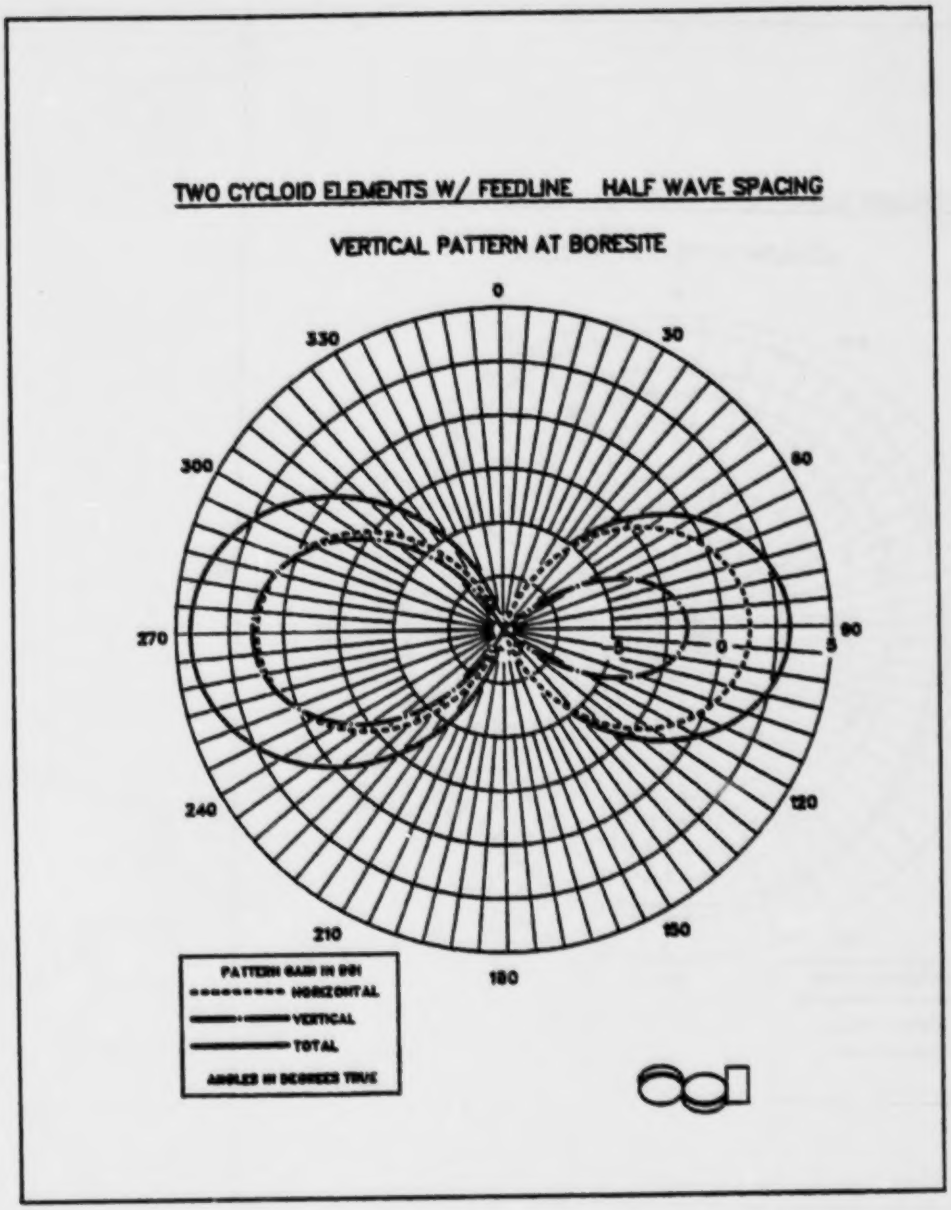

TWO CYCLOID ELEMENTS W/ FEEDLINE HALF WAVE SPACING

VERTICAL PATTERN AT BORESITE

FIGURE A 32

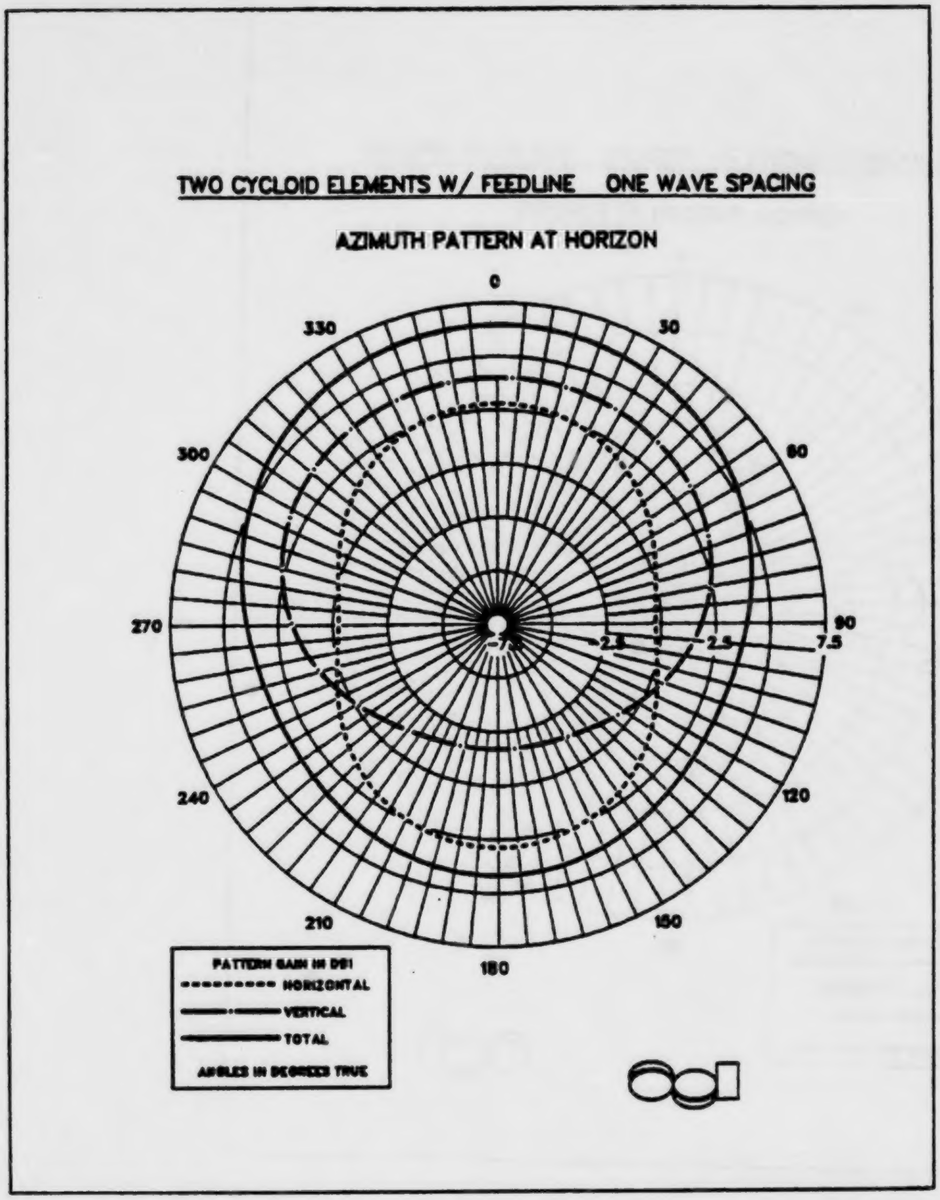

TWO CYCLOID ELEMENTS W/ FEEDLINE ONE WAVE SPACING
AZIMUTH PATTERN AT HORIZON
0
30
60
90
120
150
180
210
240
270
300
330
-7.5
-2.5
2.5
7.5
PATTERN GAIN IN DBI
HORIZONTAL
VERTICAL
TOTAL
ANGLES IN DEGREES TRUE

FIGURE A 33

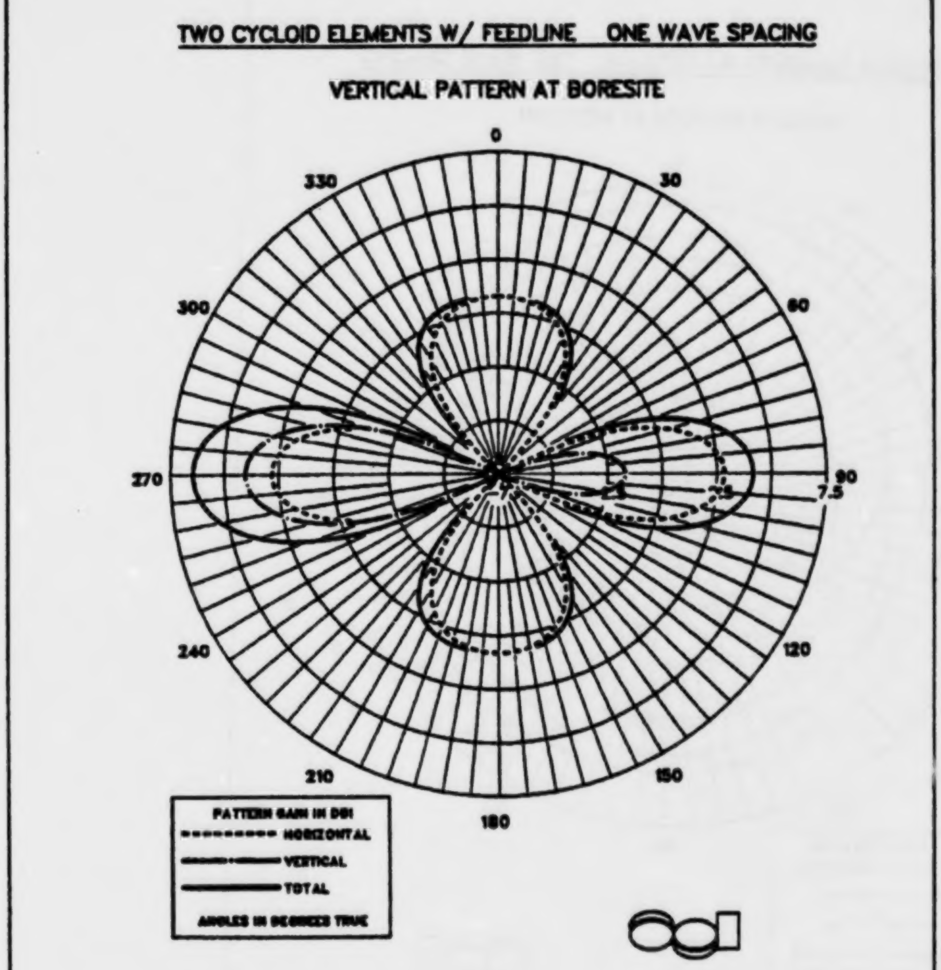
TWO CYCLOID ELEMENTS W/ FEEDLINE ONE WAVE SPACING

VERTICAL PATTERN AT BORESITE

FIGURE A 34

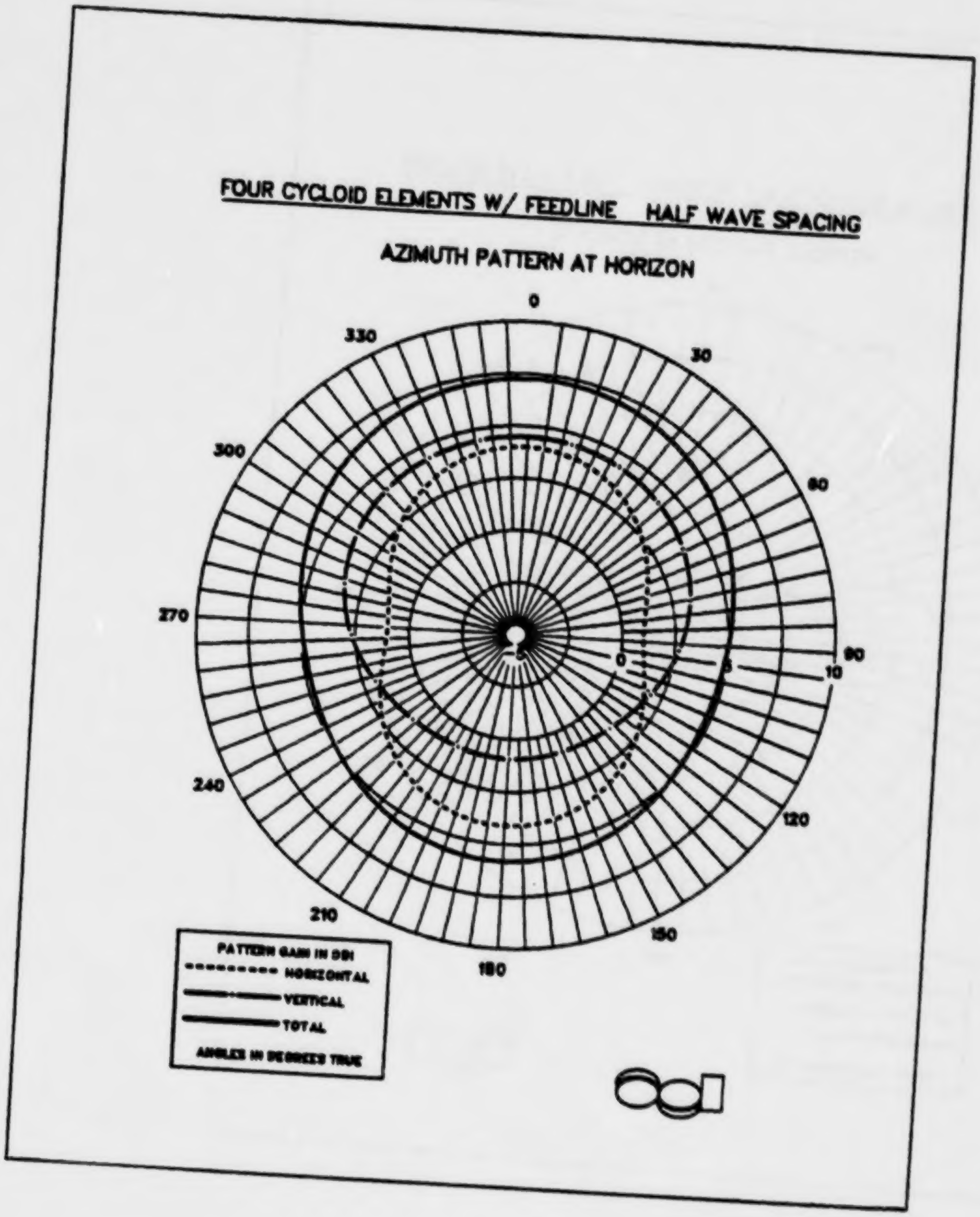
FOUR CYCLOID ELEMENTS W/ FEEDLINE HALF WAVE SPACING
AZIMUTH PATTERN AT HORIZON
0
30
60
90
120
150
180
210
240
270
300
330
-5
0
5
10
PATTERN GAIN IN DBI
HORIZONTAL
VERTICAL
TOTAL
ANGLES IN DEGREES TRUE

FIGURE A 35

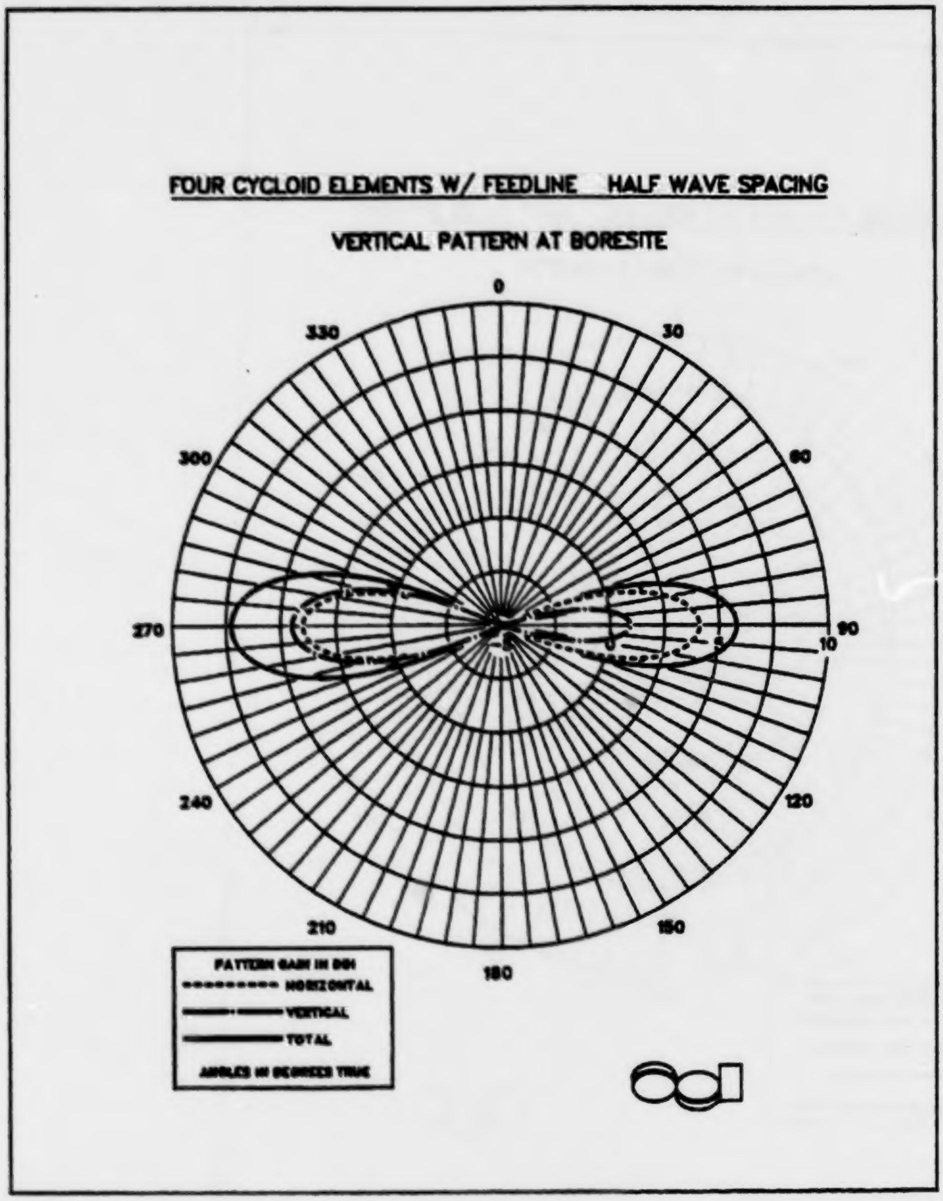
FOUR CYCLOID ELEMENTS W/ FEEDLINE HALF WAVE SPACING
VERTICAL PATTERN AT BORESITE
0
30
60
90
10
120
150
180
210
240
270
300
330
PATTERN GAIN IN DBI
HORIZONTAL
VERTICAL
TOTAL
ANGLES IN DEGREES TRUE

FIGURE A 36

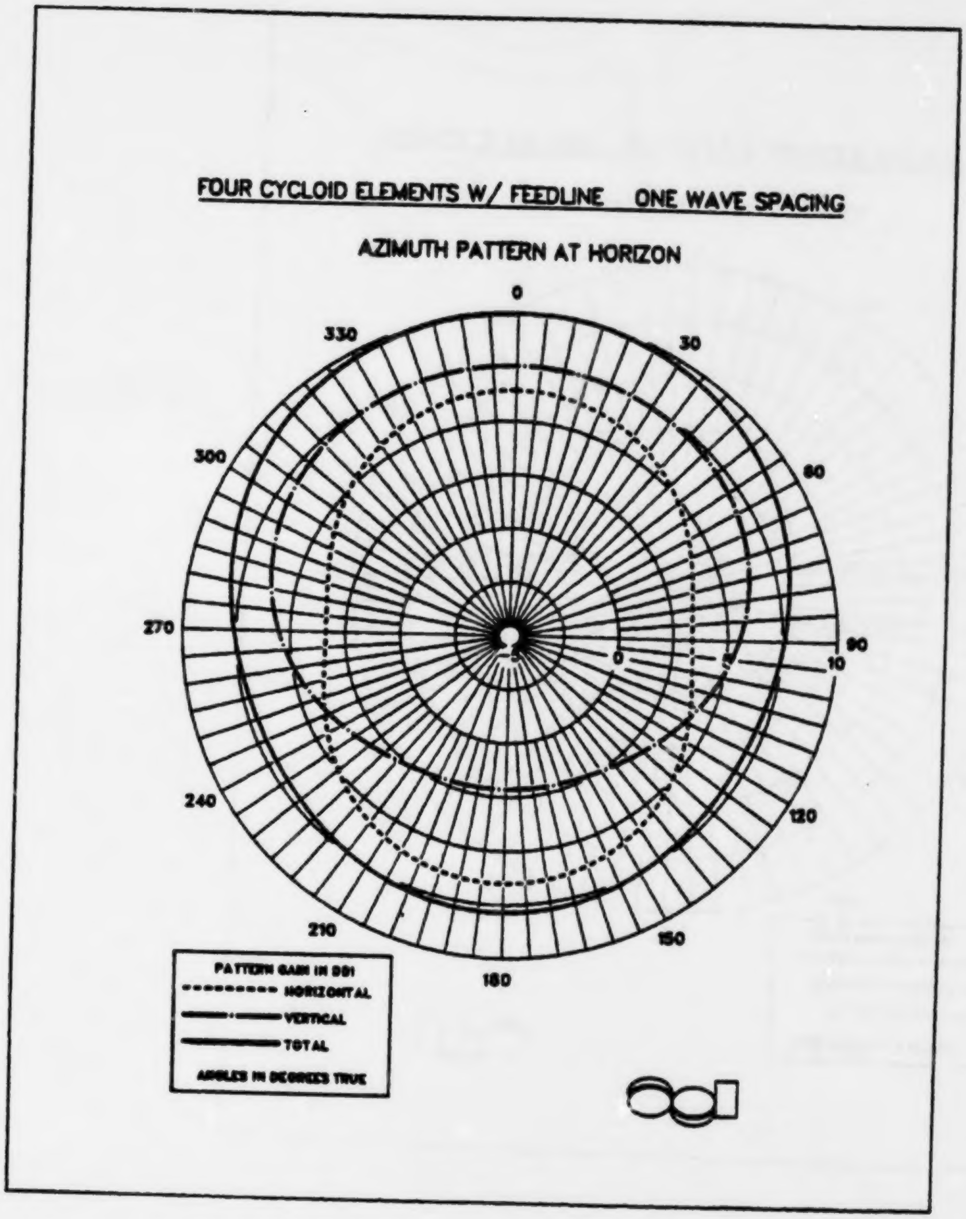

FOUR CYCLOID ELEMENTS W/ FEEDLINE ONE WAVE SPACING

AZIMUTH PATTERN AT HORIZON

FIGURE A 37

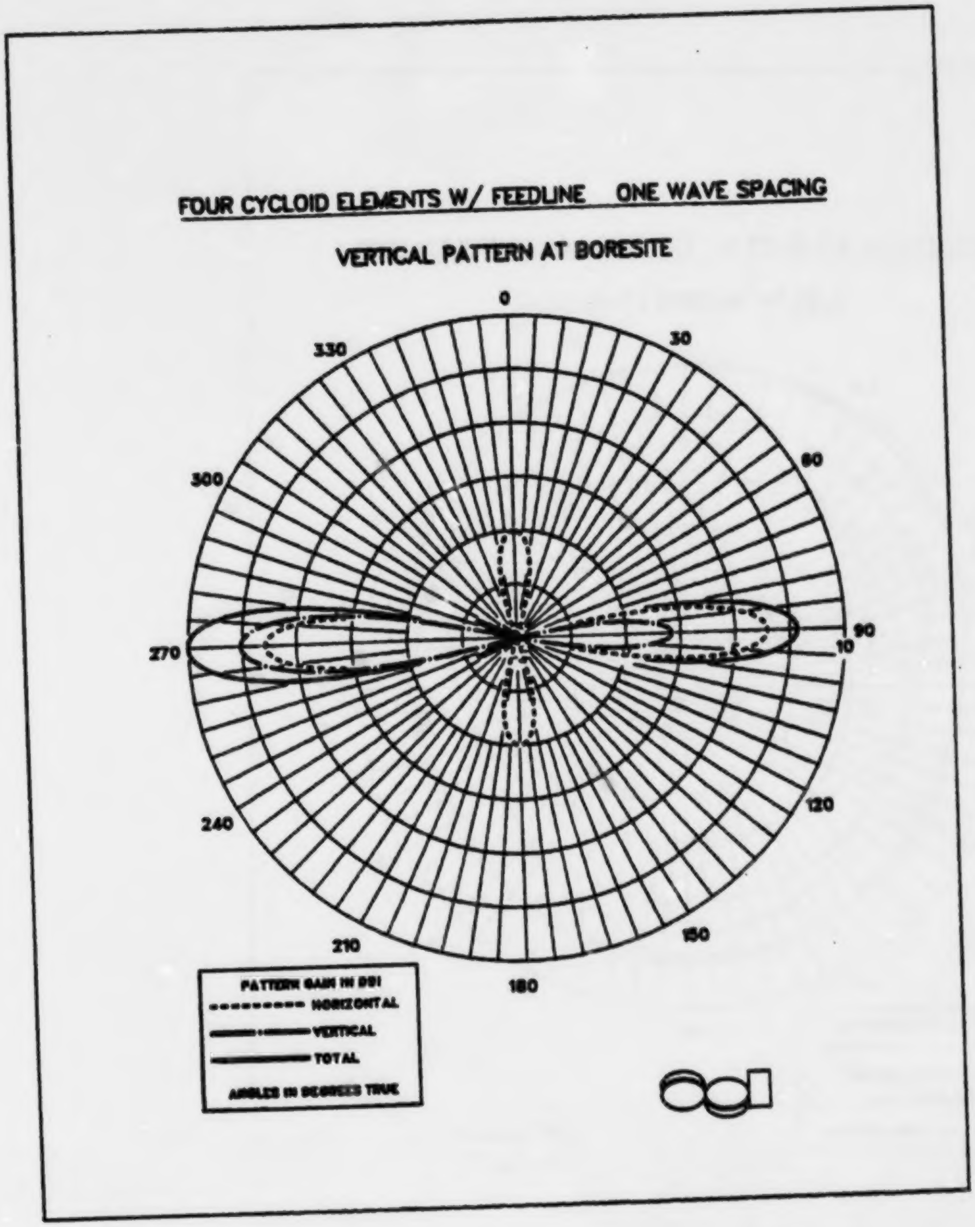
FOUR CYCLOID ELEMENTS W/ FEEDLINE ONE WAVE SPACING
VERTICAL PATTERN AT BORESITE
0
30
60
90
10
120
150
180
210
240
270
300
330
PATTERN GAIN IN DBI
HORIZONTAL
VERTICAL
TOTAL
ANGLES IN DEGREES TRUE

FIGURE A 38

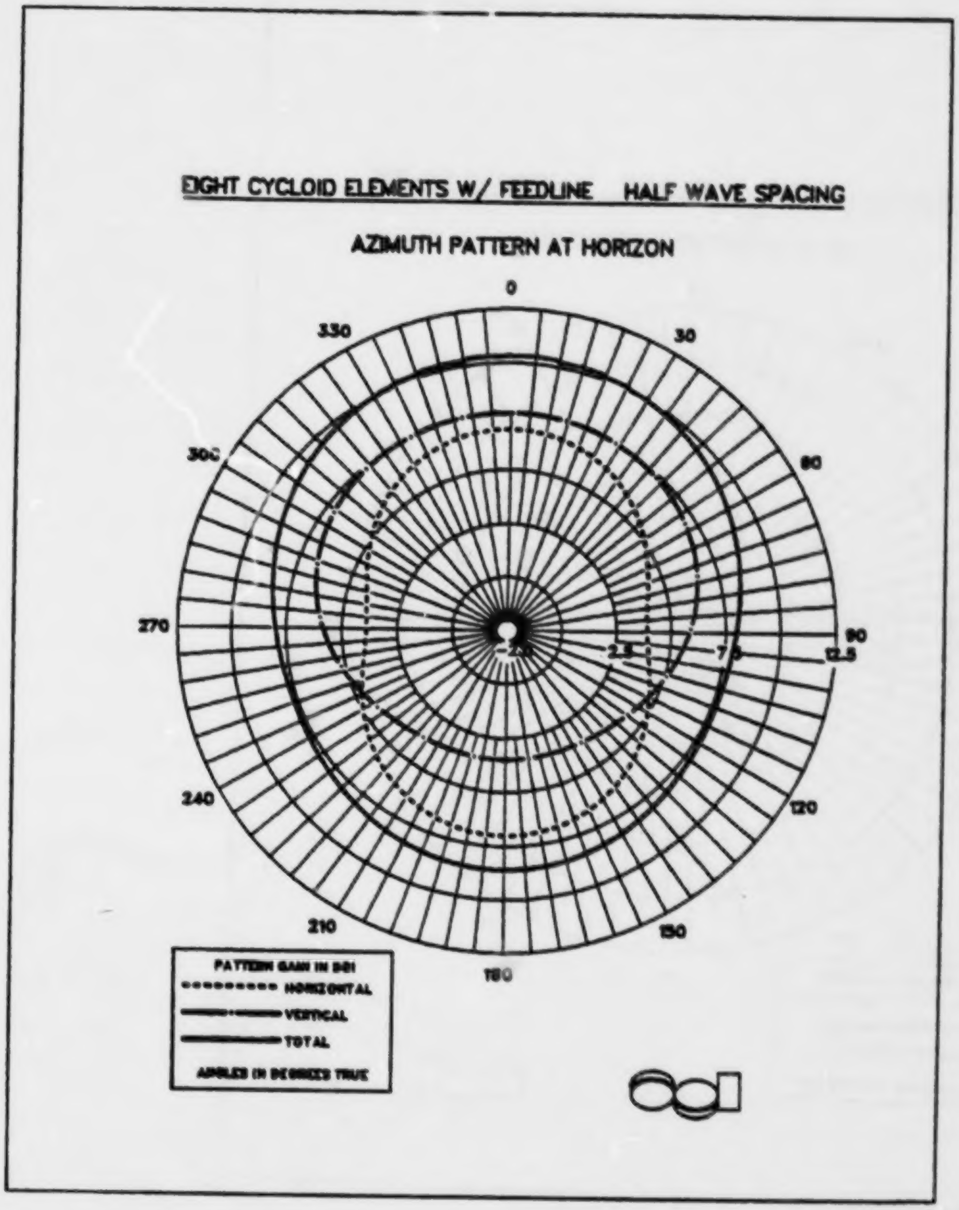

EIGHT CYCLOID ELEMENTS W/ FEEDLINE HALF WAVE SPACING

AZIMUTH PATTERN AT HORIZON

FIGURE A 39

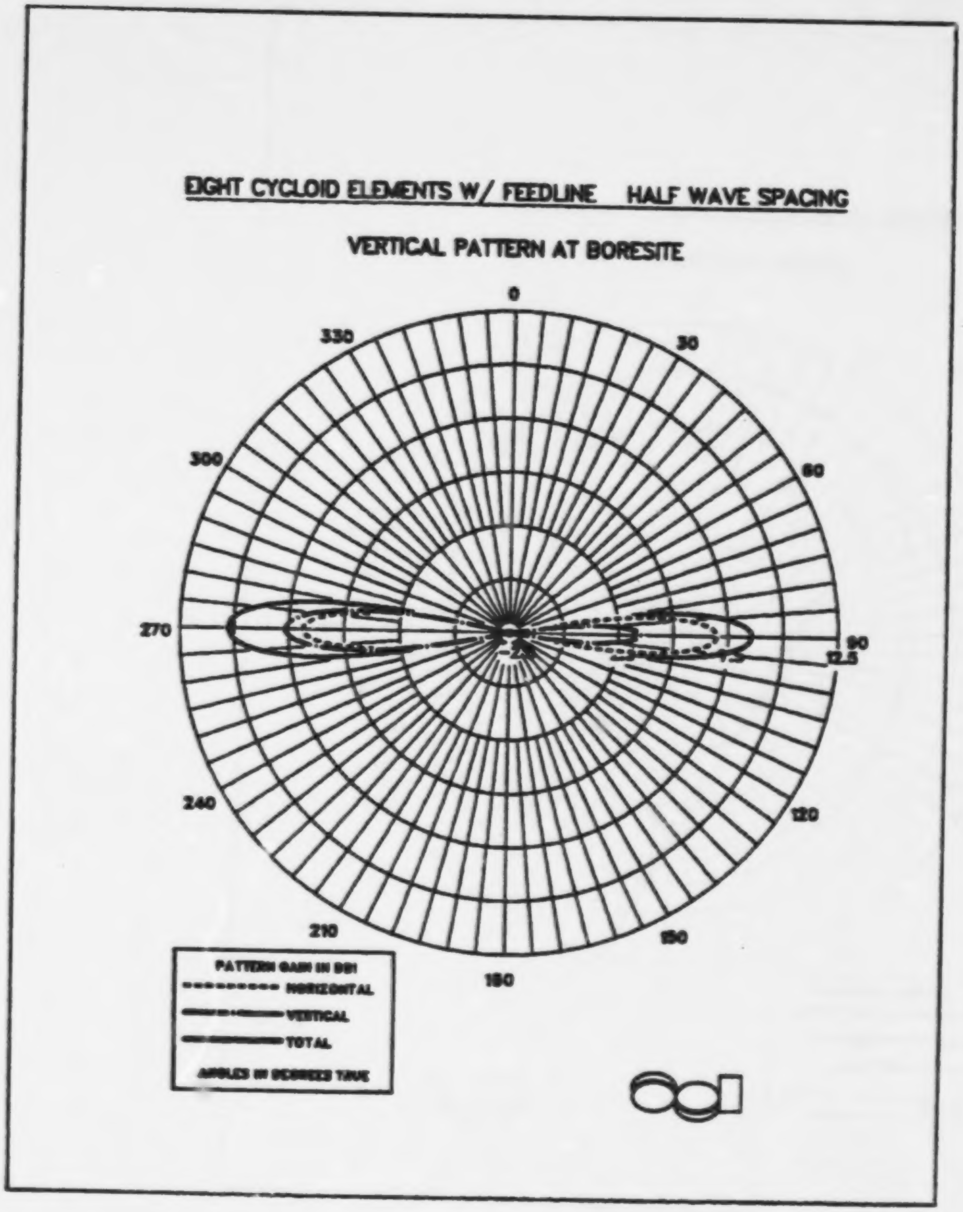

EIGHT CYCLOID ELEMENTS W/ FEEDLINE HALF WAVE SPACING

VERTICAL PATTERN AT BORESITE

FIGURE A 40

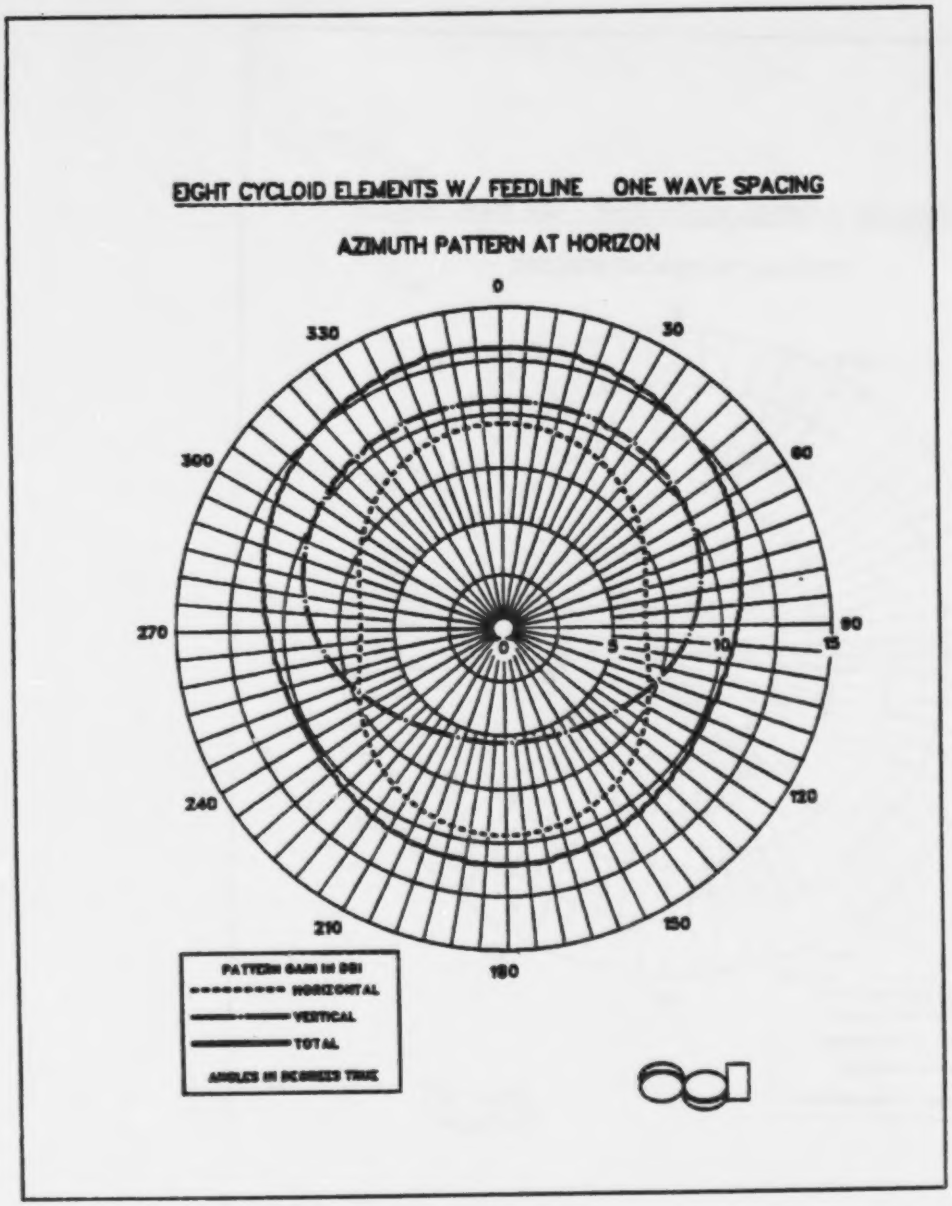
EIGHT CYCLOID ELEMENTS W/ FEEDLINE ONE WAVE SPACING
AZIMUTH PATTERN AT HORIZON
0
30
60
90
120
150
180
210
240
270
300
330
0
5
10
15
PATTERN GAIN IN DBI
HORIZONTAL
VERTICAL
TOTAL
ANGLES IN DEGREES TRUE

FIGURE A 41

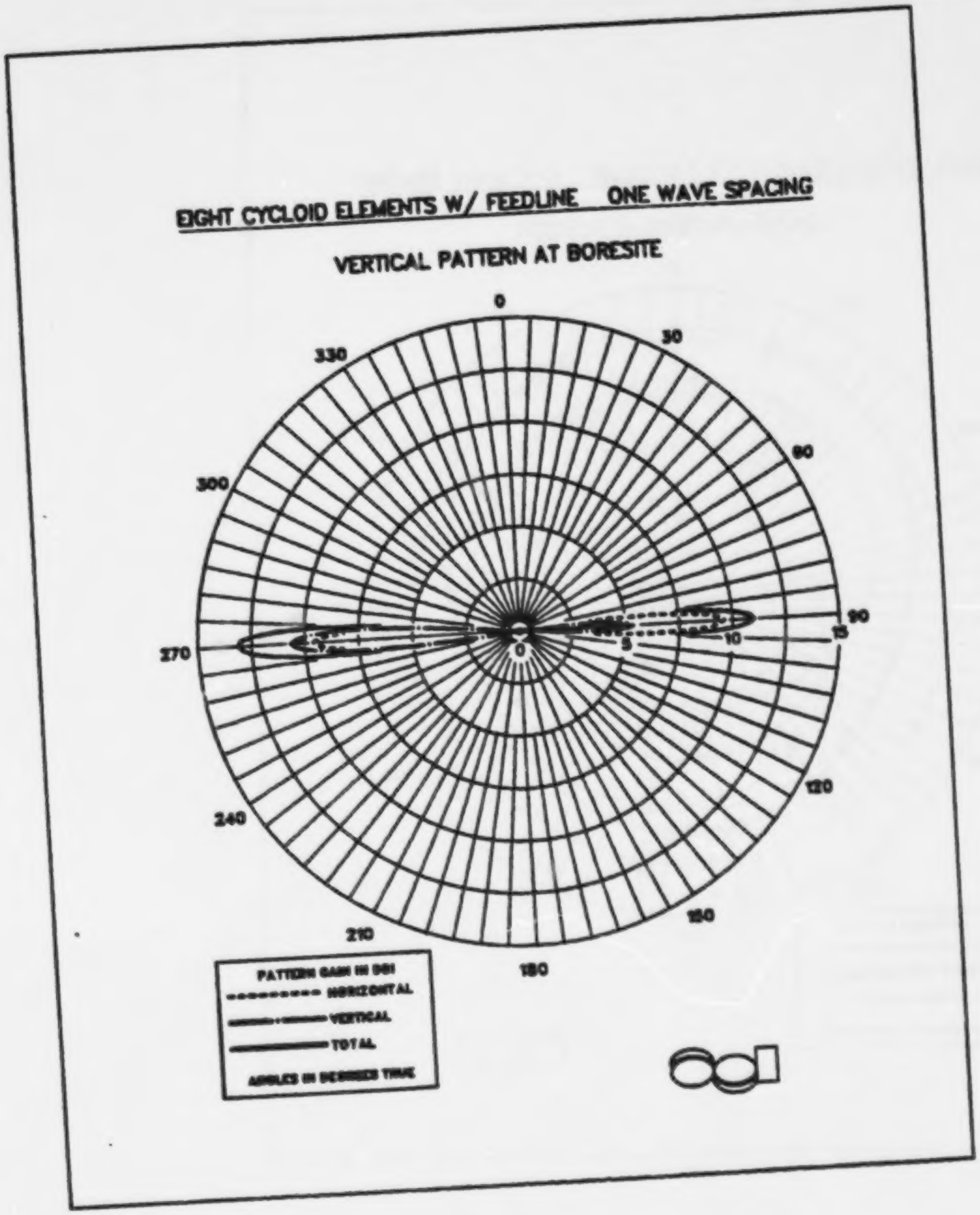

EIGHT CYCLOID ELEMENTS W/ FEEDLINE ONE WAVE SPACING

VERTICAL PATTERN AT BORESITE

FIGURE A 42

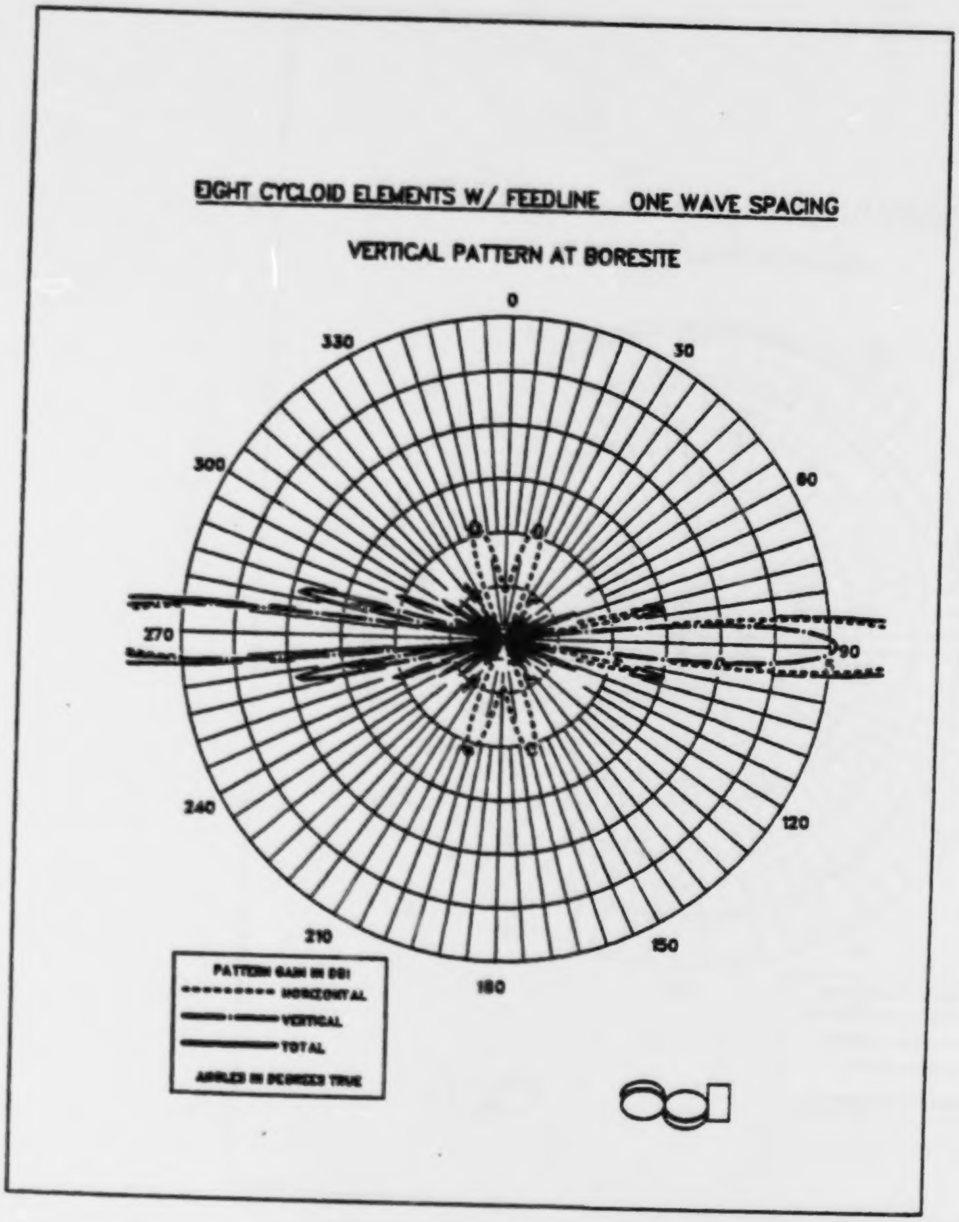
EIGHT CYCLOID ELEMENTS W/ FEEDLINE ONE WAVE SPACING
VERTICAL PATTERN AT BORESITE
0
30
60
90
120
150
180
210
240
270
300
330
PATTERN GAIN IN DBI
HORIZONTAL
VERTICAL
TOTAL
ANGLES IN DEGREES TRUE

FIGURE A 43

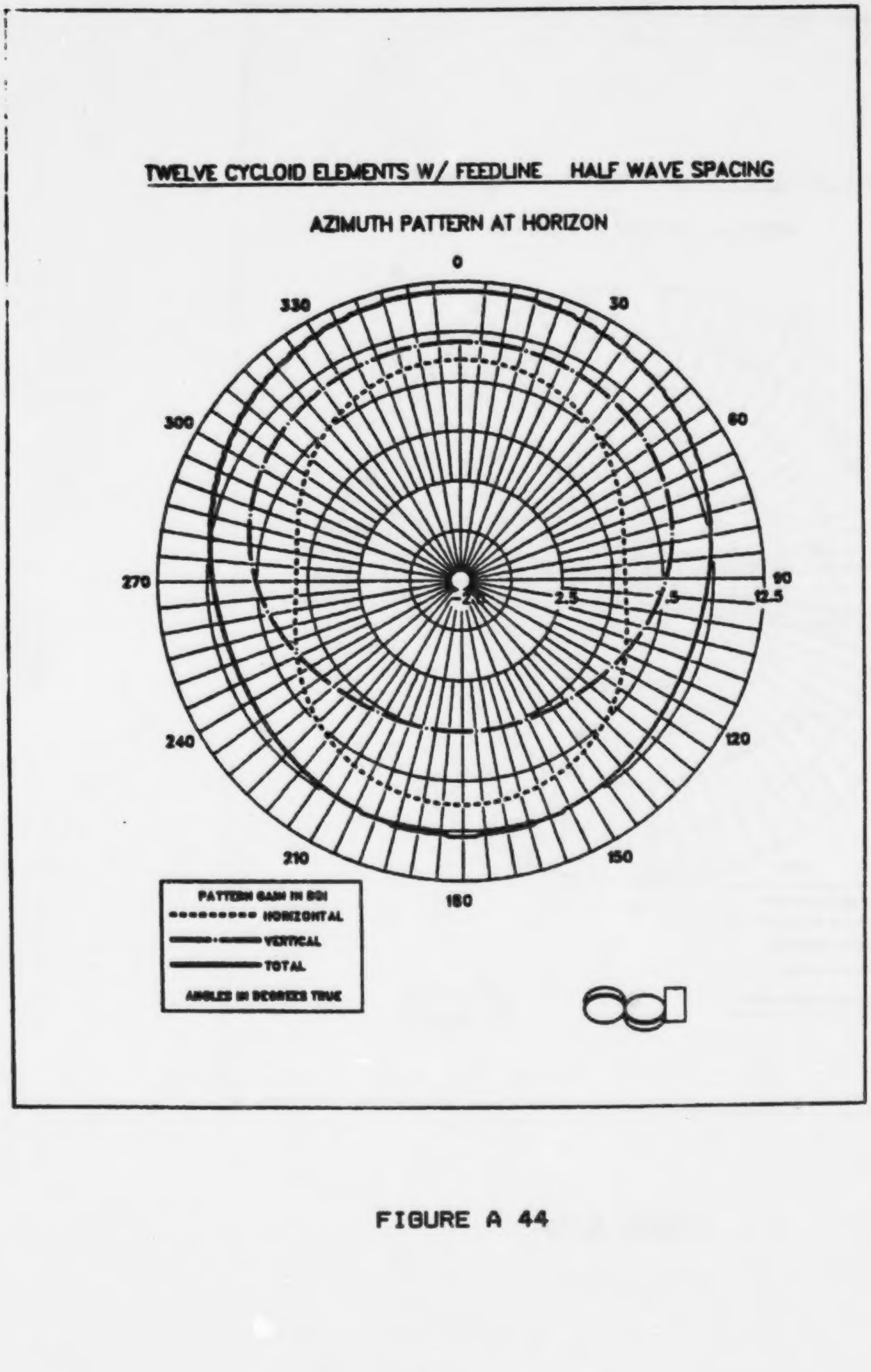

TWELVE CYCLOID ELEMENTS W/ FEEDLINE HALF WAVE SPACING

AZIMUTH PATTERN AT HORIZON

FIGURE A 44

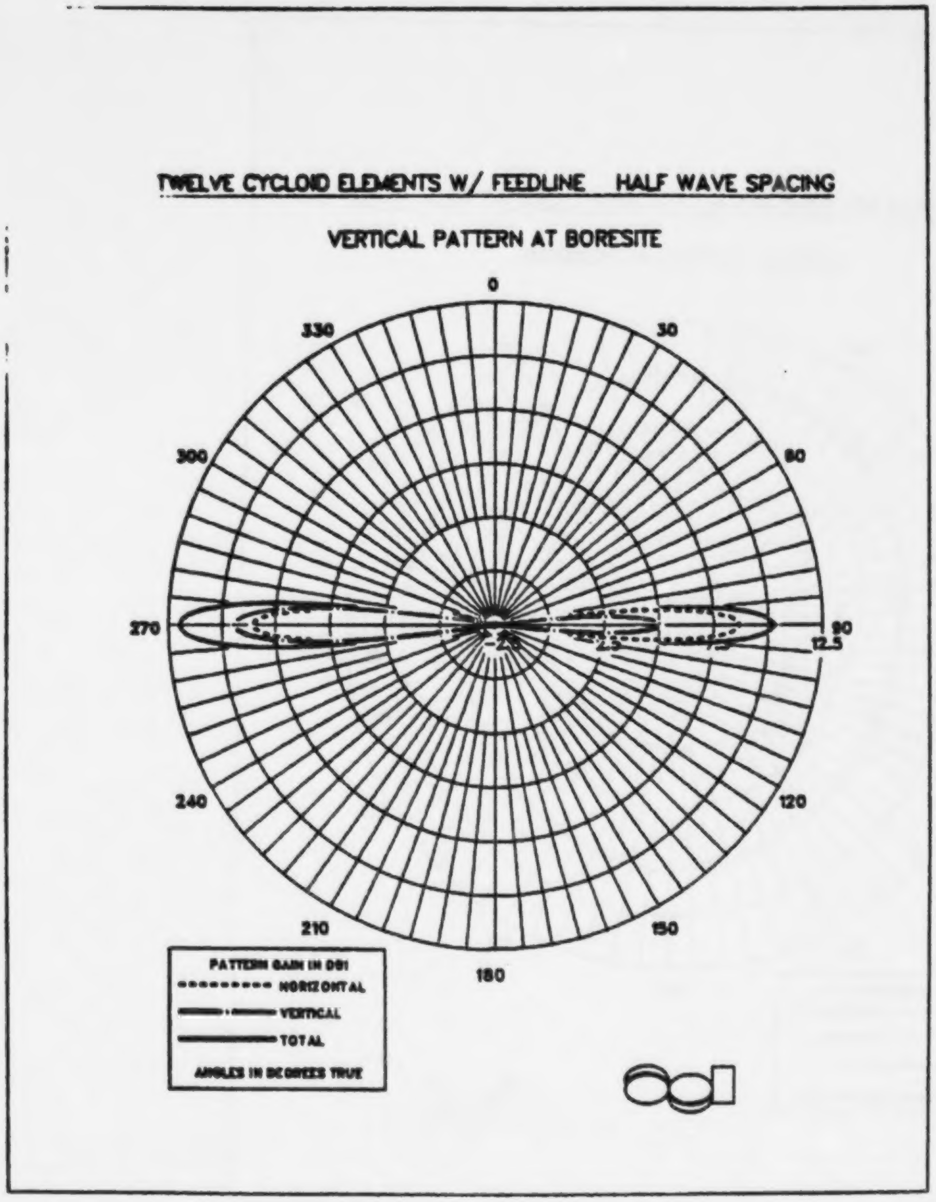
TWELVE CYCLOID ELEMENTS W/ FEEDLINE HALF WAVE SPACING
VERTICAL PATTERN AT BORESITE
0
30
60
90
120
150
180
210
240
270
300
330
-2.5
2.5
7.5
12.5
PATTERN GAIN IN DBI
HORIZONTAL
VERTICAL
TOTAL
ANGLES IN DEGREES TRUE
odl

FIGURE A 45

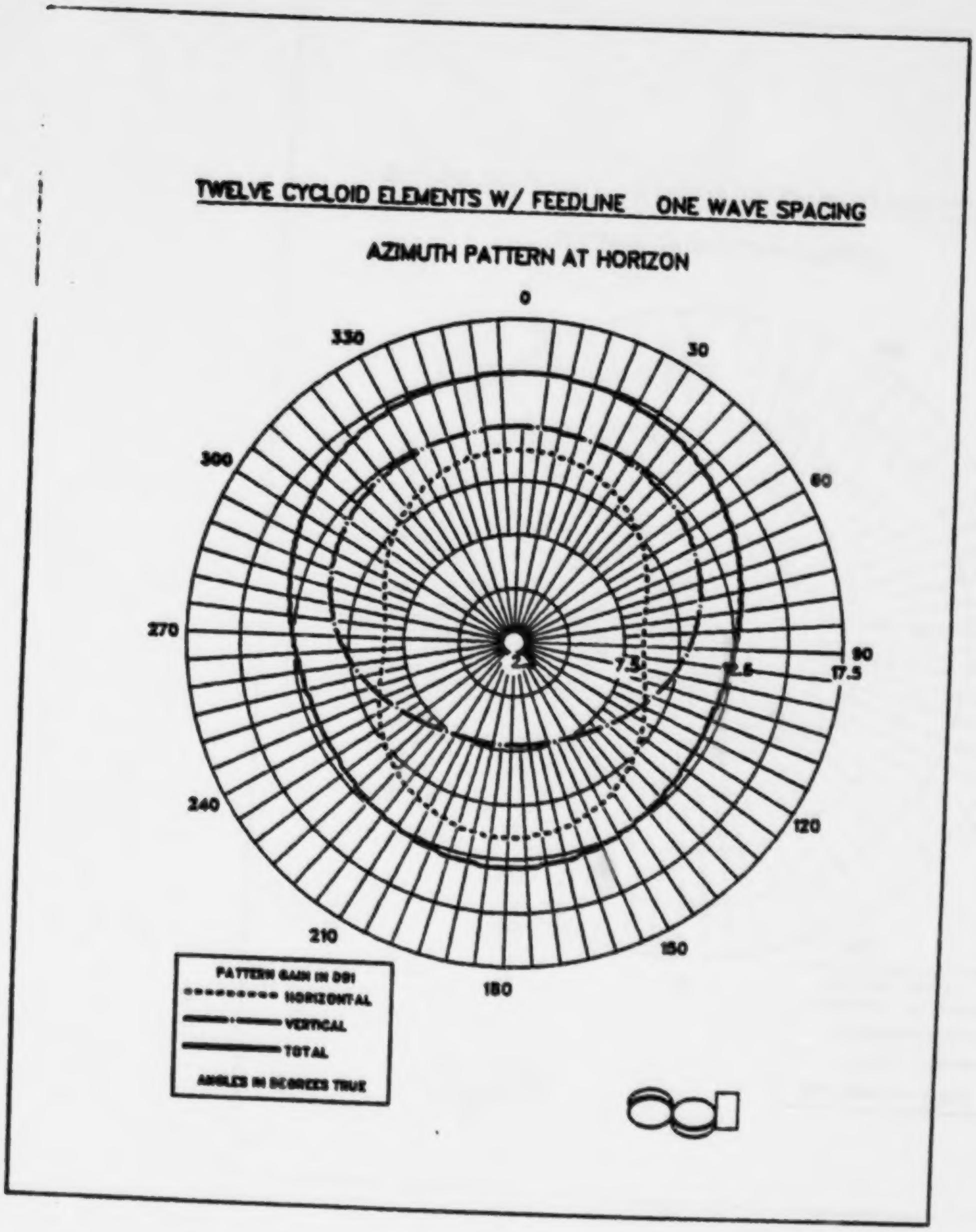

TWELVE CYCLOID ELEMENTS W/ FEEDLINE ONE WAVE SPACING

AZIMUTH PATTERN AT HORIZON

FIGURE A 46

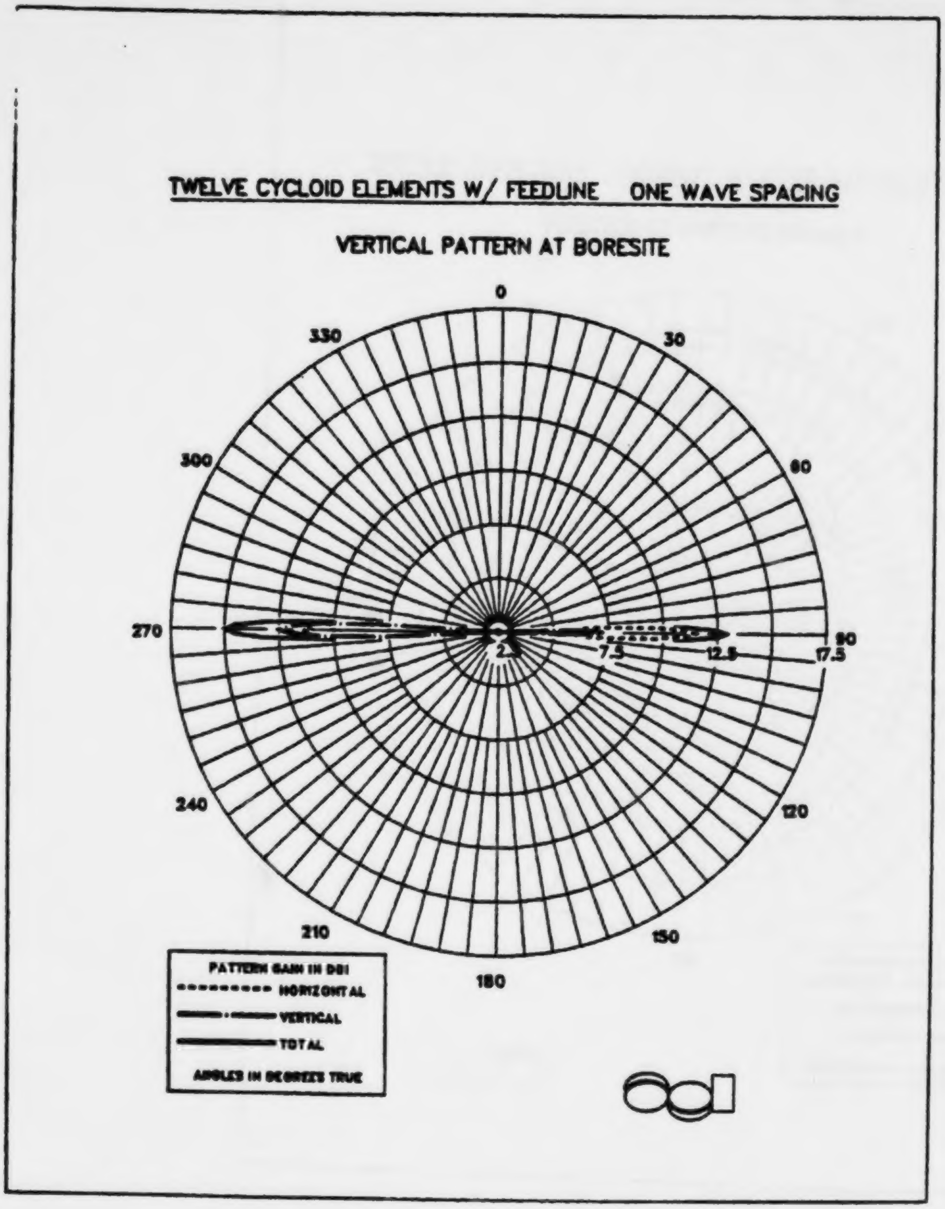

TWELVE CYCLOID ELEMENTS W/ FEEDLINE ONE WAVE SPACING

VERTICAL PATTERN AT BORESITE

FIGURE A 47

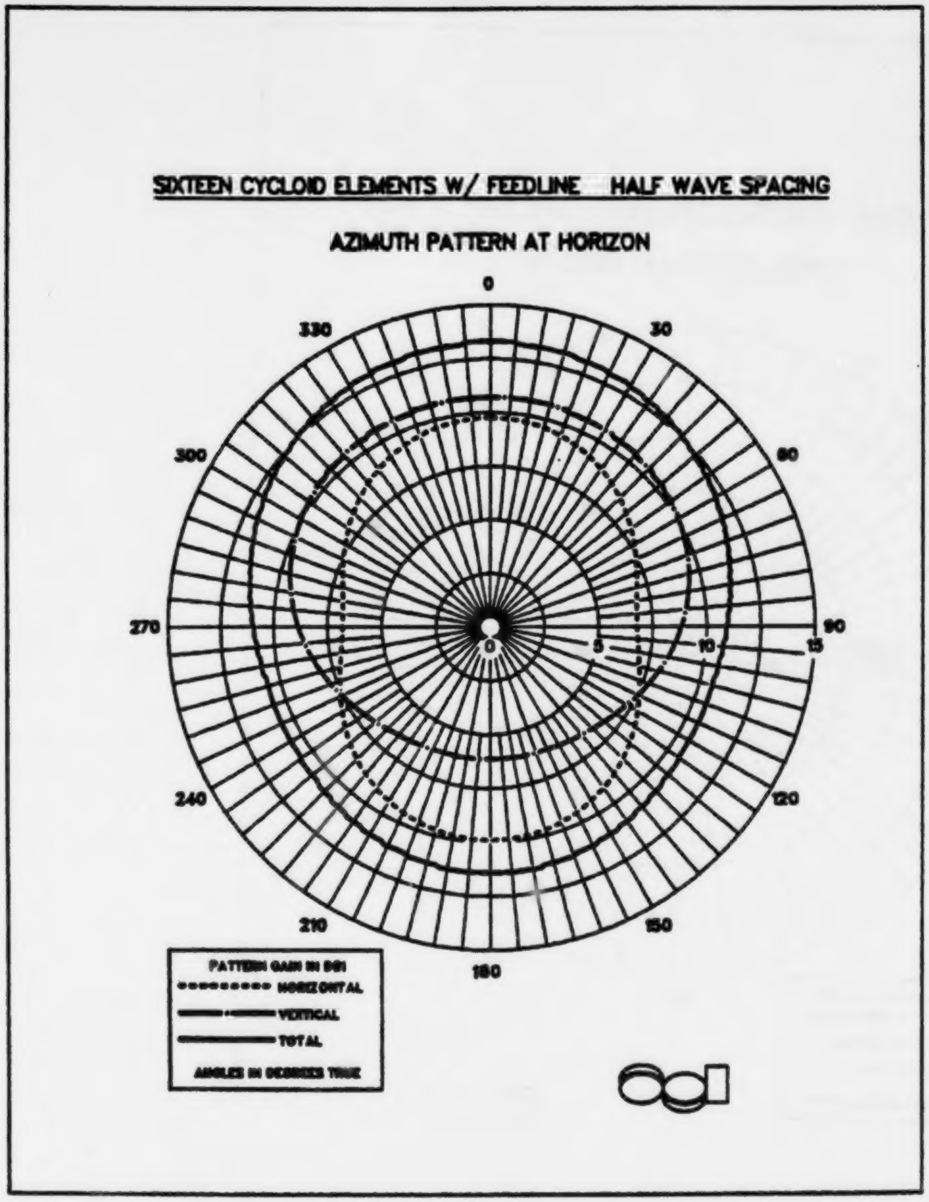
SIXTEEN CYCLOID ELEMENTS W/ FEEDLINE HALF WAVE SPACING
AZIMUTH PATTERN AT HORIZON
0
30
60
90
120
150
180
210
240
270
300
330
0
5
10
15
PATTERN GAIN IN DBI
HORIZONTAL
VERTICAL
TOTAL
ANGLES IN DEGREES TRUE

FIGURE A 48

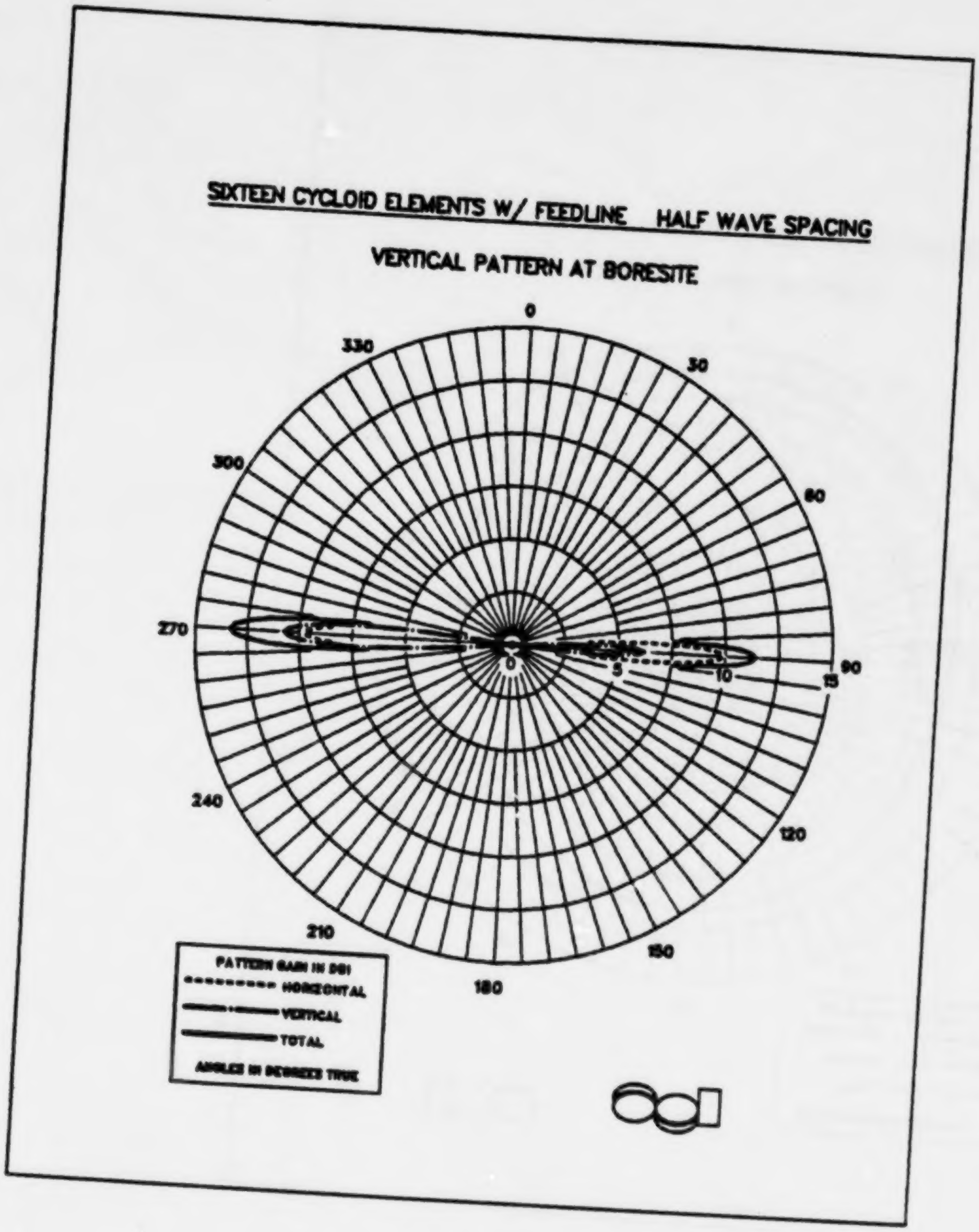

SIXTEEN CYCLOID ELEMENTS W/ FEEDLINE HALF WAVE SPACING

VERTICAL PATTERN AT BORESITE

FIGURE A 49

SIXTEEN CYCLOID ELEMENTS W/ FEEDLINE ONE WAVE SPACING

AZIMUTH PATTERN AT HORIZON

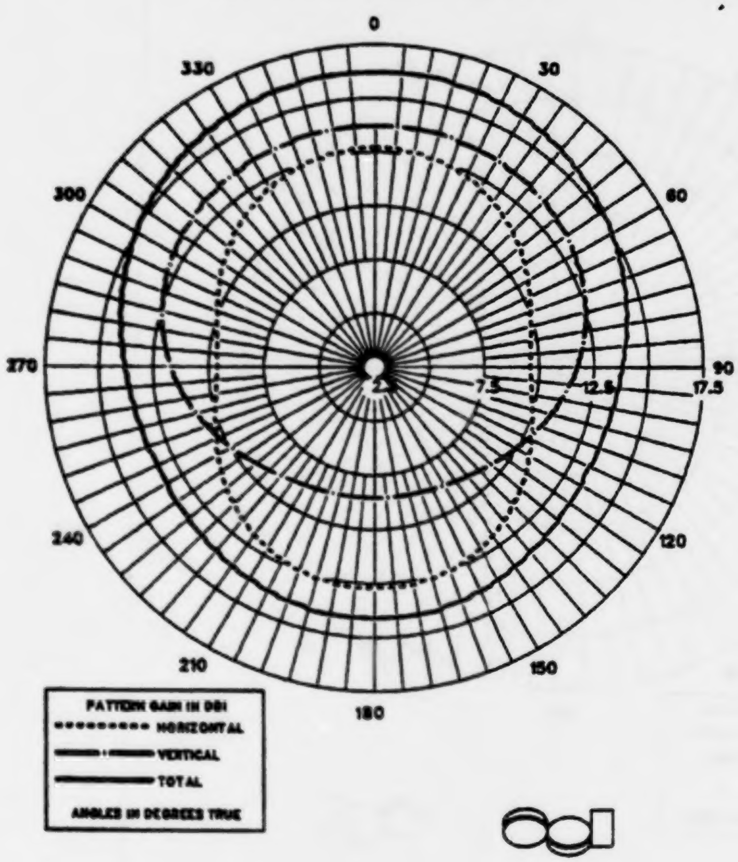

FIGURE A 50

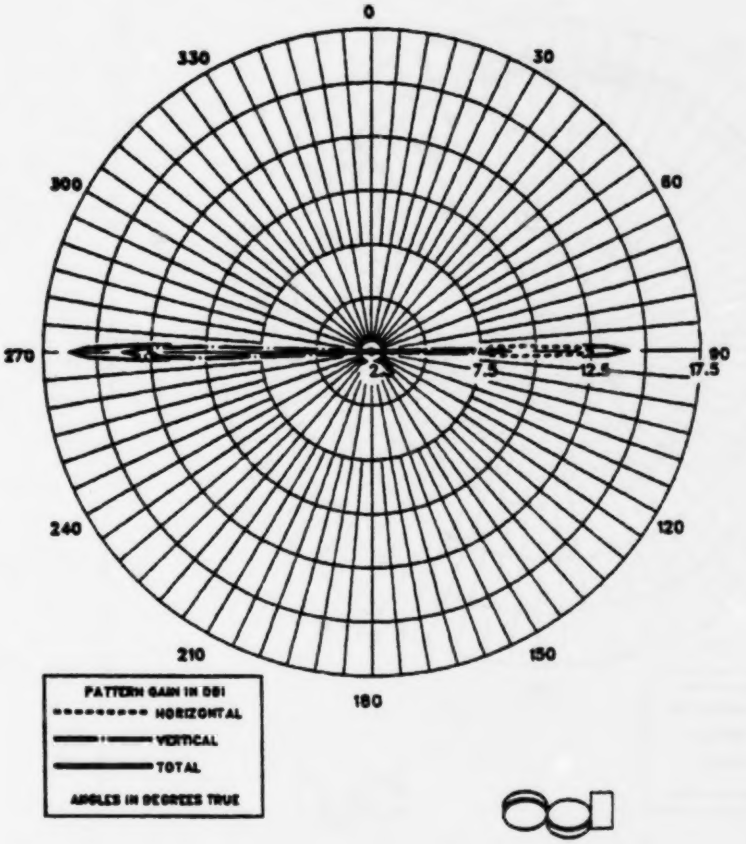

SIXTEEN CYCLOID ELEMENTS W/ FEEDLINE   ONE WAVE SPACING

VERTICAL PATTERN AT BORESITE

FIGURE A 51

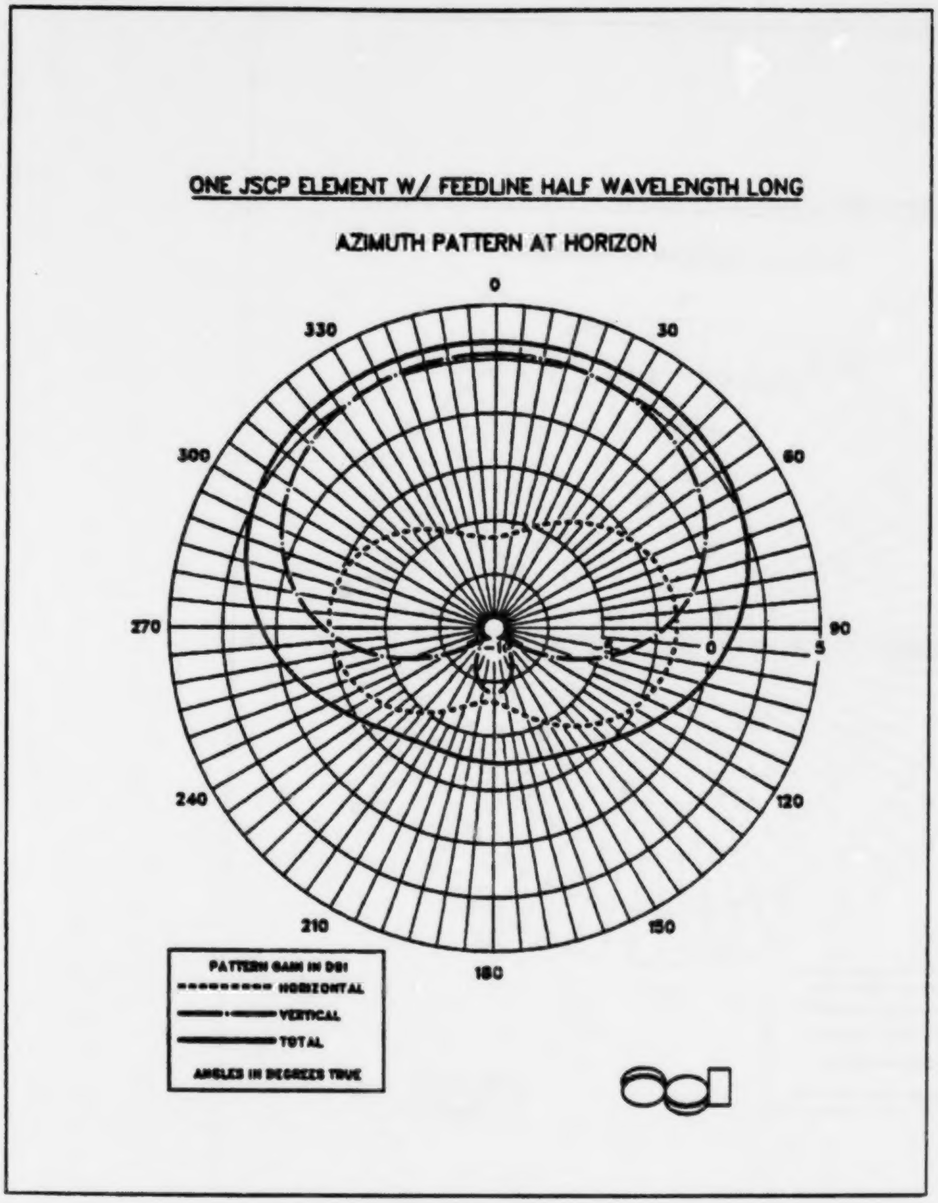
ONE JSCP ELEMENT W/ FEEDLINE HALF WAVELENGTH LONG

AZIMUTH PATTERN AT HORIZON

FIGURE A 52

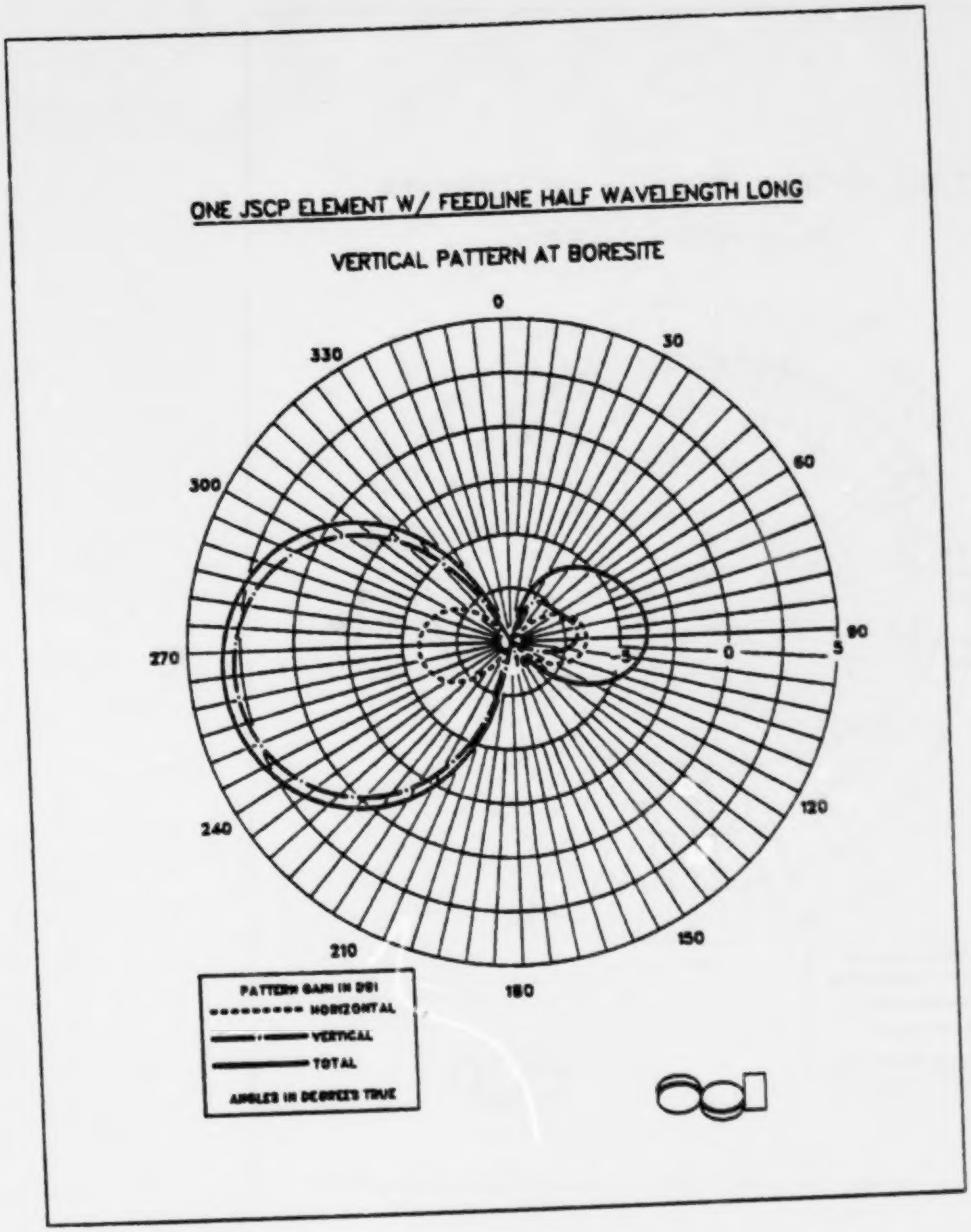

ONE JSCP ELEMENT W/ FEEDLINE HALF WAVELENGTH LONG

VERTICAL PATTERN AT BORESITE

FIGURE A 53

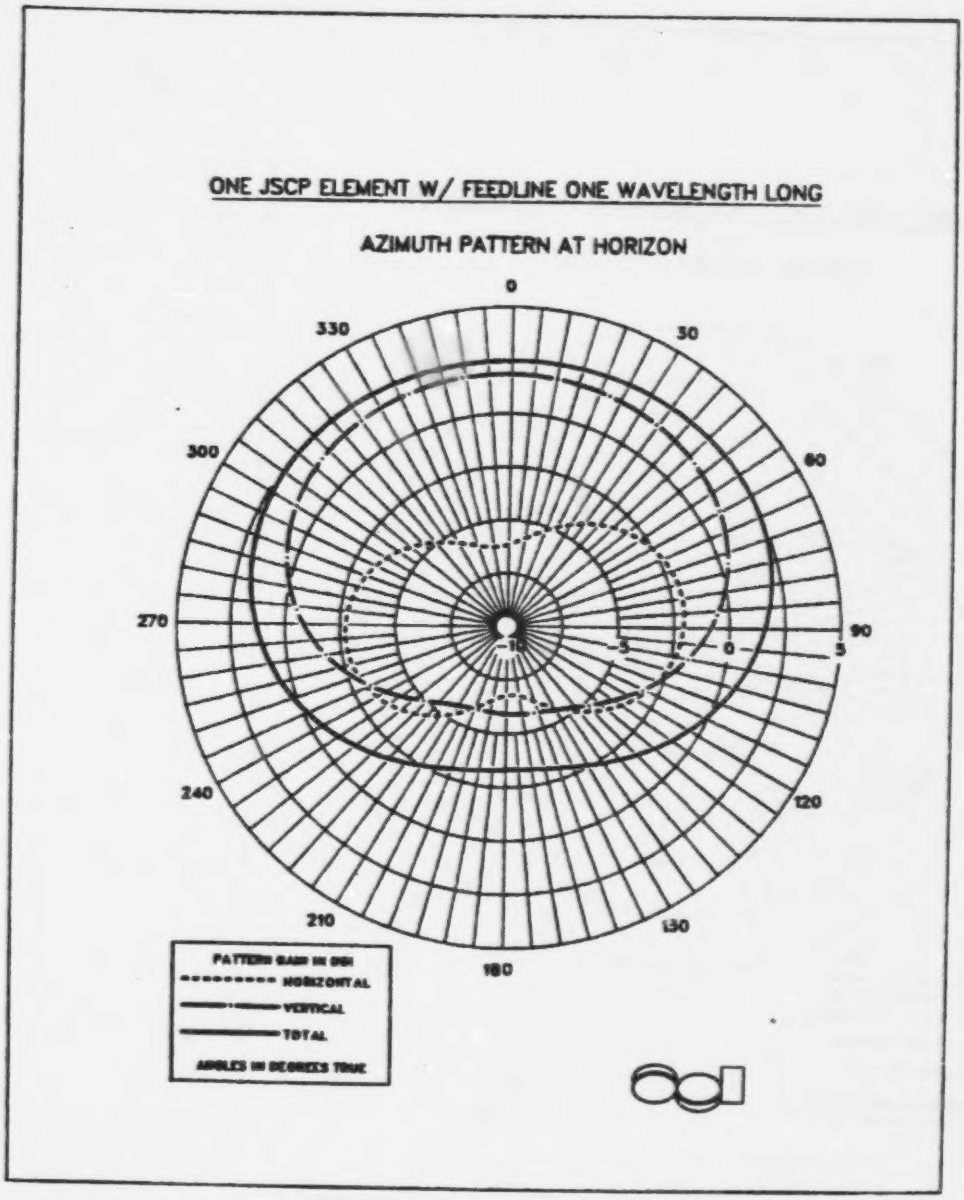
ONE JSCP ELEMENT W/ FEEDLINE ONE WAVELENGTH LONG
AZIMUTH PATTERN AT HORIZON
0
30
60
90
120
150
180
210
240
270
300
330
-10
-5
0
5
PATTERN GAIN IN DBI
HORIZONTAL
VERTICAL
TOTAL
ANGLES IN DEGREES TRUE

FIGURE A 54

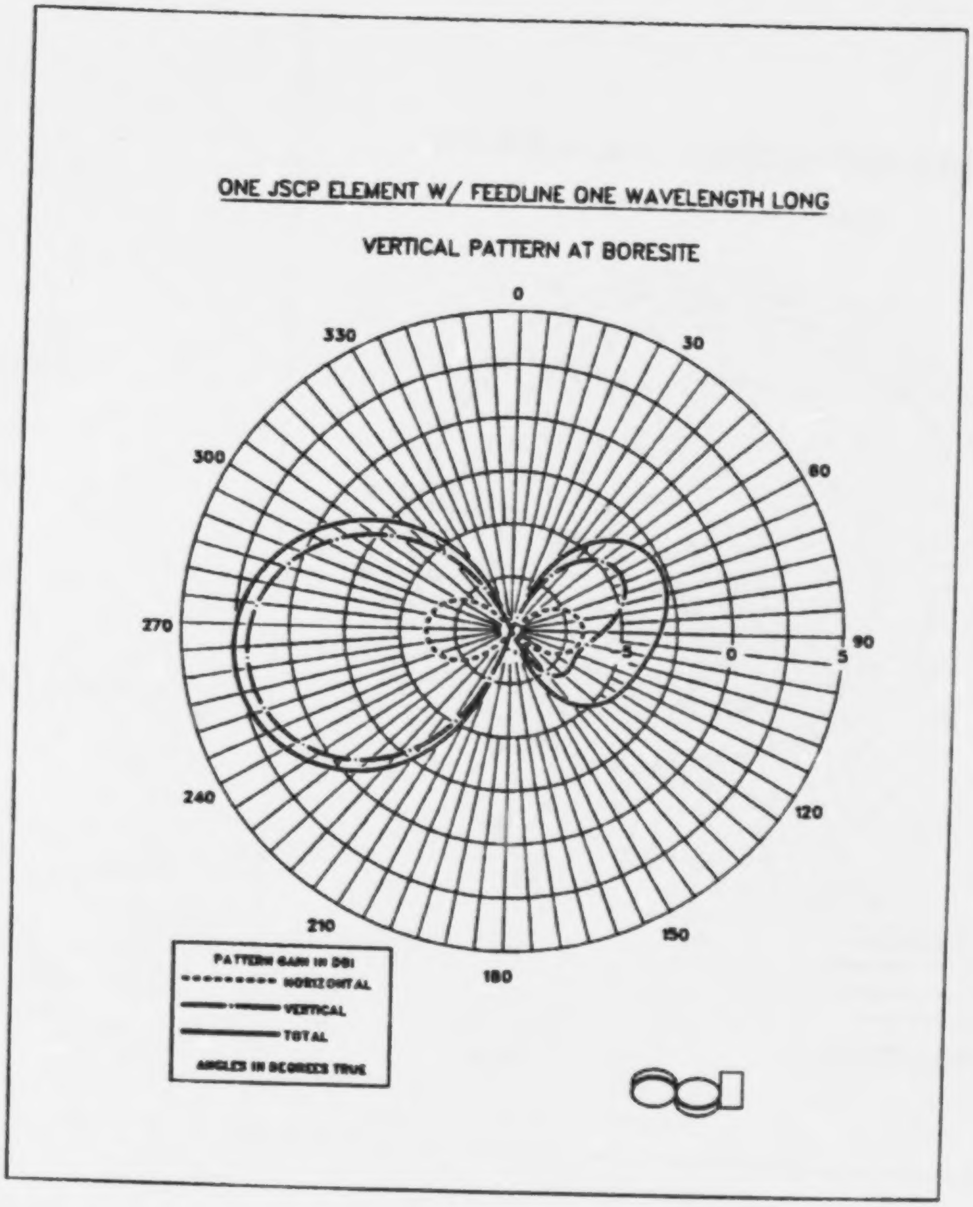

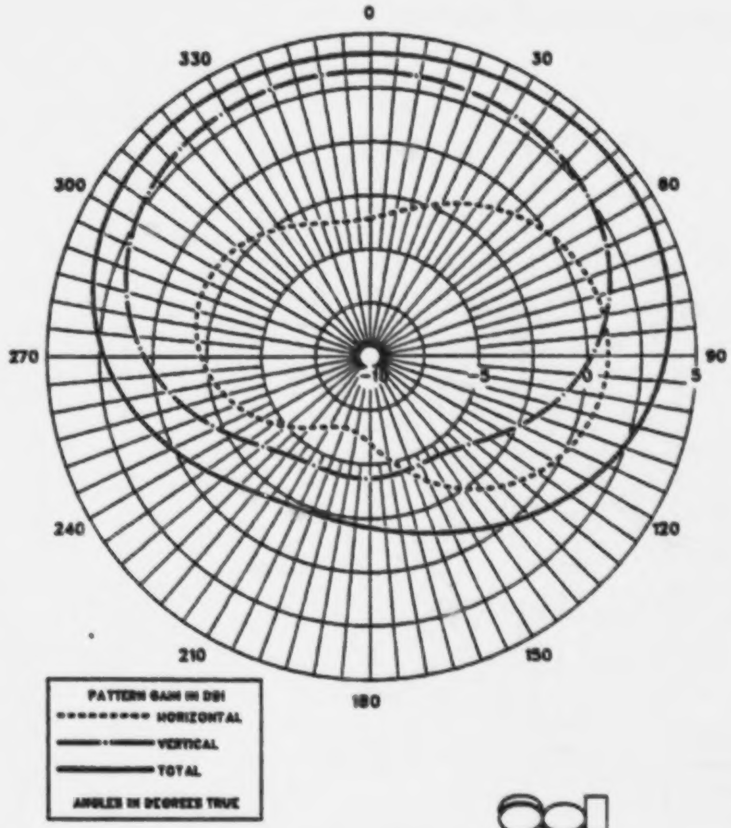

TWO JSCP ELEMENTS W/ FEEDLINE HALF WAVE SPACING

AZIMUTH PATTERN AT HORIZON

FIGURE A 56

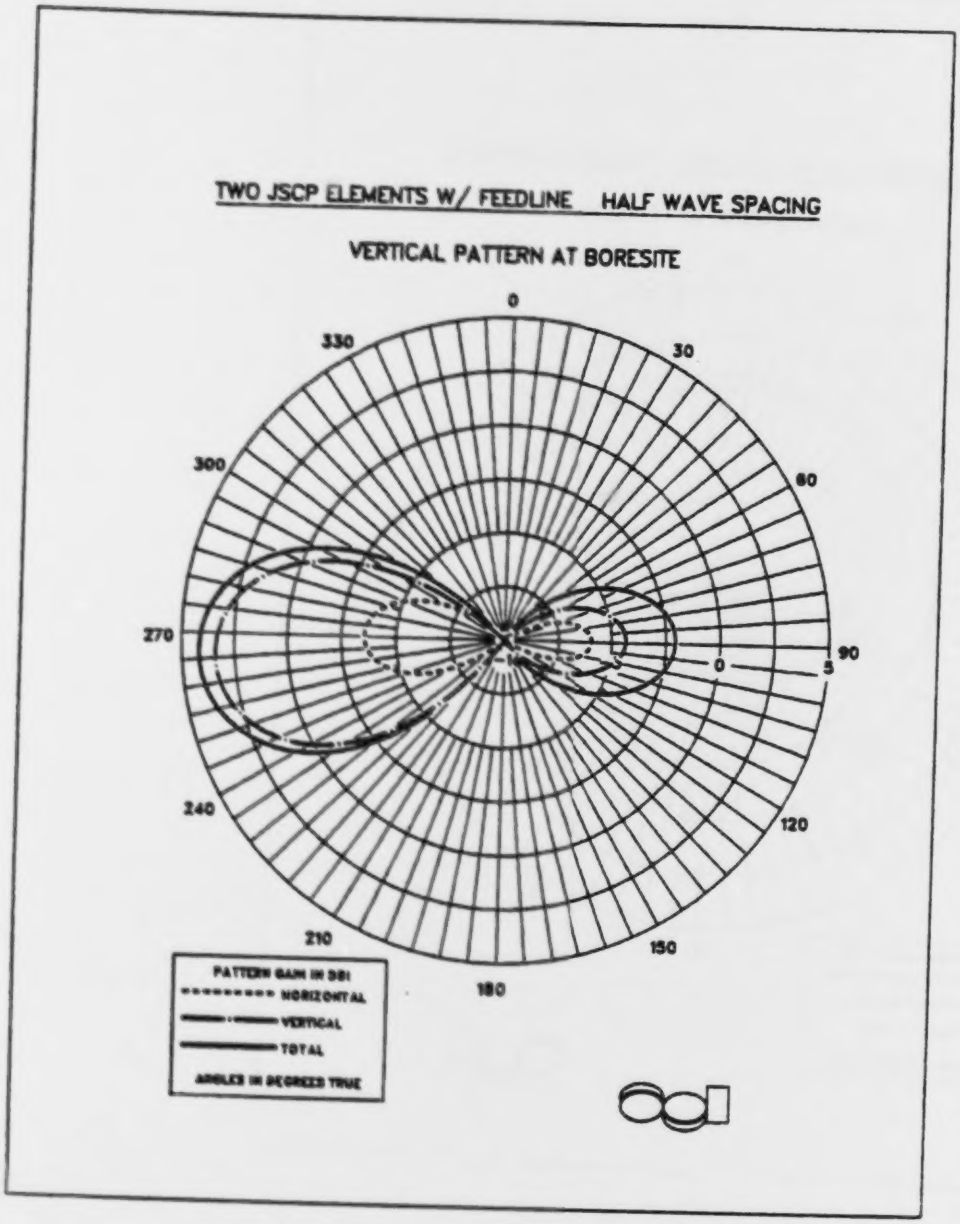

TWO JSCP ELEMENTS W/ FEEDLINE HALF WAVE SPACING

VERTICAL PATTERN AT BORESITE

FIGURE A 57

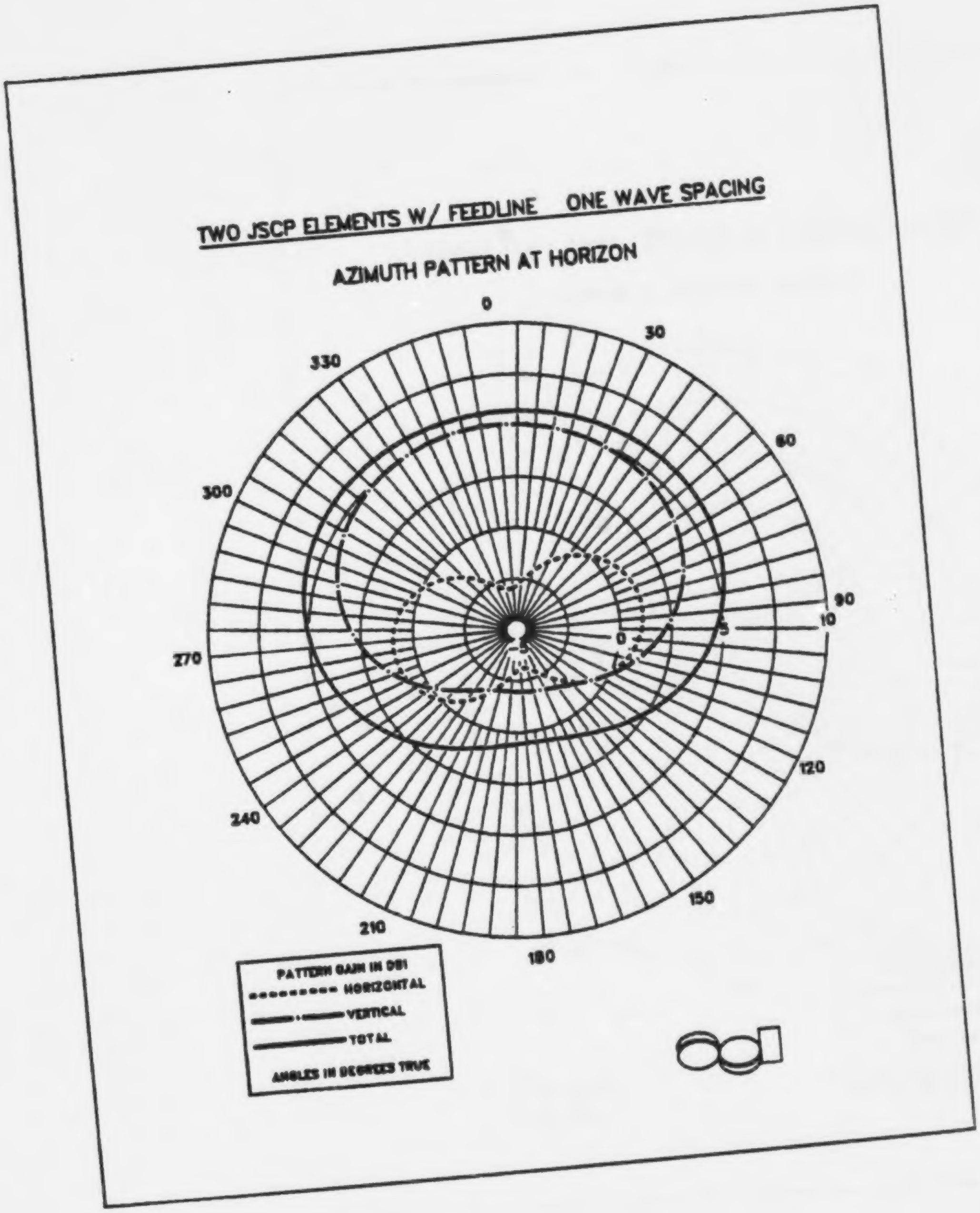
TWO JSCP ELEMENTS W/ FEEDLINE ONE WAVE SPACING

AZIMUTH PATTERN AT HORIZON

FIGURE A 58

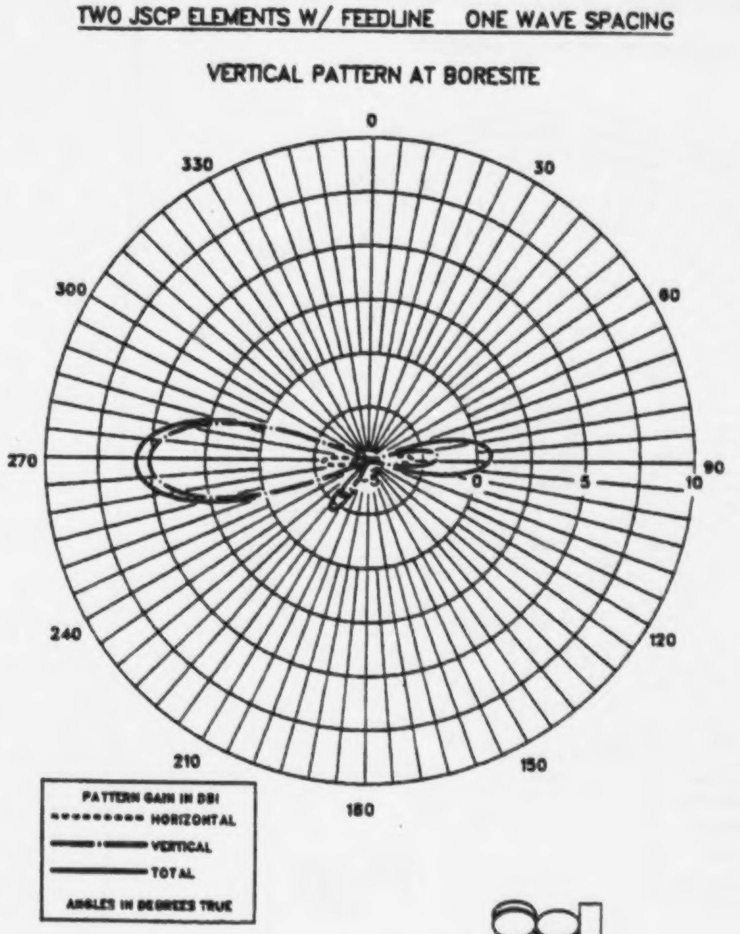

TWO JSCP ELEMENTS W/ FEEDLINE ONE WAVE SPACING

VERTICAL PATTERN AT BORESITE

FIGURE A 59

FOUR JSCP ELEMENTS W/ FEEDLINE HALF WAVE SPACING

AZIMUTH PATTERN AT HORIZON

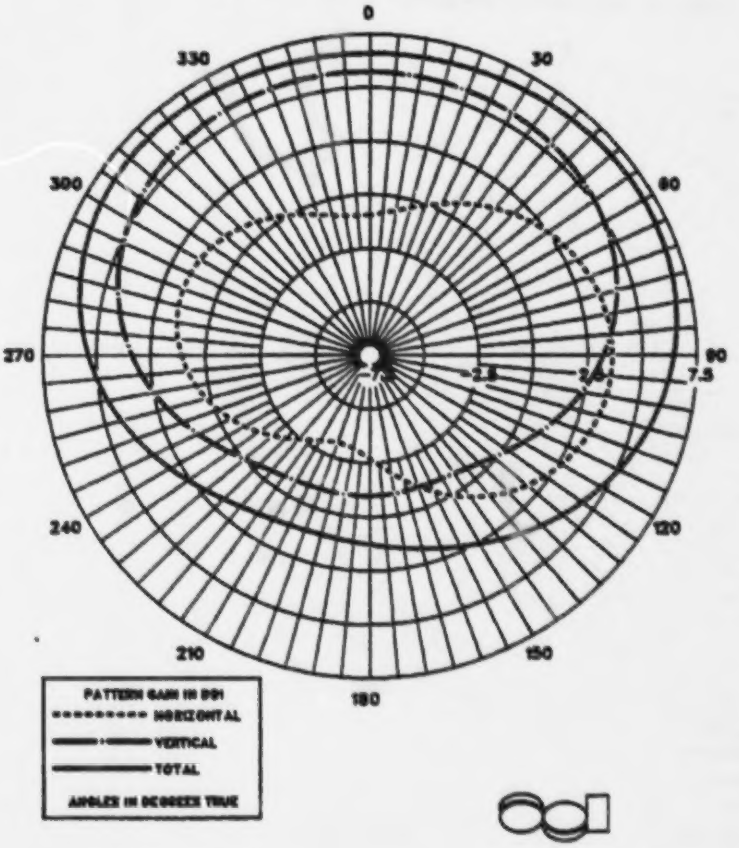

FIGURE A 60

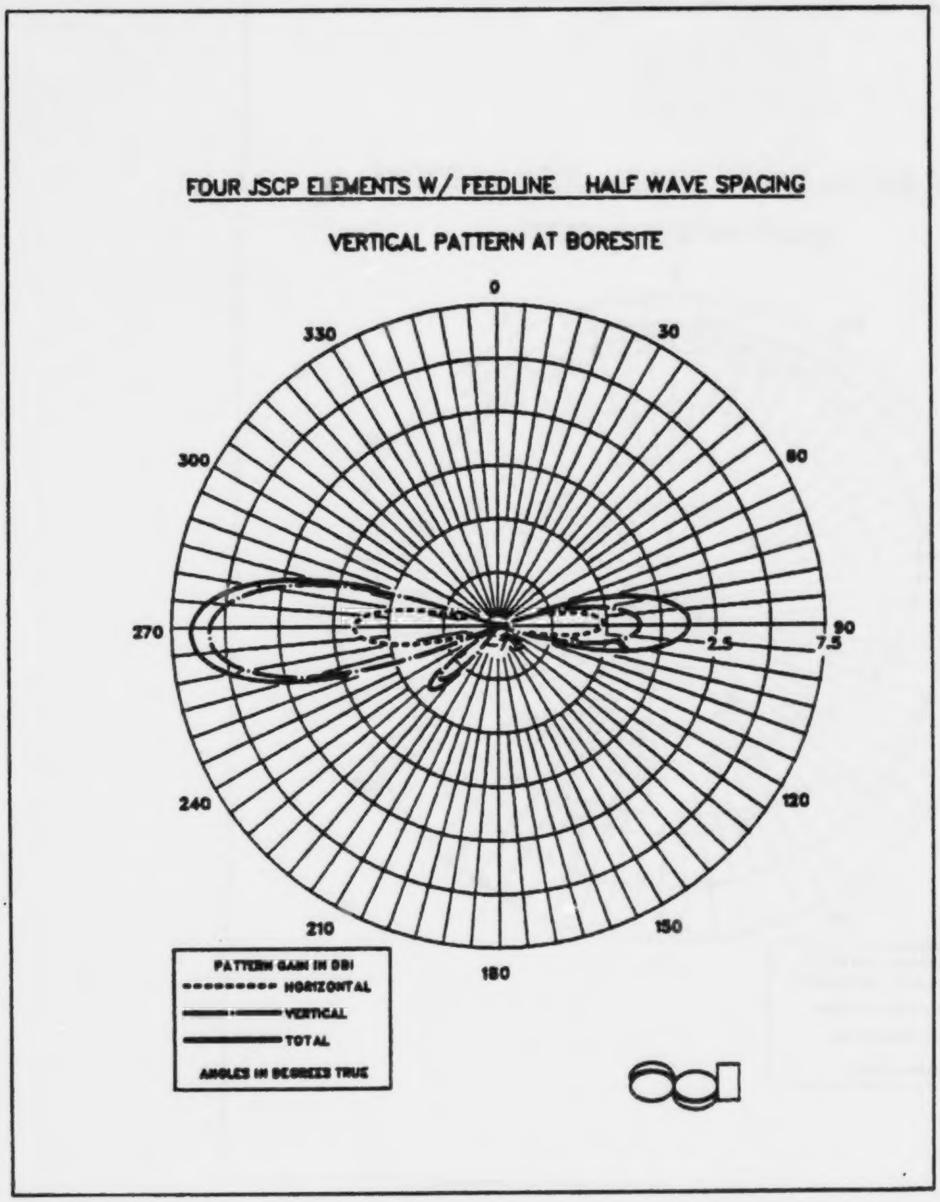
FOUR JSCP ELEMENTS W/ FEEDLINE HALF WAVE SPACING
VERTICAL PATTERN AT BORESITE
0
30
60
90
120
150
180
210
240
270
300
330
2.5
7.5
-7.5
PATTERN GAIN IN DBI
HORIZONTAL
VERTICAL
TOTAL
ANGLES IN DEGREES TRUE

FIGURE A 61

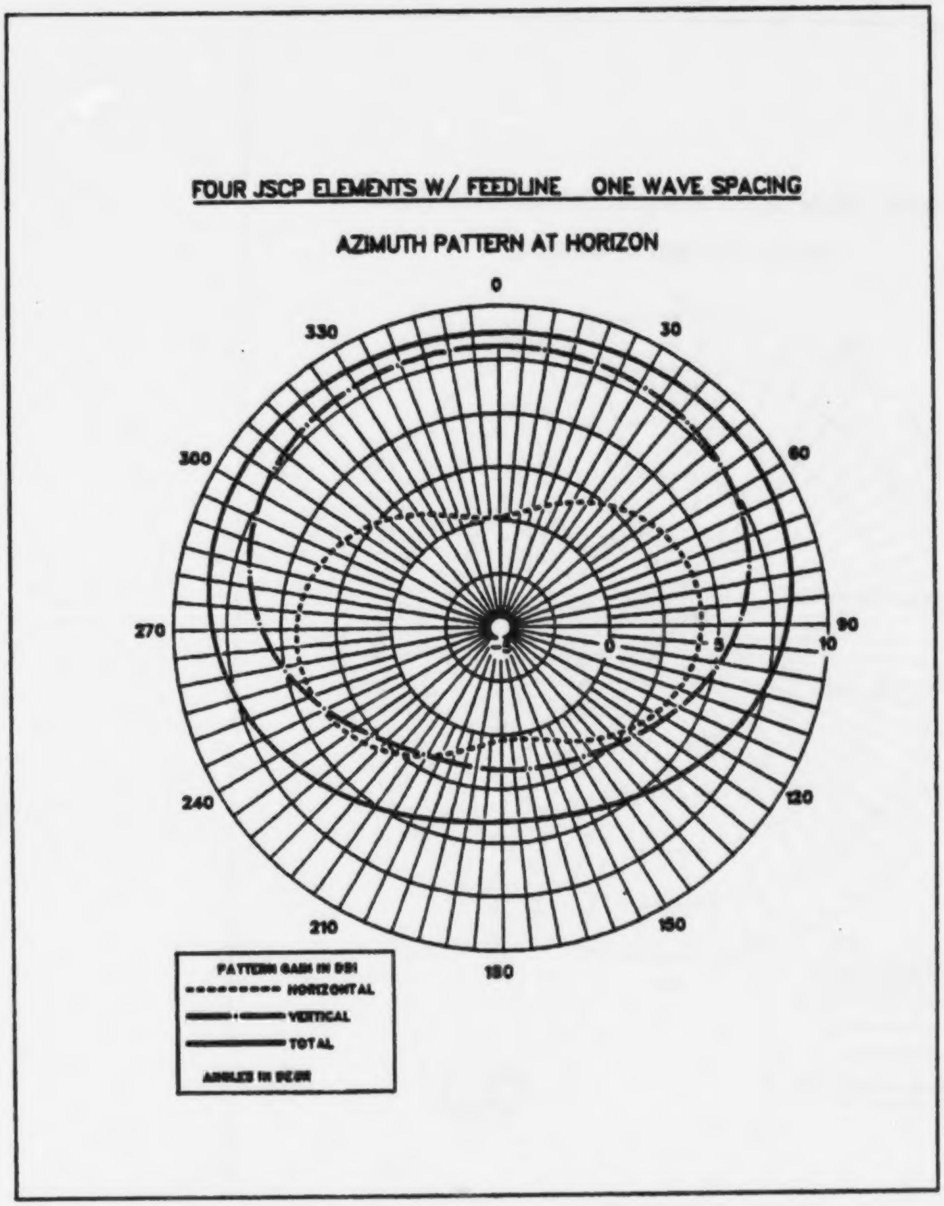

FOUR JSCP ELEMENTS W/ FEEDLINE ONE WAVE SPACING
AZIMUTH PATTERN AT HORIZON
0
30
60
90
120
150
180
210
240
270
300
330
0
5
10
PATTERN GAIN IN DBI
HORIZONTAL
VERTICAL
TOTAL
ANGLES IN DEGR

FIGURE A 62

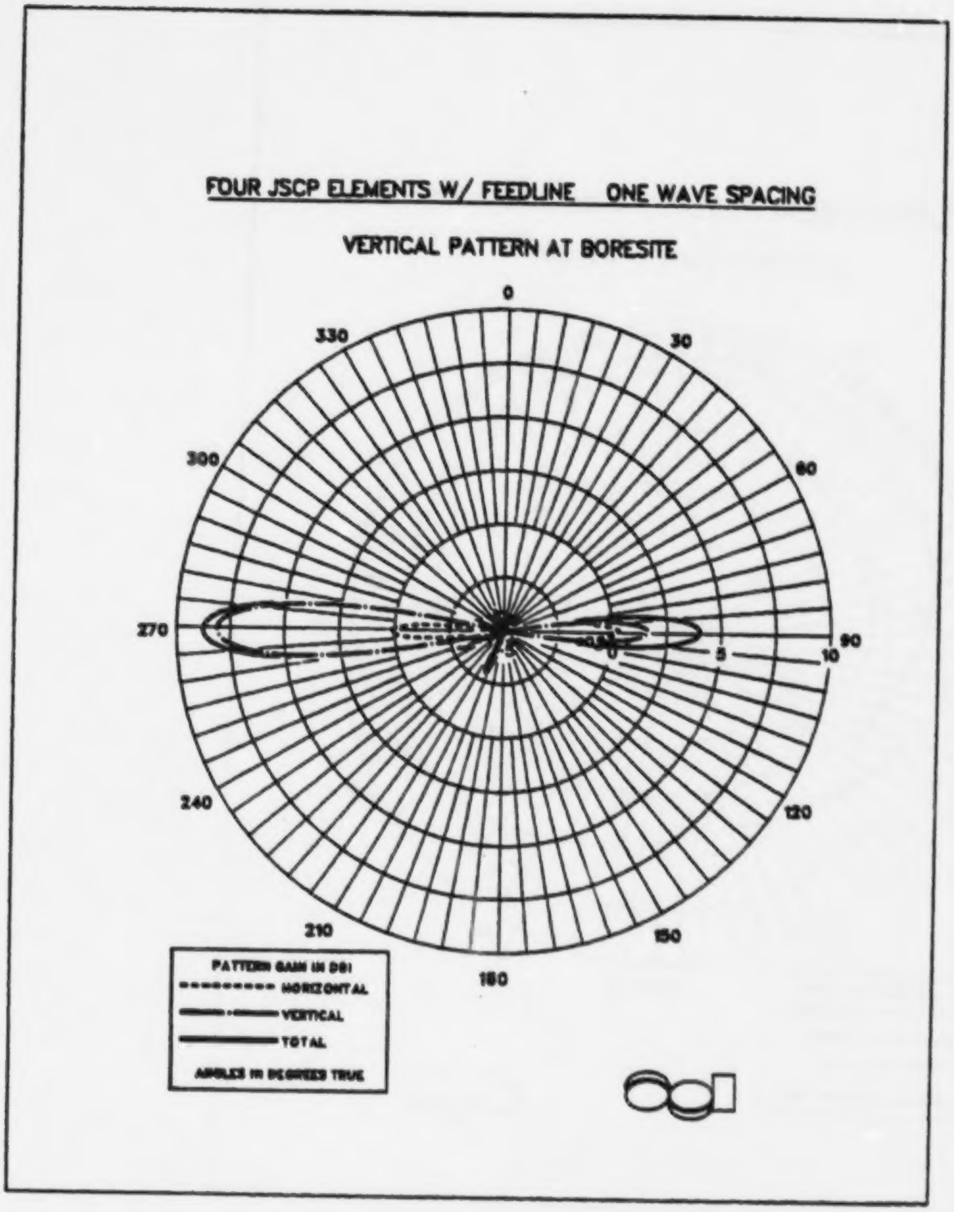
FOUR JSCP ELEMENTS W/ FEEDLINE ONE WAVE SPACING
VERTICAL PATTERN AT BORESITE
0
30
60
90
120
150
180
210
240
270
300
330
0
5
10
PATTERN GAIN IN DBI
HORIZONTAL
VERTICAL
TOTAL
ANGLES IN DEGREES TRUE

FIGURE A 63

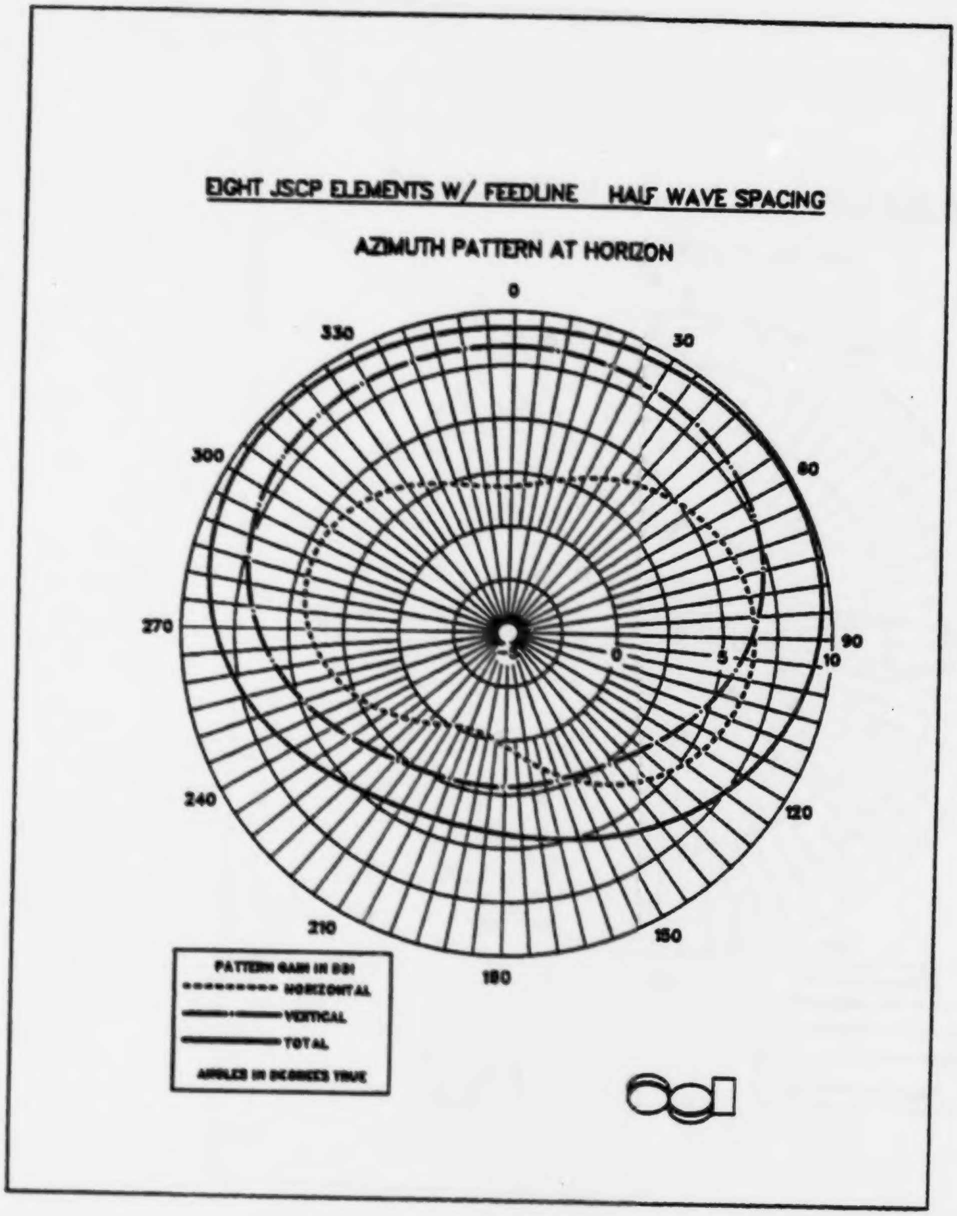
EIGHT JSCP ELEMENTS W/ FEEDLINE HALF WAVE SPACING
AZIMUTH PATTERN AT HORIZON
0
30
60
90
120
150
180
210
240
270
300
330
0
5
10
PATTERN GAIN IN DBI
HORIZONTAL
VERTICAL
TOTAL
ANGLES IN DEGREES TRUE

FIGURE A 64

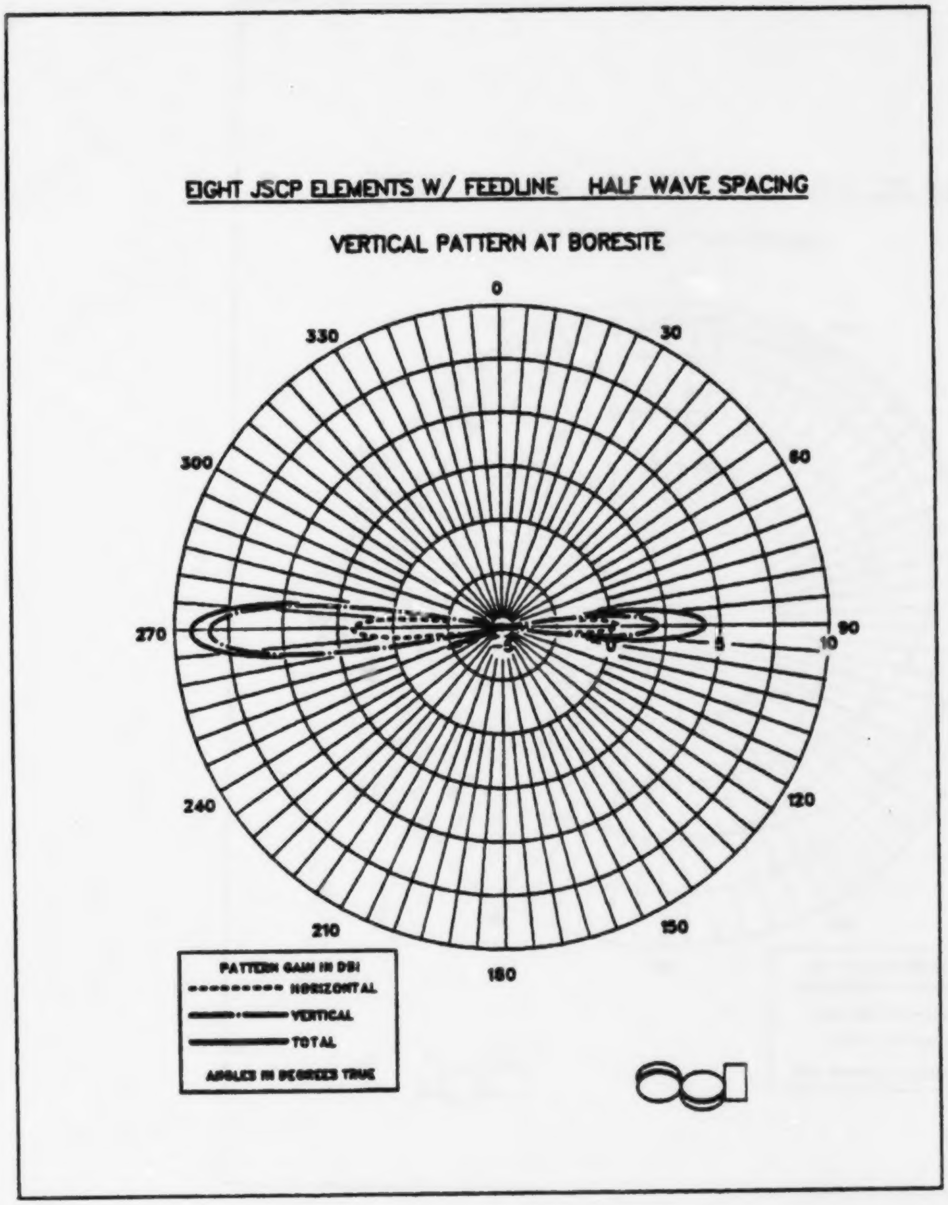
EIGHT JSCP ELEMENTS W/ FEEDLINE HALF WAVE SPACING

VERTICAL PATTERN AT BORESITE

FIGURE A 65

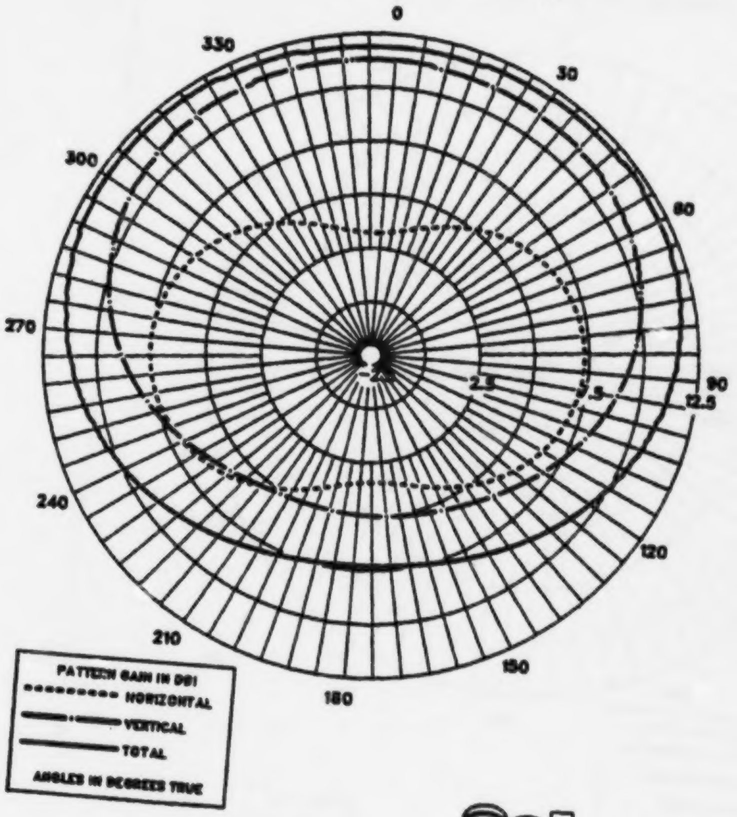

EIGHT JSCP ELEMENTS W/ FEEDLINE ONE WAVE SPACING

AZIMUTH PATTERN AT HORIZON

FIGURE A 66

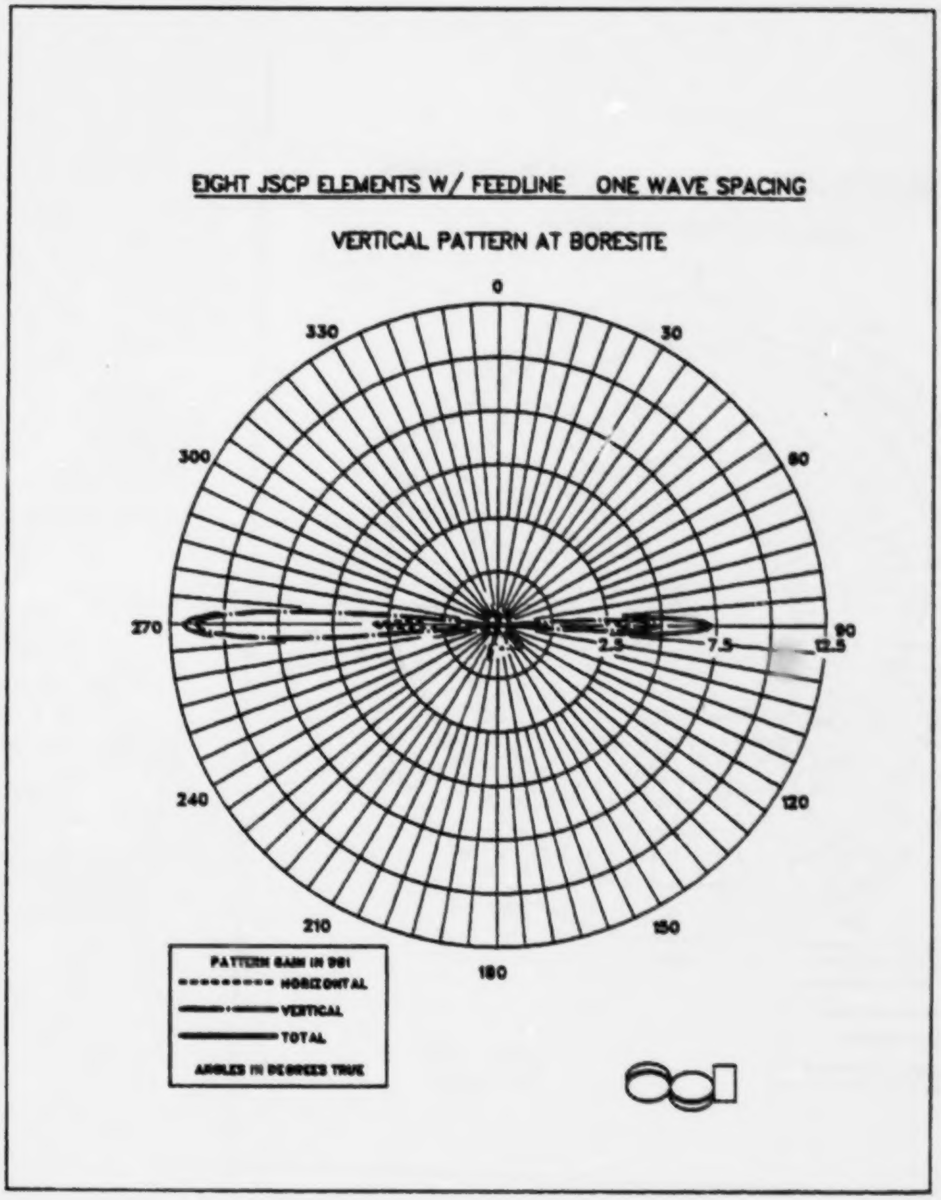
EIGHT JSCP ELEMENTS W/ FEEDLINE ONE WAVE SPACING
VERTICAL PATTERN AT BORESITE
0
30
60
90
120
150
180
210
240
270
300
330
2.5
7.5
12.5
PATTERN GAIN IN DBI
HORIZONTAL
VERTICAL
TOTAL
ANGLES IN DEGREES TRUE

FIGURE A 67

TWELVE JSCP ELEMENTS W/ FEEDLINE HALF WAVE SPACING

AZIMUTH PATTERN AT HORIZON

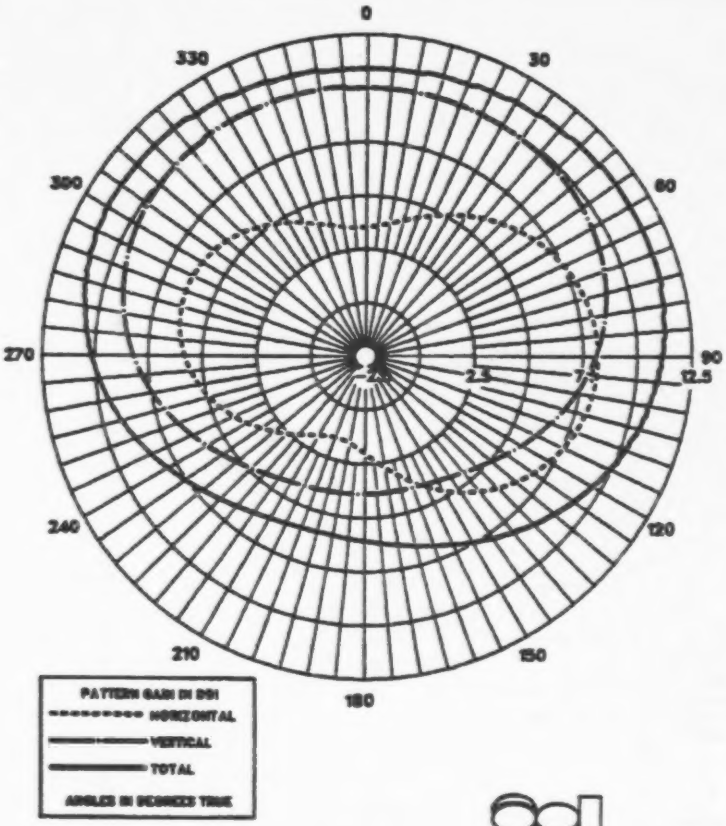

FIGURE A 68

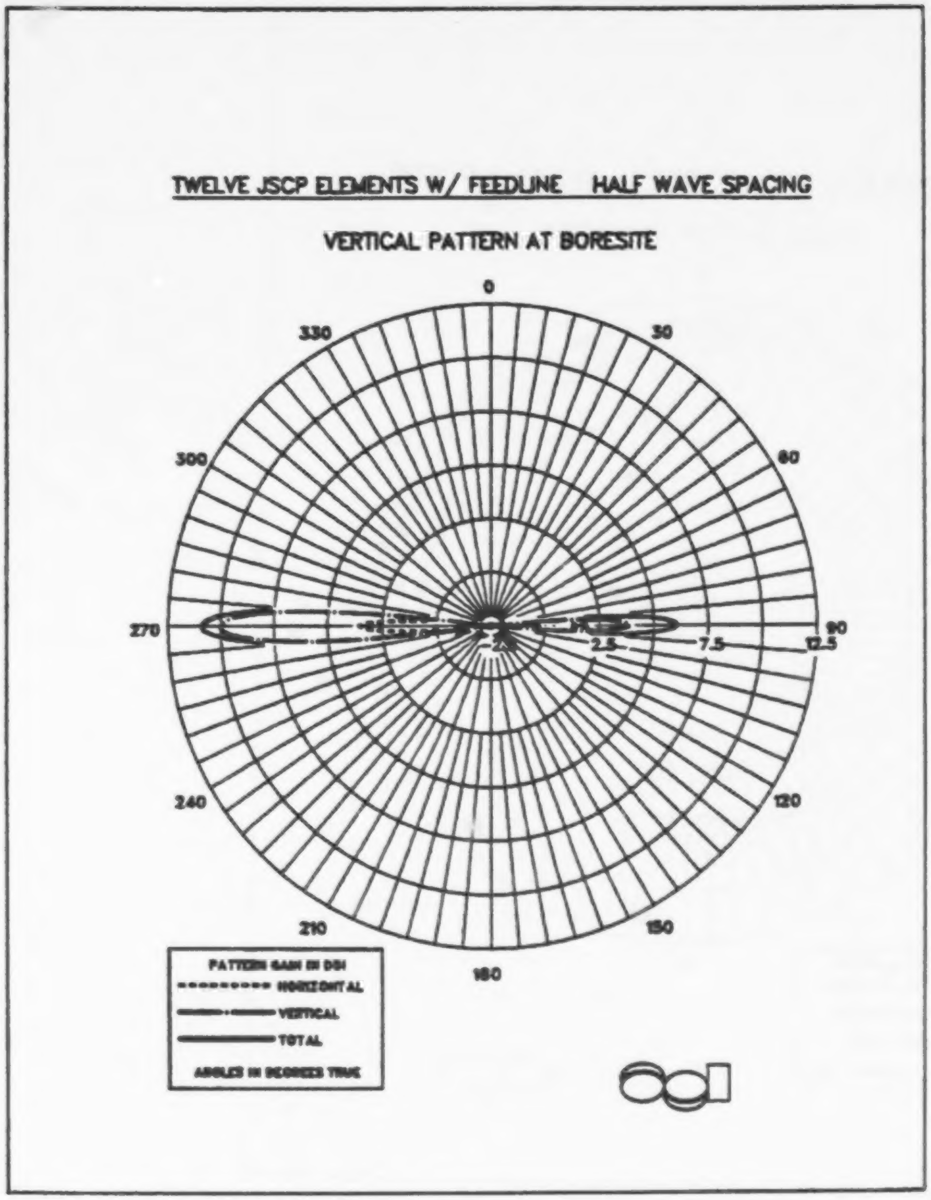
TWELVE JSCP ELEMENTS W/ FEEDLINE HALF WAVE SPACING
VERTICAL PATTERN AT BORESITE
0
30
60
90
120
150
180
210
240
270
300
330
2.5
7.5
12.5
PATTERN GAIN IN DBI
HORIZONTAL
VERTICAL
TOTAL
ANGLES IN DEGREES TRUE

FIGURE A 69

TWELVE JSCP ELEMENTS W/ FEEDLINE   ONE WAVE SPACING

AZIMUTH PATTERN AT HORIZON

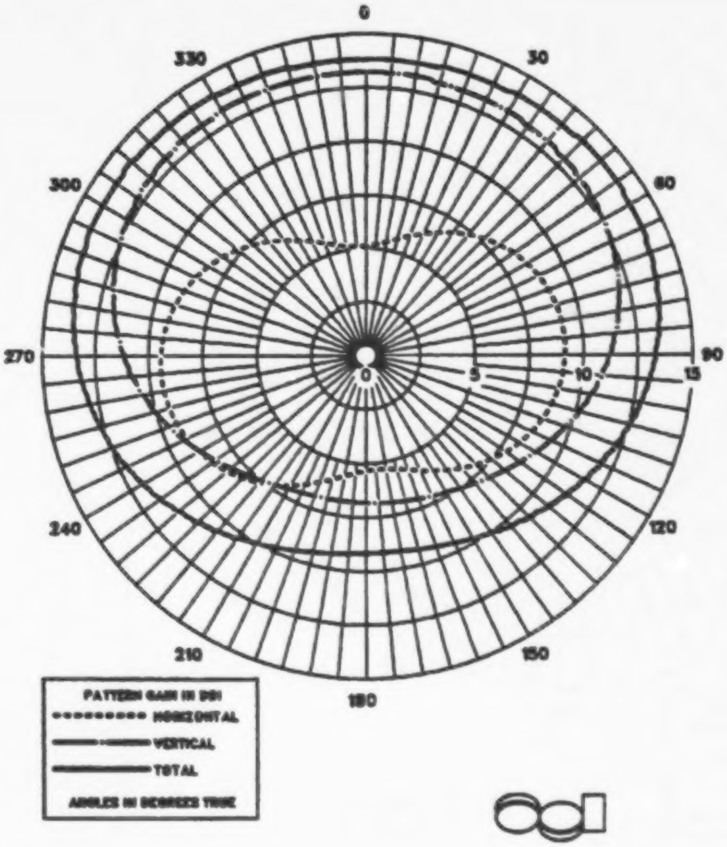

FIGURE A 70

TWELVE JSCP ELEMENTS W/ FEEDLINE ONE WAVE SPACING

VERTICAL PATTERN AT BORESITE

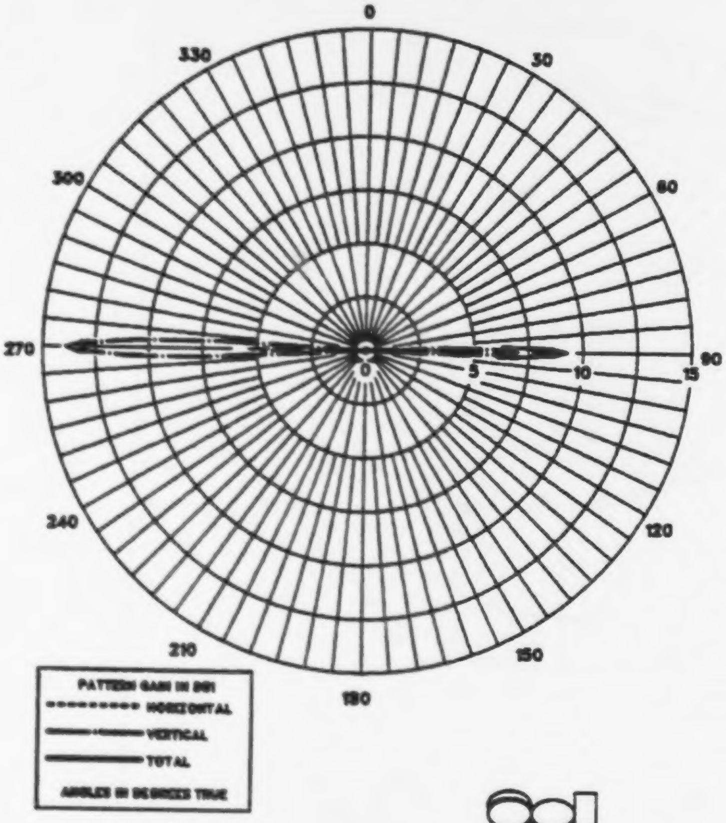

FIGURE A 71

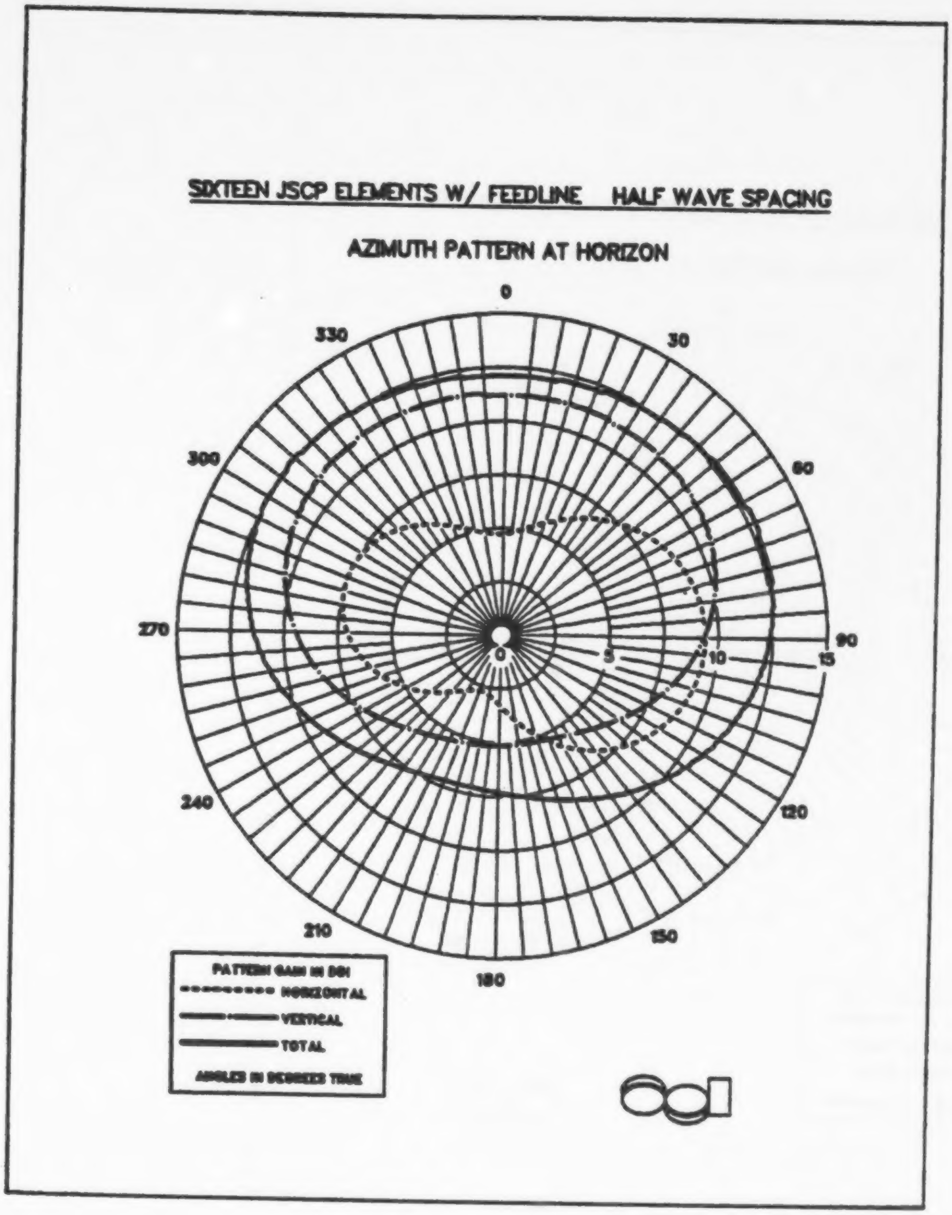
SIXTEEN JSCP ELEMENTS W/ FEEDLINE HALF WAVE SPACING
AZIMUTH PATTERN AT HORIZON
0
30
60
90
120
150
180
210
240
270
300
330
0
5
10
15
PATTERN GAIN IN DBI
HORIZONTAL
VERTICAL
TOTAL
ANGLES IN DEGREES TRUE

FIGURE A 72

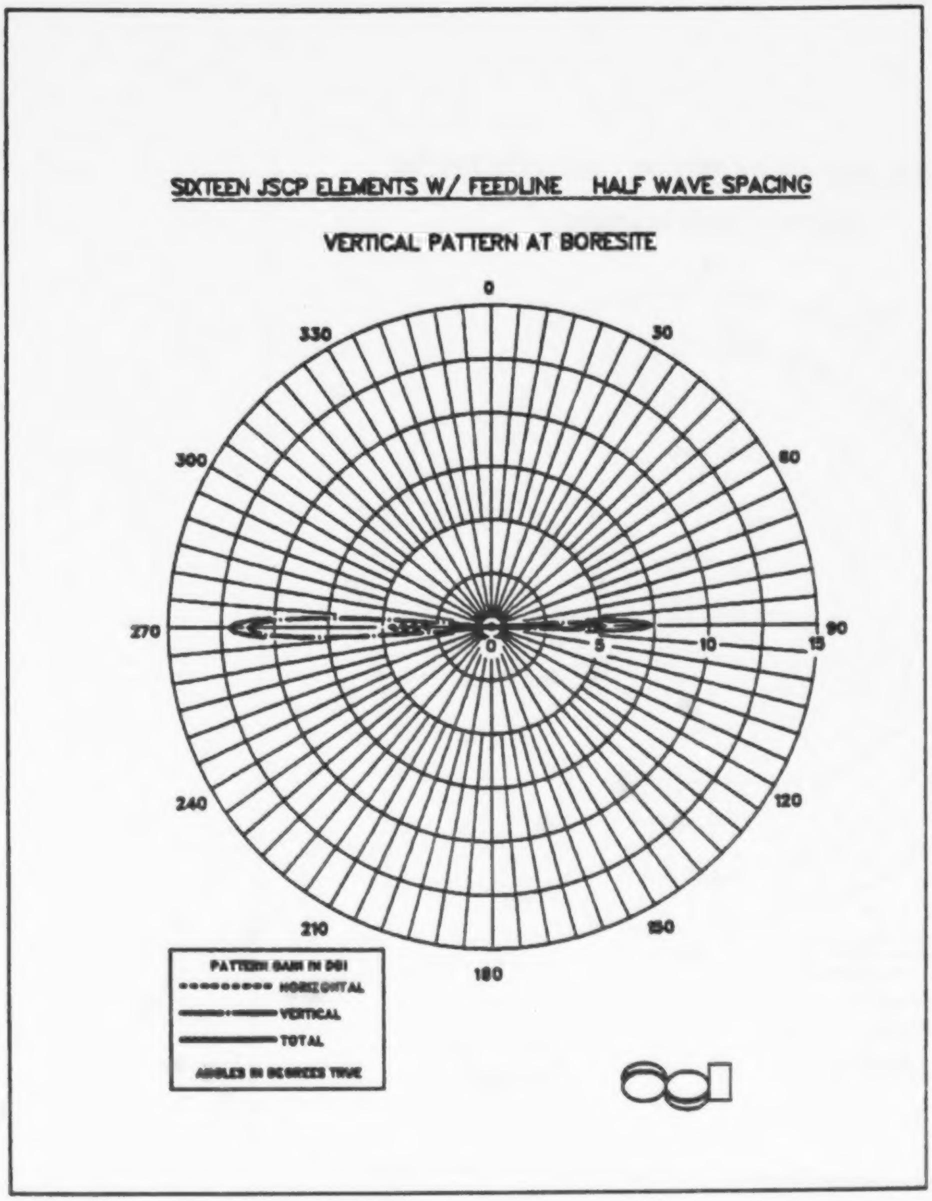

SIXTEEN JSCP ELEMENTS W/ FEEDLINE HALF WAVE SPACING

VERTICAL PATTERN AT BORESITE

FIGURE A 73

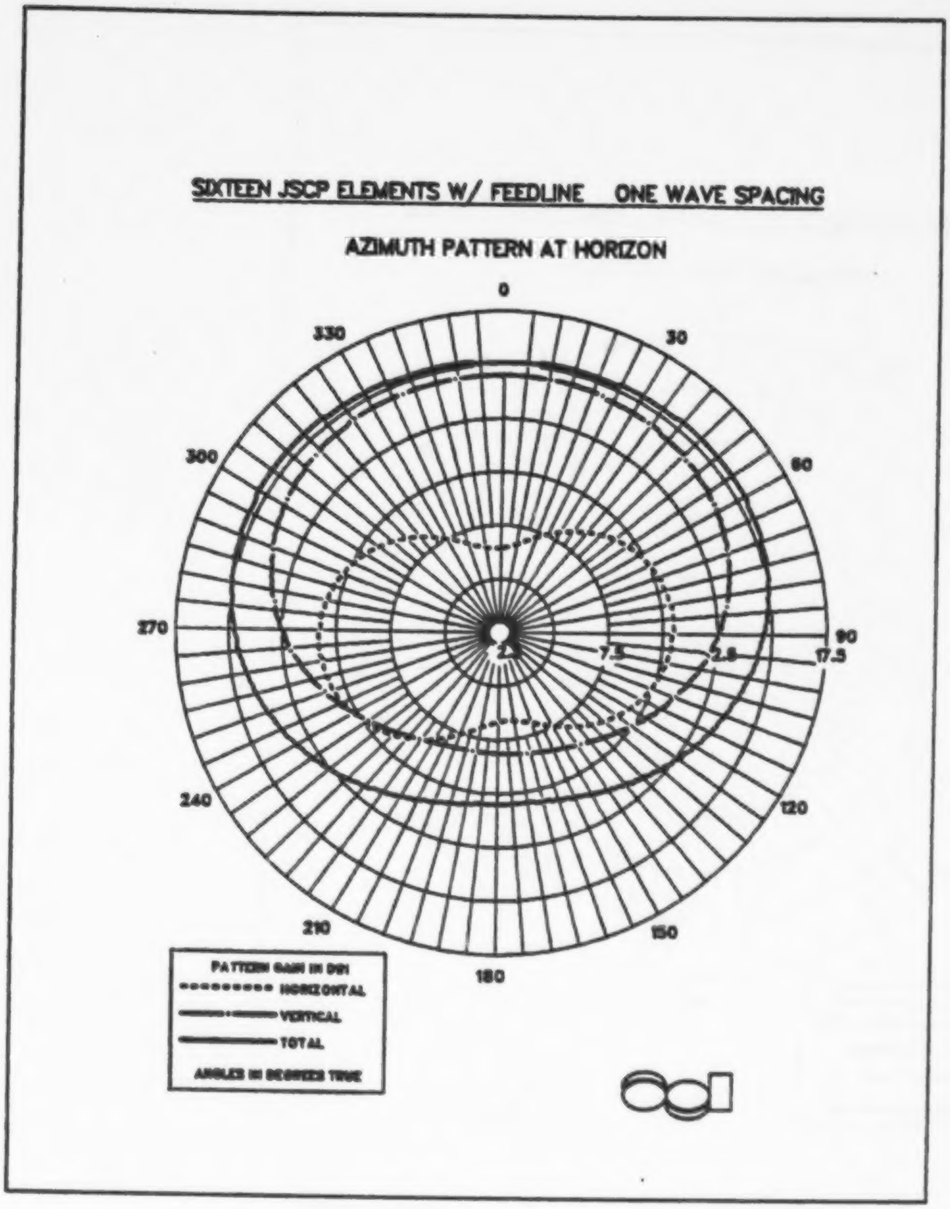
SIXTEEN JSCP ELEMENTS W/ FEEDLINE ONE WAVE SPACING
AZIMUTH PATTERN AT HORIZON
0
30
60
90
120
150
180
210
240
270
300
330
2.5
7.5
12.5
17.5
PATTERN GAIN IN DBI
HORIZONTAL
VERTICAL
TOTAL
ANGLES IN DEGREES TRUE

FIGURE A 74

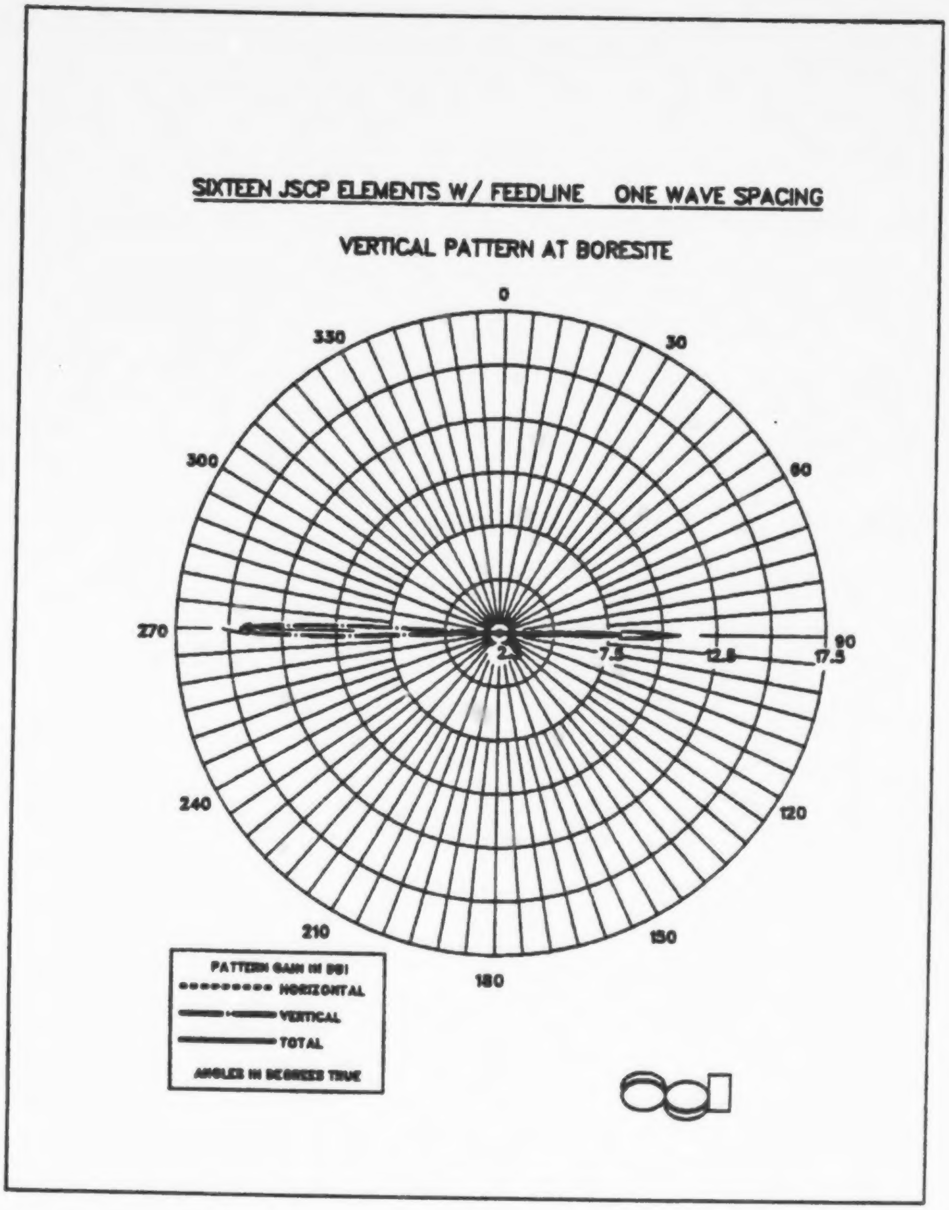
SIXTEEN JSCP ELEMENTS W/ FEEDLINE ONE WAVE SPACING
VERTICAL PATTERN AT BORESITE
0
30
60
90
120
150
180
210
240
270
300
330
2.5
7.5
12.5
17.5
PATTERN GAIN IN DBI
HORIZONTAL
VERTICAL
TOTAL
ANGLES IN DEGREES TRUE

FIGURE A 75

APPENDIX B

FM ARRAY BAY SPACING STUDY
RADIATION PATTERNS

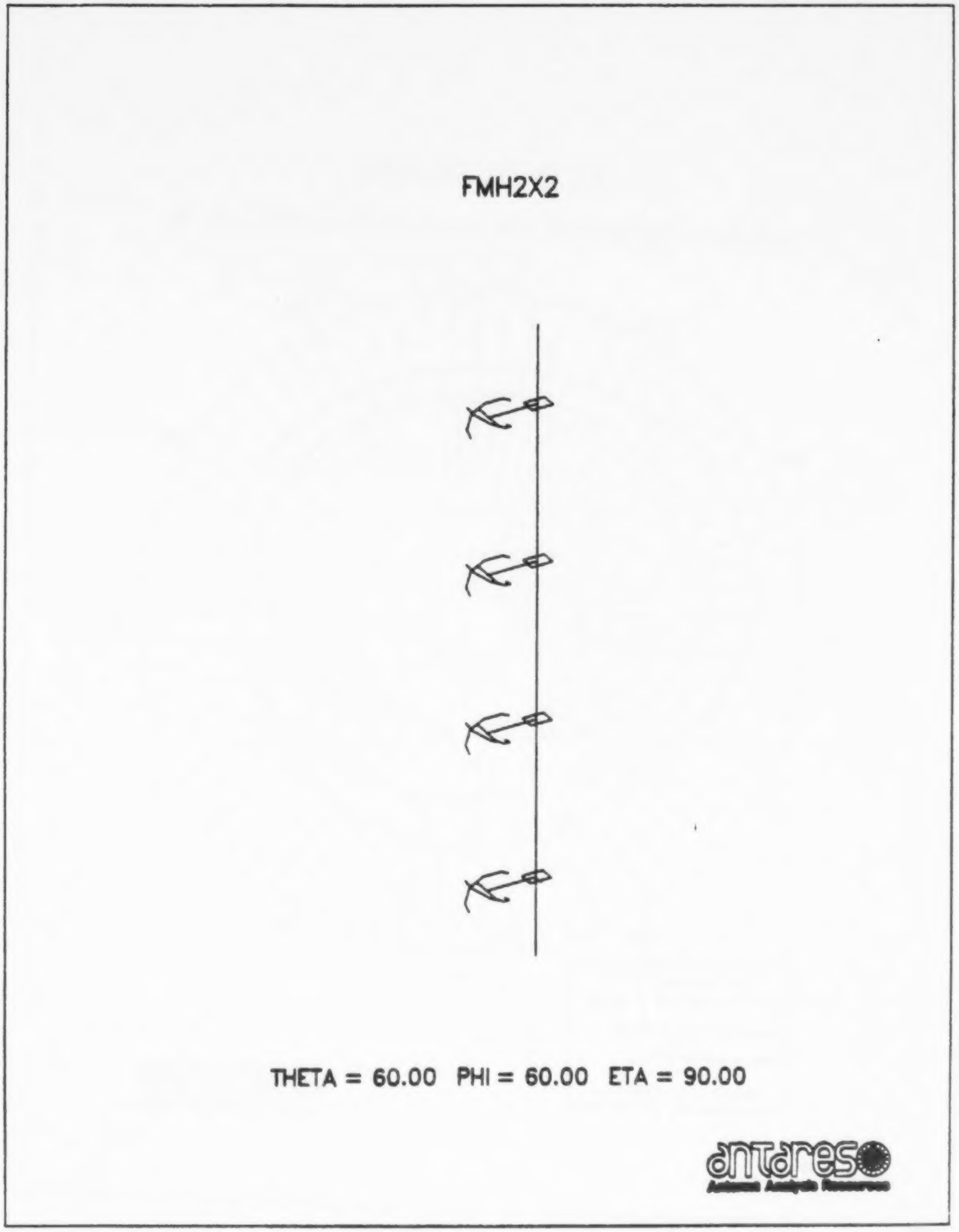
FMH2X2
THETA = 60.00 PHI = 60.00 ETA = 90.00
antares
Antenna Analysis Resources

FIGURE B 1

THE ERI FMH 2X2 ARRAY

STANDARD SPACING OF ONE WAVELENGTH BETWEEN BAYS

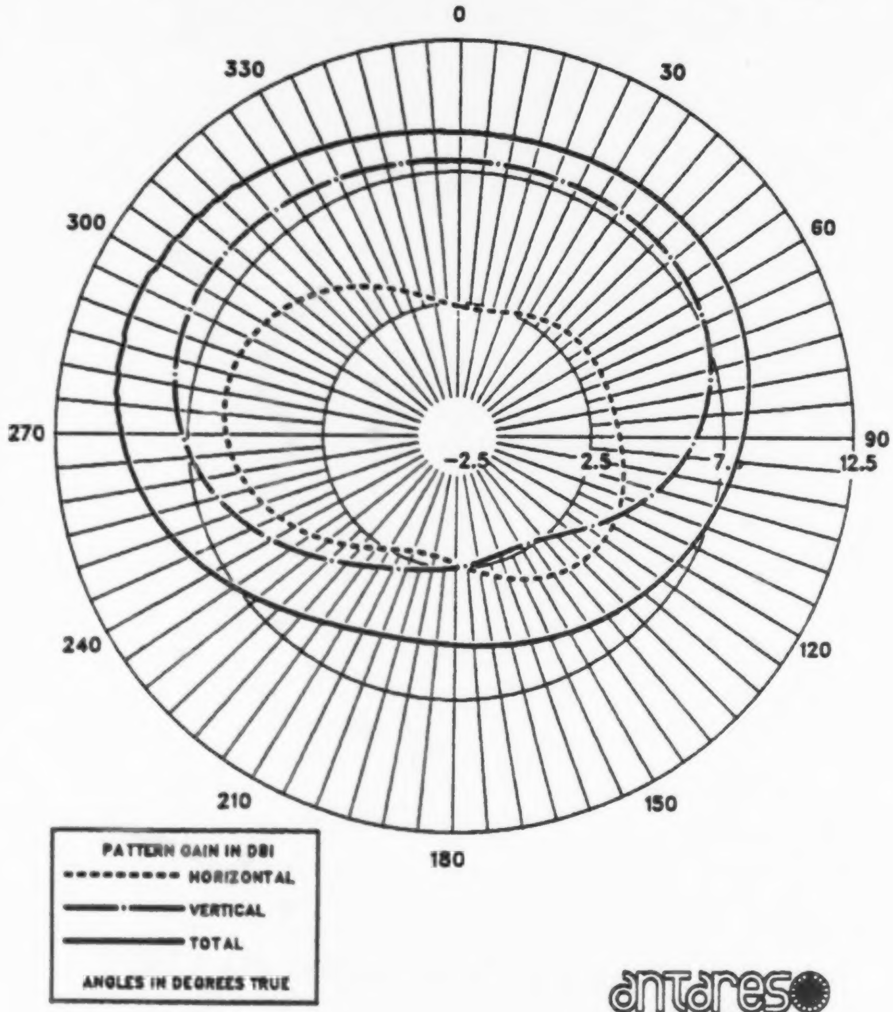

antares
Antenna Analysis Resources

FIGURE B 2

THE ERI FMH 2X2 ARRAY

STANDARD SPACING OF ONE WAVELENGTH BETWEEN BAYS

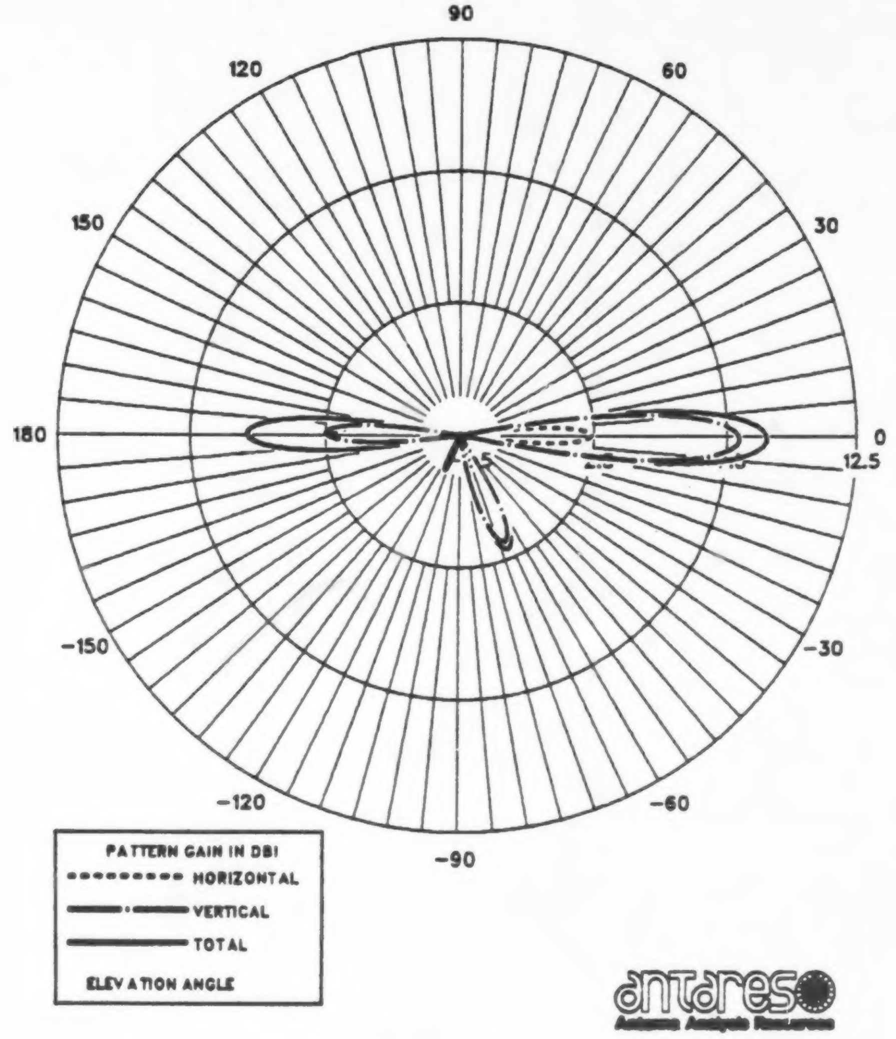

FIGURE B 3

THE ERI FMH 2X2 ARRAY

STANDARD SPACING OF ONE WAVELENGTH BETWEEN BAYS

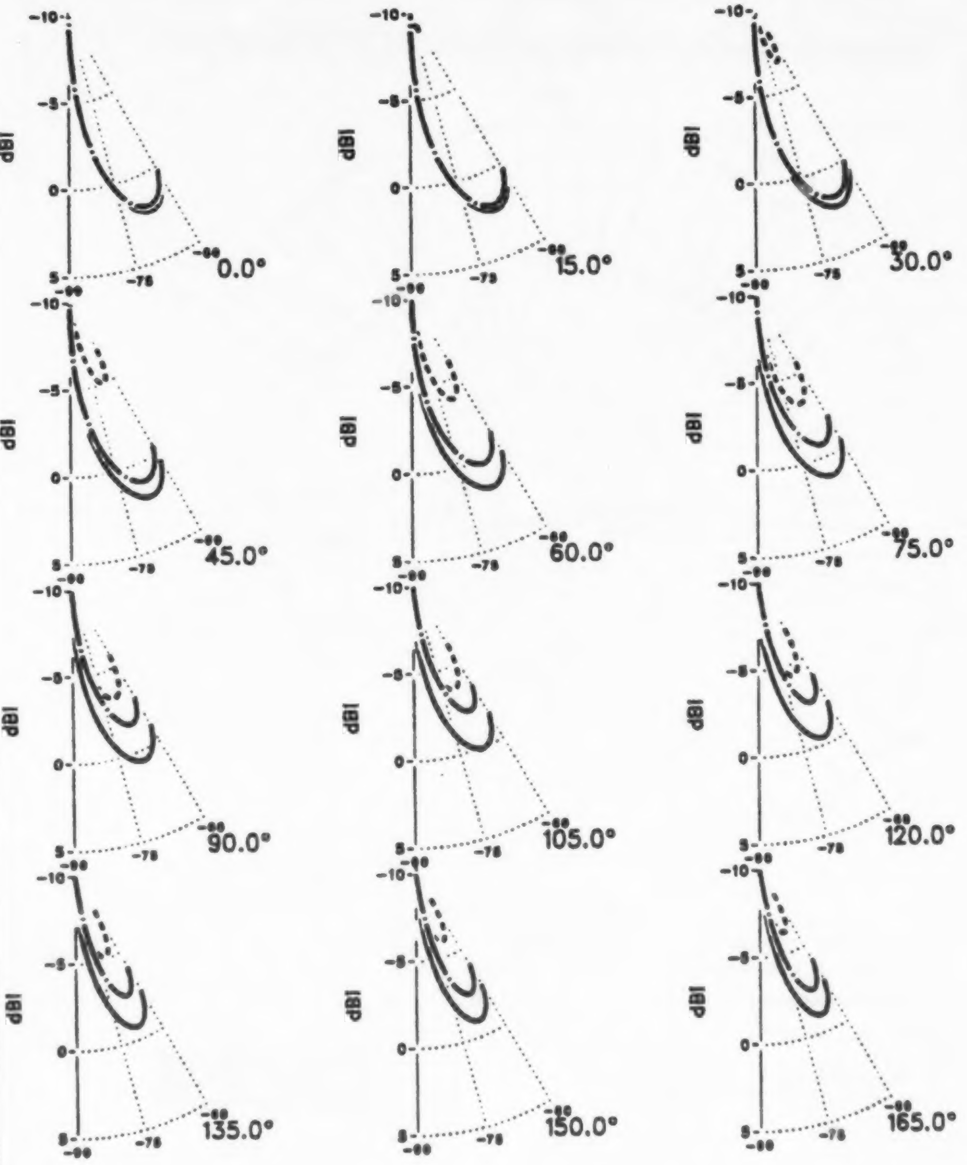

FIGURE B 4

THE ERI FMH 2X2 ARRAY

STANDARD SPACING OF ONE WAVELENGTH BETWEEN BAYS

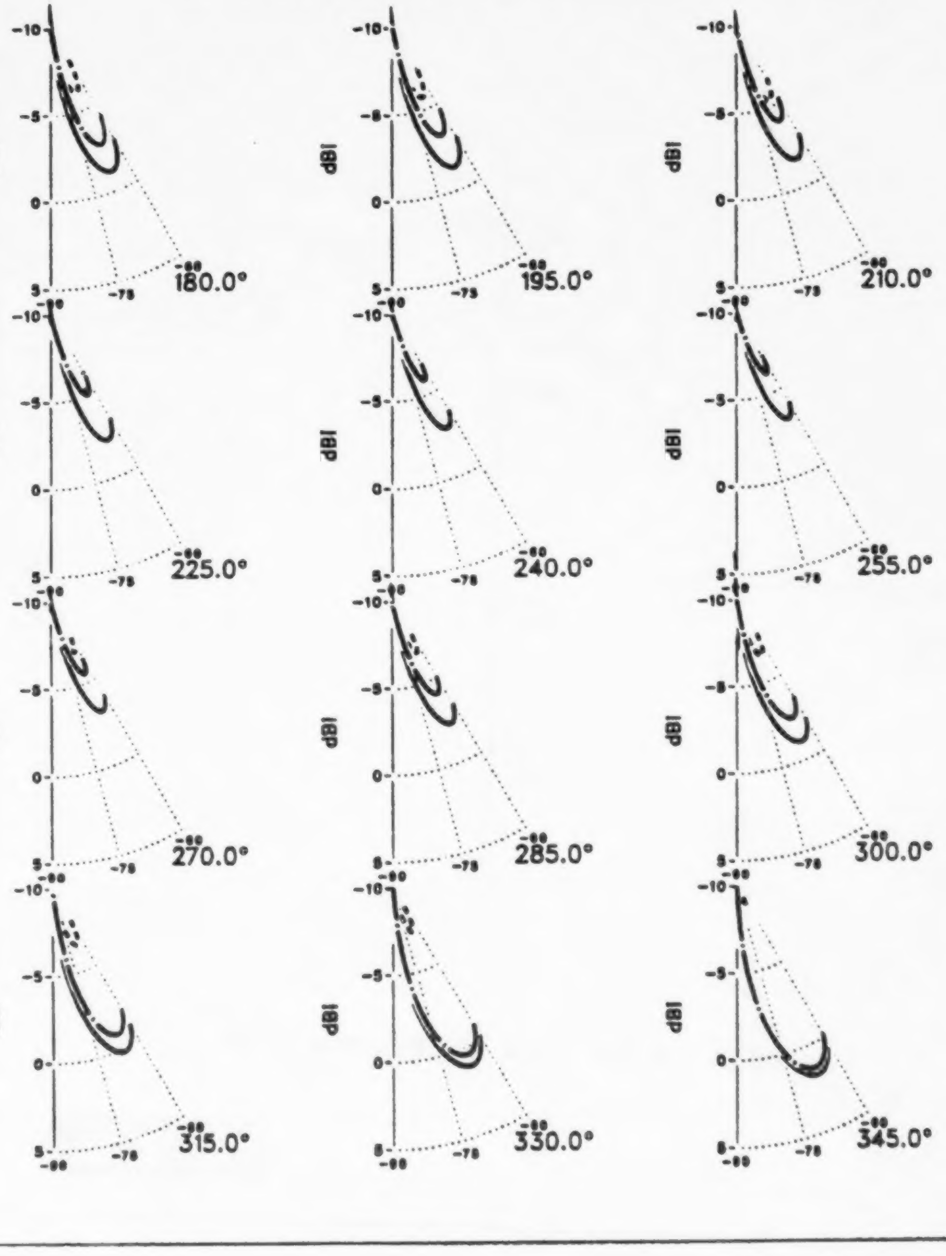

FIGURE B 5

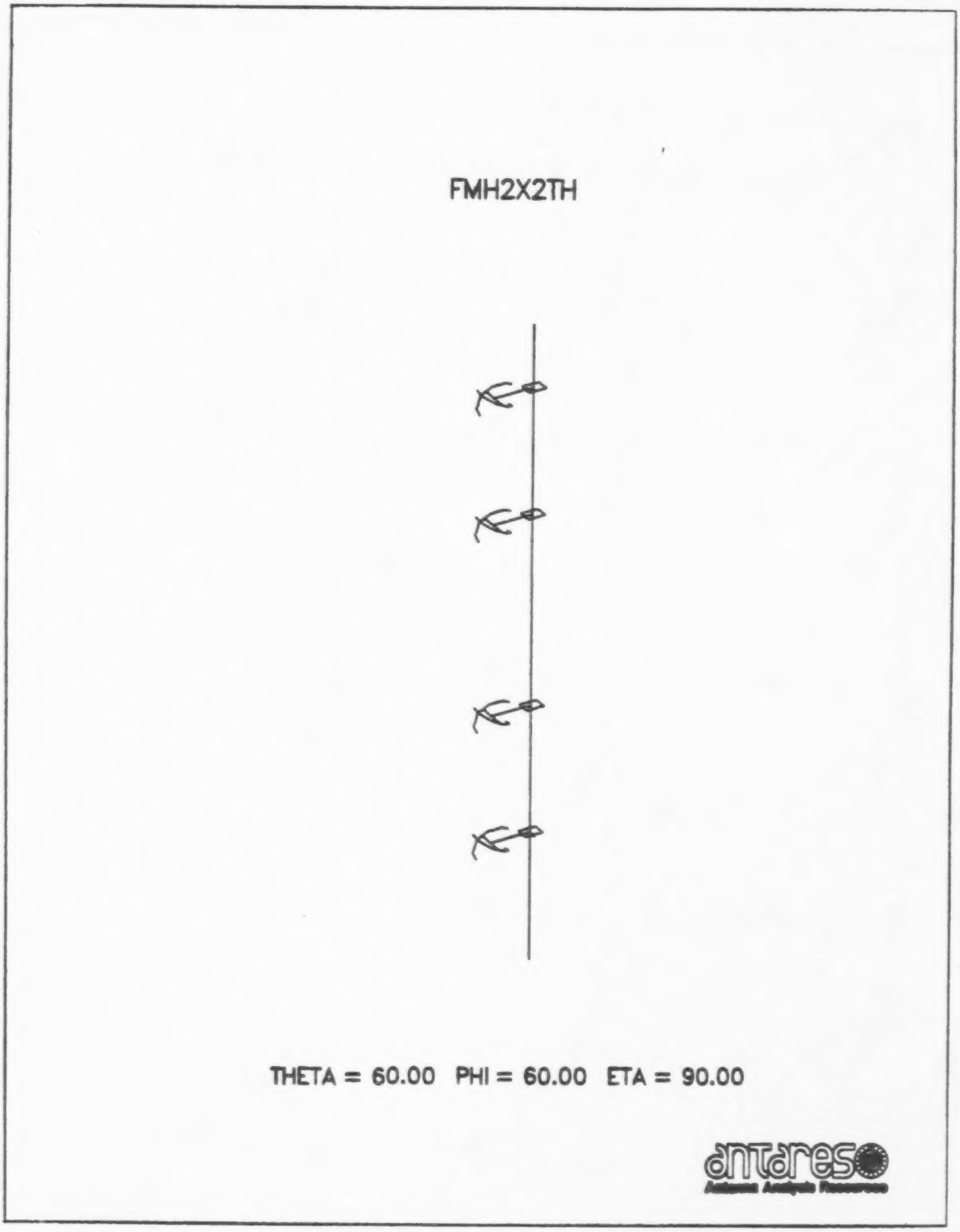
FMH2X2TH
THETA = 60.00 PHI = 60.00 ETA = 90.00
antares
Antenna Analysis Resources

FIGURE B 6

THE FMH2X2 ARRAY

3/2 WAVELENGTH SPACING BETWEEN BAYS

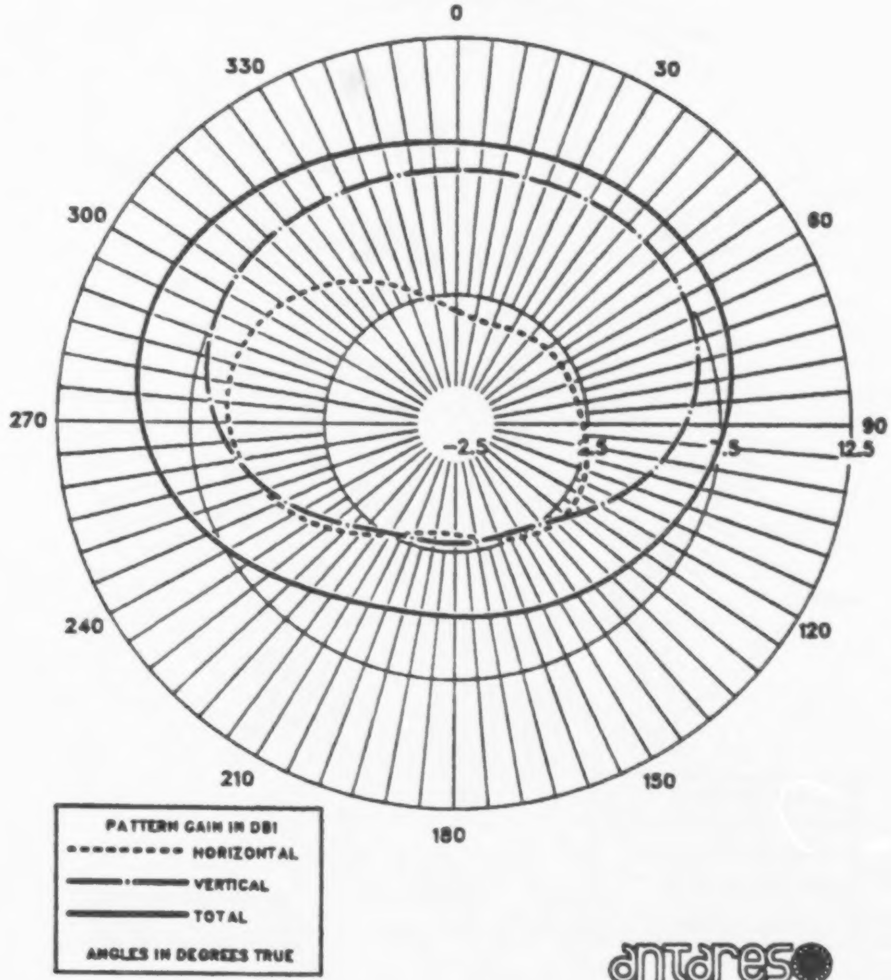

antares
Antenna Analysis Resources

FIGURE B 7

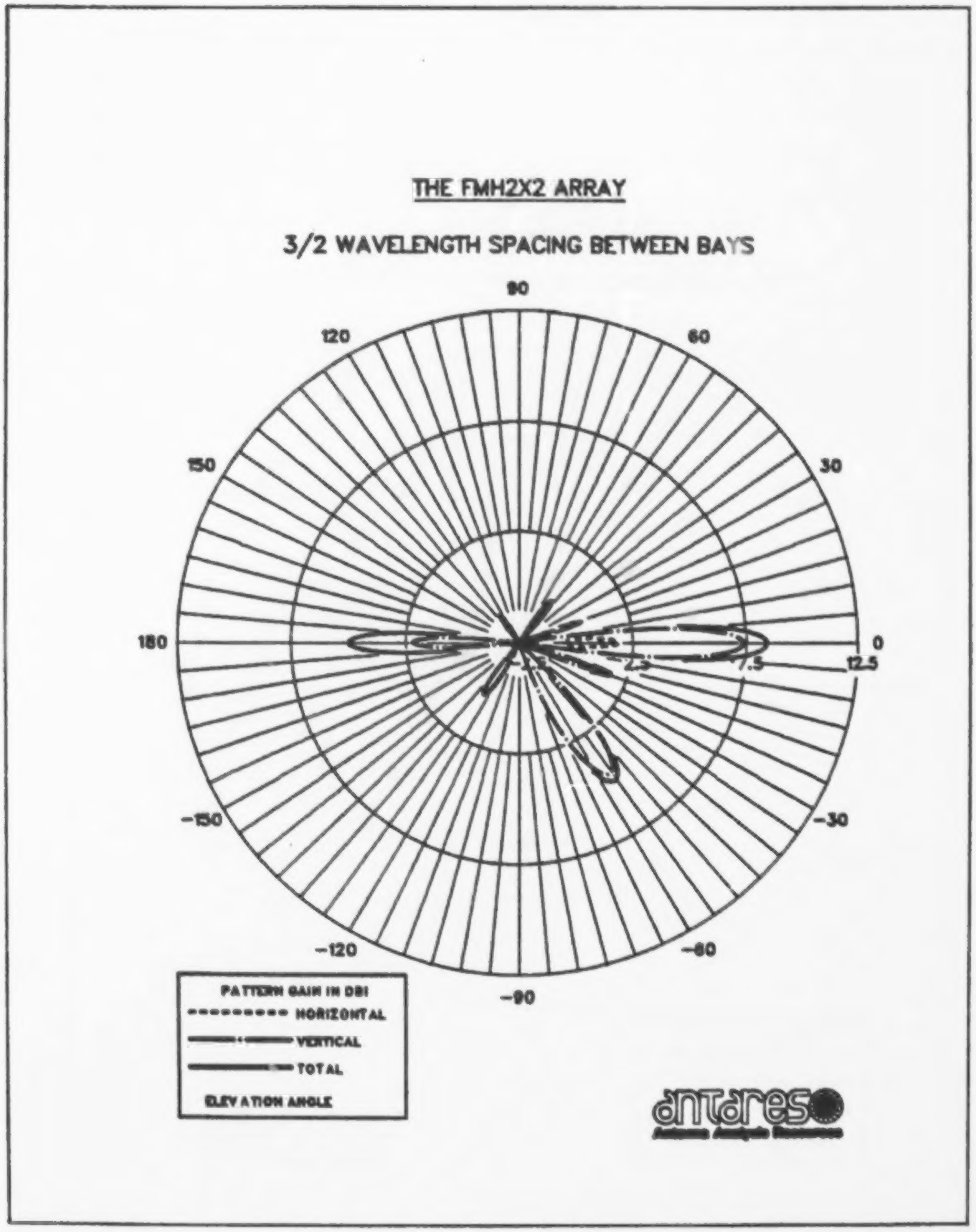

THE FMH2X2 ARRAY

3/2 WAVELENGTH SPACING BETWEEN BAYS

FIGURE B 8

THE ERI FMH2X2 ARRAY

3/2 WAVELENGTH SPACING BETWEEN BAYS

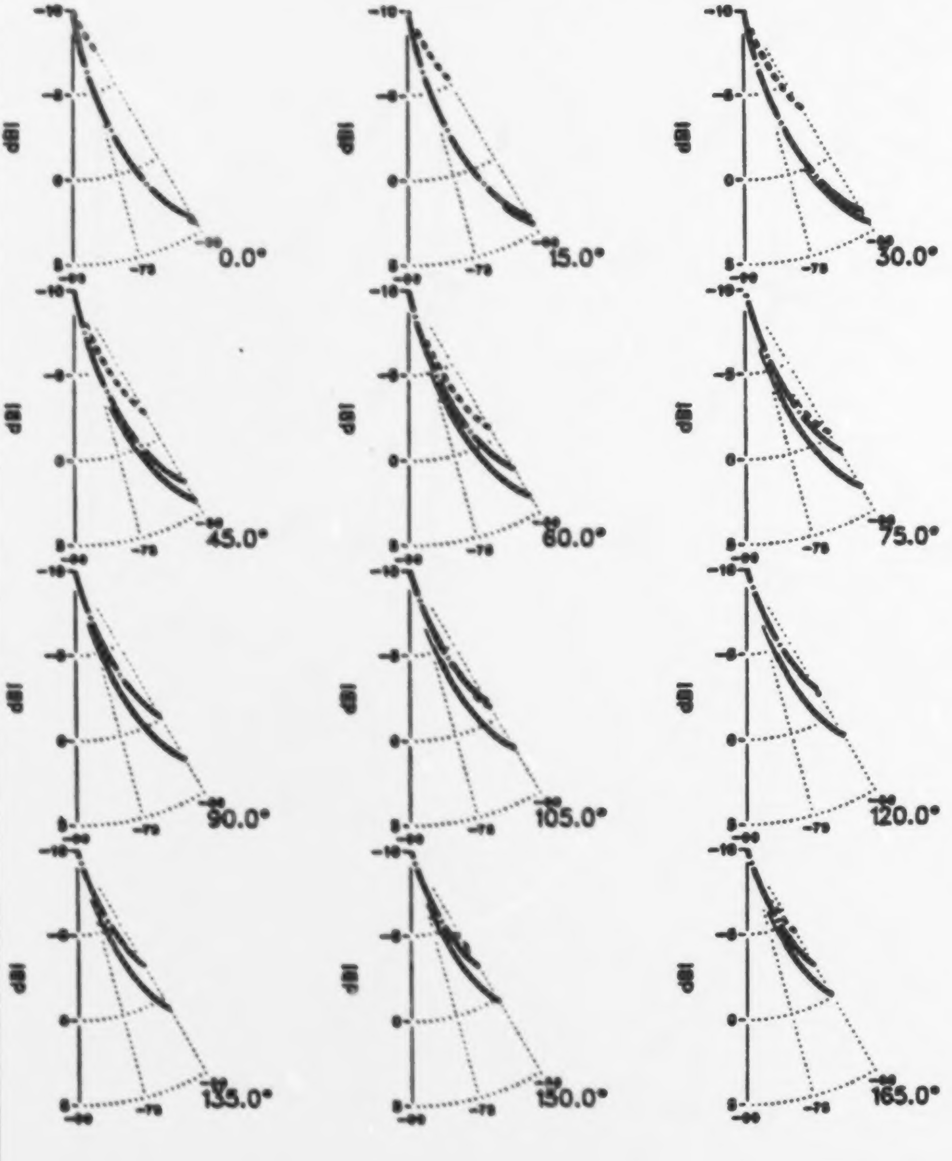

FIGURE B 7

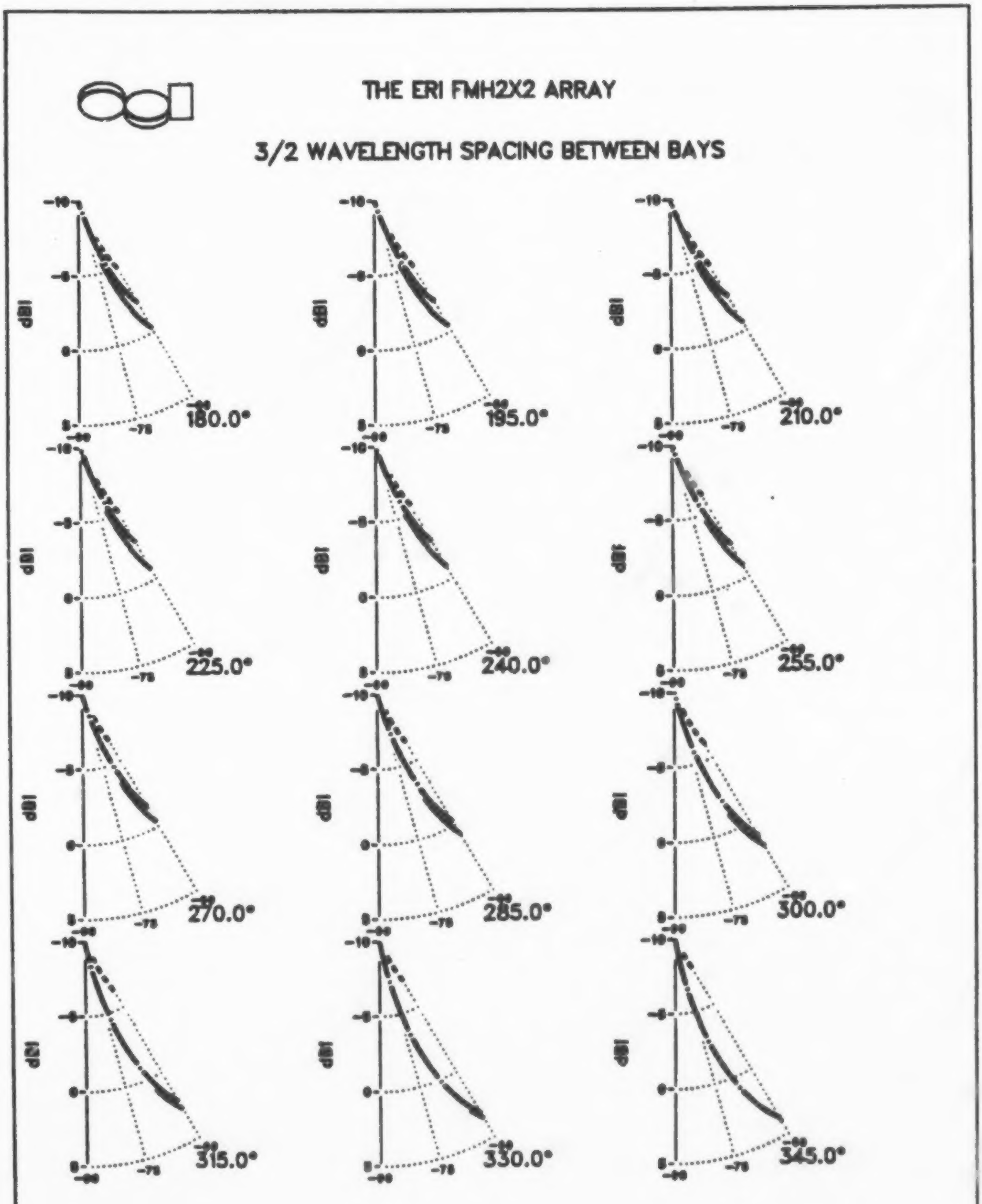

THE ERI FMH2X2 ARRAY

3/2 WAVELENGTH SPACING BETWEEN BAYS

FIGURE B 10

FMH2X2TW

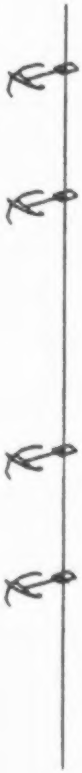

THETA = 60.00 PHI = 60.00 ETA = 90.00

FIGURE B 11

THE FMH 2X2 ARRAY

2 WAVELENGTH SPACING BETWEEN BAYS

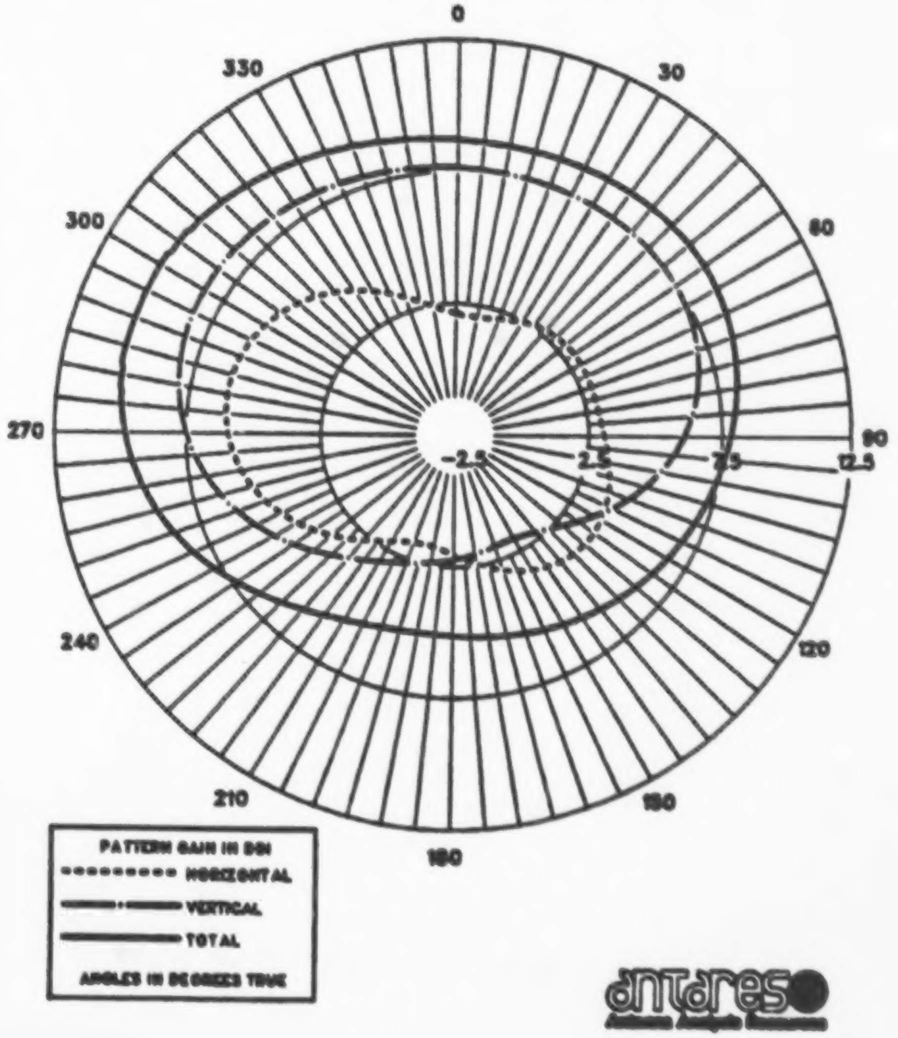

antares

FIGURE B 12

THE FMH 2X2 ARRAY

2 WAVELENGTH SPACING BETWEEN BAYS

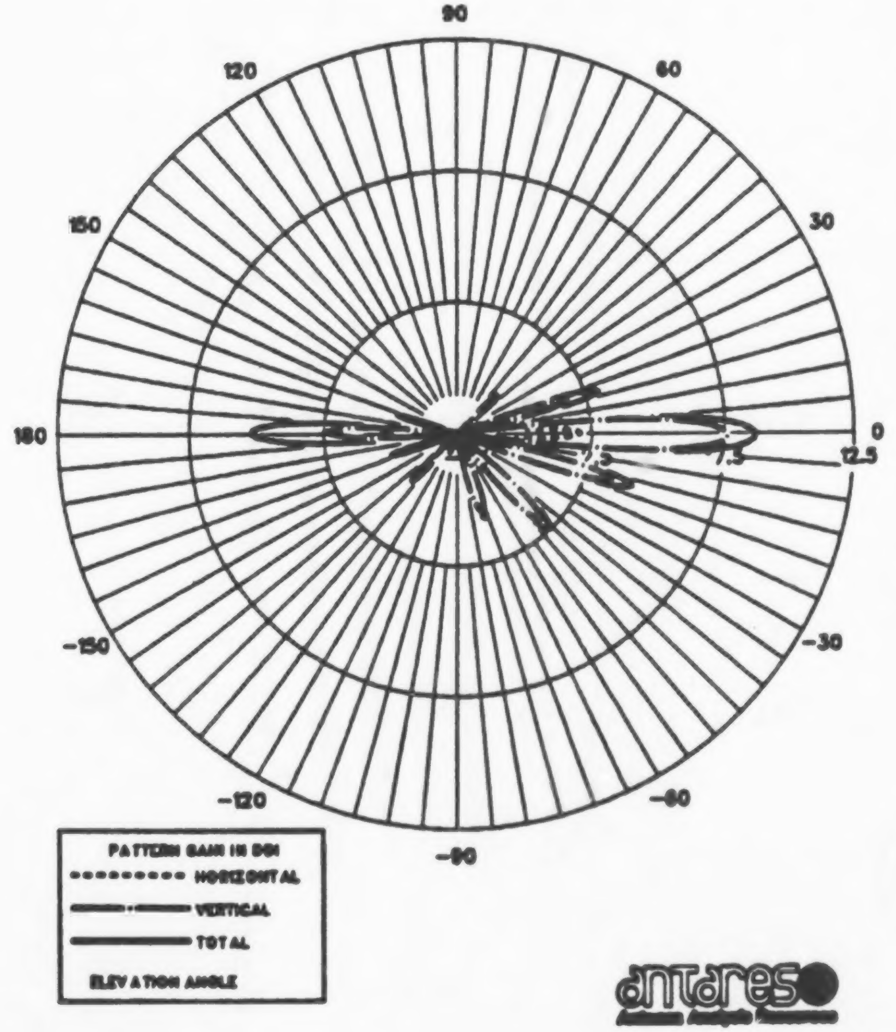

FIGURE B 13

THE ERI FMH 2X2 ARRAY

2 WAVELENGTH SPACING BETWEEN BAYS

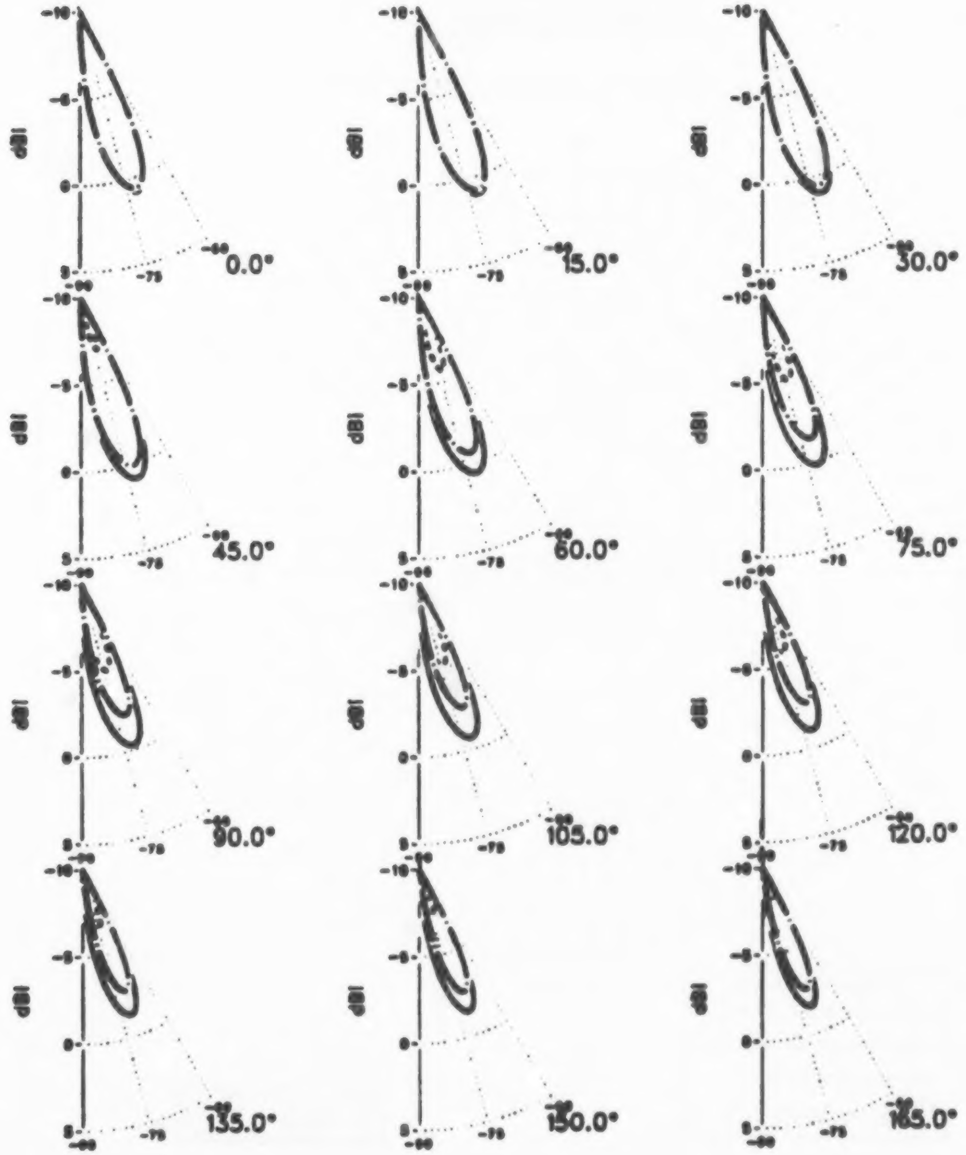

FIGURE B 14

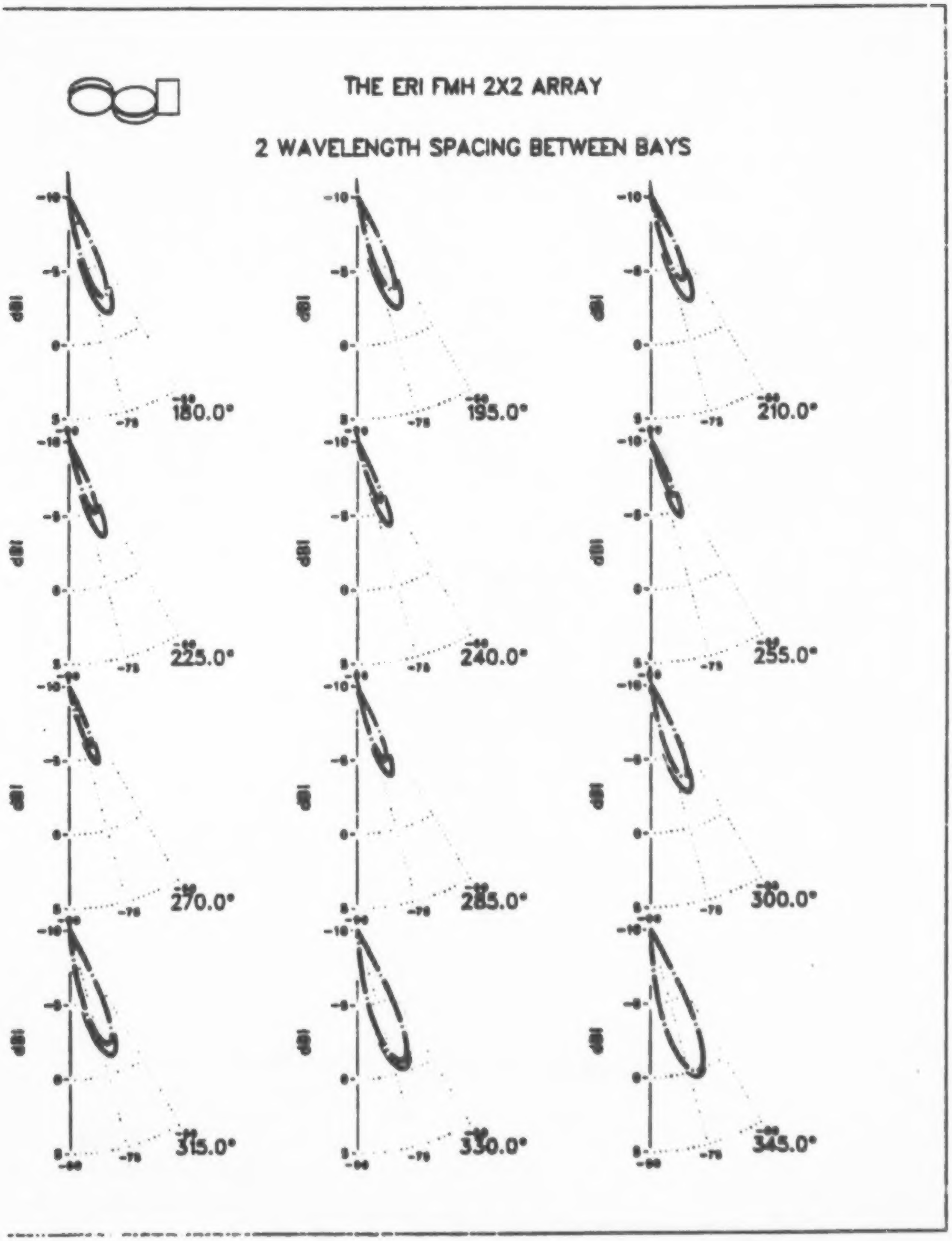

THE ERI FMH 2X2 ARRAY

2 WAVELENGTH SPACING BETWEEN BAYS

FIGURE B 15

FMH3X3

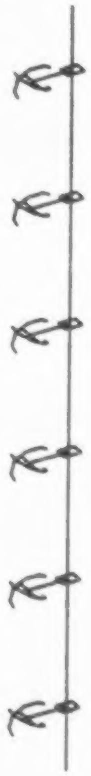

THETA = 60.00 PHI = 60.00 ETA = 90.00

187<

FIGURE B 16

THE ERI FMH 3X3 ARRAY

STANDARD SPACING OF ONE WAVELENGTH BETWEEN BAYS

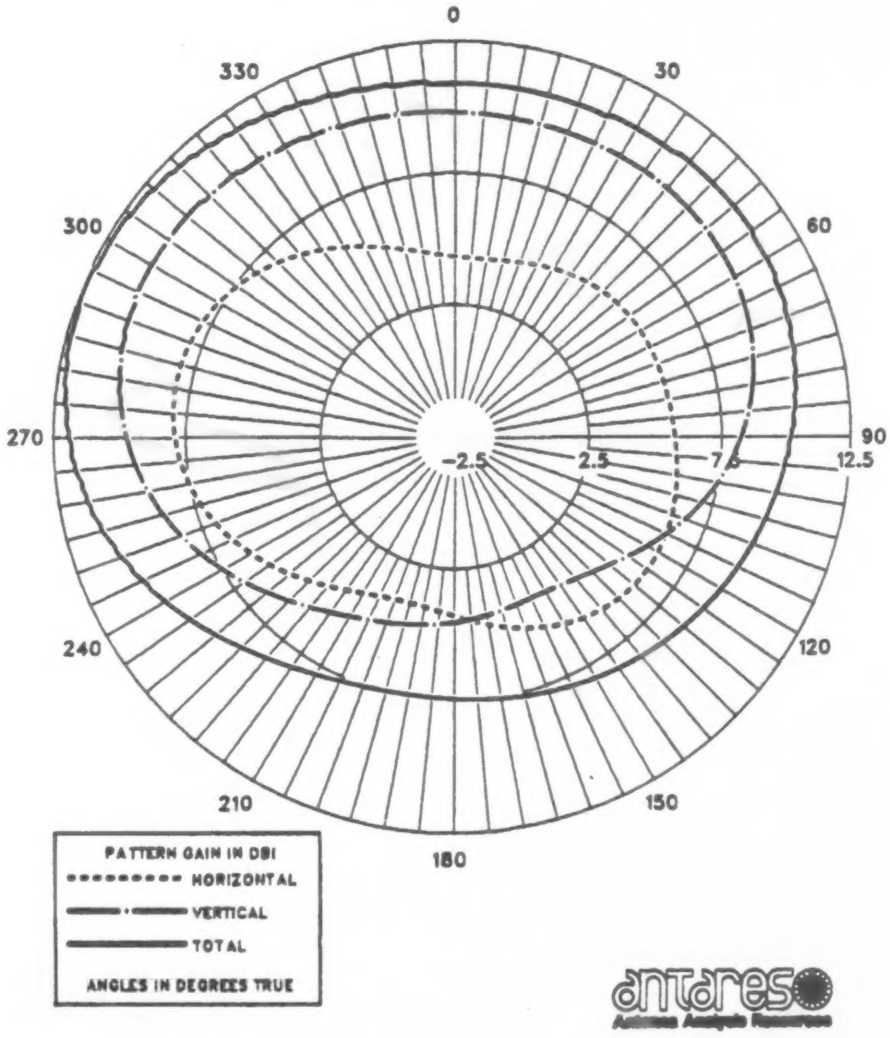

FIGURE B 17

THE ERI FMH 3X3 ARRAY

STANDARD SPACING OF ONE WAVELENGTH BETWEEN BAYS

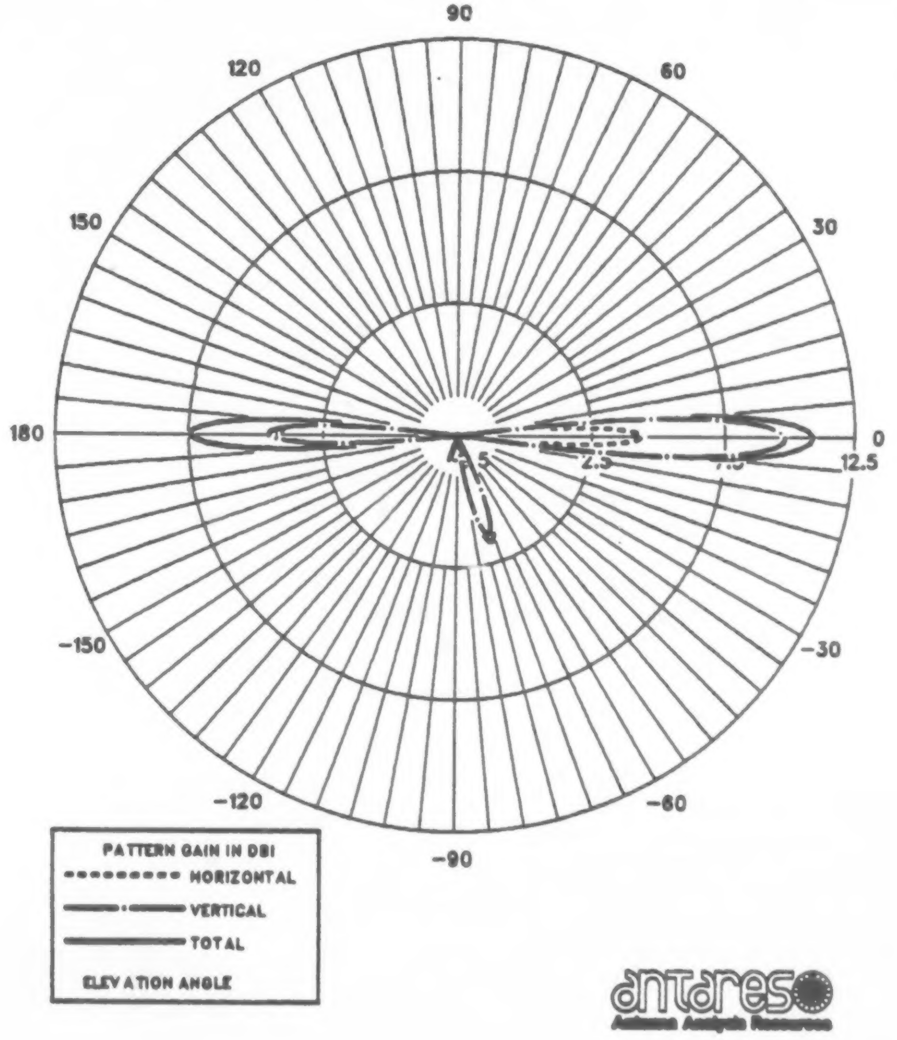

FIGURE B 18

THE ERI FMH 3X3 ARRAY

STANDARD SPAC'NG OF ONE WAVELENGTH BETWEEN BAYS

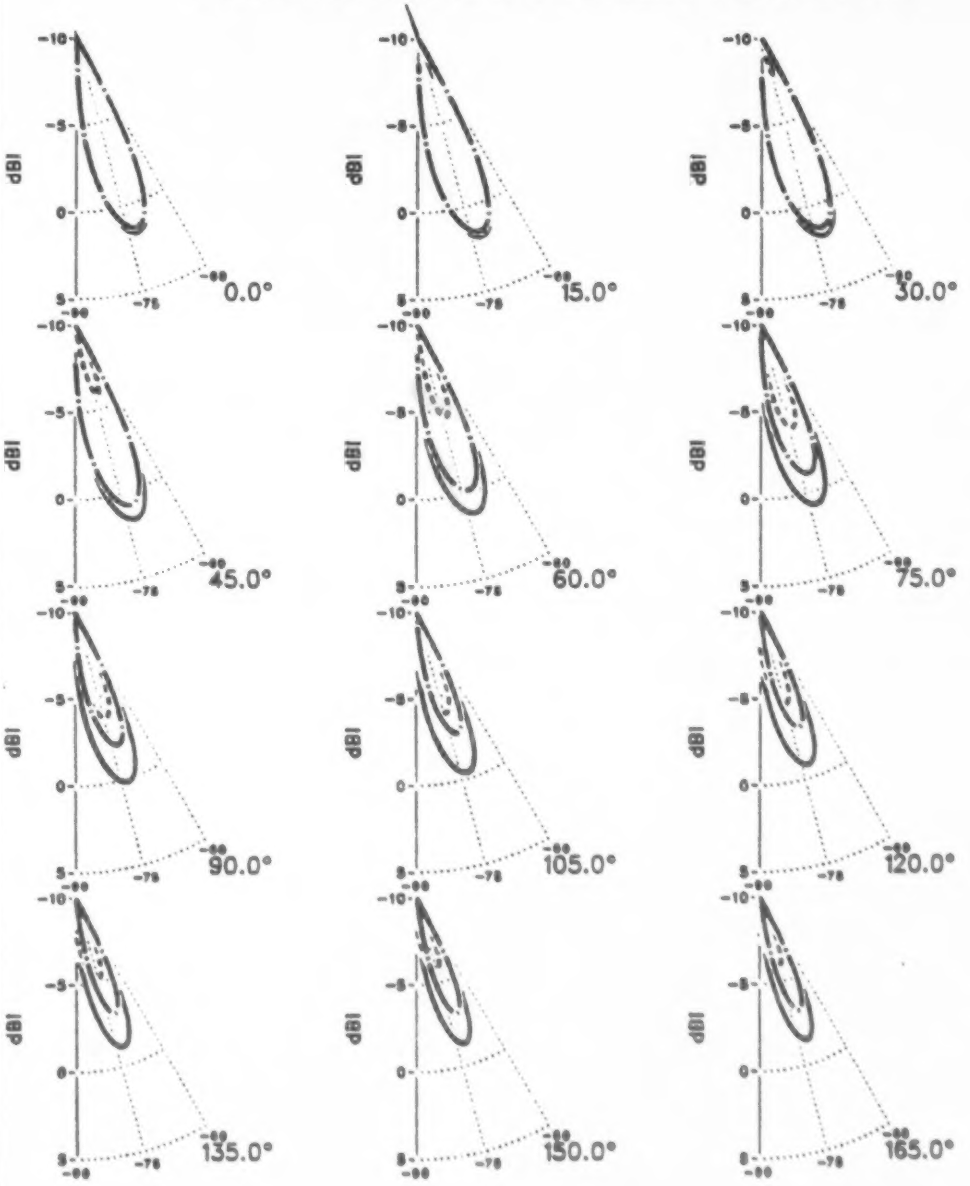

FIGURE B 19

THE ERI FMH 3X3 ARRAY

STANDARD SPACING OF ONE WAVELENGTH BETWEEN BAYS

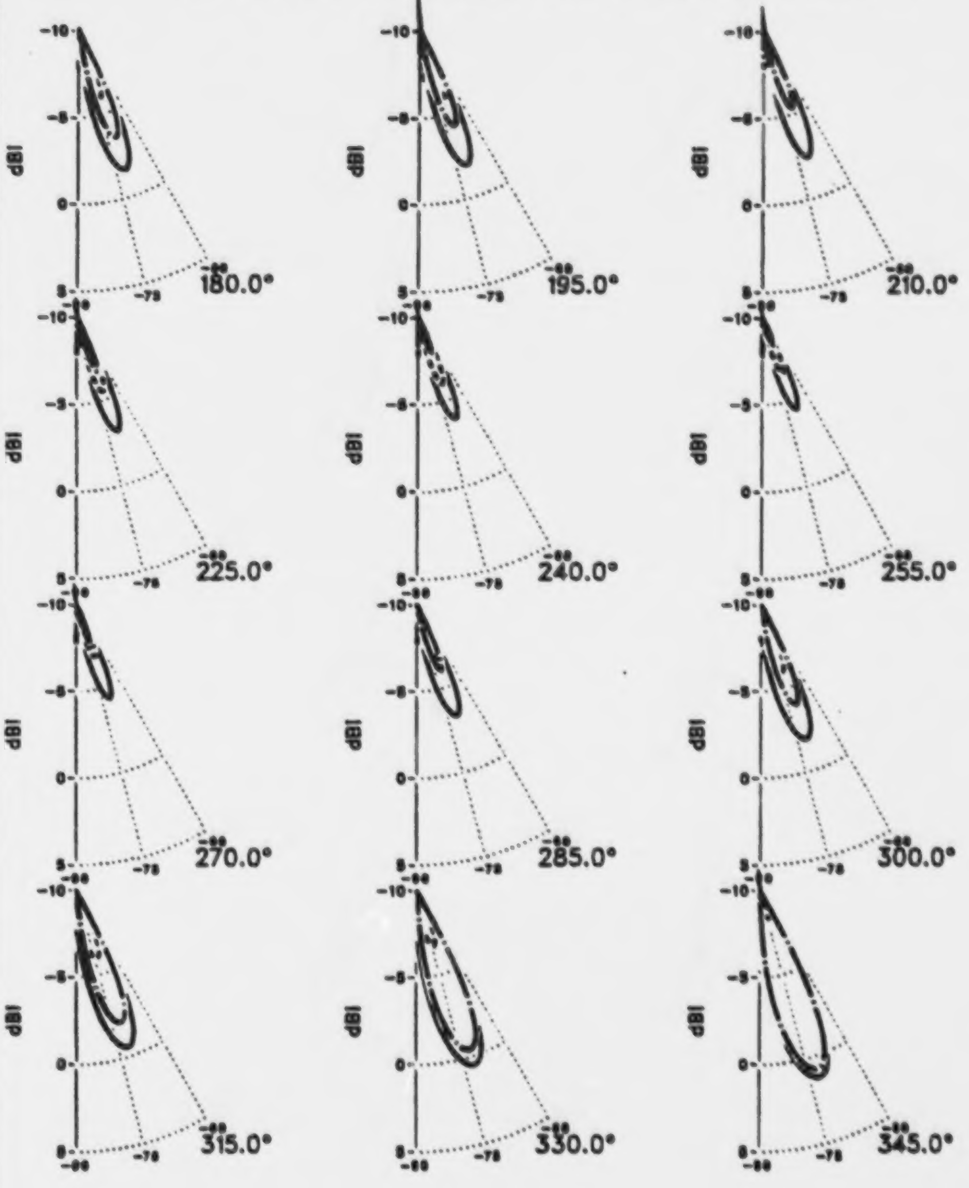

FIGURE B 20

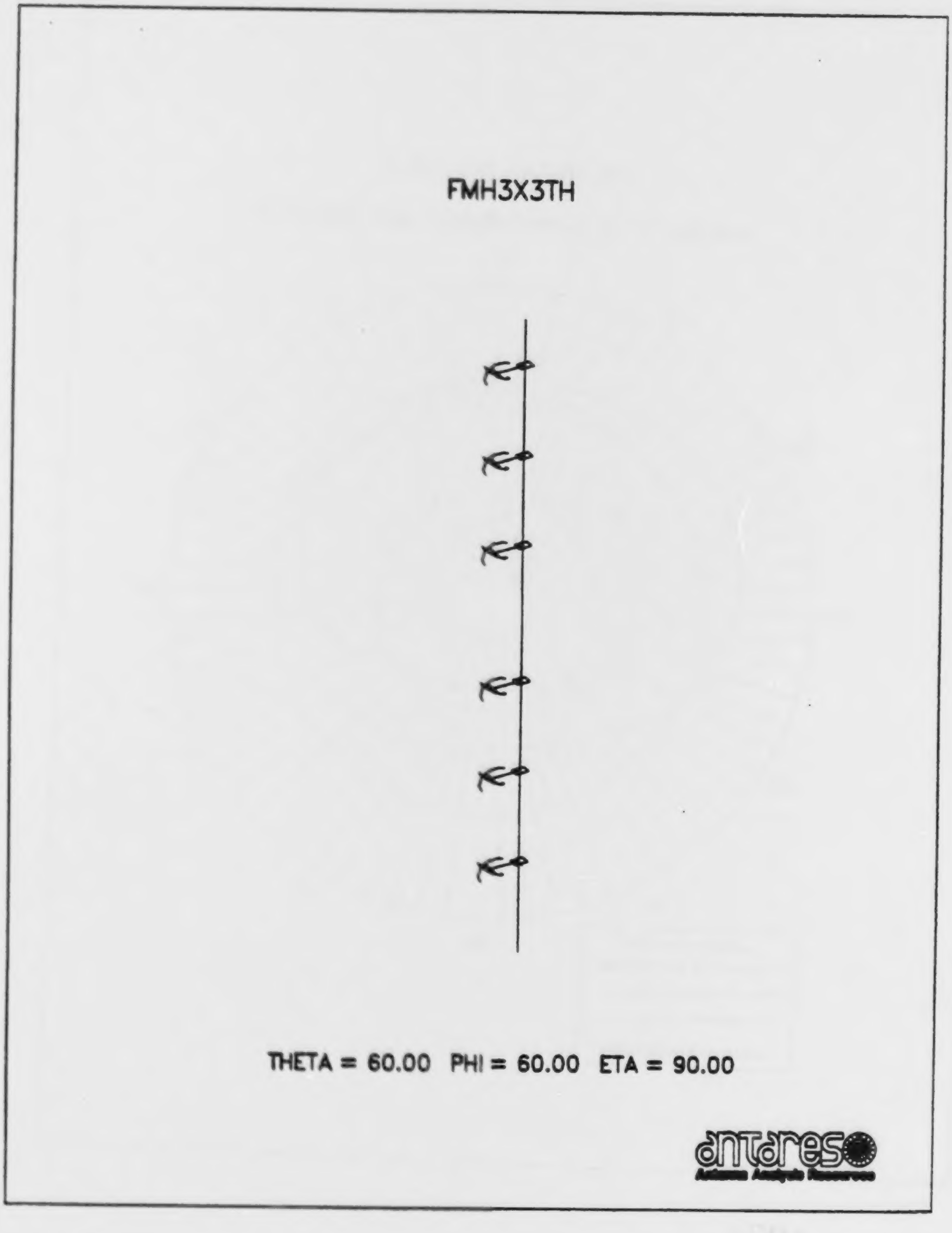
FMH3X3TH
THETA = 60.00 PHI = 60.00 ETA = 90.00
antares
Antenna Analysis Resources

FIGURE B 21

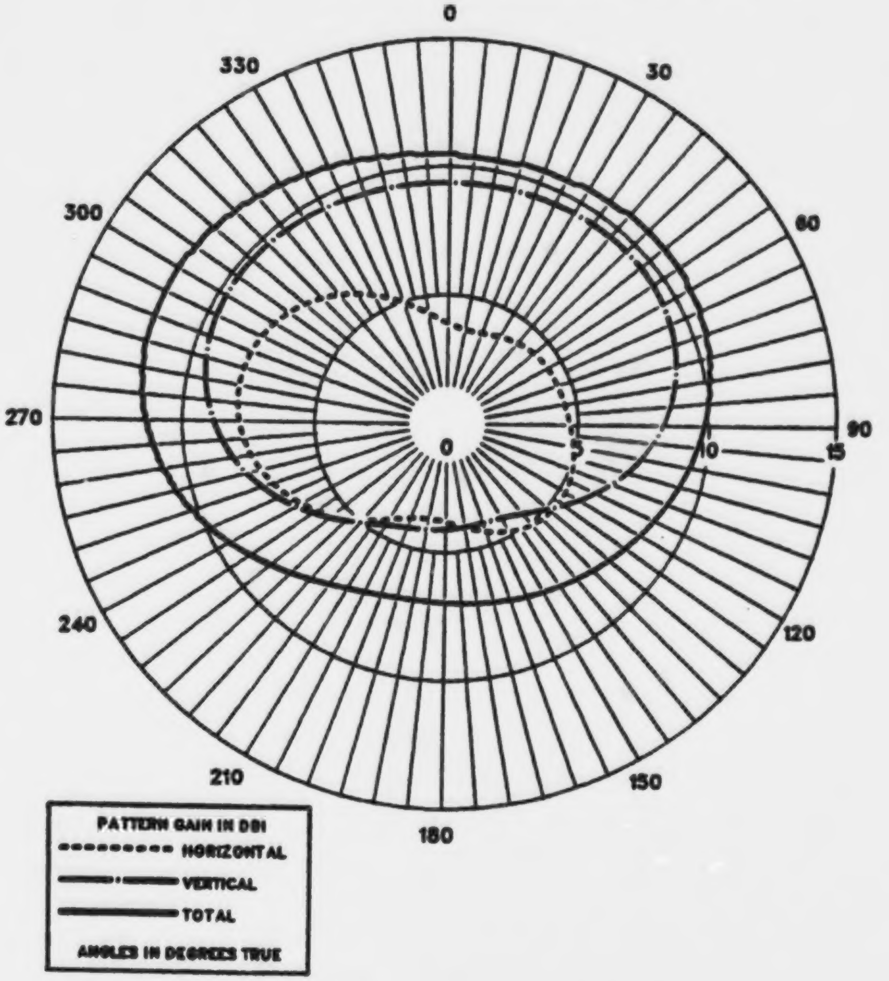

THE ERI FMH 3X3 ARRAY

SPACING OF 3/2 WAVELENGTHS BETWEEN BAYS

193<

FIGURE B 22

THE ERI FMH 3X3 ARRAY

SPACING OF 3/2 WAVELENGTHS BETWEEN BAYS

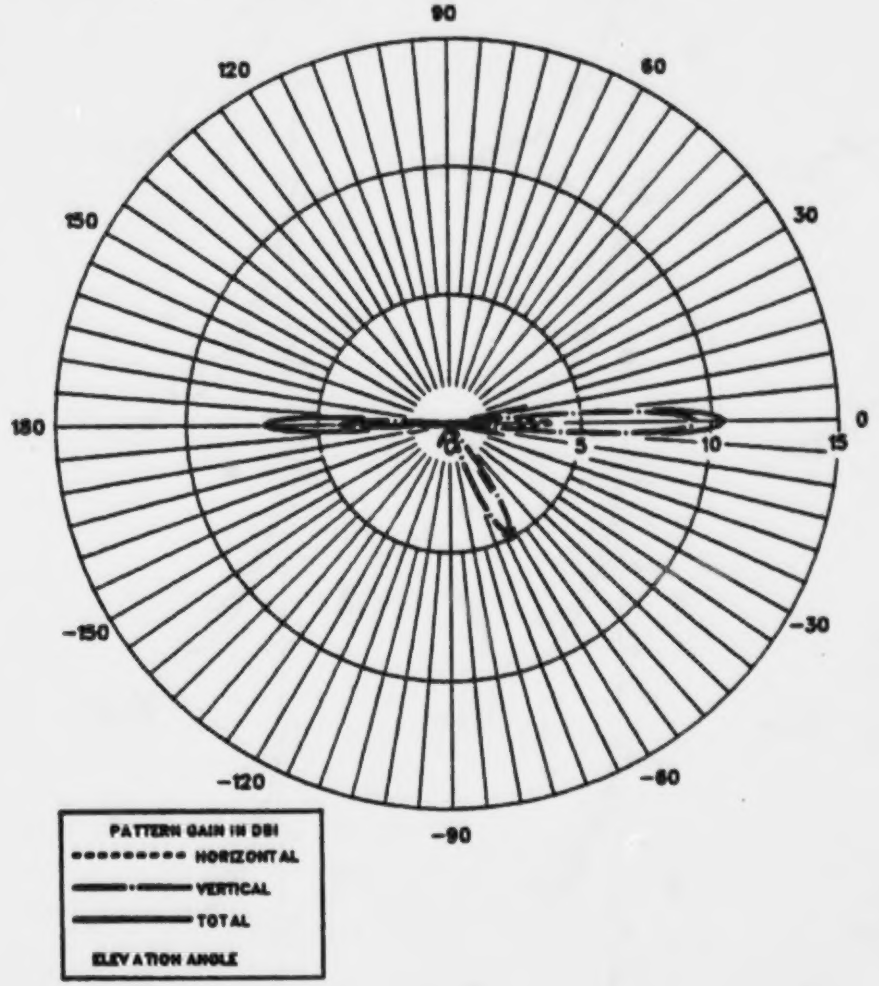

FIGURE B 23

THE ERI FMH 3X3 ARRAY

SPACING OF 3/2 WAVELENGTHS BETWEEN BAYS

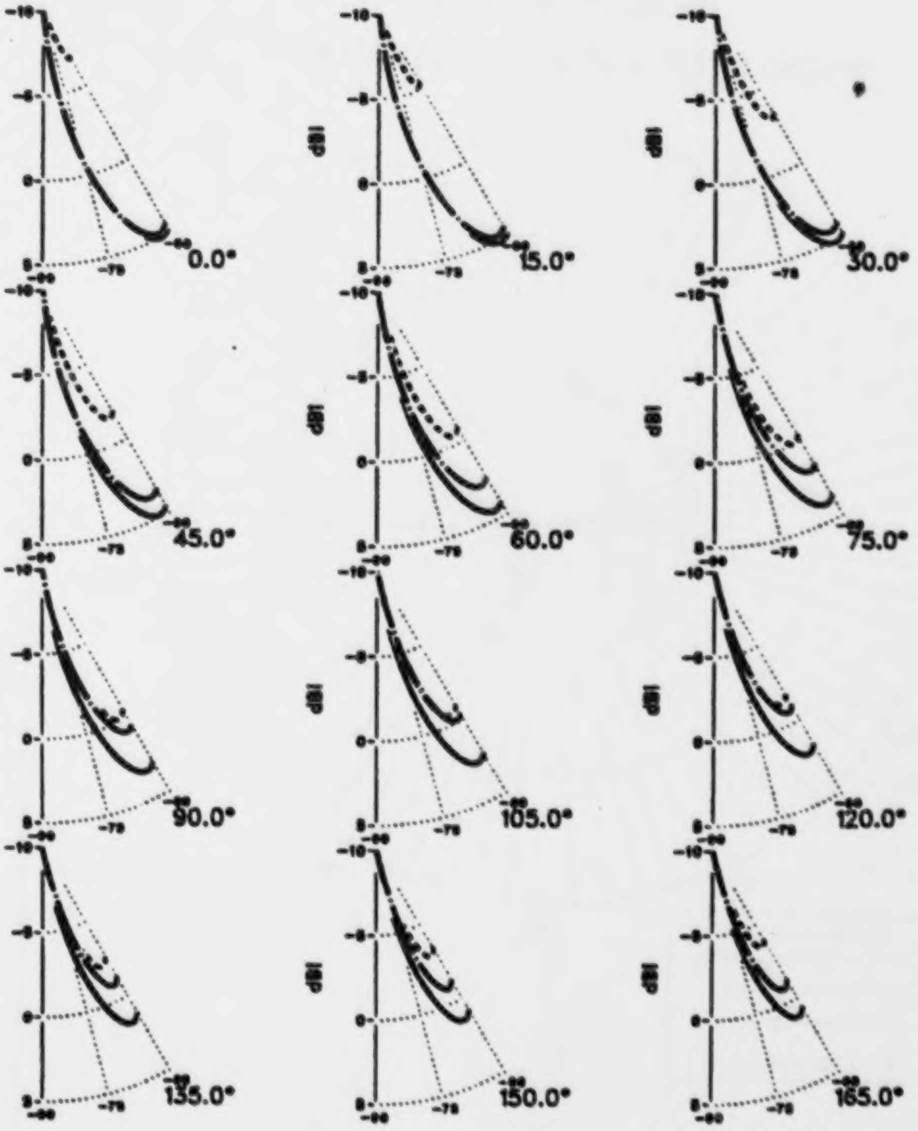

FIGURE B 24

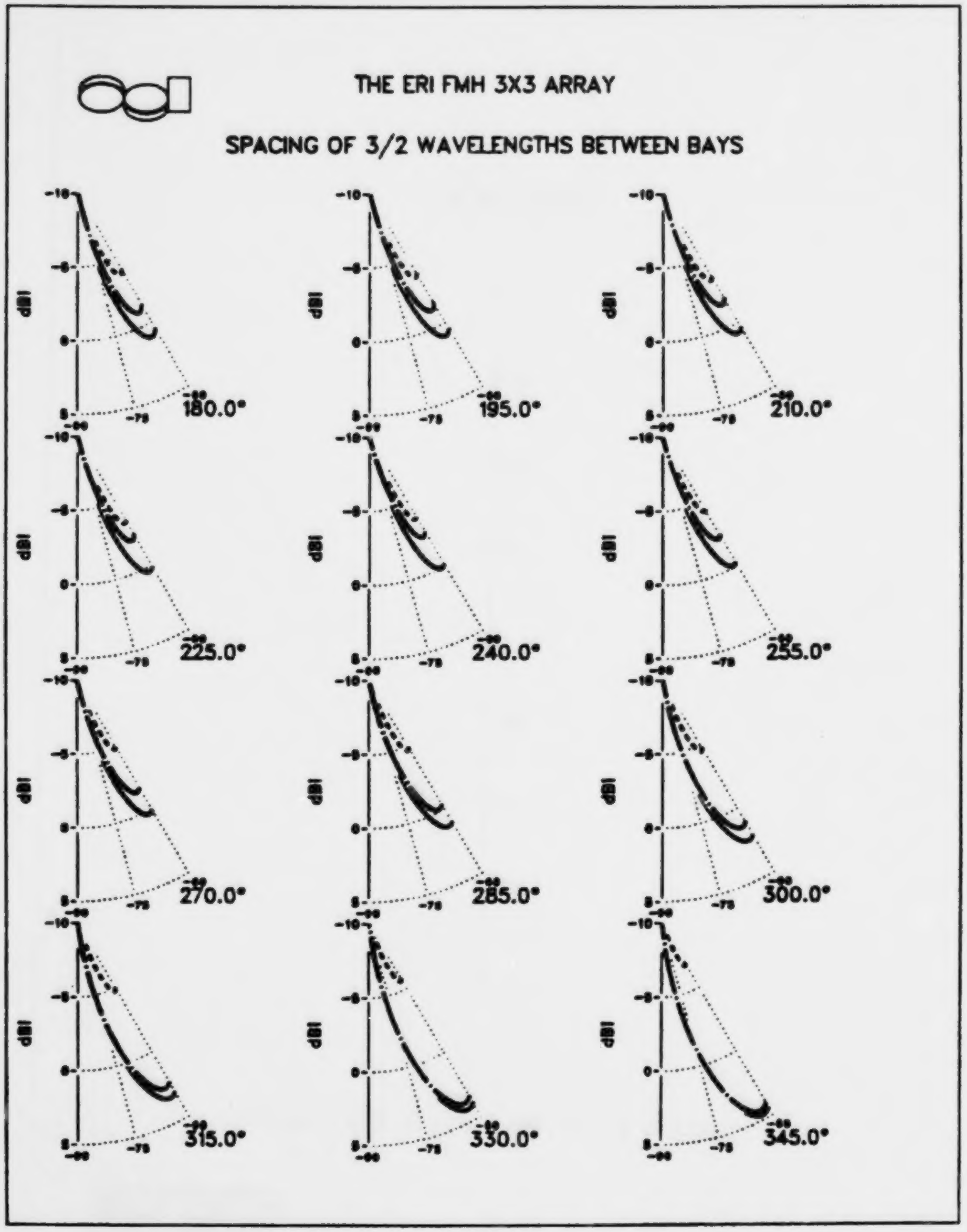

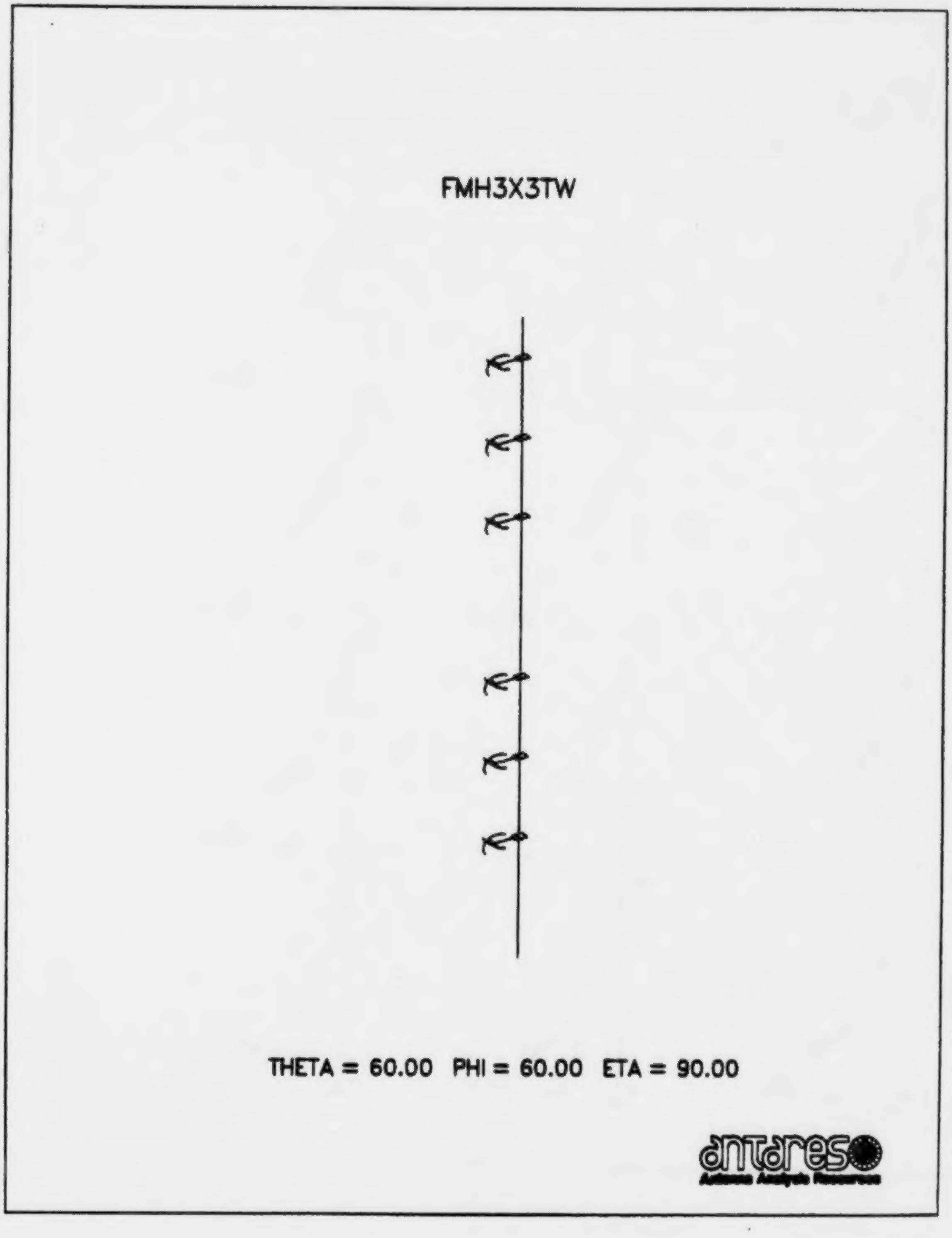
FMH3X3TW
THETA = 60.00 PHI = 60.00 ETA = 90.00
antares
Antenna Analysis Resources

FIGURE B 26

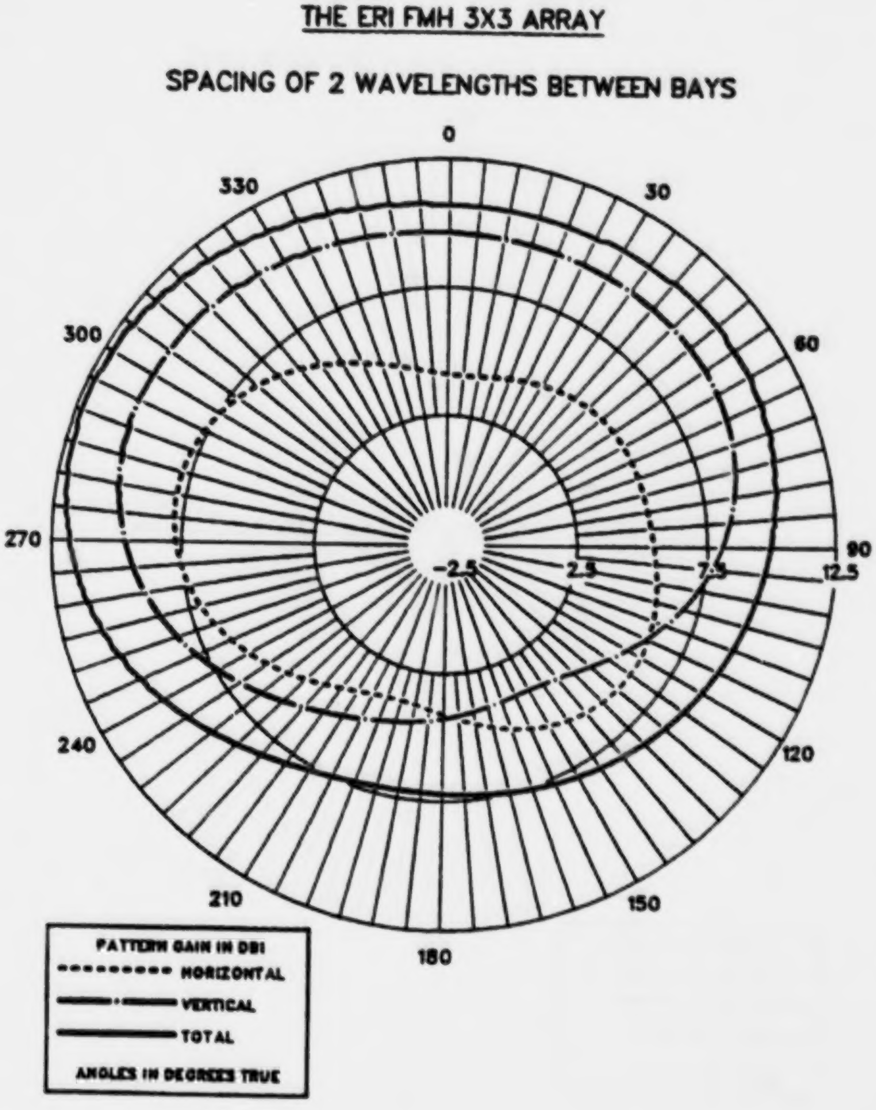

THE ERI FMH 3X3 ARRAY

SPACING OF 2 WAVELENGTHS BETWEEN BAYS

FIGURE B 27

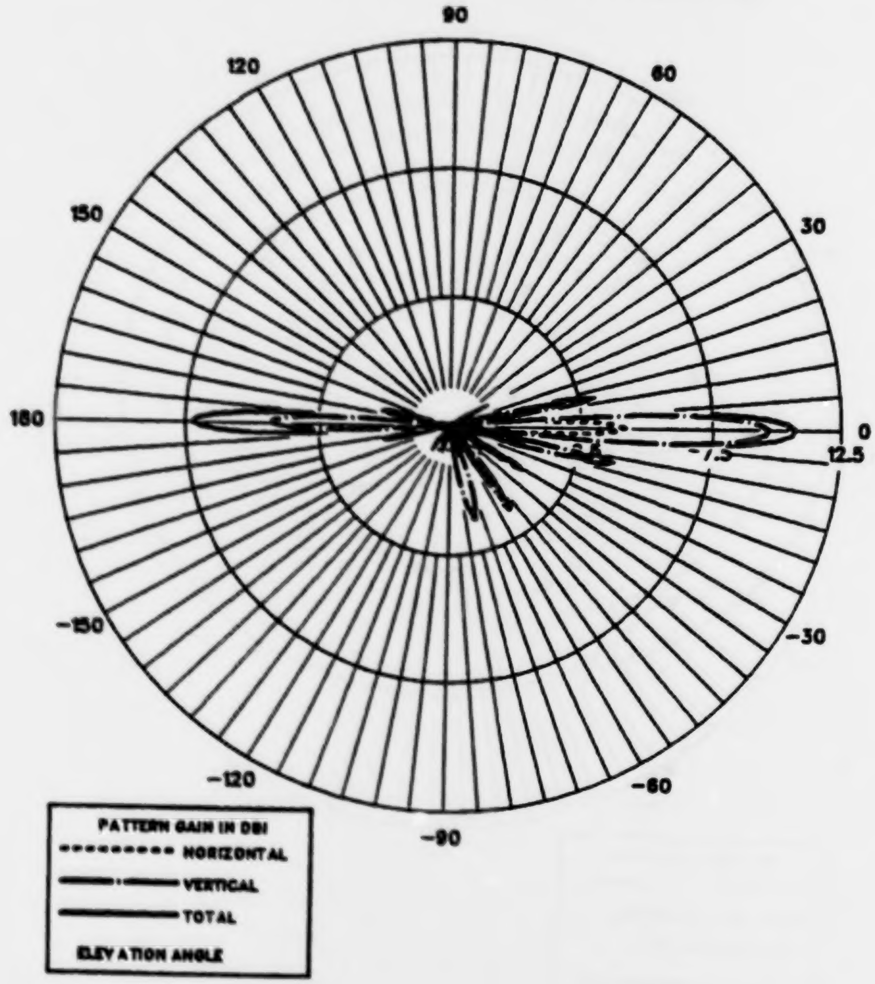

THE ERI FMH 3X3 ARRAY

SPACING OF 2 WAVELENGTHS BETWEEN BAYS

FIGURE B 28

THE ERI FMH 3X3 ARRAY

SPACING OF 2 WAVELENGTHS BETWEEN BAYS

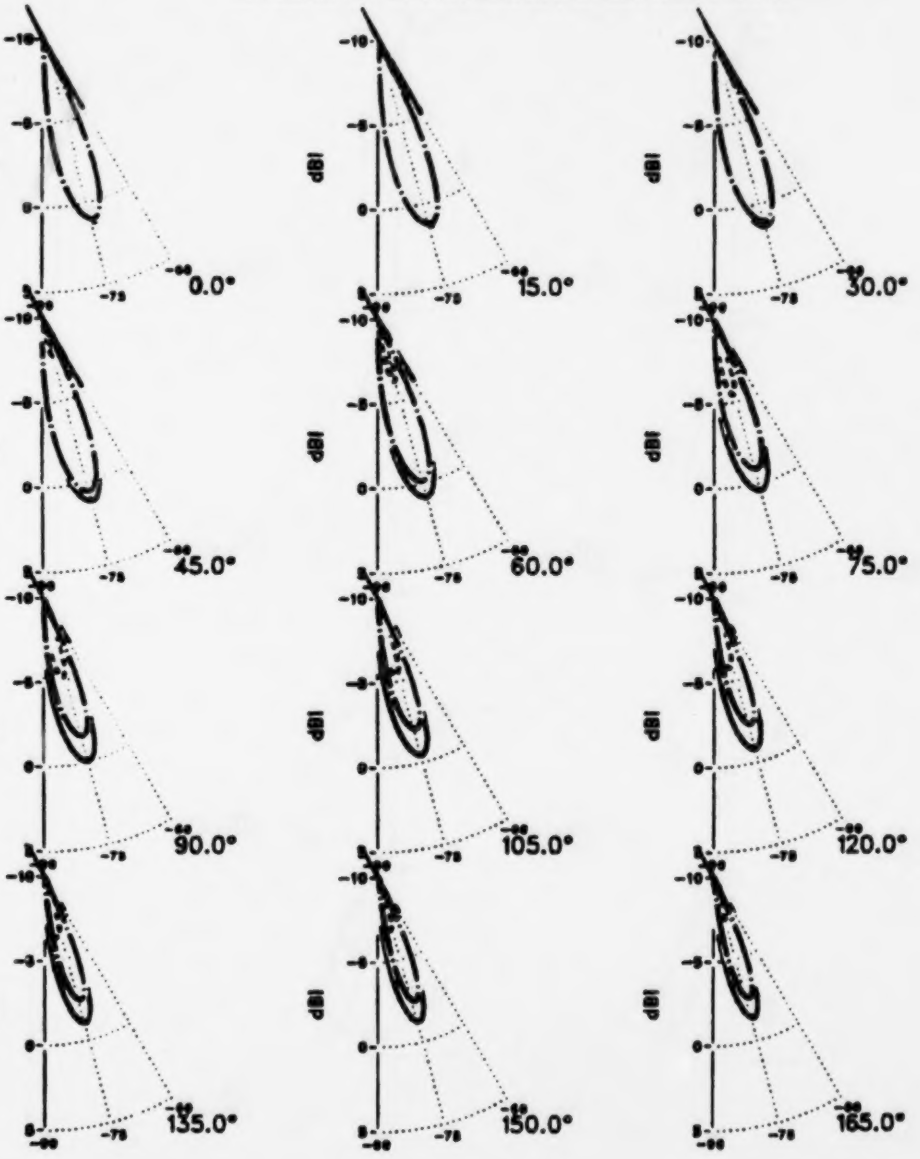

FIGURE B 29

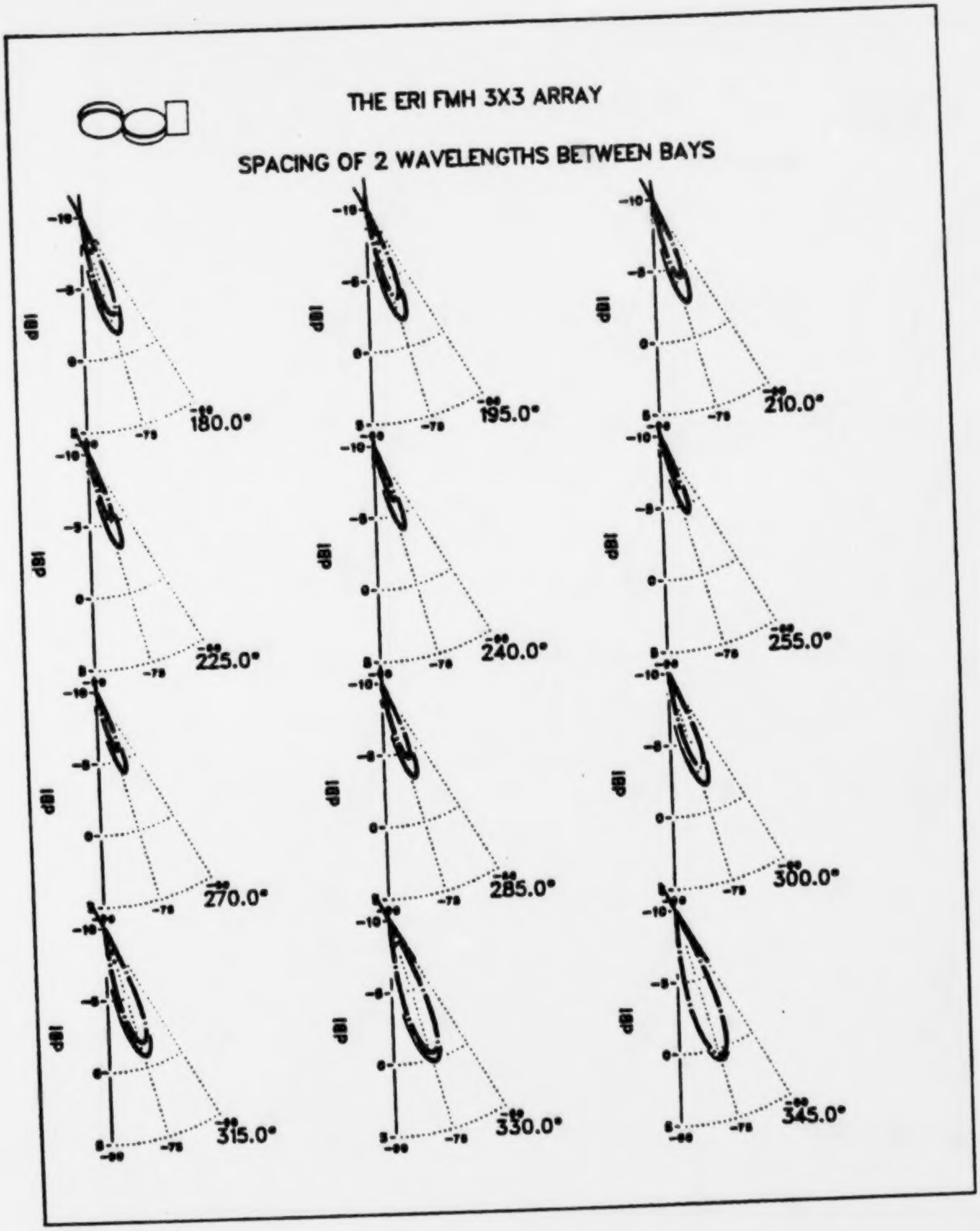

THE ERI FMH 3X3 ARRAY

SPACING OF 2 WAVELENGTHS BETWEEN BAYS

FIGURE B 30

FMH4X4

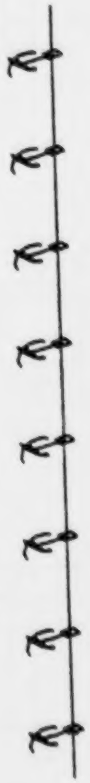

THETA = 60.00 PHI = 60.00 ETA = 90.00

FIGURE B 31

THE ERI FMH 4X4 ARRAY

STANDARD SPACING OF ONE WAVELENGTH BETWEEN BAYS

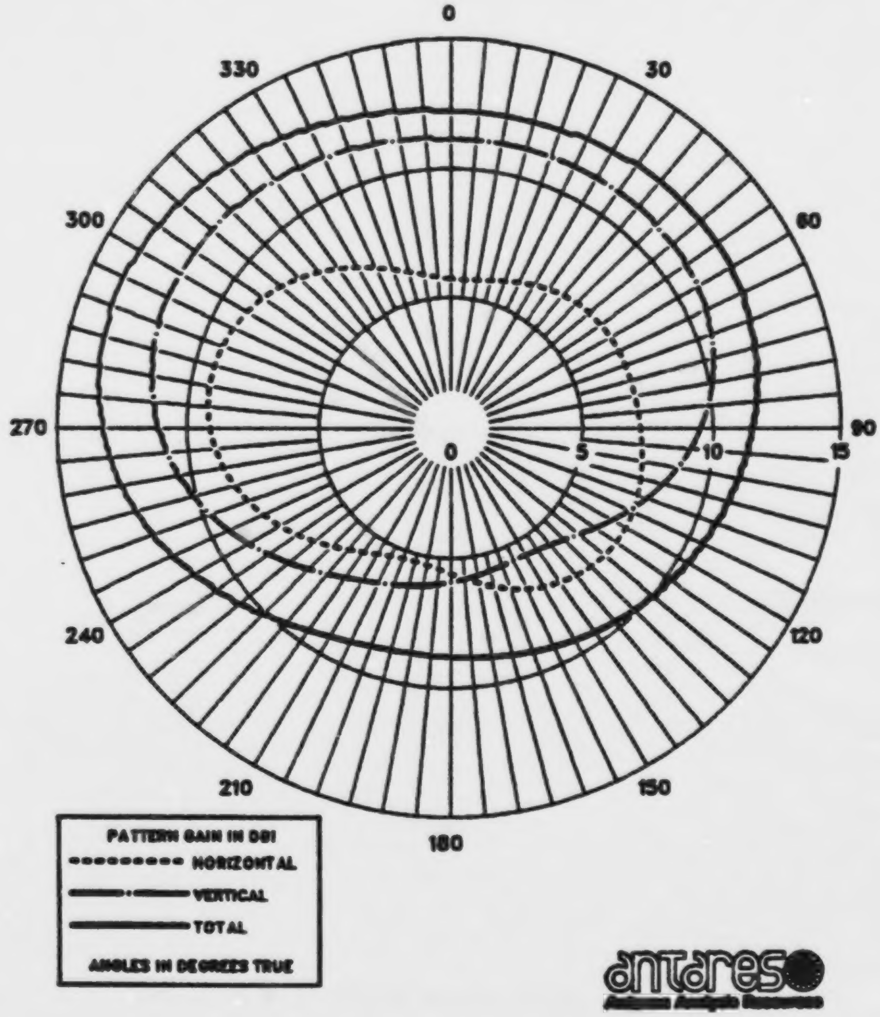

antares
Antenna Analysis Resources

203<

FIGURE B 32

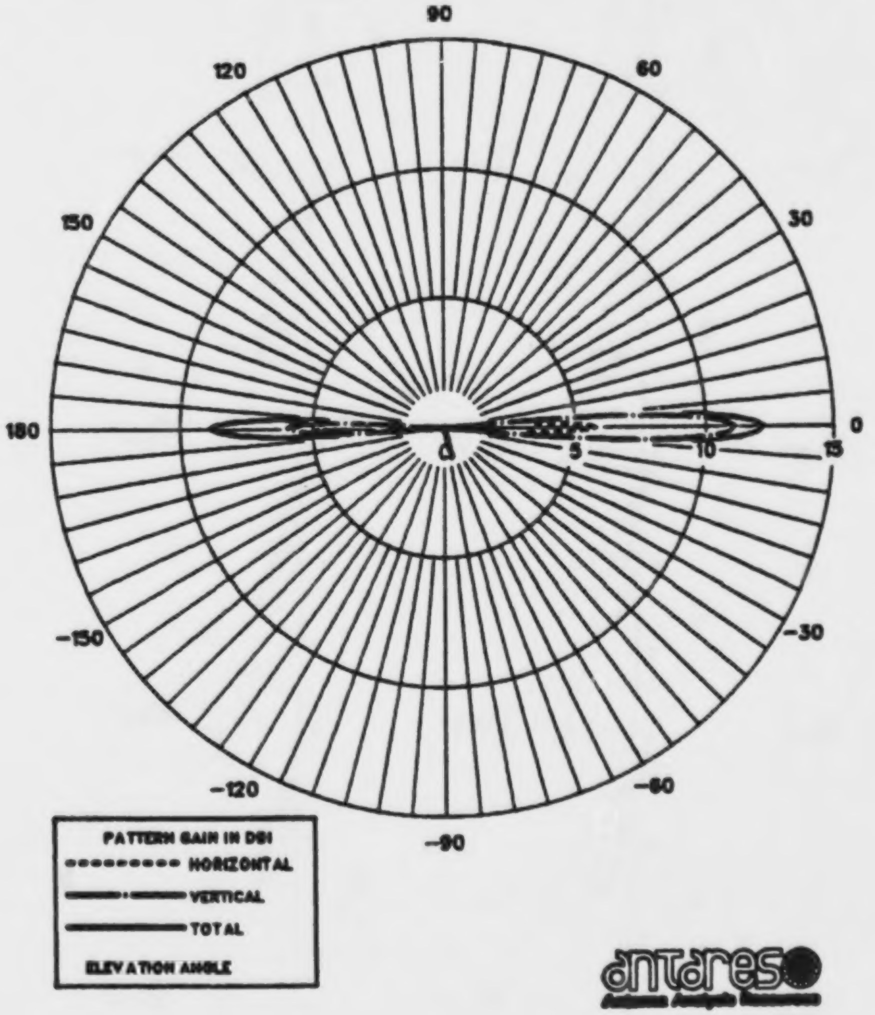
THE ERI FMH 4X4 ARRAY

STANDARD SPACING OF ONE WAVELENGTH BETWEEN BAYS

antares
Antenna Analysis Resources

FIGURE B 33

THE ERI FMH 4X4 ARRAY

STANDARD SPACING OF ONE WAVELENGTH BETWEEN BAYS

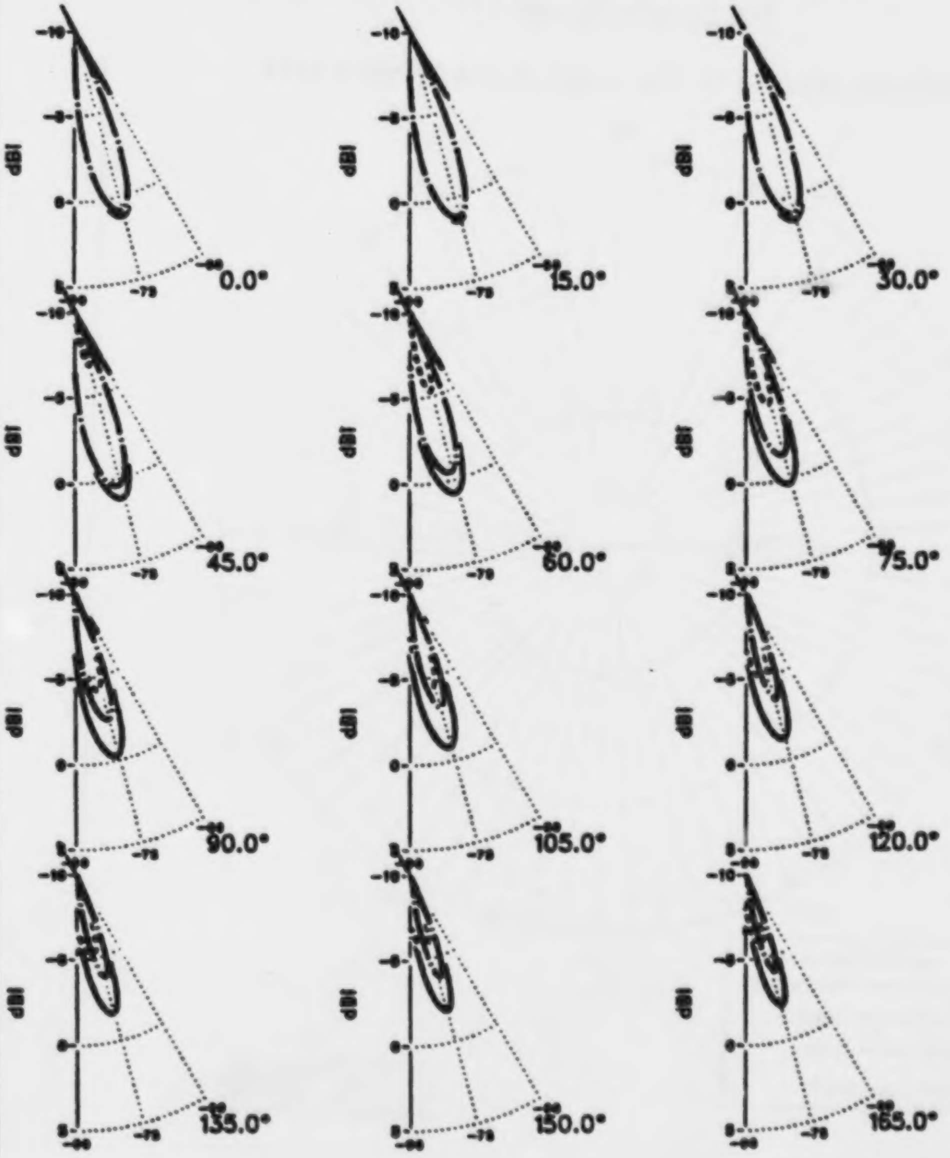

205<

FIGURE B 34

THE ERI FMH 4X4 ARRAY

STANDARD SPACING OF ONE WAVELENGTH BETWEEN BAYS

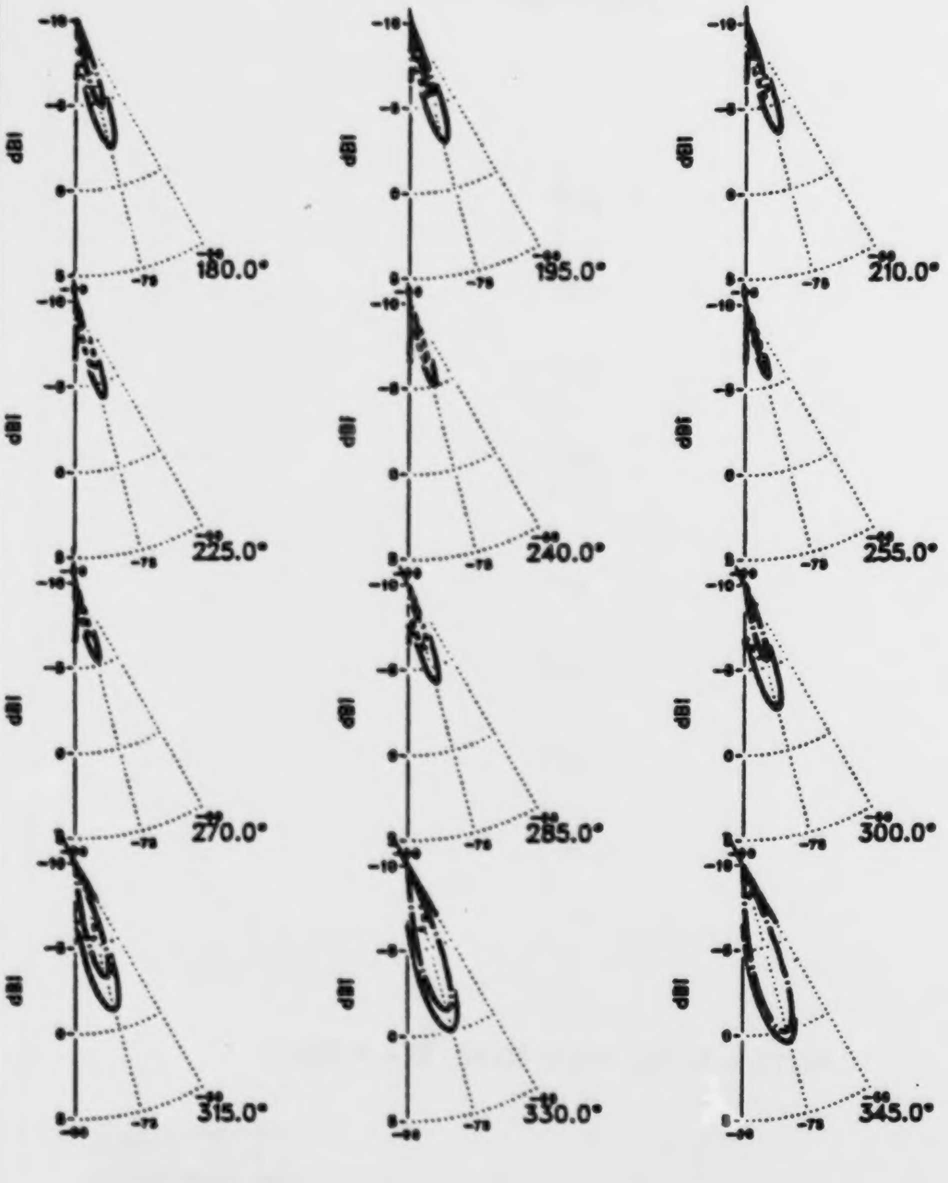

FIGURE B 35

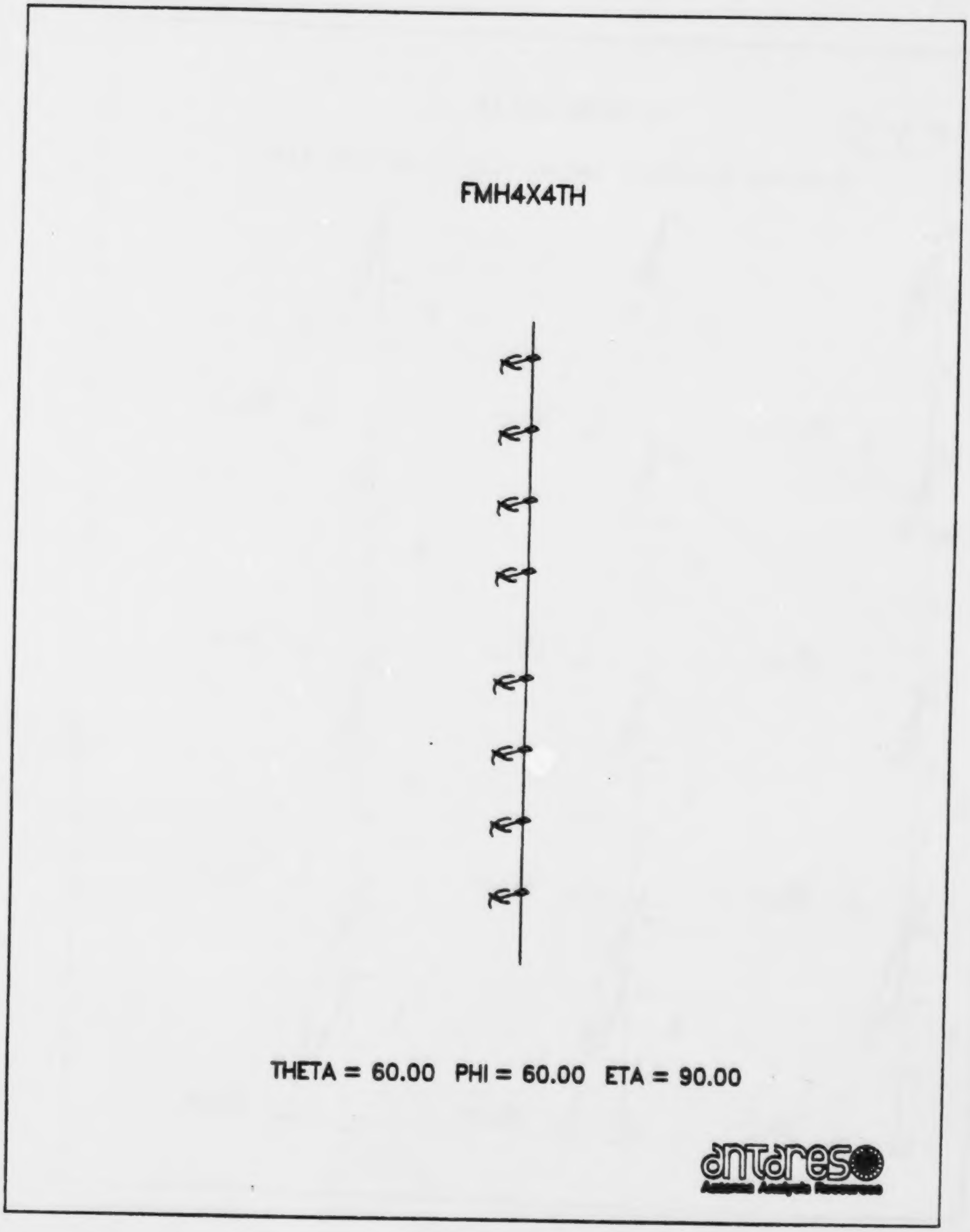
FMH4X4TH
THETA = 60.00 PHI = 60.00 ETA = 90.00
antares
Antenna Analysis Resources

FIGURE B 36

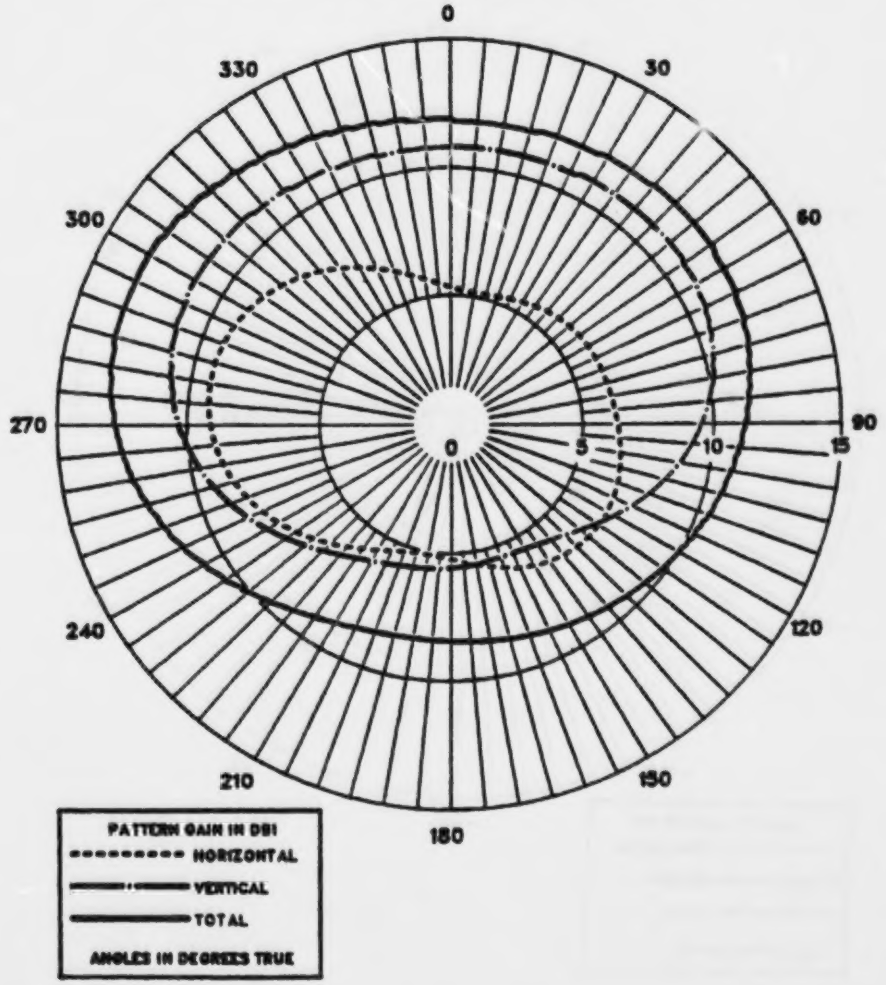

THE ERI FMH 4X4 ARRAY

SPACING OF 3/2 WAVELENGTHS BETWEEN BAYS

FIGURE B 37

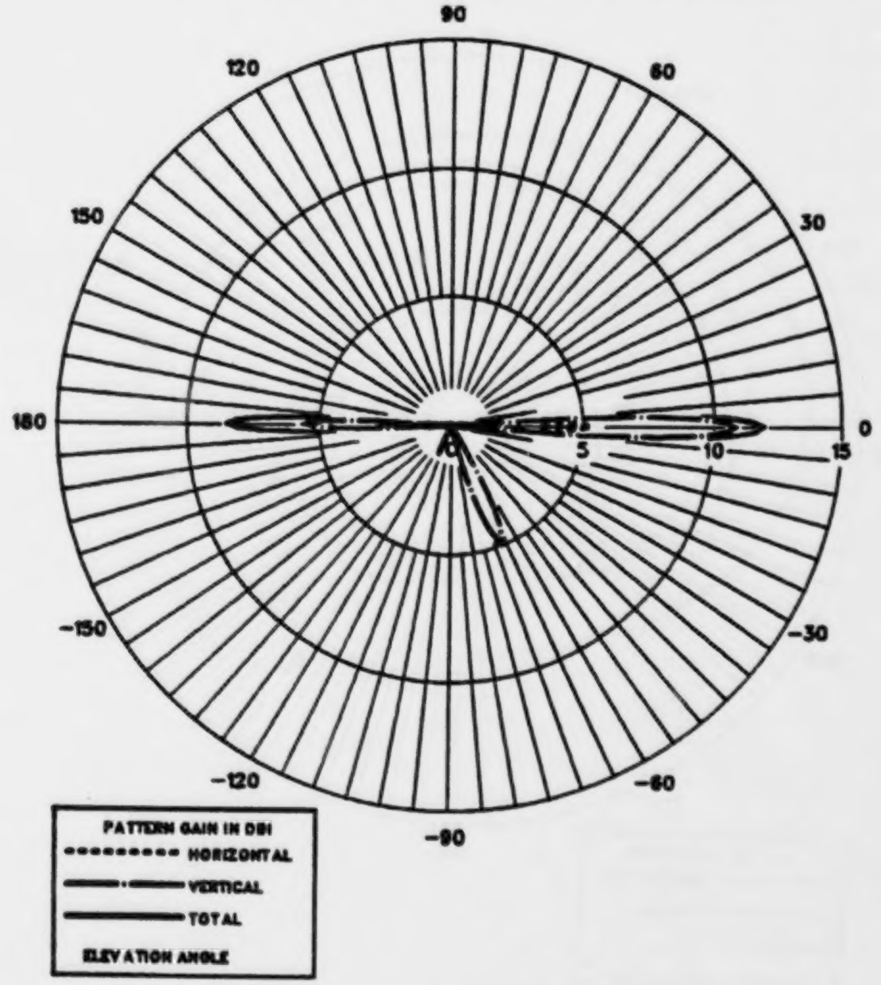

THE ERI FMH 4X4 ARRAY

SPACING OF 3/2 WAVELENGTHS BETWEEN BAYS

FIGURE B 38

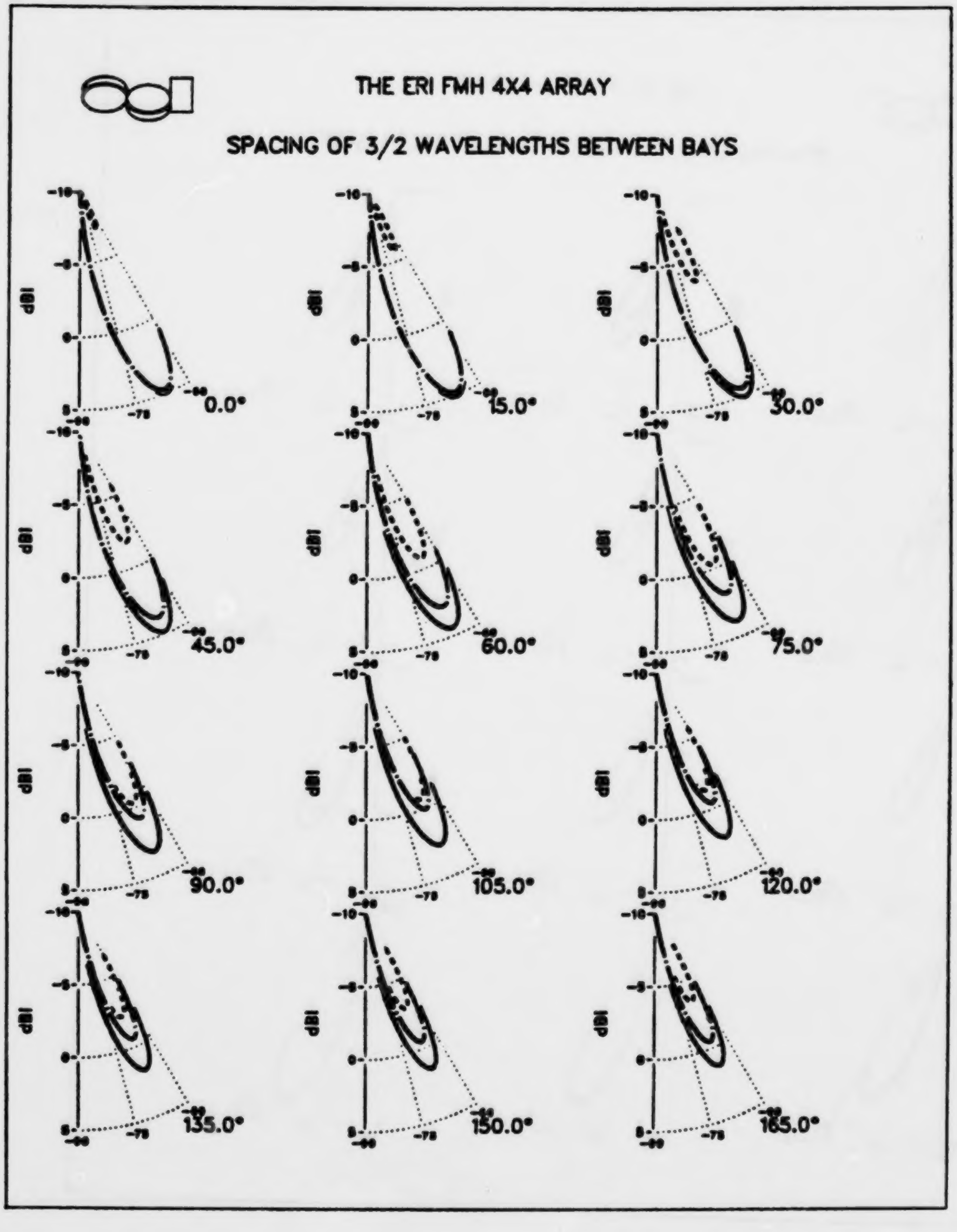
THE ERI FMH 4X4 ARRAY
SPACING OF 3/2 WAVELENGTHS BETWEEN BAYS
dBI
-10
-5
0
5
-90
-75
-60
0.0°
15.0°
30.0°
45.0°
60.0°
75.0°
90.0°
105.0°
120.0°
135.0°
150.0°
165.0°

FIGURE B 39

THE ERI FMH 4X4 ARRAY

SPACING OF 3/2 WAVELENGTHS BETWEEN BAYS

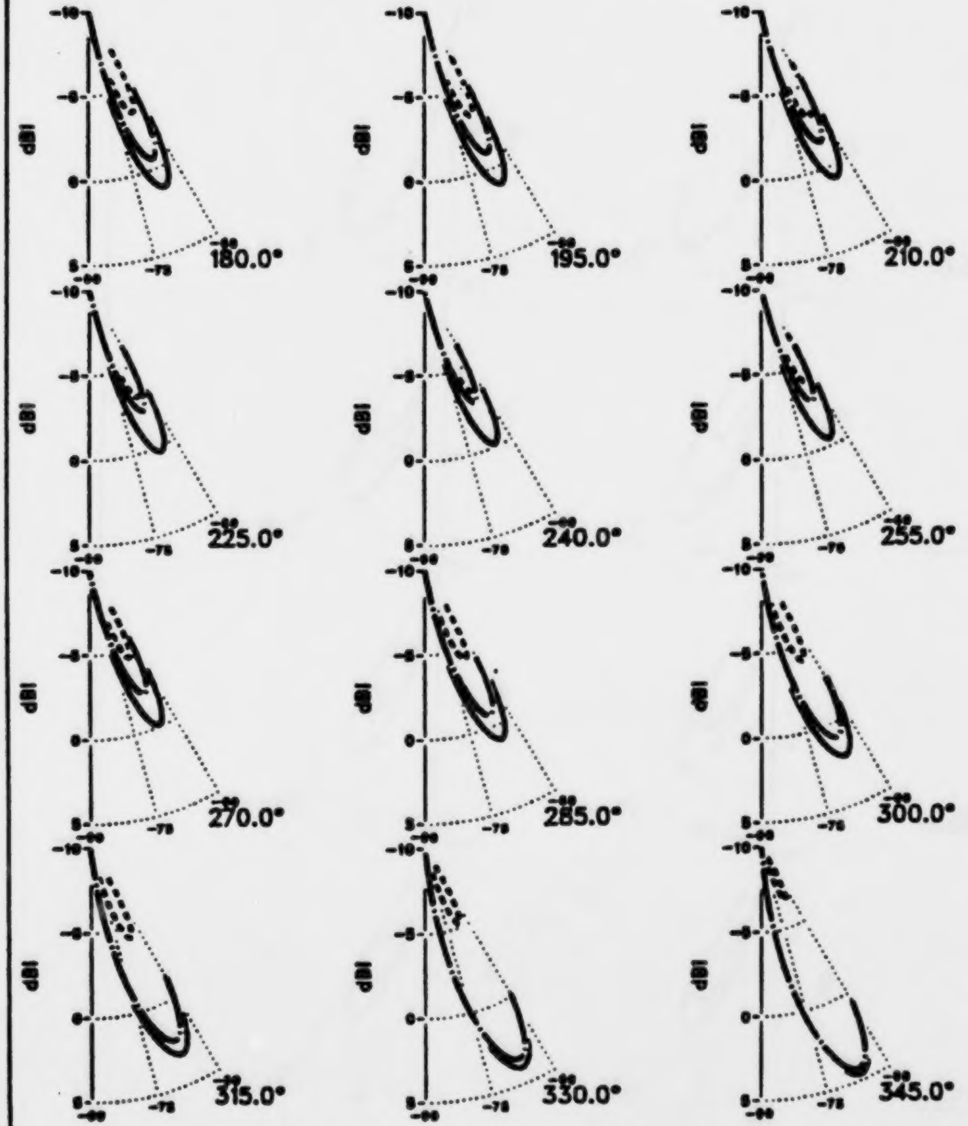

FIGURE B 40

FMH4X4TW

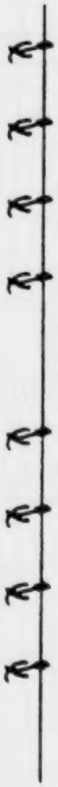

THETA = 60.00 PHI = 60.00 ETA = 90.00

antares
Antenna Analysis Resources

FIGURE B 41

212<

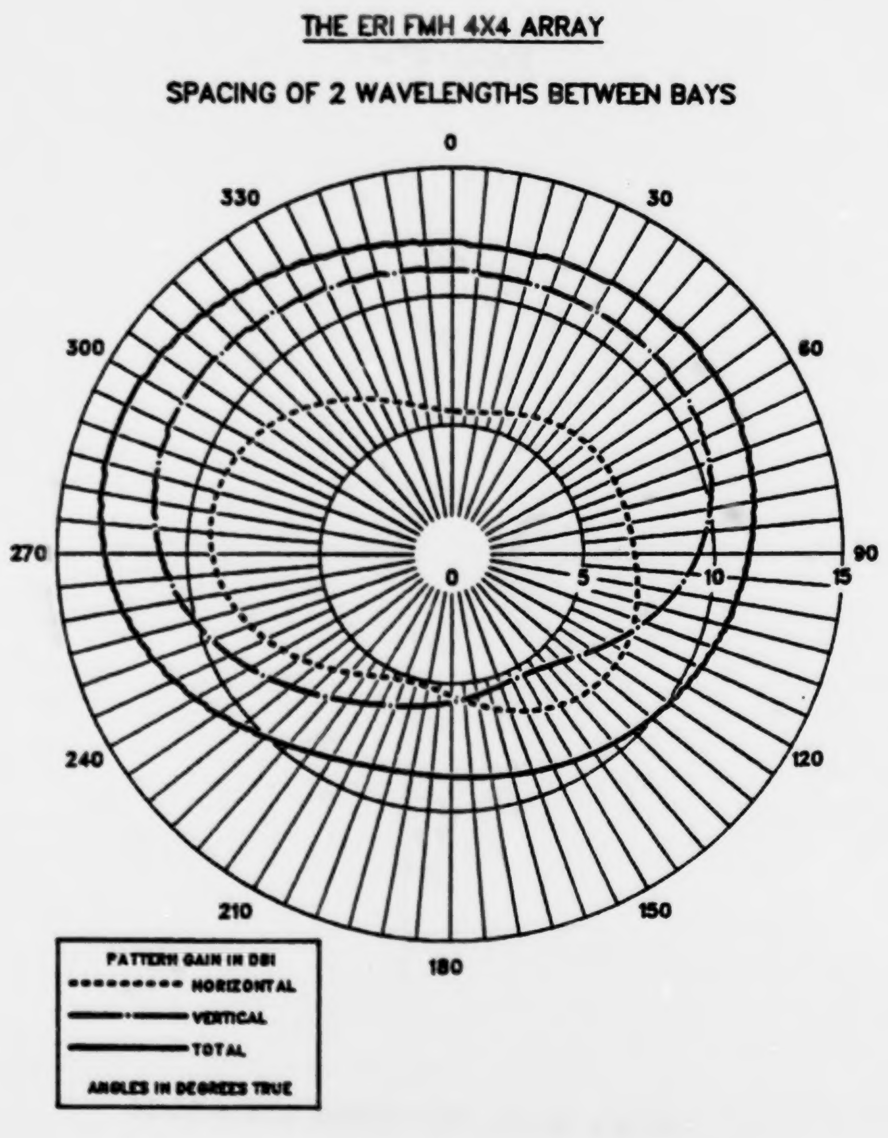
THE ERI FMH 4X4 ARRAY
SPACING OF 2 WAVELENGTHS BETWEEN BAYS
0
30
60
90
120
150
180
210
240
270
300
330
0
5
10
15
PATTERN GAIN IN DBI
HORIZONTAL
VERTICAL
TOTAL
ANGLES IN DEGREES TRUE

FIGURE B 42

THE ERI FMH 4X4 ARRAY

SPACING OF 2 WAVELENGTHS BETWEEN BAYS

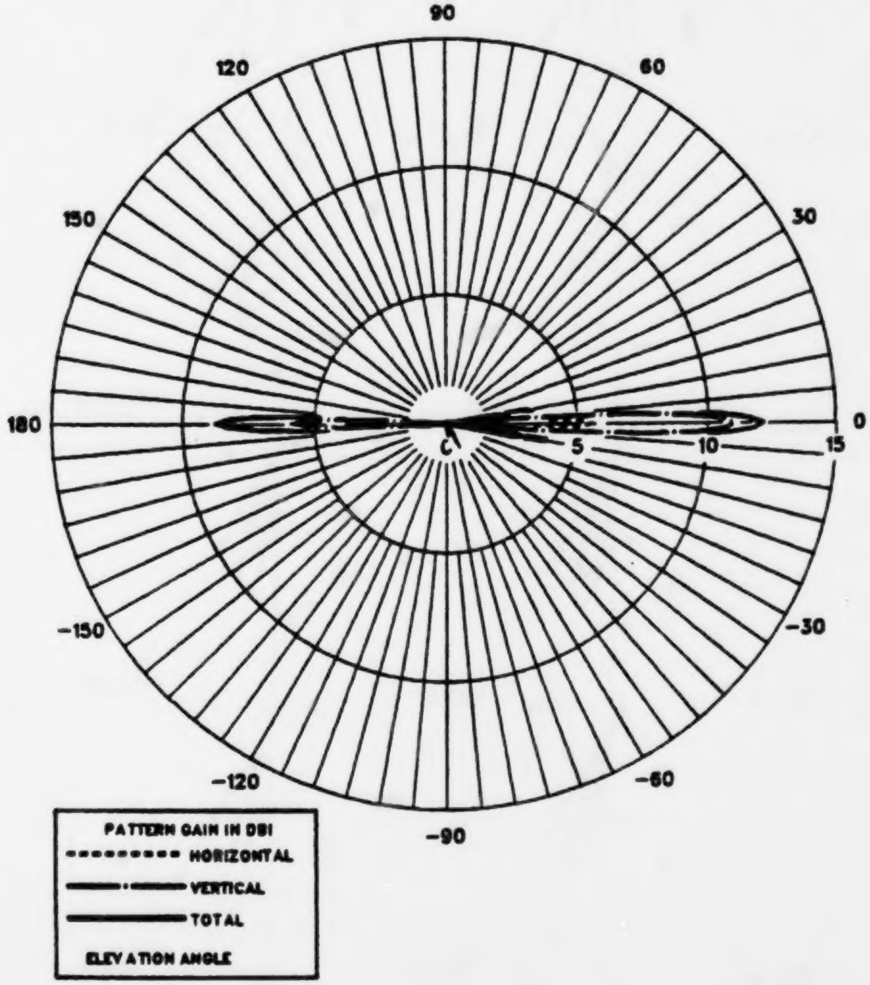

FIGURE B 43

THE ERI FMH 4X4 ARRAY

SPACING OF 2 WAVELENGTHS BETWEEN BAYS

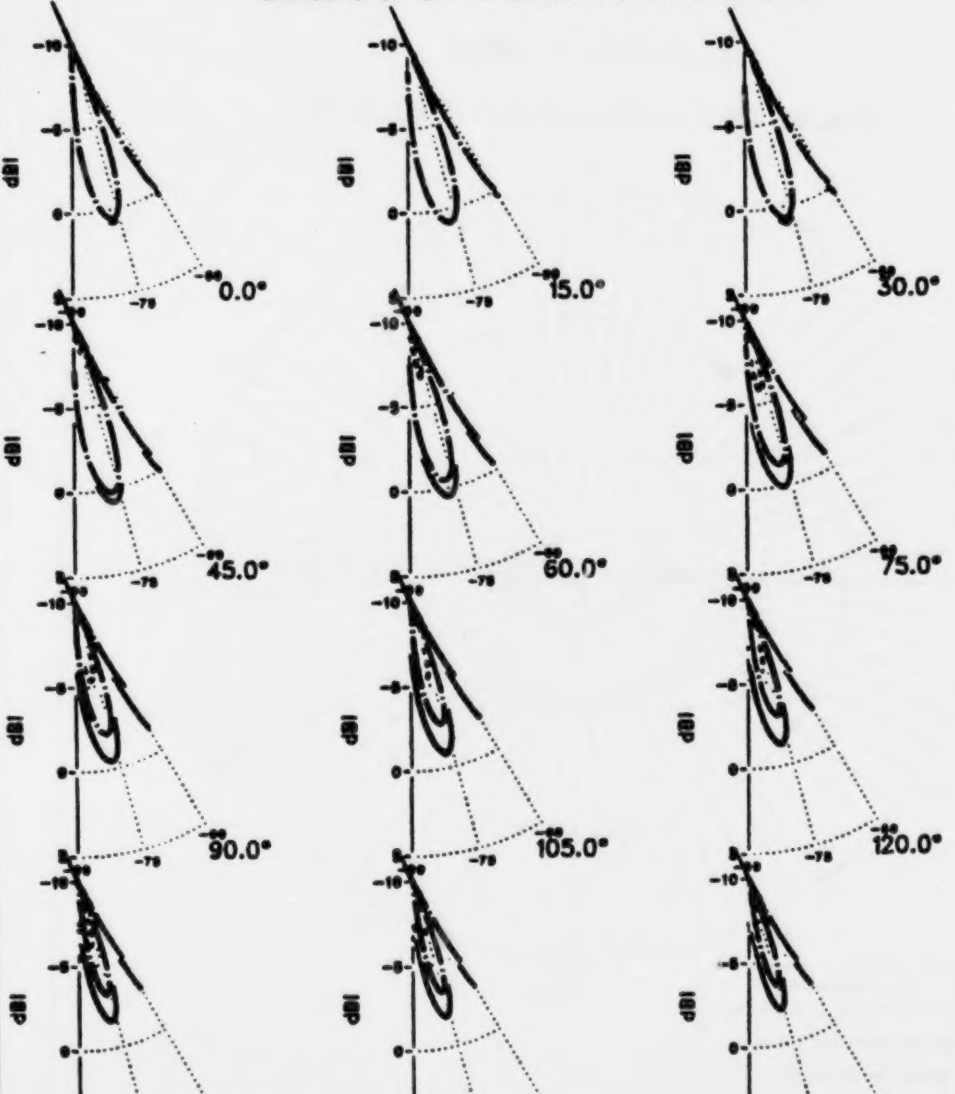

FIGURE B 44

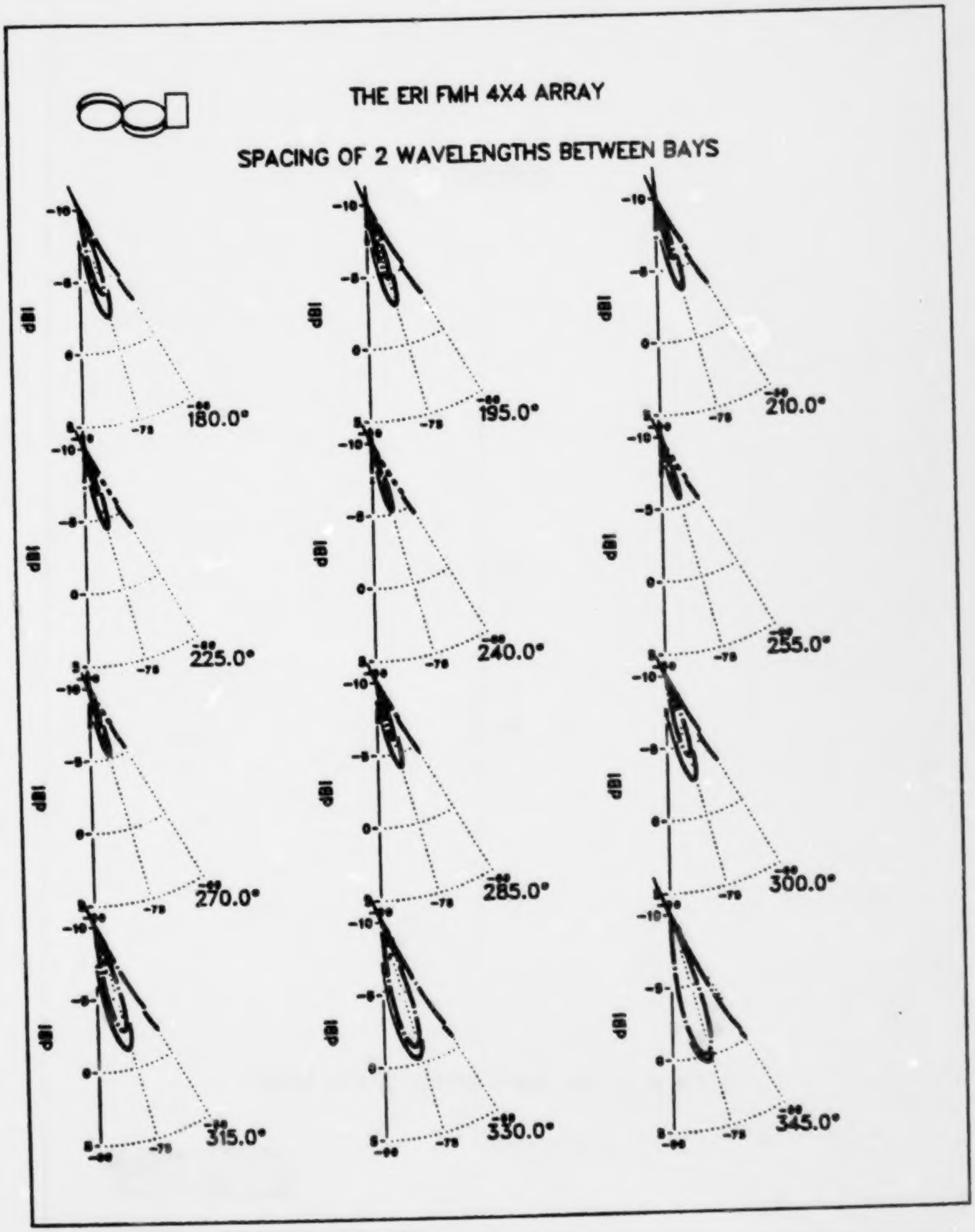
THE ERI FMH 4X4 ARRAY

SPACING OF 2 WAVELENGTHS BETWEEN BAYS

FIGURE B 45

CYC2X2

THETA = 60.00 PHI = 60.00 ETA = 90.00

antares
Antenna Analysis Resources

FIGURE B 46

THE CYCLOID 2X2 ARRAY

STANDARD SPACING OF ONE WAVELENGTH BETWEEN BAYS

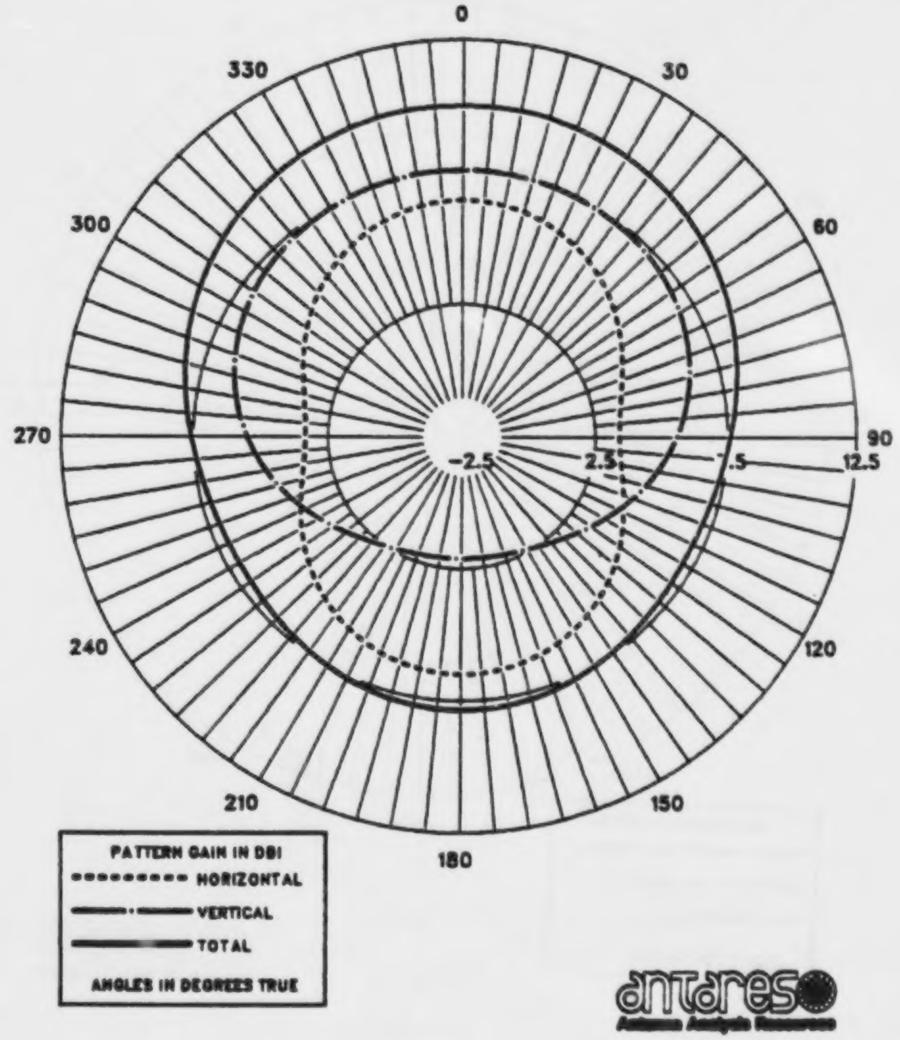

FIGURE B 47

THE CYCLOID 2X2 ARRAY

STANDARD SPACING OF ONE WAVELENGTH BETWEEN BAYS

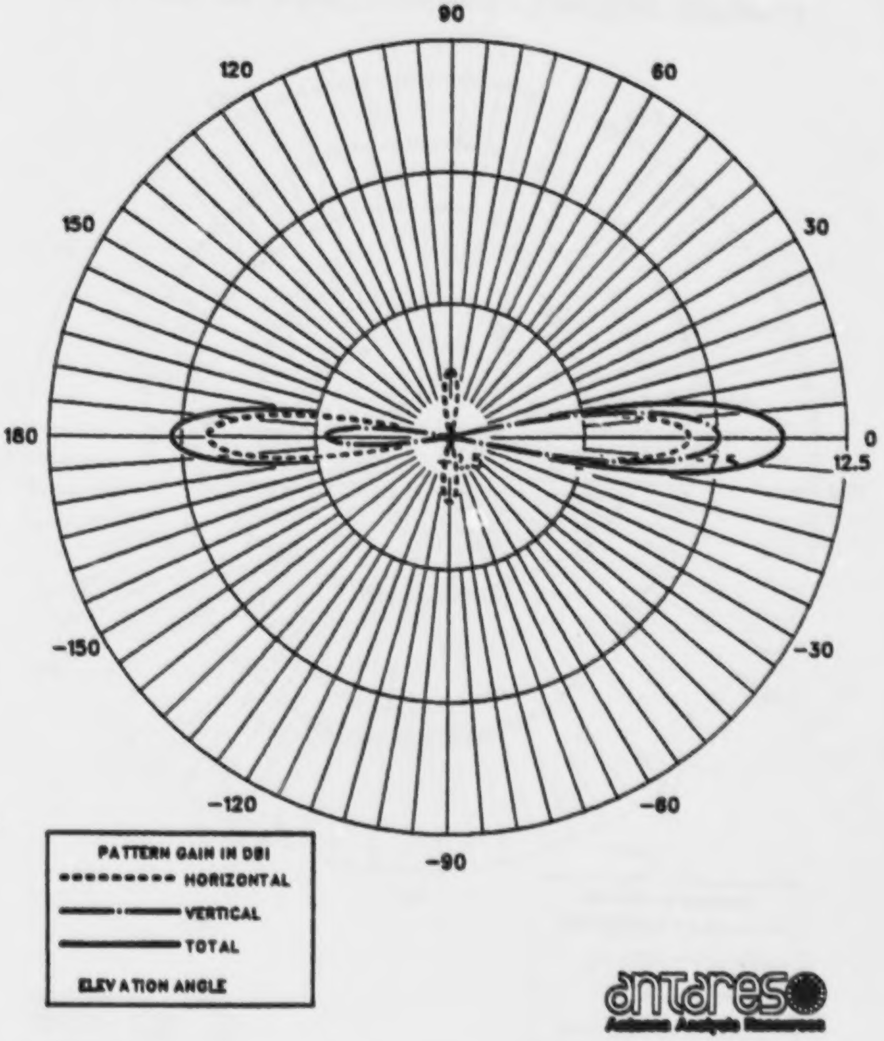

FIGURE B 48

THE CYCLOID 2X2 ARRAY

STANDARD SPACING OF ONE WAVELENGTH BETWEEN BAYS

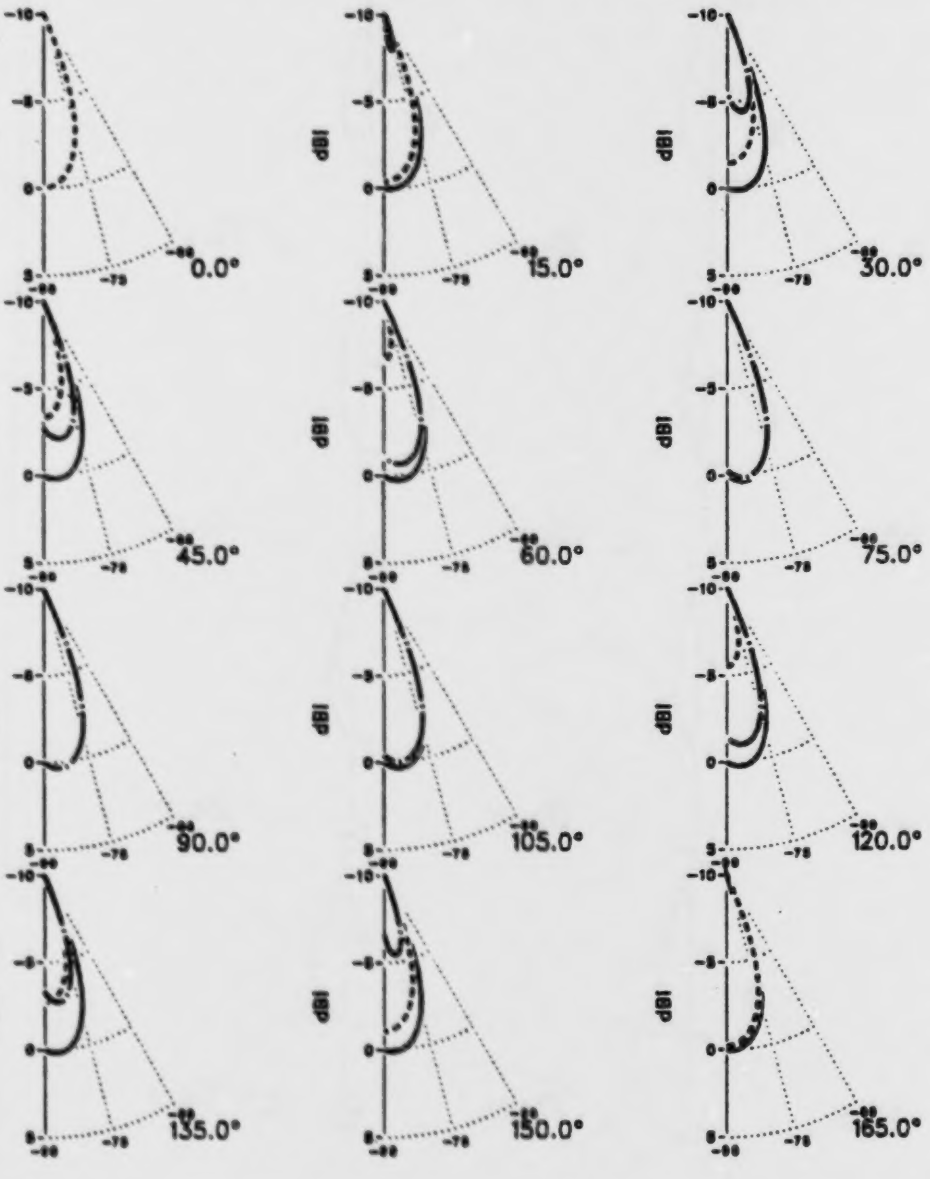

FIGURE B 49

THE CYCLOID 2X2 ARRAY

STANDARD SPACING OF ONE WAVELENGTH BETWEEN BAYS

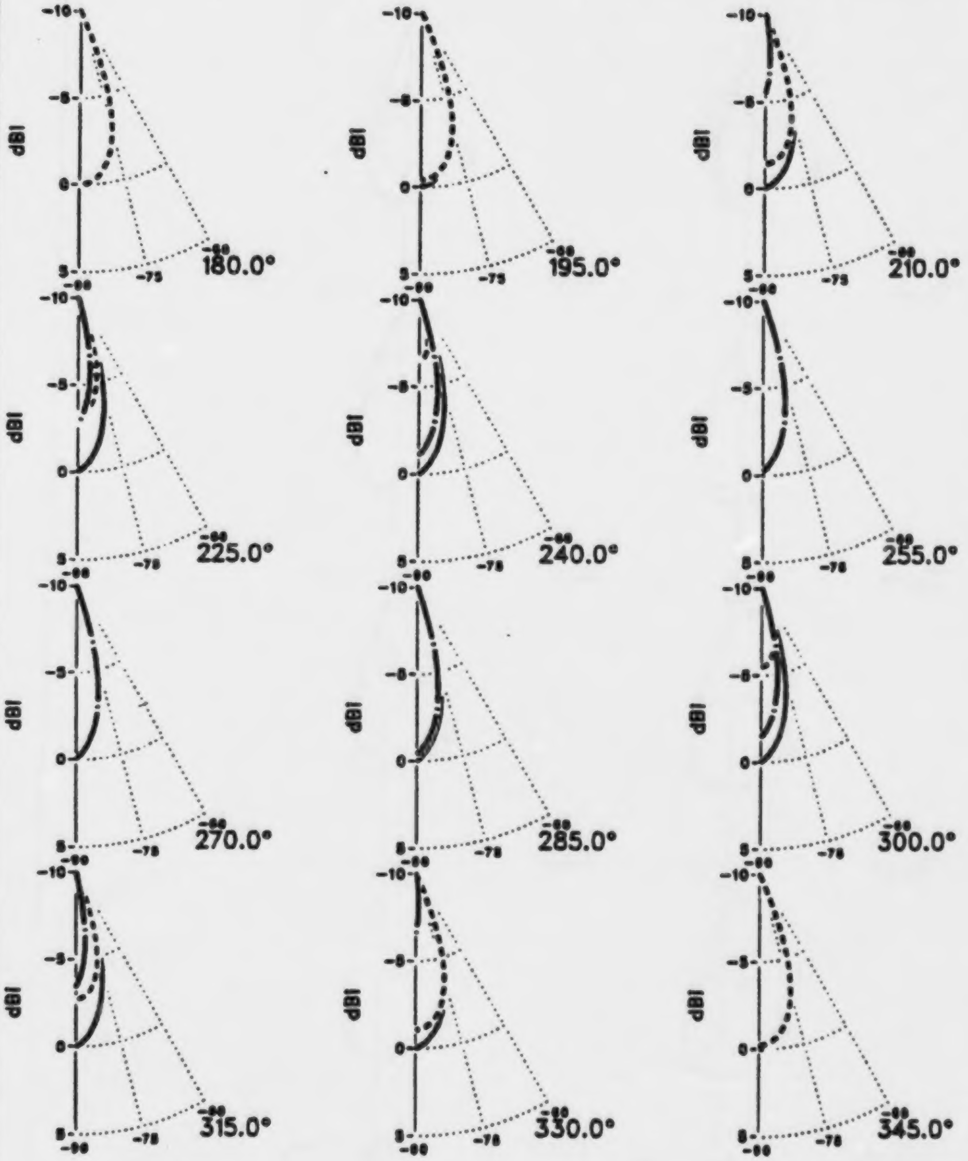

FIGURE B 50

CYC2X2TH

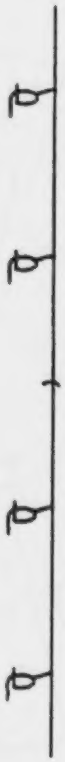

THETA = 60.00 PHI = 60.00 ETA = 90.00

antares
Antenna Analysis Resources

FIGURE B 51

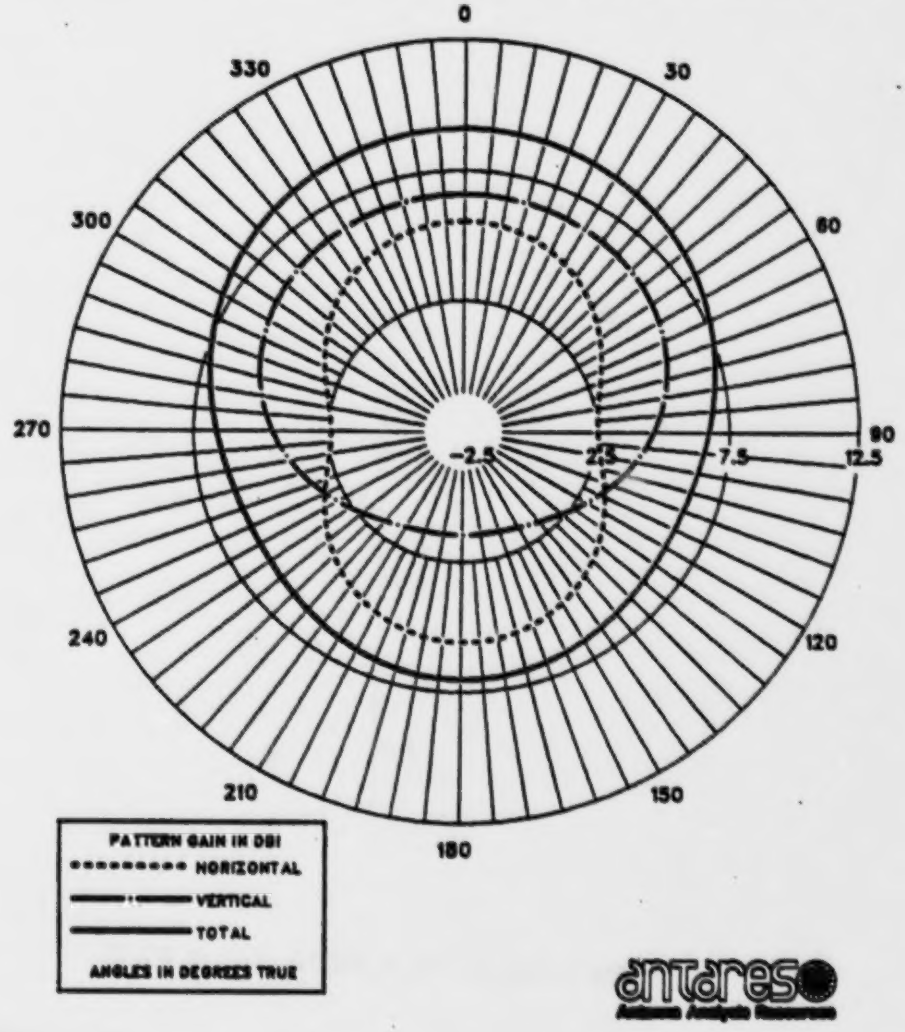
THE CYCLOID 2X2 ARRAY
SPACING OF 3/2 WAVELENGTHS BETWEEN UPPER & LOWER BAYS
0
30
60
90
120
150
180
210
240
270
300
330
-2.5
2.5
7.5
12.5
PATTERN GAIN IN DBI
HORIZONTAL
VERTICAL
TOTAL
ANGLES IN DEGREES TRUE
antares
Antenna Analysis Resources

FIGURE B 52

THE CYCLOID 2X2 ARRAY

SPACING OF 3/2 WAVELENGTHS BETWEEN UPPER & LOWER BAYS

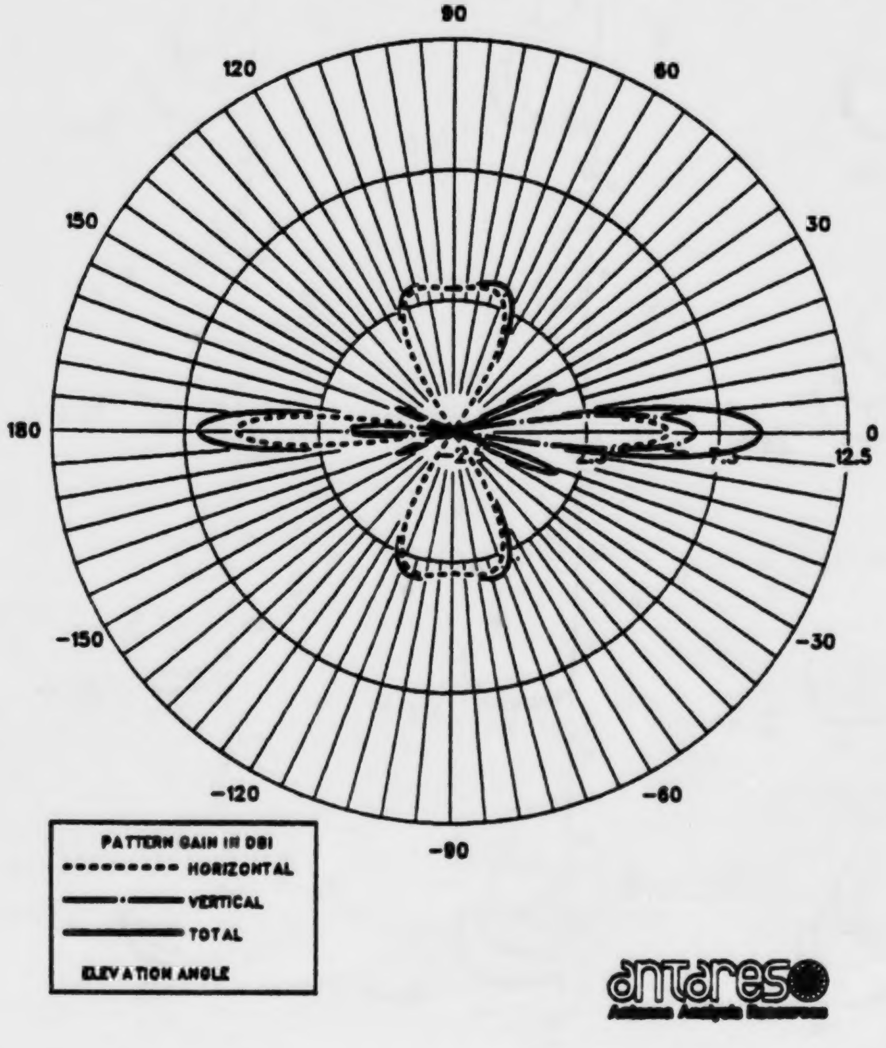

FIGURE B 53

THE CYCLOID 2X2 ARRAY

SPACING OF 3/2 WAVELENGTHS BETWEEN UPPER & LOWER BAYS

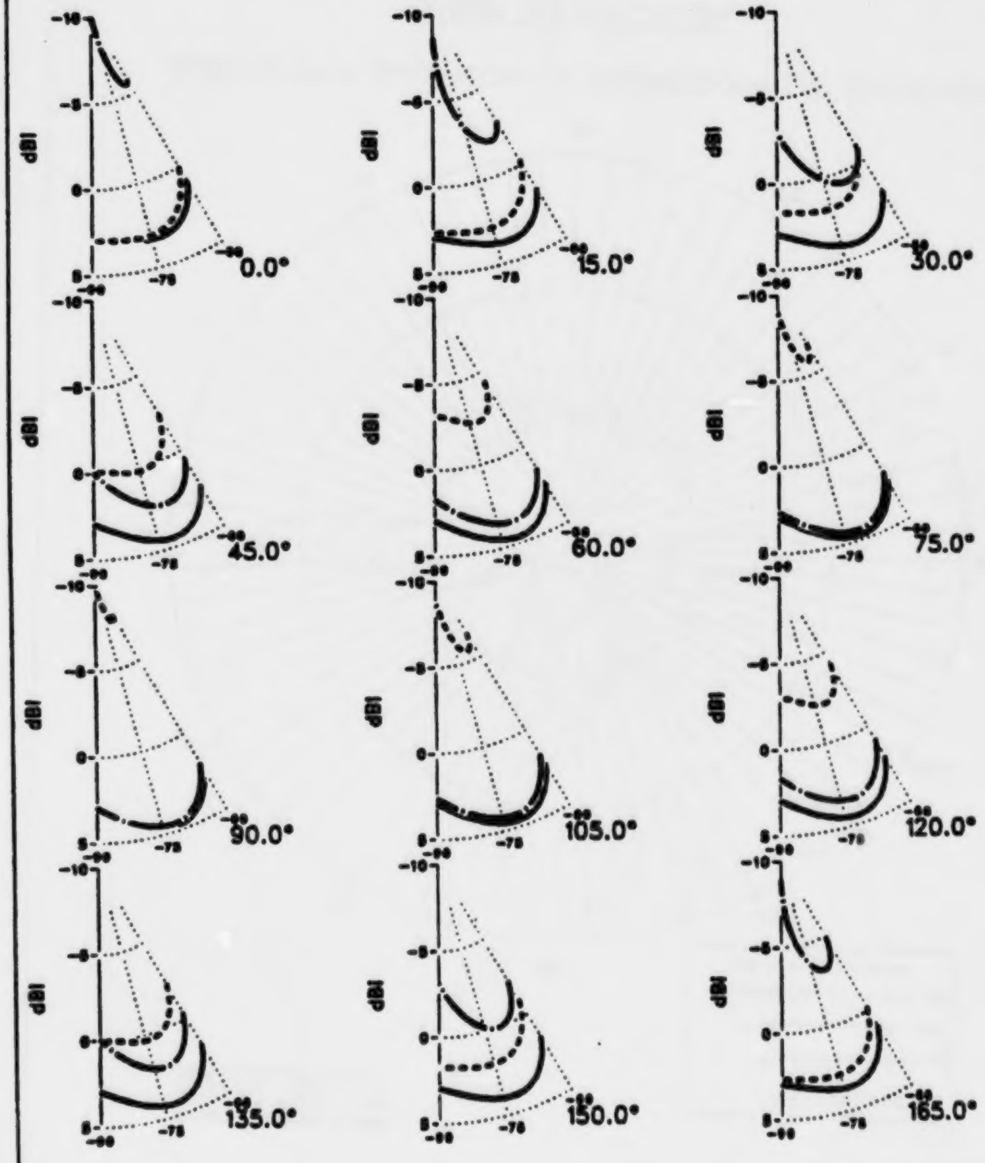

FIGURE B 54

THE CYCLOID 2X2 ARRAY

SPACING OF 3/2 WAVELENGTHS BETWEEN UPPER & LOWER BAYS

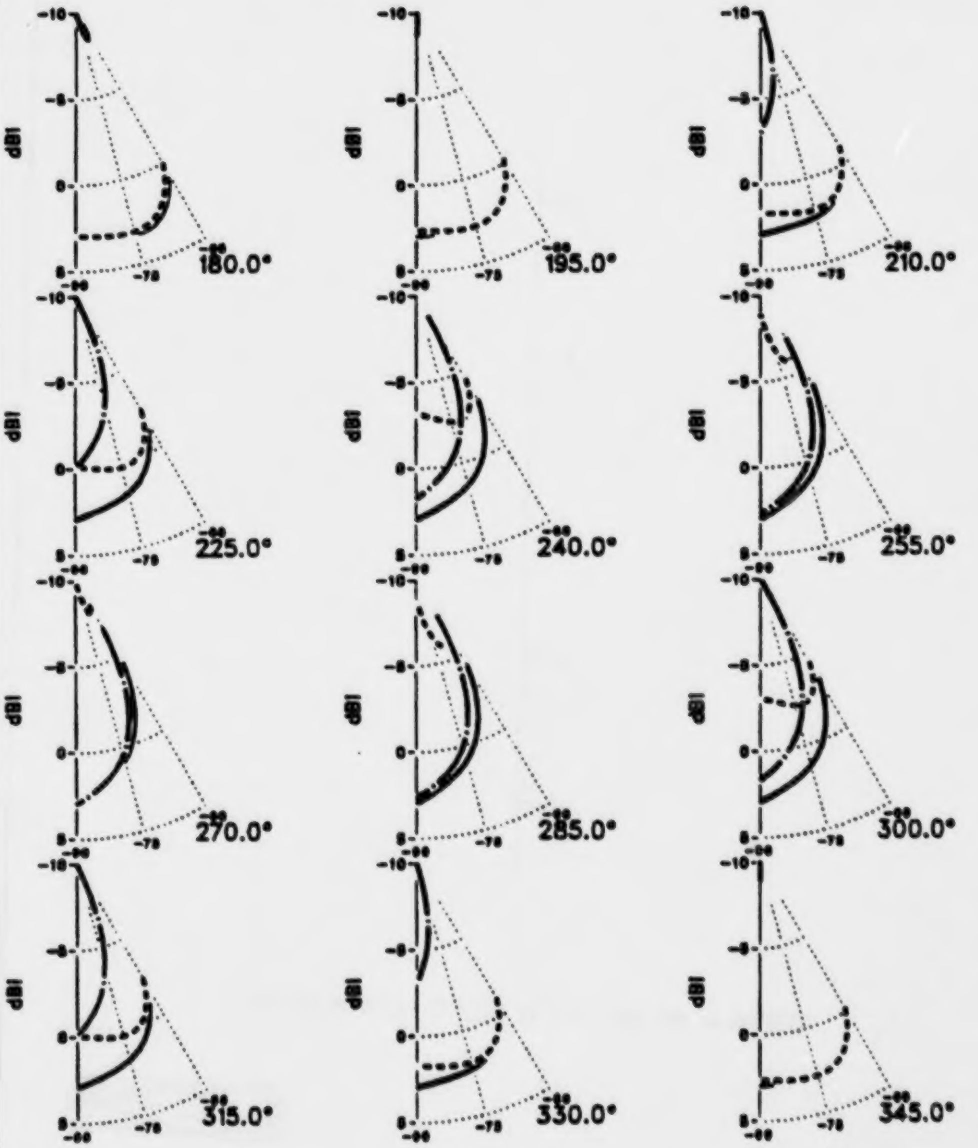

FIGURE B 55

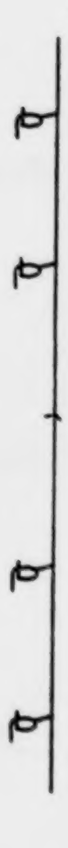

CYC2X2TW

THETA = 60.00 PHI = 60.00 ETA = 90.00

FIGURE B 56

THE CYCLOID 2X2 ARRAY

SPACING OF TWO WAVELENGTHS BETWEEN BAYS

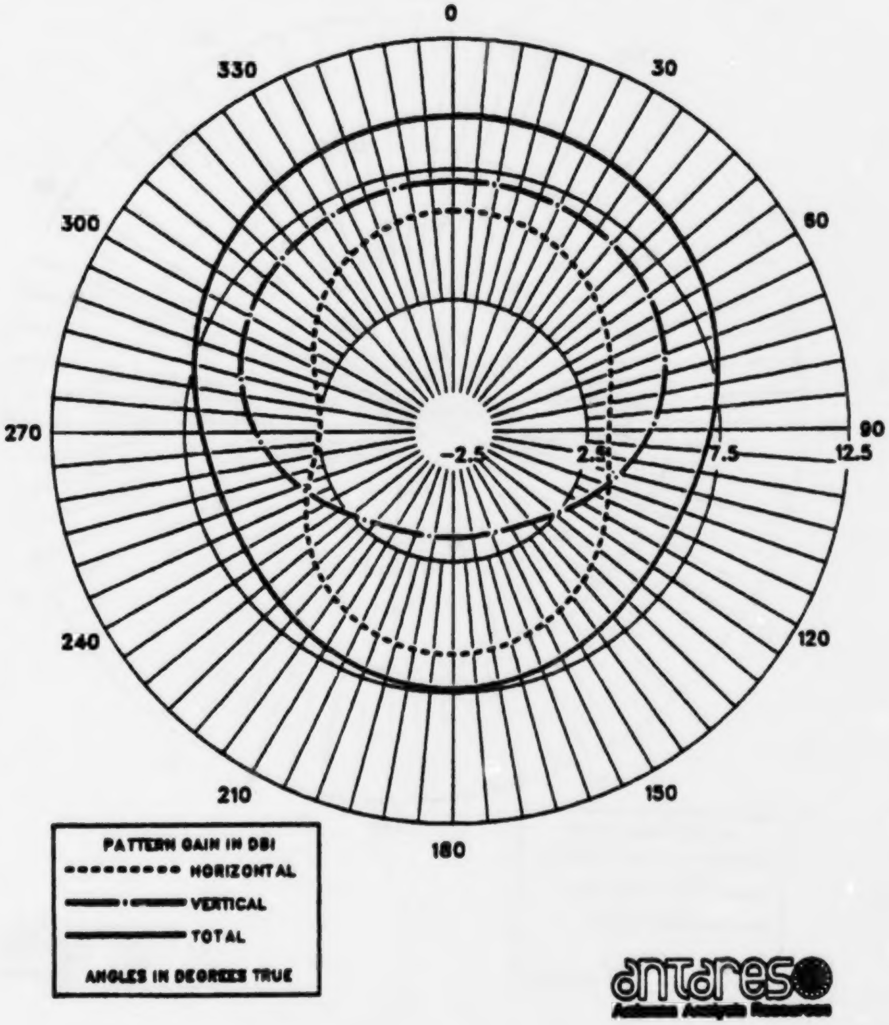

antares
Antenna Analysis Resources

FIGURE B 57

THE CYCLOID 2X2 ARRAY

SPACING OF TWO WAVELENGTHS BETWEEN BAYS

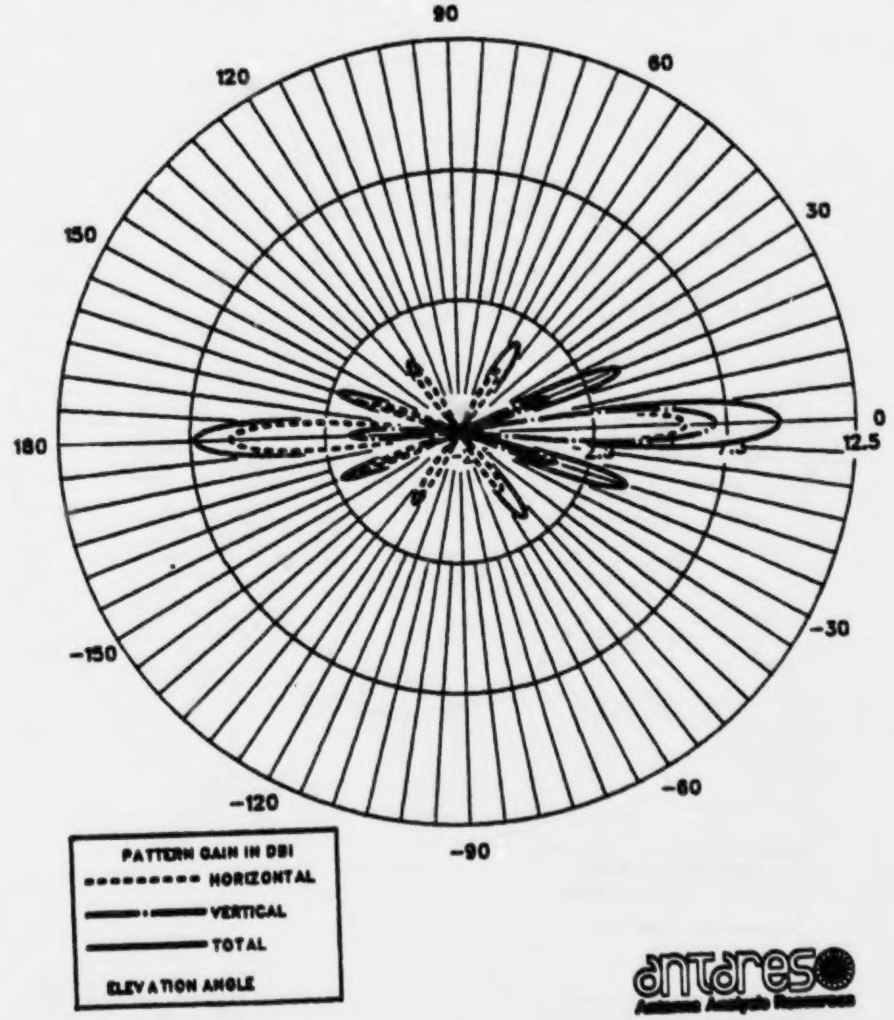

FIGURE B 58

THE CYCLOID 2X2 ARRAY

SPACING OF TWO WAVELENGTHS BETWEEN UPPER & LOWER BAYS

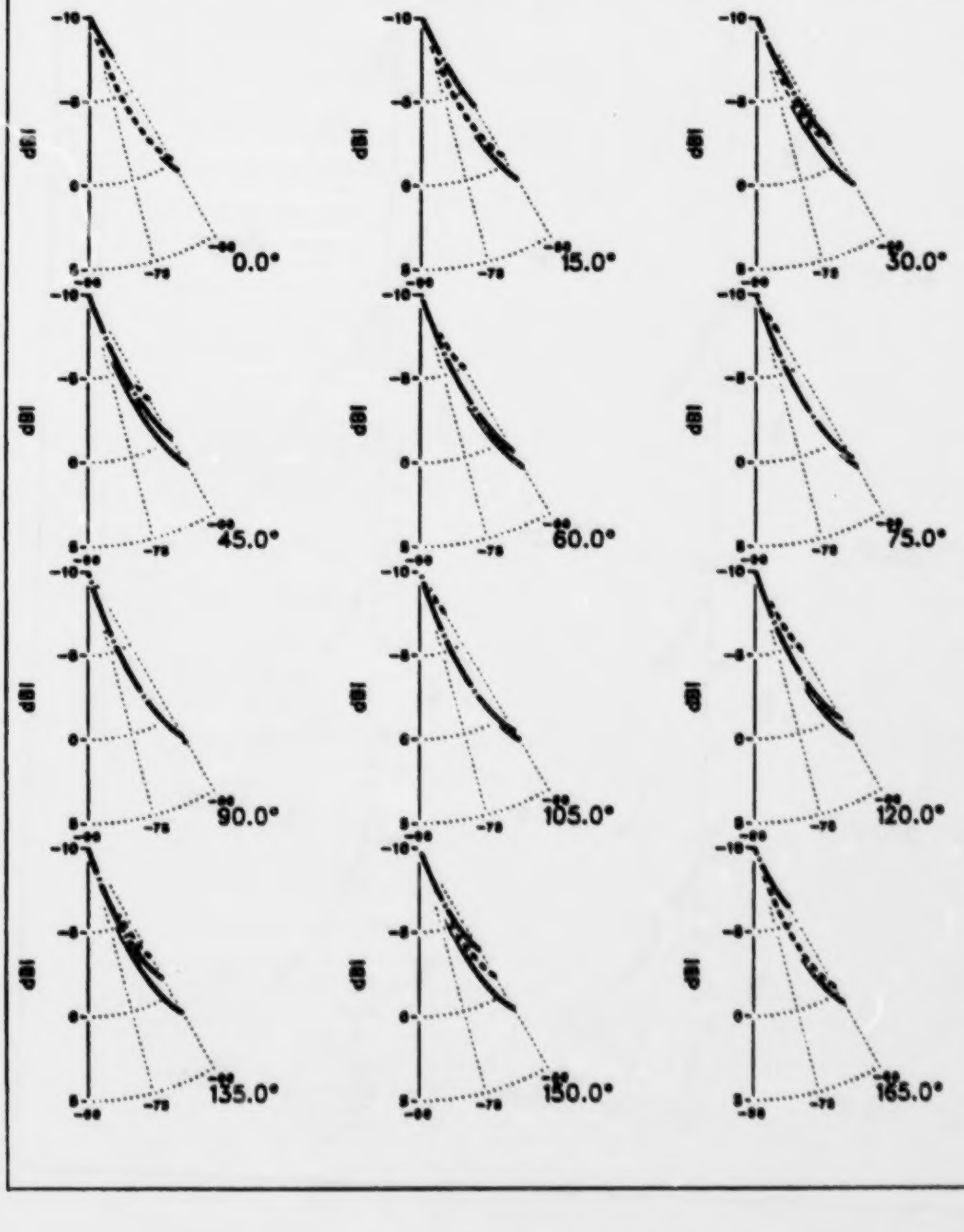

FIGURE B 59

THE CYCLOID 2X2 ARRAY

SPACING OF TWO WAVELENGTHS BETWEEN UPPER & LOWER BAYS

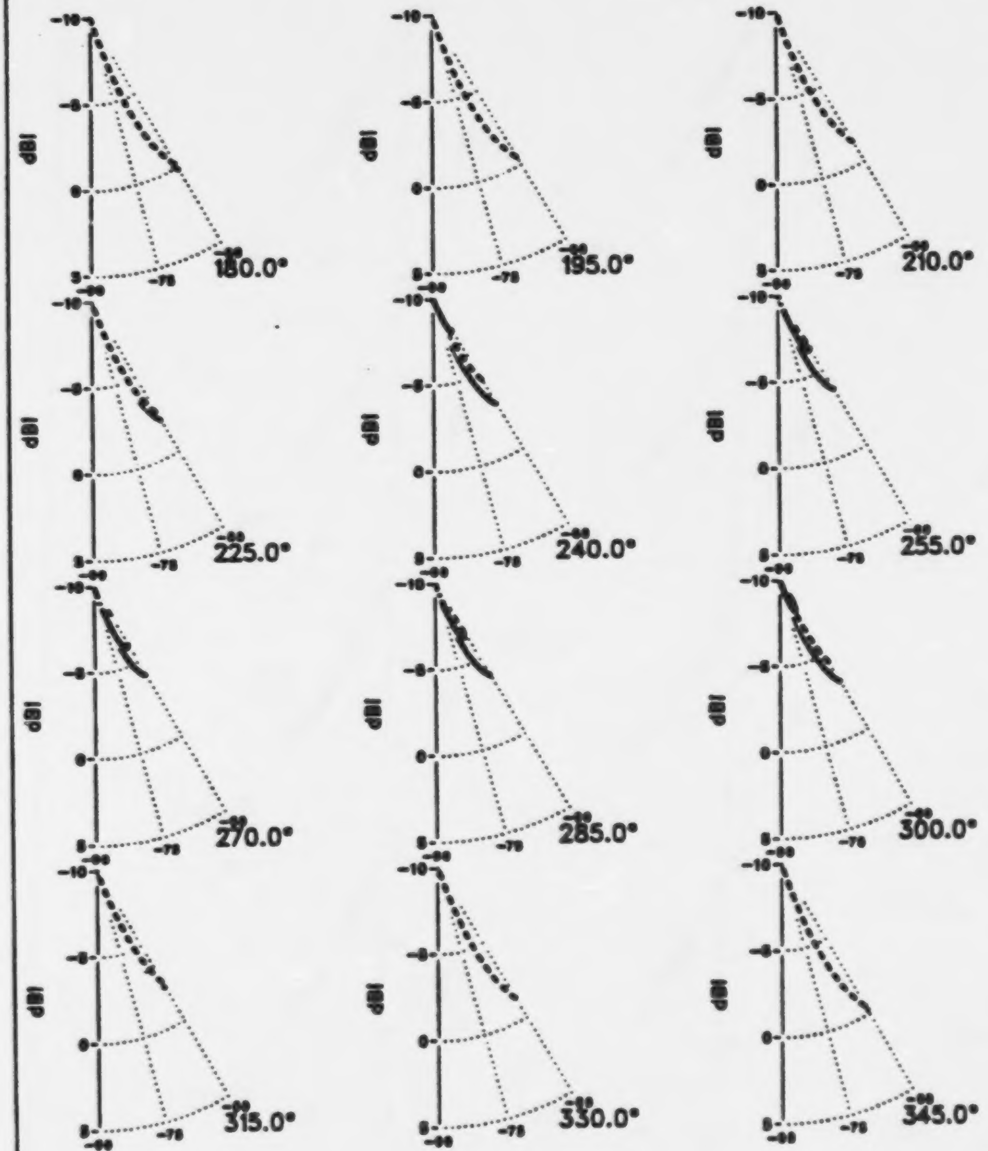

FIGURE B 60

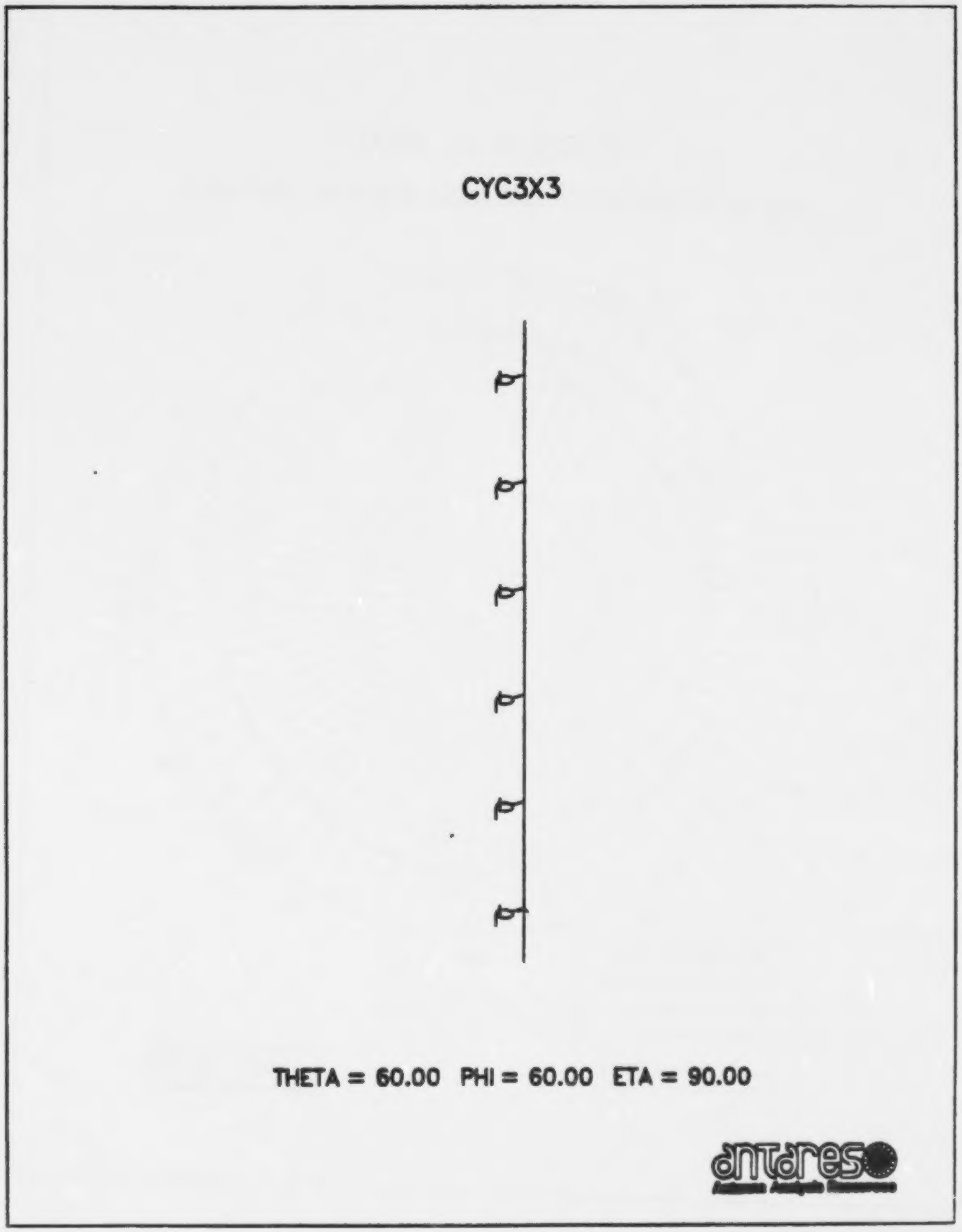

FIGURE B 61

THE CYCLOID 3X3 ARRAY

STANDARD SPACING OF ONE WAVELENGTH BETWEEN BAYS

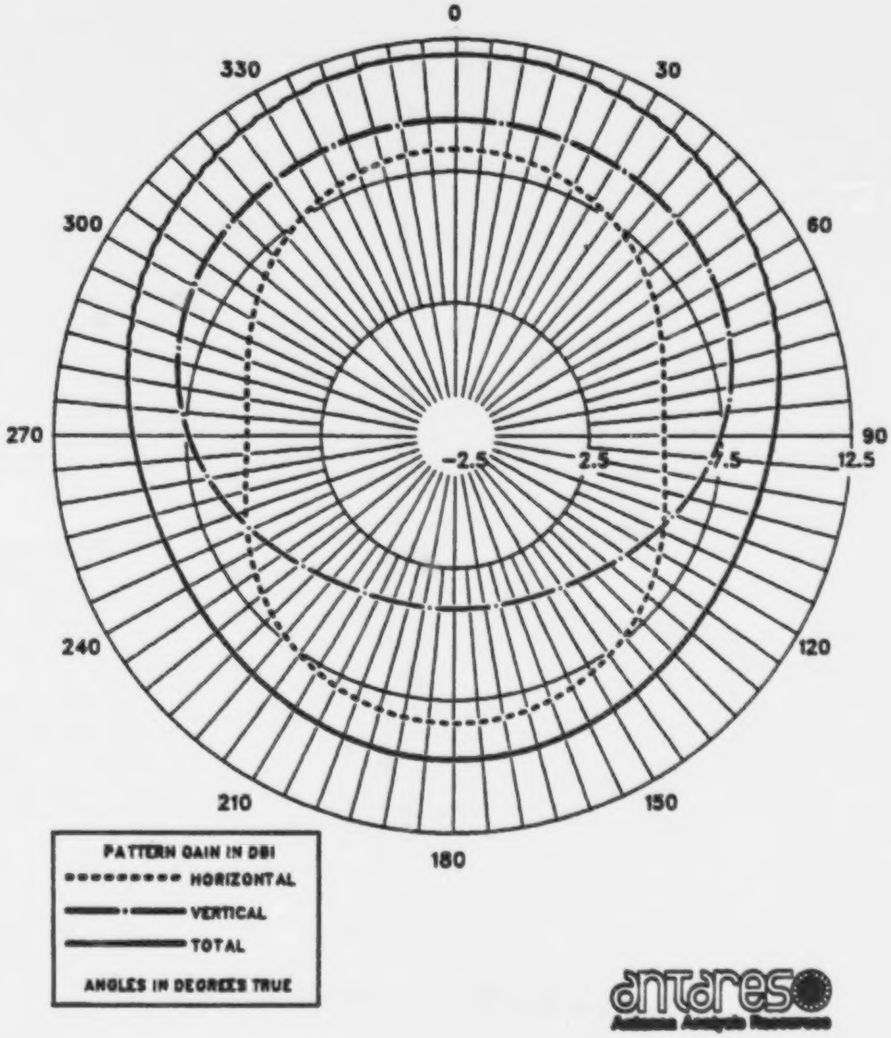

antares
Antenna Analysis Resources

233<

FIGURE B 62

THE CYCLOID 3X3 ARRAY

STANDARD SPACING OF ONE WAVELENGTH BETWEEN BAYS

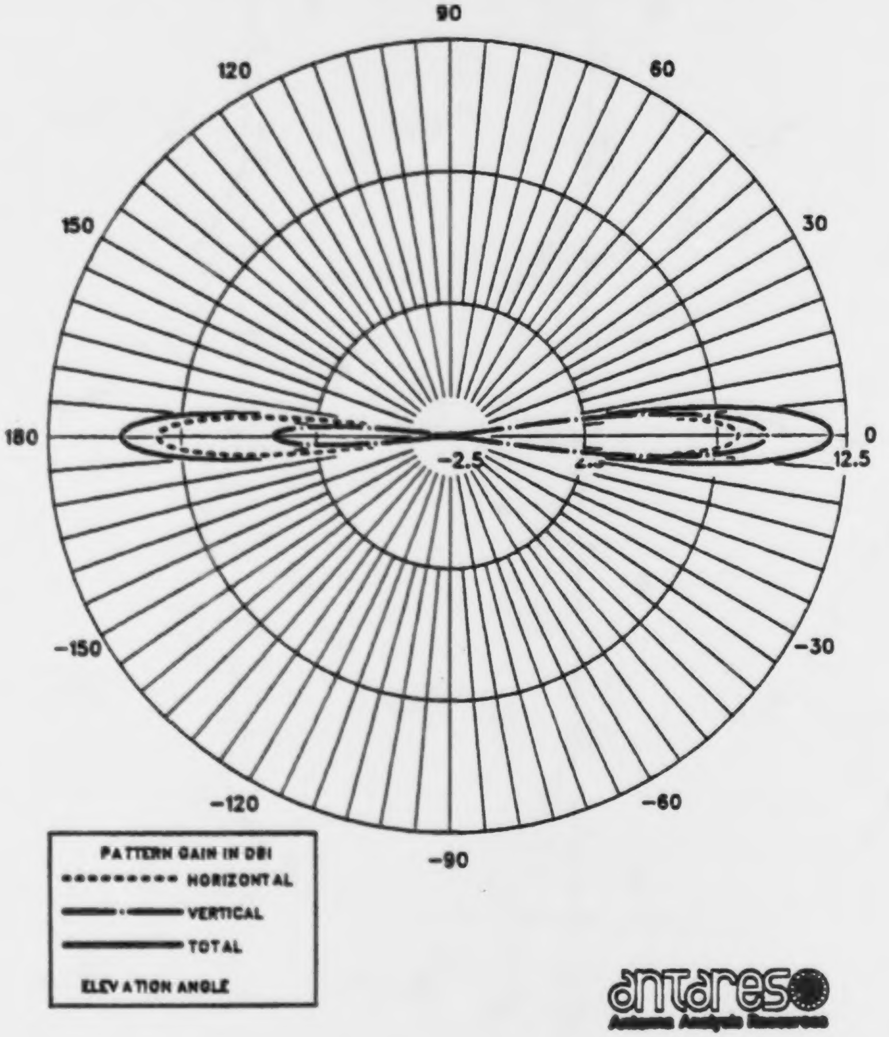

antares
Antenna Analysis Resources

FIGURE B 63

THE CYCLOID 3X3 ARRAY

STANDARD SPACING OF ONE WAVELENGTH BETWEEN BAYS

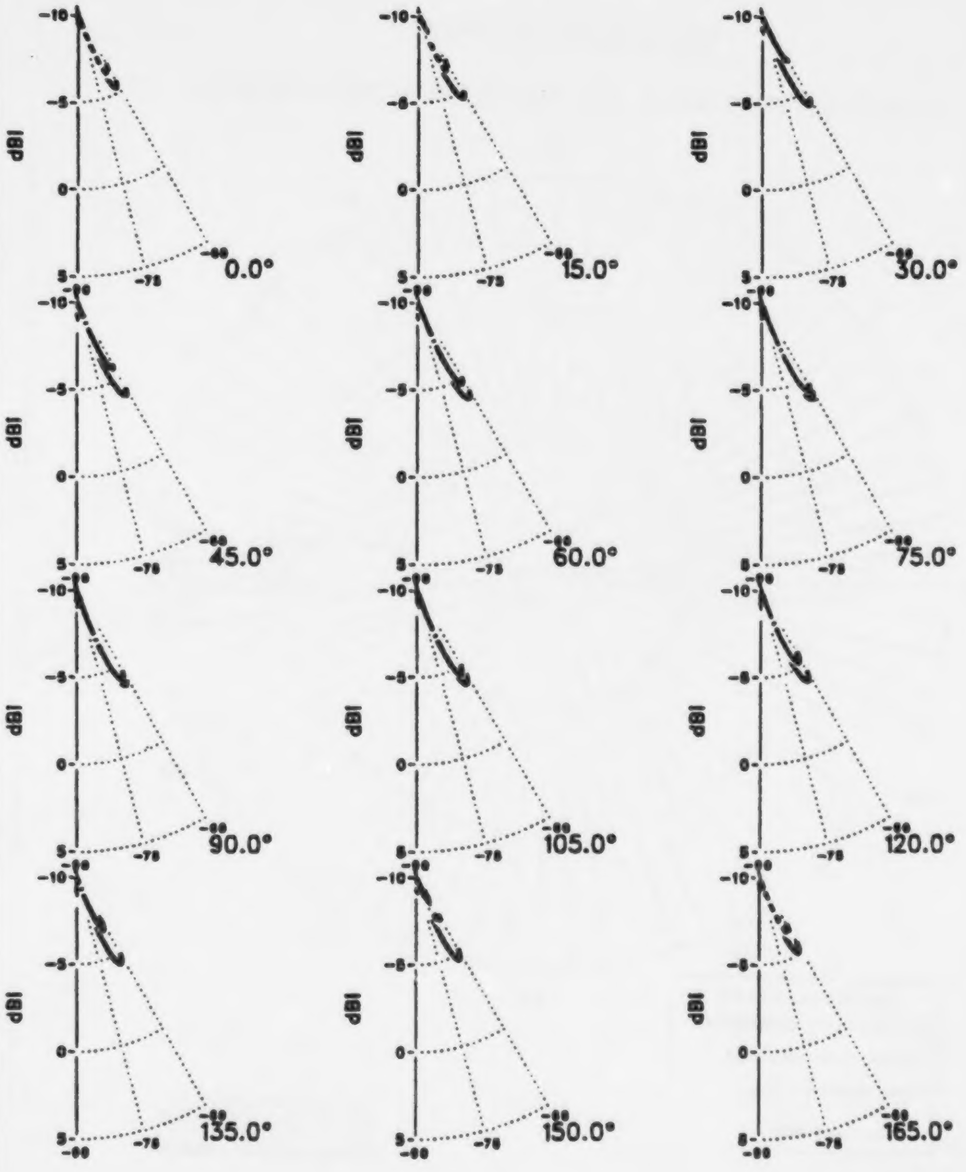

FIGURE B 64

THE CYCLOID 3X3 ARRAY

STANDARD SPACING OF ONE WAVELENGTH BETWEEN BAYS

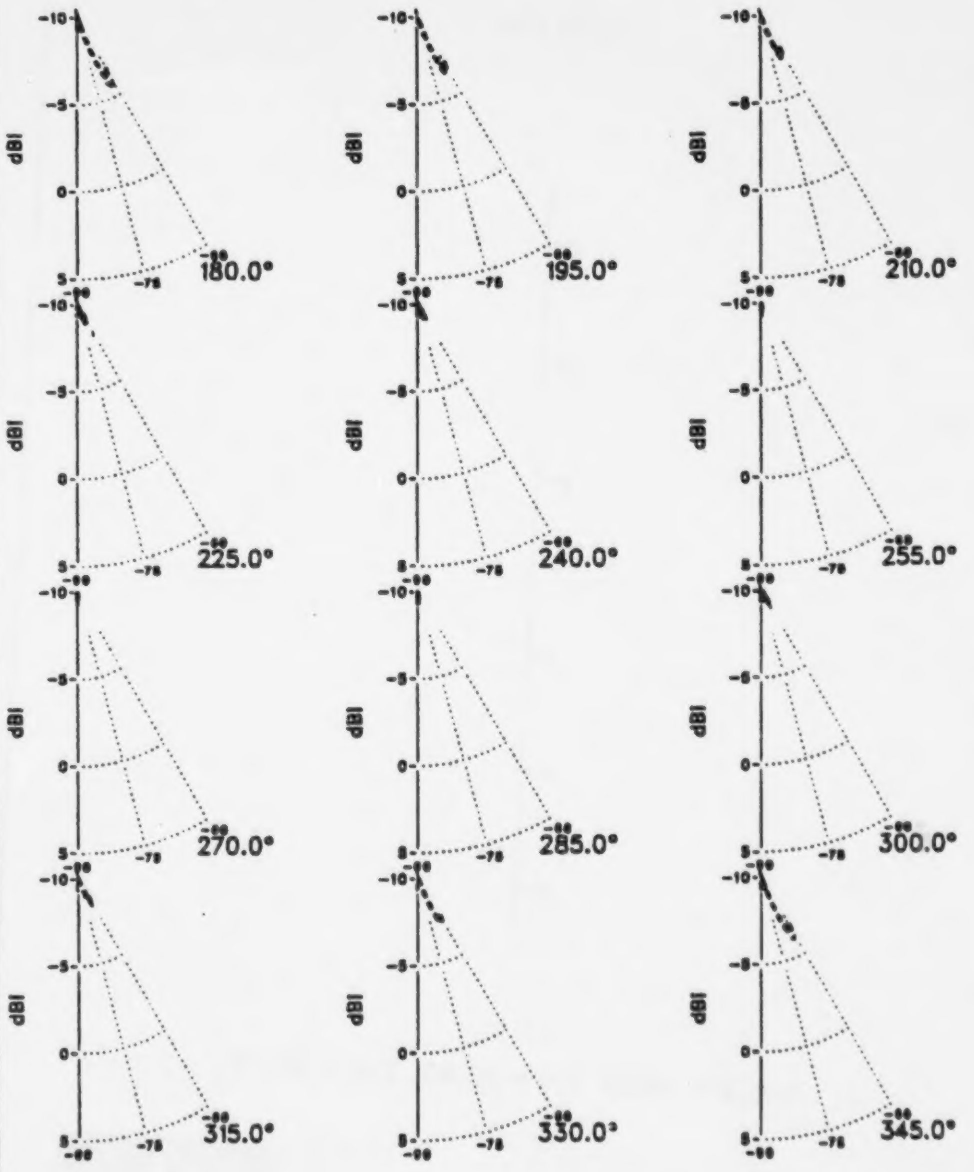

FIGURE B 65

CYC3X3TH

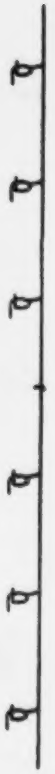

THETA = 60.00 PHI = 60.00 ETA = 90.00

antares
Antenna Analysis Resources

FIGURE B 66

THE CYCLOID 3X3 ARRAY

SPACING OF 3/2 WAVELENGTHS BETWEEN UPPER & LOWER BAYS

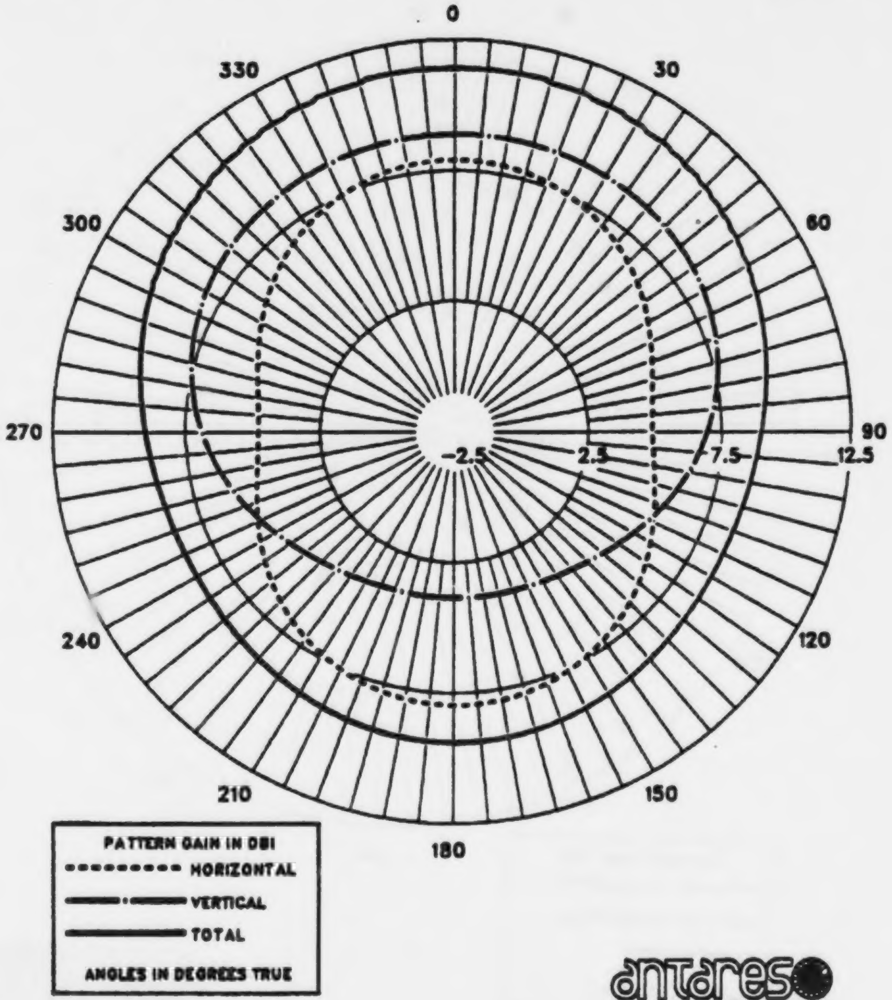

antares
Antares Analysis Resources

FIGURE B 67

THE CYCLOID 3X3 ARRAY

SPACING OF 3/2 WAVELENGTHS BETWEEN UPPER & LOWER BAYS

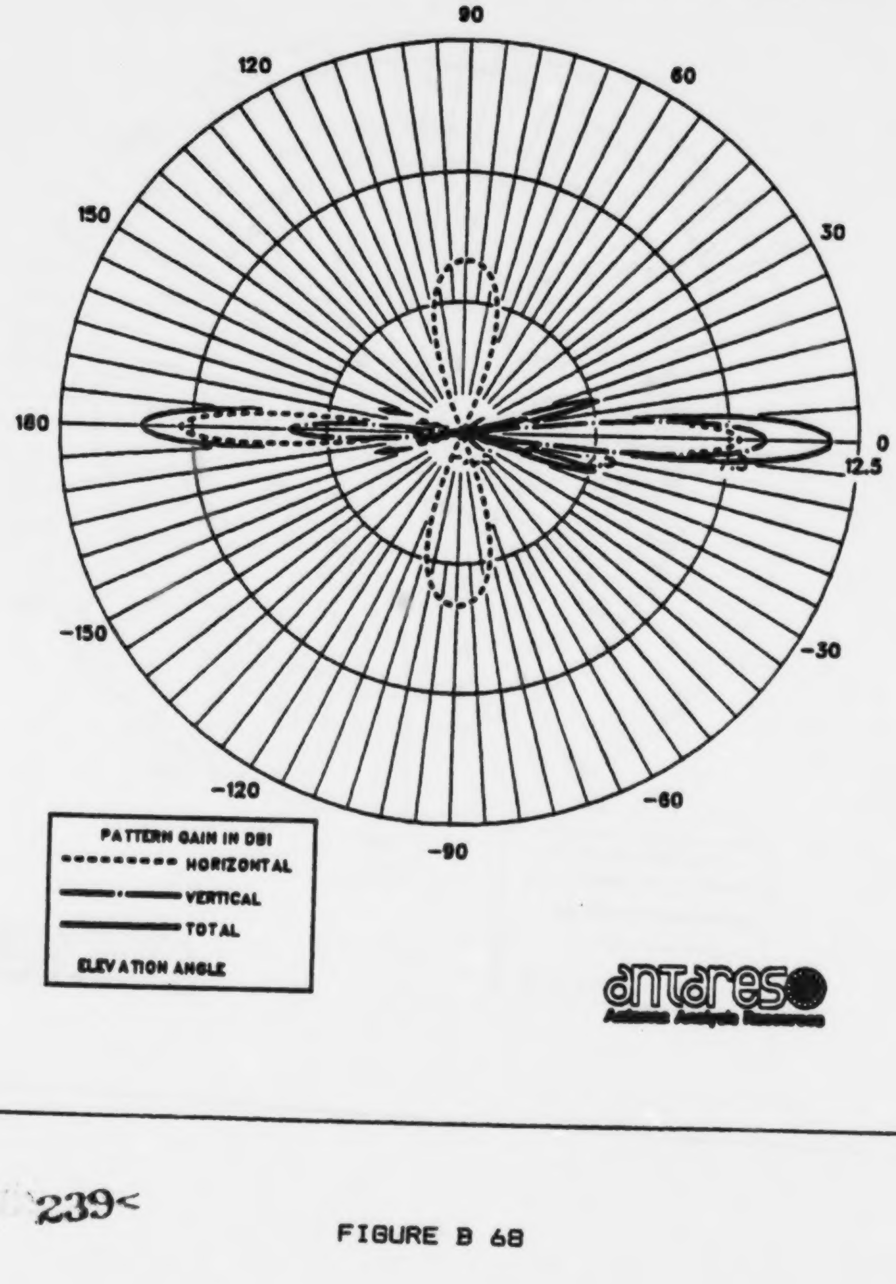

antares
Antenna Analysis Resources

FIGURE B 68

THE CYCLOID 3X3 ARRAY

SPACING OF 3/2 WAVELENGTHS BETWEEN UPPER & LOWER BAYS

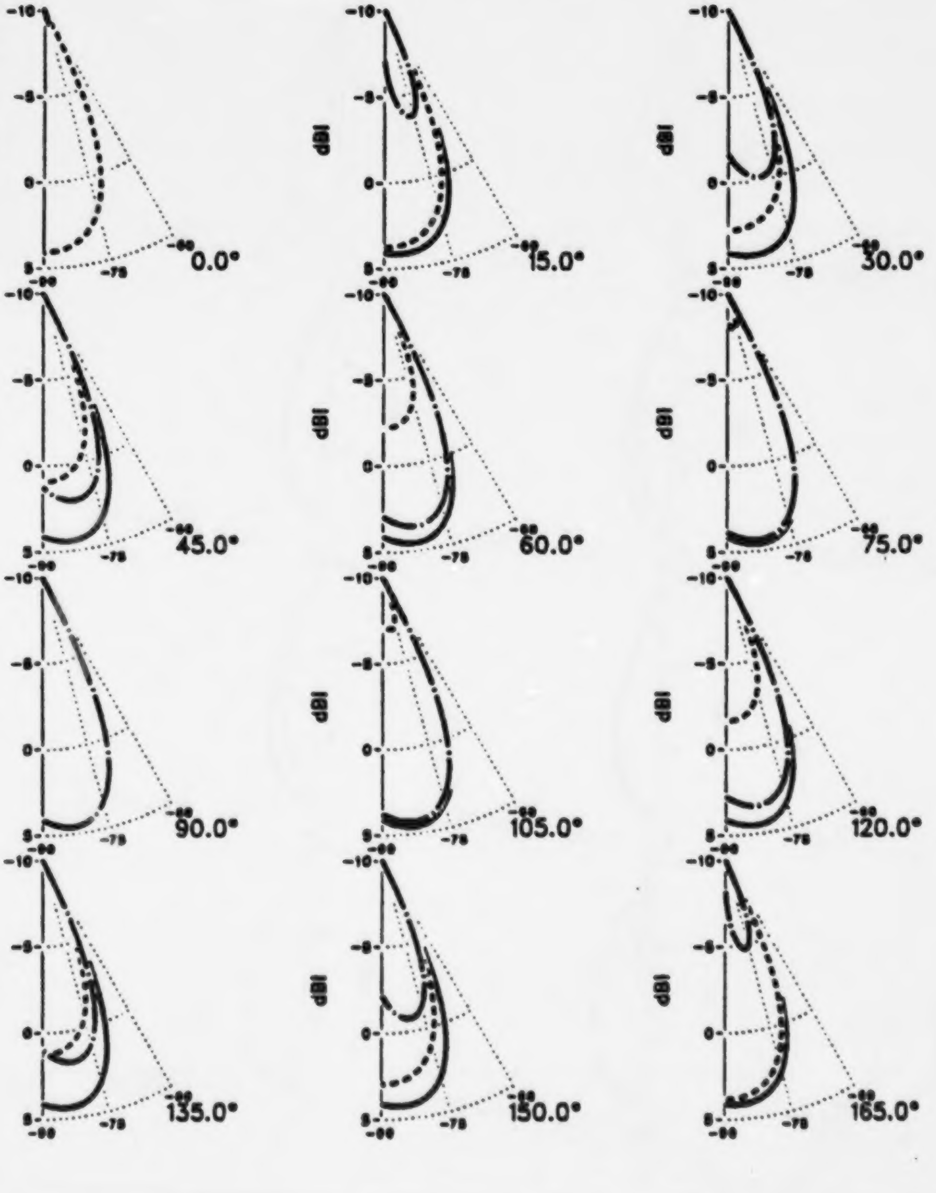

FIGURE B 69

THE CYCLOID 3X3 ARRAY

SPACING OF 3/2 WAVELENGTHS BETWEEN UPPER & LOWER BAYS

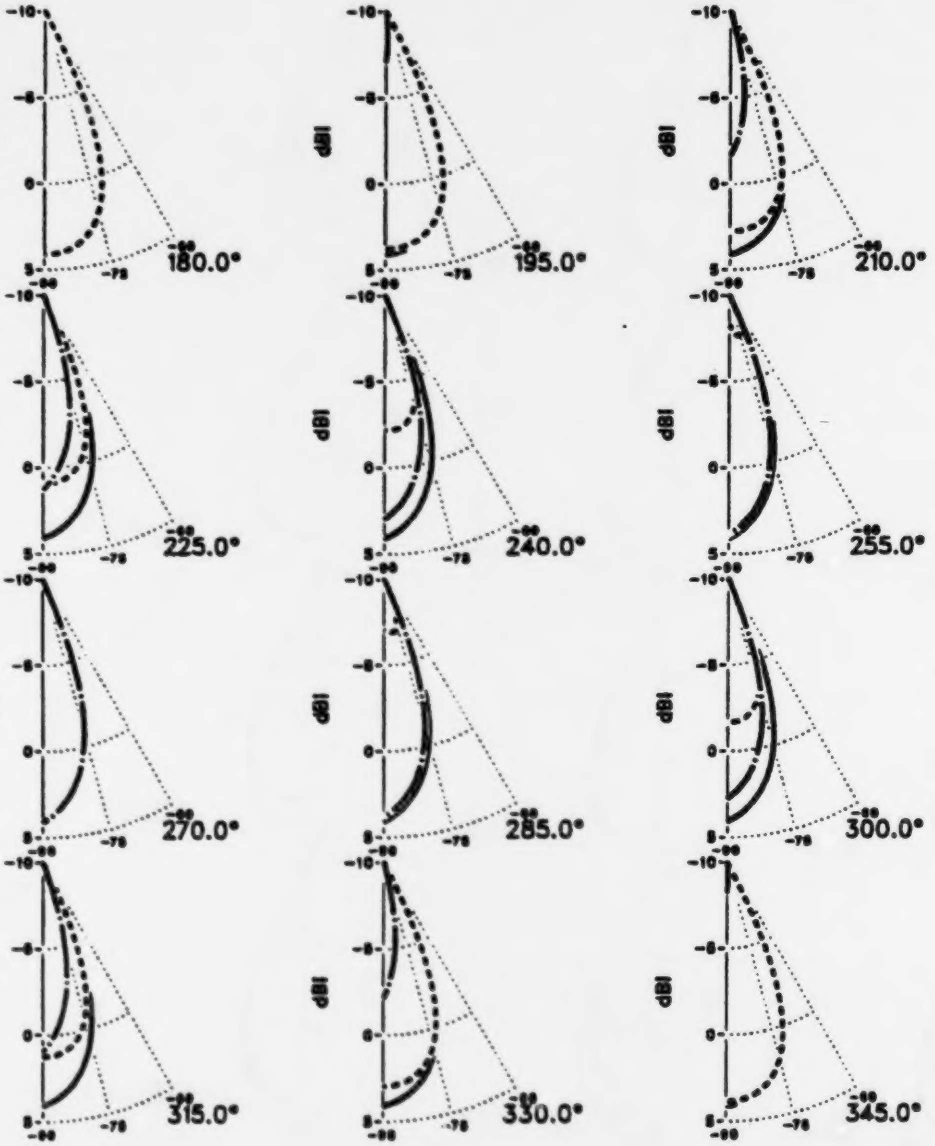

FIGURE B 70

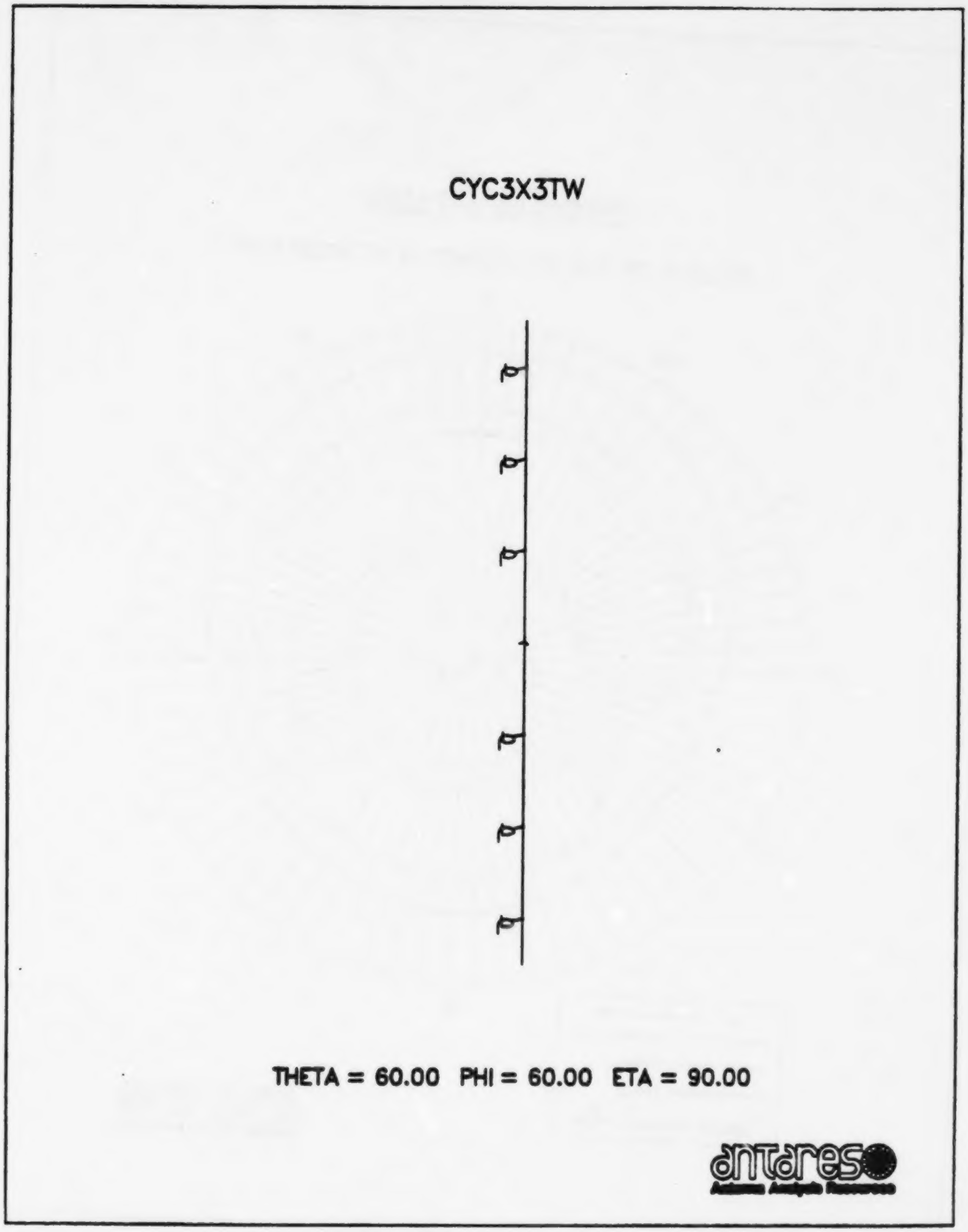
CYC3X3TW
THETA = 60.00 PHI = 60.00 ETA = 90.00
antares
Antenna Analysis Resources

FIGURE B 71

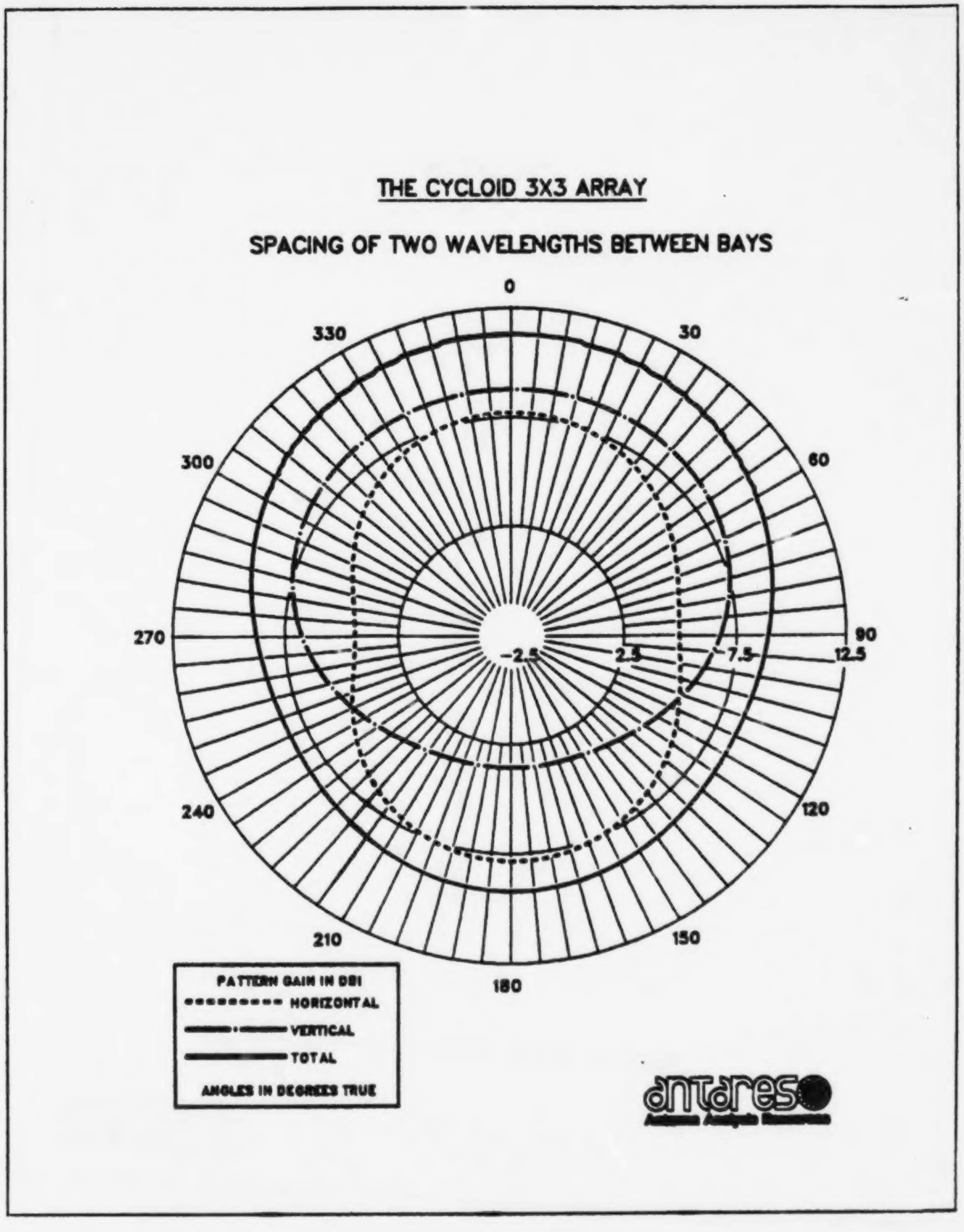
THE CYCLOID 3X3 ARRAY

SPACING OF TWO WAVELENGTHS BETWEEN BAYS

FIGURE B 72

THE CYCLOID 3X3 ARRAY

SPACING OF TWO WAVELENGTHS BETWEEN BAYS

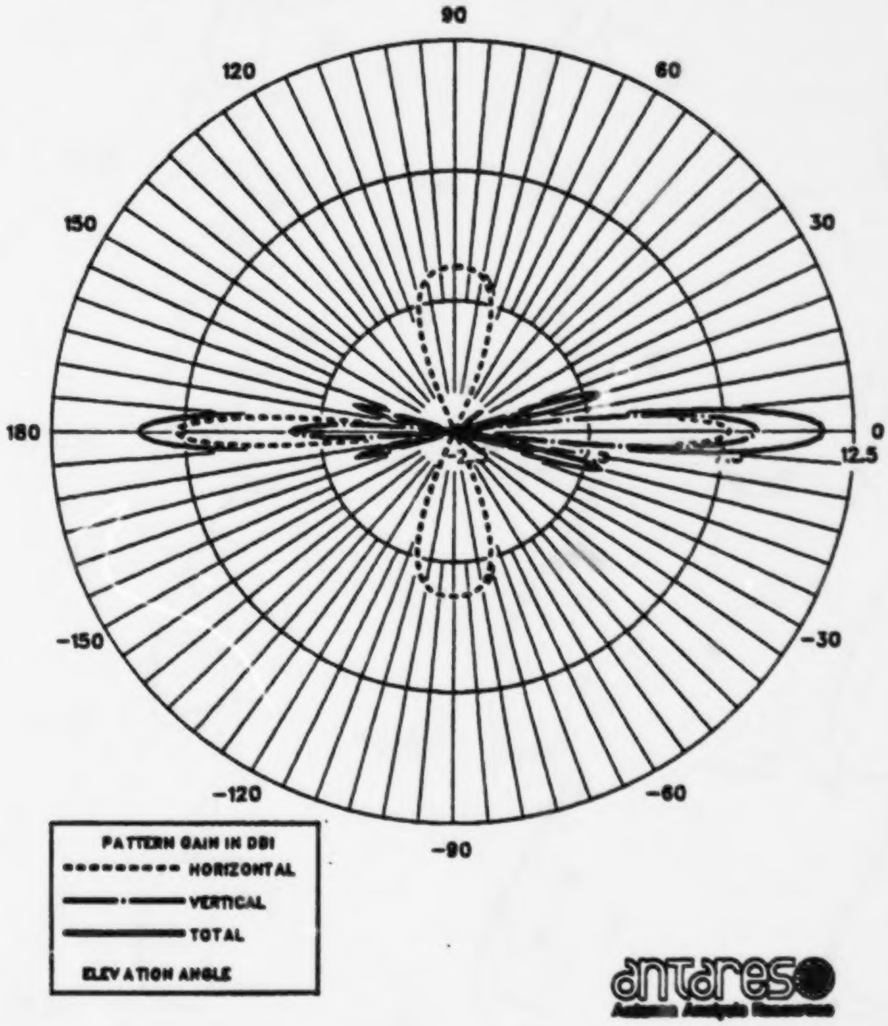

antares
Antenna Analysis Resources

FIGURE B 73

THE CYCLOID 3X3 ARRAY

SPACING OF 2 WAVELENGTHS BETWEEN BAYS

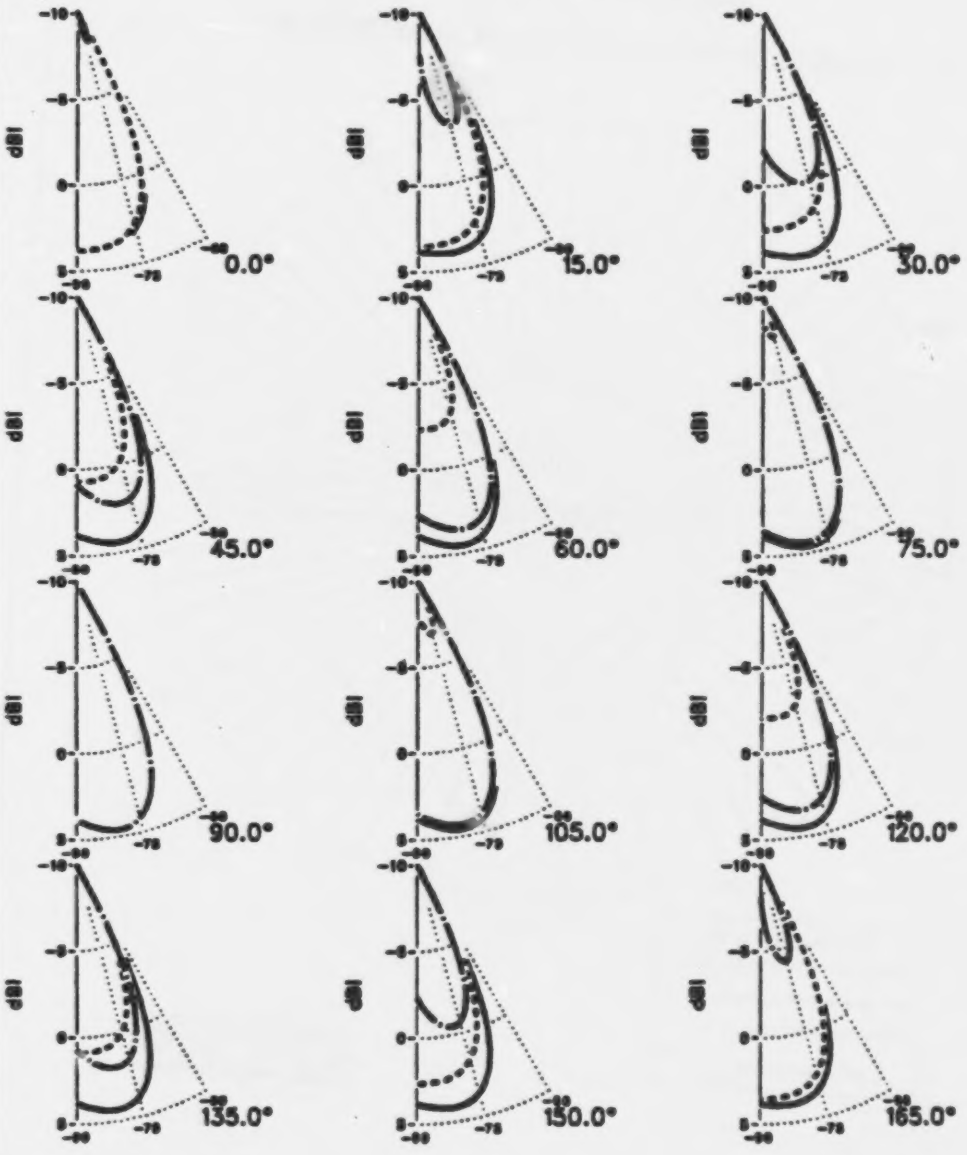

FIGURE B 74

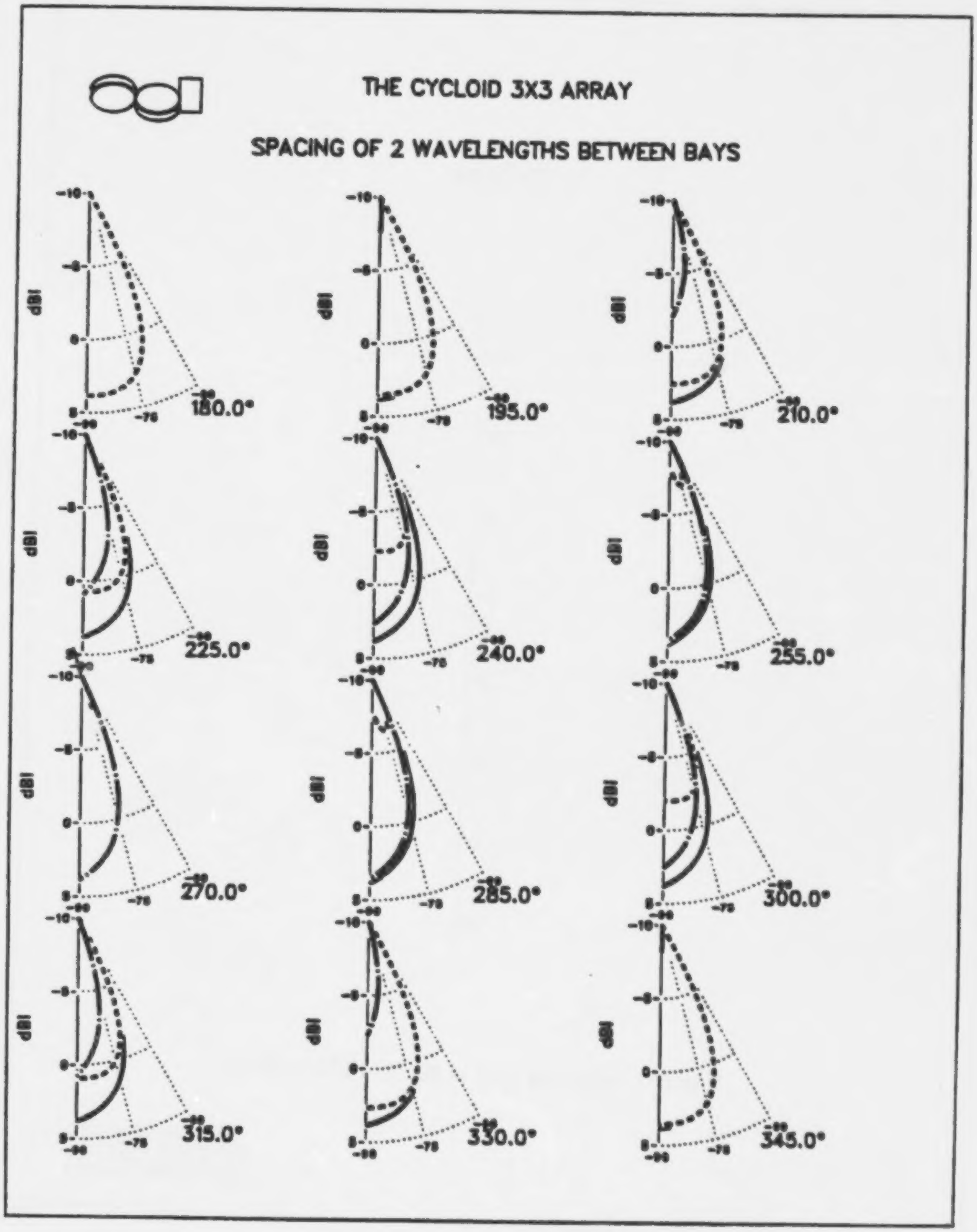

THE CYCLOID 3X3 ARRAY

SPACING OF 2 WAVELENGTHS BETWEEN BAYS

FIGURE B 75

CYC4X4

THETA = 60.00 PHI = 60.00 ETA = 90.00

247<

FIGURE B 76

THE CYCLOID 4X4 ARRAY

STANDARD SPACING OF ONE WAVELENGTH BETWEEN BAYS

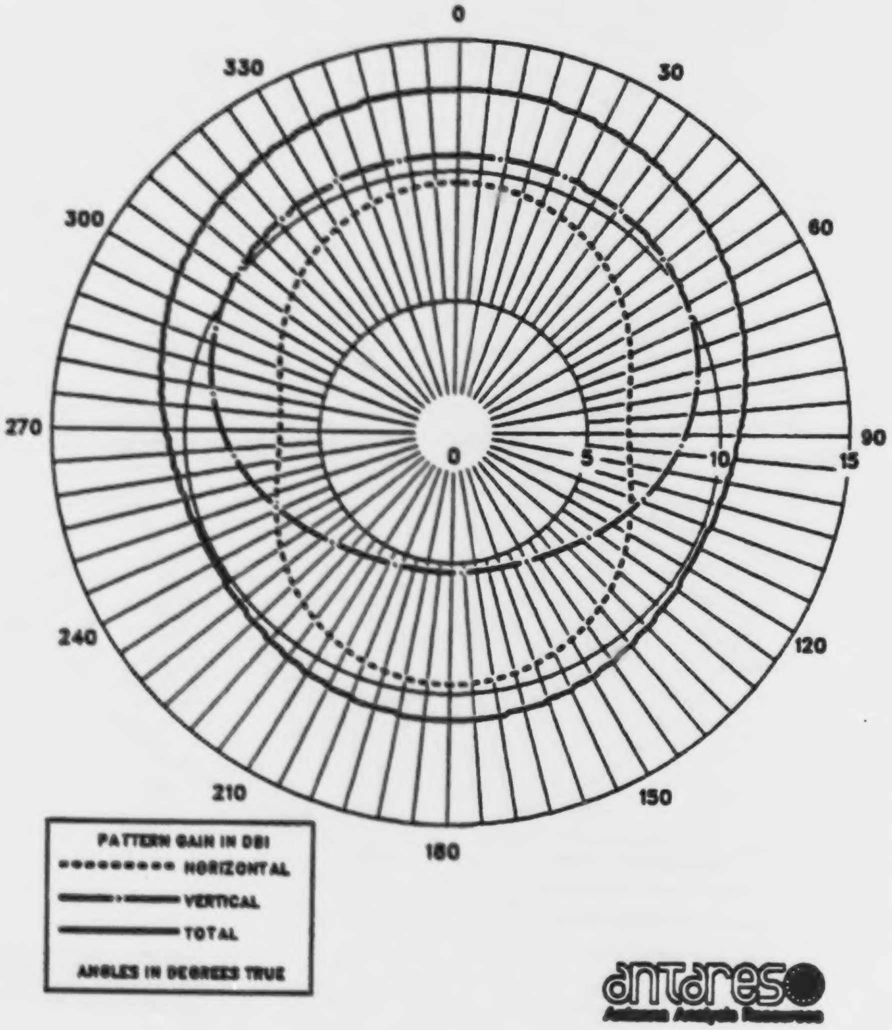

FIGURE B 77

THE CYCLOID 4X4 ARRAY

STANDARD SPACING OF ONE WAVELENGTH BETWEEN BAYS

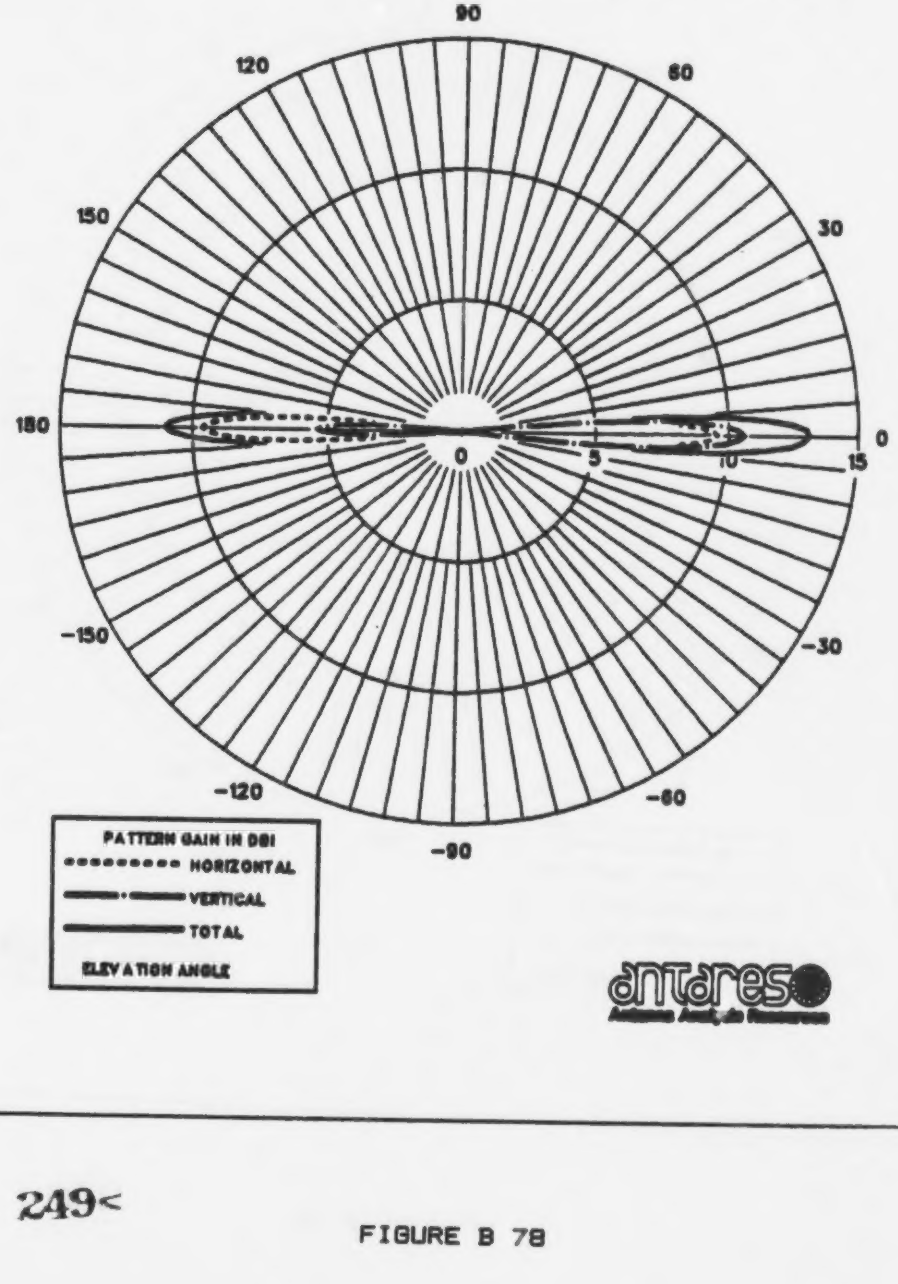

antares
Antenna Analysis Resources

249<

FIGURE B 78

THE CYCLOID 4X4 ARRAY

STANDARD SPACING OF ONE WAVELENGTH BETWEEN BAYS

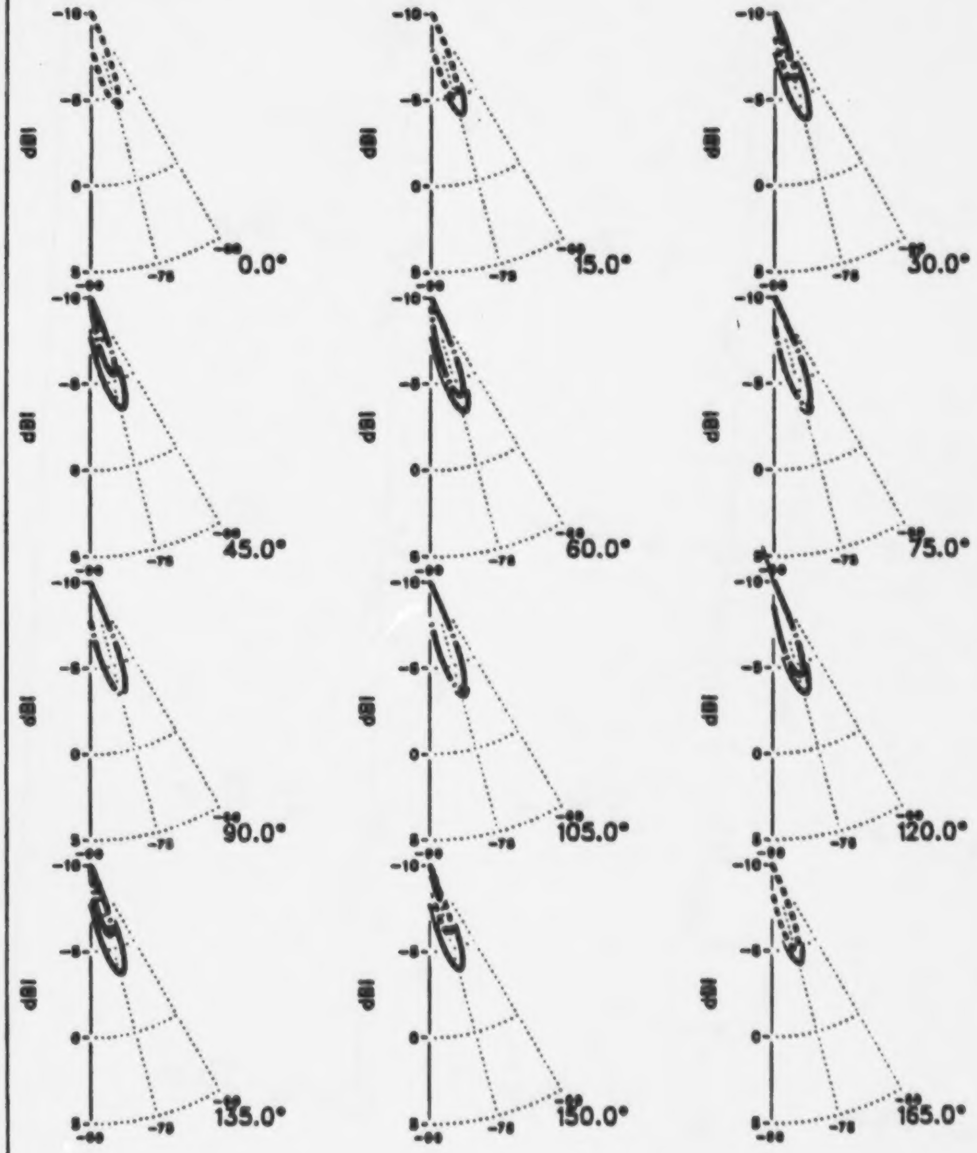

FIGURE B 79

250<

THE CYCLOID 4X4 ARRAY

STANDARD SPACING OF ONE WAVELENGTH BETWEEN BAYS

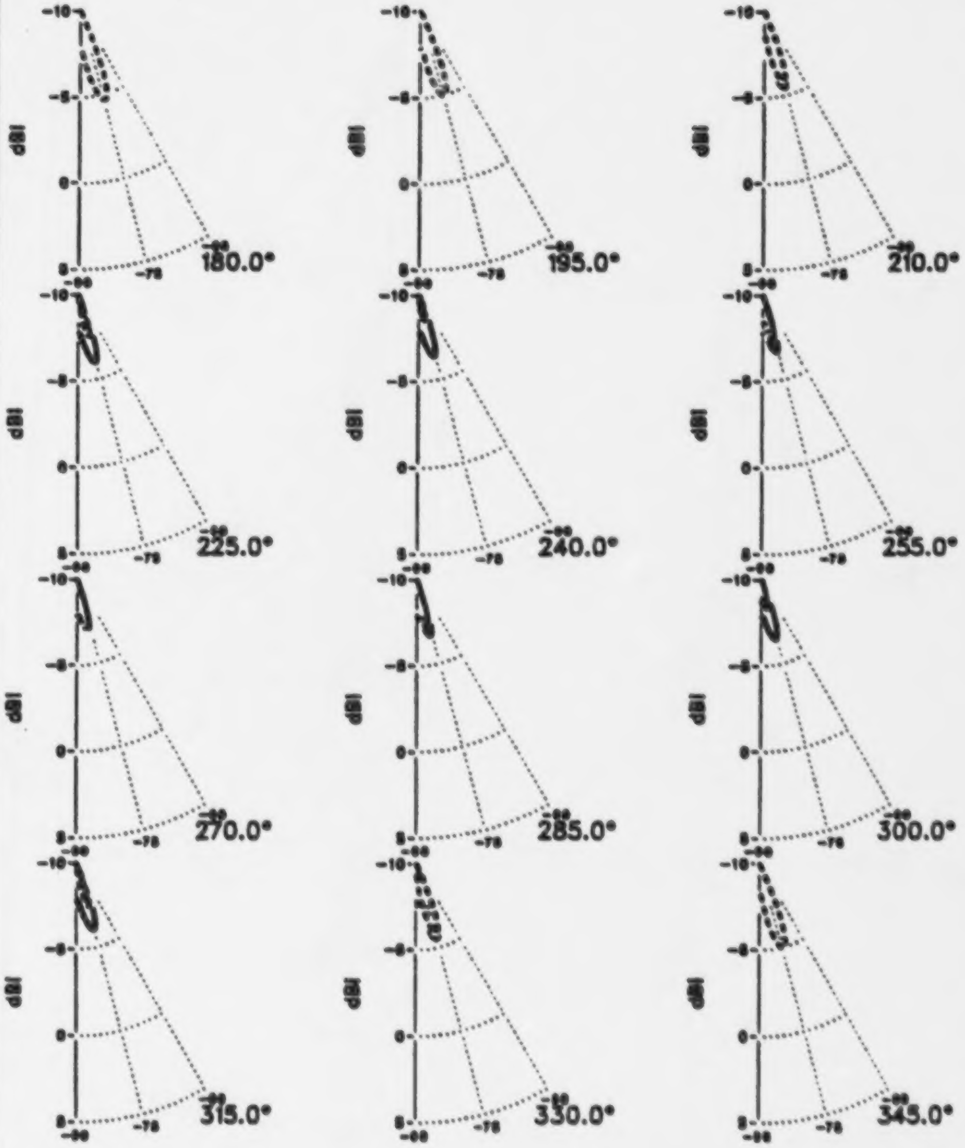

FIGURE B 80

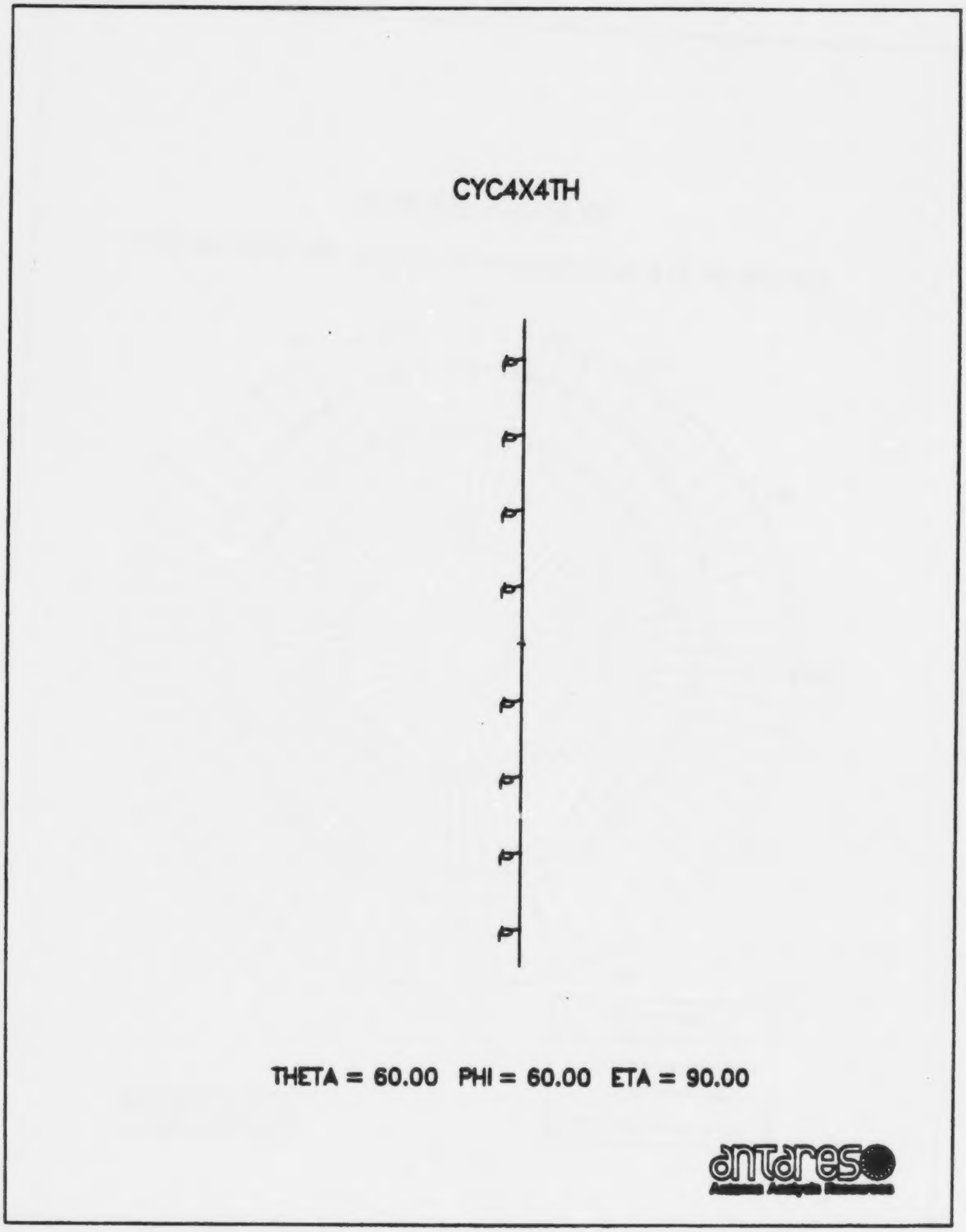
CYC4X4TH
THETA = 60.00 PHI = 60.00 ETA = 90.00
antares
Antenna Analysis Resources

FIGURE B 81

THE CYCLOID 4X4 ARRAY

SPACING OF 3/2 WAVELENGTHS BETWEEN UPPER & LOWER BAYS

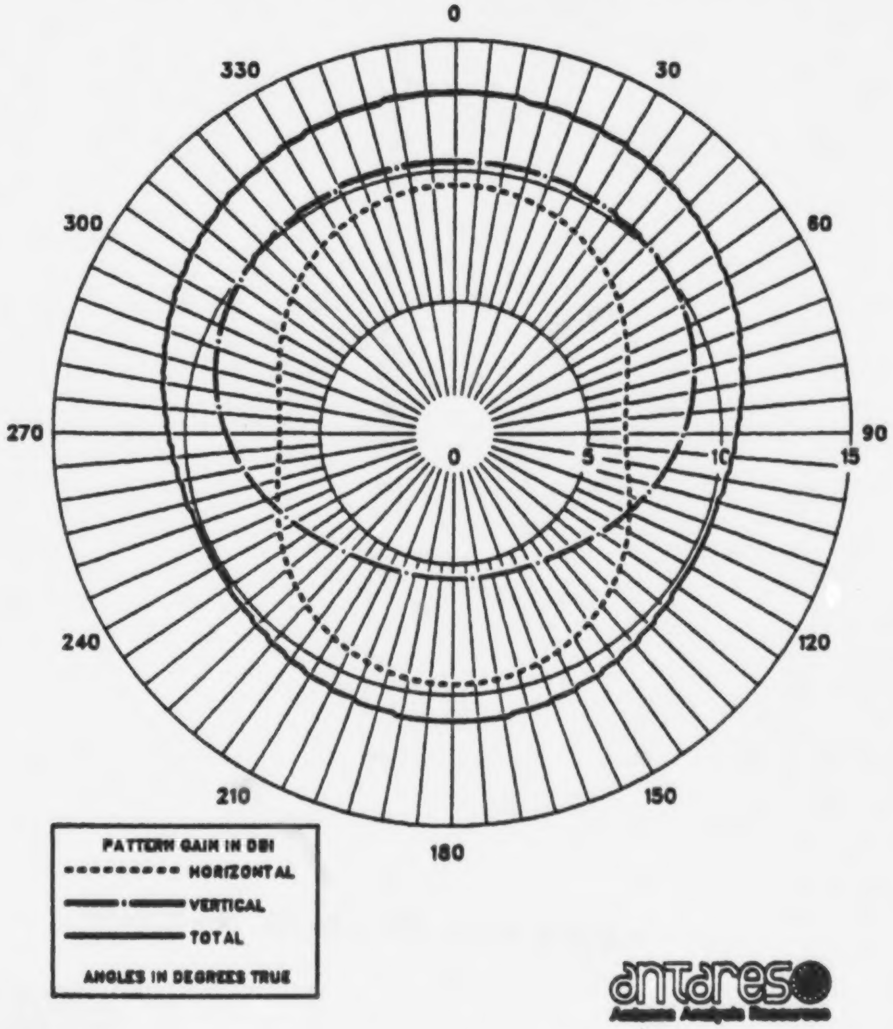

antares
Antenna Analysis Resources

FIGURE B 82

THE CYCLOID 4X4 ARRAY

SPACING OF 3/2 WAVELENGTHS BETWEEN UPPER & LOWER BAYS

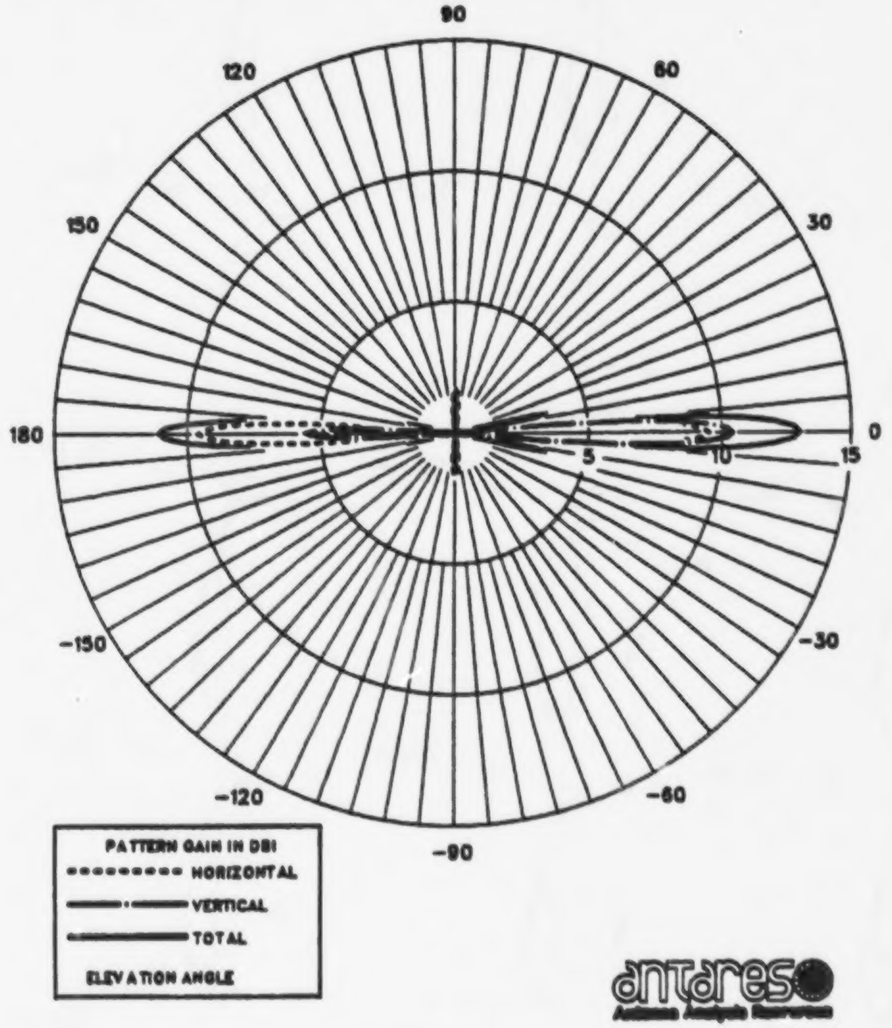

antares

FIGURE B 83

THE CYCLOID 4X4 ARRAY

SPACING OF 3/2 WAVELENGTHS BETWEEN UPPER & LOWER BAYS

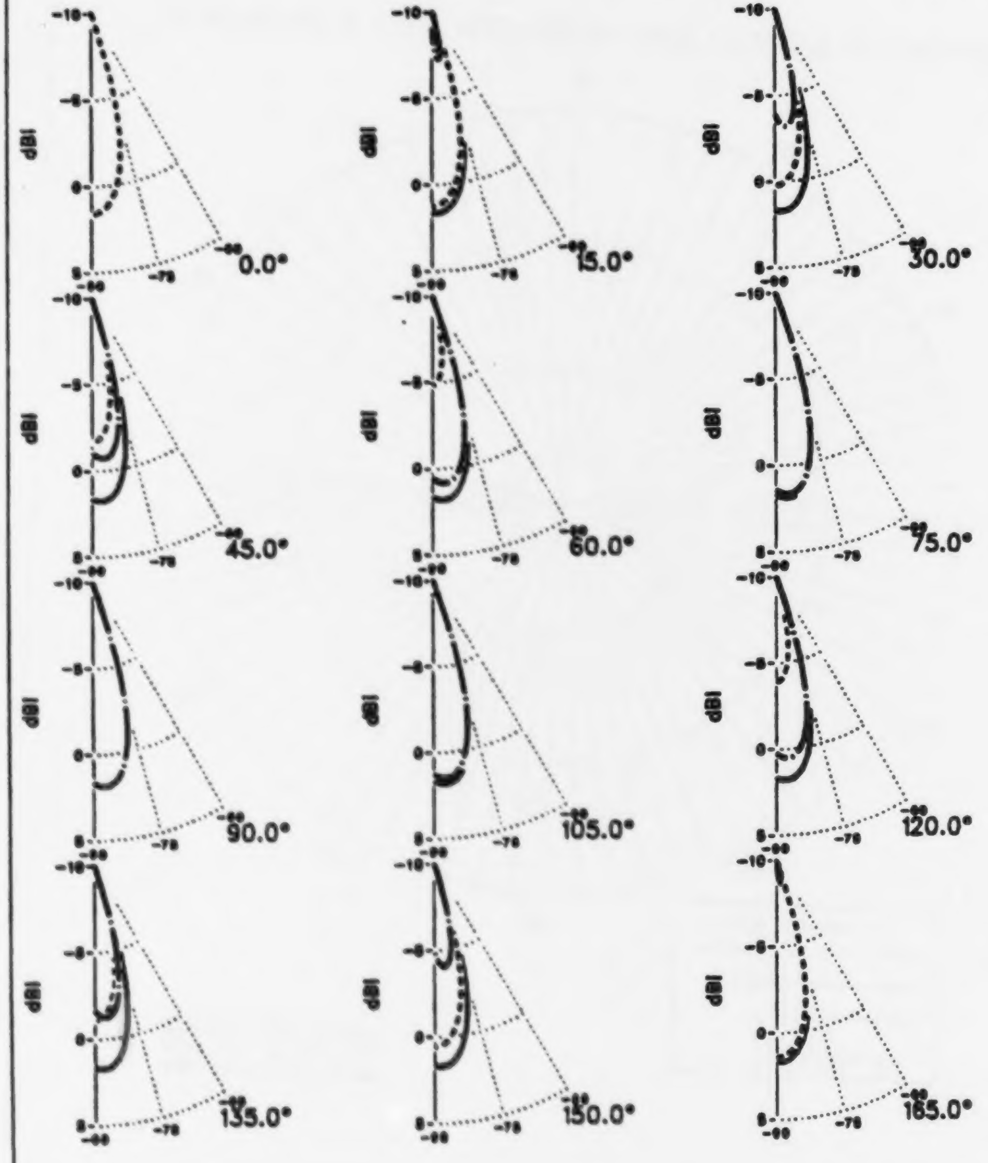

FIGURE B 84

THE CYCLOID 4X4 ARRAY

SPACING OF 3/2 WAVELENGTHS BETWEEN UPPER & LOWER BAYS

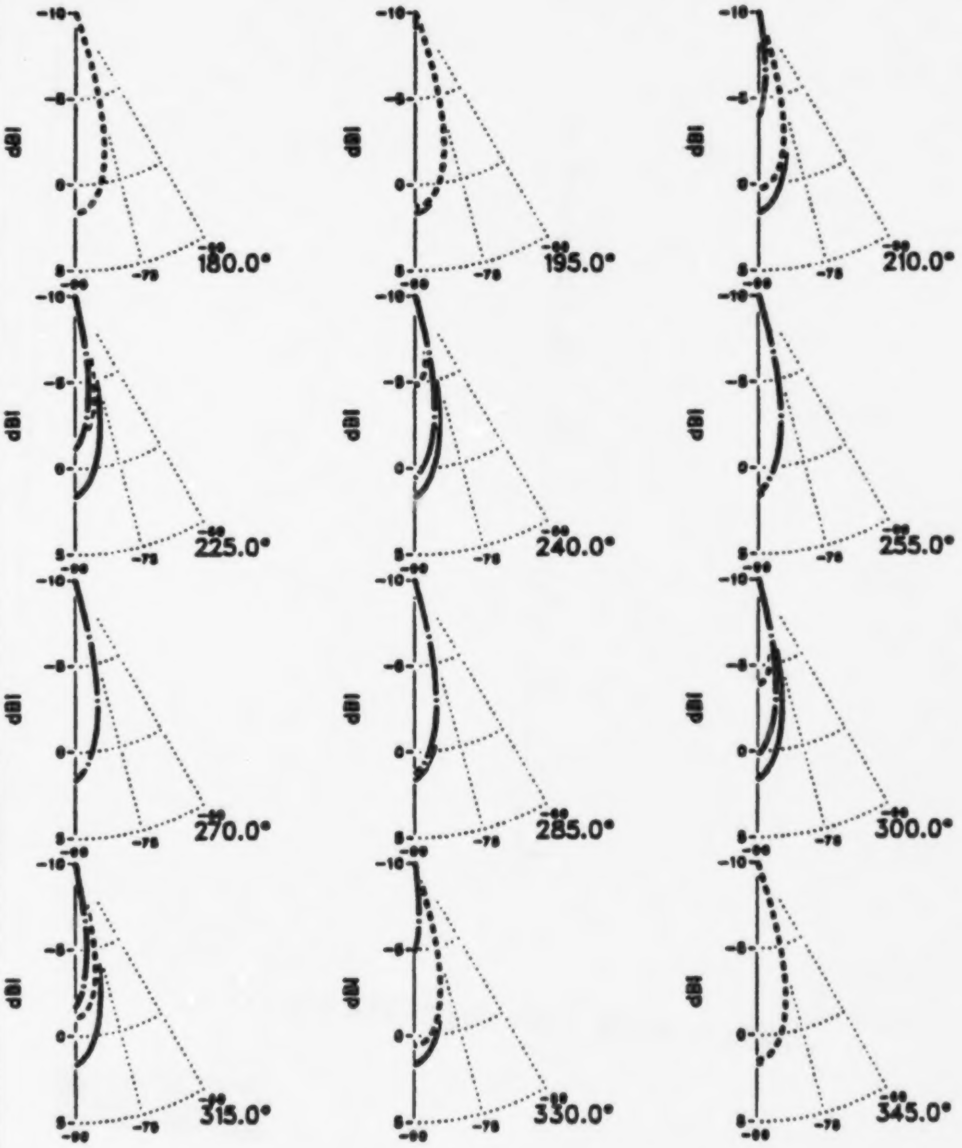

FIGURE B 85

CYC4X4TW

THETA = 60.00 PHI = 60.00 ETA = 90.00

257<

FIGURE B 86

THE CYCLOID 4X4 ARRAY

SPACING OF TWO WAVELENGTHS BETWEEN UPPER & LOWER BAYS

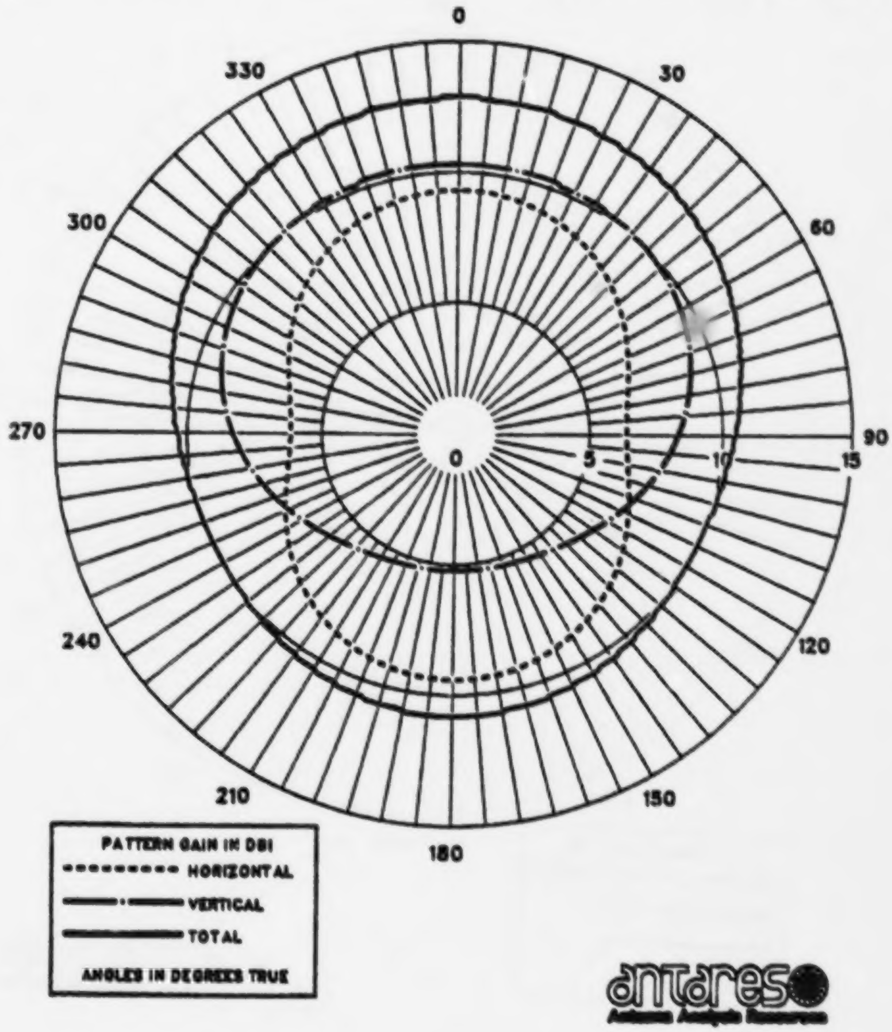

antares
Antenna Analysis Resources

FIGURE B 87

THE CYCLOID 4X4 ARRAY

SPACING OF TWO WAVELENGTHS BETWEEN UPPER & LOWER BAYS

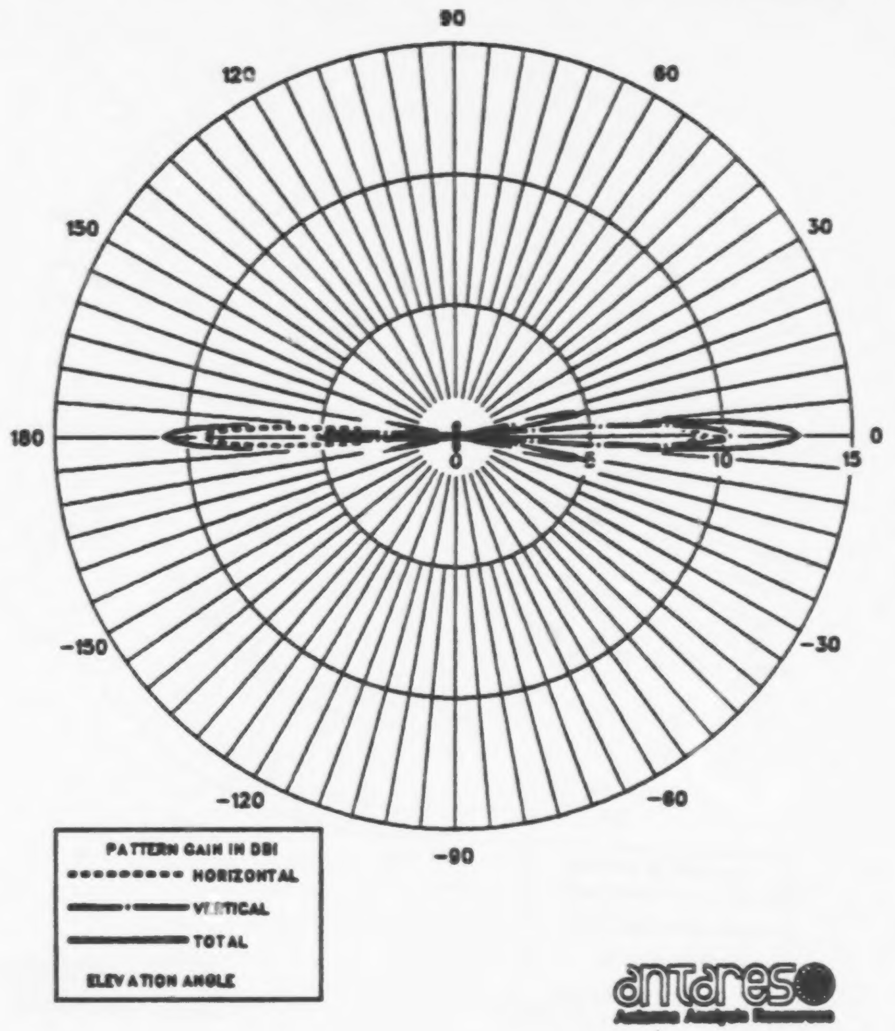

antares
Antenna Analysis Resources

FIGURE B 88

THE CYCLOID 4X4 ARRAY

SPACING OF TWO WAVELENGTHS BETWEEN UPPER & LOWER BAYS

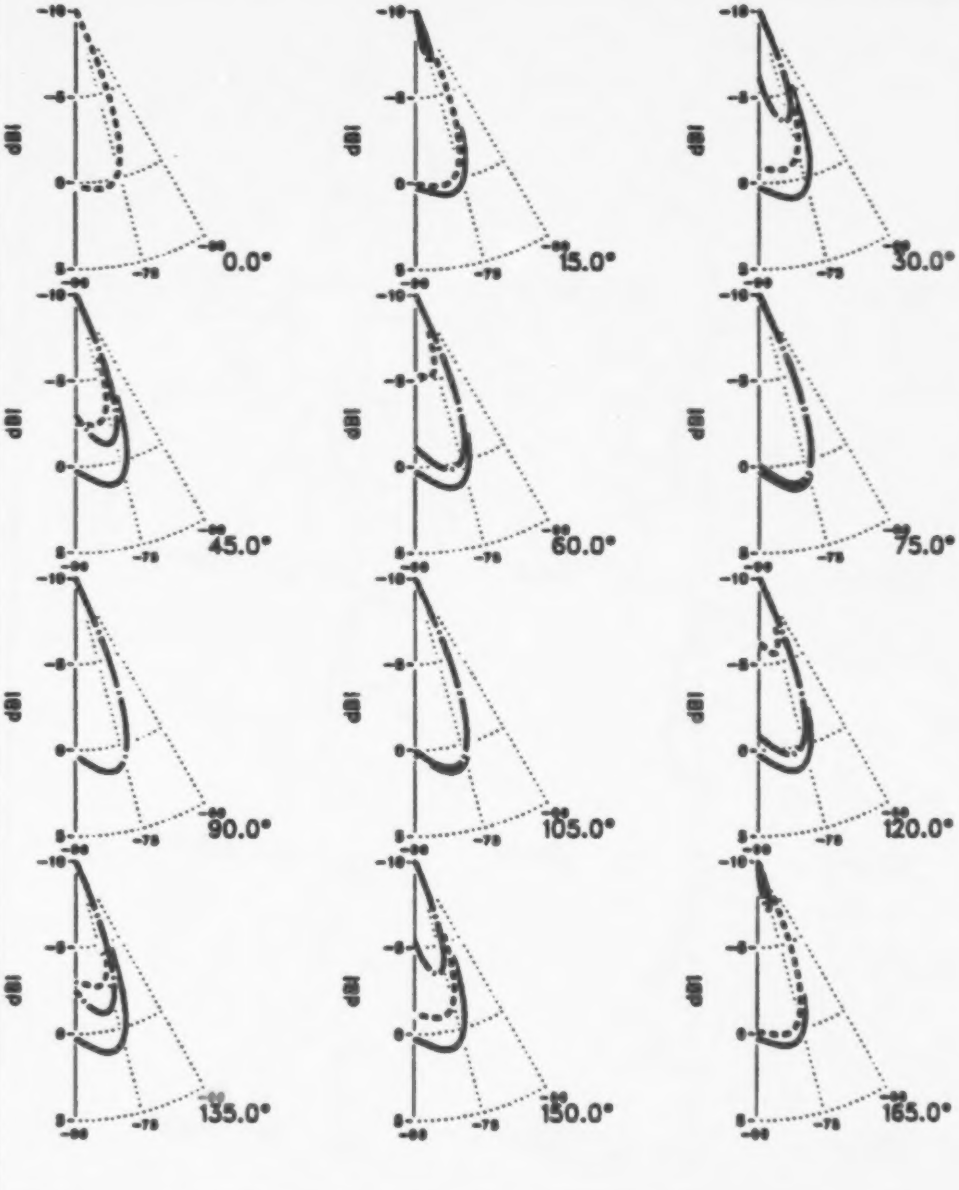

FIGURE B 89

THE CYCLOID 4X4 ARRAY

SPACING OF TWO WAVELENGTHS BETWEEN UPPER & LOWER BAYS

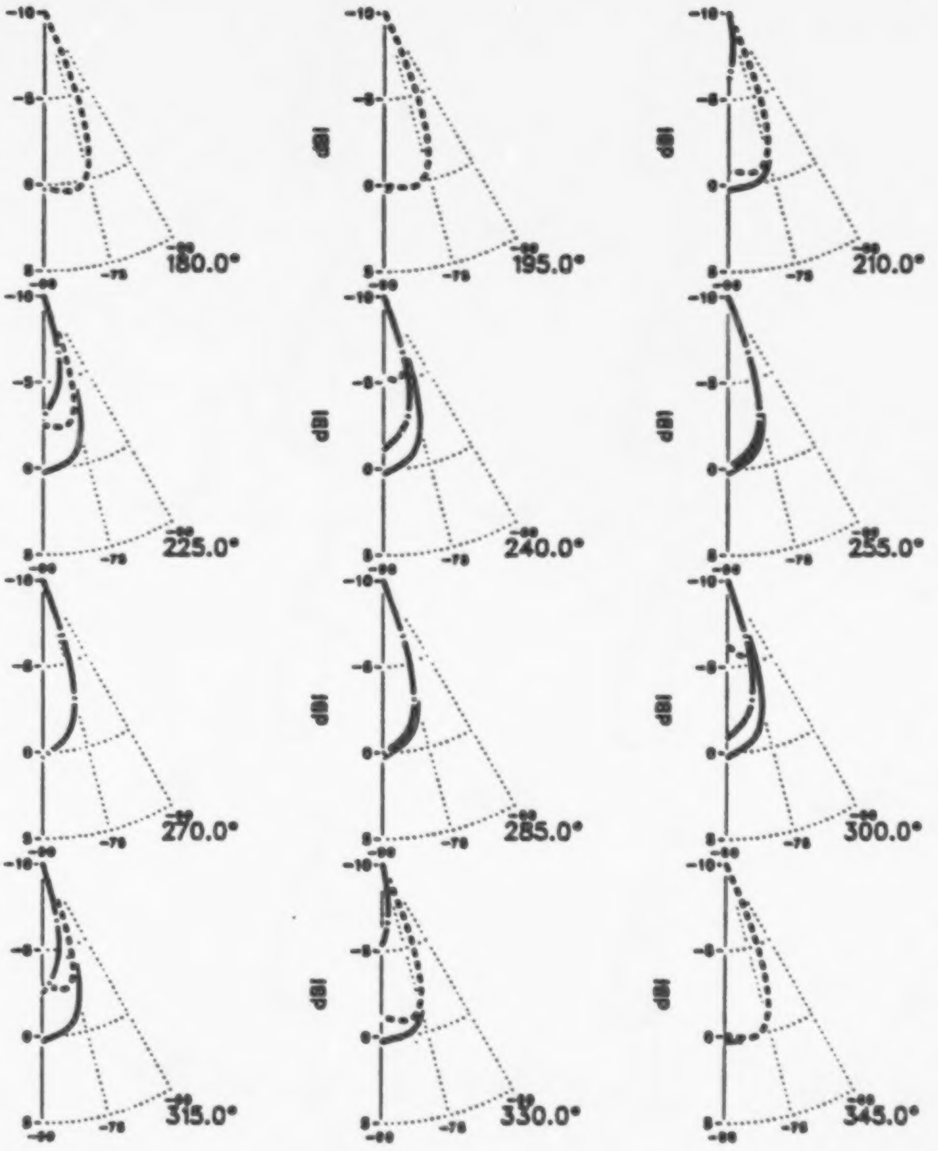

FIGURE B 90

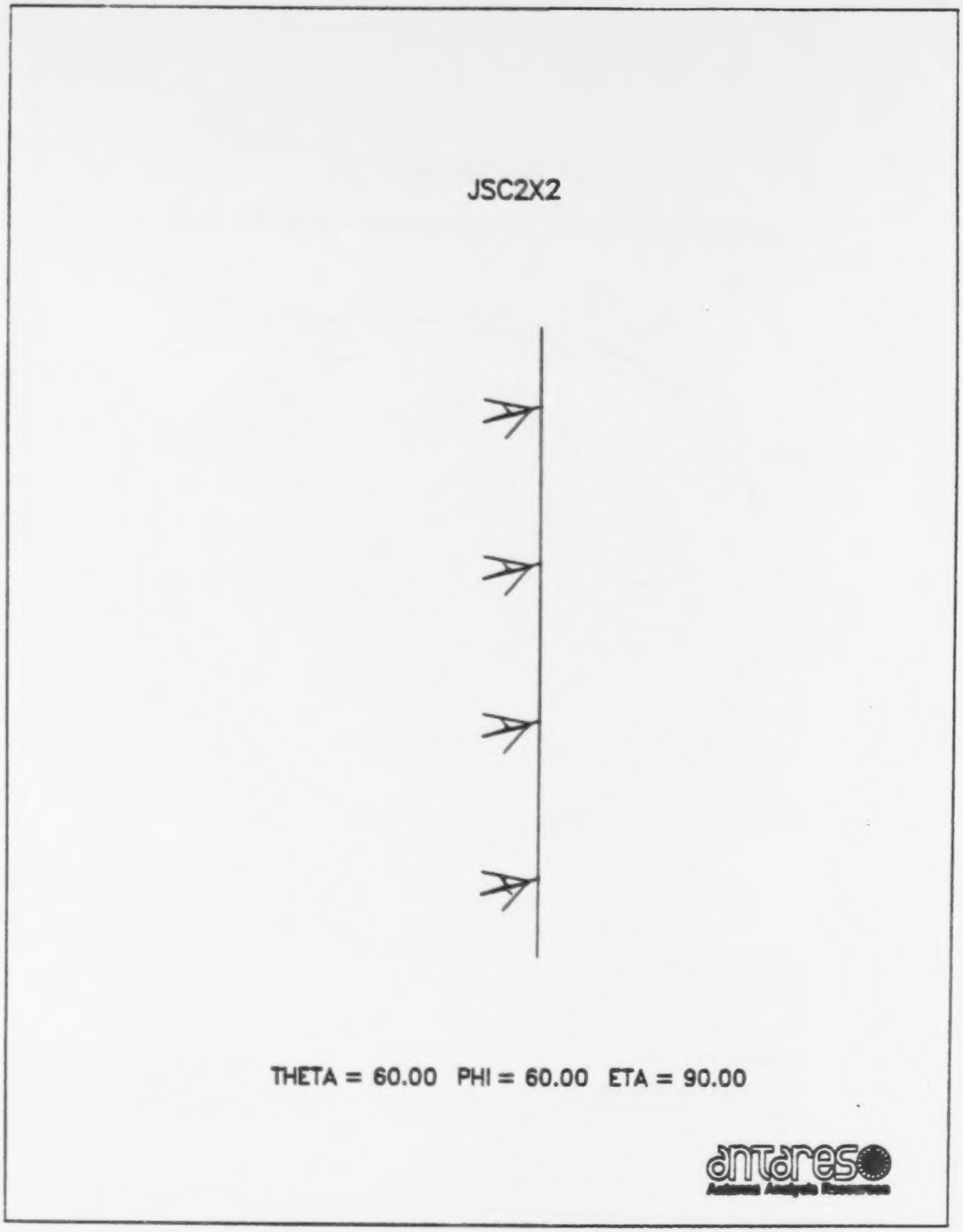
JSC2X2
THETA = 60.00 PHI = 60.00 ETA = 90.00
antares
Antenna Analysis Resources

FIGURE B 91

THE JSCP 2X2 ARRAY

STANDARD SPACING OF ONE WAVELENGTH BETWEEN BAYS

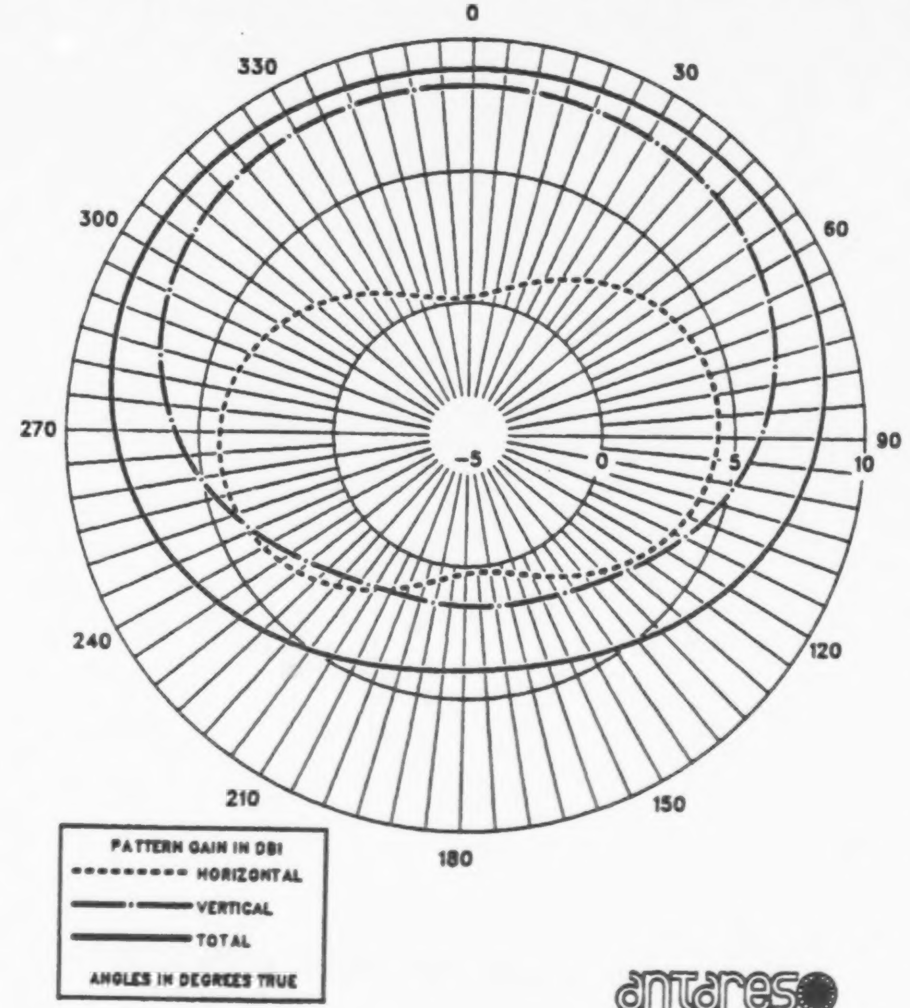

antares
Antenna Analysis Resources

263<

FIGURE B 92

THE JSCP 2X2 ARRAY

STANDARD SPACING OF ONE WAVELENGTH BETWEEN BAYS

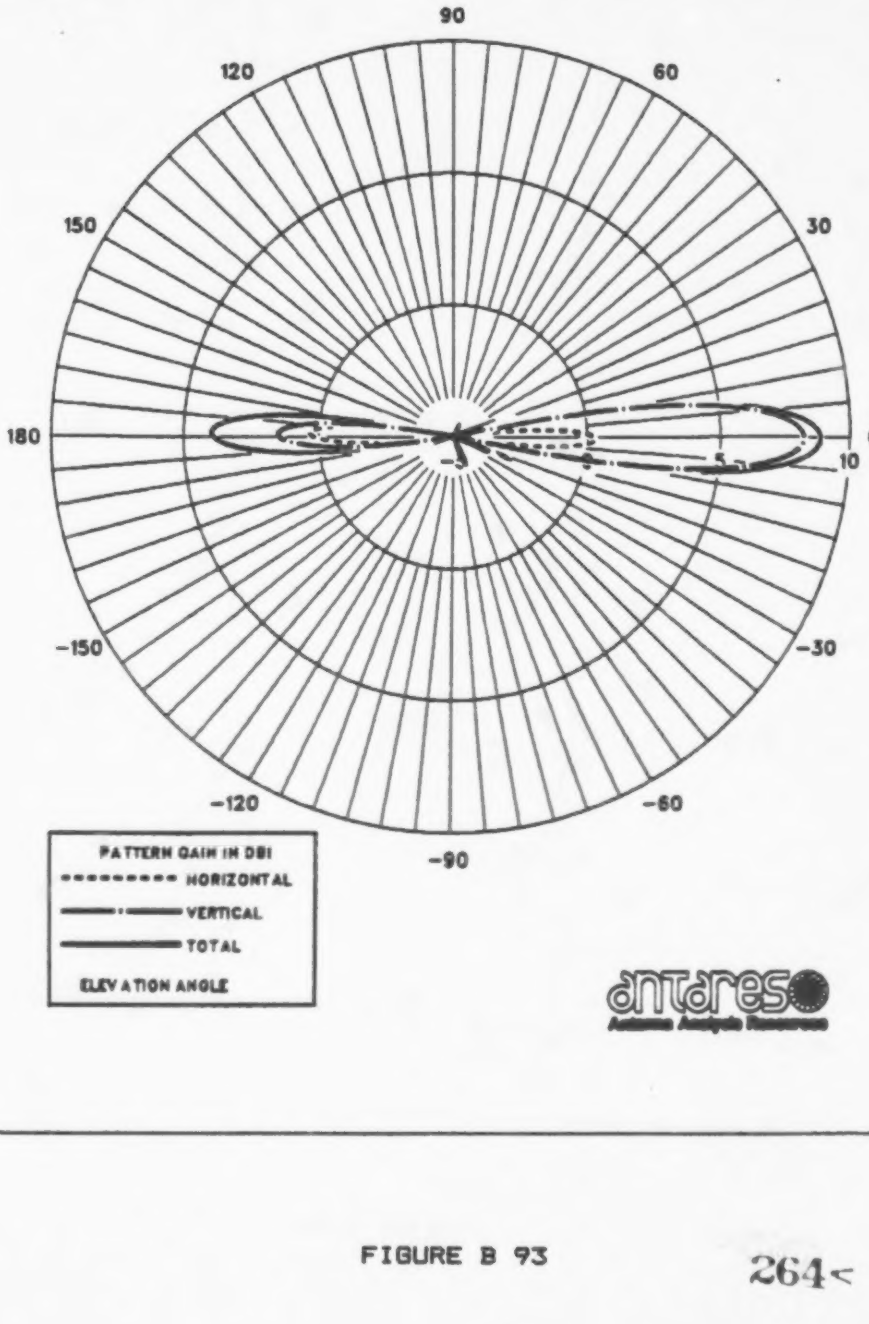

FIGURE B 93

THE JSCP 2X2 ARRAY

STANDARD SPACING OF ONE WAVELENGTH BETWEEN BAYS

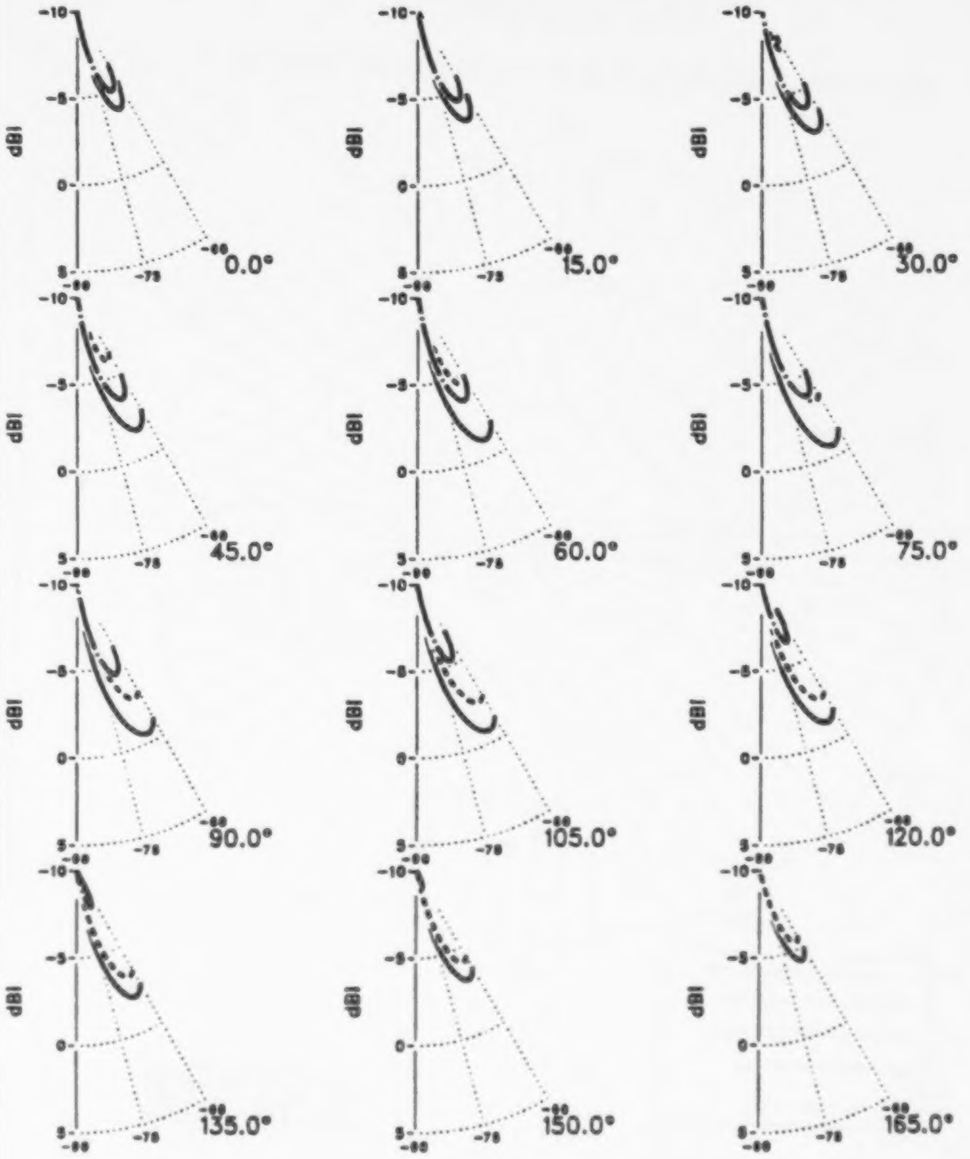

FIGURE B 94

THE JSCP 2X2 ARRAY

STANDARD SPACING OF ONE WAVELENGTH BETWEEN BAYS

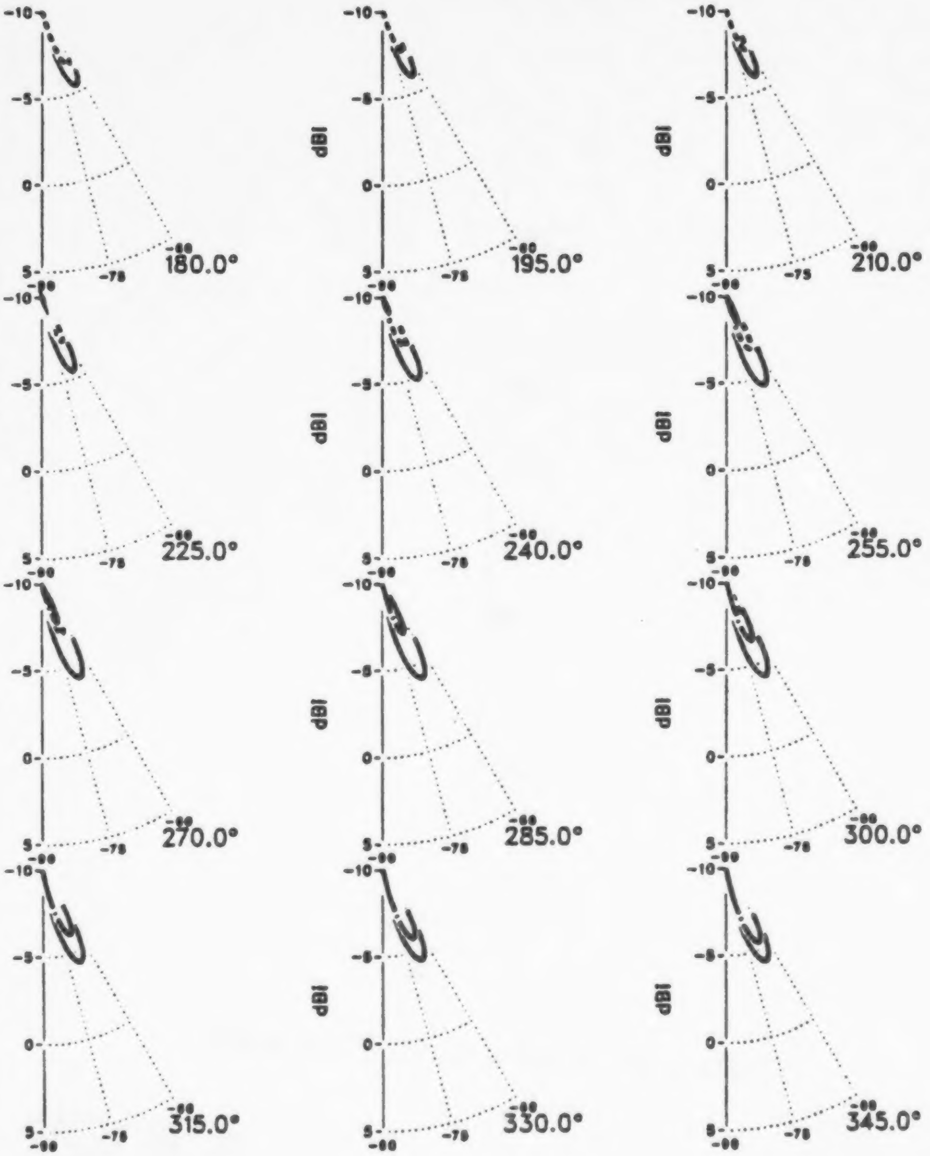

FIGURE B 95

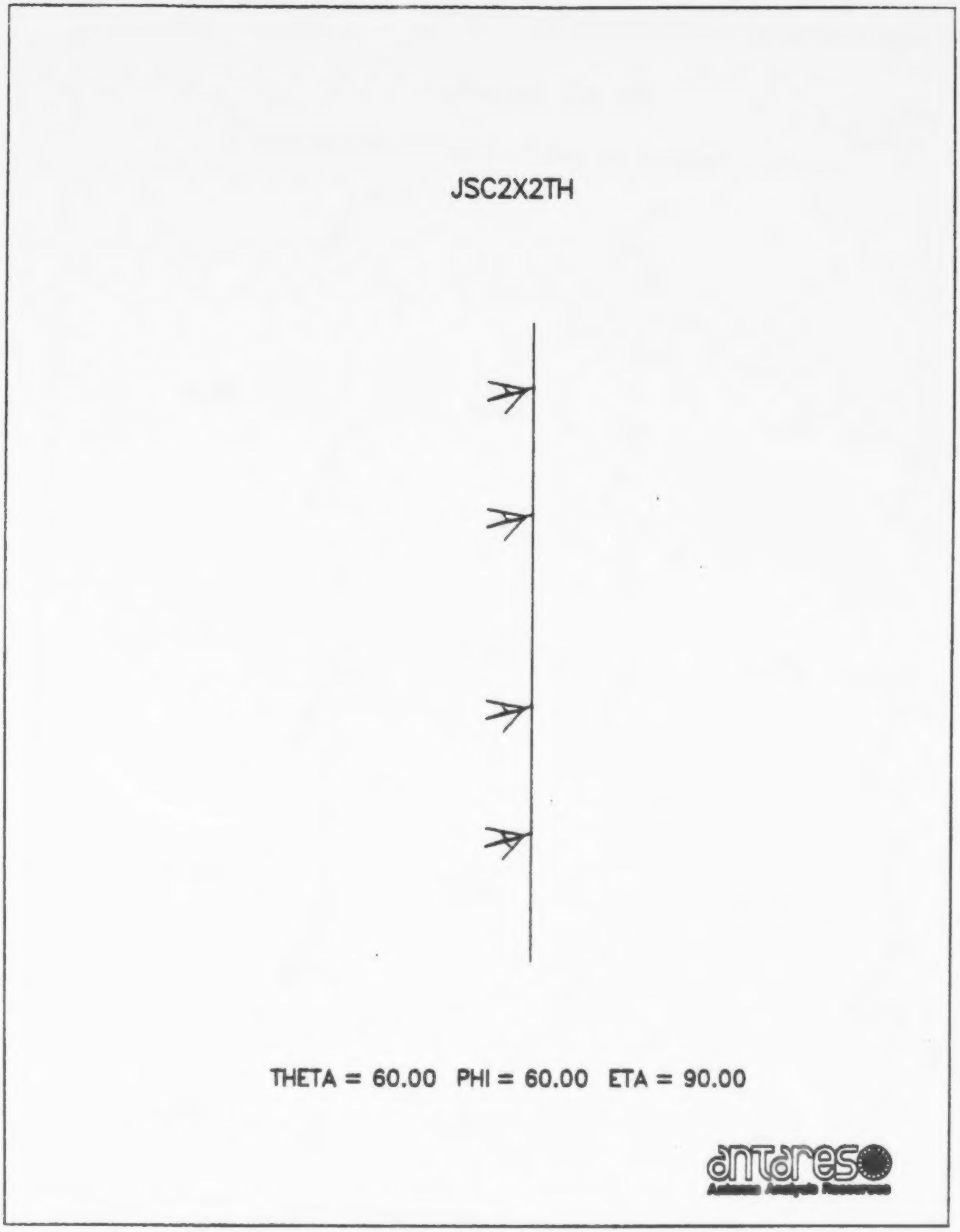

FIGURE B 96

THE JSCP 2X2 ARRAY

SPACING OF 3/2 WAVELENGTHS BETWEEN UPPER & LOWER BAYS

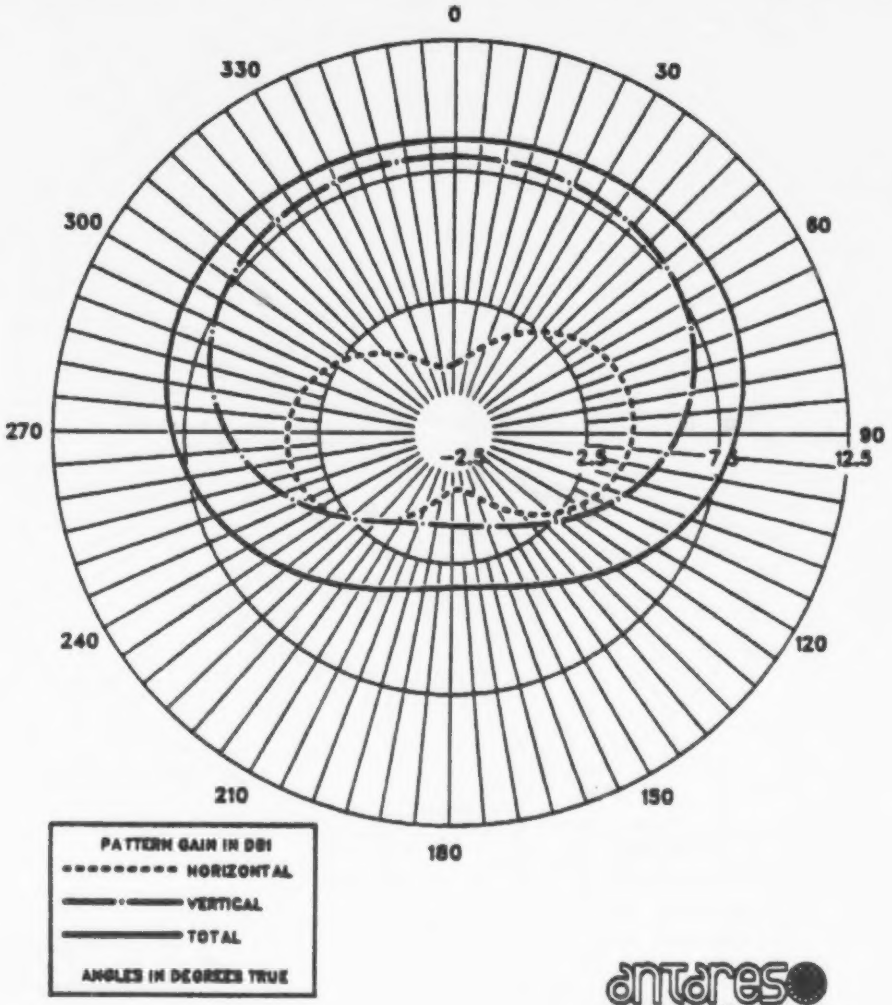

FIGURE B 97

THE JSCP 2X2 ARRAY

SPACING OF 3/2 WAVELENGTHS BETWEEN UPPER & LOWER BAYS

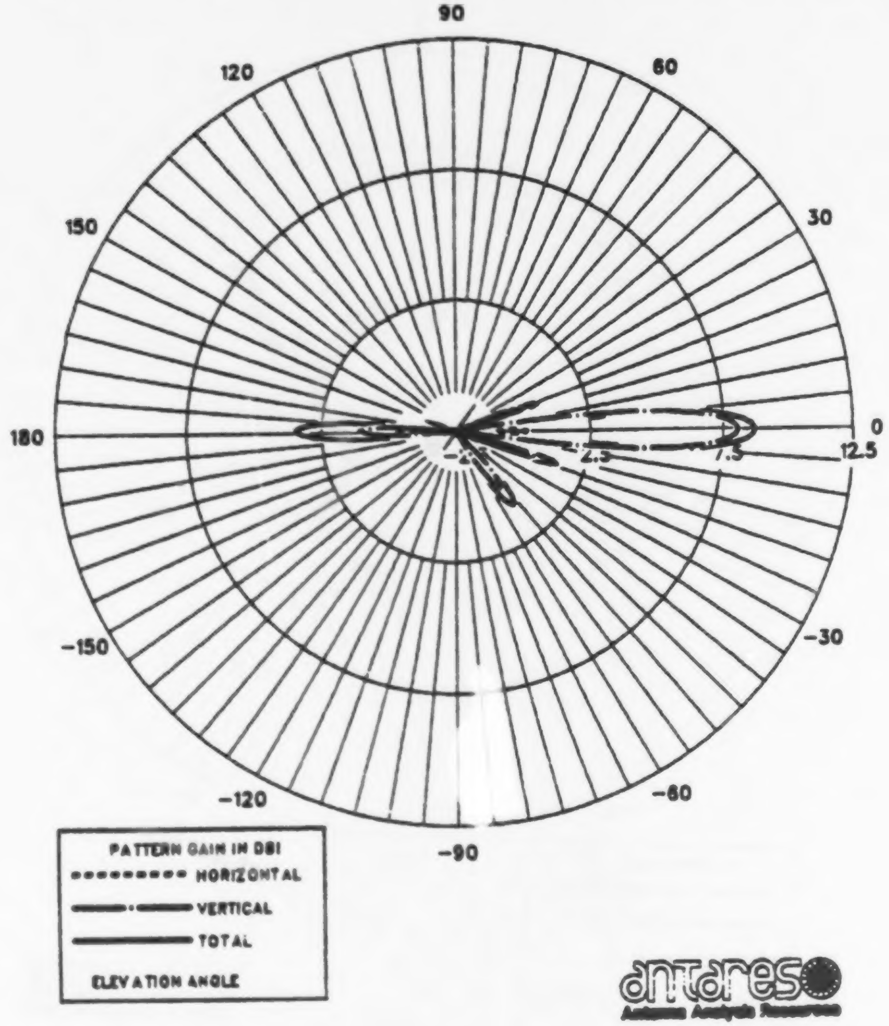

antares
Antenna Analysis Resources

FIGURE B 98

THE JSCP 2X2 ARRAY

SPACING OF 3/2 WAVELENGTHS BETWEEN UPPER & LOWER BAYS

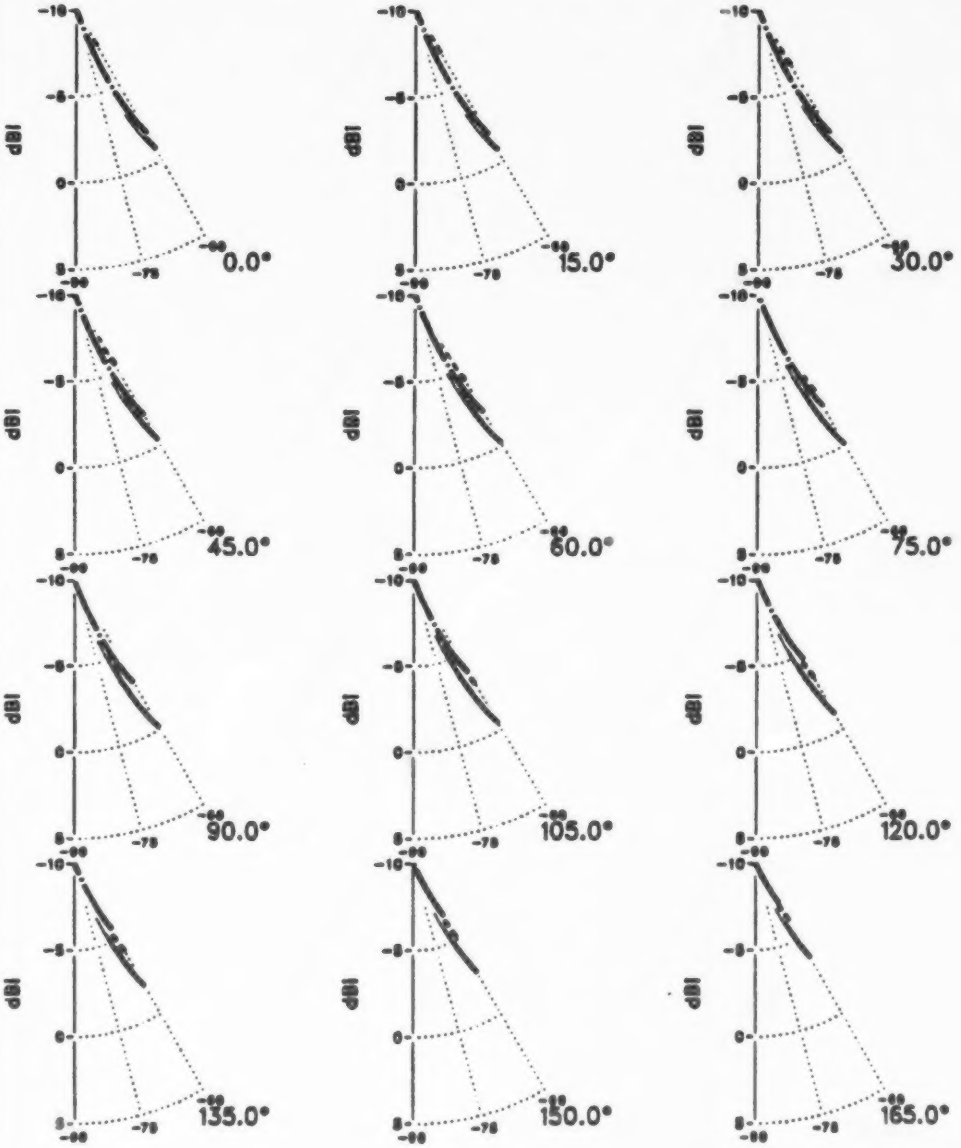

FIGURE B 99

THE JSCP 2X2 ARRAY

SPACING OF 3/2 WAVELENGTHS BETWEEN UPPER & LOWER BAYS

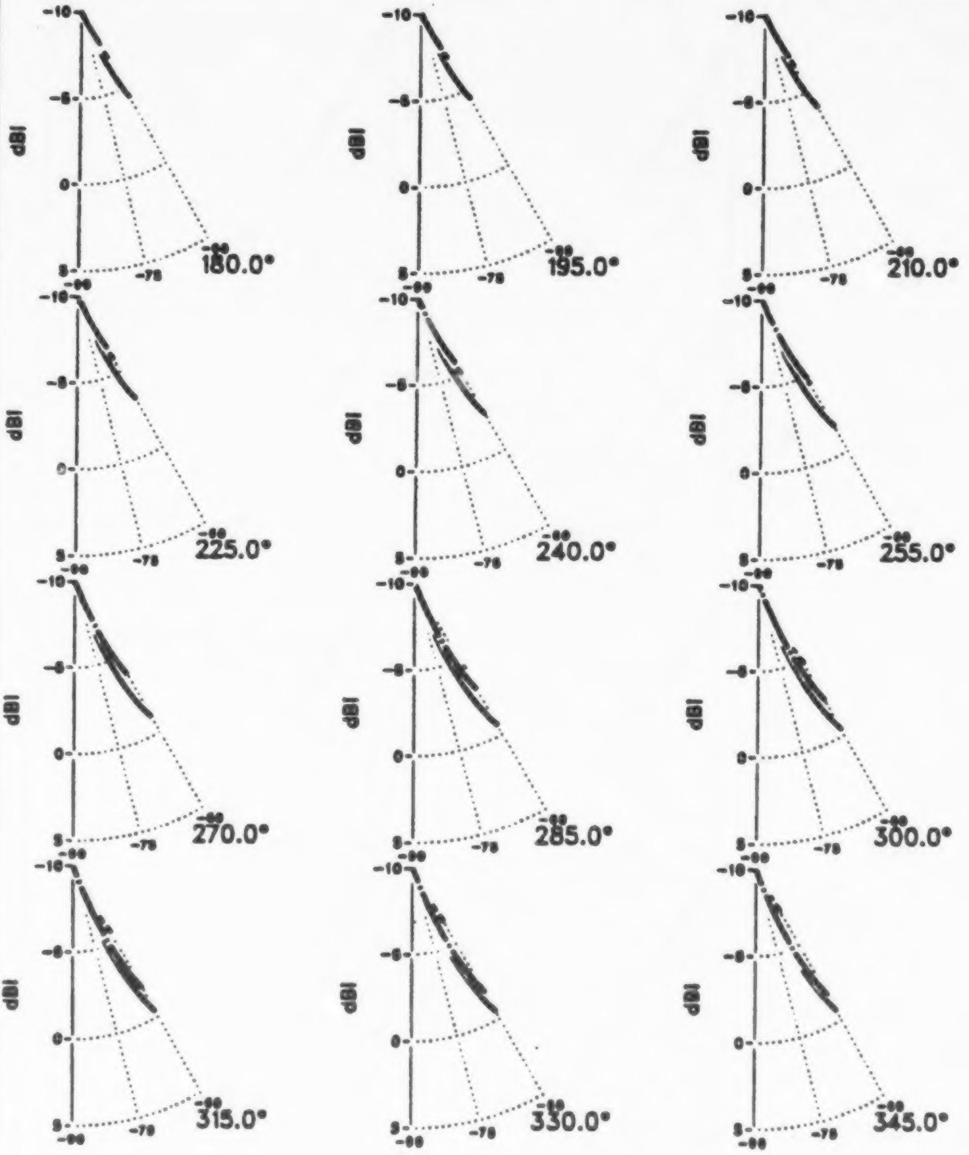

FIGURE B 100

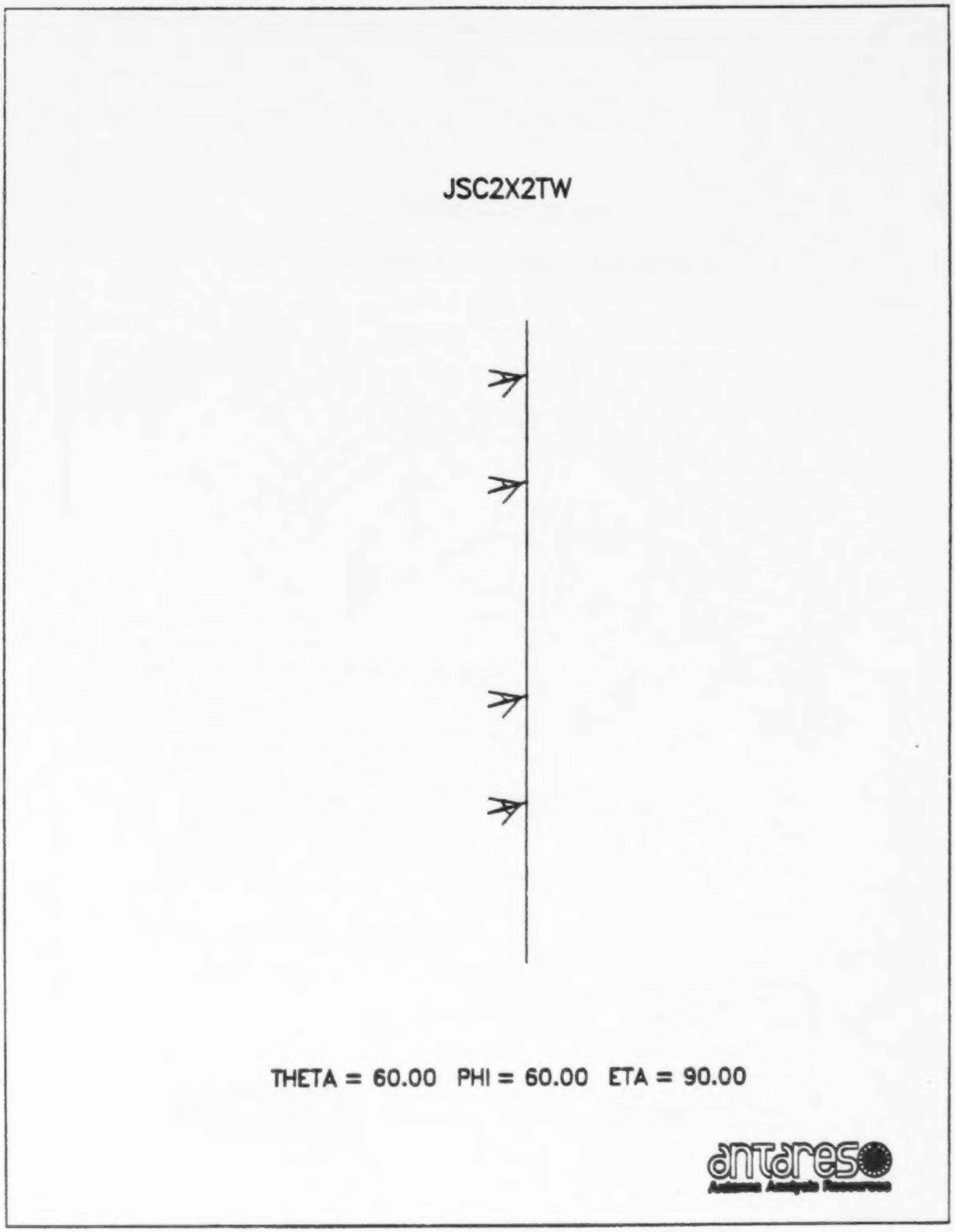
JSC2X2TW
THETA = 60.00 PHI = 60.00 ETA = 90.00
antares
Antenna Analysis Resources

FIGURE B 101

THE JSCP 2X2 ARRAY

2 WAVELENGTH SPACING BETWEEN BAYS

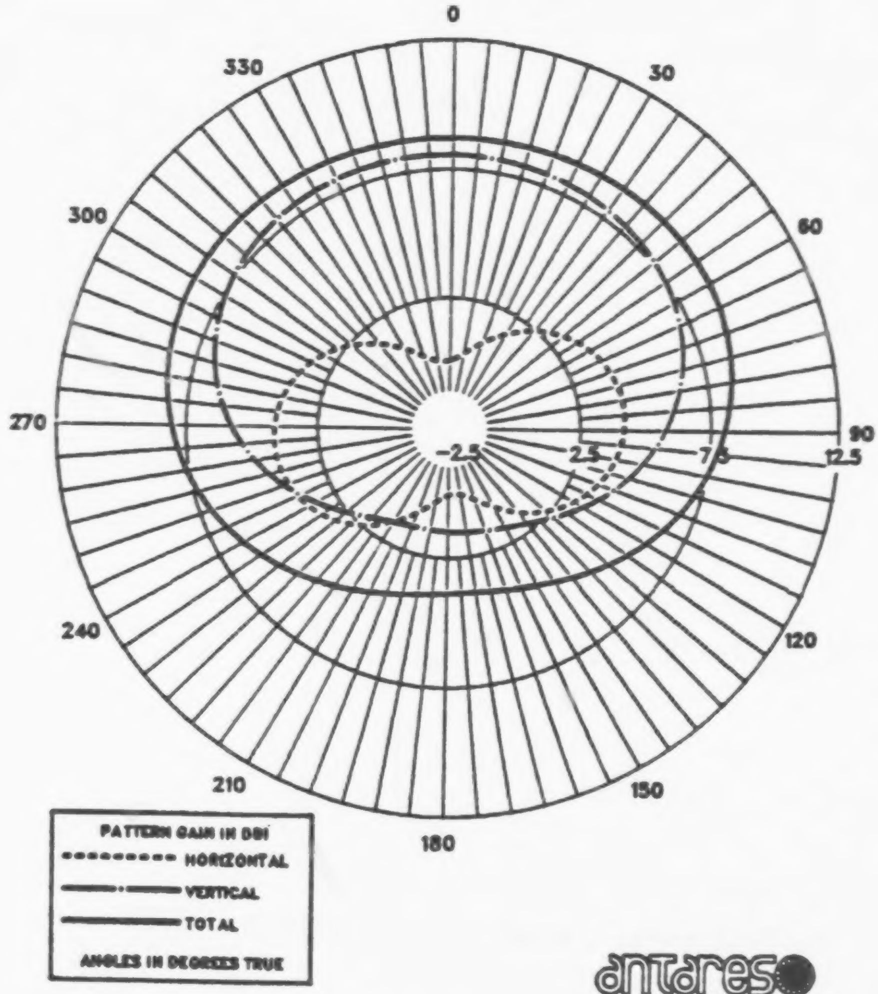

antares
Antenna Analysis Resources

273<

FIGURE B 102

THE JSCP 2X2 ARRAY

2 WAVELENGTH SPACING BETWEEN BAYS

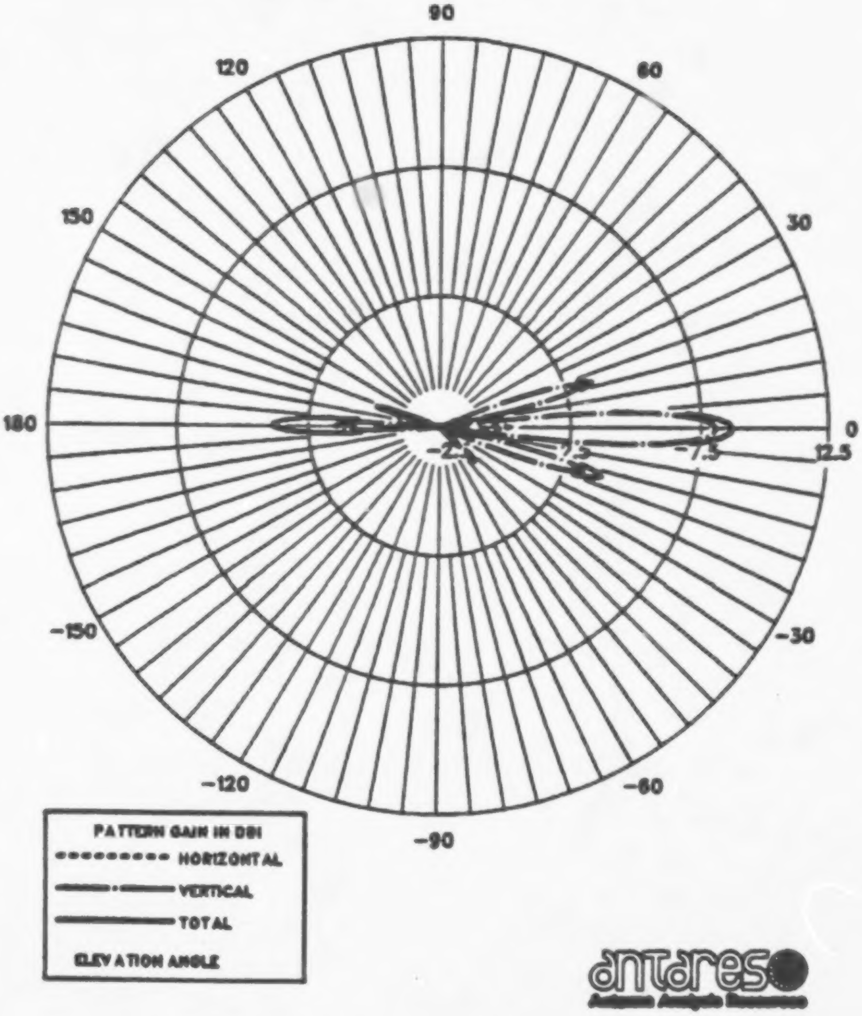

FIGURE B 103

THE JSCP 2X2 ARRAY

2 WAVELENGTH SPACING BETWEEN BAYS

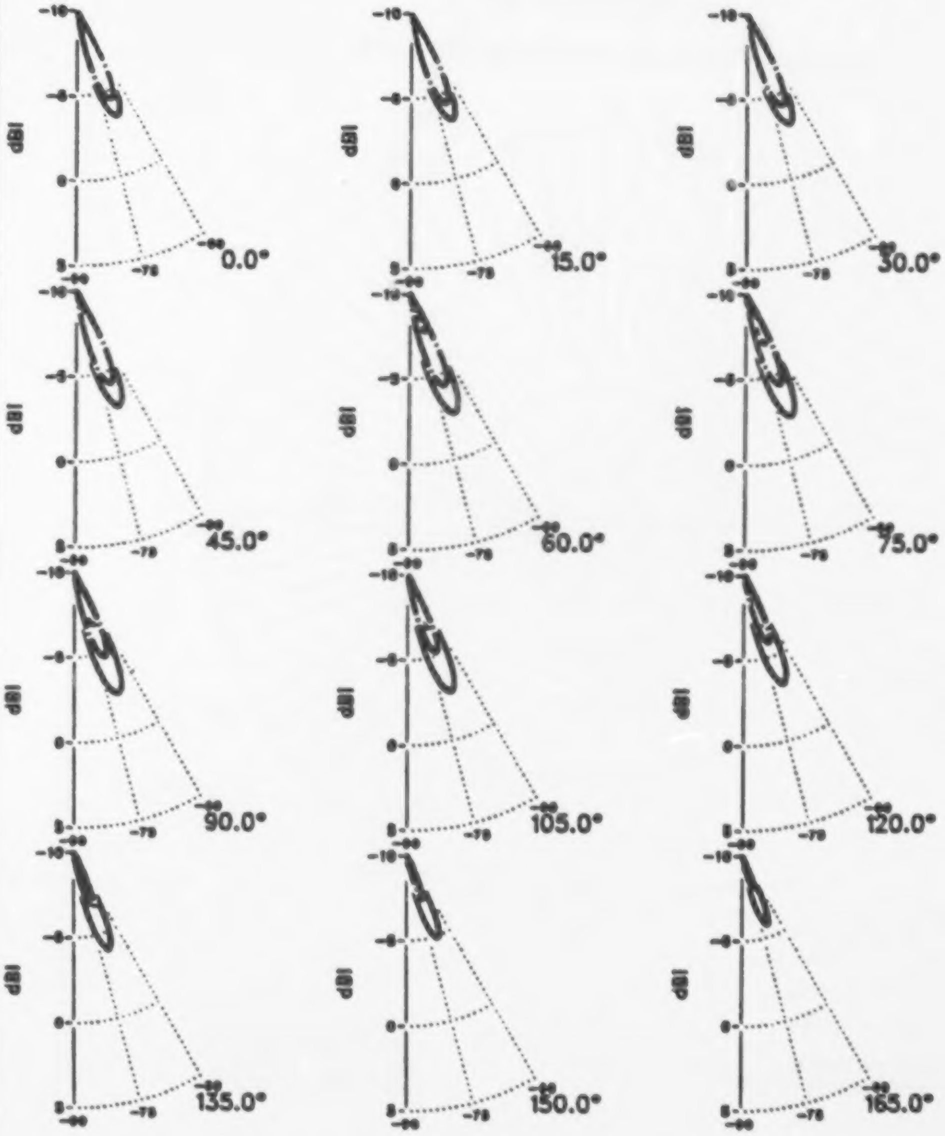

FIGURE B 104

THE JSCP 2X2 ARRAY

2 WAVELENGTH SPACING BETWEEN BAYS

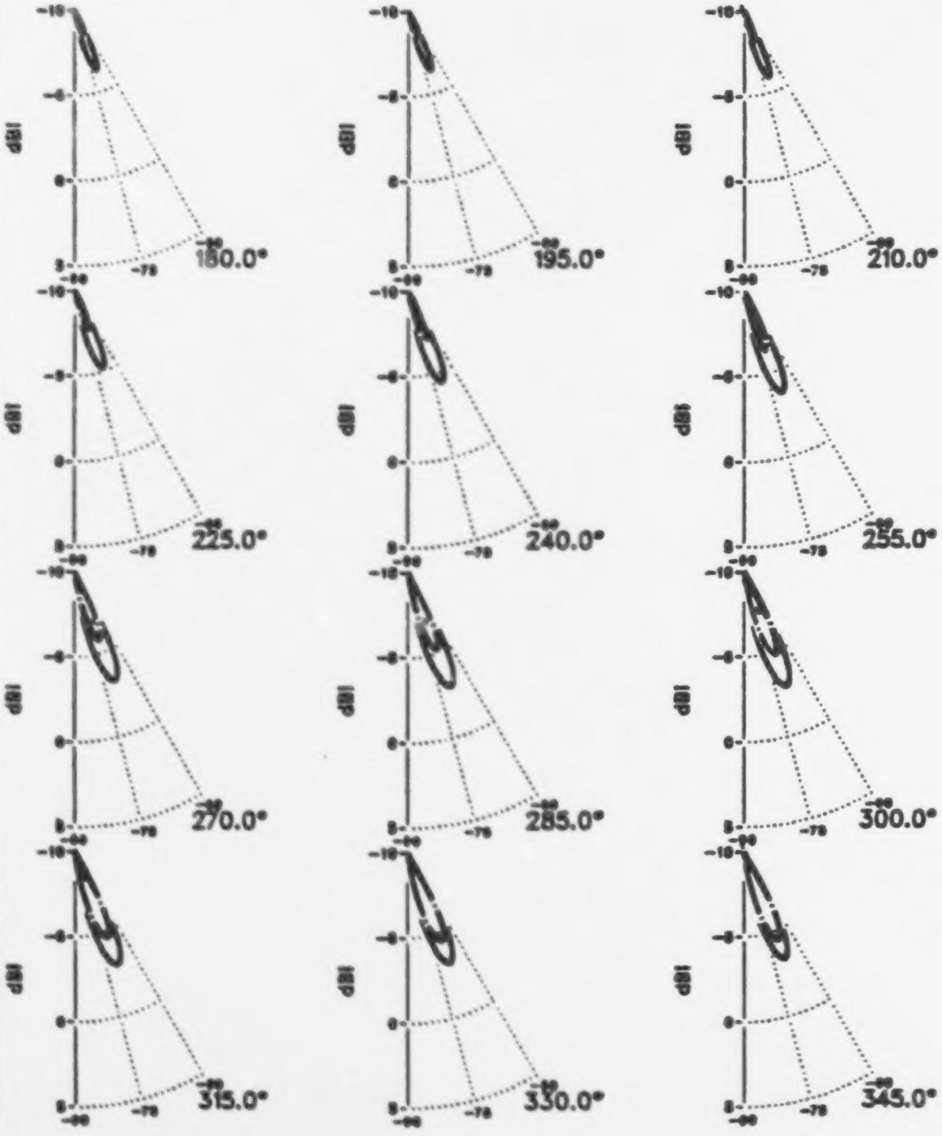

FIGURE B 105

JSC3X3

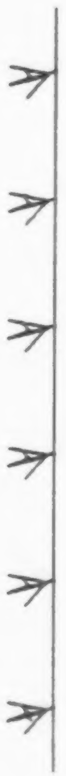

THETA = 60.00 PHI = 60.00 ETA = 90.00

277<

FIGURE B 106

THE JSCP 3X3 ARRAY

STANDARD SPACING OF ONE WAVELENGTH BETWEEN BAYS

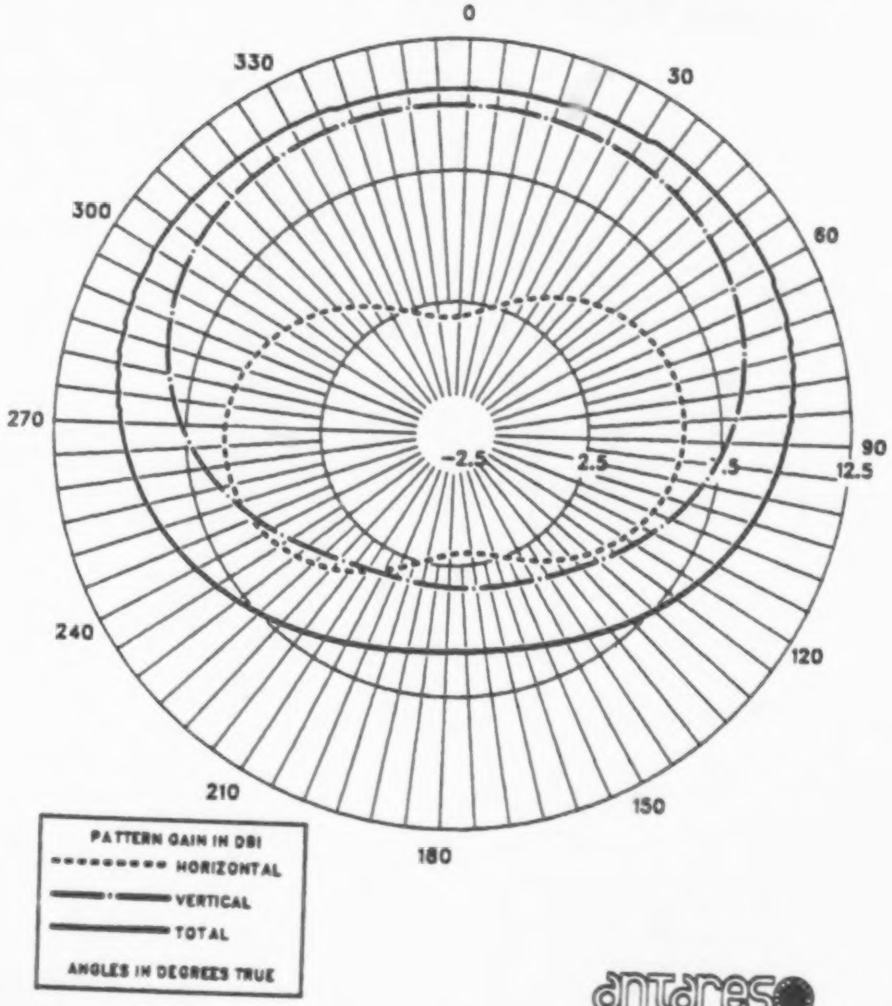

antares
Antenna Analysis Resources

FIGURE B 107

THE JSCP 3X3 ARRAY

STANDARD SPACING OF ONE WAVELENGTH BETWEEN BAYS

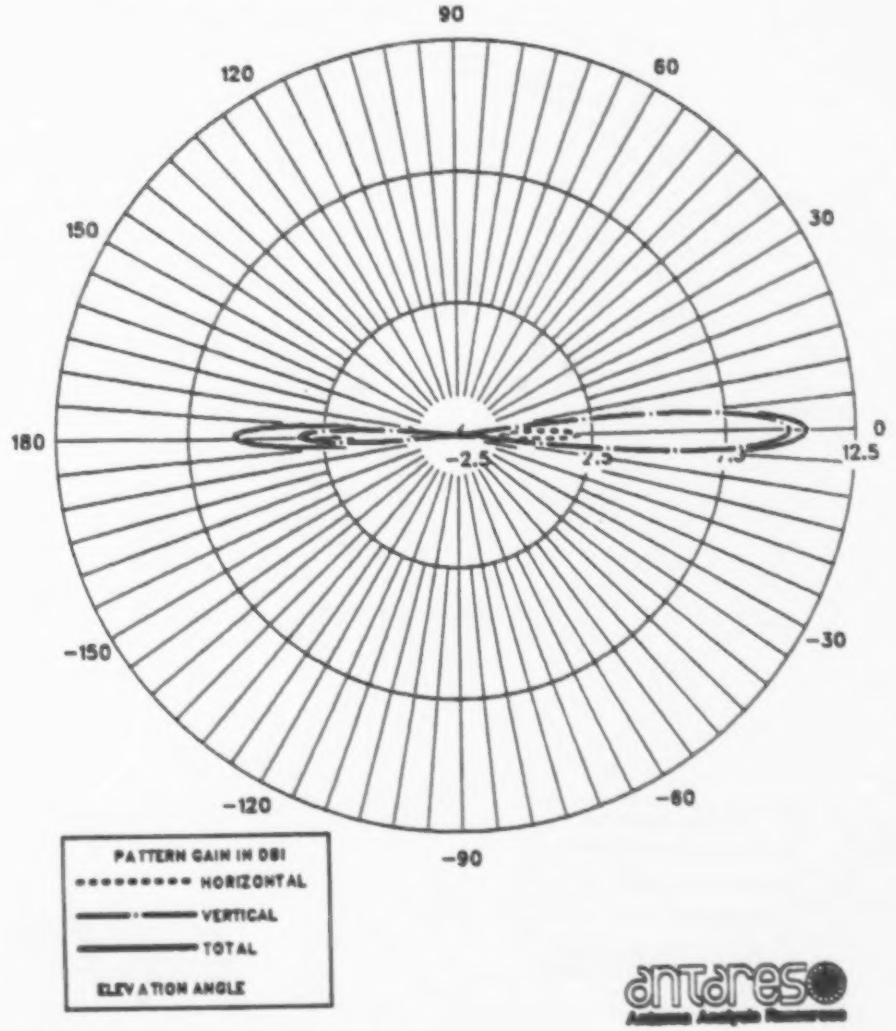

FIGURE B 108

THE JSCP 3X3 ARRAY

STANDARD SPACING OF ONE WAVELENGTH BETWEEN BAYS

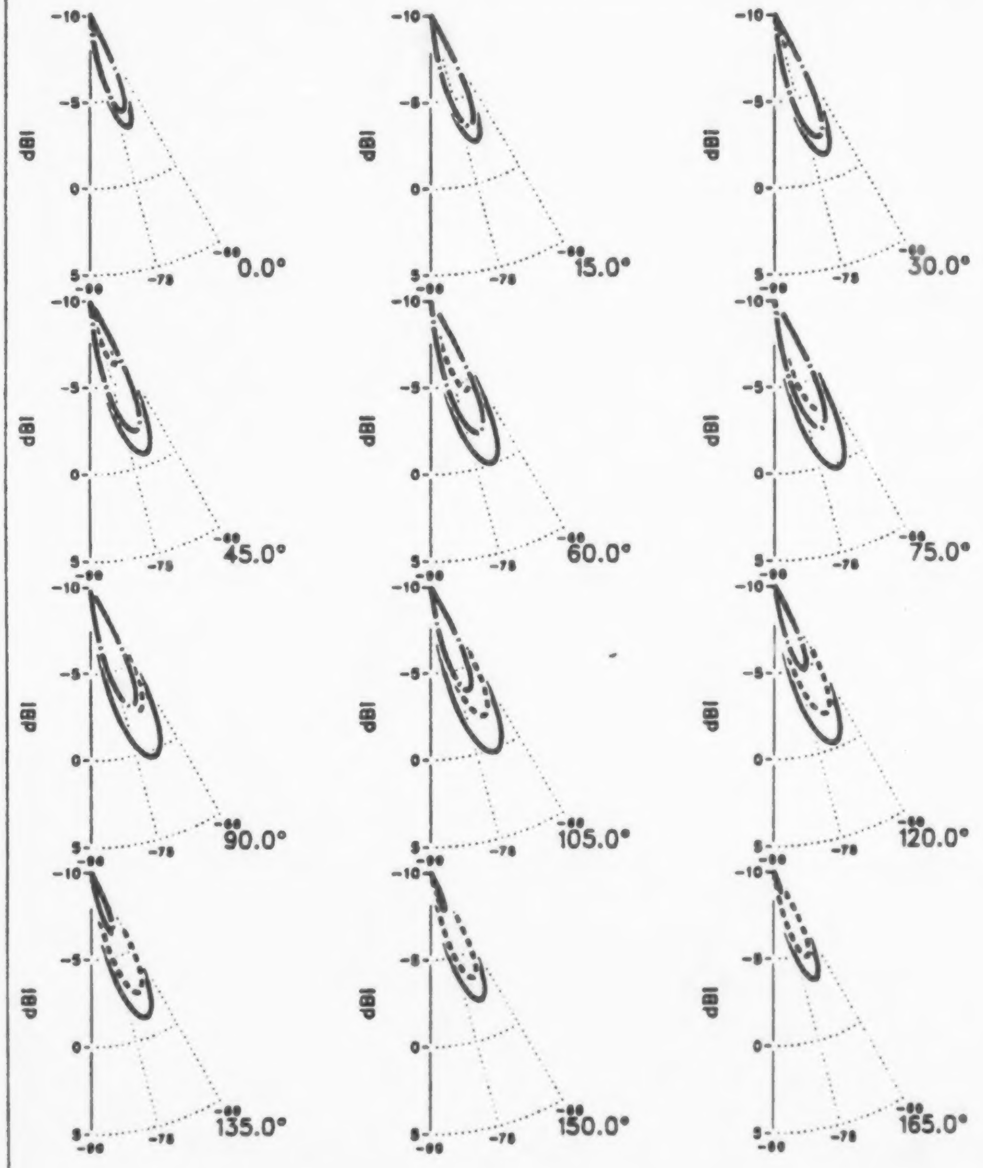

FIGURE B 109

280<

THE JSCP 3X3 ARRAY

STANDARD SPACING OF ONE WAVELENGTH BETWEEN BAYS

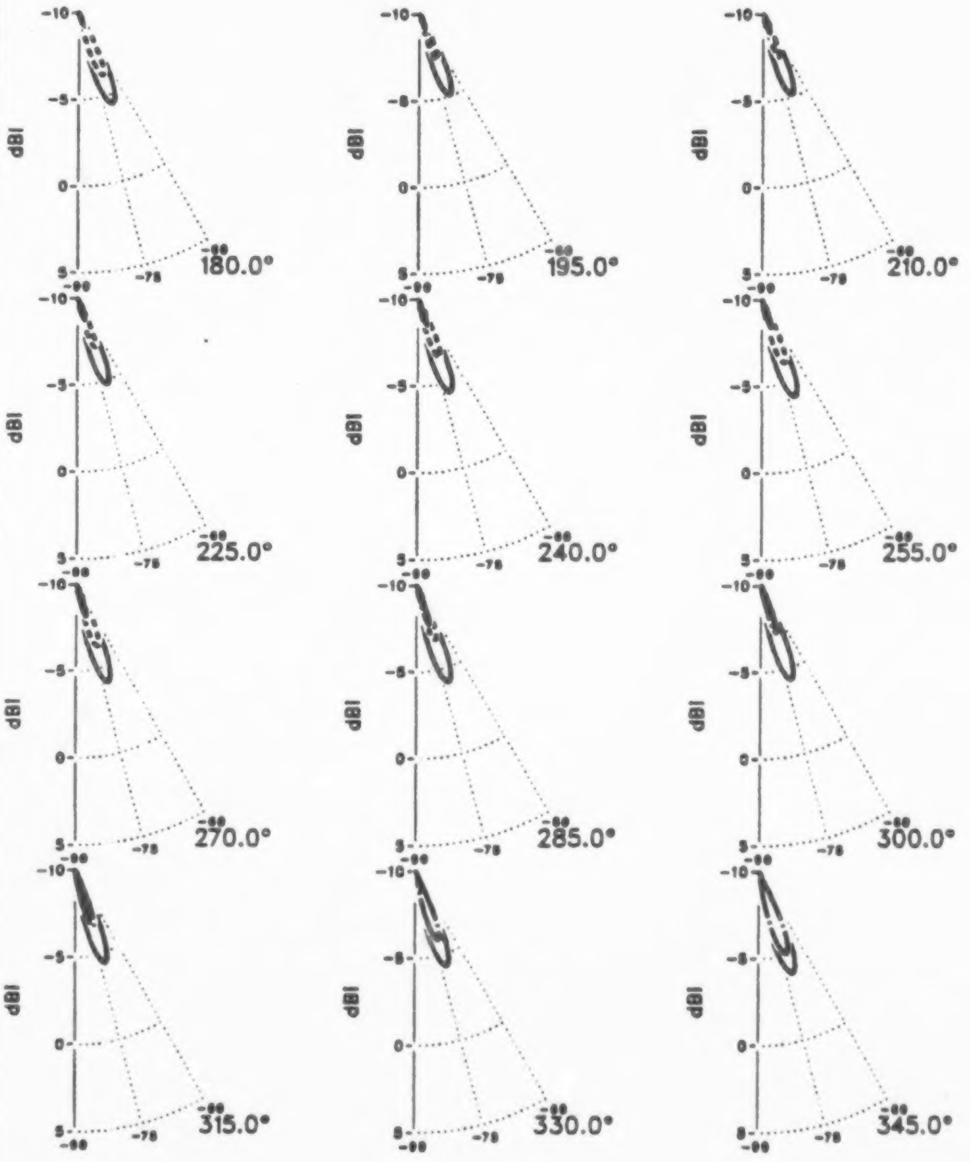

FIGURE B 110

JSC3X3TH

THETA = 60.00 PHI = 60.00 ETA = 90.00

FIGURE B 111

THE JSCP 3X3 ARRAY

3/2 WAVELENGTH SPACING BETWEEN BAYS

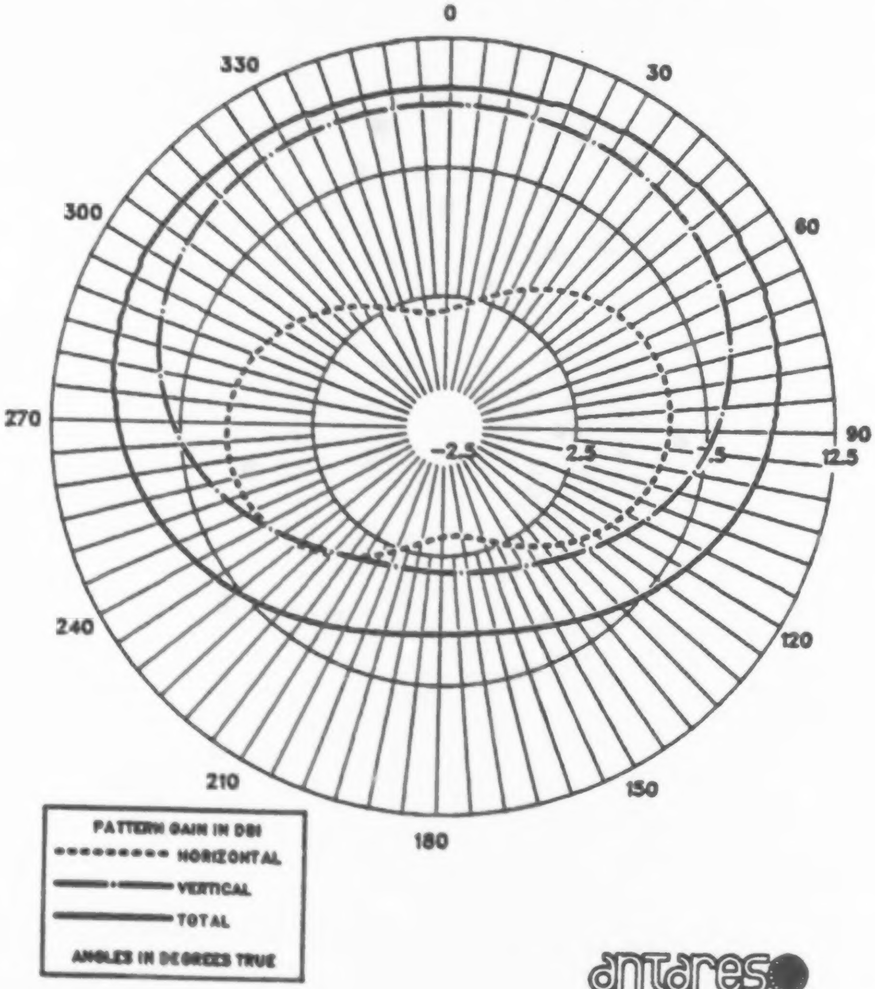

antares
Antenna Analysis Resources

FIGURE B 112

THE JSCP 3X3 ARRAY

3/2 WAVELENGTH SPACING BETWEEN BAYS

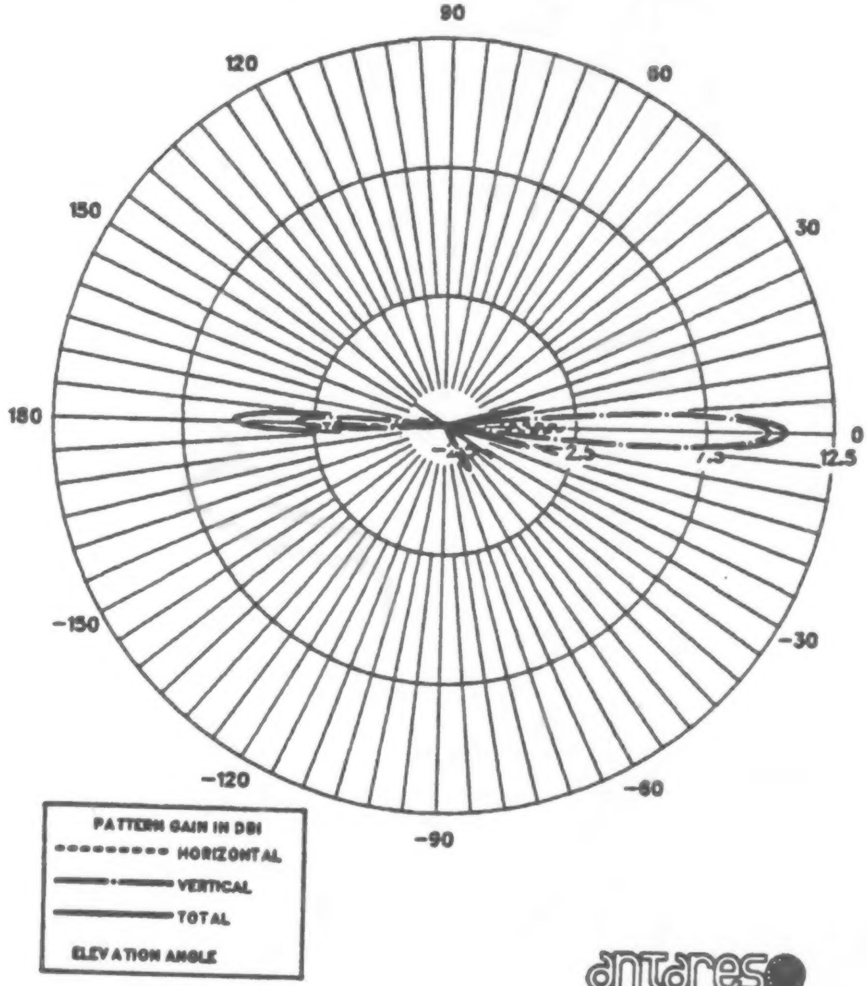

antares
Antenna Analysis Resources

FIGURE B 113

THE JSCP 3X3 ARRAY

3/2 WAVELENGTH SPACING BETWEEN BAYS

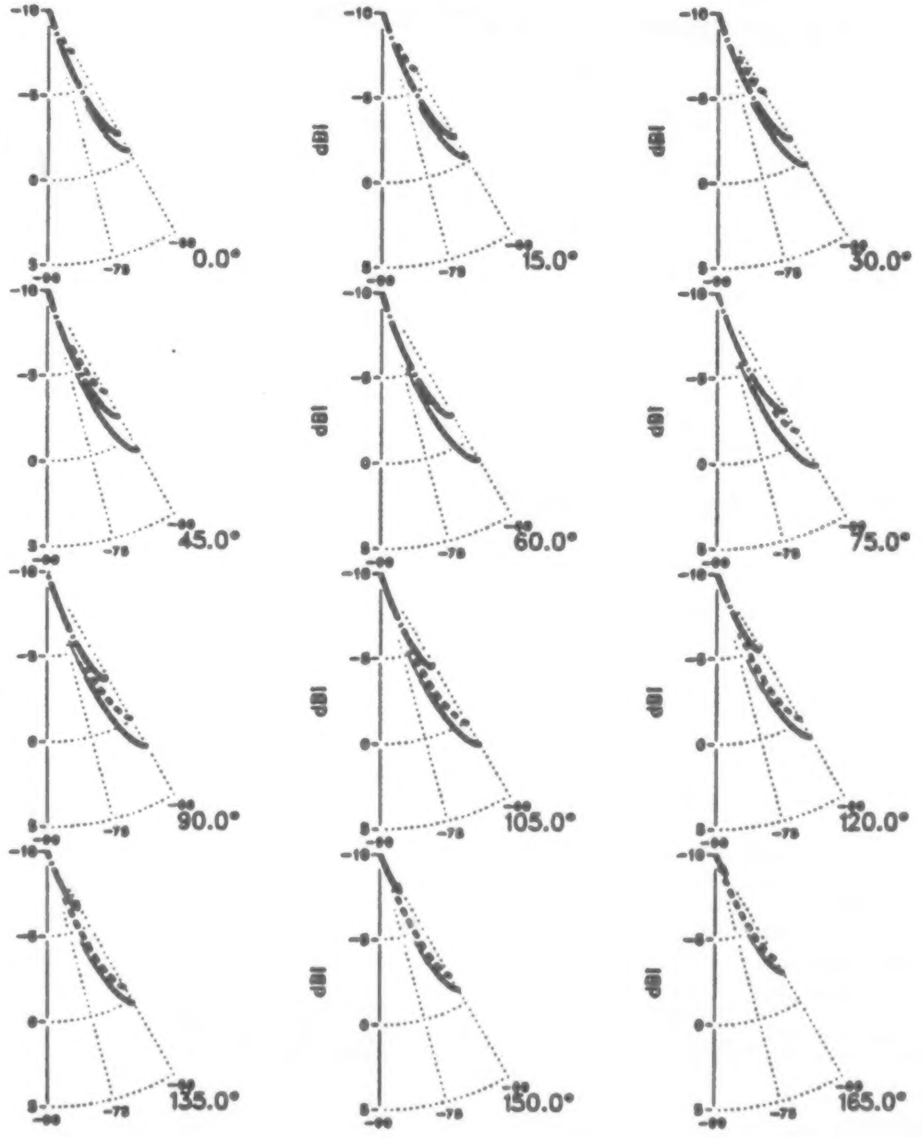

FIGURE B 114

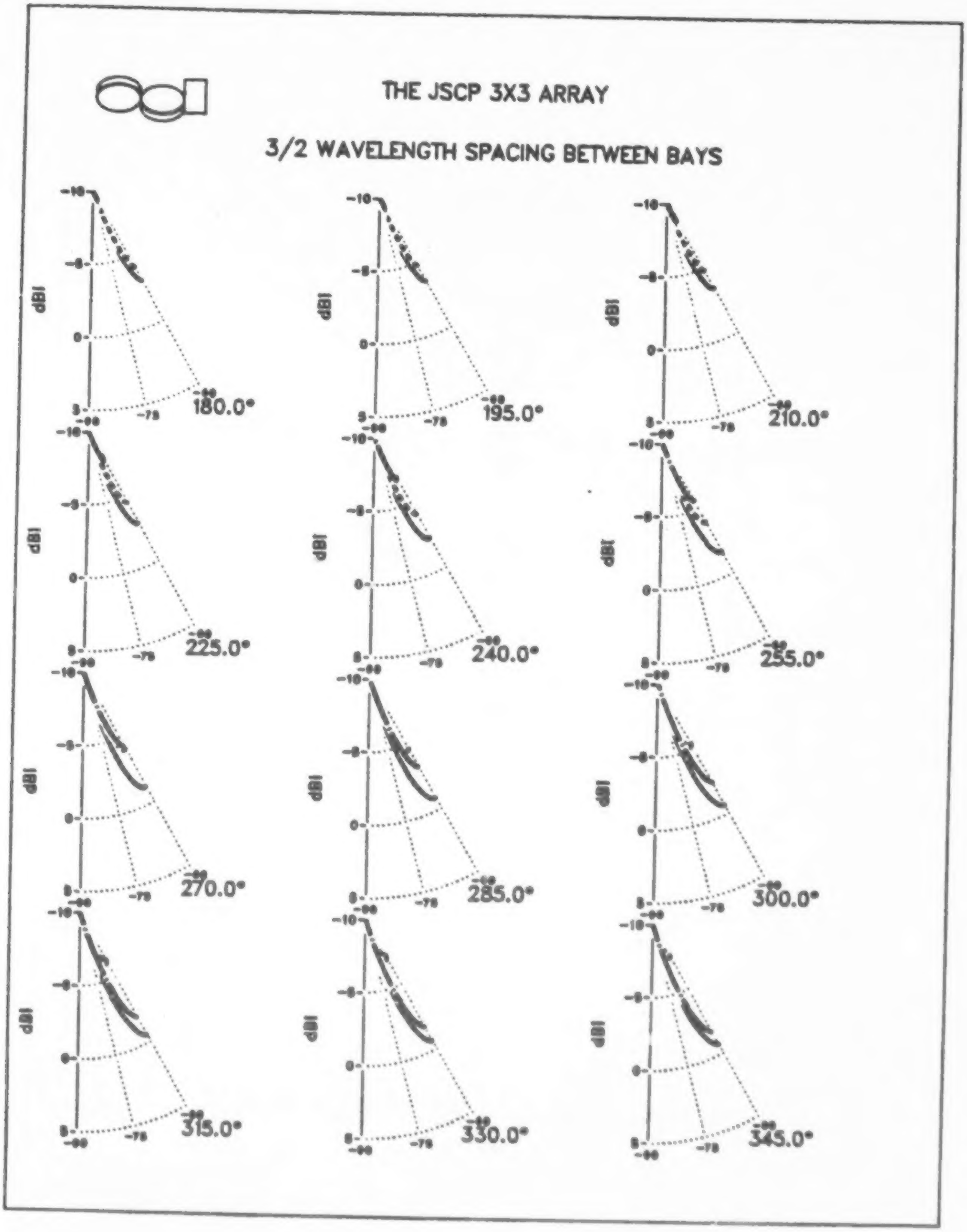
THE JSCP 3X3 ARRAY
3/2 WAVELENGTH SPACING BETWEEN BAYS
dBi
-10
-5
0
5
-90
-75
-60
180.0°
195.0°
210.0°
225.0°
240.0°
255.0°
270.0°
285.0°
300.0°
315.0°
330.0°
345.0°

FIGURE B 115

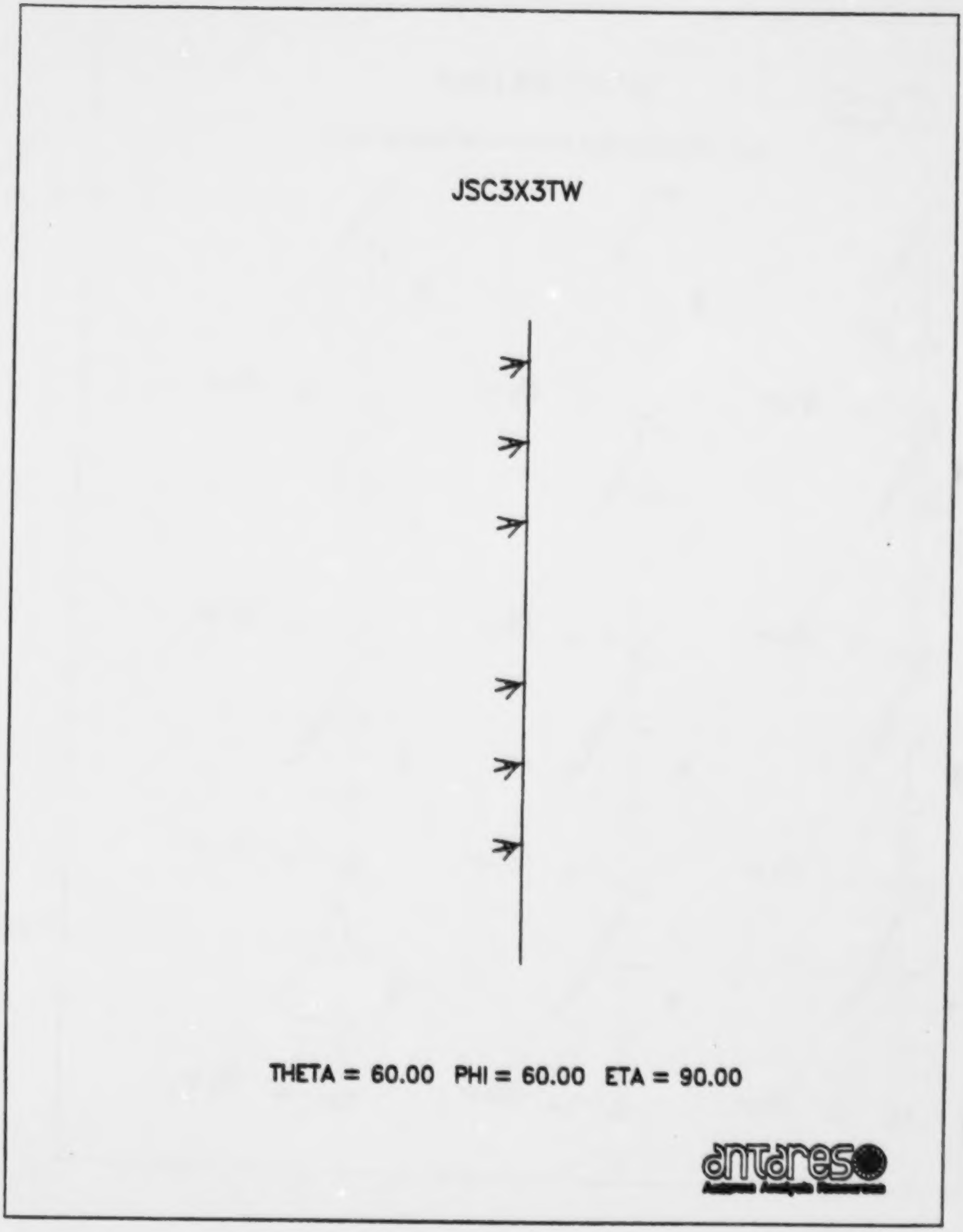

FIGURE B 116

THE JSCP 3X3 ARRAY

2 WAVELENGTH SPACING BETWEEN BAYS

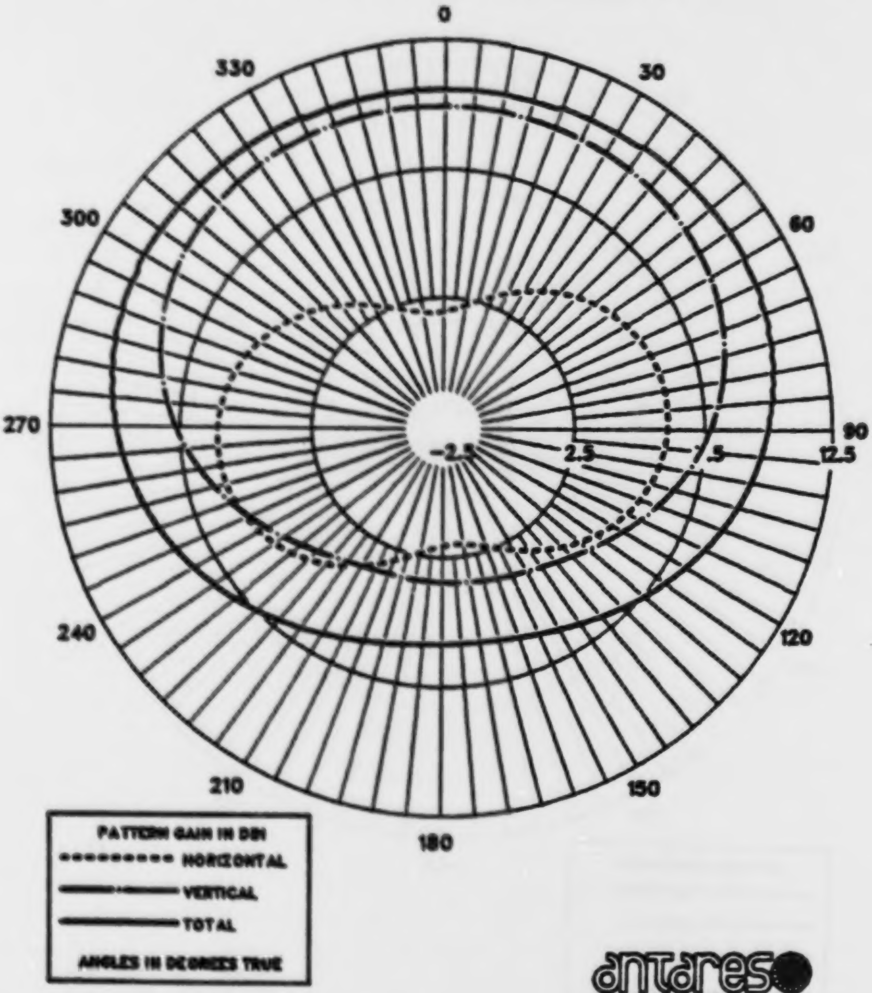

antares
Antenna Analysis Resources

FIGURE B 117

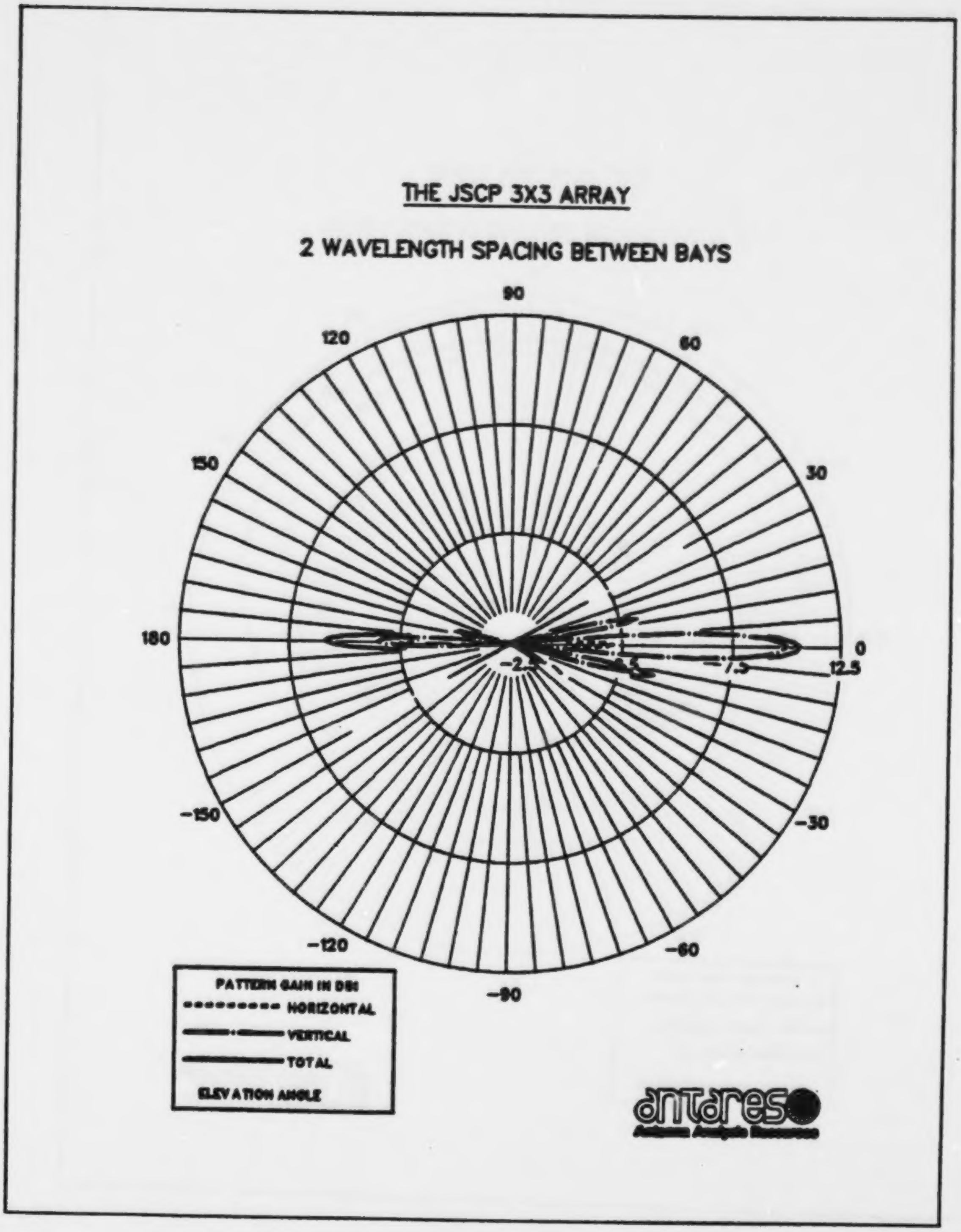

THE JSCP 3X3 ARRAY

2 WAVELENGTH SPACING BETWEEN BAYS

FIGURE B 118

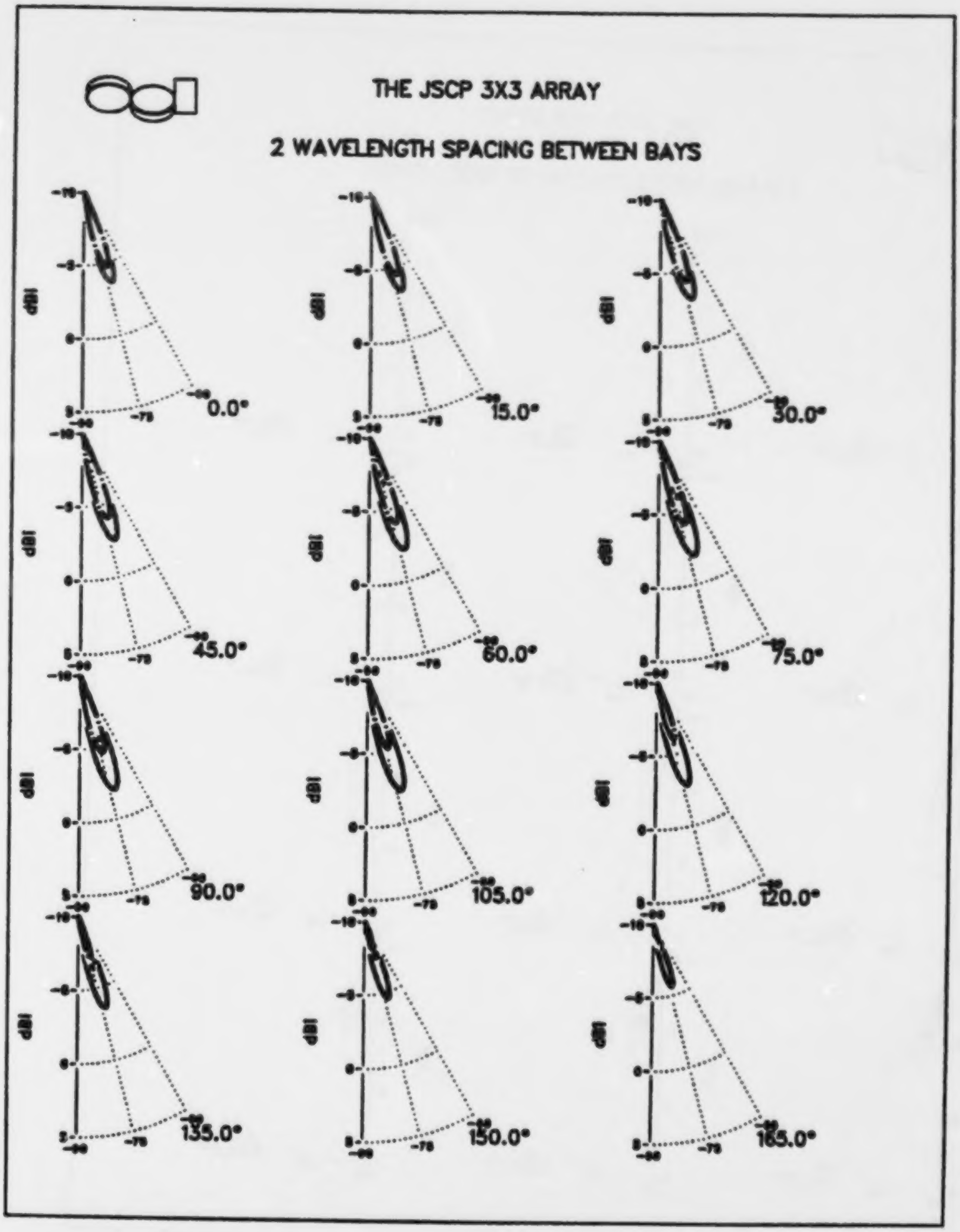

THE JSCP 3X3 ARRAY

2 WAVELENGTH SPACING BETWEEN BAYS

FIGURE B 119

290<

THE JSCP 3X3 ARRAY

2 WAVELENGTH SPACING BETWEEN BAYS

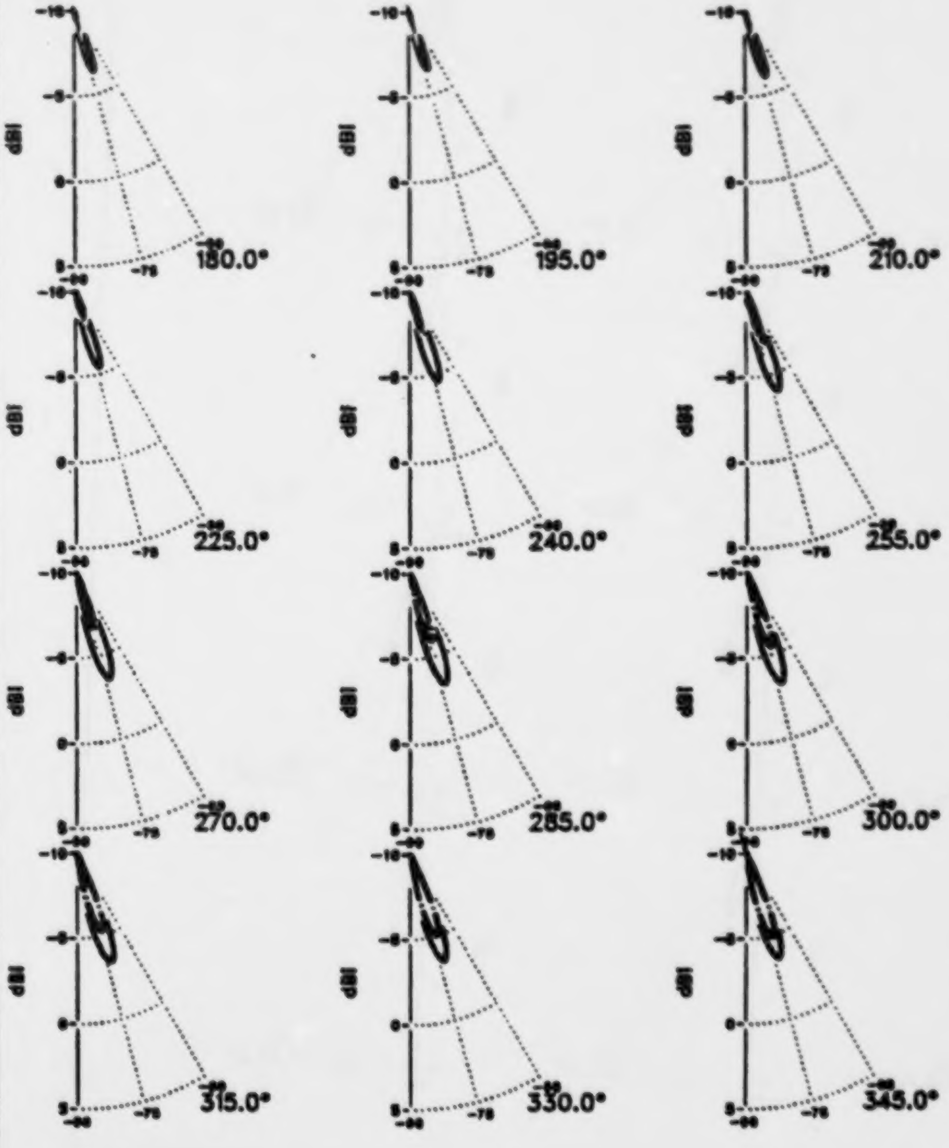

FIGURE B 120

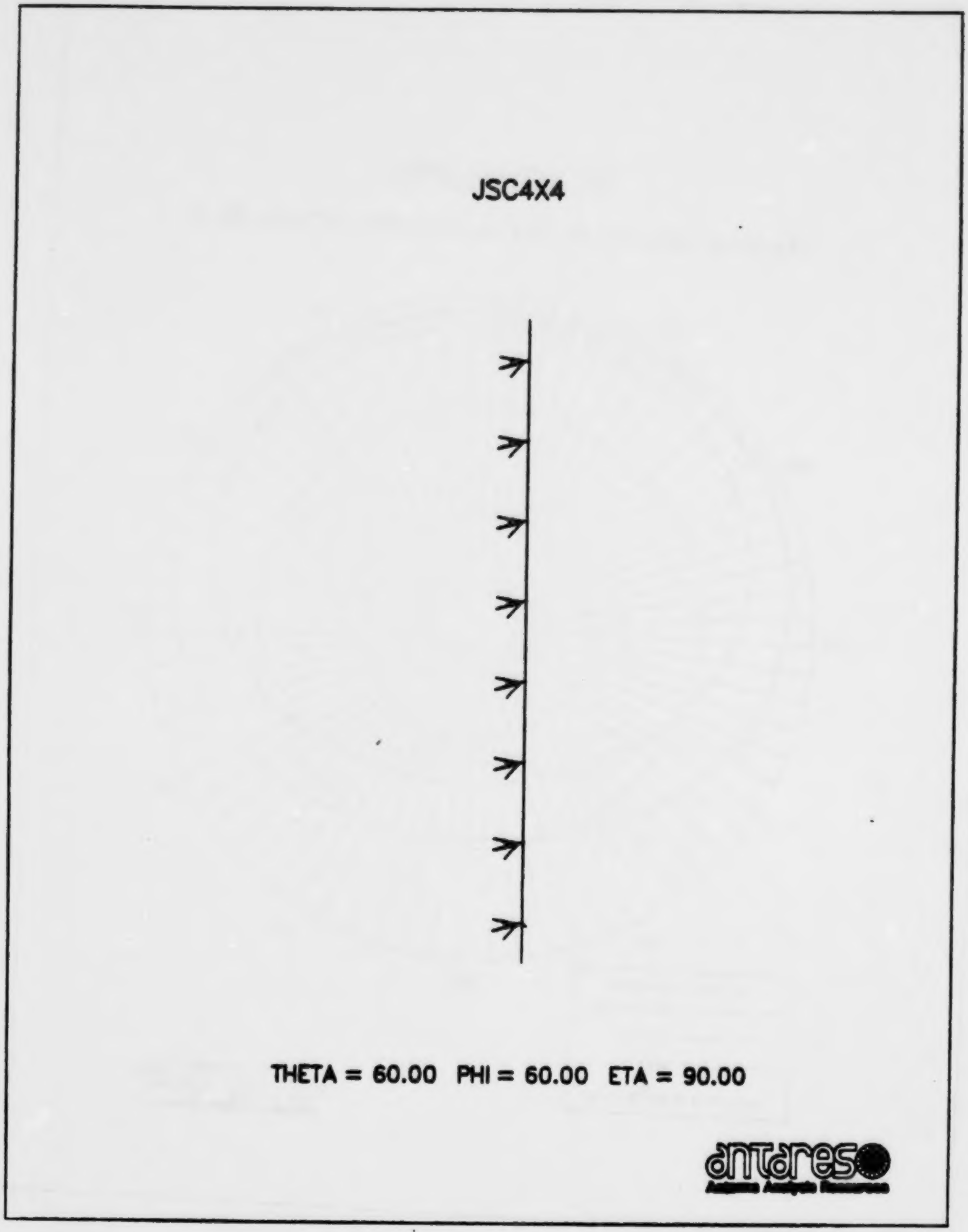

FIGURE B 121

THE JSCP 4X4 ARRAY

STANDARD SPACING OF ONE WAVELENGTH BETWEEN BAYS

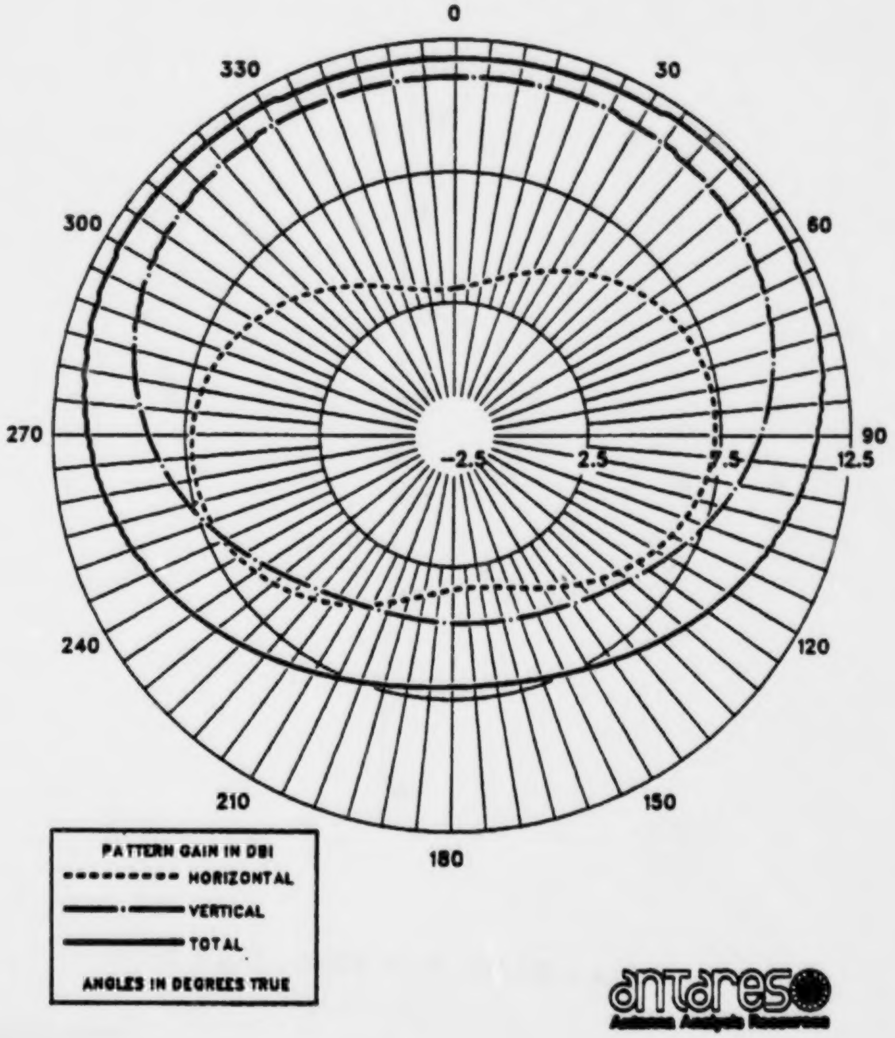

antares
Antenna Analysis Resources

FIGURE B 122

THE JSCP 4X4 ARRAY

STANDARD SPACING OF ONE WAVELENGTH BETWEEN BAYS

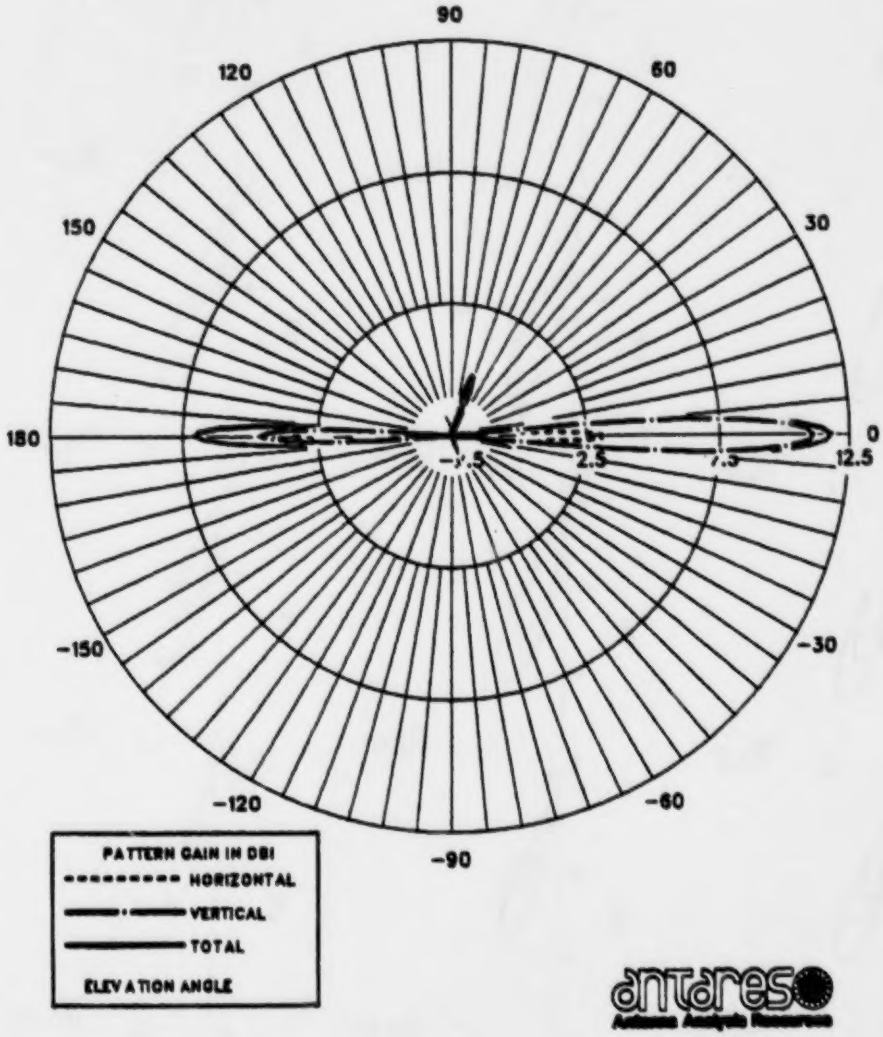

antares
Antenna Analysis Resources

FIGURE B 123

THE JSCP 4X4 ARRAY

STANDARD SPACING OF ONE WAVELENGTH BETWEEN BAYS

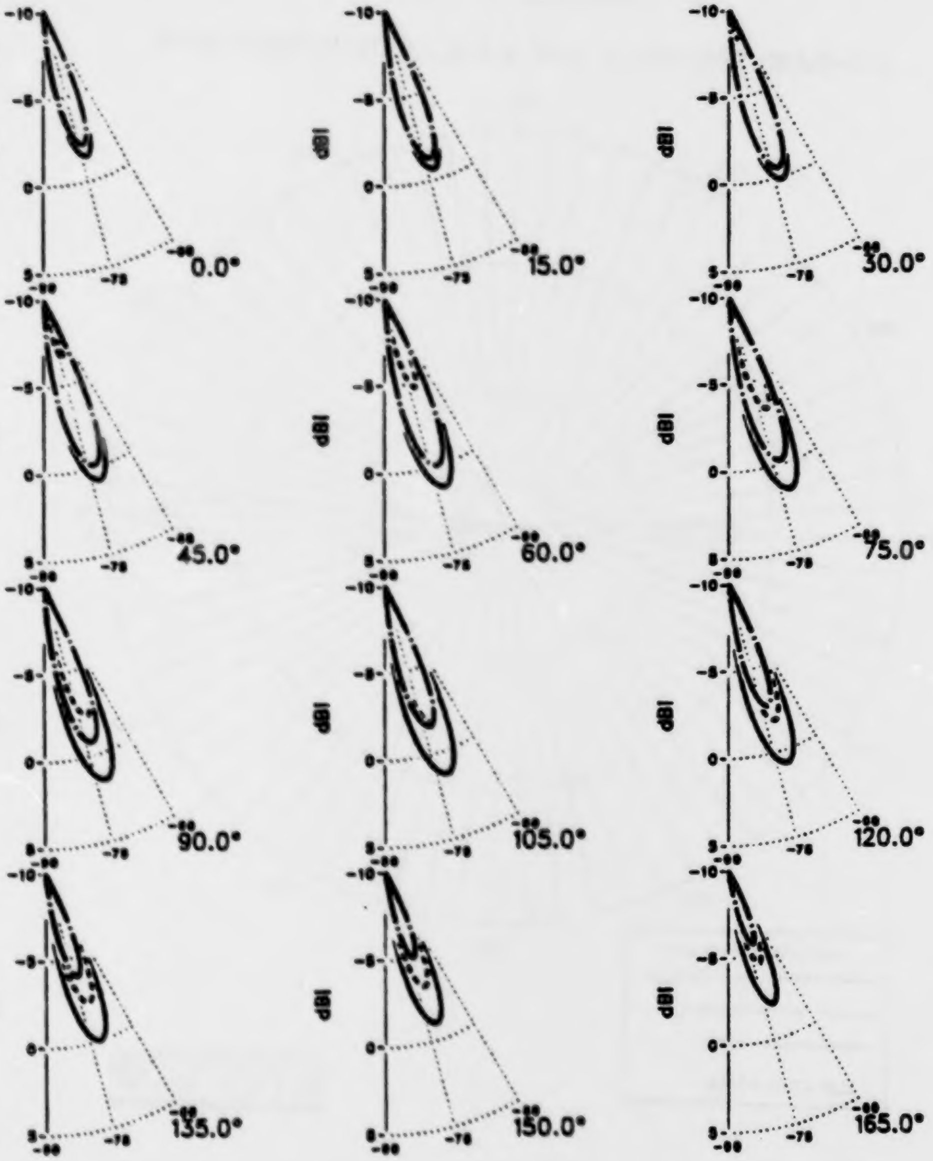

FIGURE B 124

THE JSCP 4X4 ARRAY

STANDARD SPACING OF ONE WAVELENGTH BETWEEN BAYS

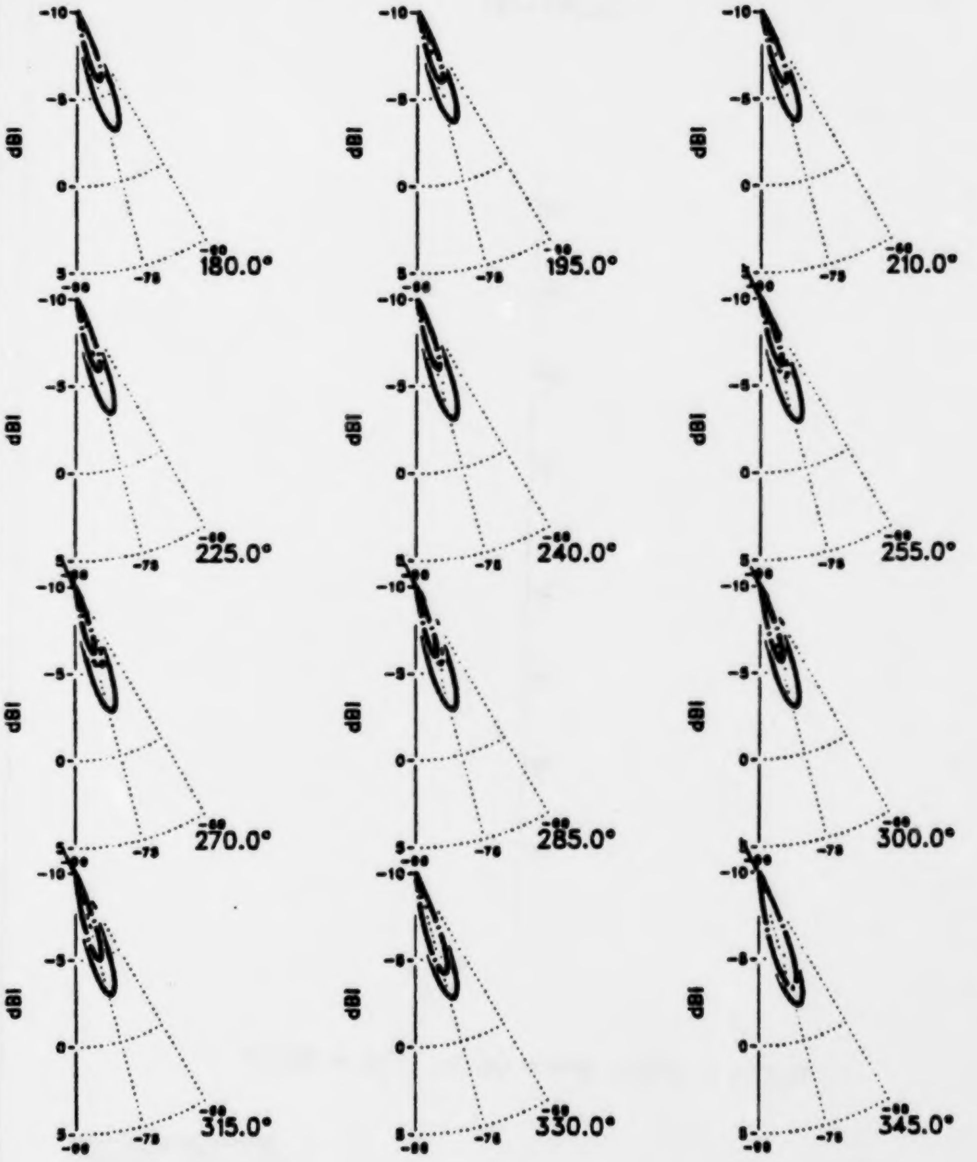

FIGURE B 125

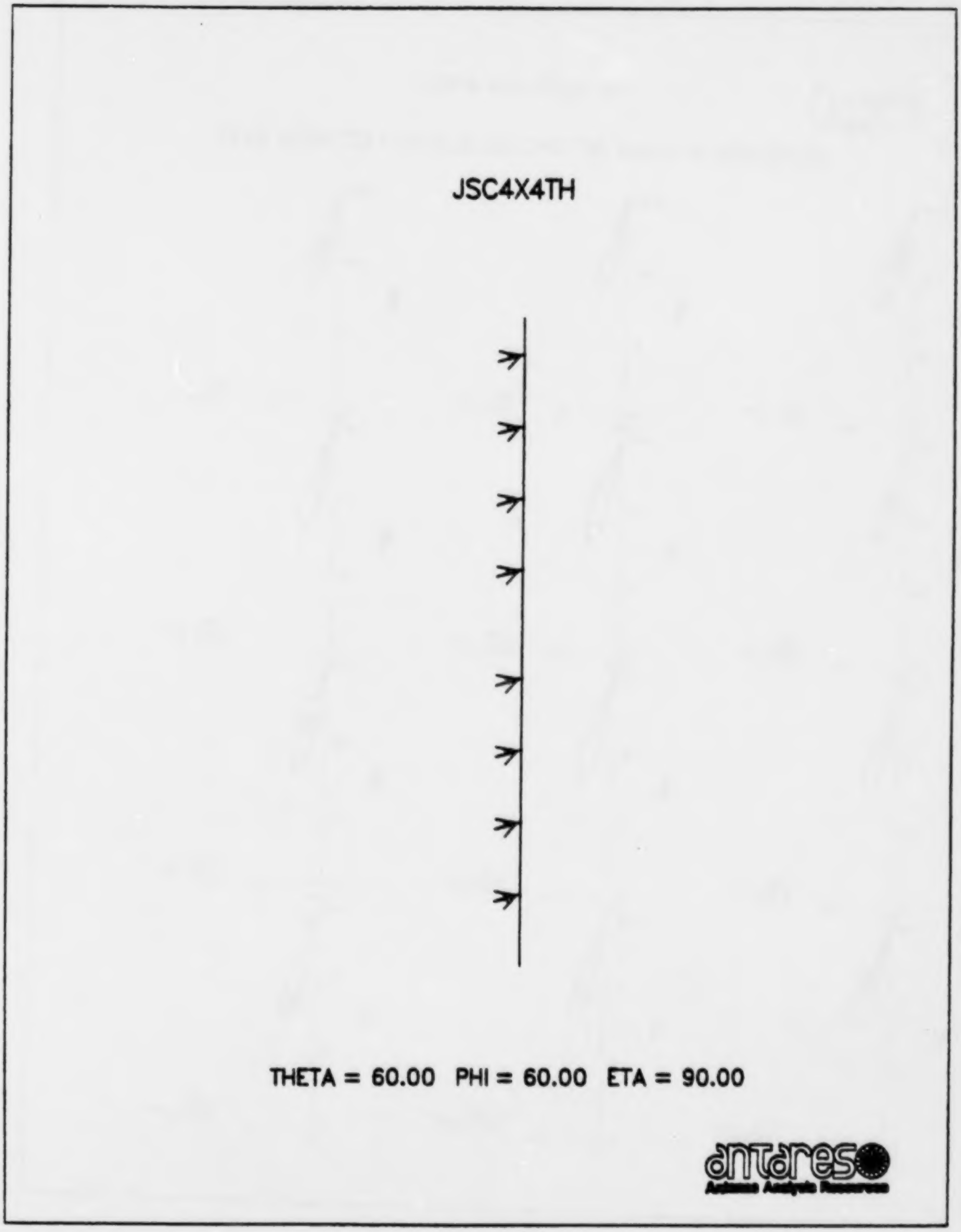
JSC4X4TH
THETA = 60.00 PHI = 60.00 ETA = 90.00
antares
Antares Analysis Resources

FIGURE B 126

THE JSCP 4X4 ARRAY

3/2 WAVELENGTH SPACING BETWEEN BAYS

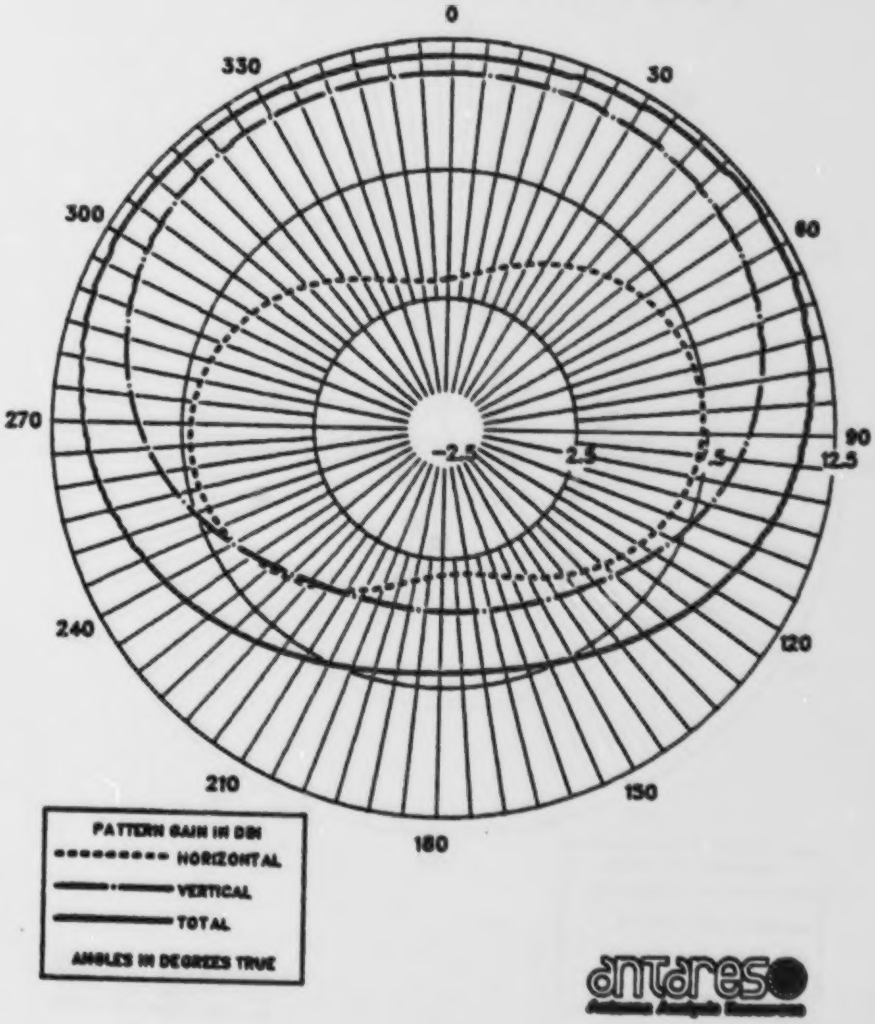

antares
Antenna Analysis Resources

FIGURE B 127

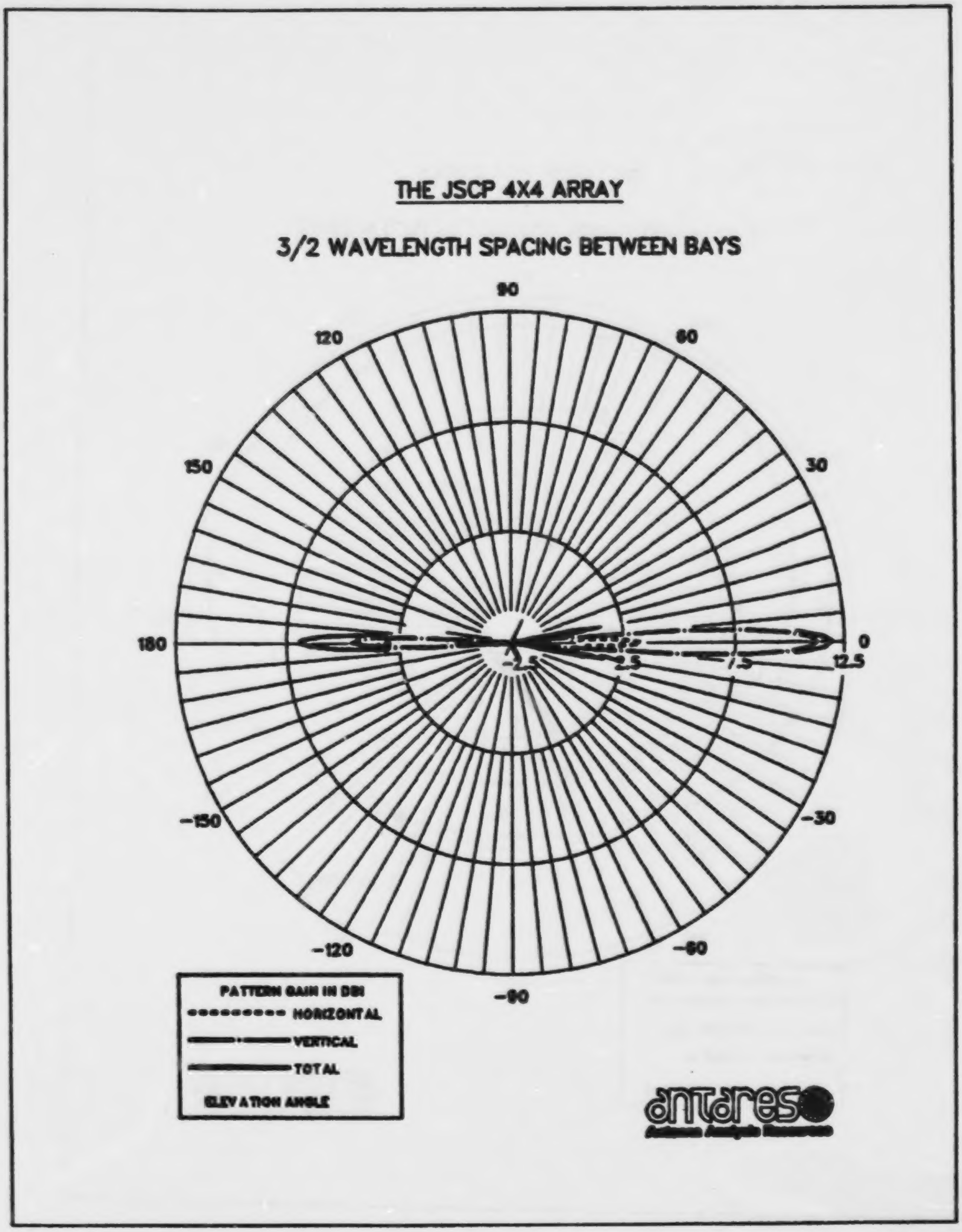
THE JSCP 4X4 ARRAY

3/2 WAVELENGTH SPACING BETWEEN BAYS

FIGURE B 128

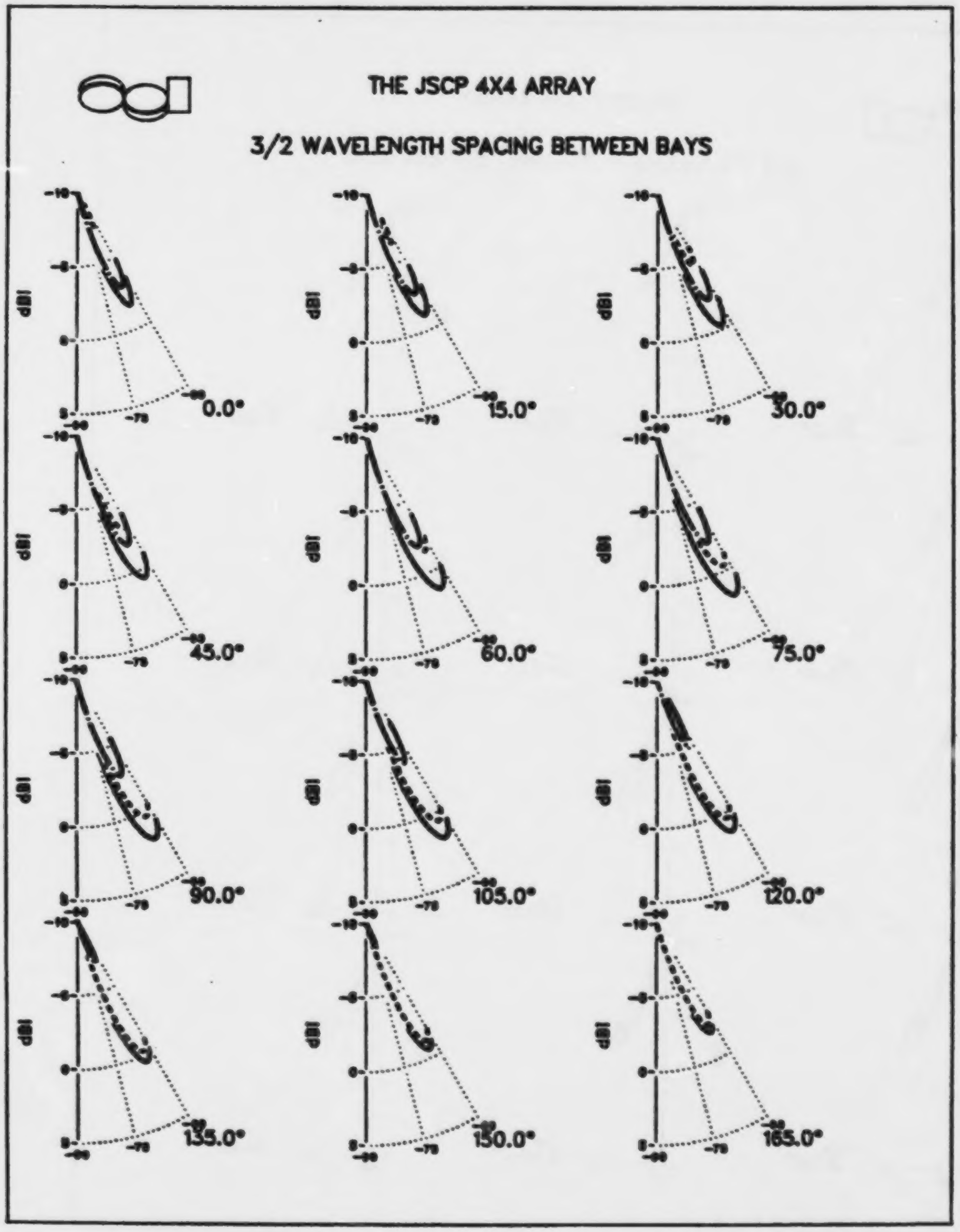

THE JSCP 4X4 ARRAY

3/2 WAVELENGTH SPACING BETWEEN BAYS

FIGURE B 129

THE JSCP 4X4 ARRAY

3/2 WAVELENGTH SPACING BETWEEN BAYS

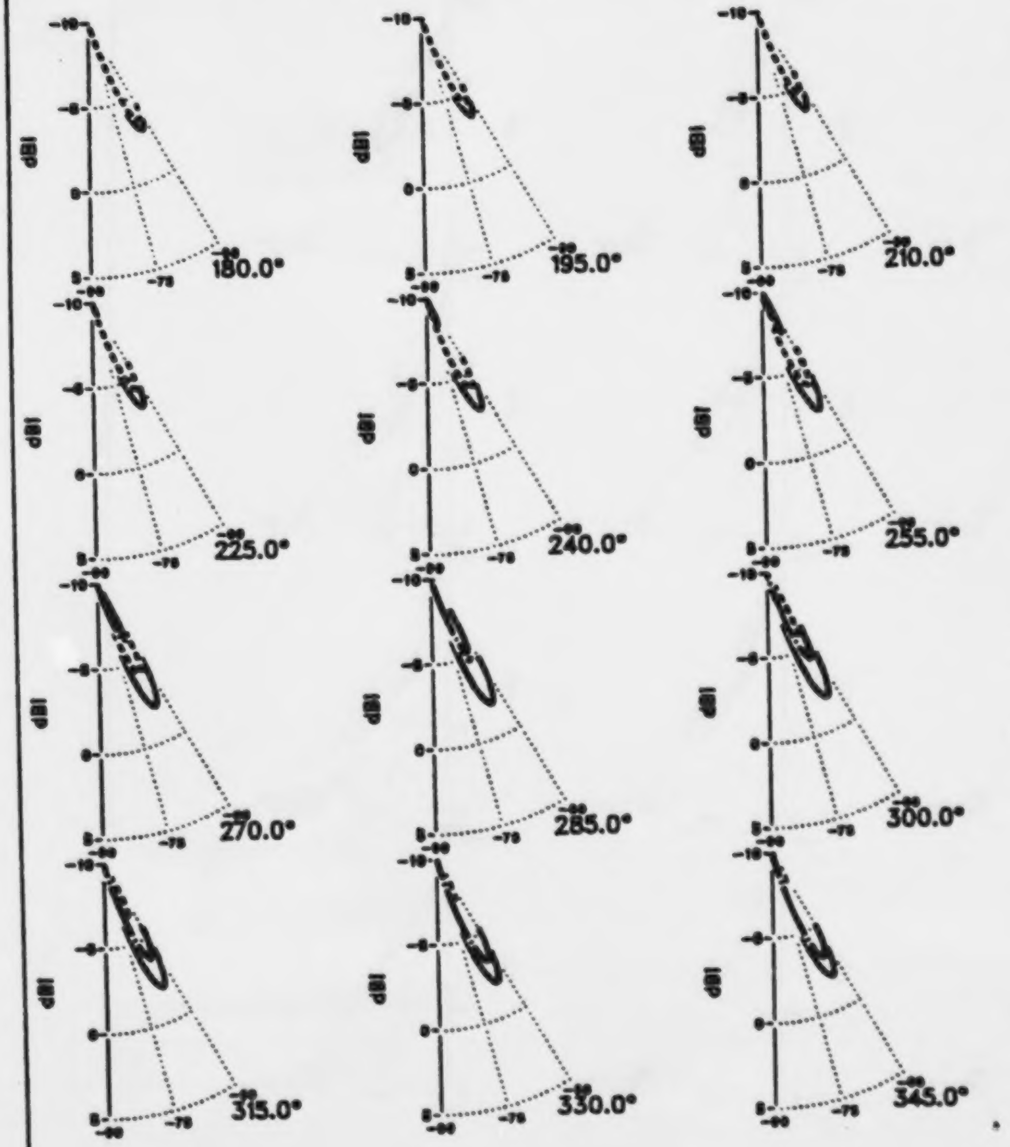

FIGURE B 130

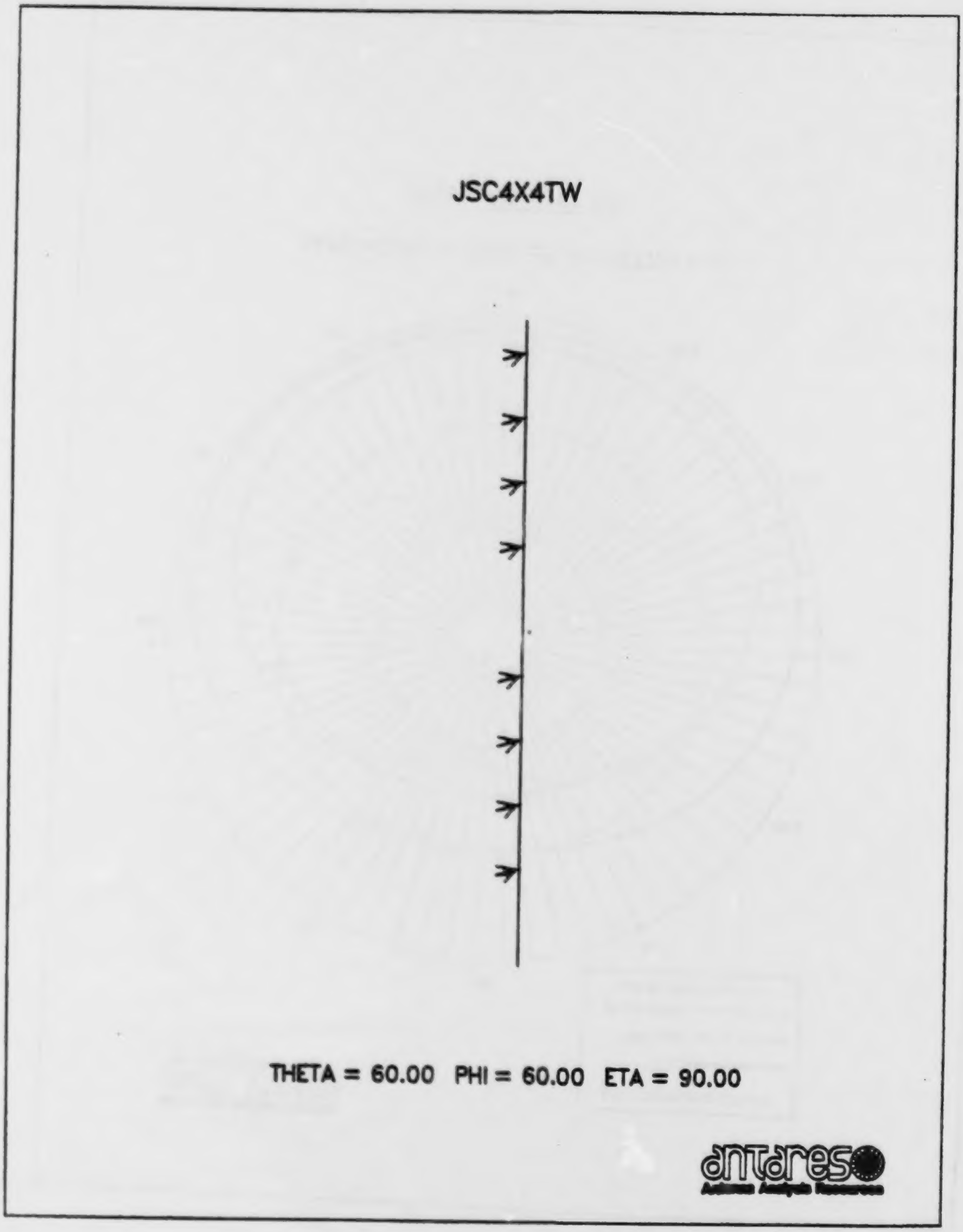
JSC4X4TW
THETA = 60.00 PHI = 60.00 ETA = 90.00
antares
Antenna Analysis Resources

FIGURE B 131

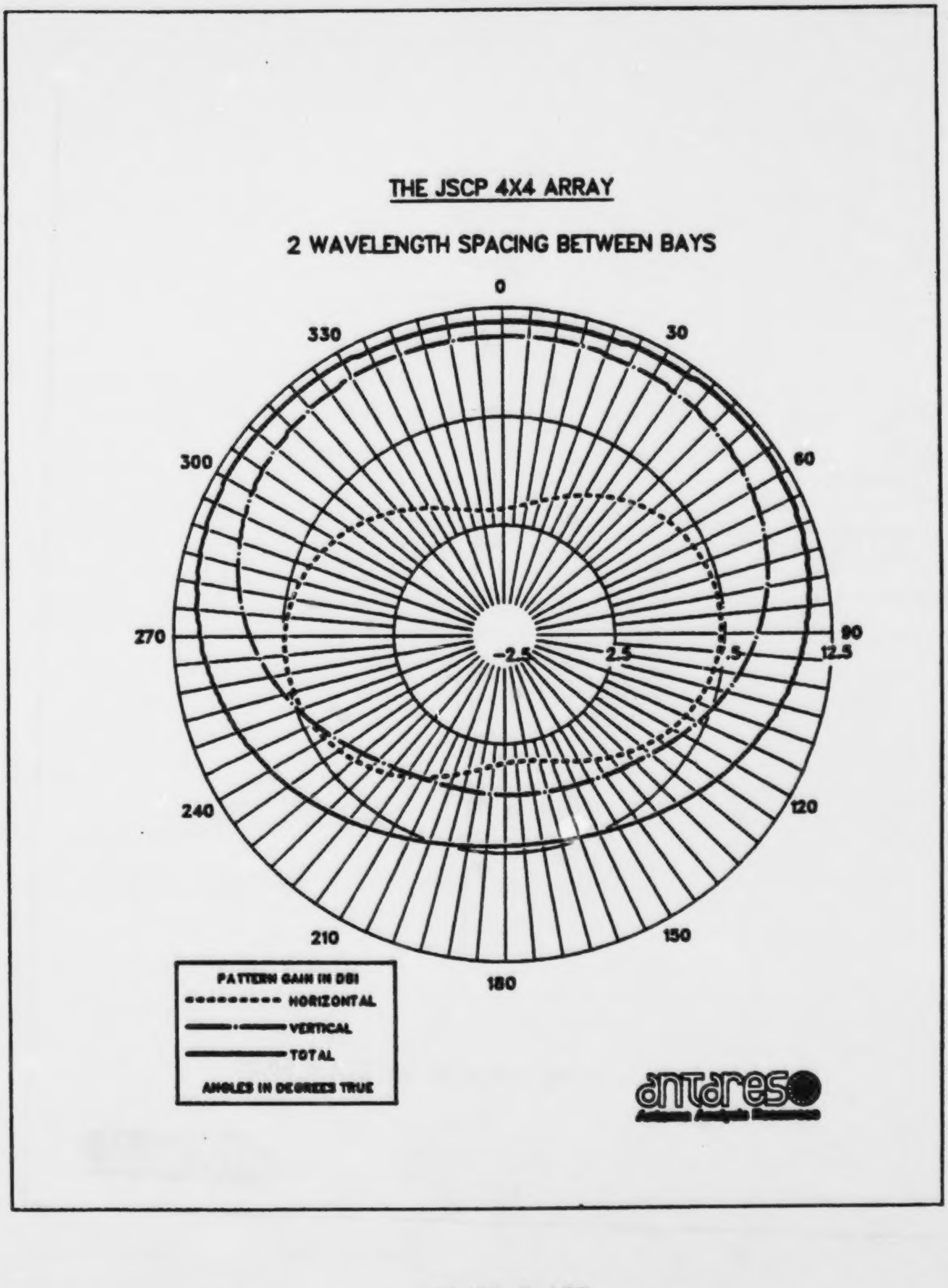
THE JSCP 4X4 ARRAY
2 WAVELENGTH SPACING BETWEEN BAYS
0
30
60
90
120
150
180
210
240
270
300
330
-2.5
2.5
7.5
12.5
PATTERN GAIN IN DBI
HORIZONTAL
VERTICAL
TOTAL
ANGLES IN DEGREES TRUE
antares
Antenna Analysis Resource

FIGURE B 132

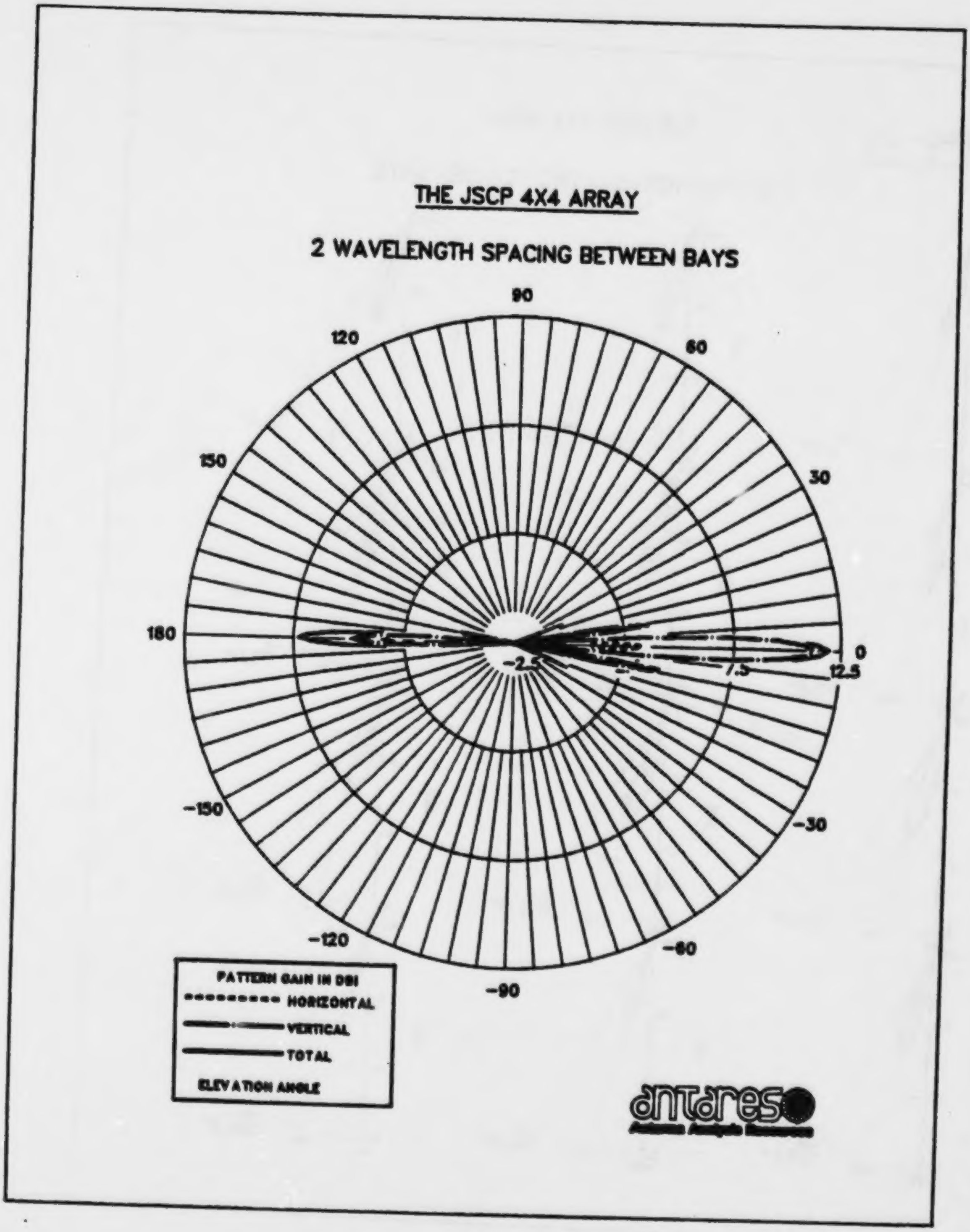

THE JSCP 4X4 ARRAY

2 WAVELENGTH SPACING BETWEEN BAYS

FIGURE B 133

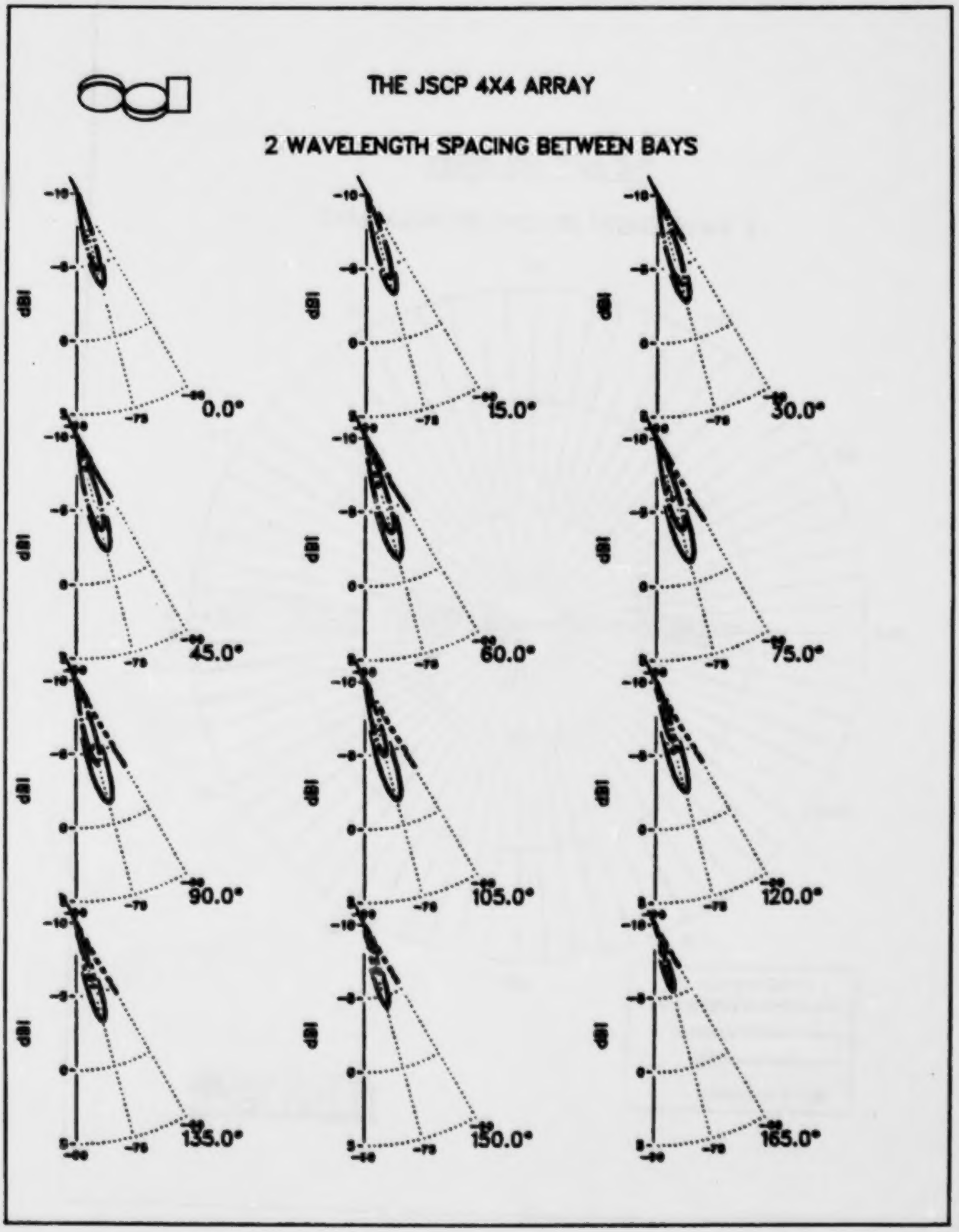

THE JSCP 4X4 ARRAY

2 WAVELENGTH SPACING BETWEEN BAYS

FIGURE B 134

THE JSCP 4X4 ARRAY

2 WAVELENGTH SPACING BETWEEN BAYS

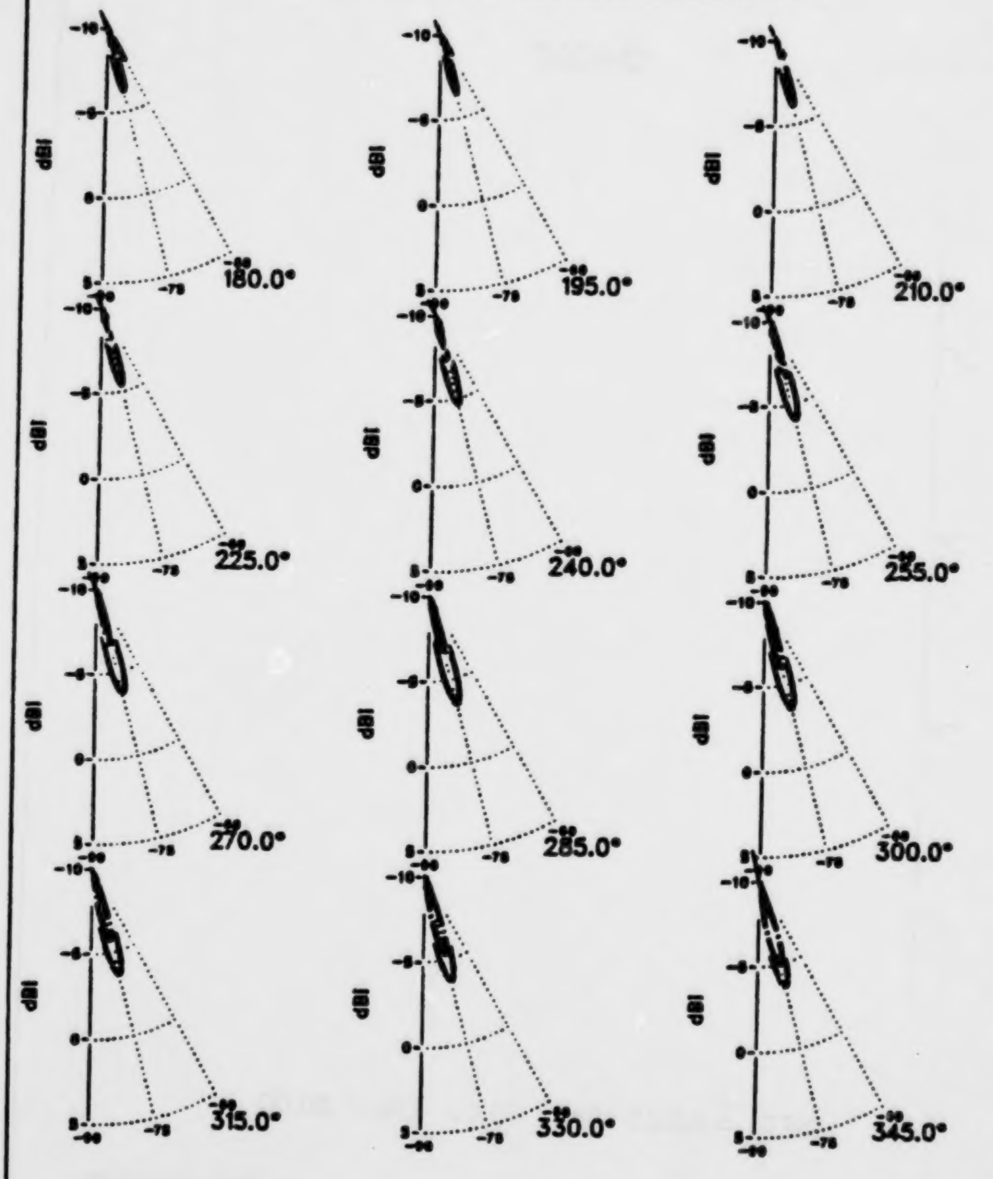

FIGURE B 135

CMK2X2

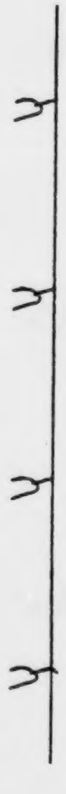

THETA = 60.00 PHI = 60.00 ETA = 90.00

antares
Antenna Analysis Resources

FIGURE B 136

THE COMARK 2X2 ARRAY

STANDARD SPACING OF ONE WAVELENGTH BETWEEN BAYS

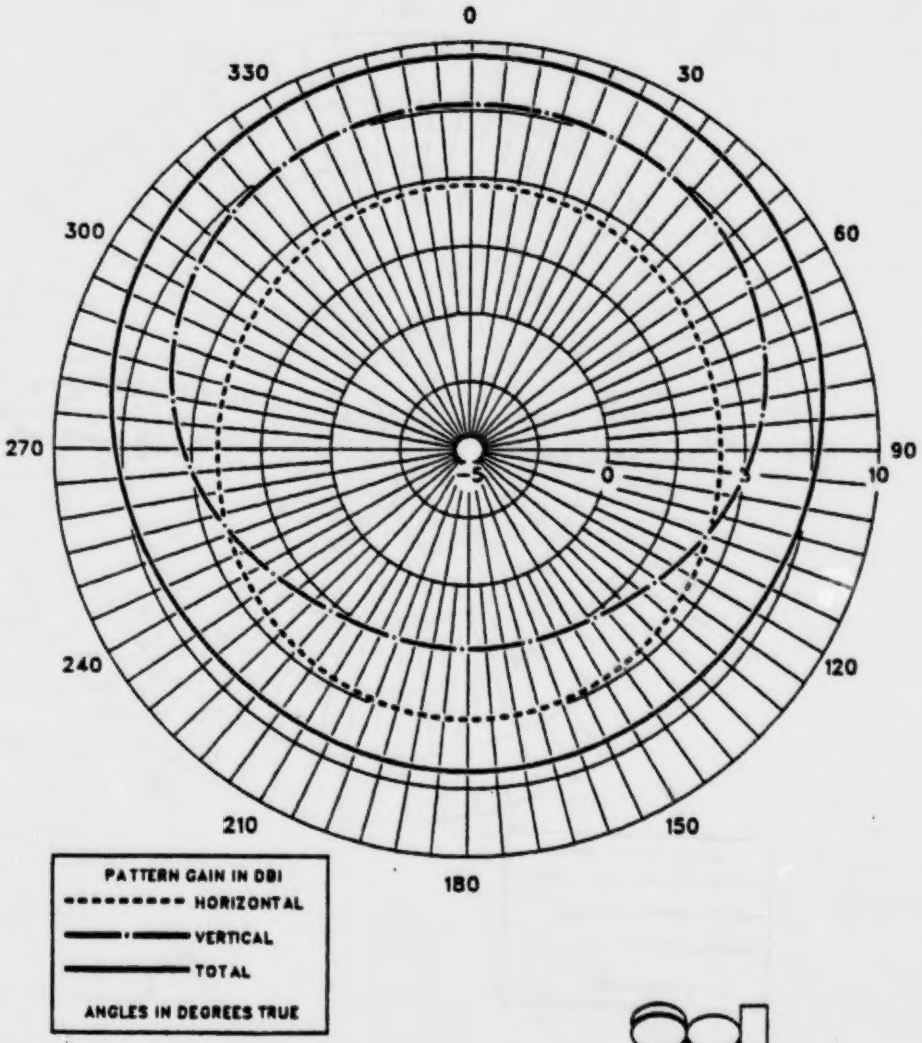

FIGURE B 137

THE COMARK 2X2 ARRAY

STANDARD SPACING OF ONE WAVELENGTH BETWEEN BAYS

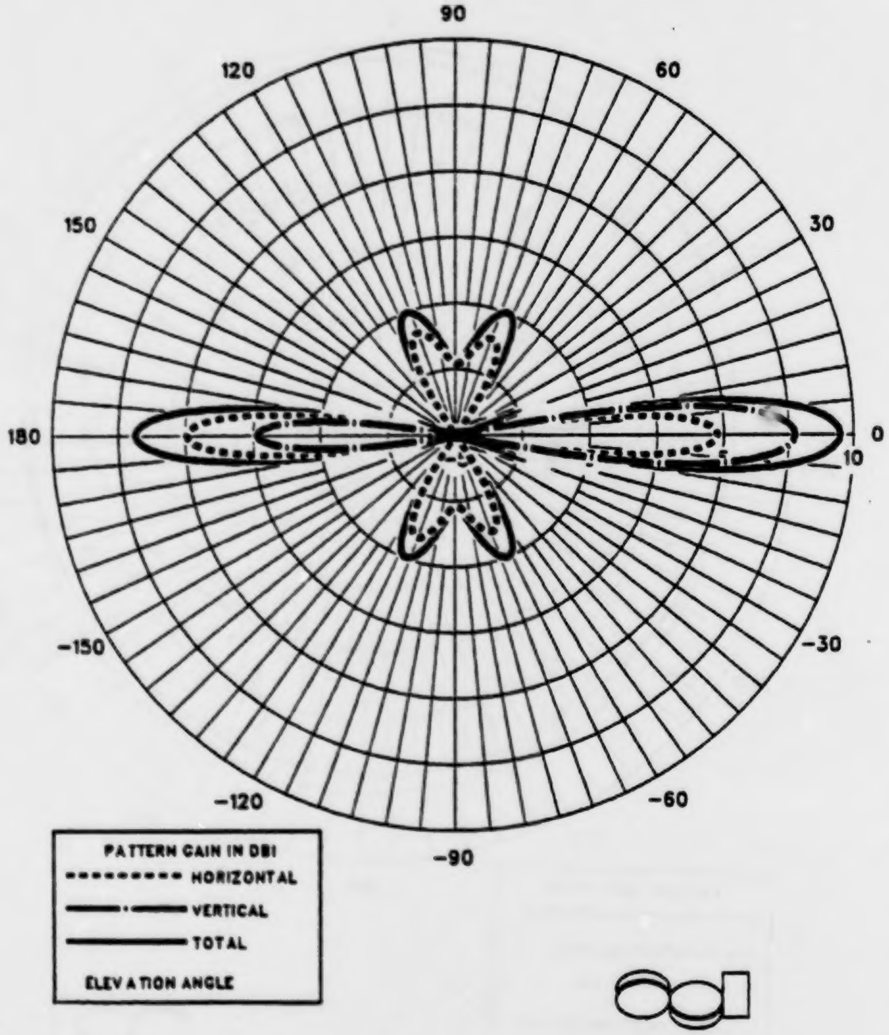

FIGURE B 138

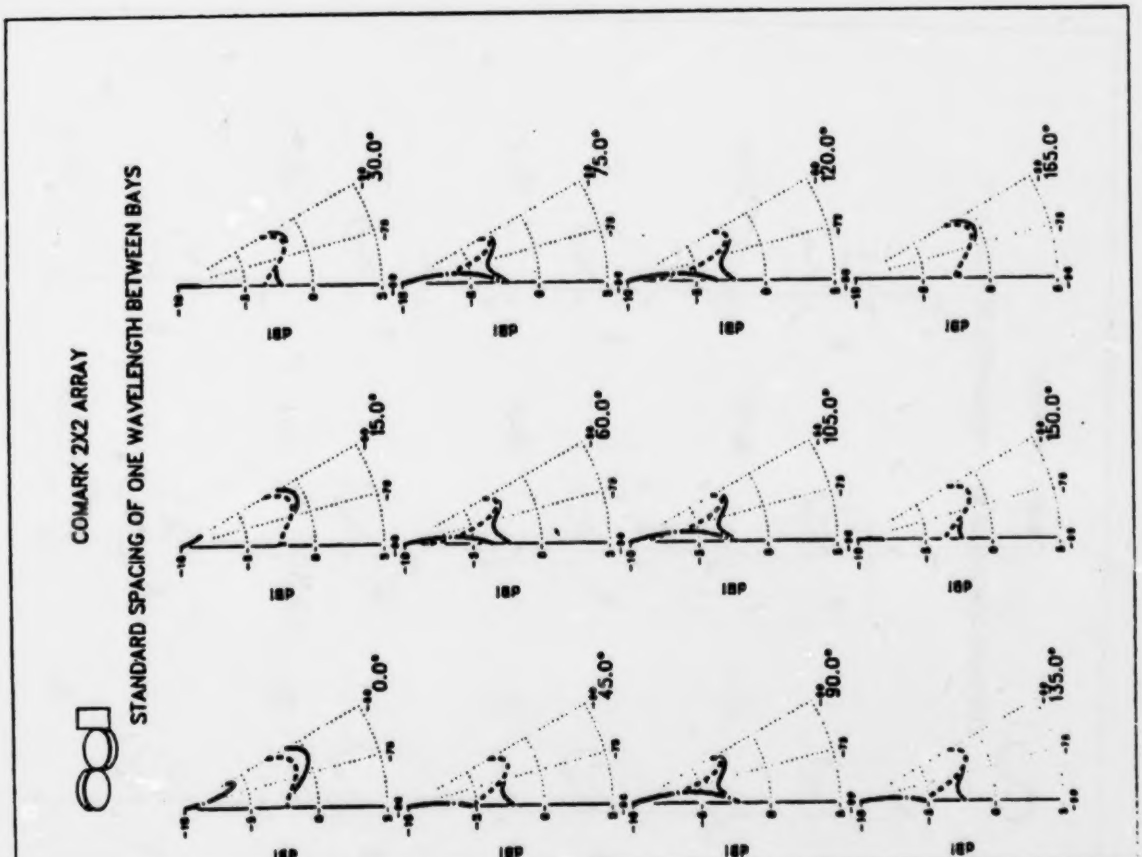
COMARK 2X2 ARRAY
STANDARD SPACING OF ONE WAVELENGTH BETWEEN BAYS
0.0°
15.0°
30.0°
45.0°
60.0°
75.0°
90.0°
105.0°
120.0°
135.0°
150.0°
165.0°
IBP

FIGURE B 139

COMARK 2X2 ARRAY

STANDARD SPACING OF ONE WAVELENGTH BETWEEN BAYS

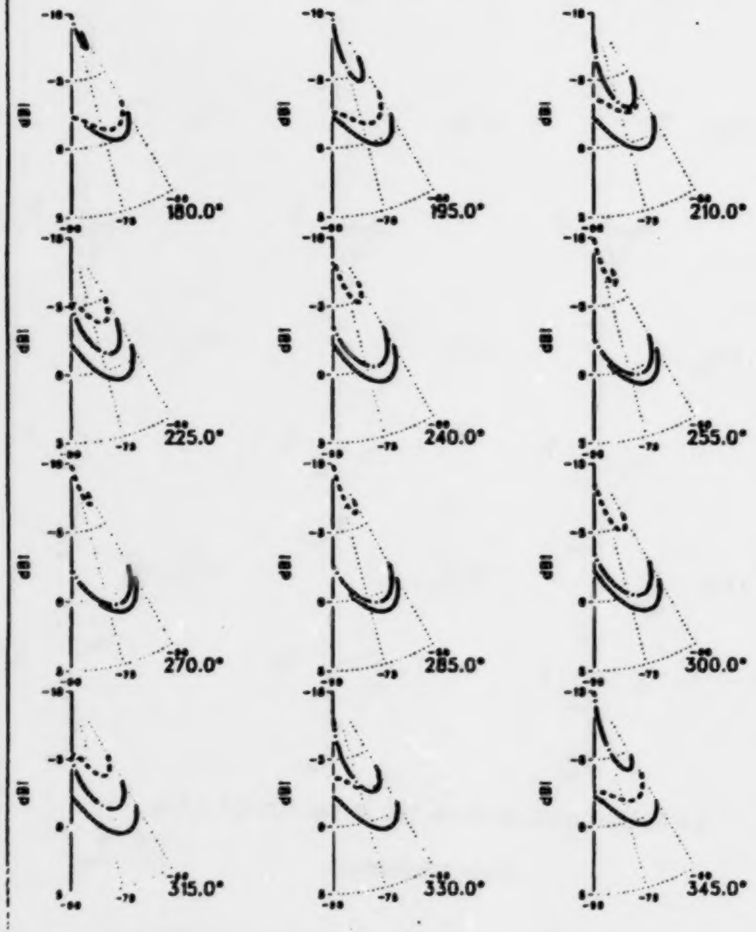

FIGURE B 140

CMK2X2TH

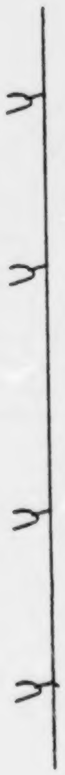

THETA = 60.00 PHI = 60.00 ETA = 90.00

FIGURE B 141

THE COMARK 2X2 ARRAY

SPACING OF 3/2 WAVELENGTHS BETWEEN UPPER & LOWER BAYS

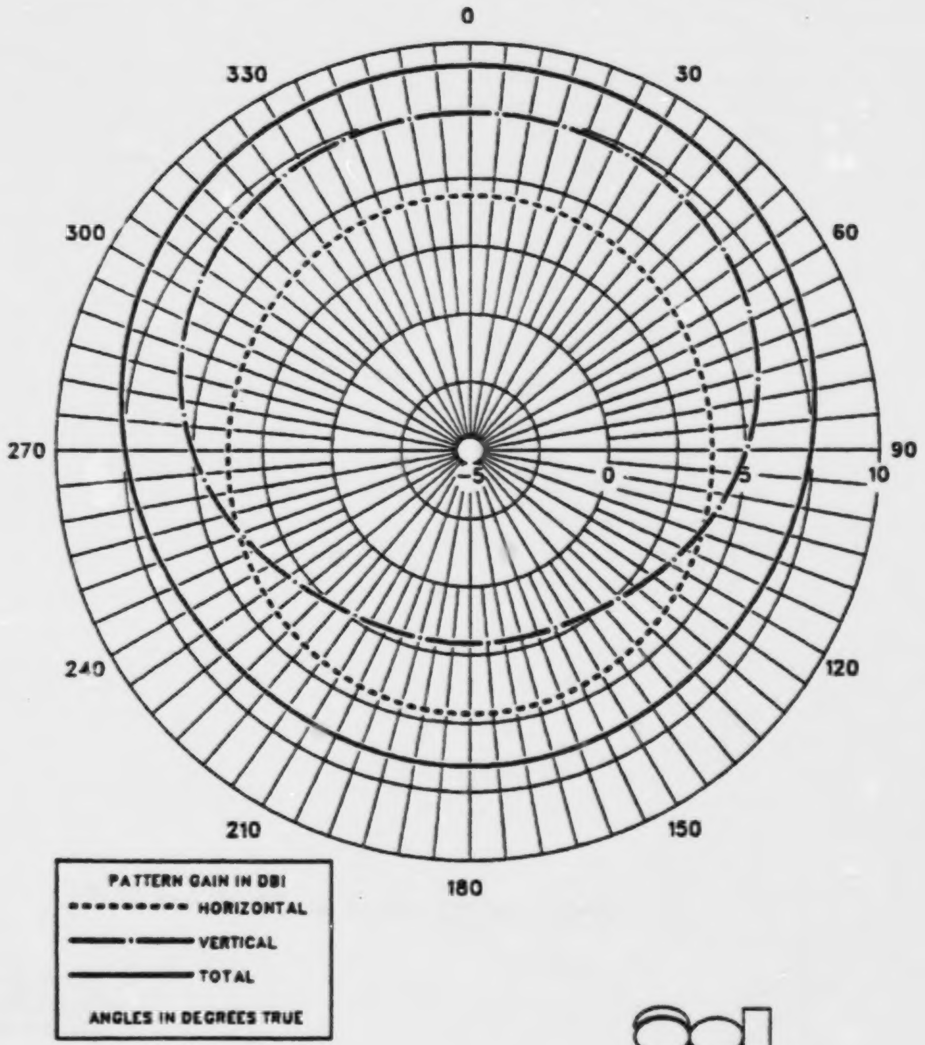

FIGURE B 142

THE COMARK 2X2 ARRAY

SPACING OF 3/2 WAVELENGTHS BETWEEN UPPER & LOWER BAYS

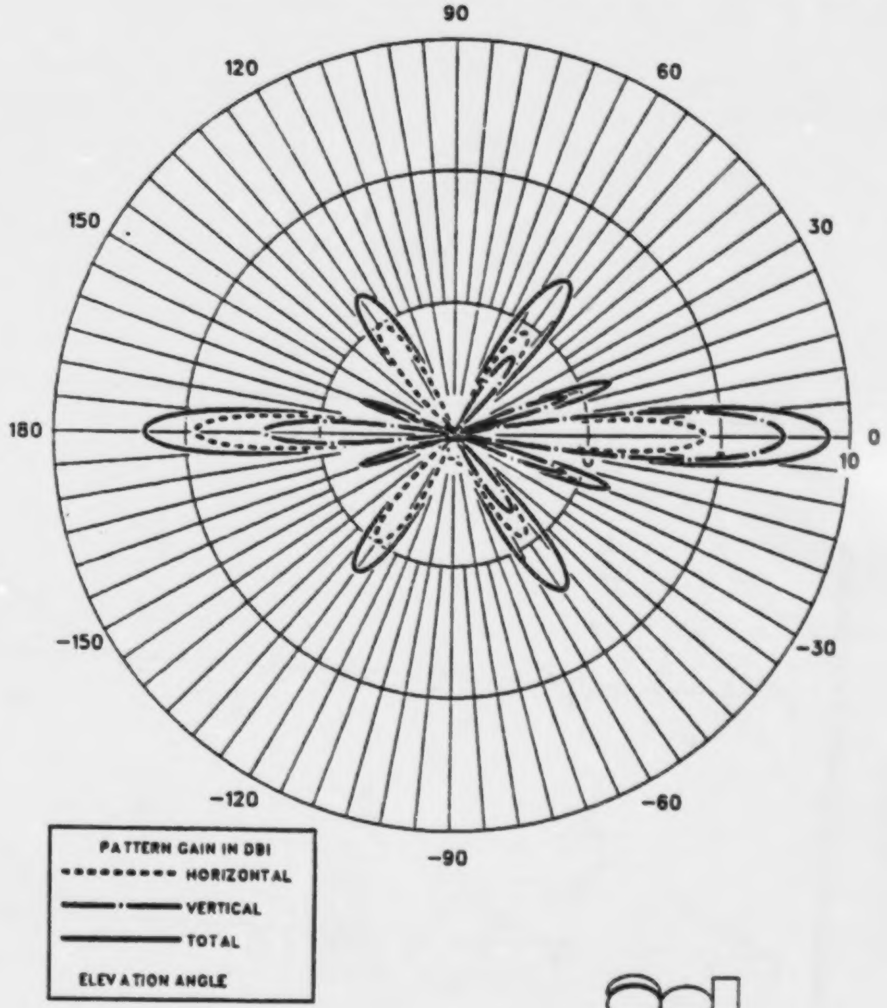

FIGURE B 143

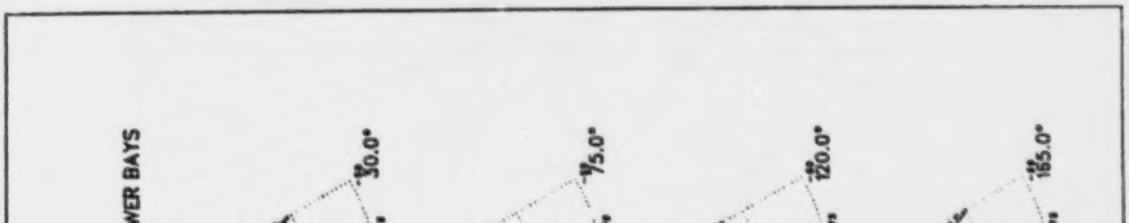
COMARK 2X2 ARRAY
SPACING OF 3/2 WAVELENGTHS BETWEEN UPPER & LOWER BAYS
0.0°
15.0°
30.0°
45.0°
60.0°
75.0°
90.0°
105.0°
120.0°
135.0°
150.0°
165.0°
IBP
IBP
IBP
IBP
IBP
IBP
IBP
IBP
IBP
IBP
IBP
IBP

FIGURE B 144

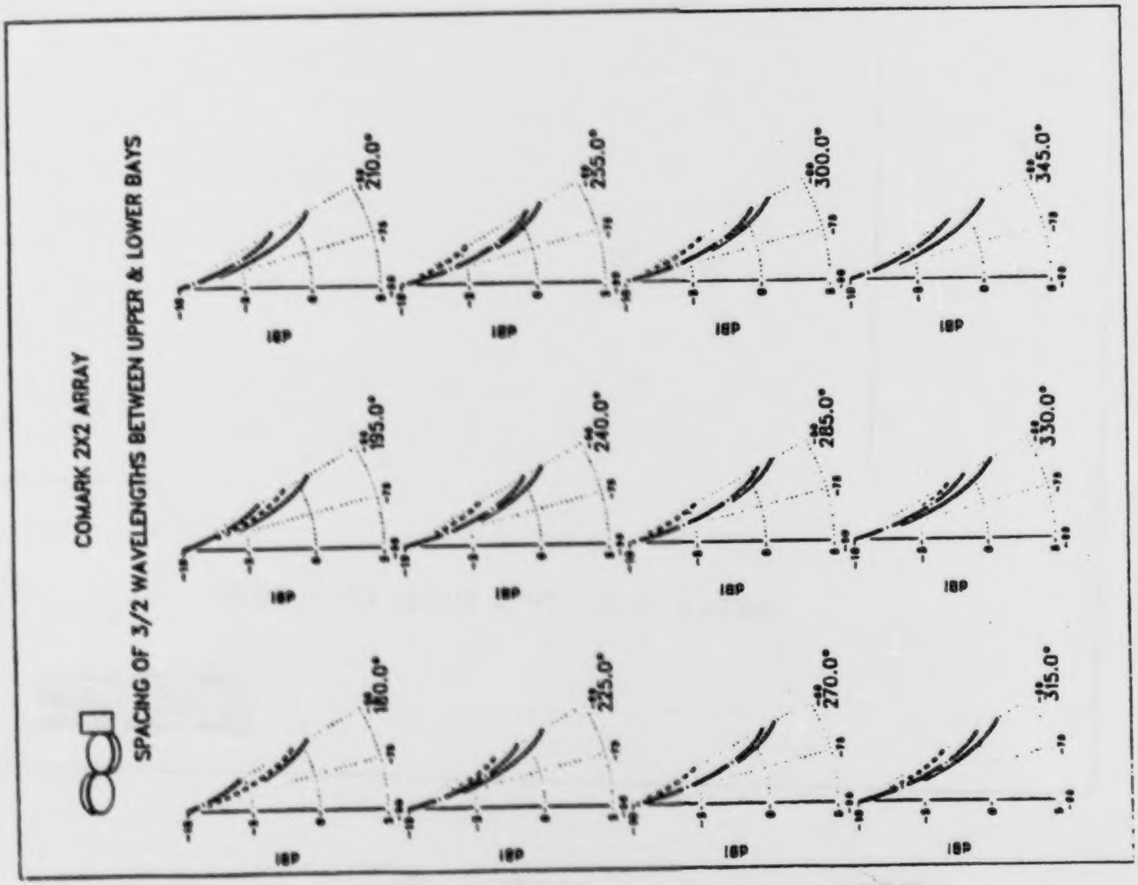
COMARK 2X2 ARRAY
SPACING OF 3/2 WAVELENGTHS BETWEEN UPPER & LOWER BAYS
180.0°
195.0°
210.0°
225.0°
240.0°
255.0°
270.0°
285.0°
300.0°
315.0°
330.0°
345.0°
IBP

FIGURE B 145

CMK2X2TW

THETA = 60.00 PHI = 60.00 ETA = 90.00

FIGURE B 146

THE COMARK 2X2 ARRAY

SPACING OF TWO WAVELENGTHS BETWEEN UPPER & LOWER BAYS

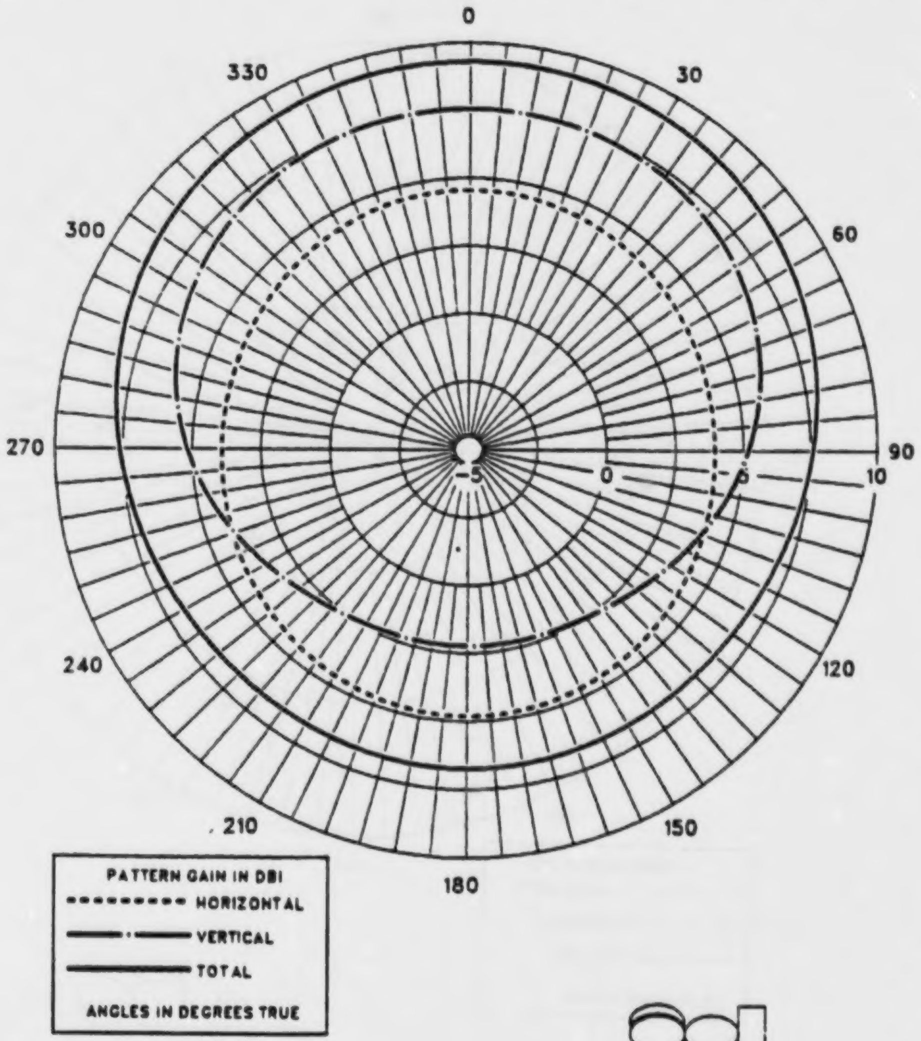

FIGURE B 147

THE COMARK 2X2 ARRAY

SPACING OF TWO WAVELENGTHS BETWEEN UPPER & LOWER BAYS

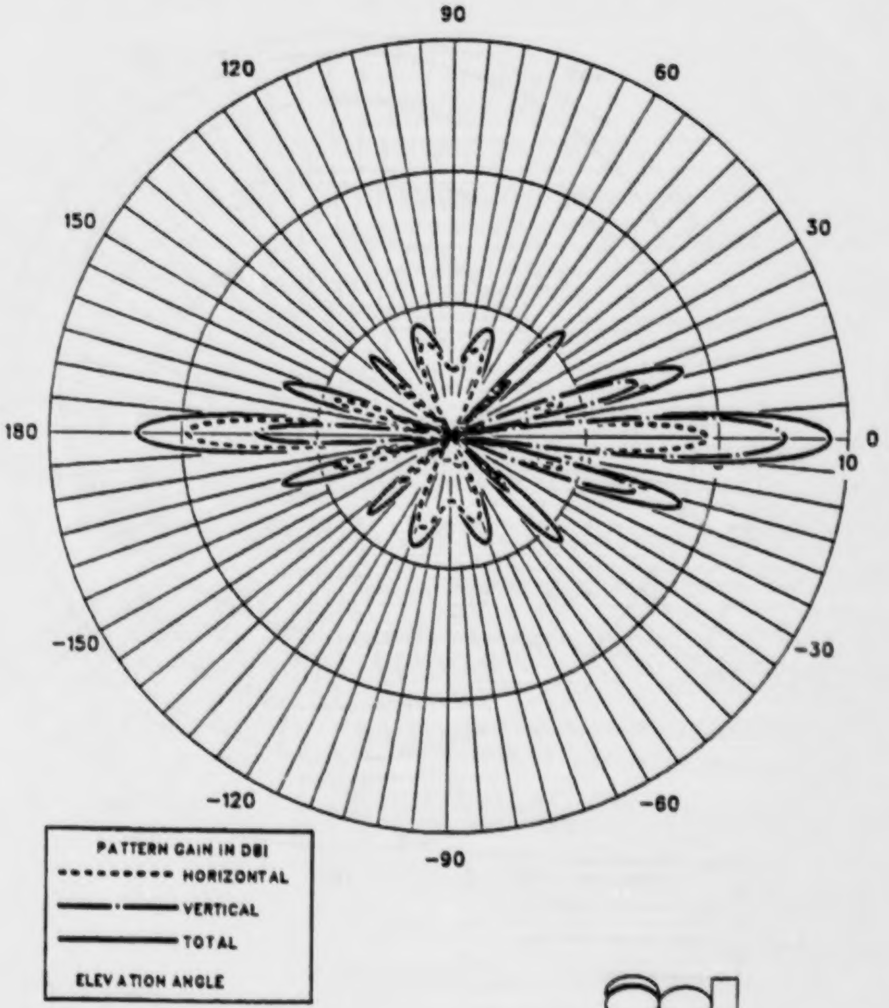

FIGURE B 148

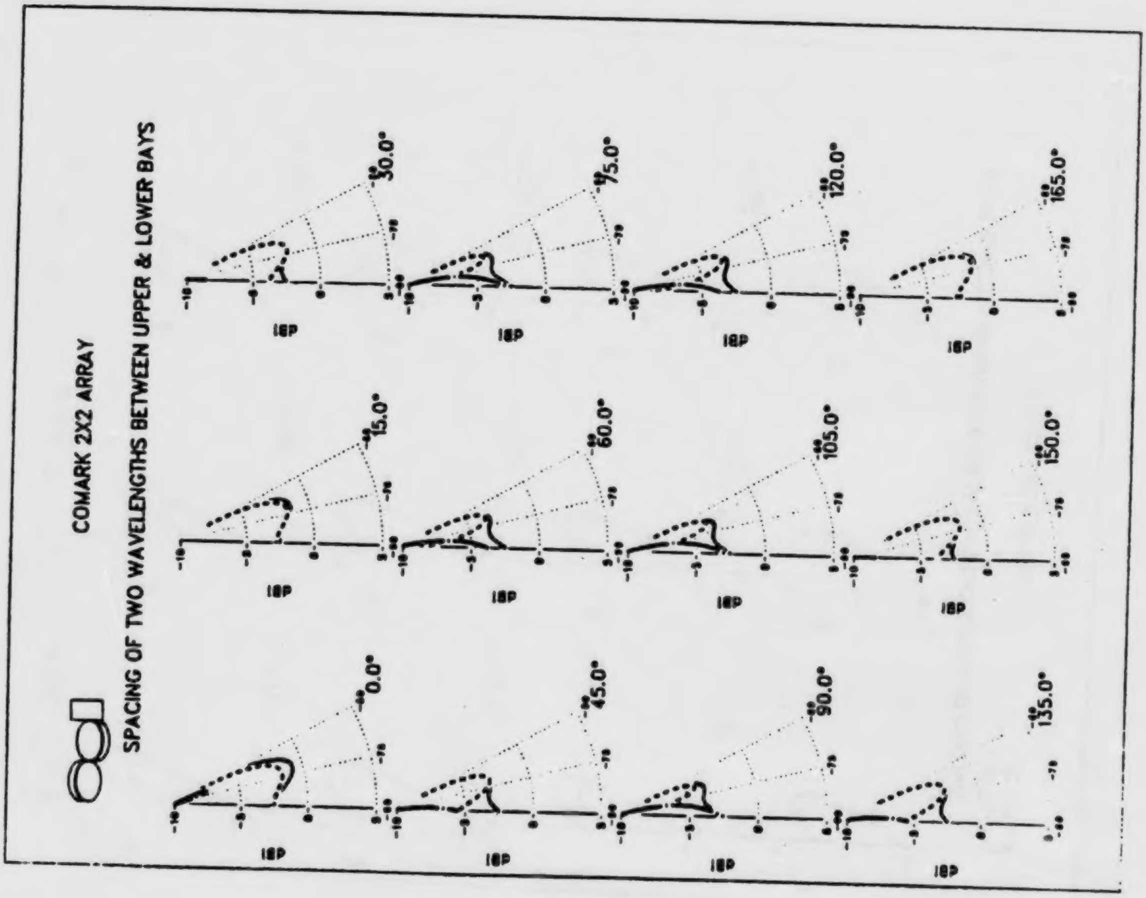
COMARK 2X2 ARRAY
SPACING OF TWO WAVELENGTHS BETWEEN UPPER & LOWER BAYS
0.0°
15.0°
30.0°
45.0°
60.0°
75.0°
90.0°
105.0°
120.0°
135.0°
150.0°
165.0°
IBP

FIGURE B 149

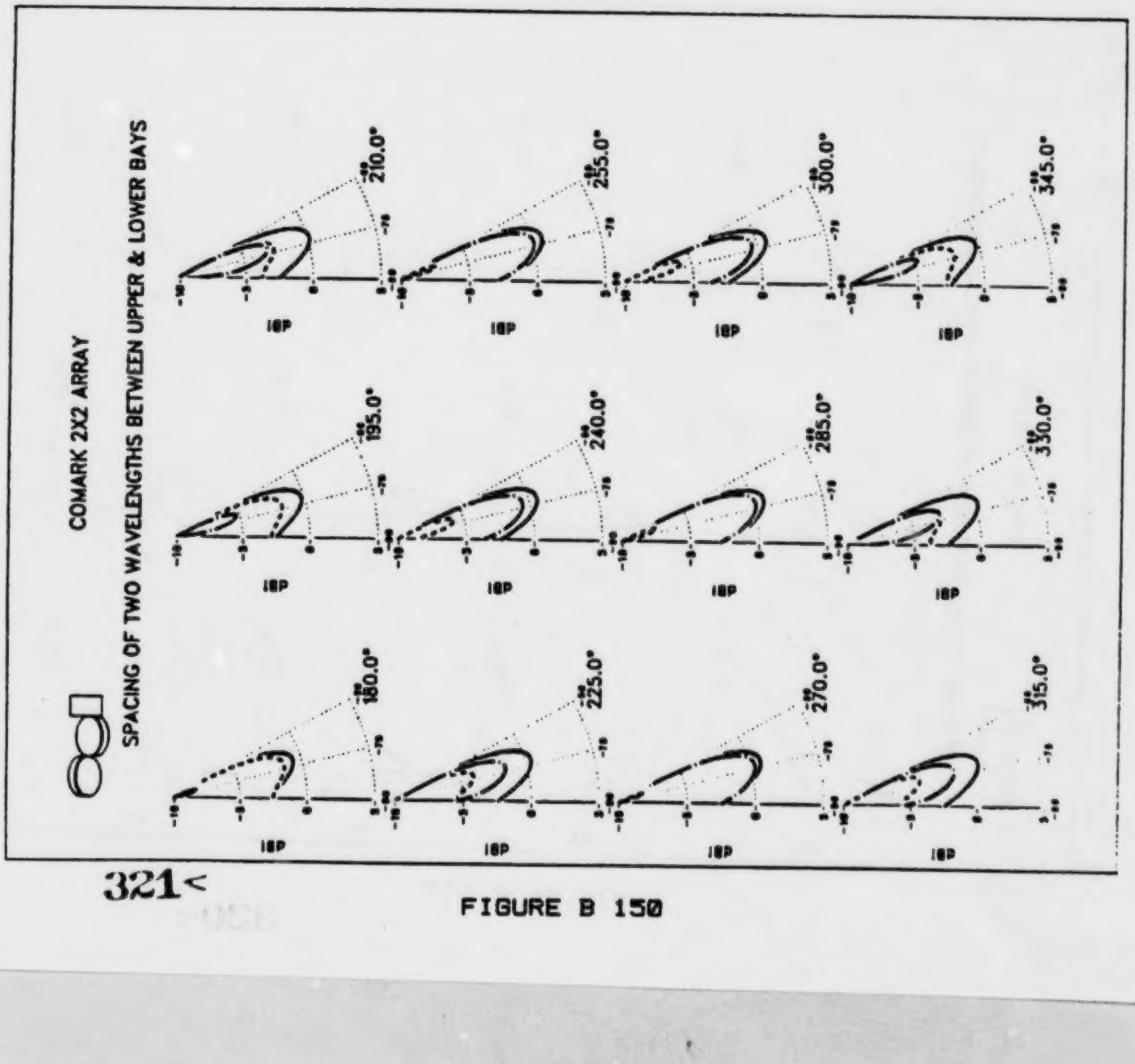
COMARK 2X2 ARRAY
SPACING OF TWO WAVELENGTHS BETWEEN UPPER & LOWER BAYS
180.0°
195.0°
210.0°
225.0°
240.0°
255.0°
270.0°
285.0°
300.0°
315.0°
330.0°
345.0°
IBP

FIGURE B 150

THE COMARK 2X2 ARRAY

STANDARD SPACING OF ONE WAVELENGTH BETWEEN BAYS

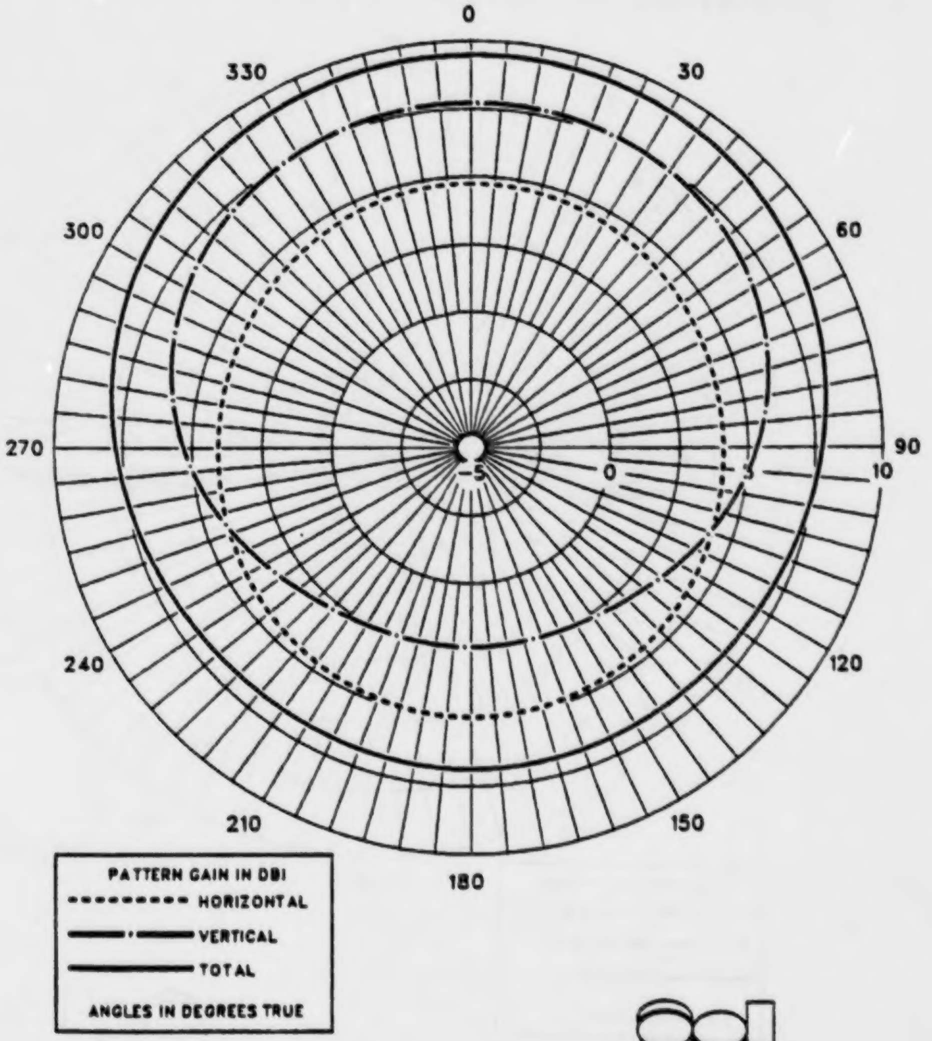

FIGURE B 151

THE COMARK 2X2 ARRAY

STANDARD SPACING OF ONE WAVELENGTH BETWEEN BAYS

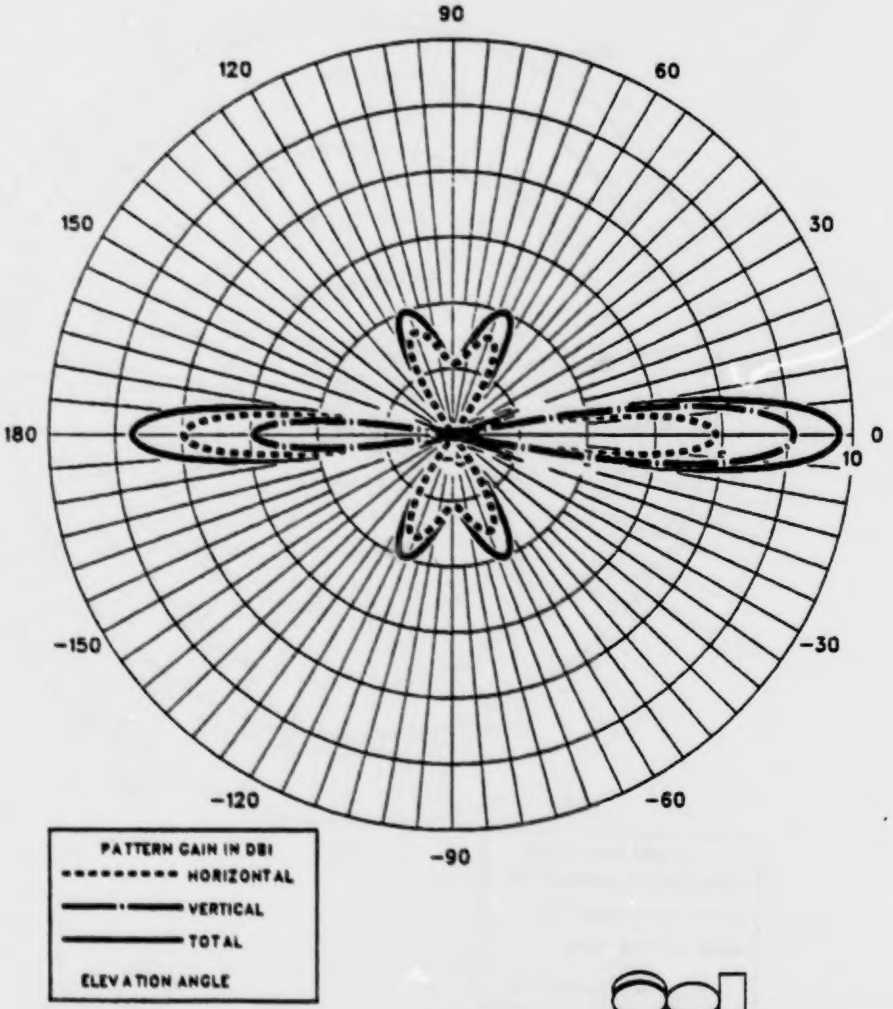

FIGURE B 152

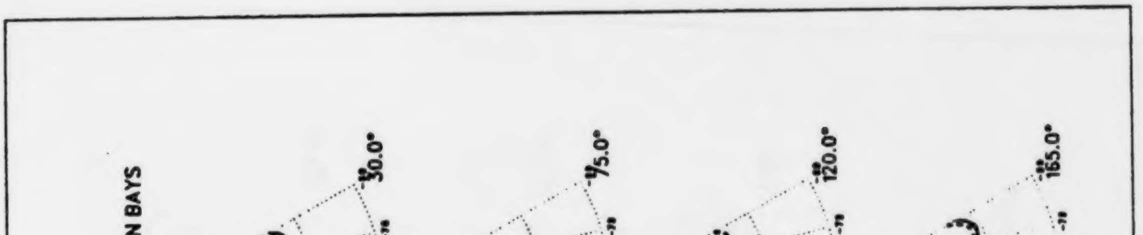
COMARK 2X2 ARRAY
STANDARD SPACING OF ONE WAVELENGTH BETWEEN BAYS
0.0°
15.0°
30.0°
45.0°
60.0°
75.0°
90.0°
105.0°
120.0°
135.0°
150.0°
165.0°
IBP

FIGURE B 153

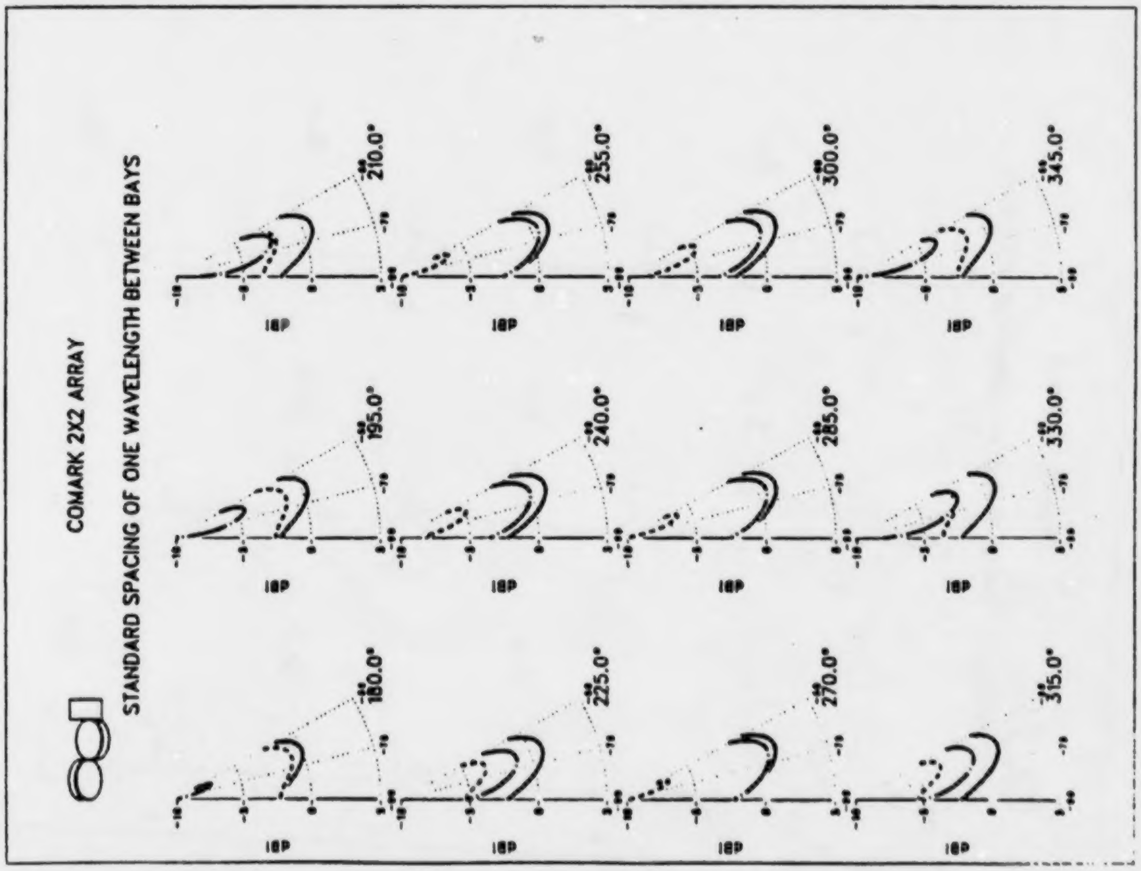

FIGURE B 154

325<

THE COMARK 2X2 ARRAY

SPACING OF 3/2 WAVELENGTHS BETWEEN UPPER & LOWER BAYS

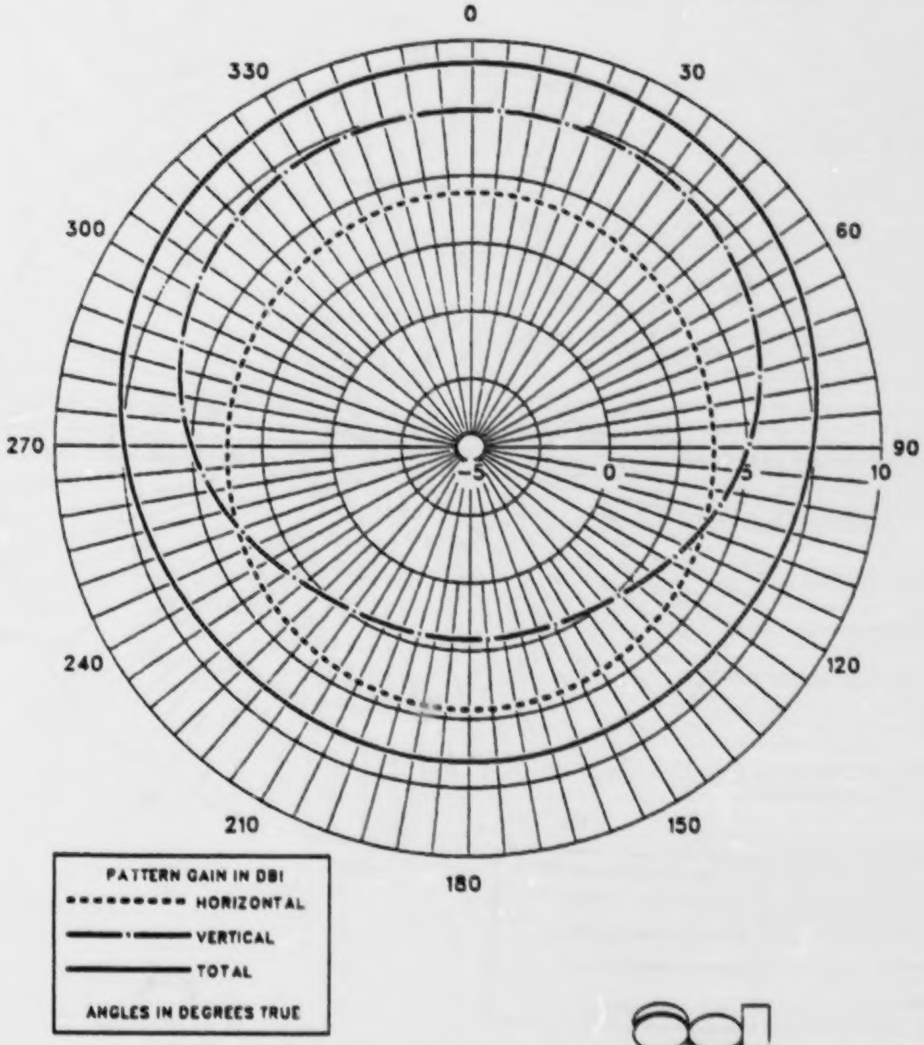

FIGURE B 155

THE COMARK 2X2 ARRAY

SPACING OF 3/2 WAVELENGTHS BETWEEN UPPER & LOWER BAYS

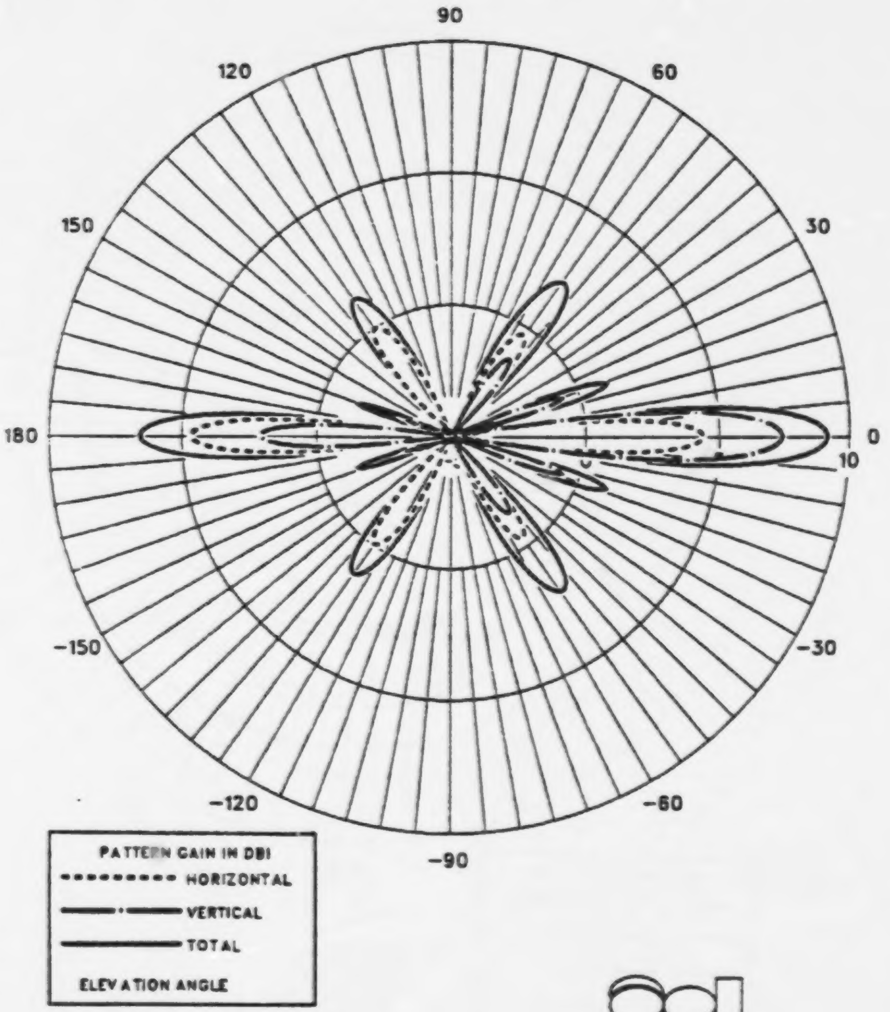

FIGURE B 156

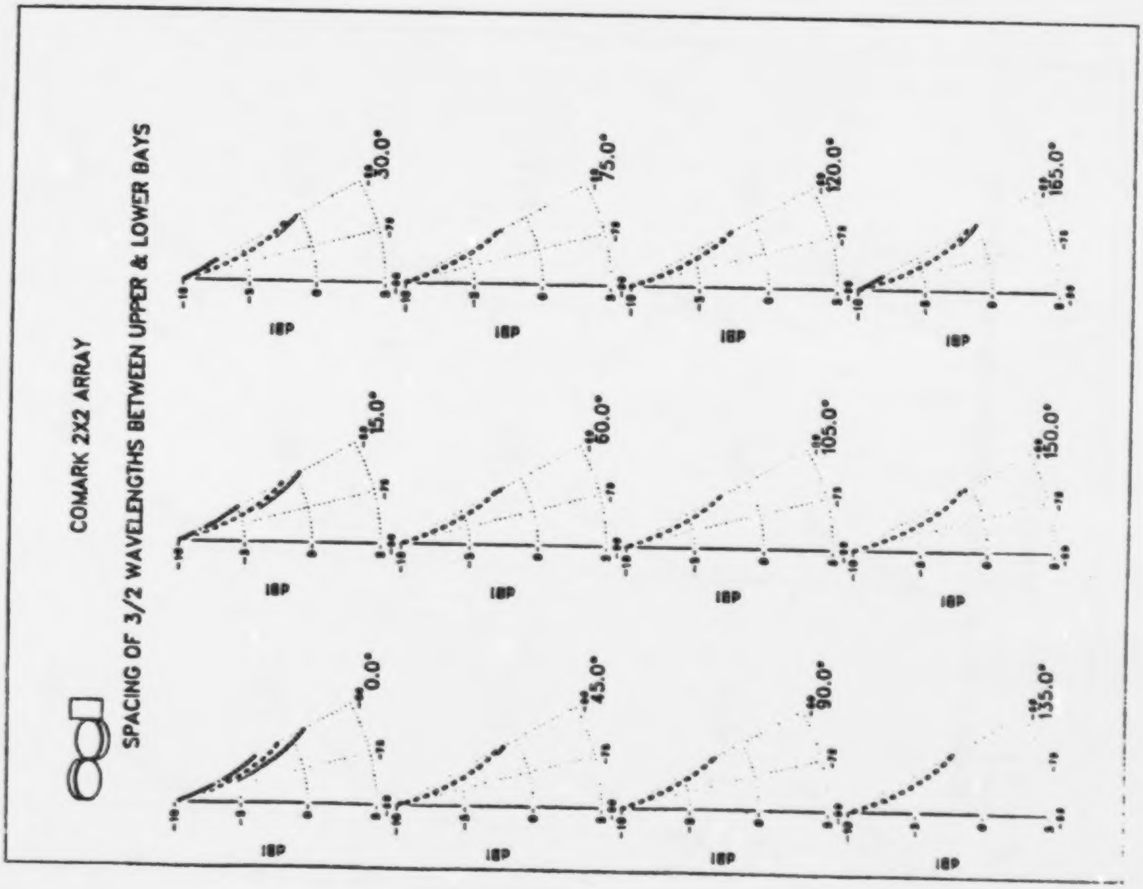

COMARK 2X2 ARRAY

SPACING OF 3/2 WAVELENGTHS BETWEEN UPPER & LOWER BAYS

FIGURE B 157

COMARK 2X2 ARRAY

SPACING OF 3/2 WAVELENGTHS BETWEEN UPPER & LOWER BAYS

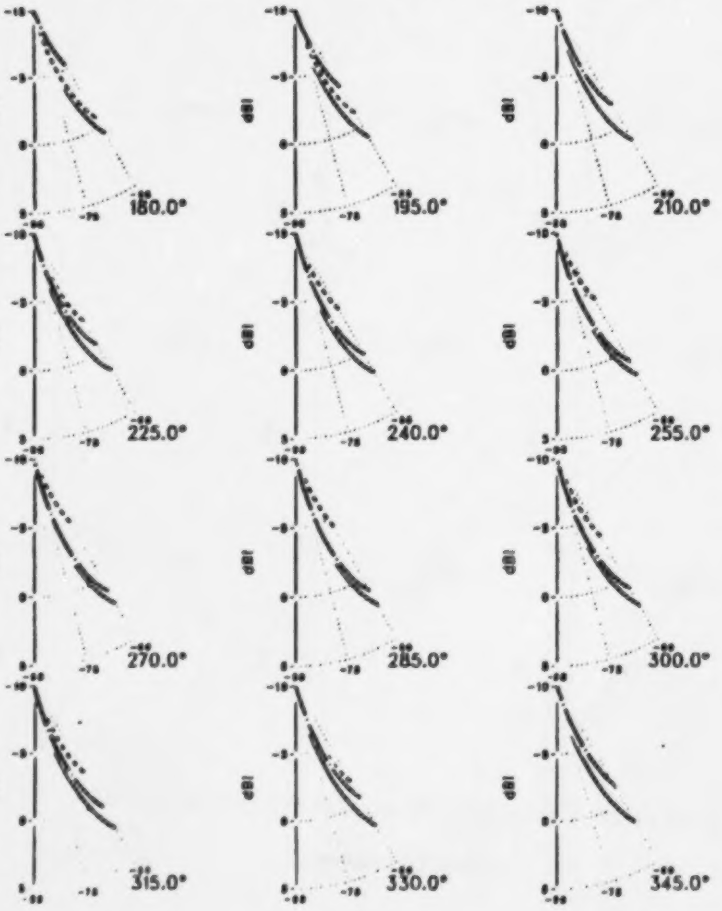

FIGURE B 158

THE COMARK 2X2 ARRAY

SPACING OF TWO WAVELENGTHS BETWEEN UPPER & LOWER BAYS

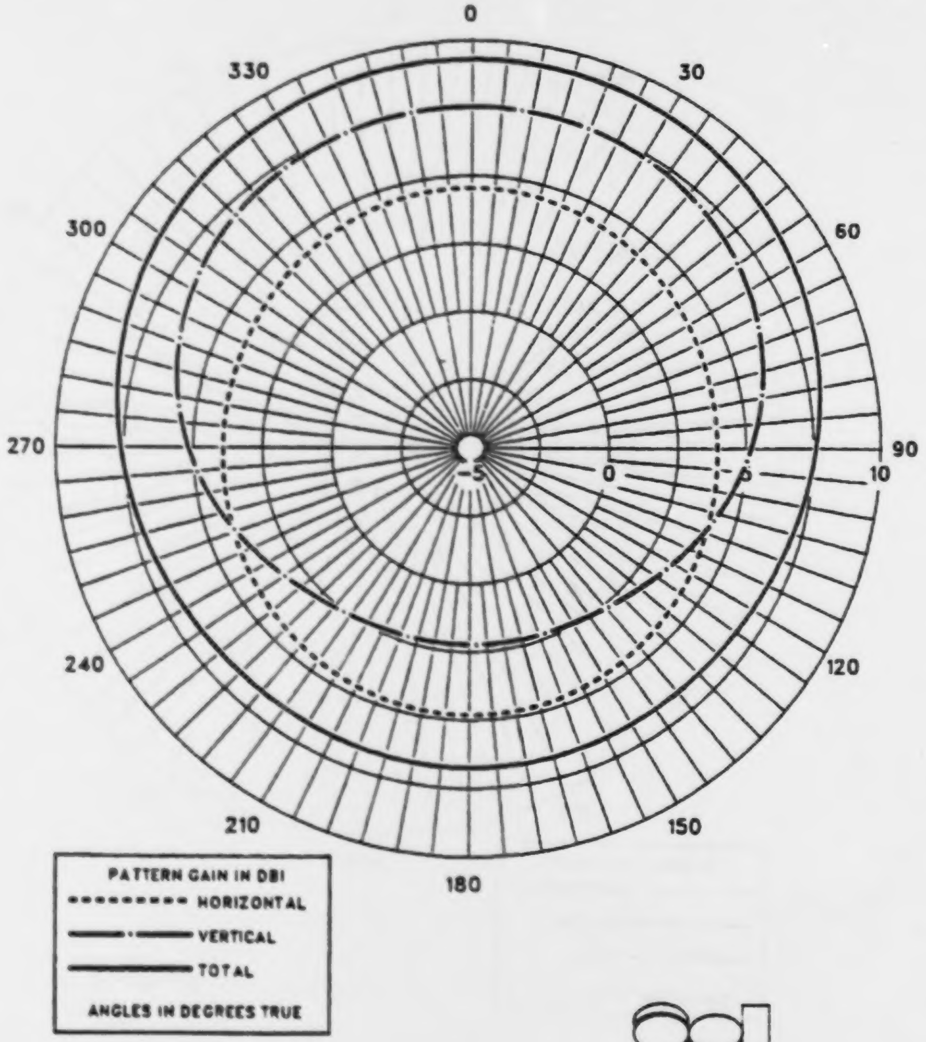

FIGURE B 159

THE COMARK 2X2 ARRAY

SPACING OF TWO WAVELENGTHS BETWEEN UPPER & LOWER BAYS

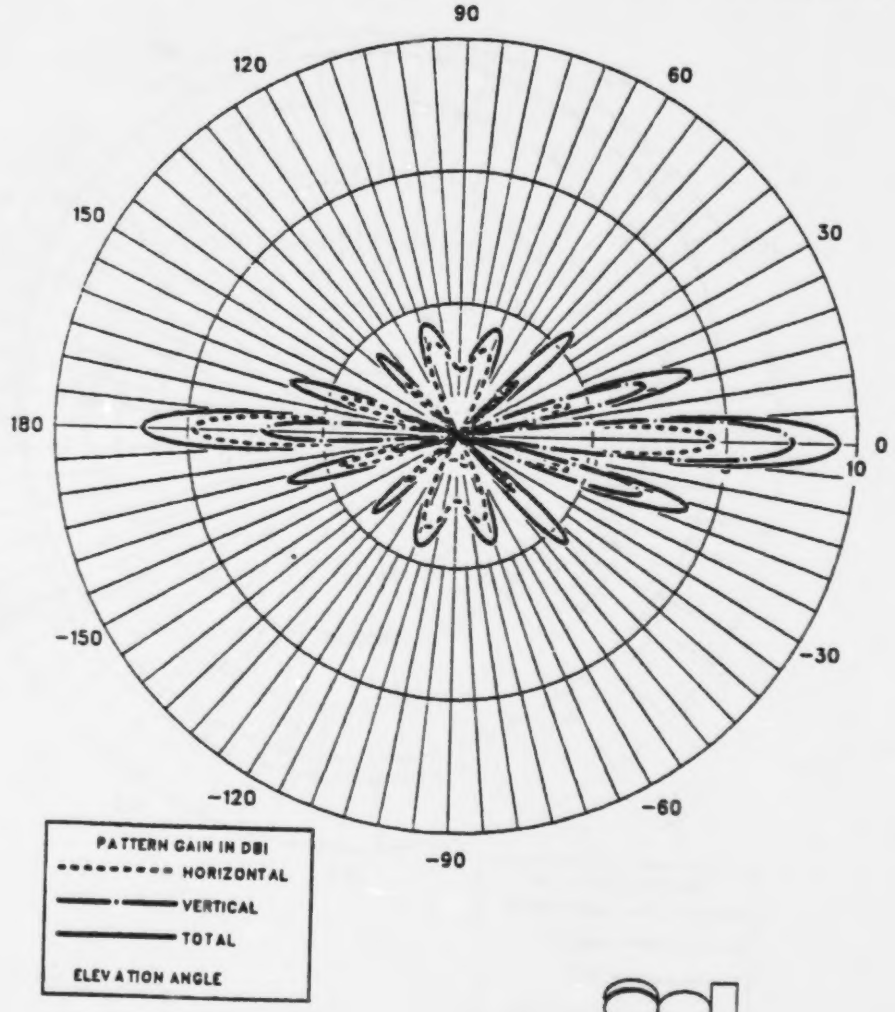

FIGURE B 160

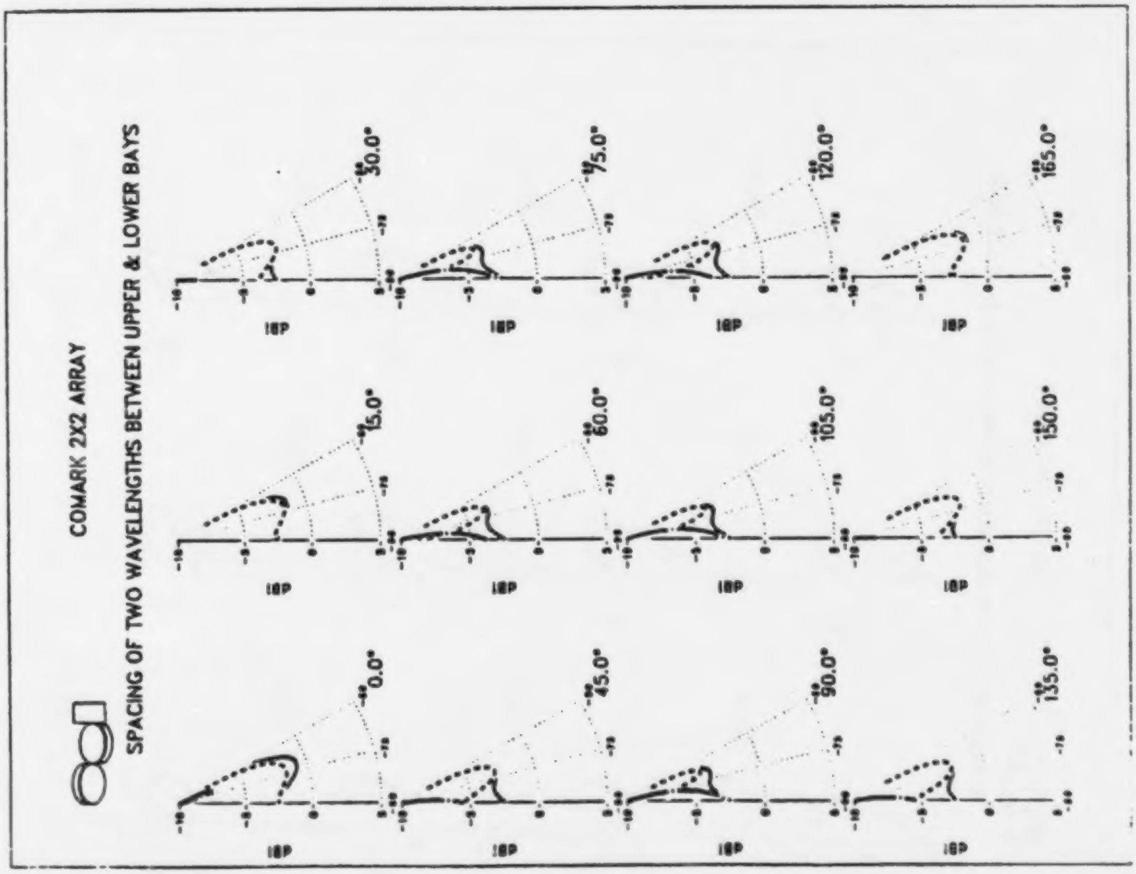
COMARK 2X2 ARRAY
SPACING OF TWO WAVELENGTHS BETWEEN UPPER & LOWER BAYS
0.0°
15.0°
30.0°
45.0°
60.0°
75.0°
90.0°
105.0°
120.0°
135.0°
150.0°
165.0°
IBP

FIGURE B 161

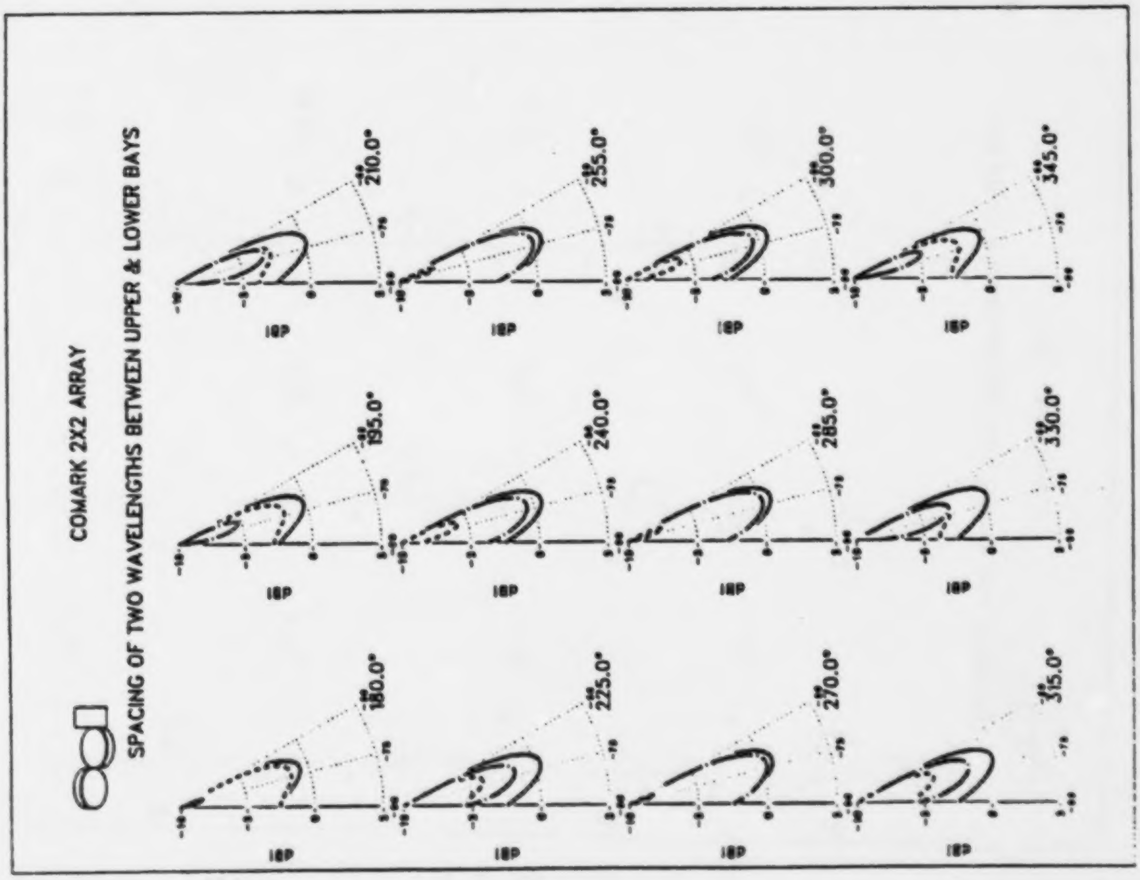
COMARK 2X2 ARRAY
SPACING OF TWO WAVELENGTHS BETWEEN UPPER & LOWER BAYS
180.0°
195.0°
210.0°
225.0°
240.0°
255.0°
270.0°
285.0°
300.0°
315.0°
330.0°
345.0°

FIGURE B 162

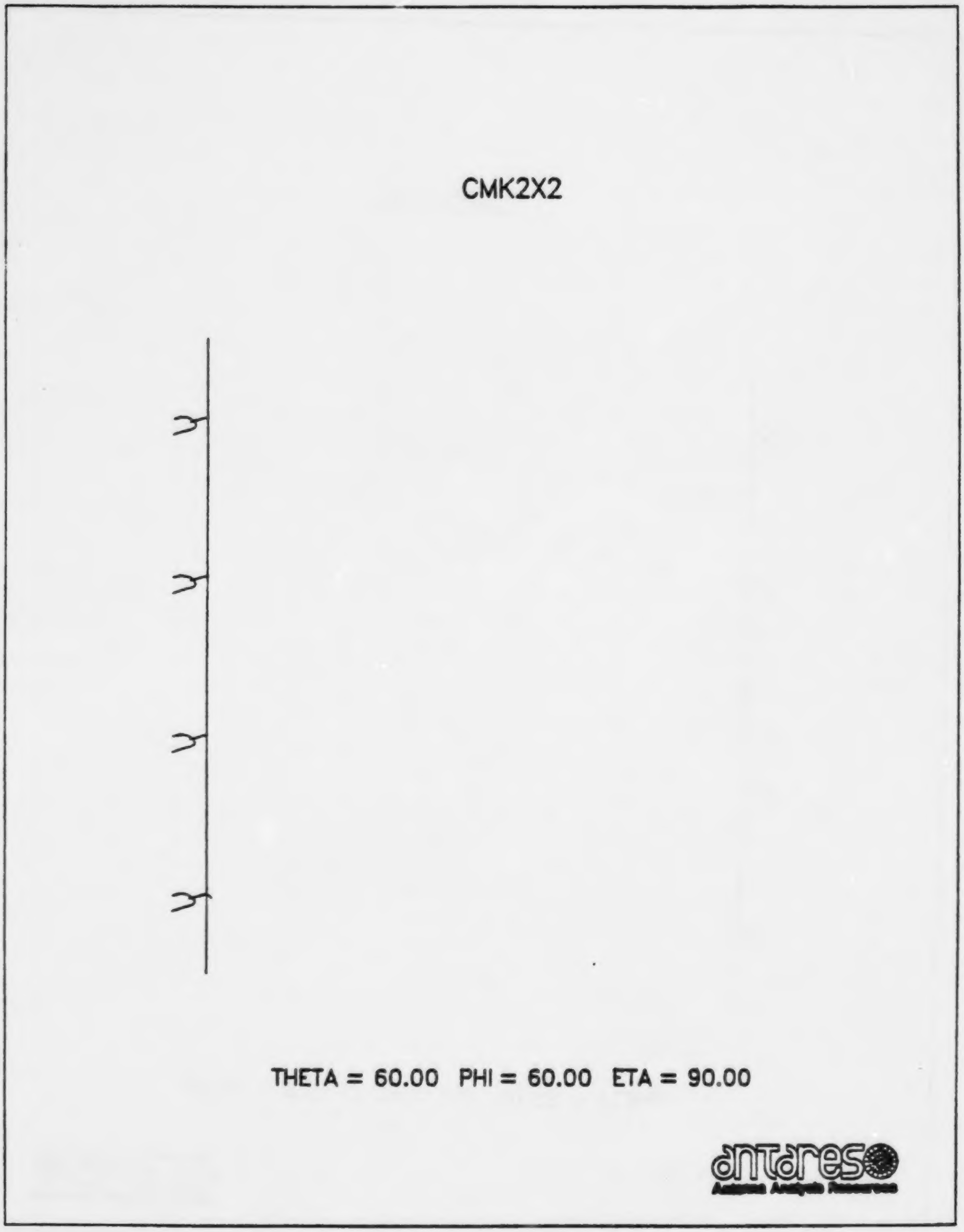
CMK2X2
THETA = 60.00 PHI = 60.00 ETA = 90.00
antares
Antenna Analysis Resources

FIGURE B 163

CMK2X2TH

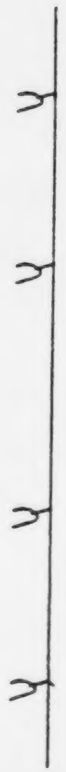

THETA = 60.00 PHI = 60.00 ETA = 90.00

FIGURE B 164

CMK2X2TW

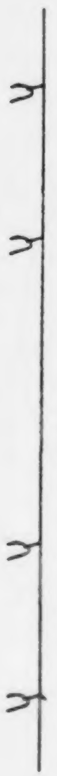

THETA = 60.00 PHI = 60.00 ETA = 90.00

antares
Antenna Analysis Resources

FIGURE B 165

THE COMARK 2X2 ARRAY

STANDARD SPACING OF ONE WAVELENGTH BETWEEN BAYS

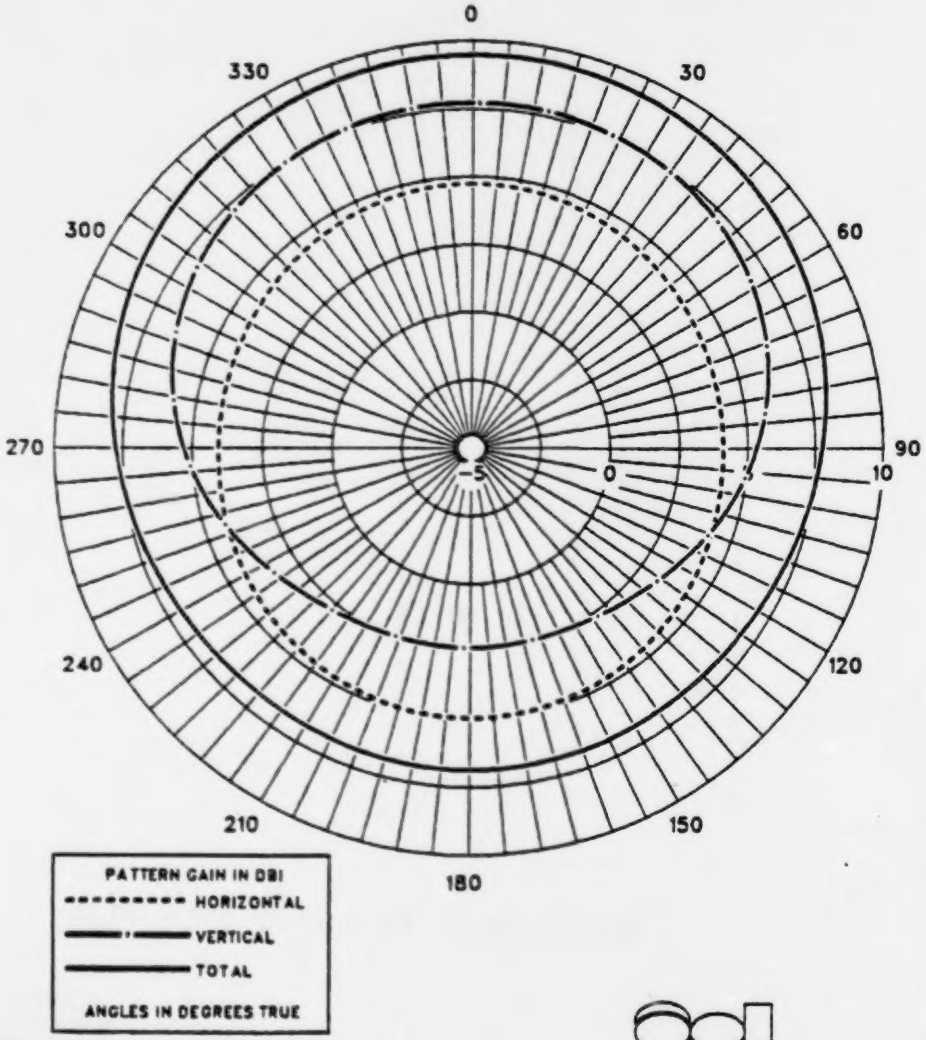

FIGURE B 166

THE COMARK 2X2 ARRAY

STANDARD SPACING OF ONE WAVELENGTH BETWEEN BAYS

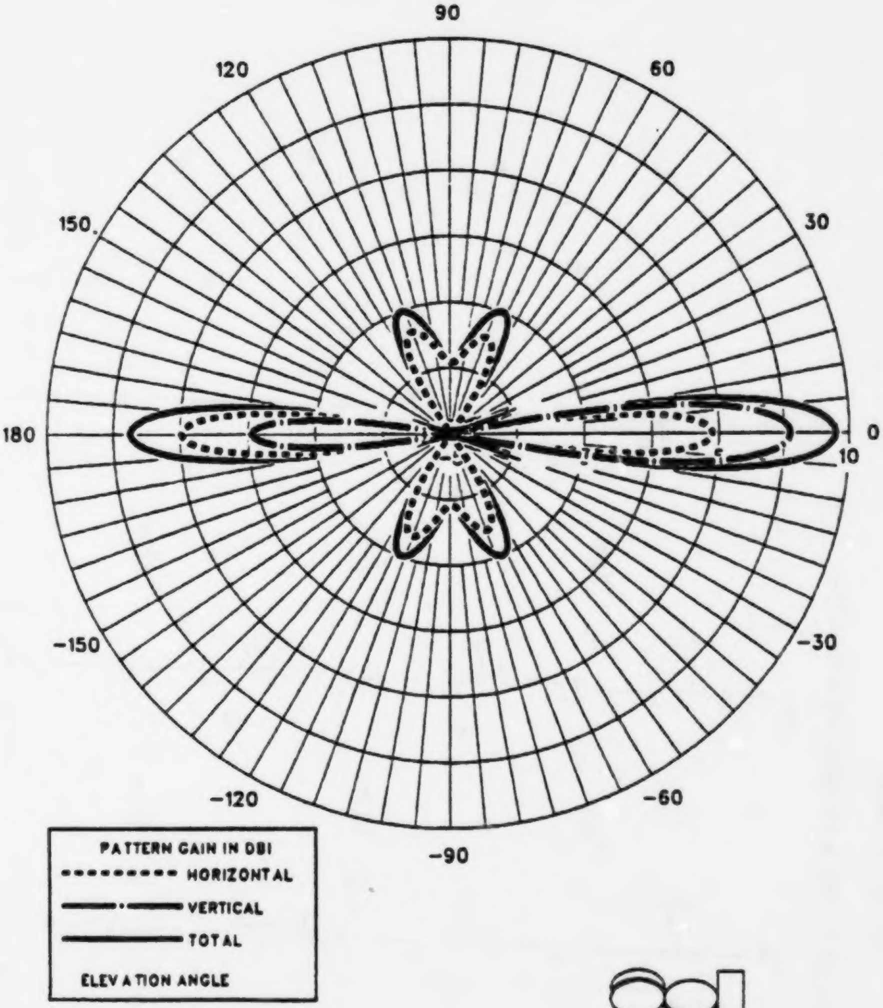

FIGURE B 167

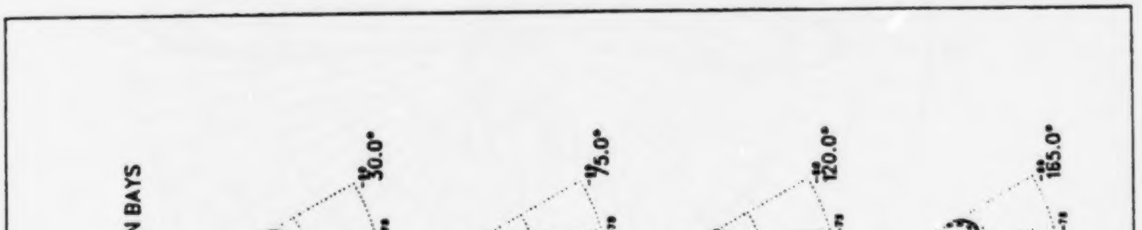
COMARK 2X2 ARRAY
STANDARD SPACING OF ONE WAVELENGTH BETWEEN BAYS
0.0°
15.0°
30.0°
45.0°
60.0°
75.0°
90.0°
105.0°
120.0°
135.0°
150.0°
165.0°
IBP

FIGURE B 168

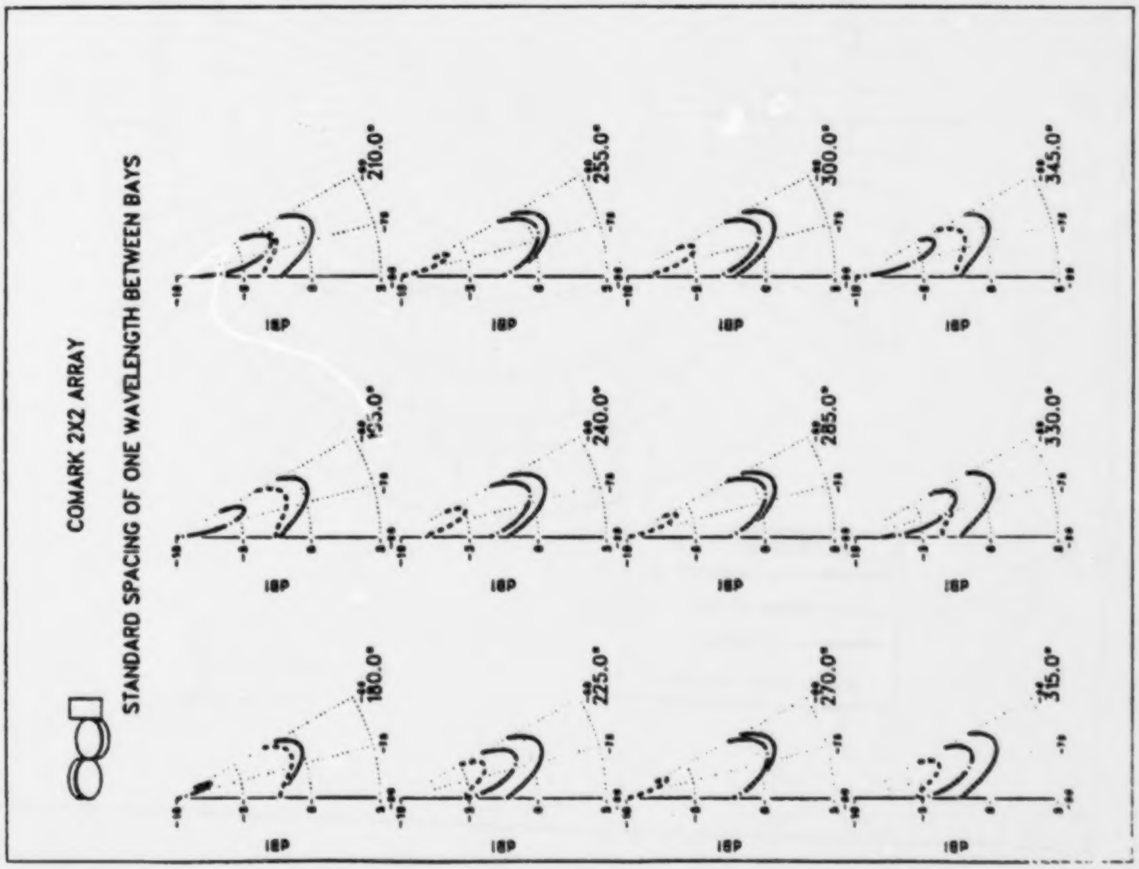
COMARK 2X2 ARRAY
STANDARD SPACING OF ONE WAVELENGTH BETWEEN BAYS
180.0°
195.0°
210.0°
225.0°
240.0°
255.0°
270.0°
285.0°
300.0°
315.0°
330.0°
345.0°
IBP

FIGURE B 169

THE COMARK 2X2 ARRAY

SPACING OF 3/2 WAVELENGTHS BETWEEN UPPER & LOWER BAYS

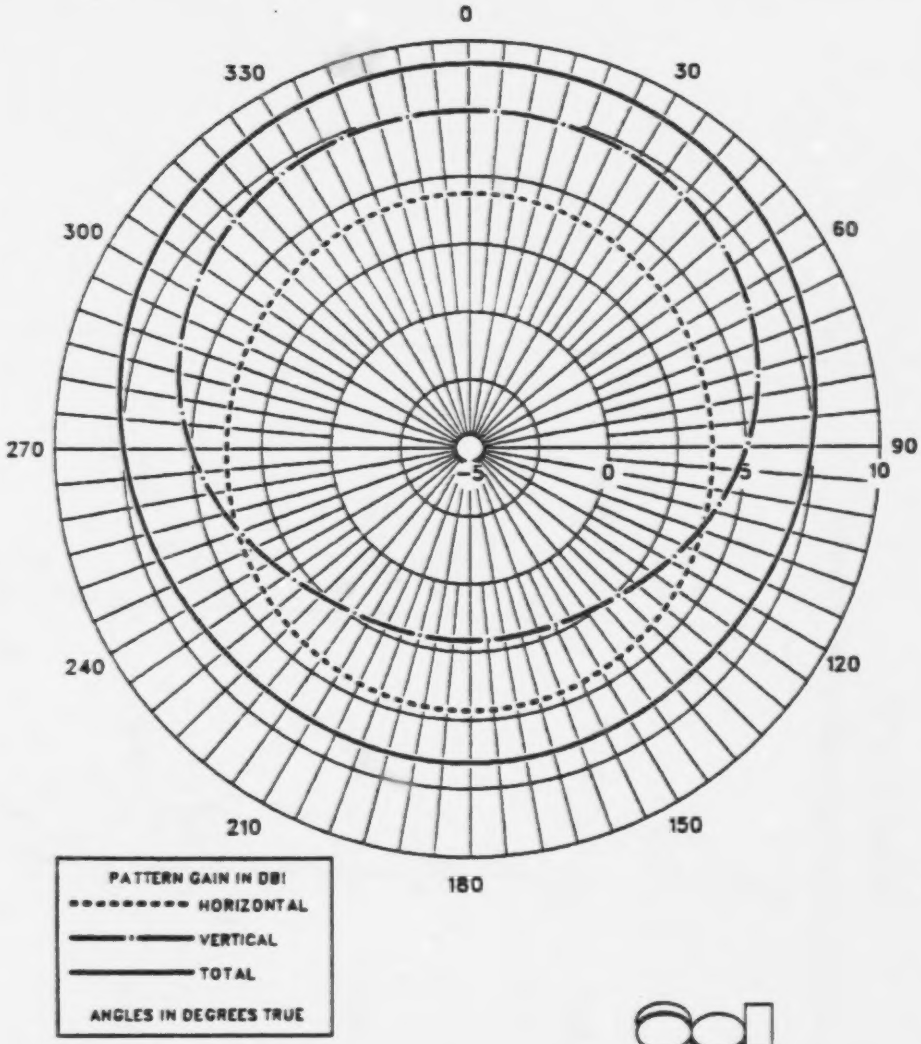

FIGURE B 170

THE COMARK 2X2 ARRAY

SPACING OF 3/2 WAVELENGTHS BETWEEN UPPER & LOWER BAYS

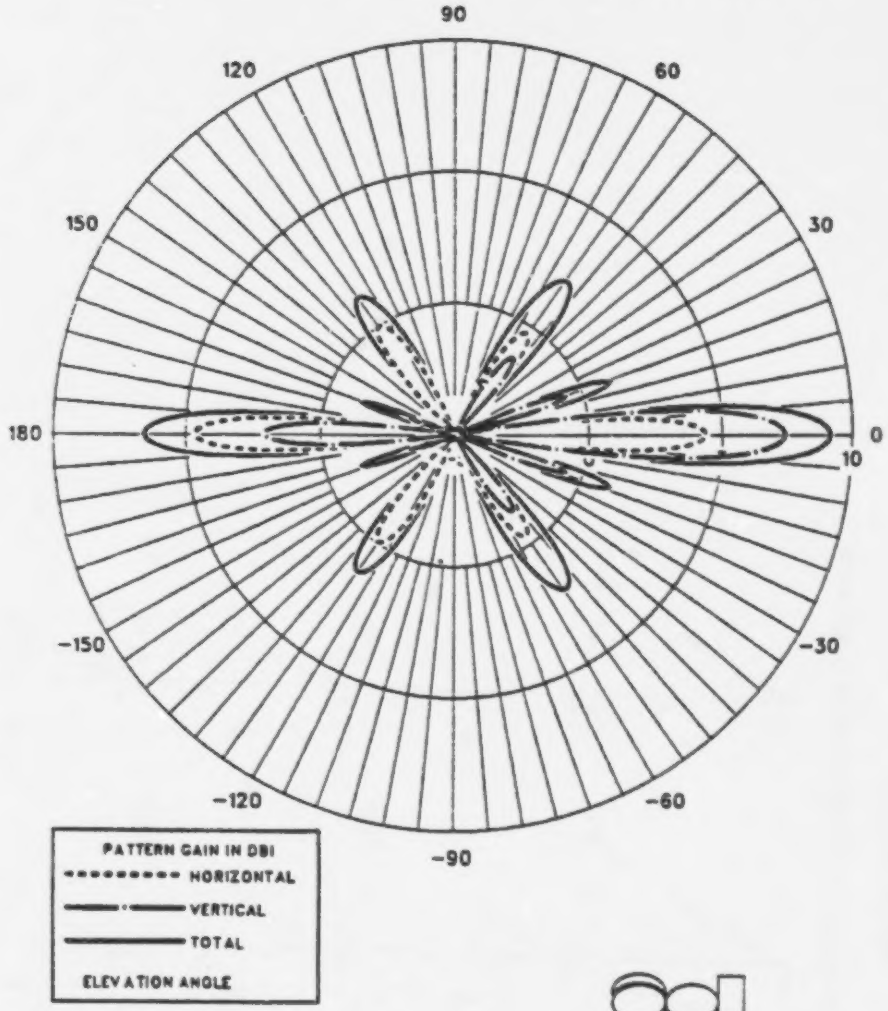

FIGURE B 171

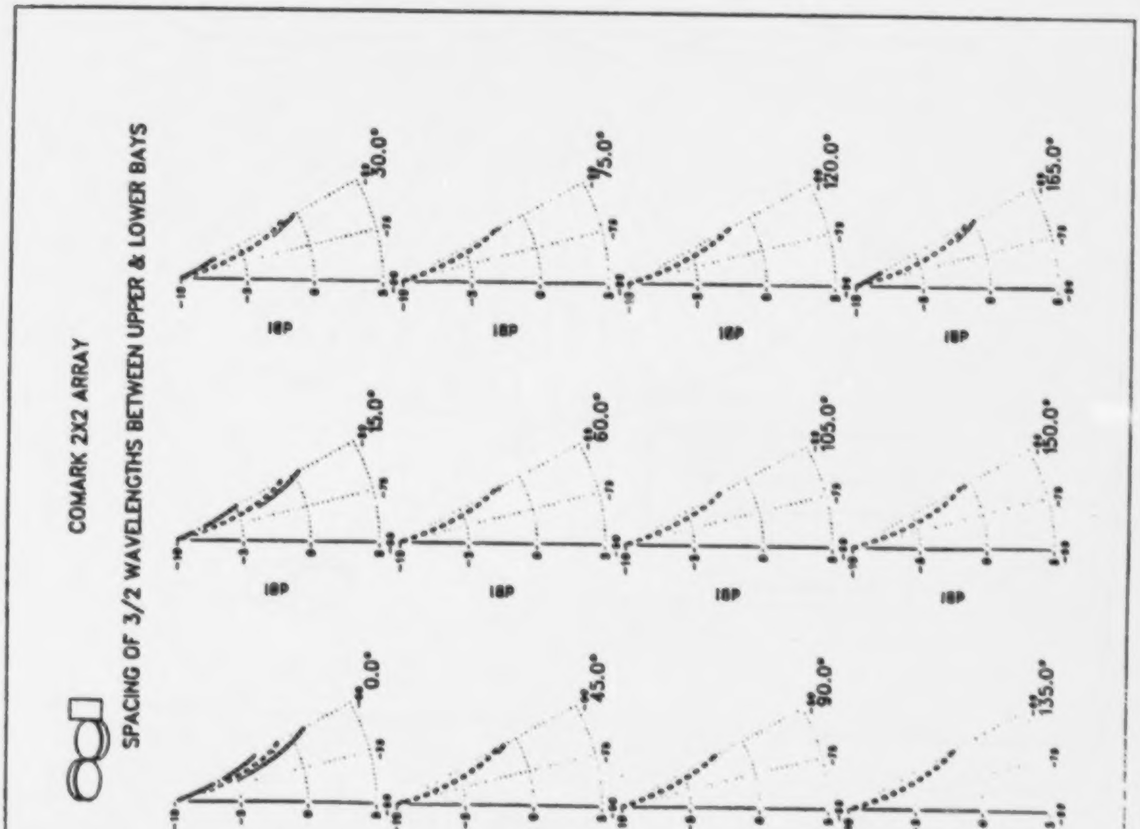
COMARK 2X2 ARRAY
SPACING OF 3/2 WAVELENGTHS BETWEEN UPPER & LOWER BAYS
0.0°
15.0°
30.0°
45.0°
60.0°
75.0°
90.0°
105.0°
120.0°
135.0°
150.0°
165.0°
IBP

FIGURE B 172

COMARK 2X2 ARRAY

SPACING OF 3/2 WAVELENGTHS BETWEEN UPPER & LOWER BAYS

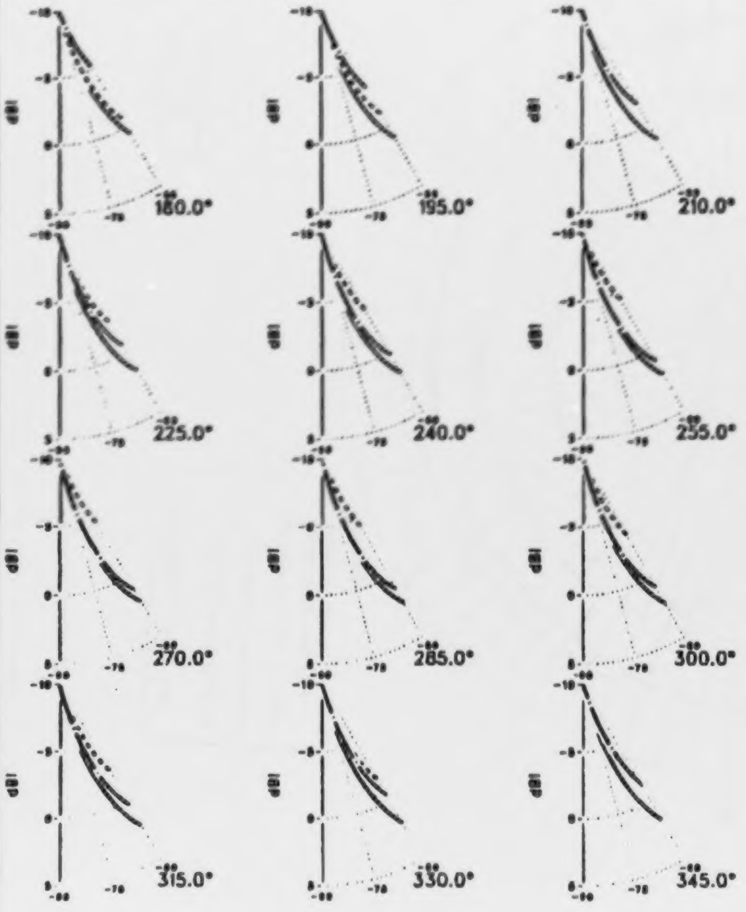

FIGURE B 173

THE COMARK 2X2 ARRAY

SPACING OF TWO WAVELENGTHS BETWEEN UPPER & LOWER BAYS

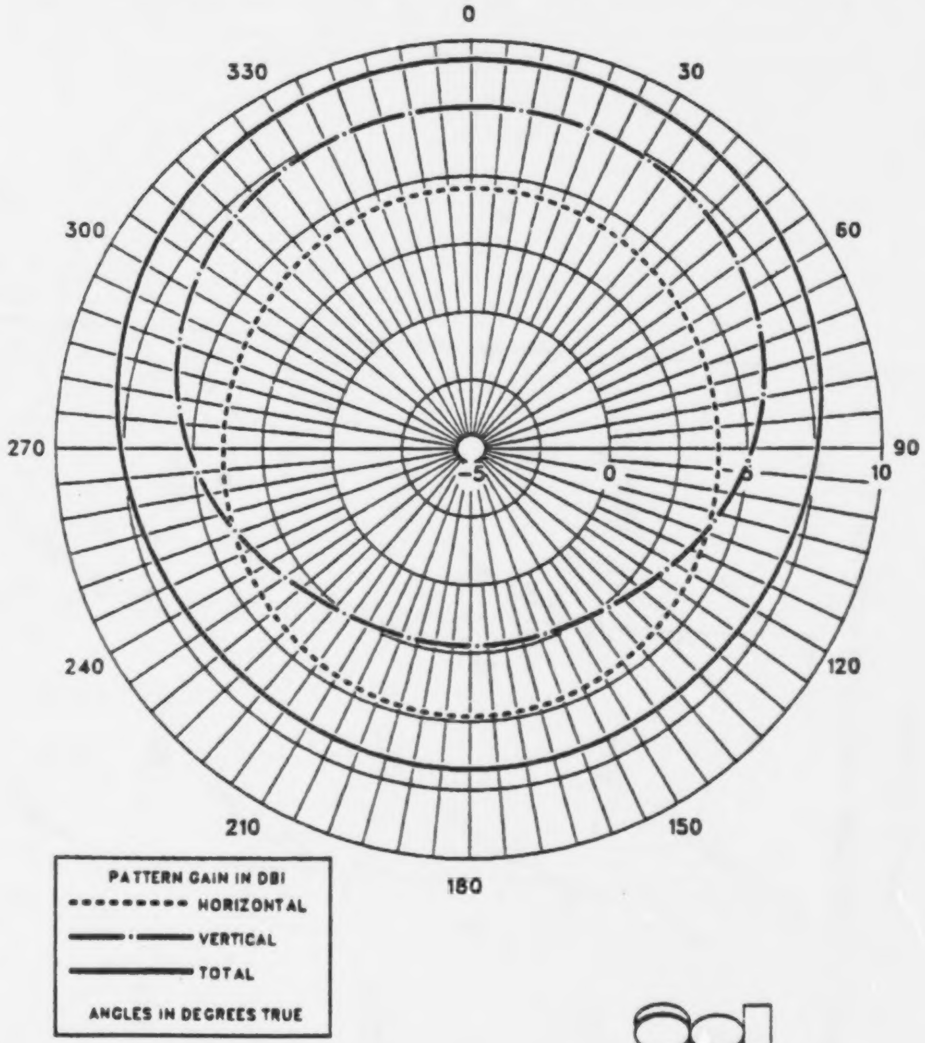

FIGURE B 174

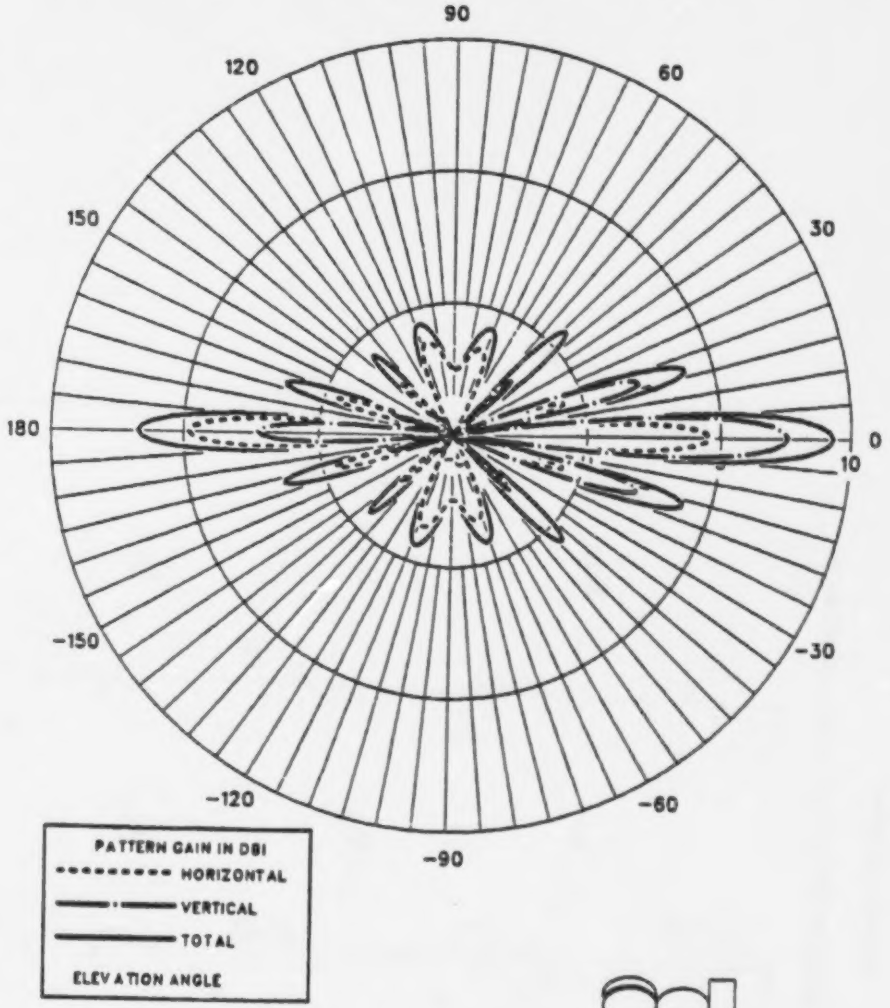

THE COMARK 2X2 ARRAY

SPACING OF TWO WAVELENGTHS BETWEEN UPPER & LOWER BAYS

FIGURE B 175

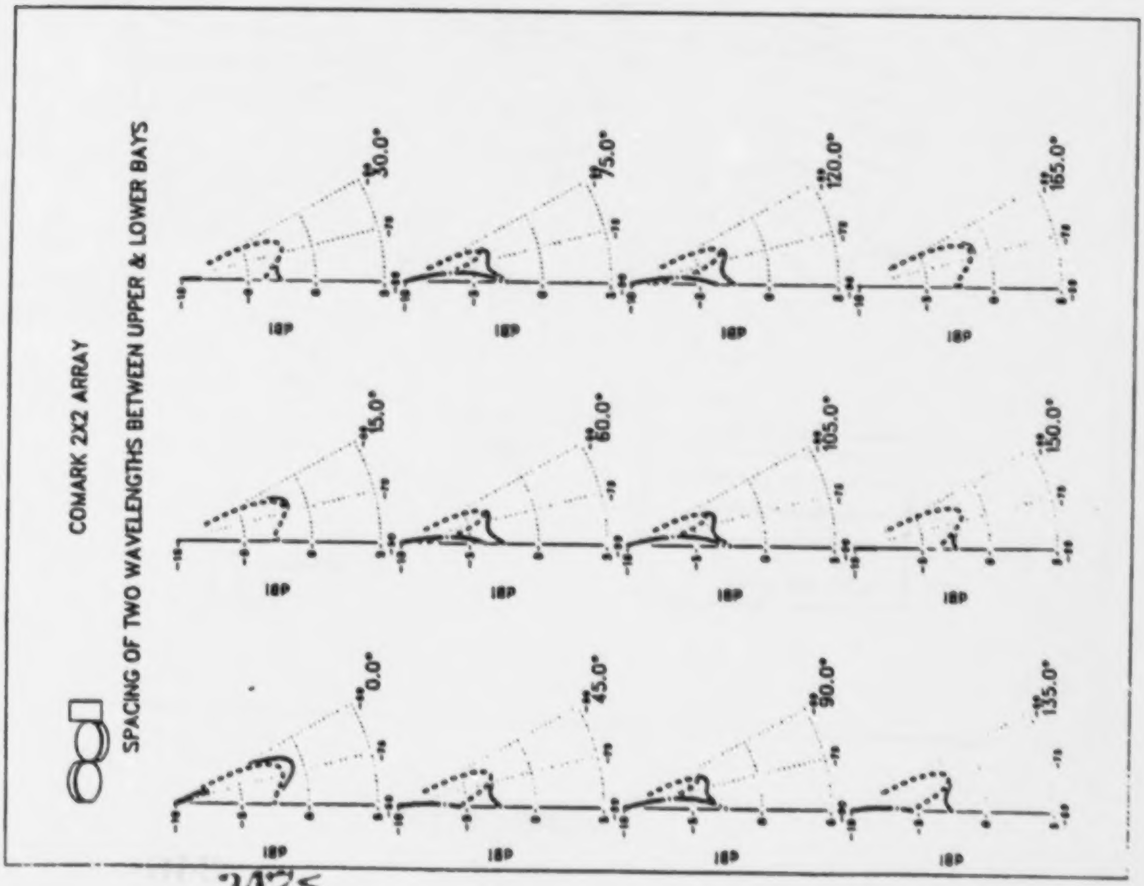
COMARK 2X2 ARRAY
SPACING OF TWO WAVELENGTHS BETWEEN UPPER & LOWER BAYS
0.0°
15.0°
30.0°
45.0°
60.0°
75.0°
90.0°
105.0°
120.0°
135.0°
150.0°
165.0°
IBP

FIGURE B 176

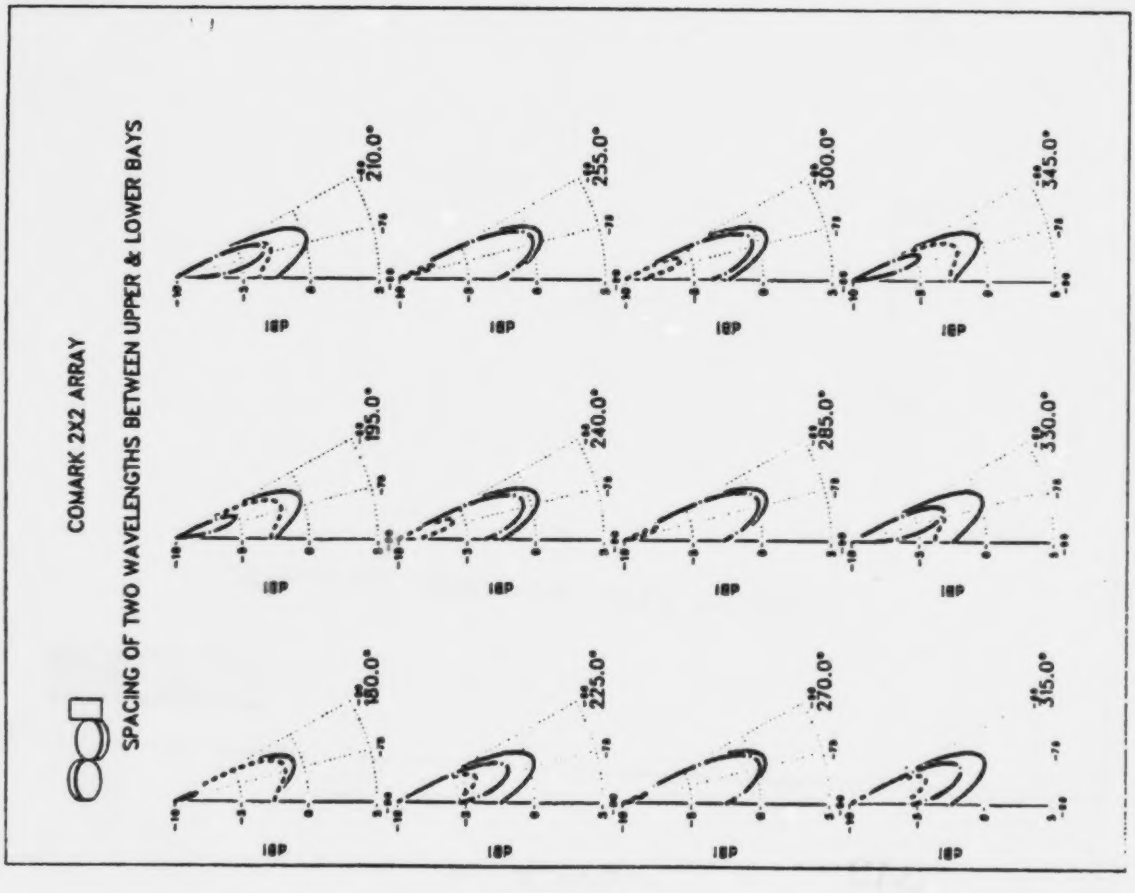COMARK 2X2 ARRAY
SPACING OF TWO WAVELENGTHS BETWEEN UPPER & LOWER BAYS
180.0°
195.0°
210.0°
225.0°
240.0°
255.0°
270.0°
285.0°
300.0°
315.0°
330.0°
345.0°
IBP

FIGURE B 177

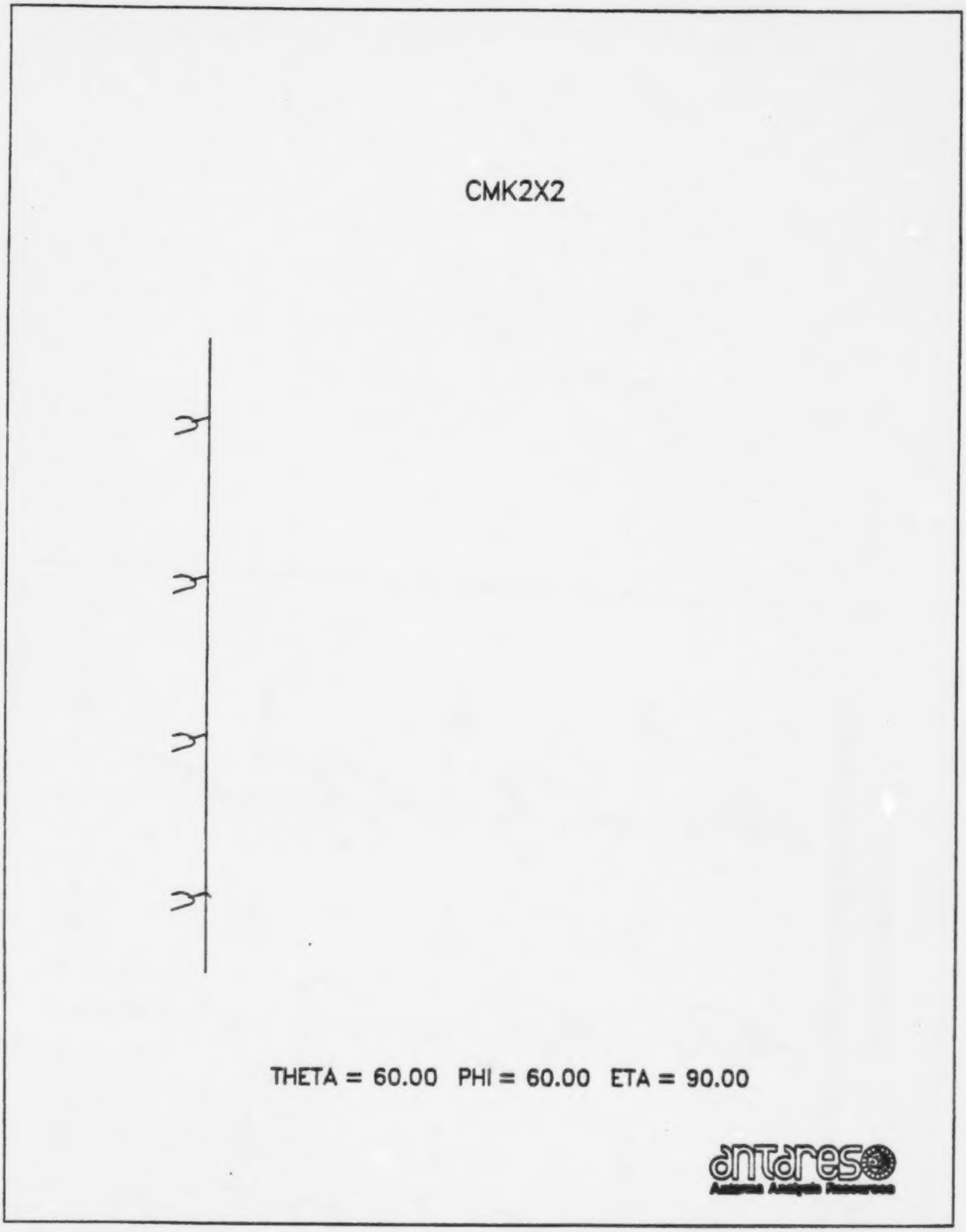

FIGURE B 178

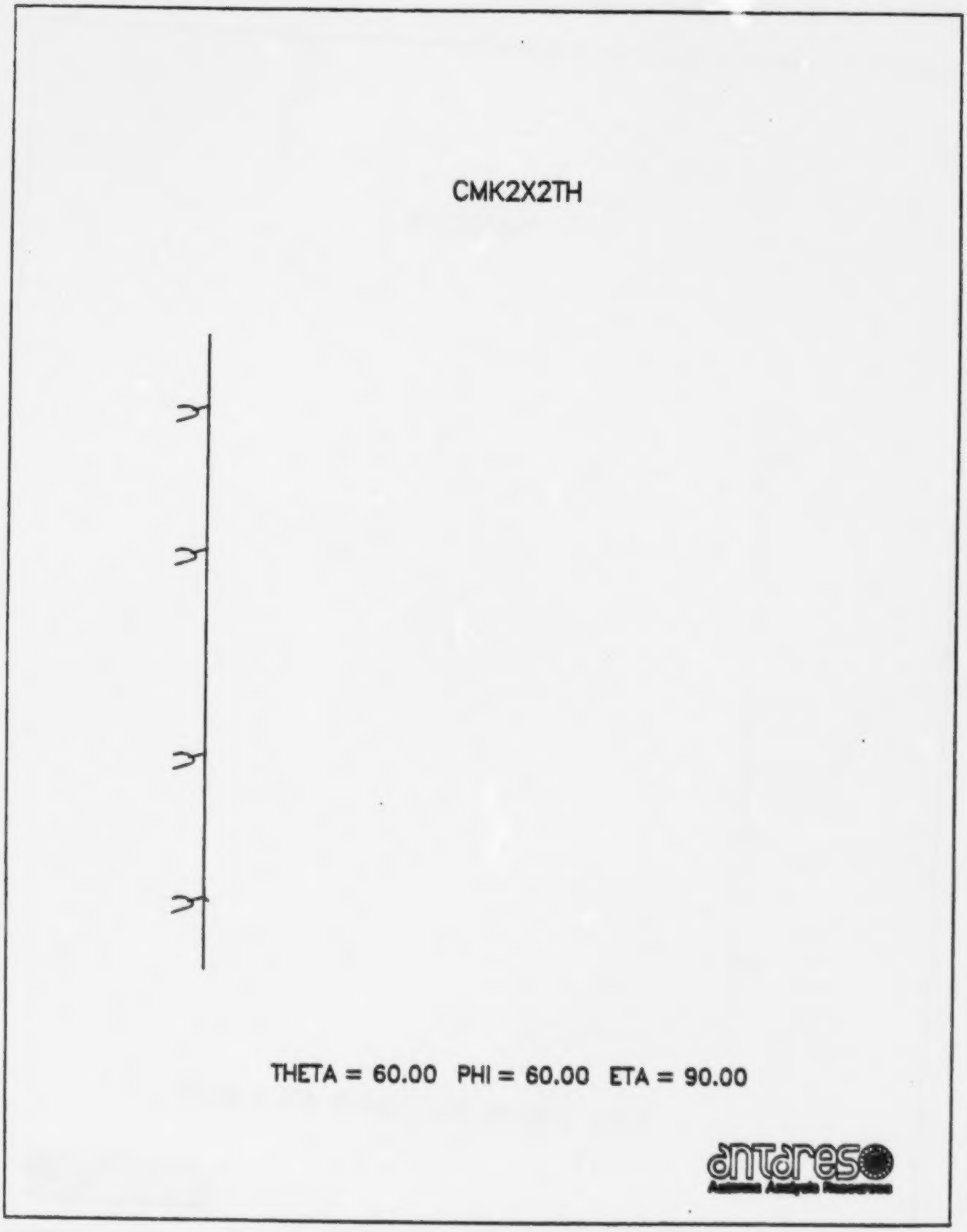
CMK2X2TH
THETA = 60.00 PHI = 60.00 ETA = 90.00
antares
Antenna Analysis Resources

FIGURE B 179

CMK2X2TW

THETA = 60.00 PHI = 60.00 ETA = 90.00

antares Antenna Analysis Resources

351<

FIGURE B 180

APPENDIX C

TV ARRAY BAY SPACING STUDY
RADIATION PATTERNS

CETEC JAT TURNSTILE ANTENNA

SINGLE ELEMENT -- CHANNEL 2

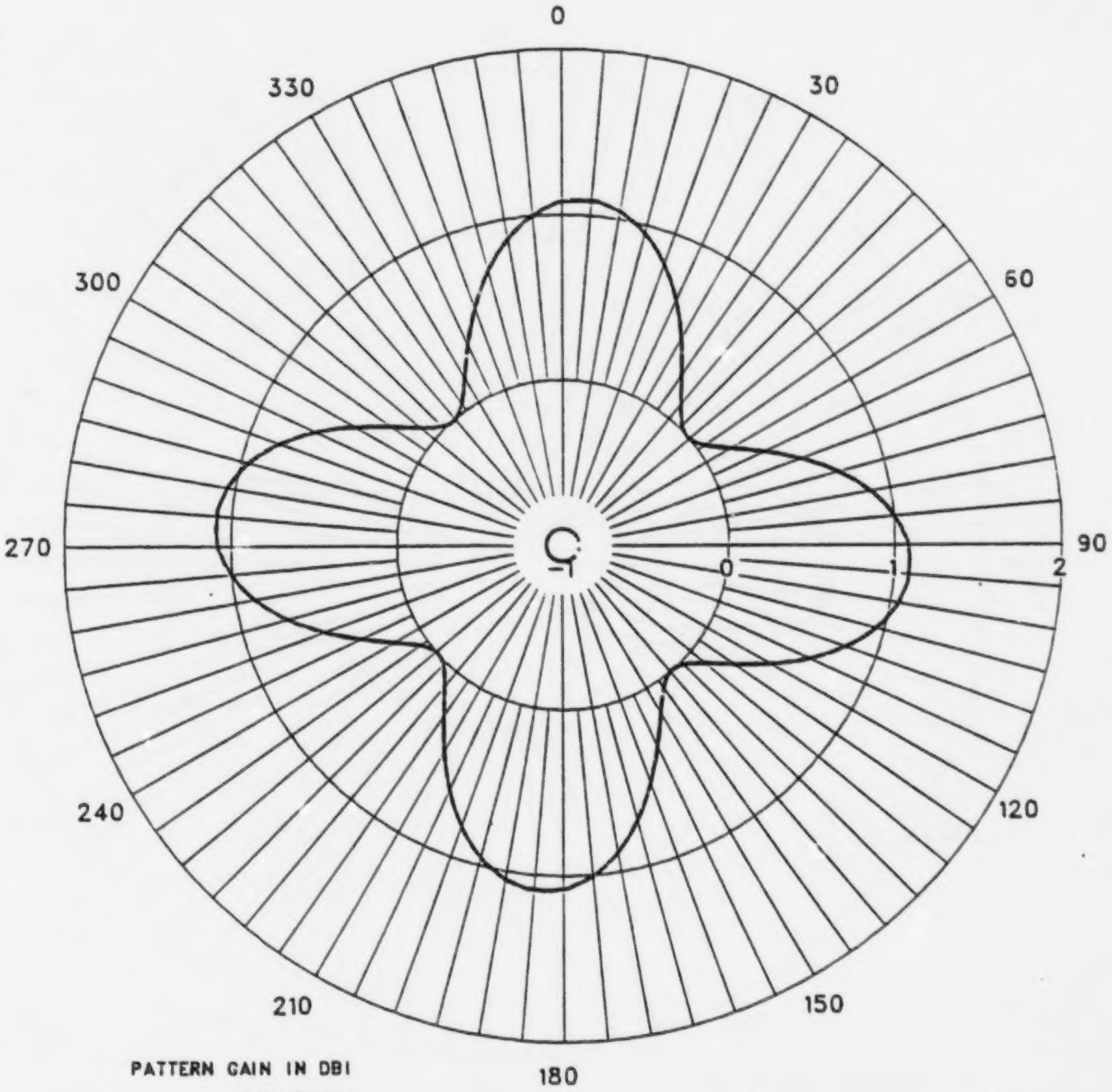

PATTERN GAIN IN DBI
--------- HORIZONTAL
——·—— VERTICAL
———— TOTAL

ANGLES IN DEGREES TRUE

FIGURE C 1

CETEC JAT TURNSTILE ANTENNA

SINGLE ELEMENT -- CHANNEL 2

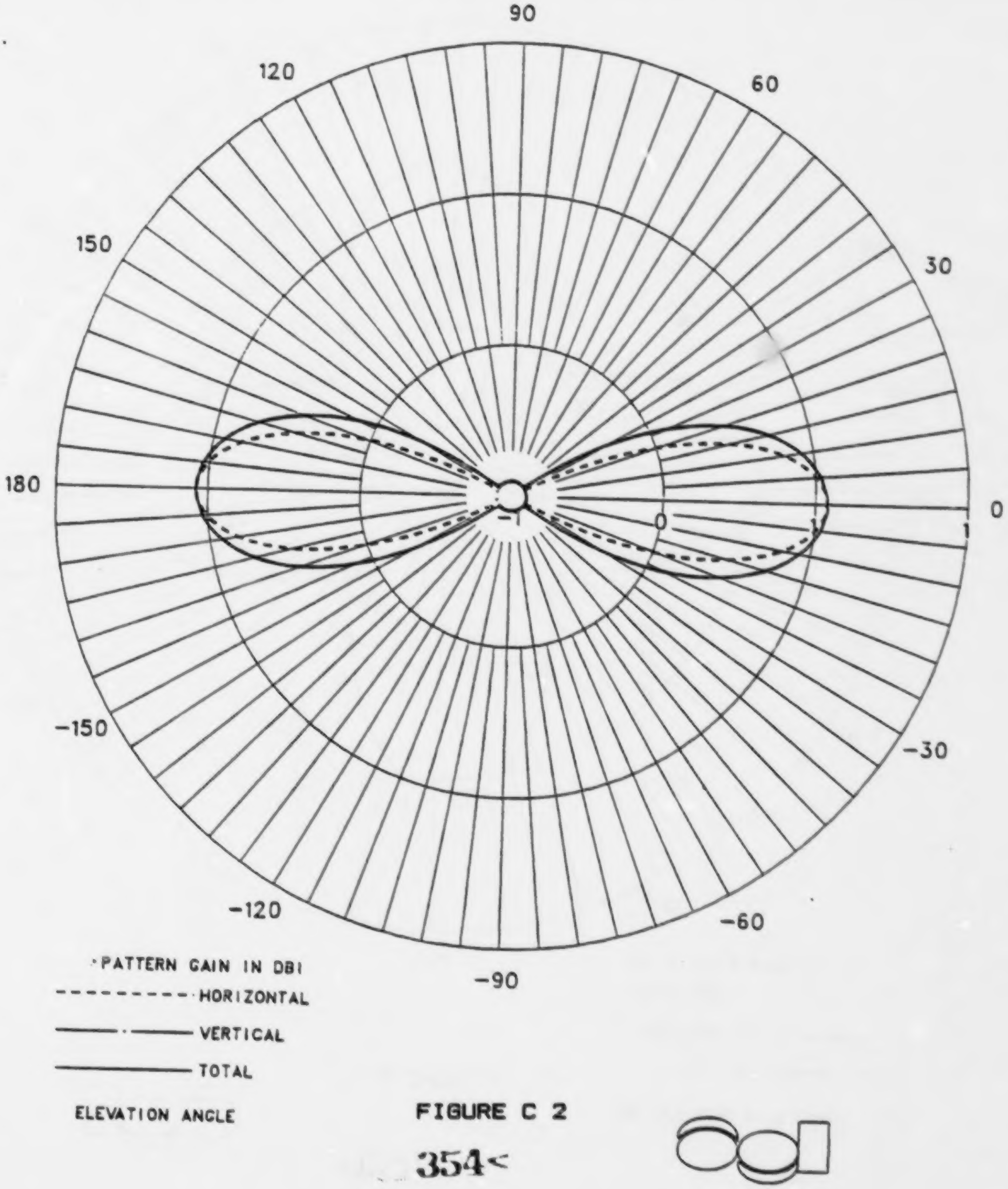

FIGURE C 2

CETEC JAT TURNSTILE ANTENNA

SINGLE ELEMENT -- CHANNEL 2

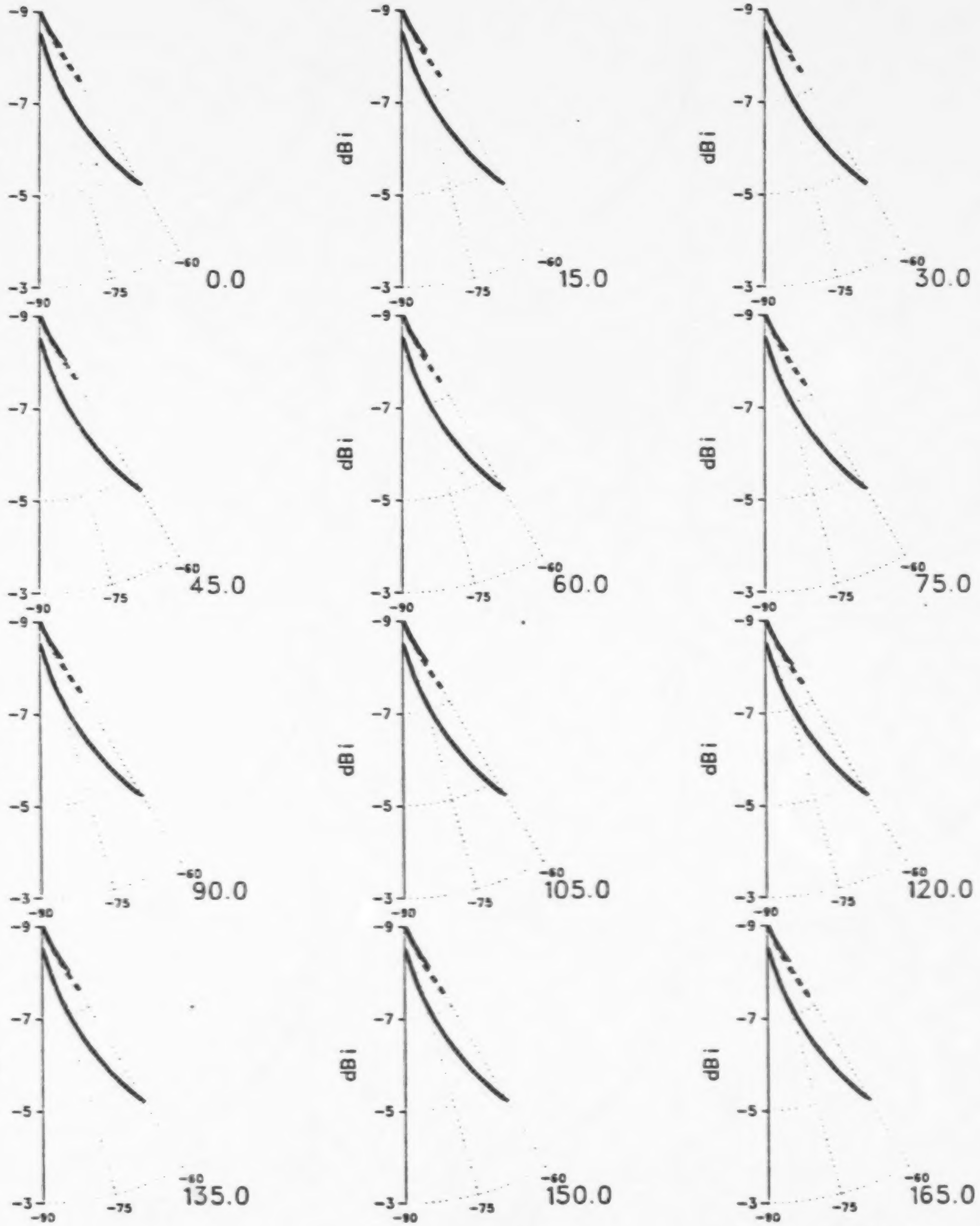

FIGURE C 3

CETEC JAT TURNSTILE ANTENNA

SINGLE ELEMENT -- CHANNEL 2

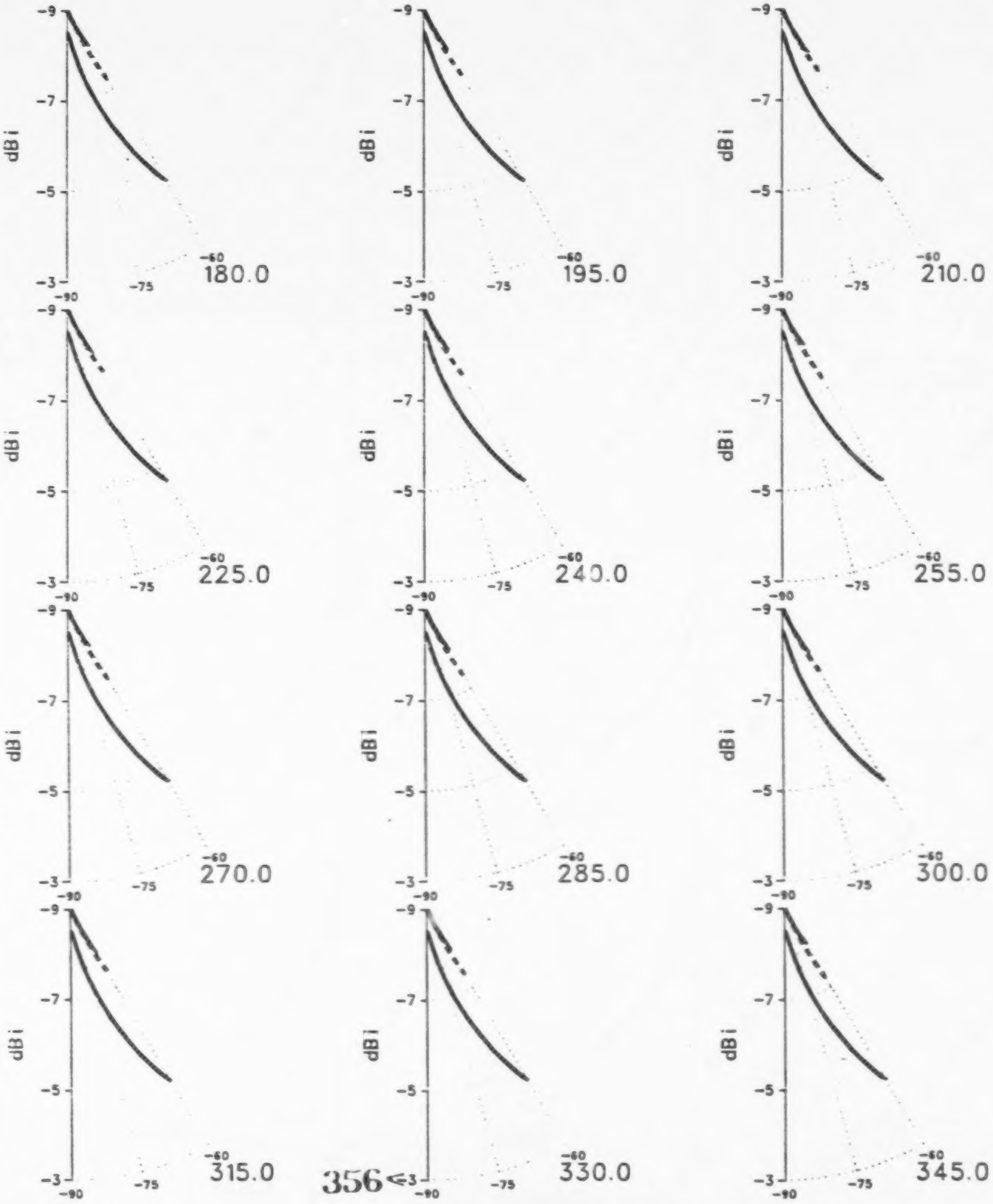

FIGURE C 4

CETEC JAT TURNSTILE ANTENNA

4 BAYS -- STANDARD SPACING -- CHANNEL 2

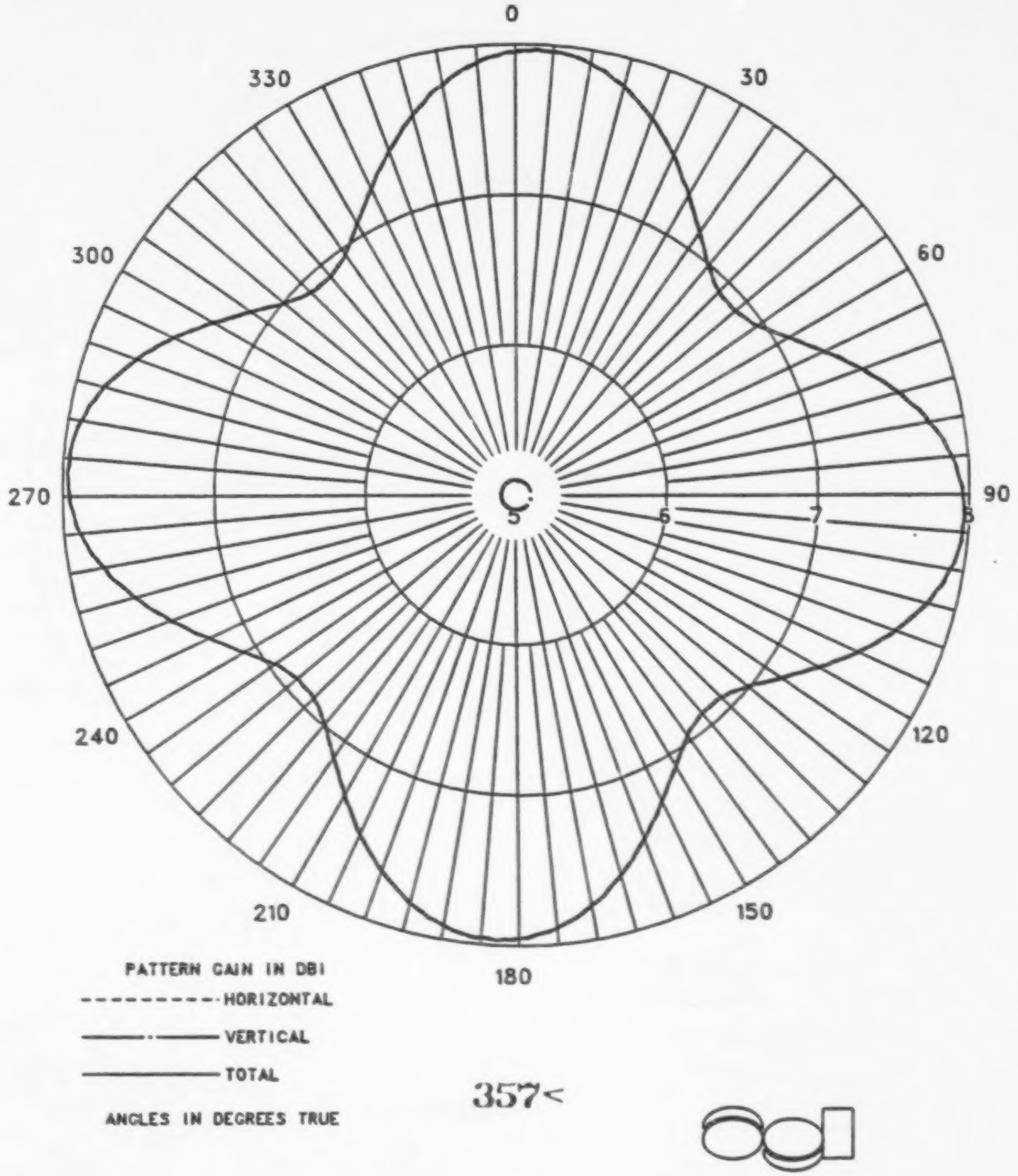

FIGURE C 5

CETEC JAT TURNSTILE ANTENNA

4 BAYS -- STANDARD SPACING -- CHANNEL 2

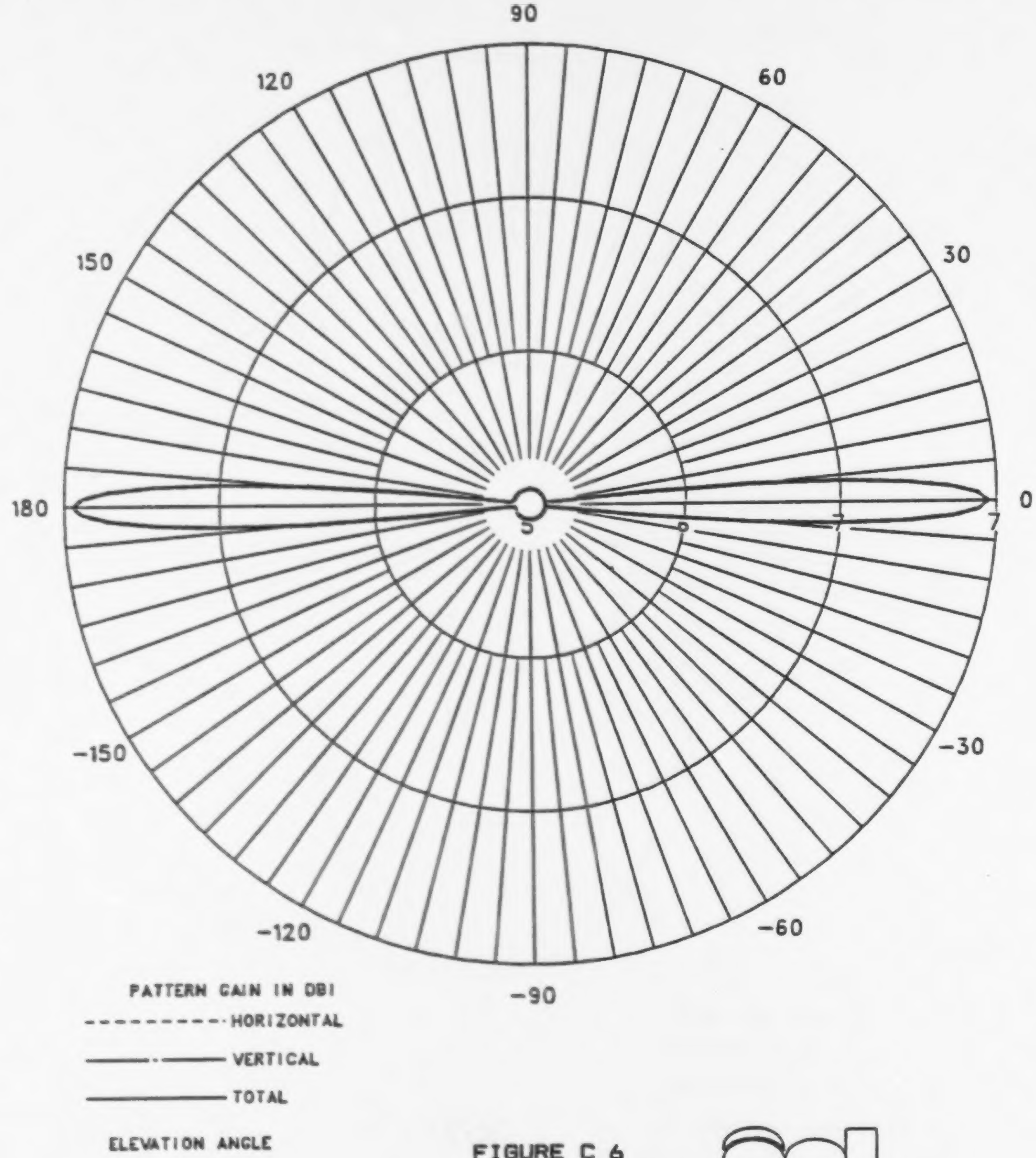

FIGURE C 6

CETEC JAT TURNSTILE ANTENNA

4 BAYS -- STANDARD SPACING -- CHANNEL 2

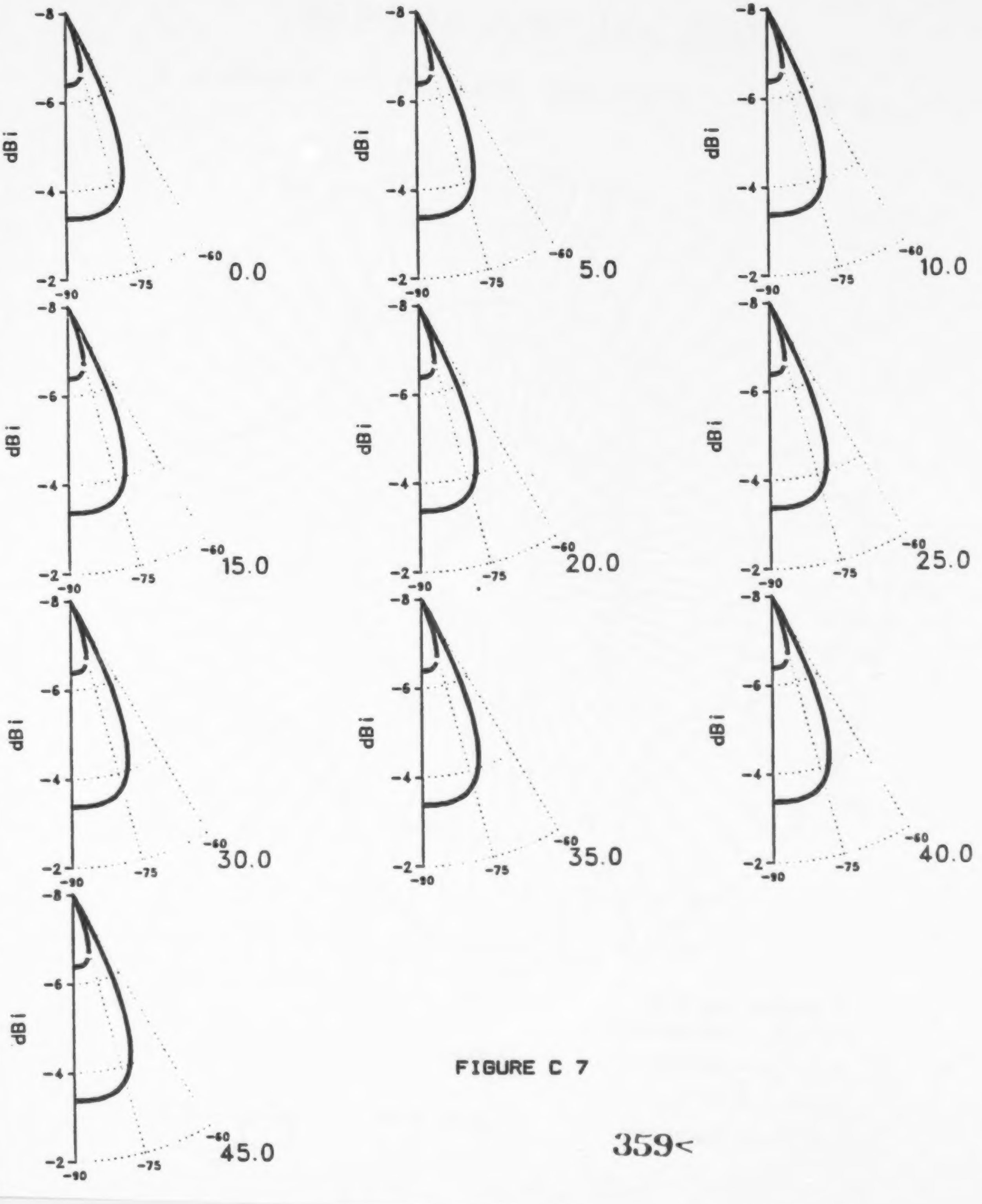

FIGURE C 7

CETEC JAT TURNSTILE ANTENNA

6 BAYS -- STANDARD SPACING -- CHANNEL 2

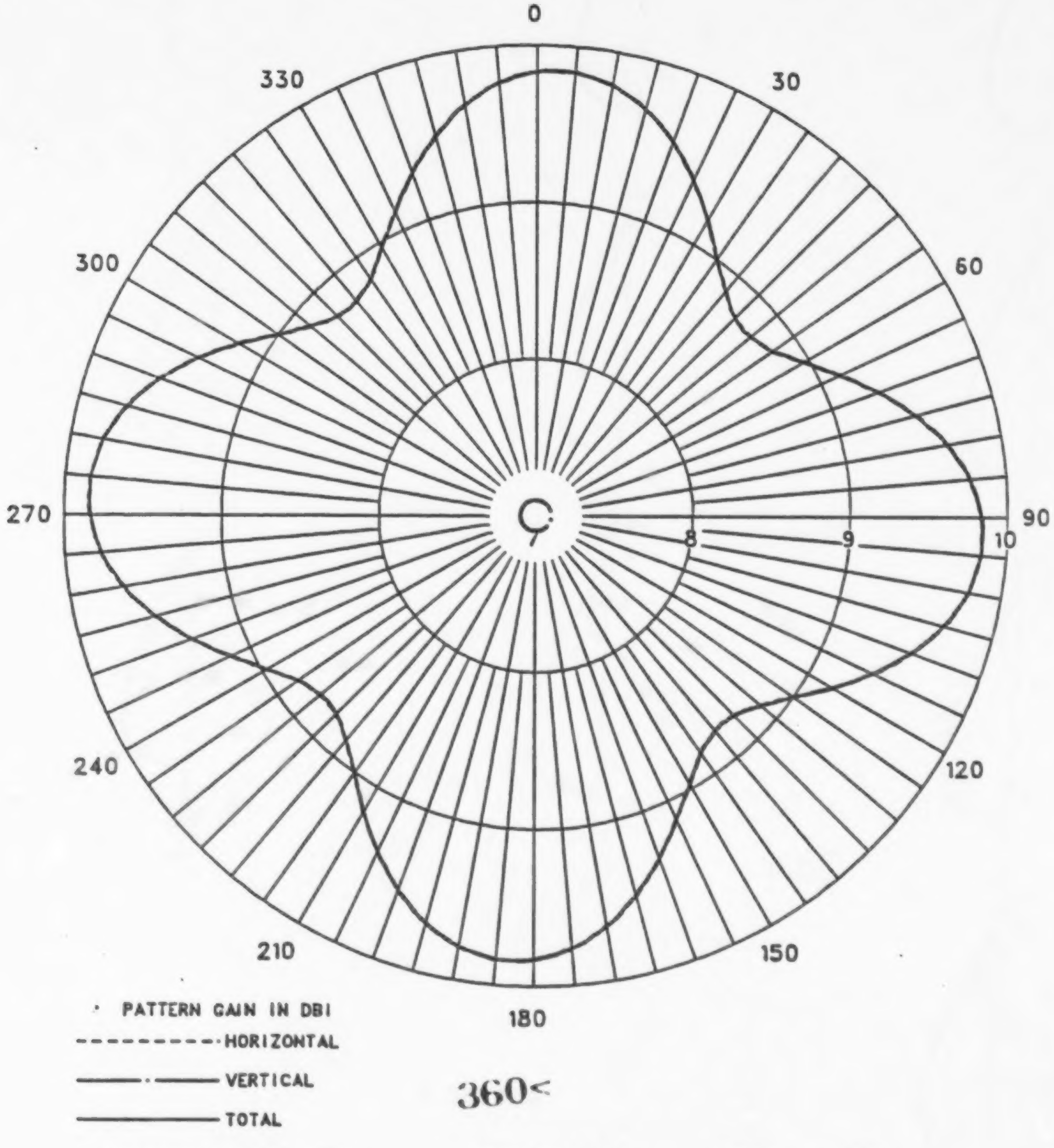

360<

ANGLES IN DEGREES TRUE

FIBURE C 8

CETEC JAT TURNSTILE ANTENNA

6 BAYS -- STANDARD SPACING -- CHANNEL 2

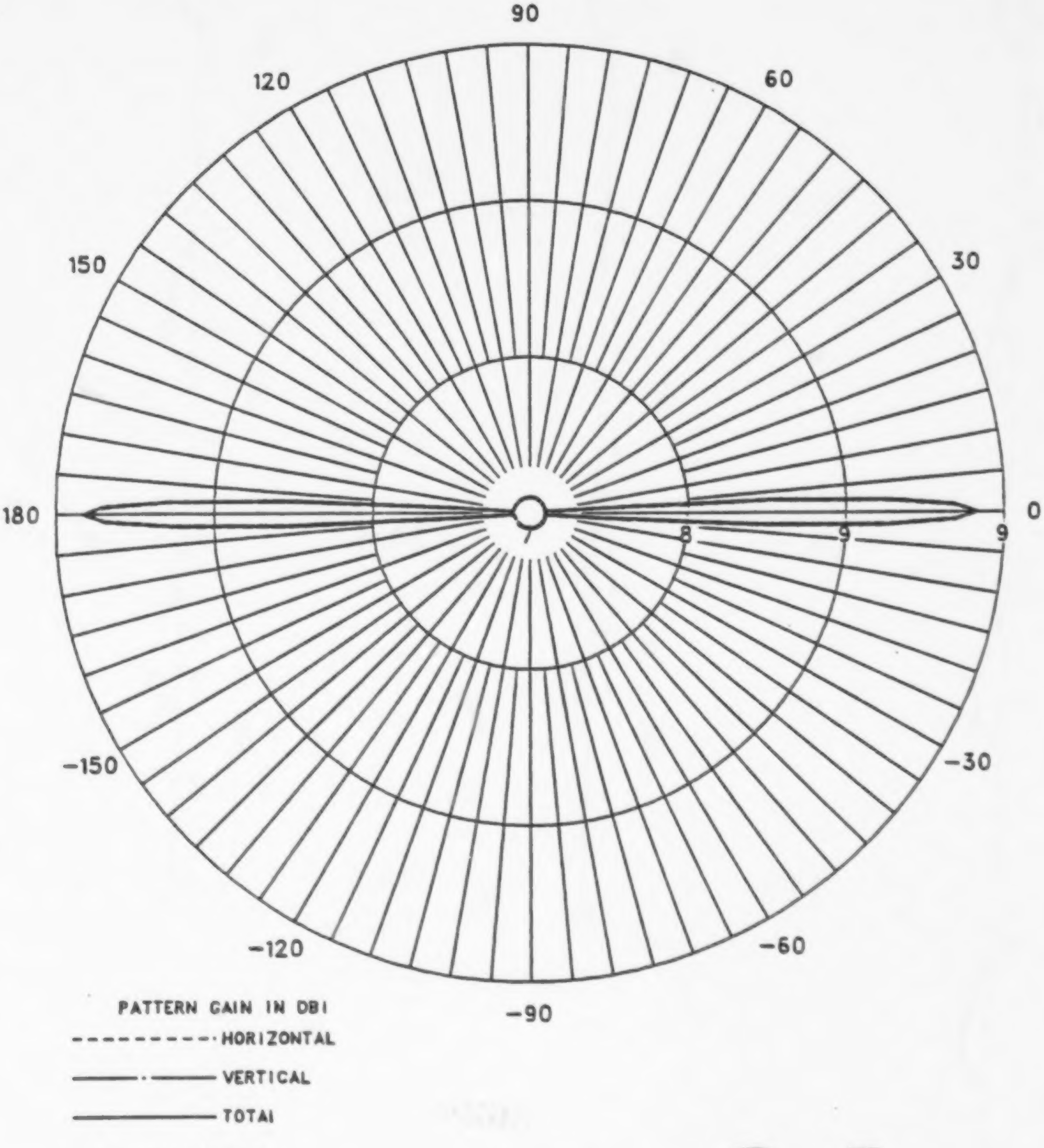

FIGURE C 9

CETEC JAT TURNSTILE ANTENNA

6 BAYS -- STANDARD SPACING -- CHANNEL 2

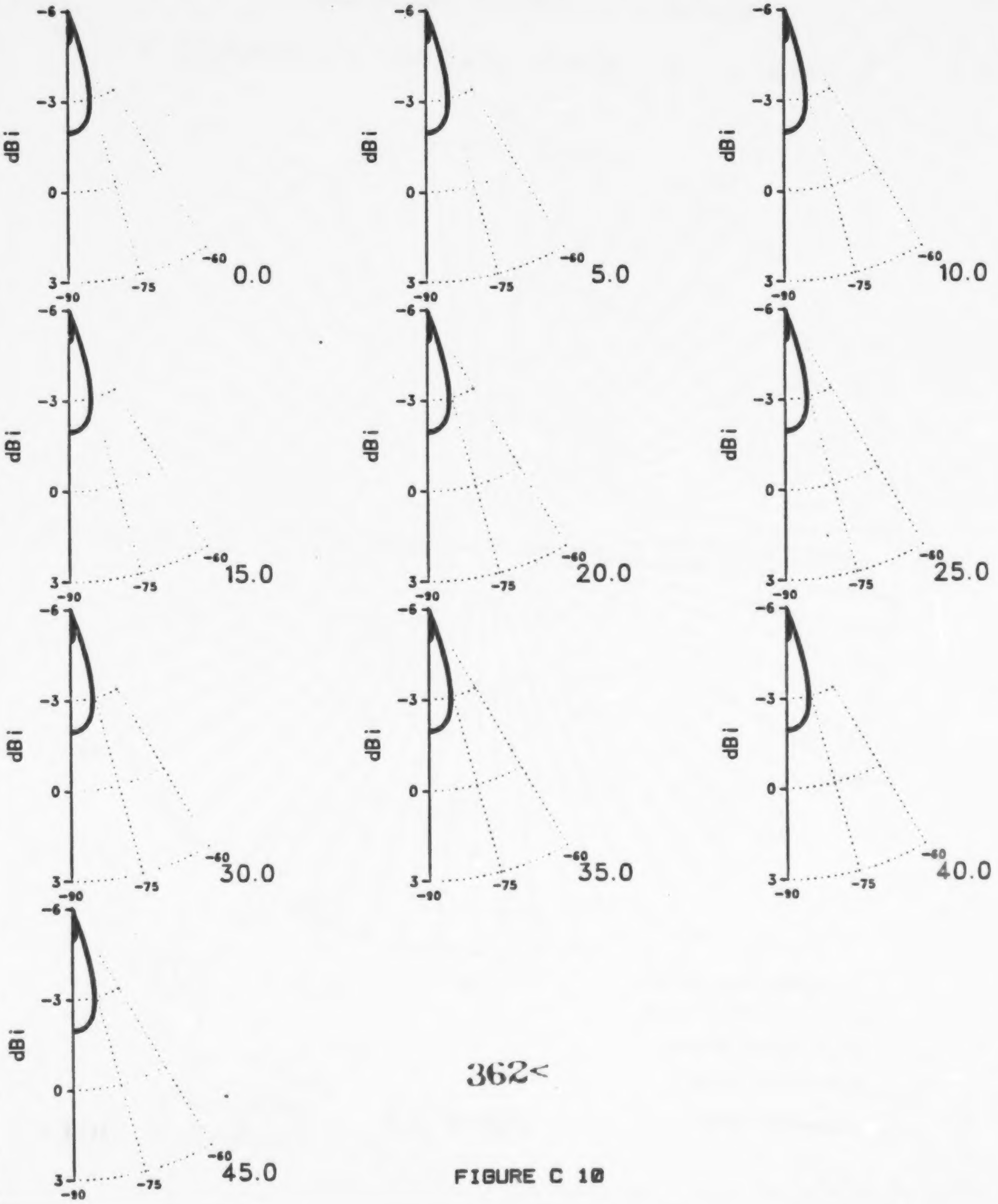

362<

FIGURE C 10

CETEC JAT TURNSTILE ANTENNA

8 BAYS -- STANDARD SPACING -- CHANNEL 2

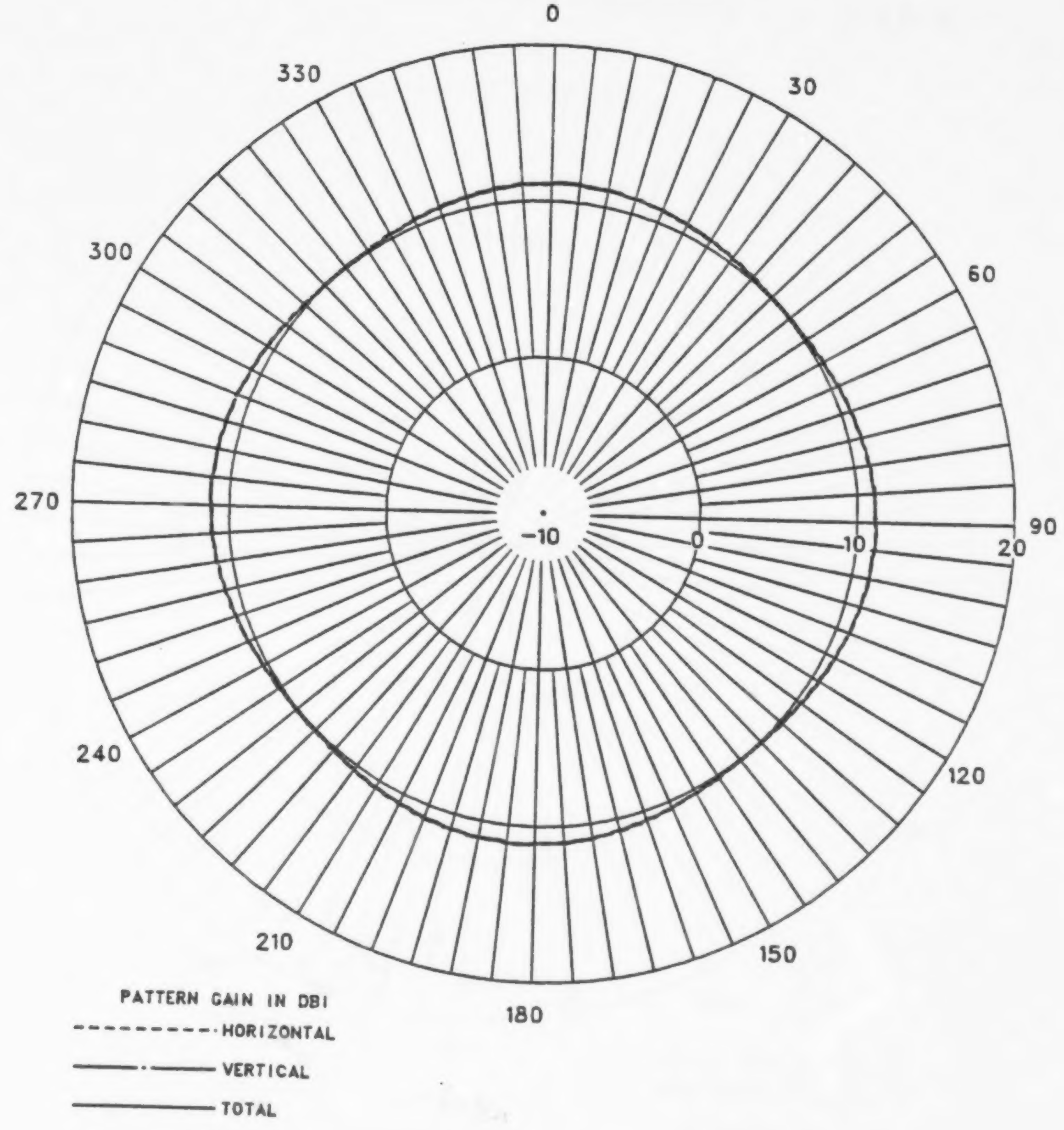

ANGLES IN DEGREES TRUE

FIGURE C 11

CETEC JAT TURNSTILE ANTENNA

8 BAYS -- STANDARD SPACING -- CHANNEL 2

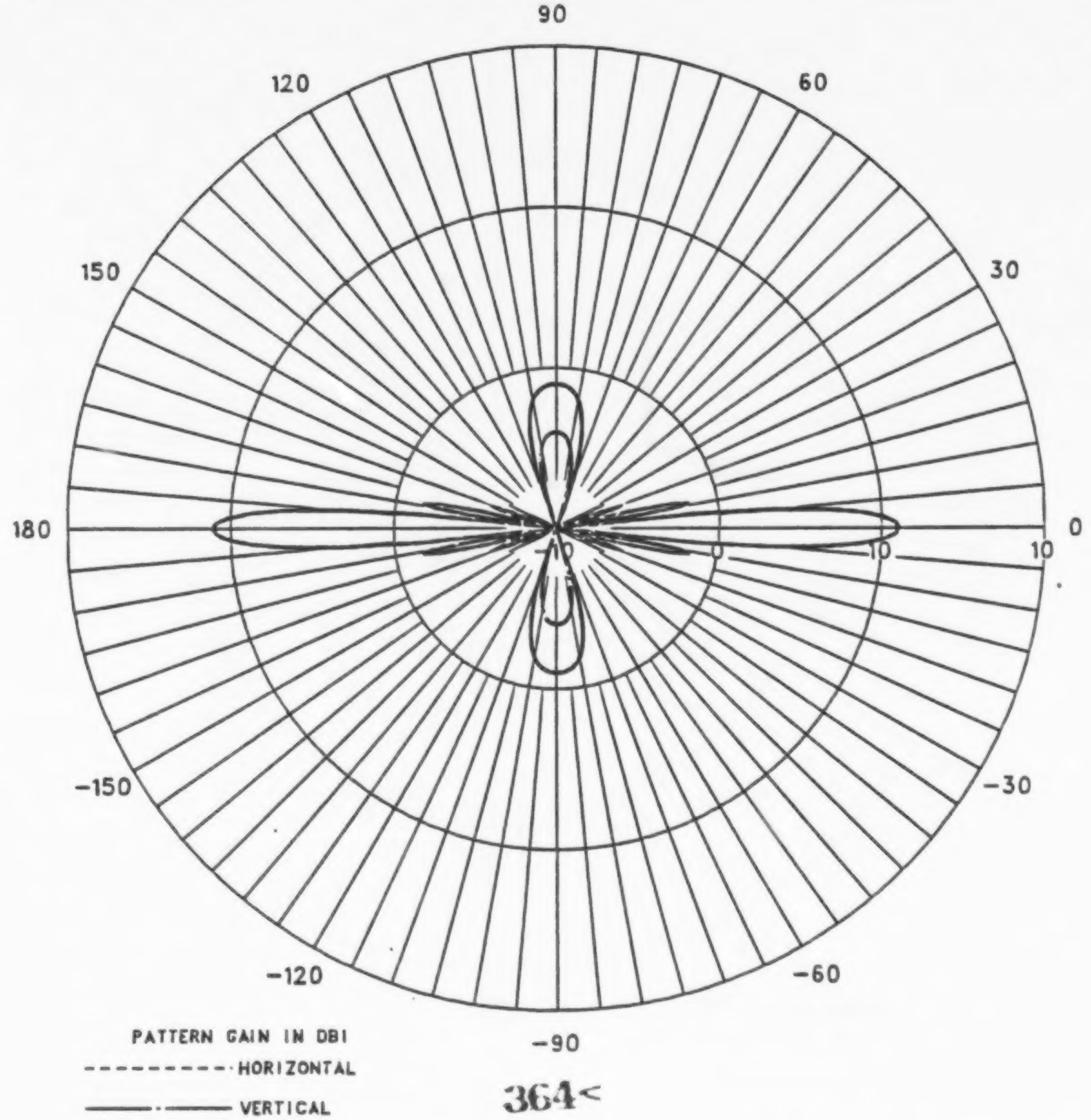

FIGURE C 12

CETEC JAT TURNSTILE ANTENNA

8 BAYS -- STANDARD SPACING -- CHANNEL 2

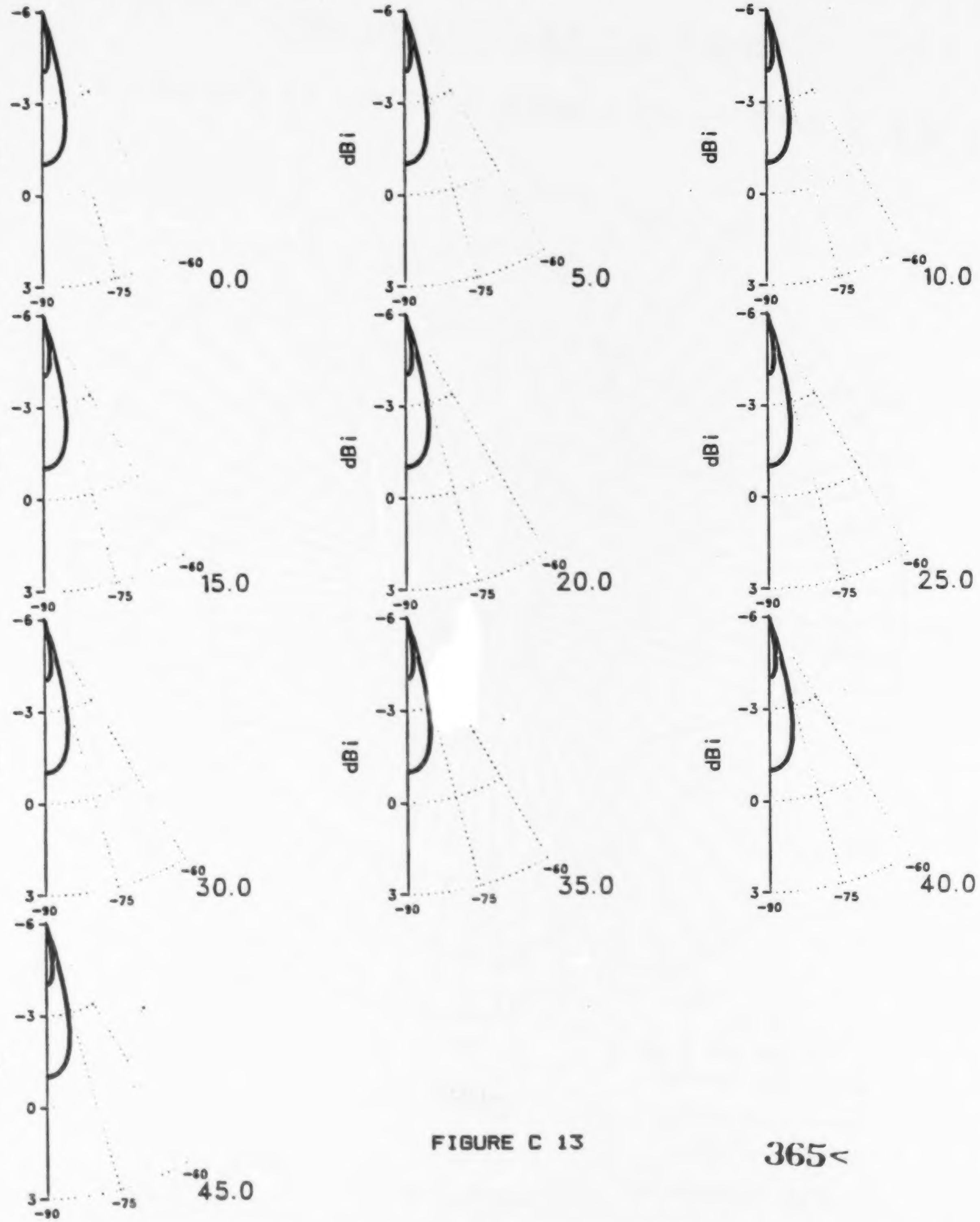

FIGURE C 13

CETEC JAT TURNSTILE ANTENNA

2 X 2 BAYS -- 1.5 LAMBDA SPACING -- CHANNEL 2

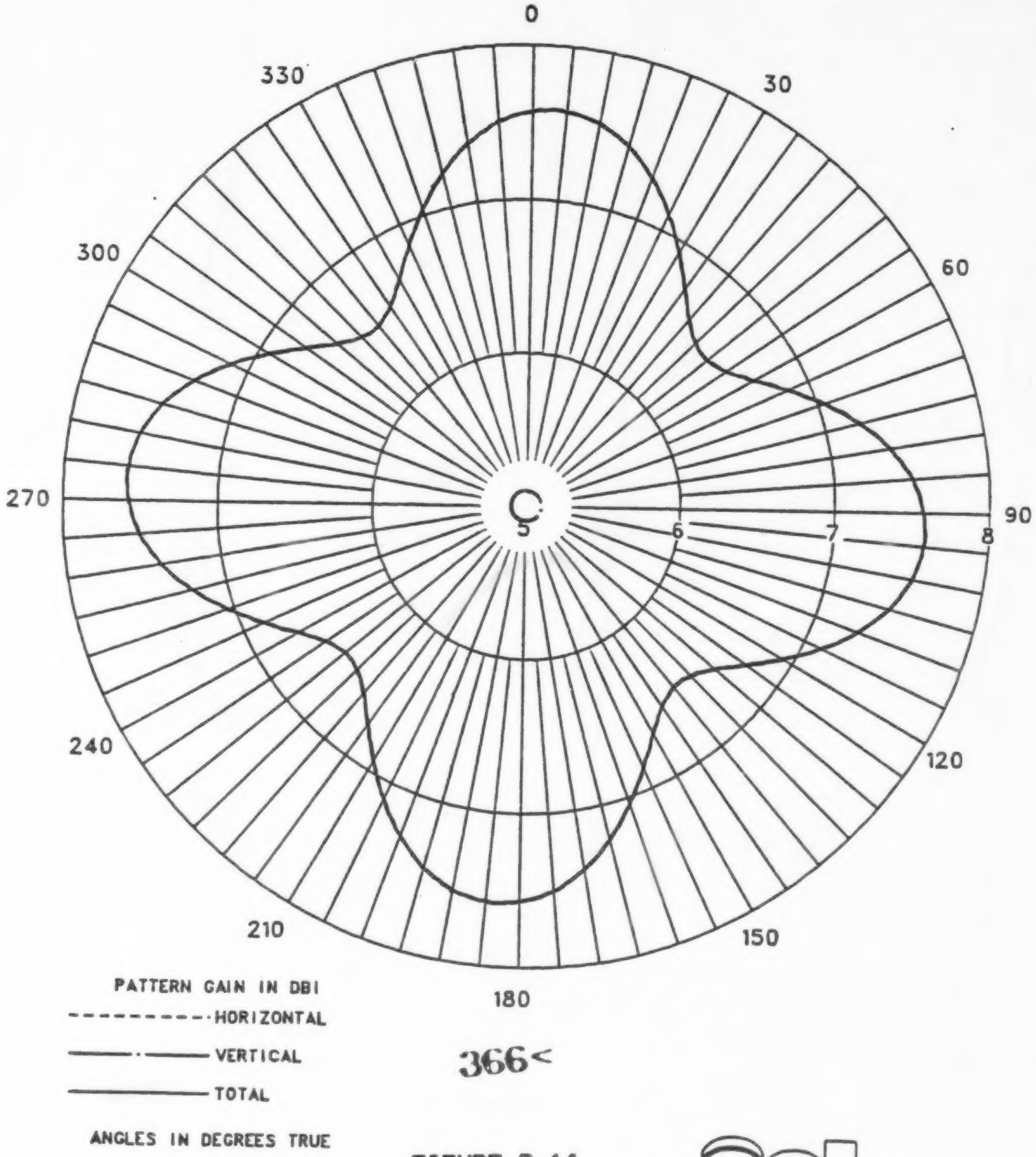

366<

FIBURE C 14

CETEC JAT TURNSTILE ANTENNA

2 X 2 BAYS -- 1.5 LAMBDA SPACING -- CHANNEL 2

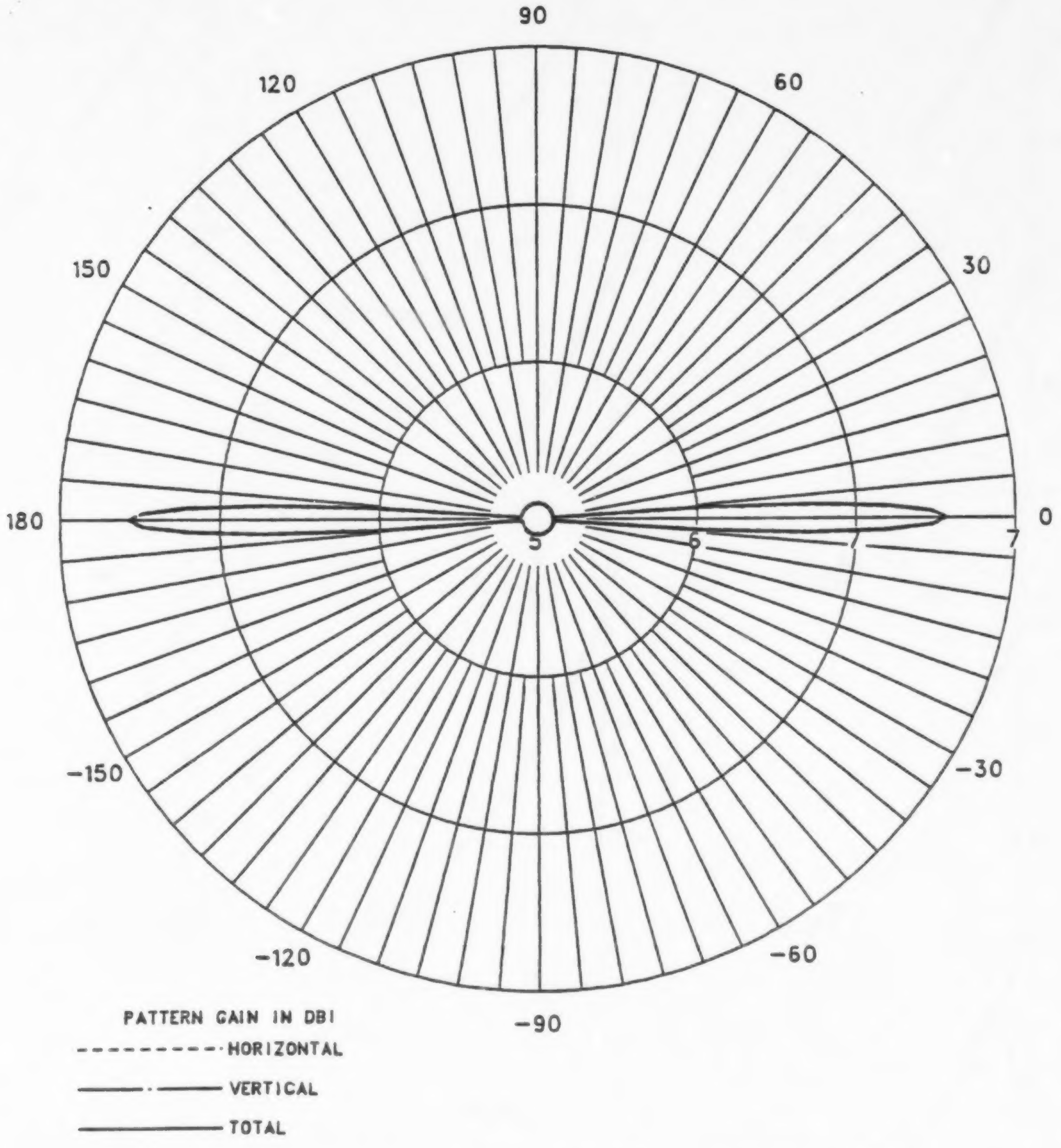

FIGURE C 15

CETEC JAT TURNSTILE ANTENNA

2 X 2 BAYS -- 1.5 LAMBDA SPACING -- CHANNEL 2

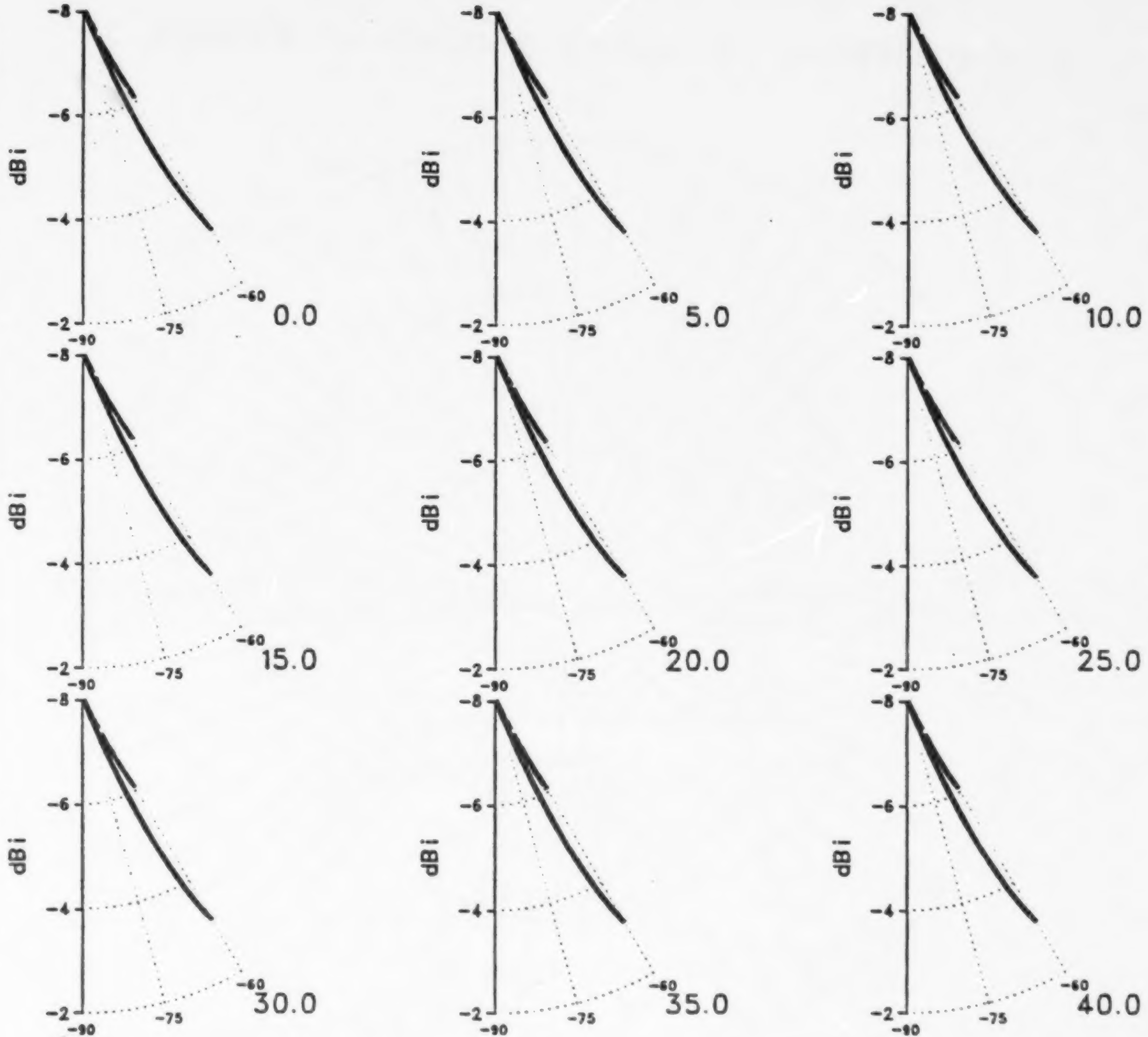

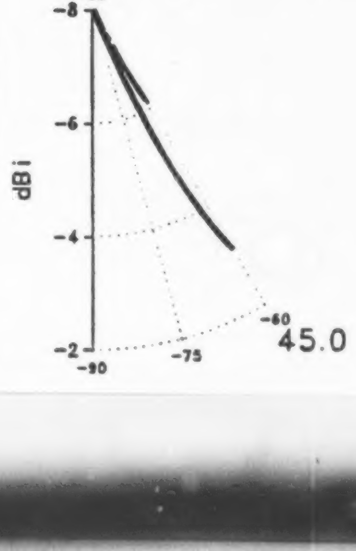

FIGURE C 16

CETEC JAT TURNSTILE ANTENNA

3 X 3 BAYS -- 1.5 LAMBDA SPACING -- CHANNEL 2

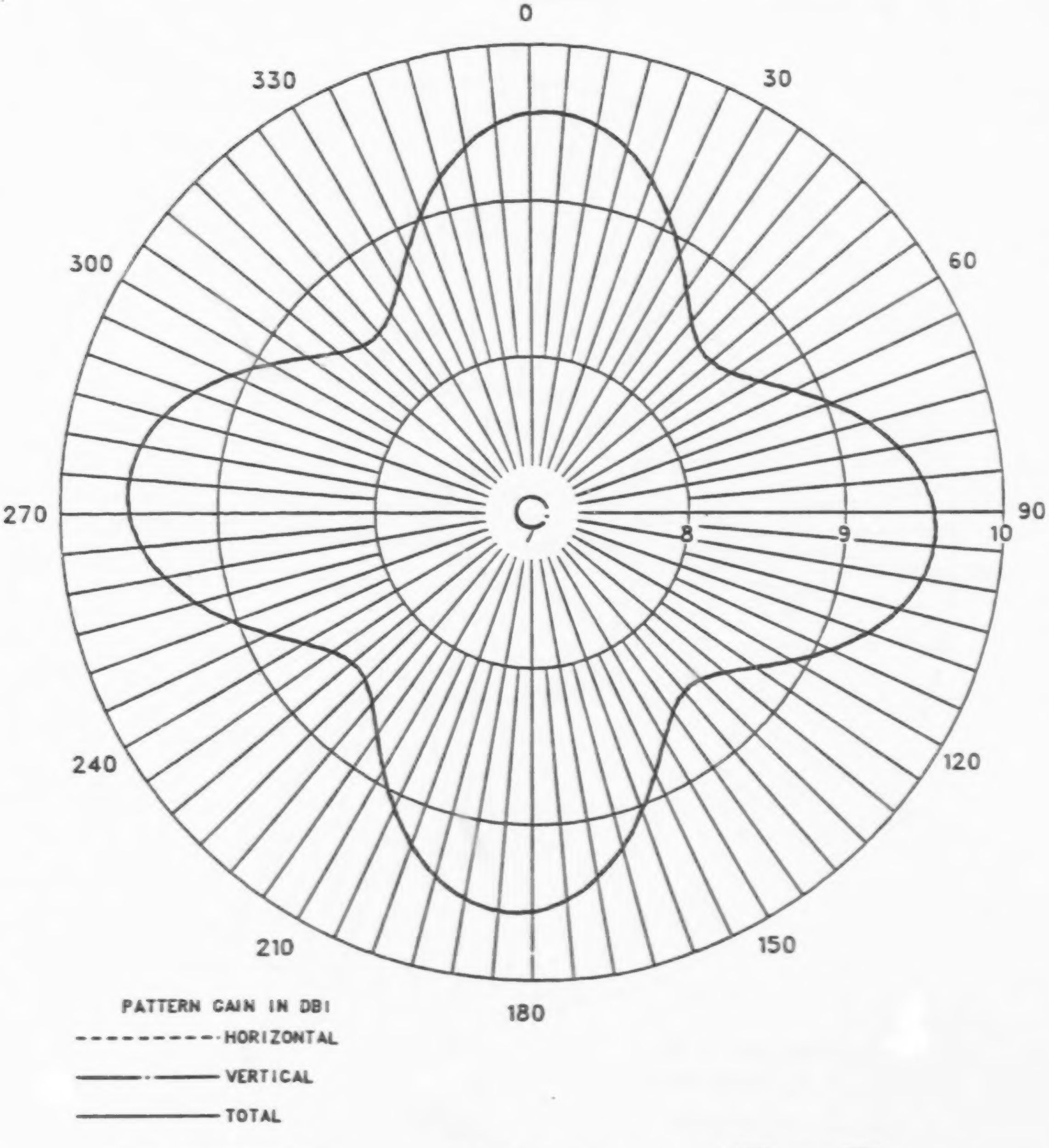

ANGLES IN DEGREES TRUE

FIGURE C 17

CETEC JAT TURNSTILE ANTENNA

3 X 3 BAYS -- 1.5 LAMBDA SPACING -- CHANNEL 2

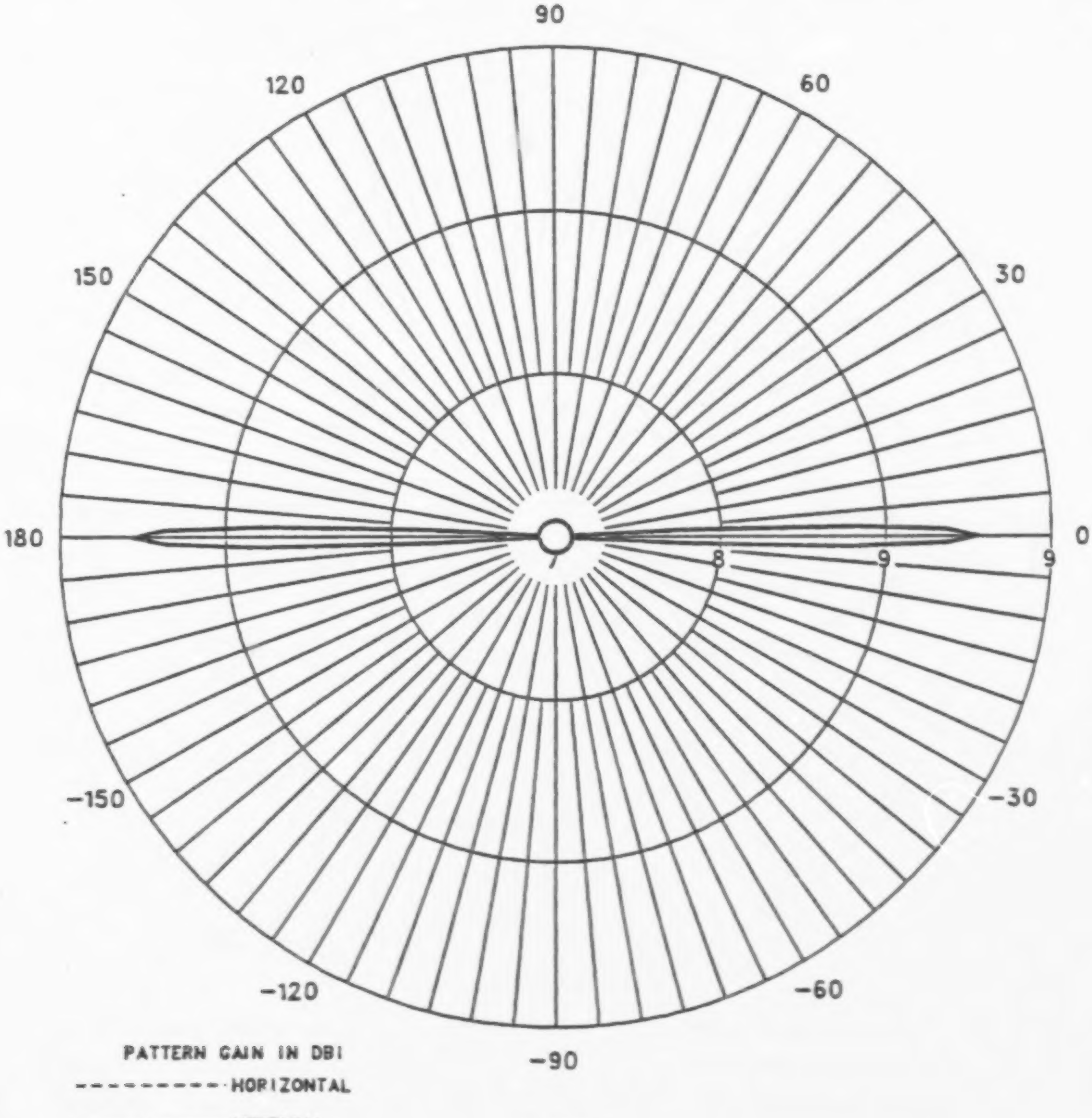

370<

FIGURE C 18

CETEC JAT TURNSTILE ANTENNA

3 X 3 BAYS -- 1.5 LAMBDA SPACING -- CHANNEL 2

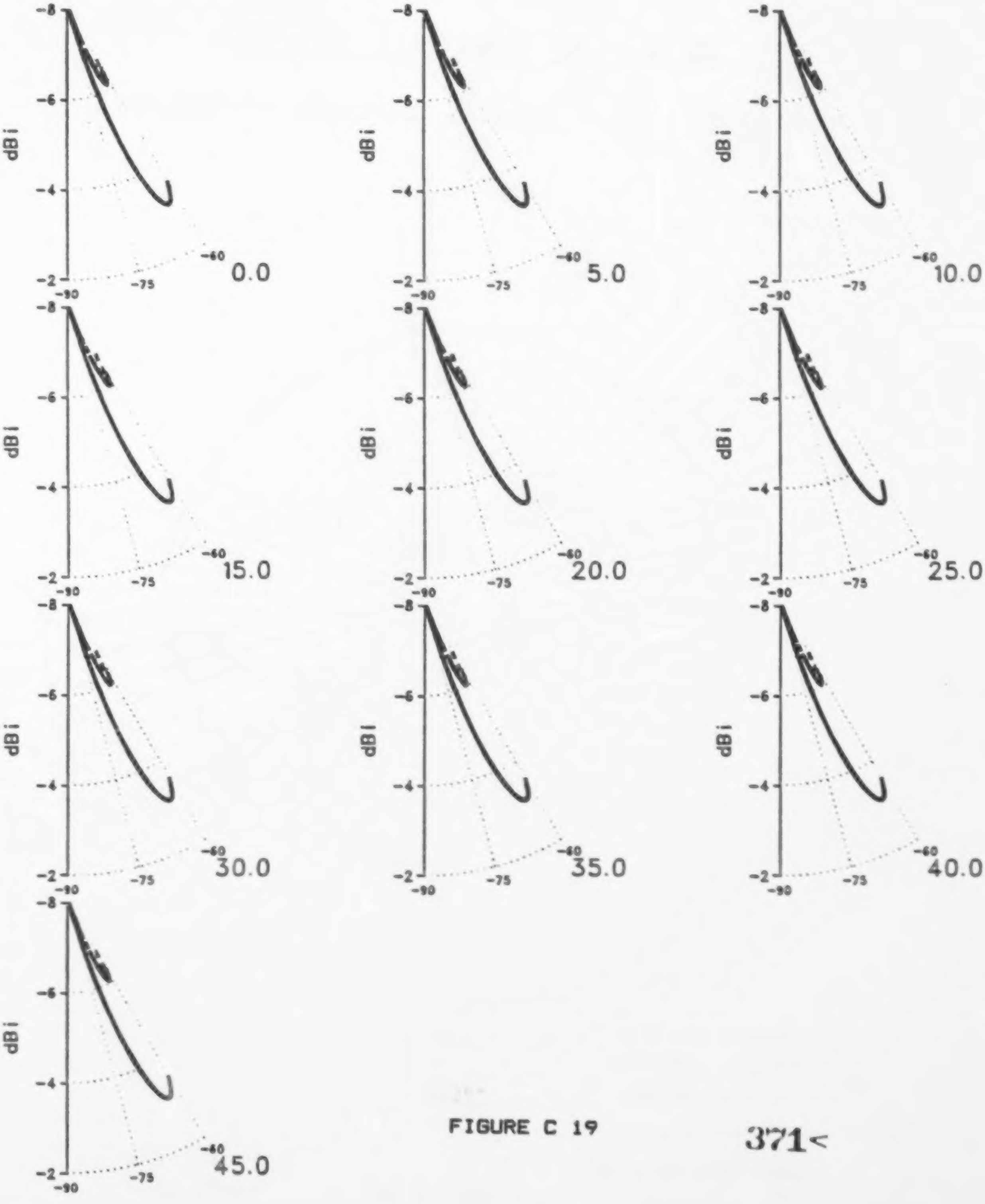

FIGURE C 19

CETEC JAT TURNSTILE ANTENNA

4 X 4 BAYS -- 1.5 LAMBDA SPACING -- CHANNEL 2

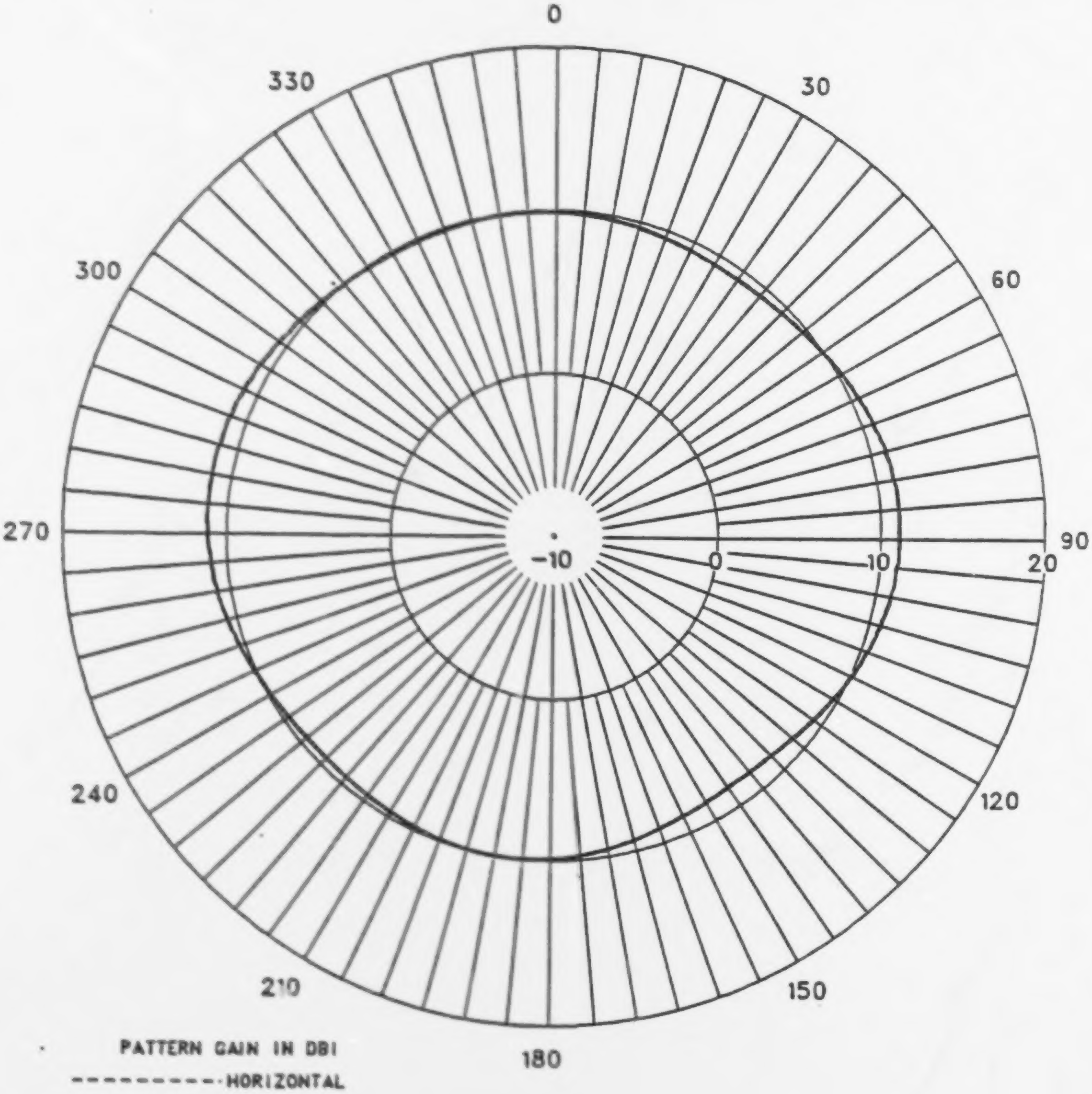

PATTERN GAIN IN DBI
- - - - - - - - - HORIZONTAL
——·—— VERTICAL
———— TOTAL

ANGLES IN DEGREES TRUE

372<

FIGURE C 20

CETEC JAT TURNSTILE ANTENNA

4 X 4 BAYS -- 1.5 LAMBDA SPACING -- CHANNEL 2

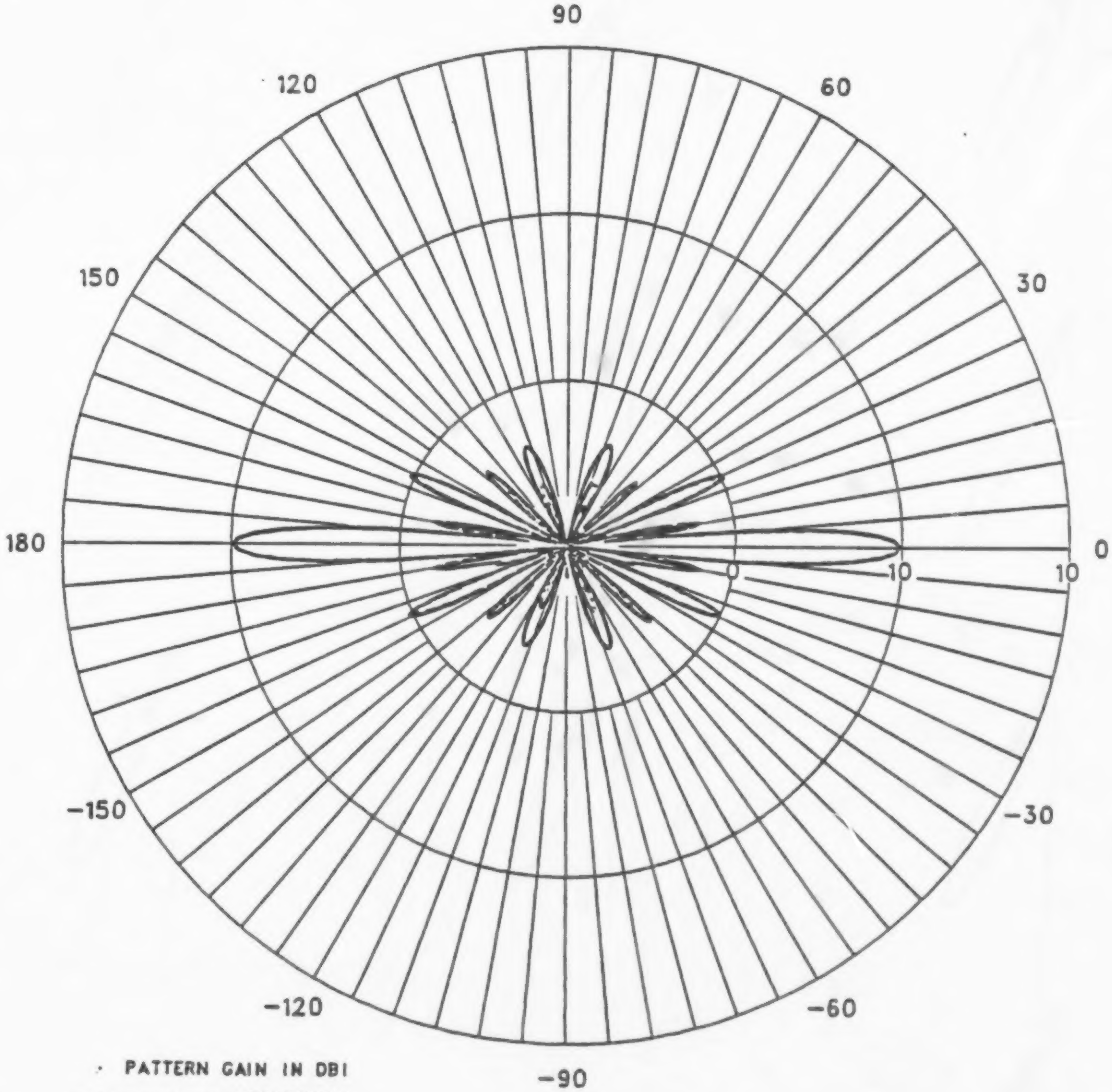

· PATTERN GAIN IN DBI
---------- HORIZONTAL
———·——— VERTICAL
———————— TOTAL

ELEVATION ANGLE

373<

FIGURE C 21

CETEC JAT TURNSTILE ANTENNA

4 X 4 BAYS -- 1.5 LAMBDA SPACING -- CHANNEL 2

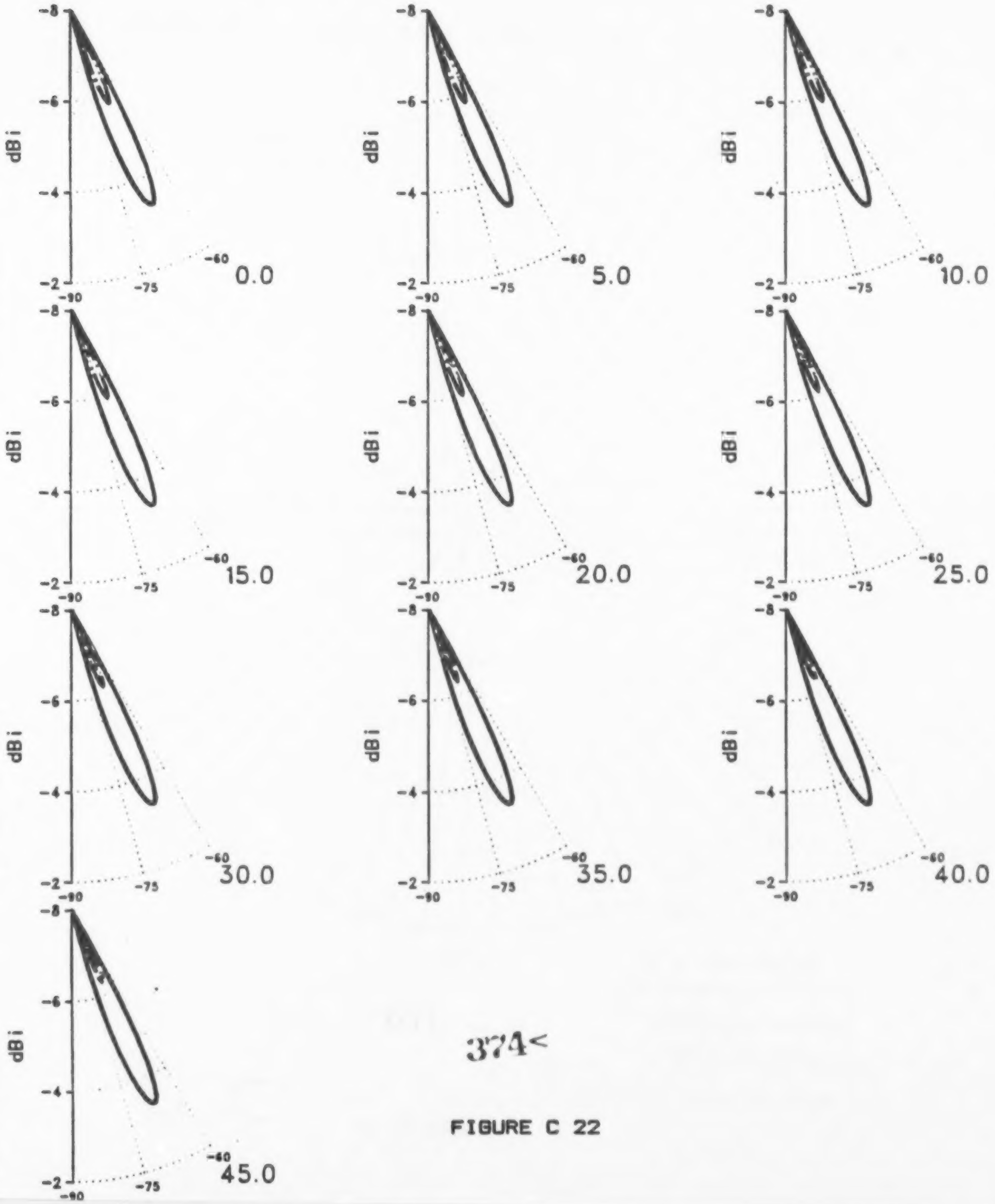

FIGURE C 22

CETEC JAT TURNSTILE ANTENNA

SINGLE ELEMENT -- CHANNEL 10

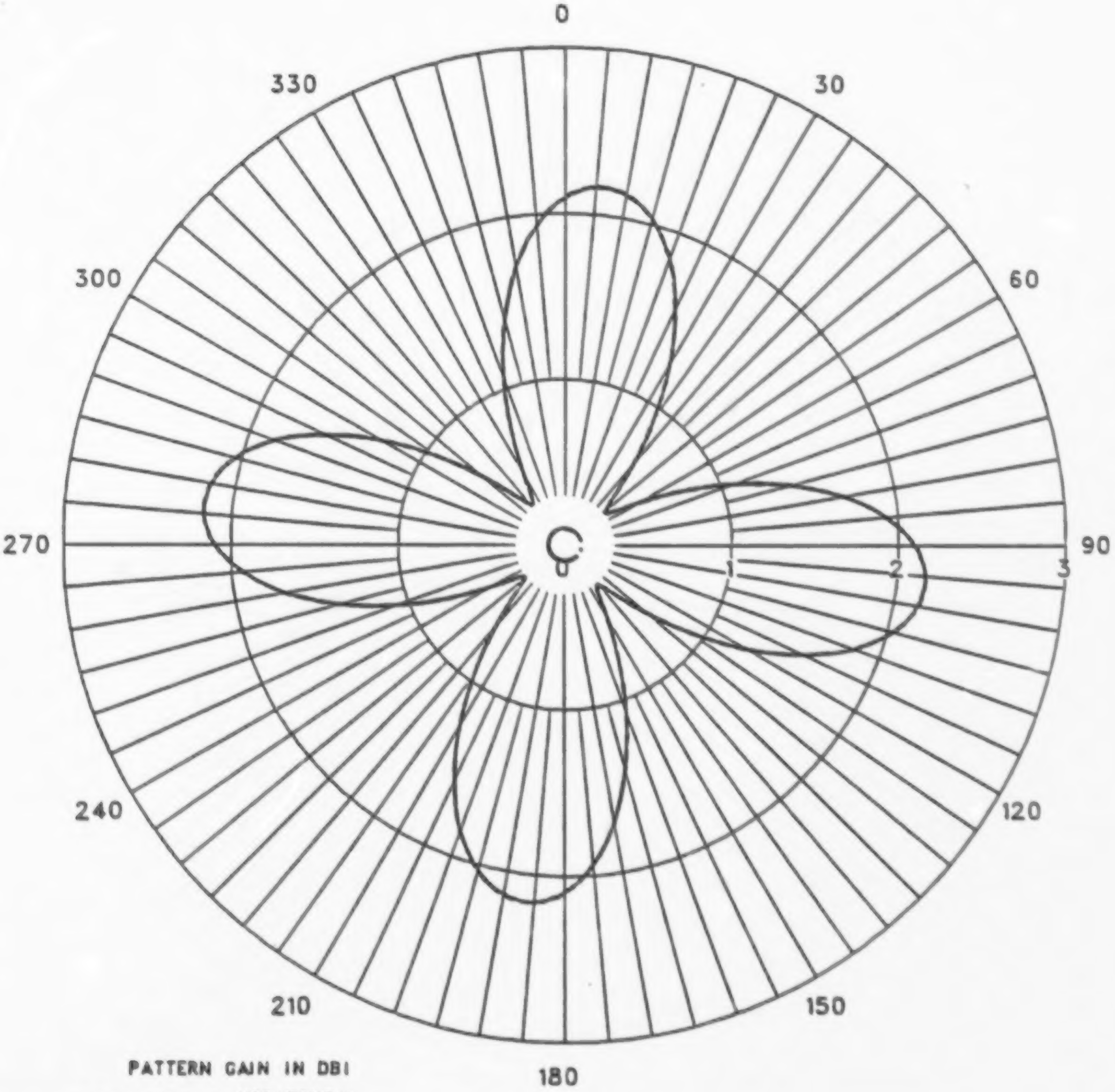

PATTERN GAIN IN DBI
---------- HORIZONTAL
——·—— VERTICAL
———— TOTAL

ANGLES IN DEGREES TRUE

375<

FIGURE C 23

CETEC JAT TURNSTILE ANTENNA

SINGLE ELEMENT -- CHANNEL 10

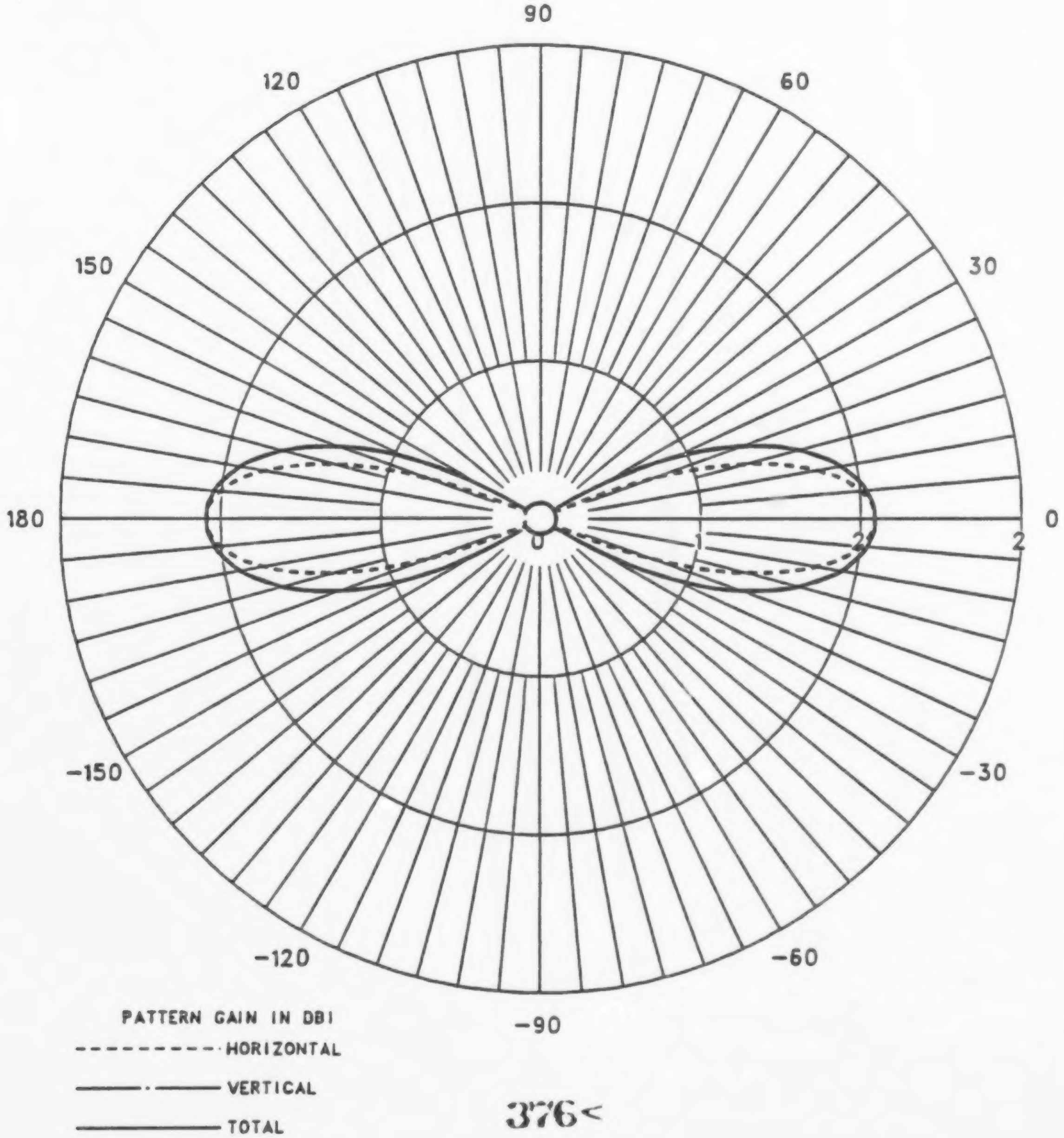

PATTERN GAIN IN DBI
- - - - - - - - - HORIZONTAL
———·——— VERTICAL
——————— TOTAL

ELEVATION ANGLE

FIGURE C 24

CETEC JAT TURNSTILE ANTENNA

SINGLE ELEMENT -- CHANNEL 10

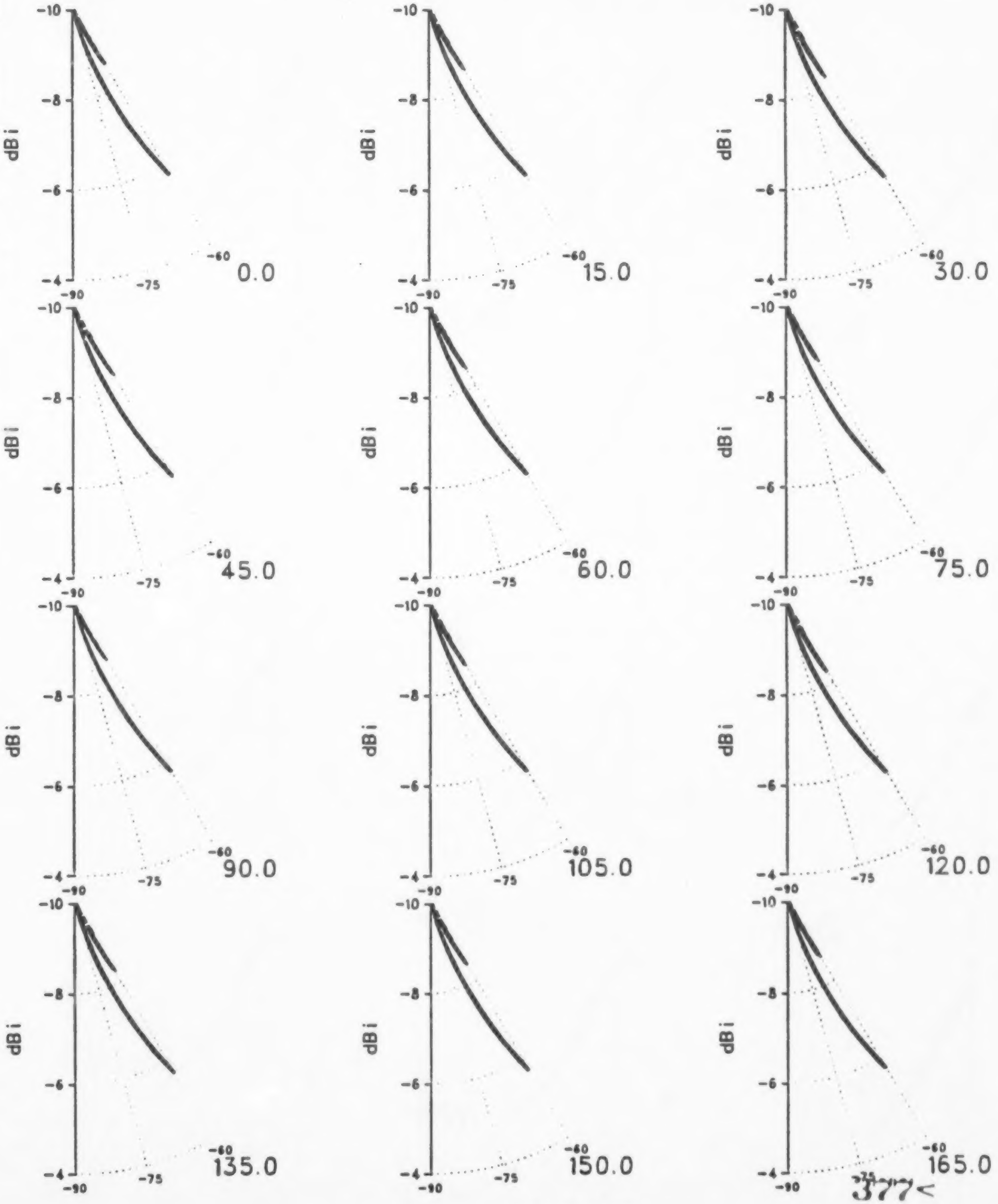

FIGURE C 25

CETEC JAT TURNSTILE ANTENNA

SINGLE ELEMENT -- CHANNEL 10

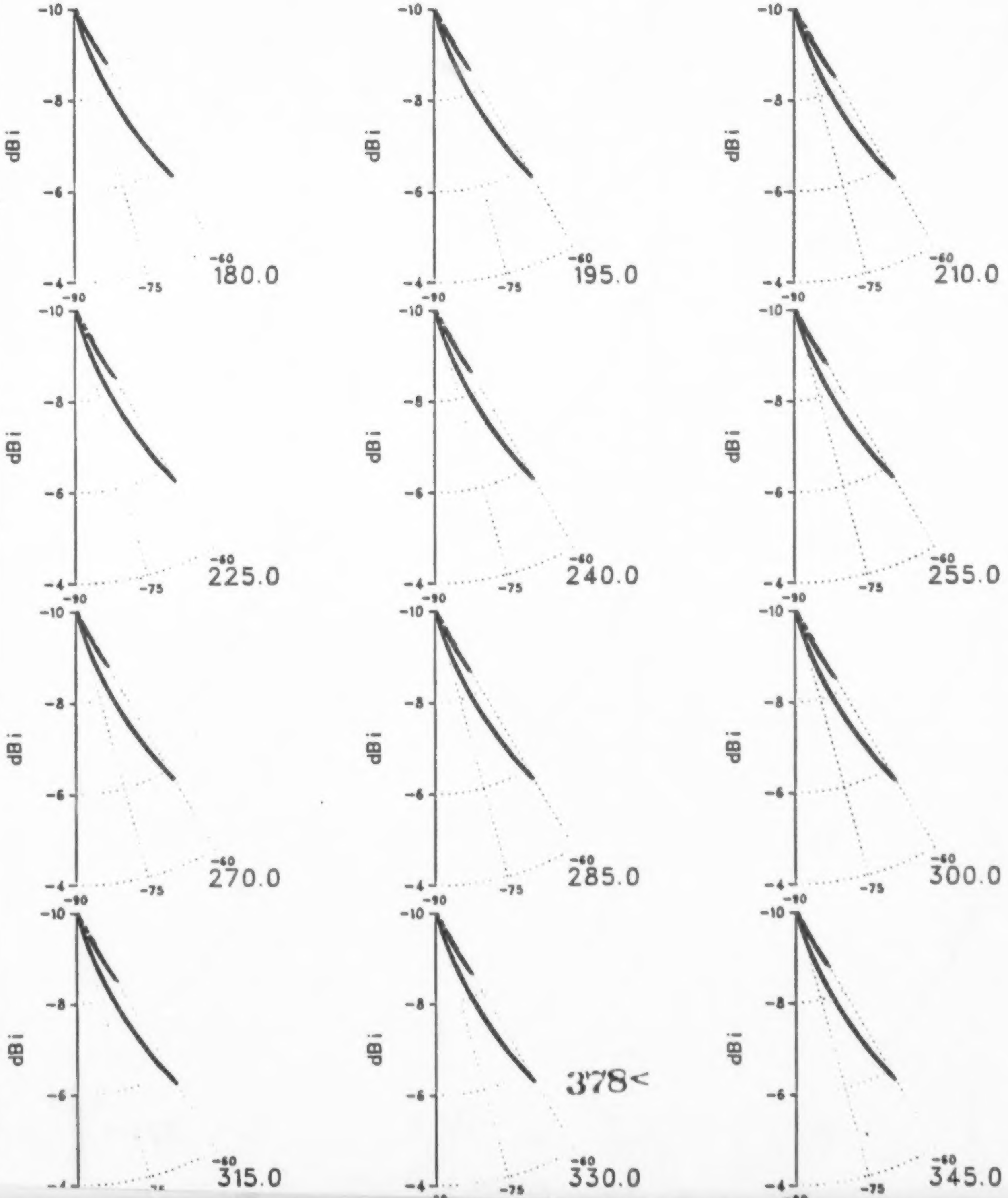

CETEC JAT TURNSTILE ANTENNA

4 BAYS -- STANDARD SPACING -- CHANNEL 10

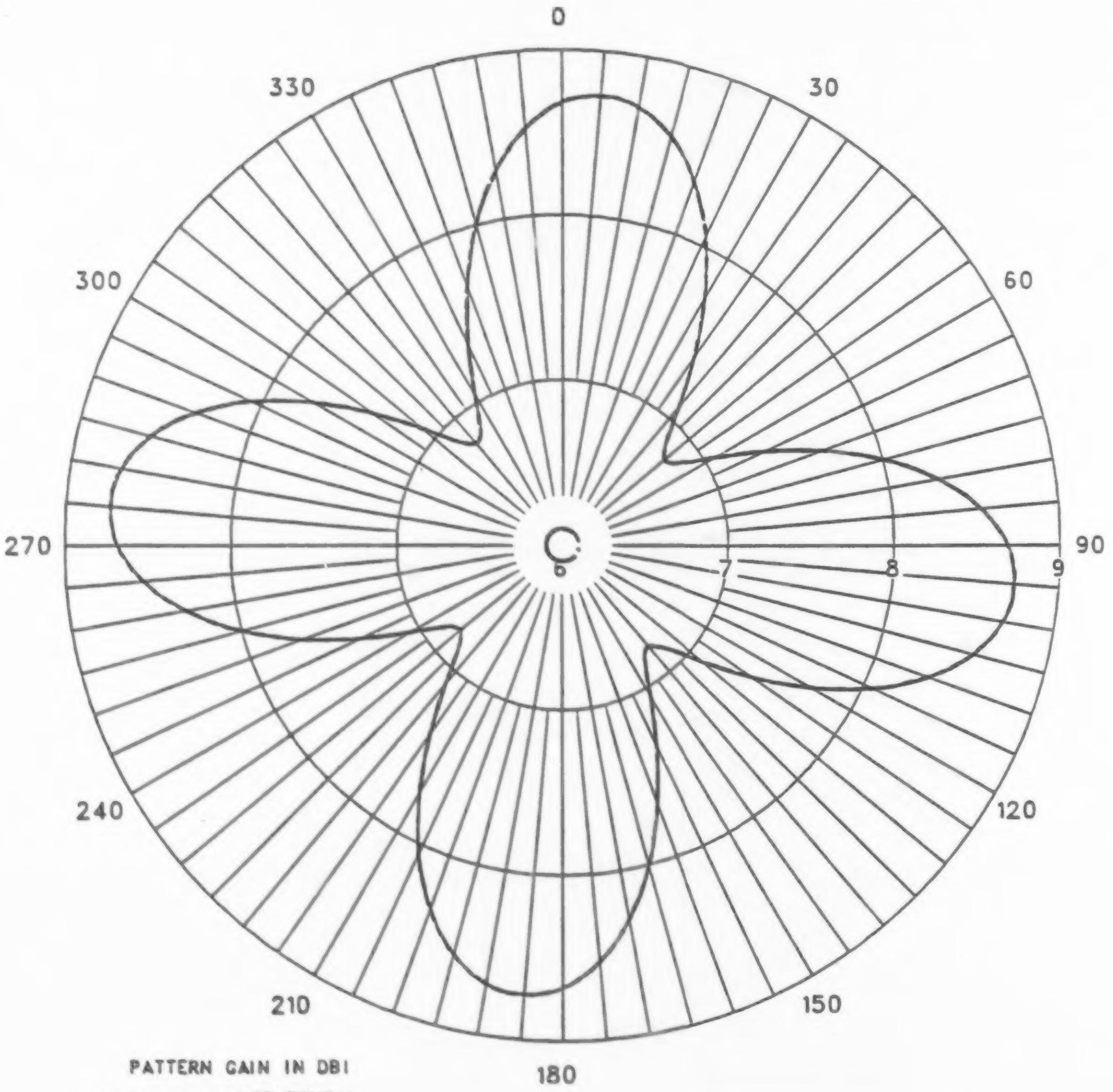

PATTERN GAIN IN DBI
---------- HORIZONTAL
——·—— VERTICAL
———— TOTAL

ANGLES IN DEGREES TRUE

FIGURE C 27

CETEC JAT TURNSTILE ANTENNA

4 BAYS -- STANDARD SPACING -- CHANNEL 10

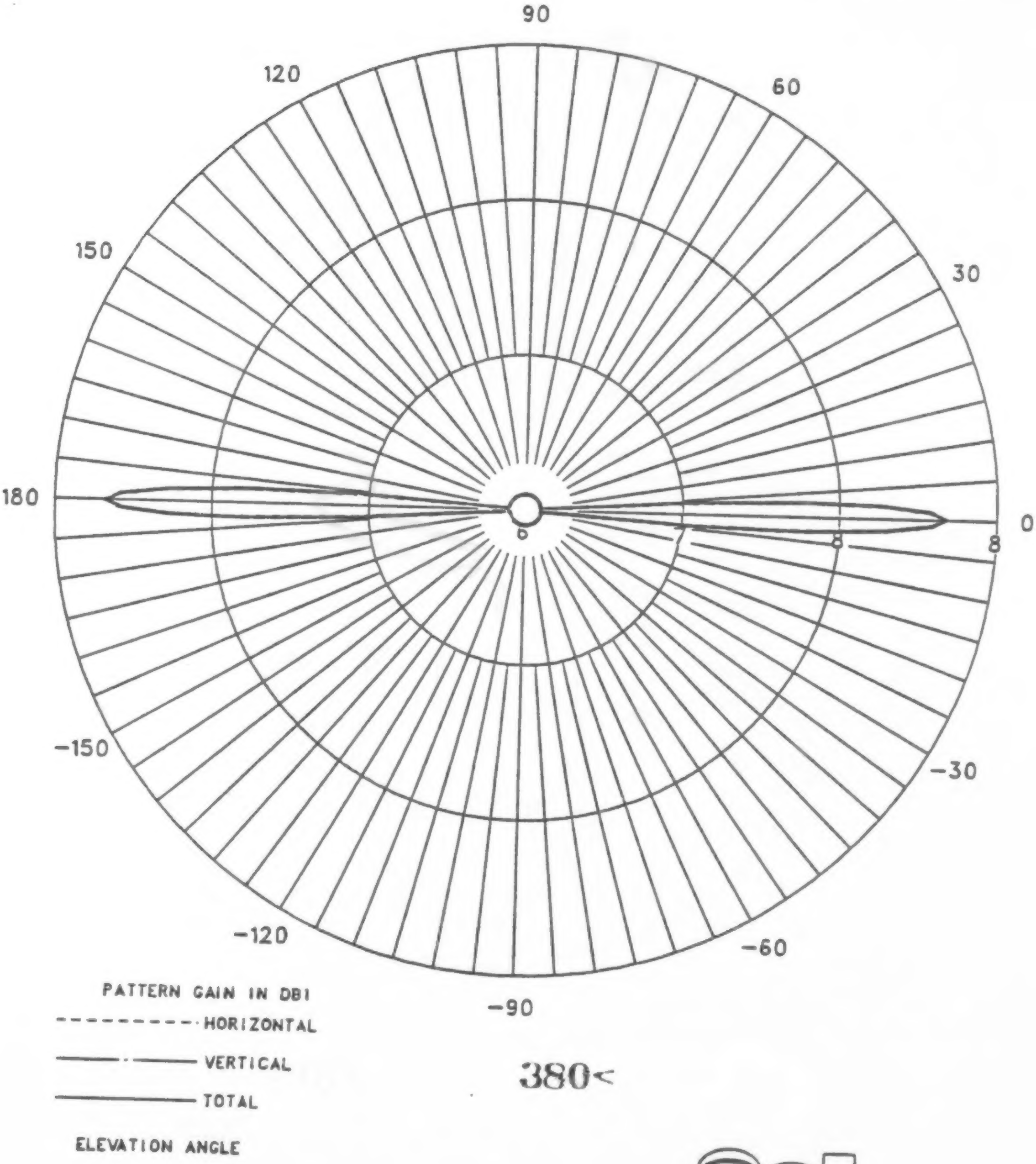

FIGURE C 28

CETEC JAT TURNSTILE ANTENNA

4 BAYS -- STANDARD SPACING -- CHANNEL 10

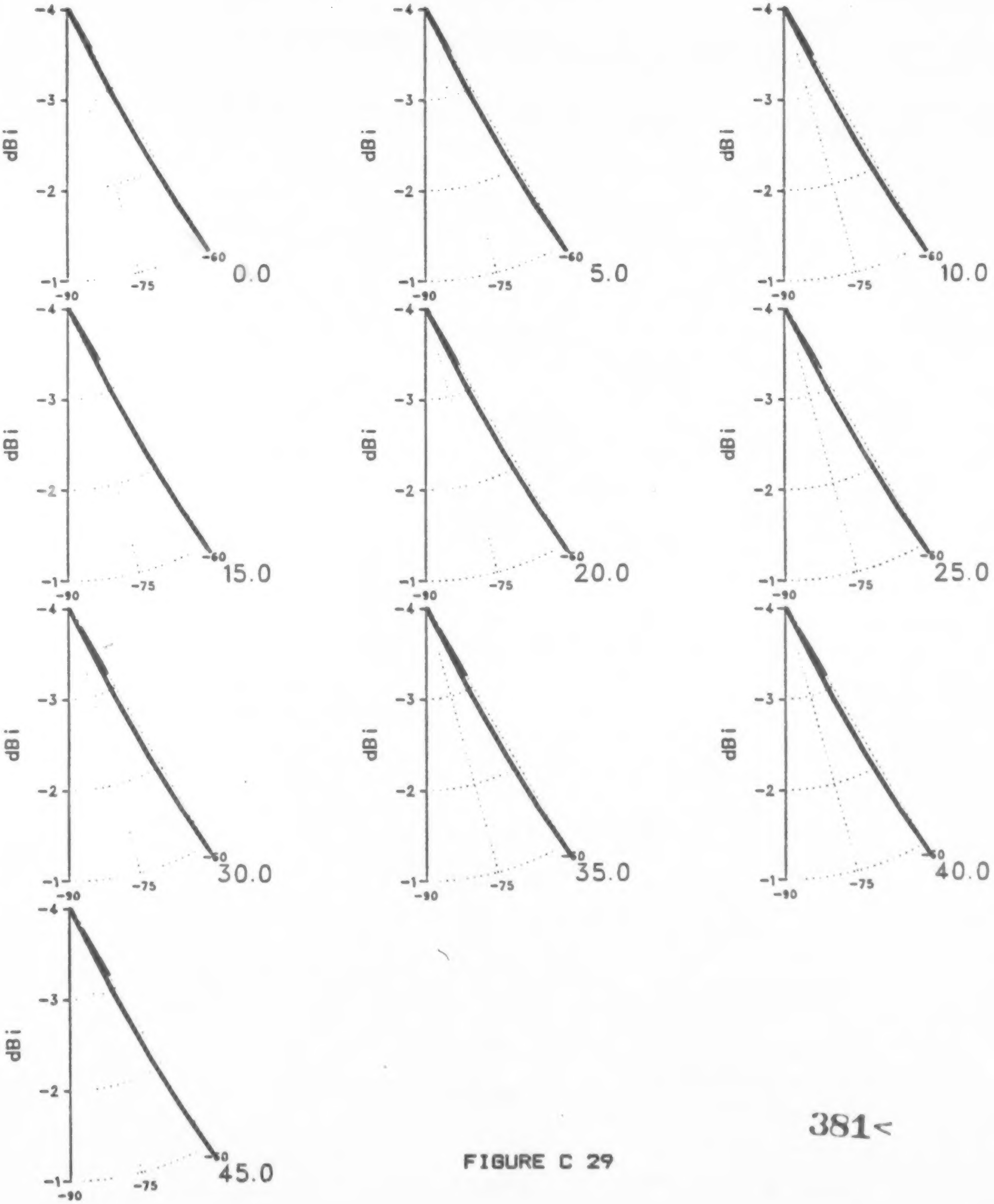

FIGURE C 29

CETEC JAT TURNSTILE ANTENNA

6 BAYS -- STANDARD SPACING -- CHANNEL 10

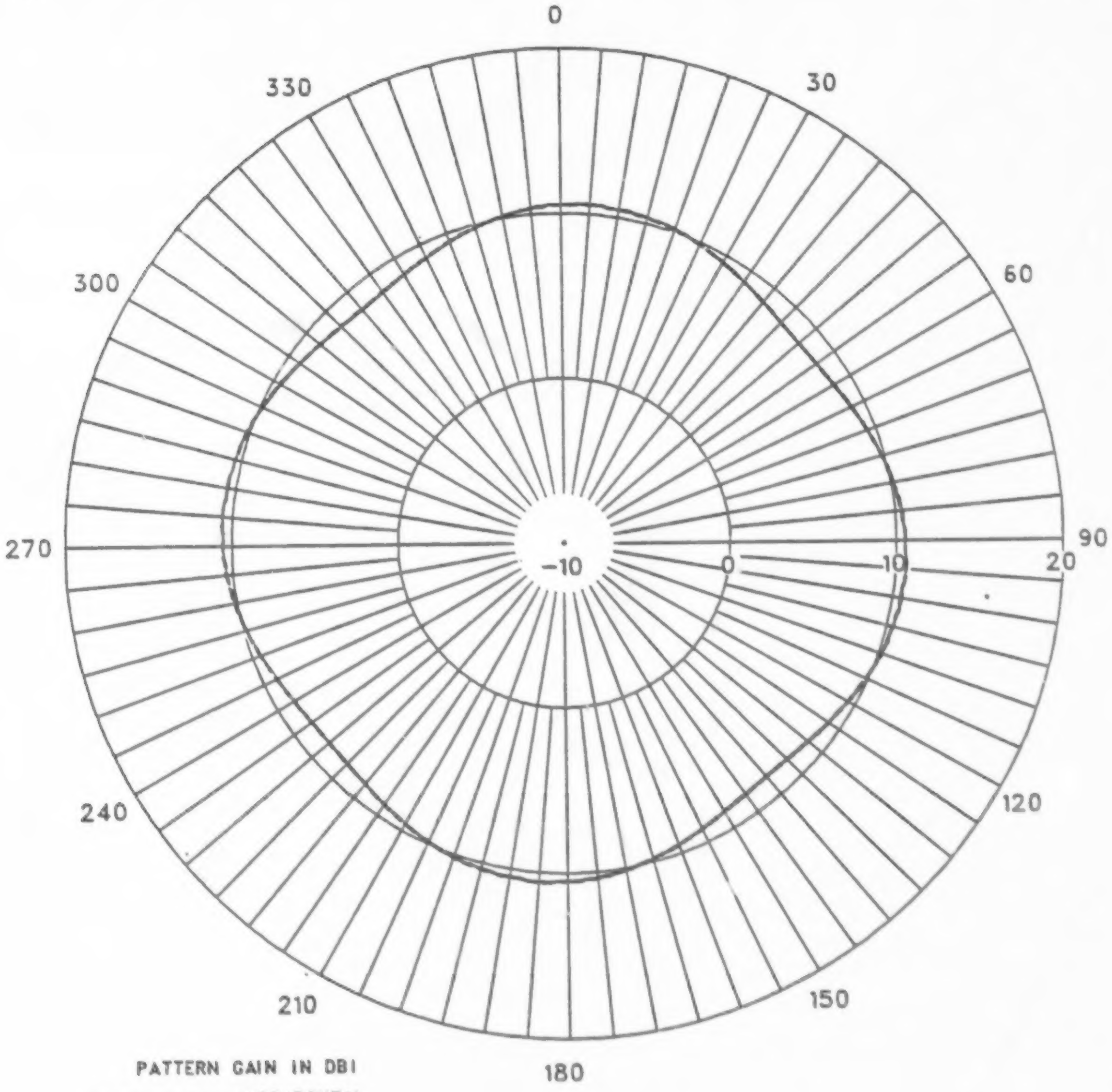

PATTERN GAIN IN DBI

- - - - - - - - - - HORIZONTAL

———·——— VERTICAL

———————— TOTAL

ANGLES IN DEGREES TRUE

382<

FIGURE C 30

CETEC JAT TURNSTILE ANTENNA

6 BAYS -- STANDARD SPACING -- CHANNEL 10

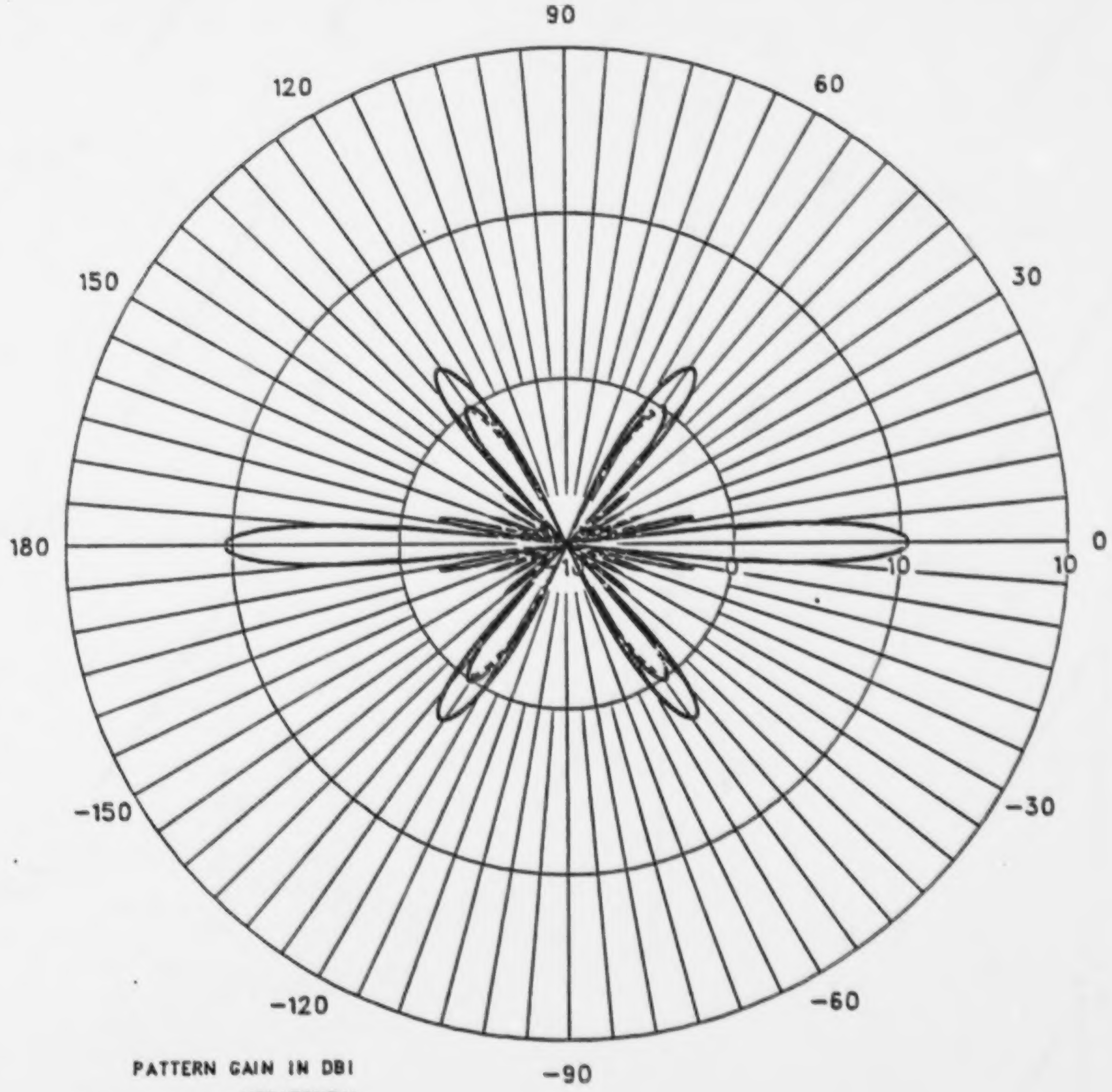

PATTERN GAIN IN DBI
- - - - - - - - - HORIZONTAL
———·——— VERTICAL
——————— TOTAL

ELEVATION ANGLE

FIGURE C 31

CETEC JAT TURNSTILE ANTENNA

6 BAYS -- STANDARD SPACING -- CHANNEL 10

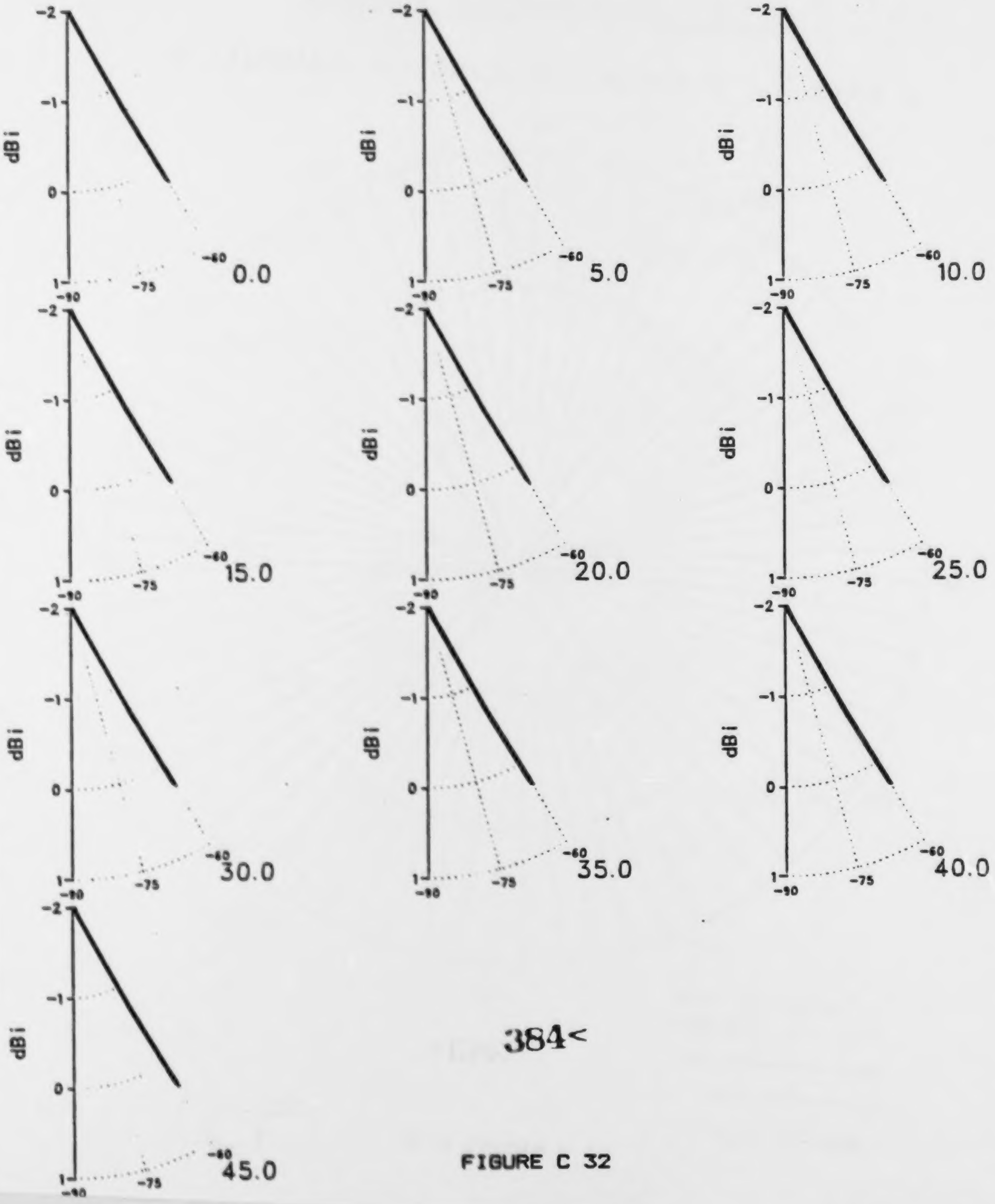

FIGURE C 32

CETEC JAT TURNSTILE ANTENNA

8 BAYS -- STANDARD SPACING -- CHANNEL 10

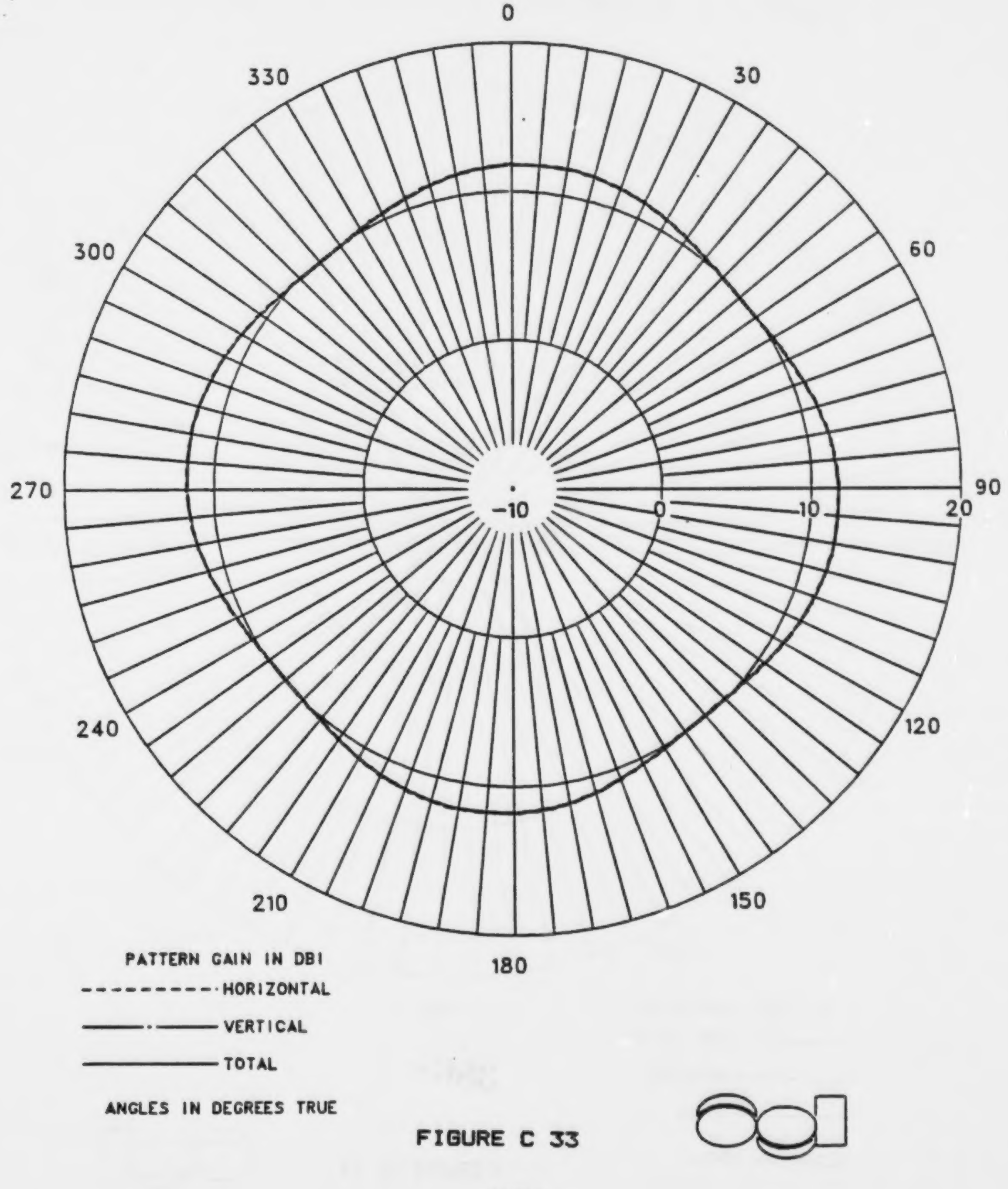

FIGURE C 33

CETEC JAT TURNSTILE ANTENNA

8 BAYS -- STANDARD SPACING -- CHANNEL 10

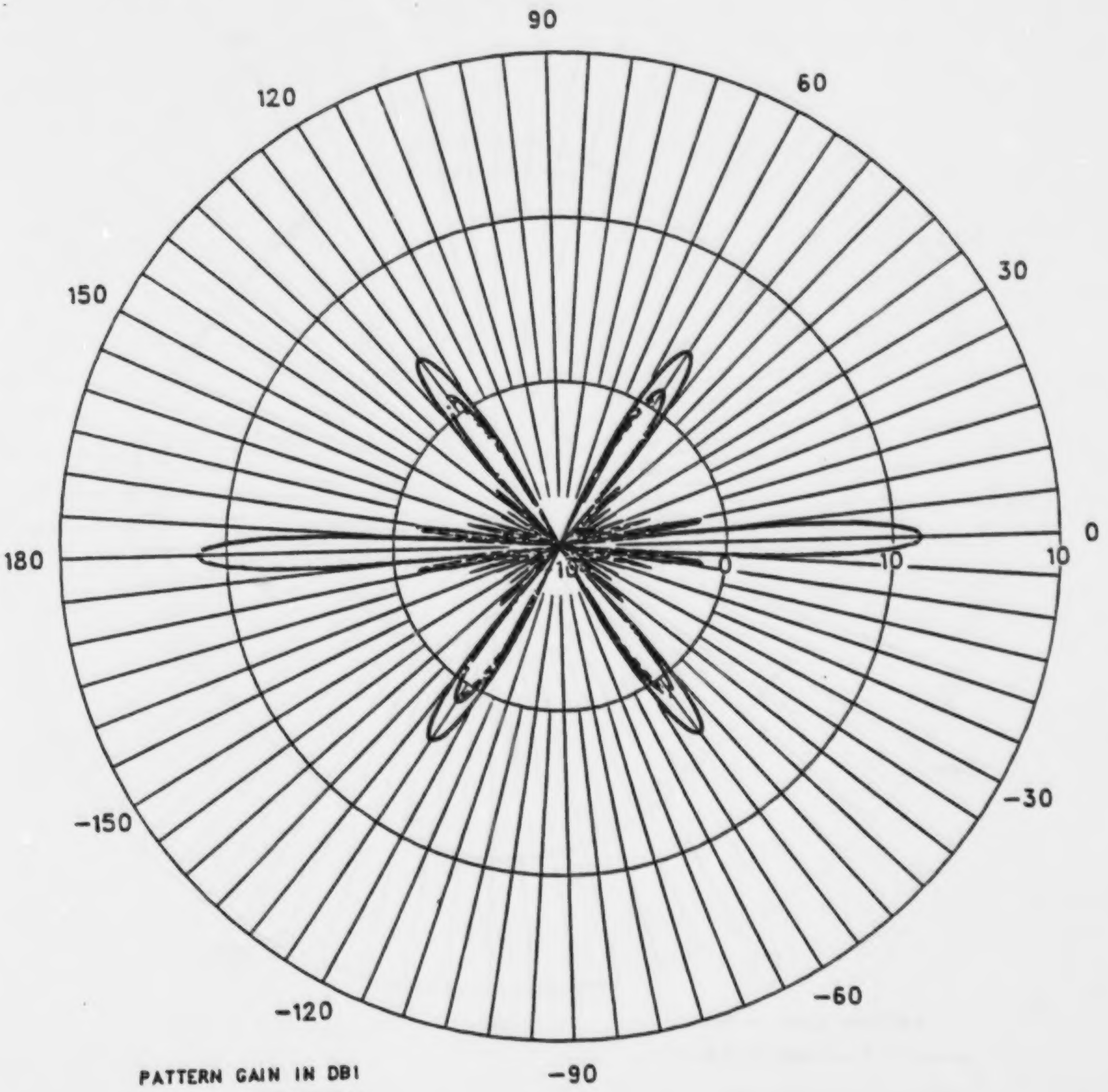

PATTERN GAIN IN DBI

---------- HORIZONTAL

——·—— VERTICAL

———— TOTAL

ELEVATION ANGLE

386<

FIGURE C 34

CETEC JAT TURNSTILE ANTENNA

8 BAYS -- STANDARD SPACING -- CHANNEL 10

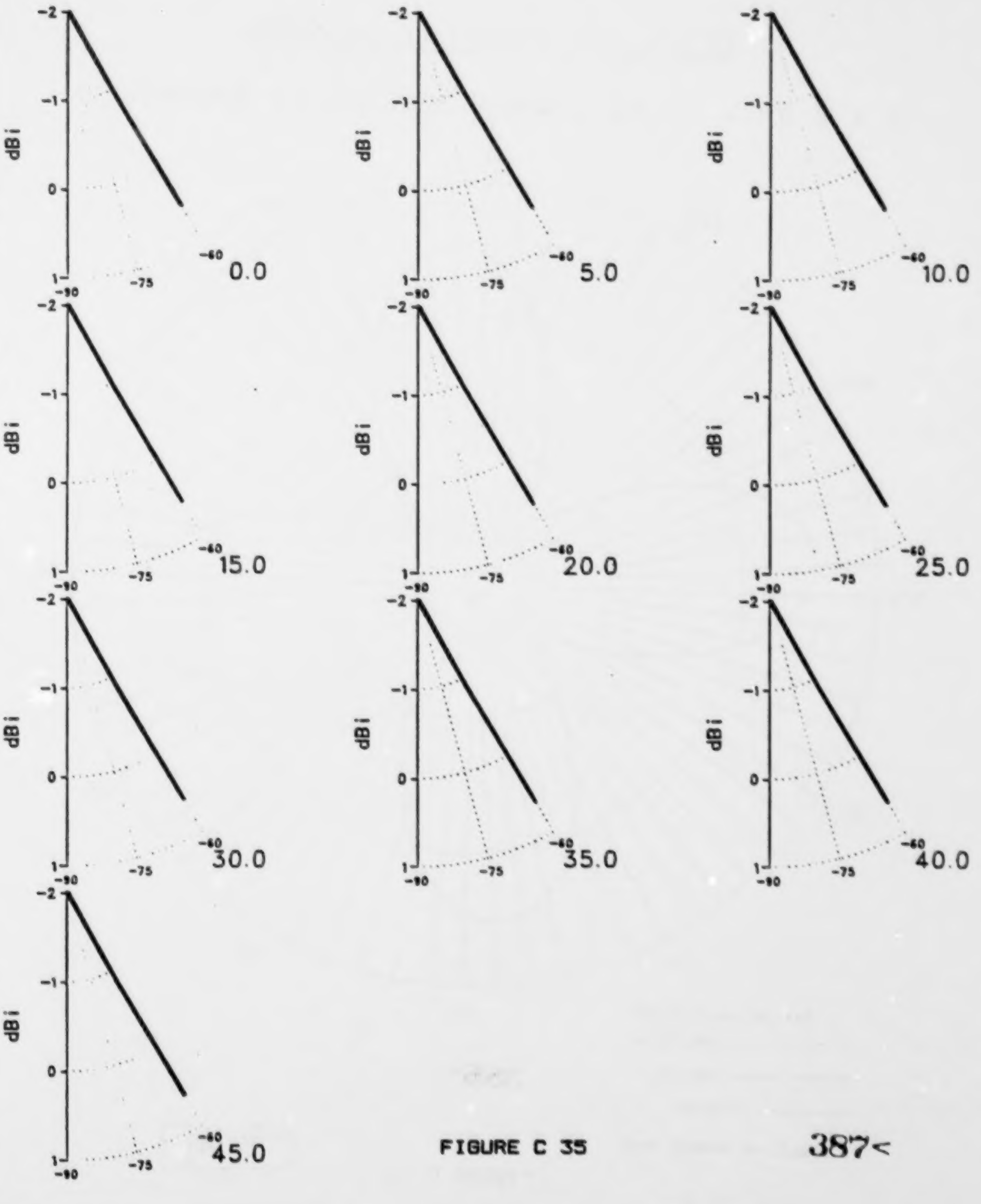

FIGURE C 35

CETEC JAT TURNSTILE ANTENNA

2 X 2 BAYS -- 1.5 LAMBDA SPACING -- CHANNEL 10

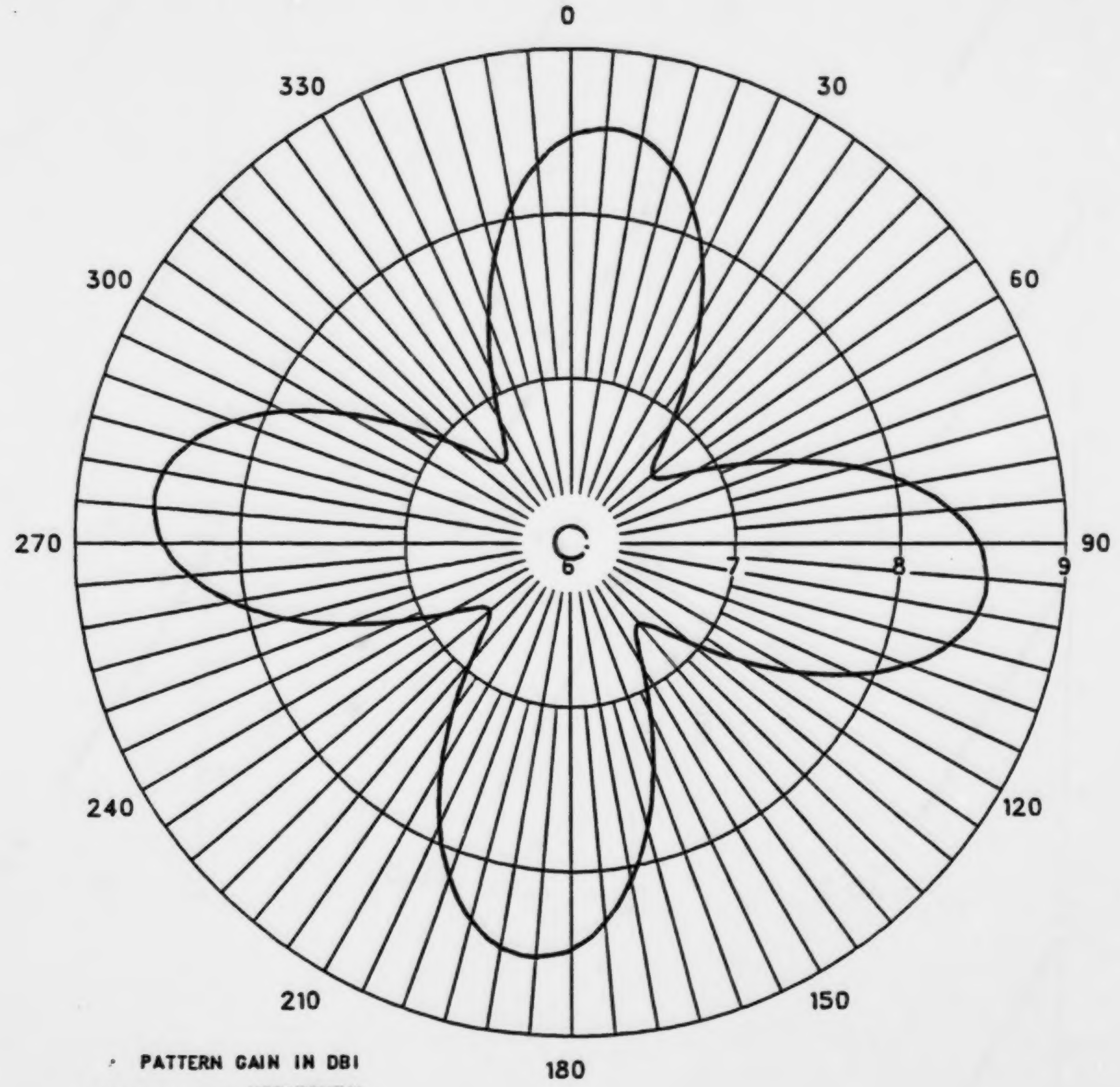

PATTERN GAIN IN DBI

---------- HORIZONTAL

——·—— VERTICAL

———— TOTAL

ANGLES IN DEGREES TRUE

388<

FIGURE C 36

CETEC JAT TURNSTILE ANTENNA

2 X 2 BAYS -- 1.5 LAMBDA SPACING -- CHANNEL 10

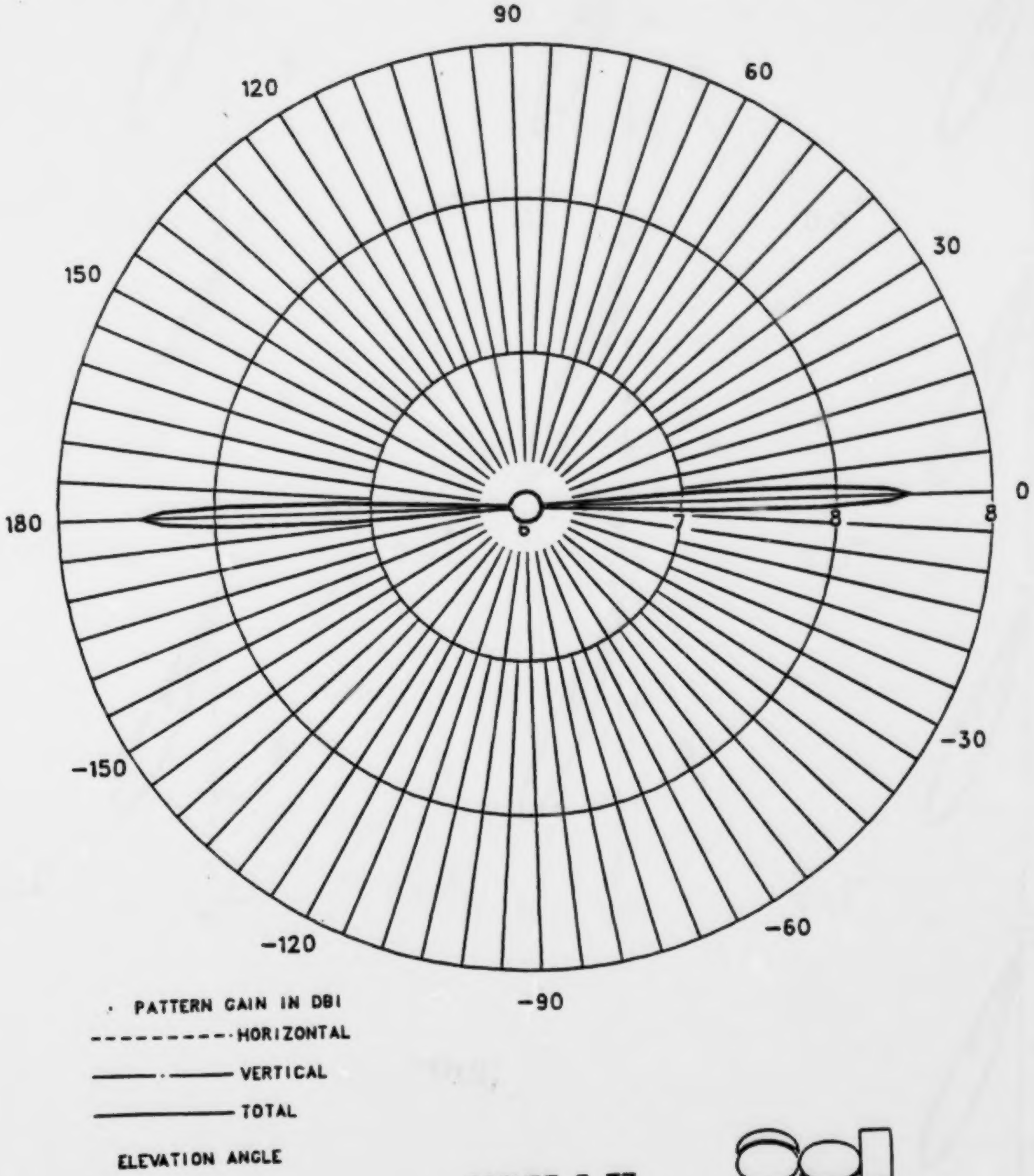

FIGURE C 37

CETEC JAT TURNSTILE ANTENNA

2 X 2 BAYS -- 1.5 LAMBDA SPACING -- CHANNEL 10

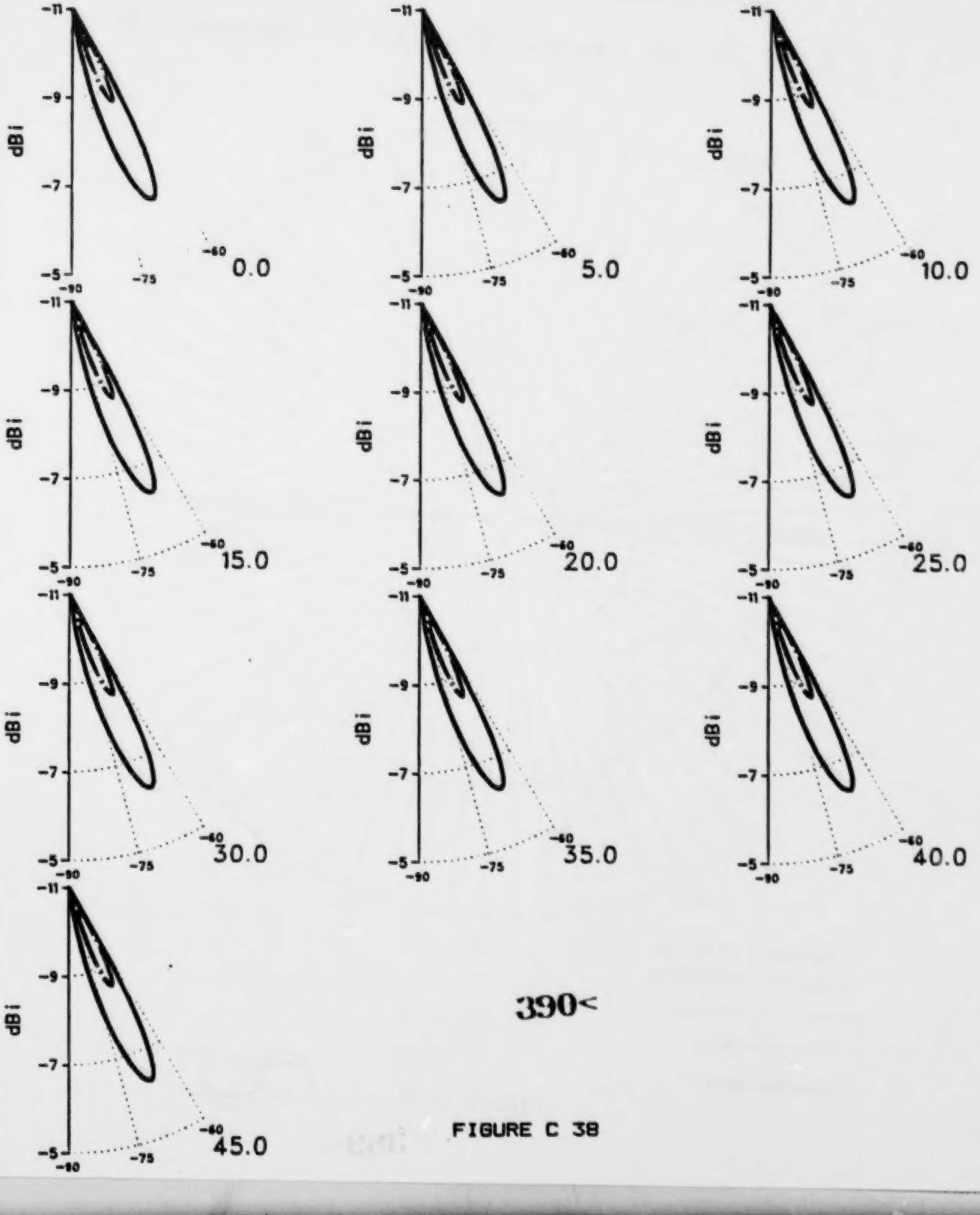

FIGURE C 38

CETEC JAT TURNSTILE ANTENNA

3 X 3 BAYS -- 1.5 LAMBDA SPACING -- CHANNEL 10

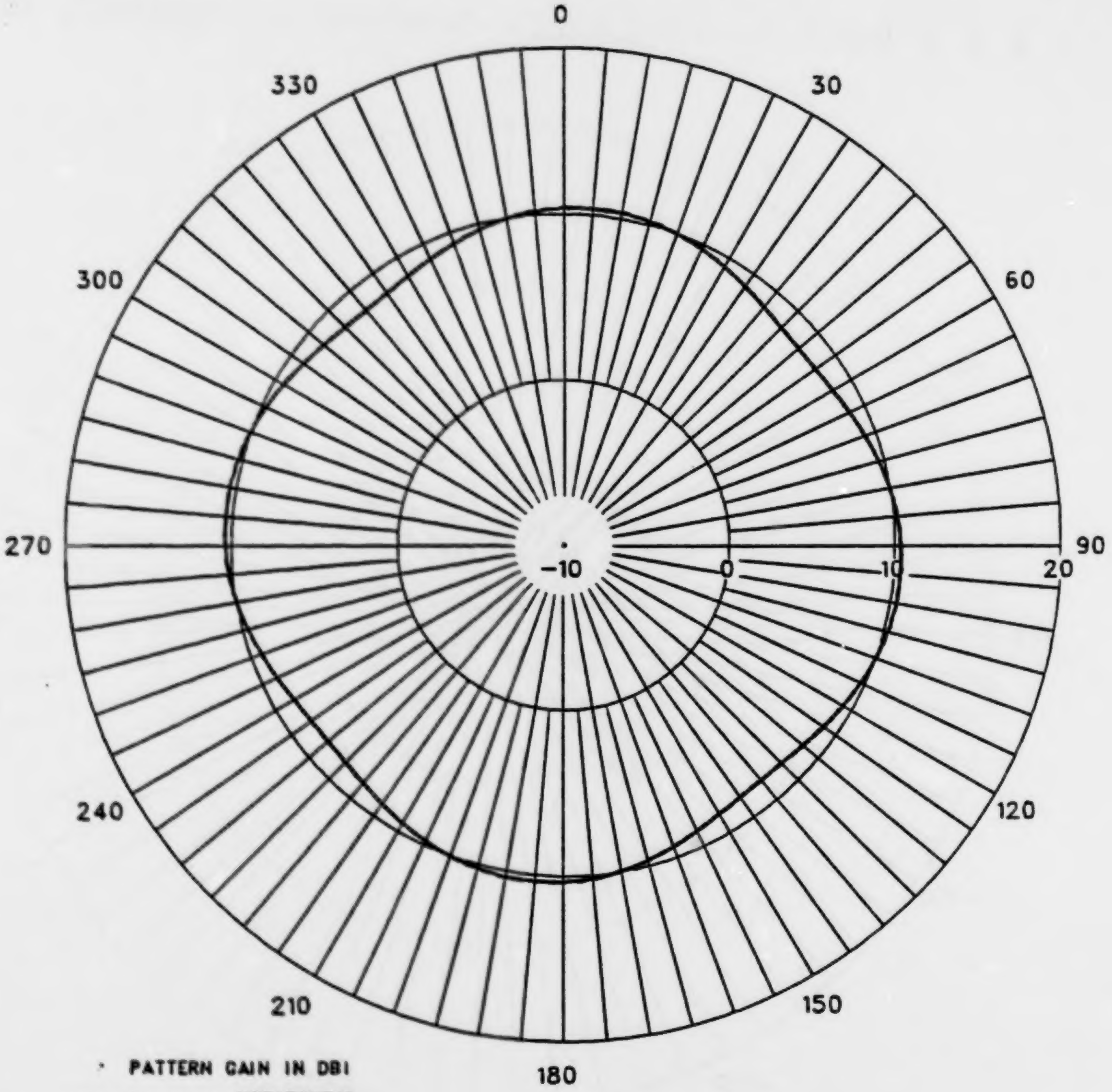

· PATTERN GAIN IN DBI

---------- HORIZONTAL

——·—— VERTICAL

———— TOTAL

ANGLES IN DEGREES TRUE

FIGURE C 39

CETEC JAT TURNSTILE ANTENNA

3 X 3 BAYS -- 1.5 LAMBDA SPACING -- CHANNEL 10

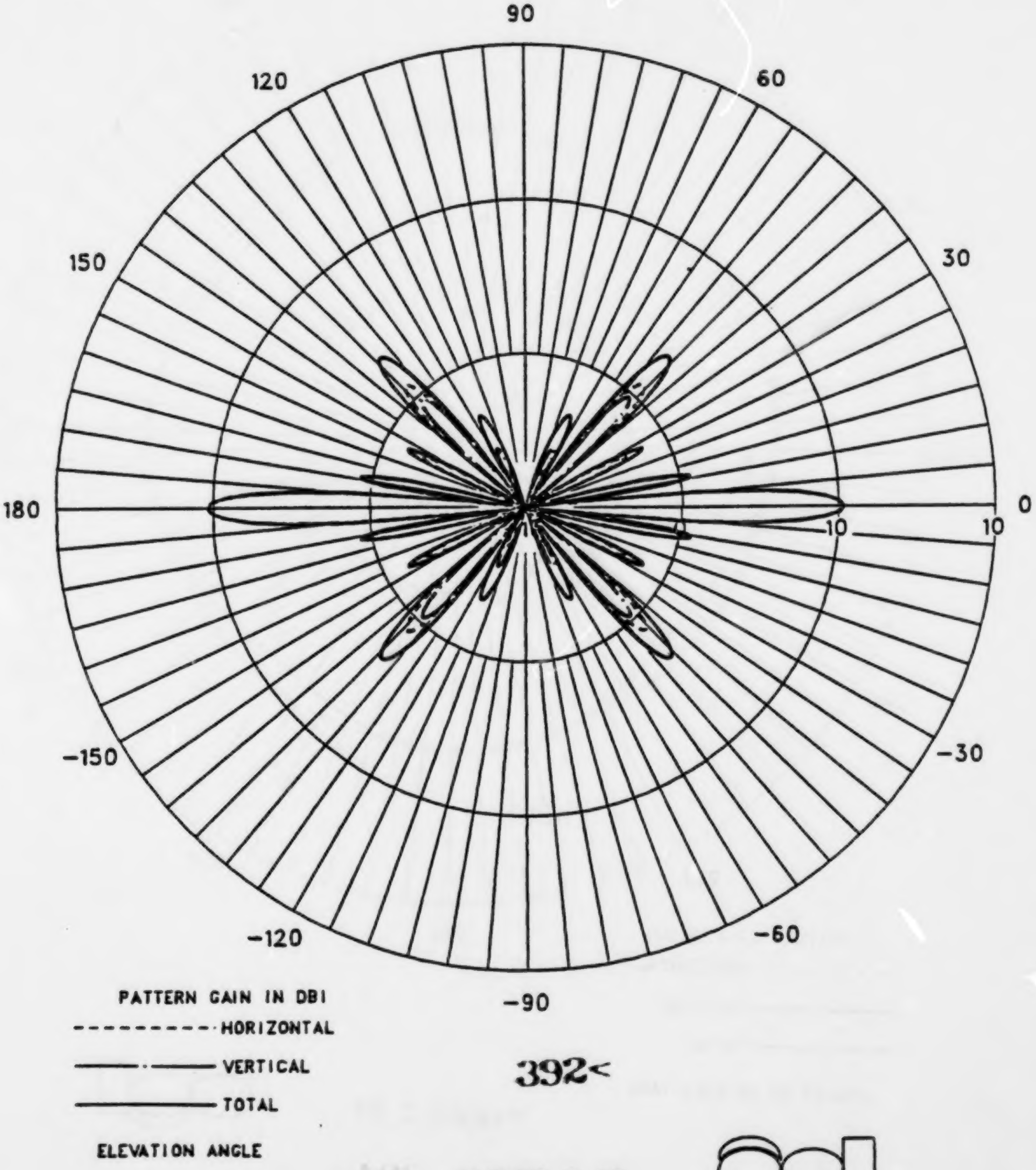

FIGURE C 40

CETEC JAT TURNSTILE ANTENNA

3 X 3 BAYS -- 1.5 LAMBDA SPACING -- CHANNEL 10

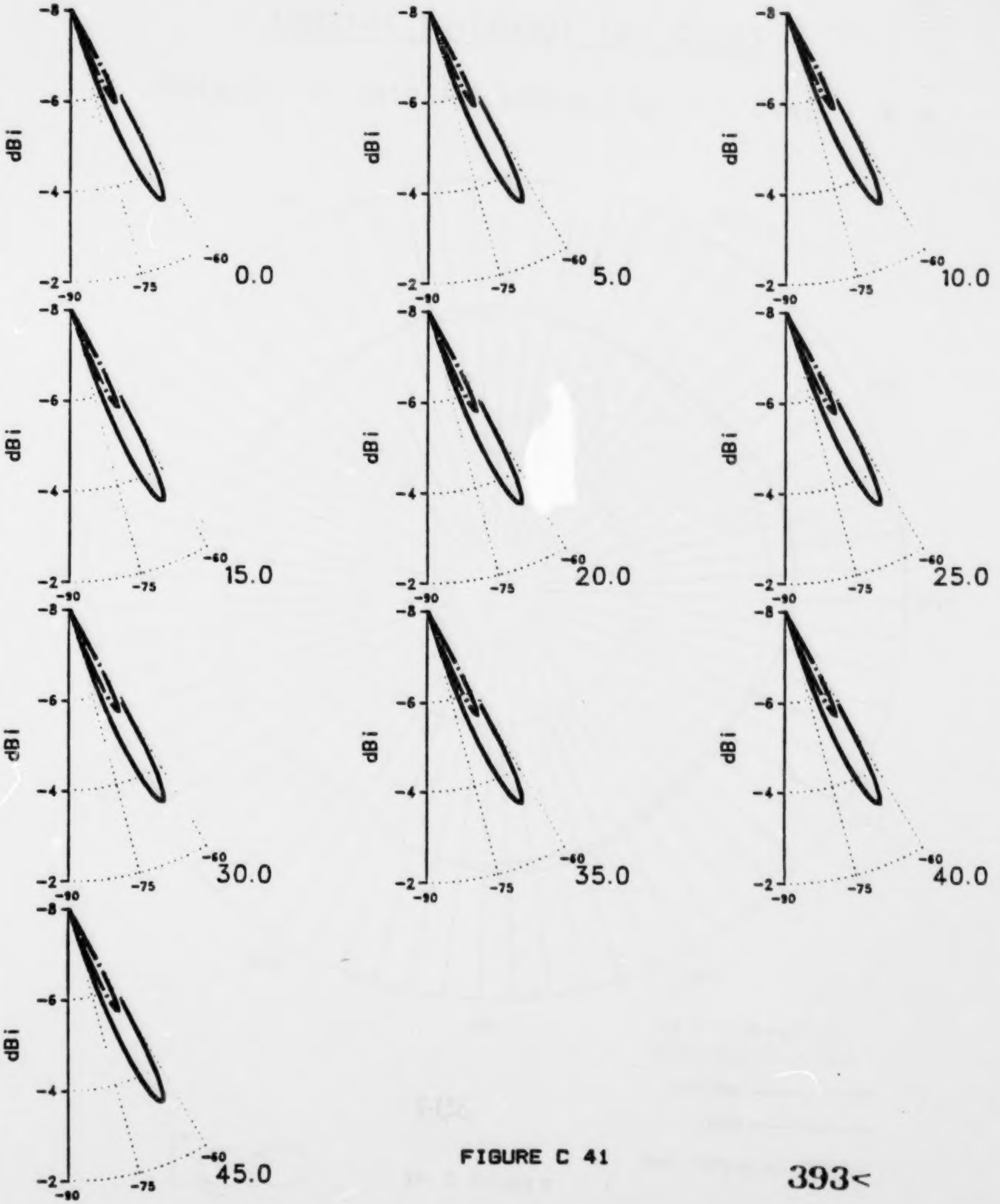

FIGURE C 41

CETEC JAT TURNSTILE ANTENNA

4 X 4 BAYS -- 1.5 LAMBDA SPACING -- CHANNEL 10

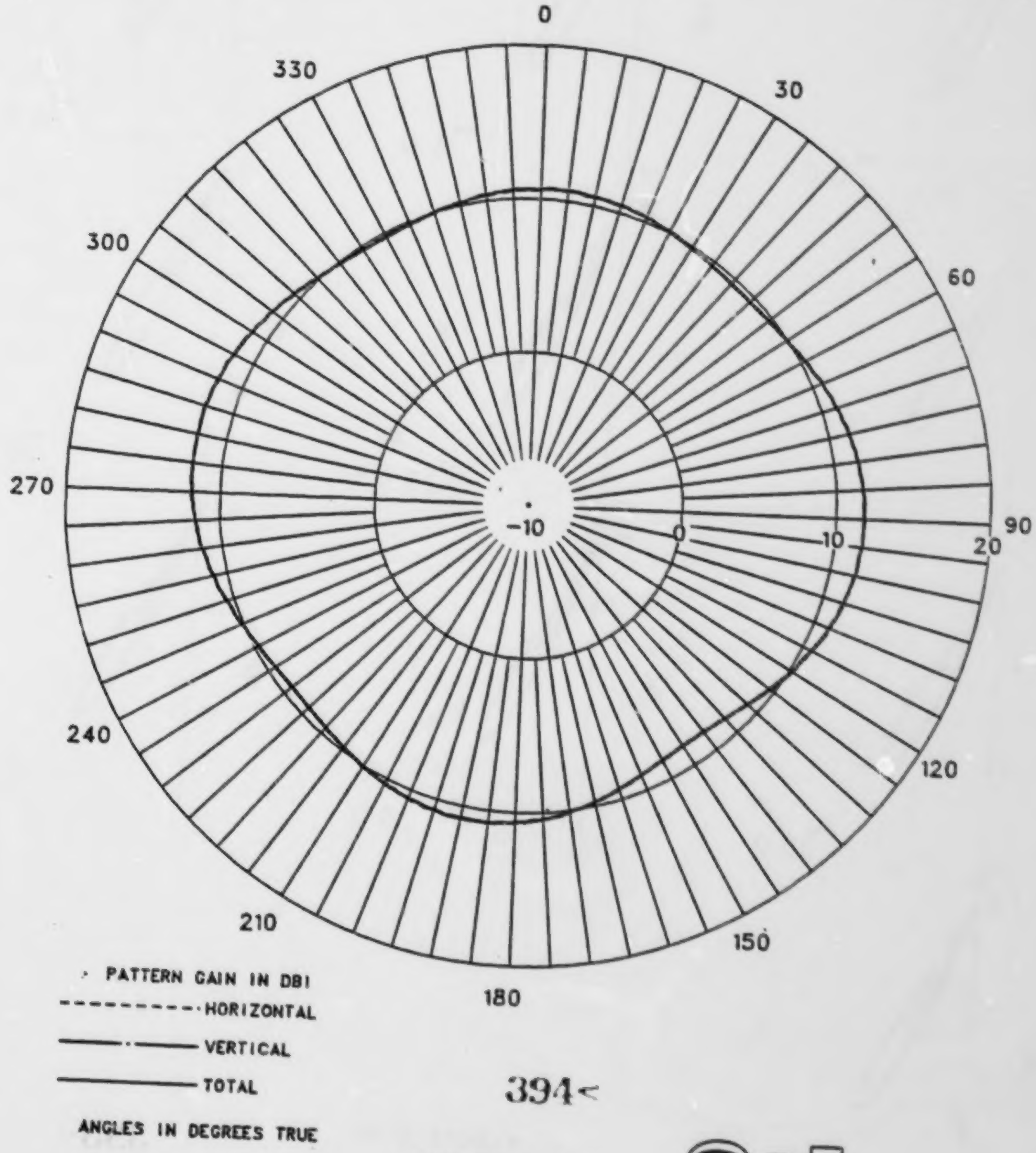

FIGURE C 42

CETEC JAT TURNSTILE ANTENNA

4 X 4 BAYS -- 1.5 LAMBDA SPACING -- CHANNEL 10

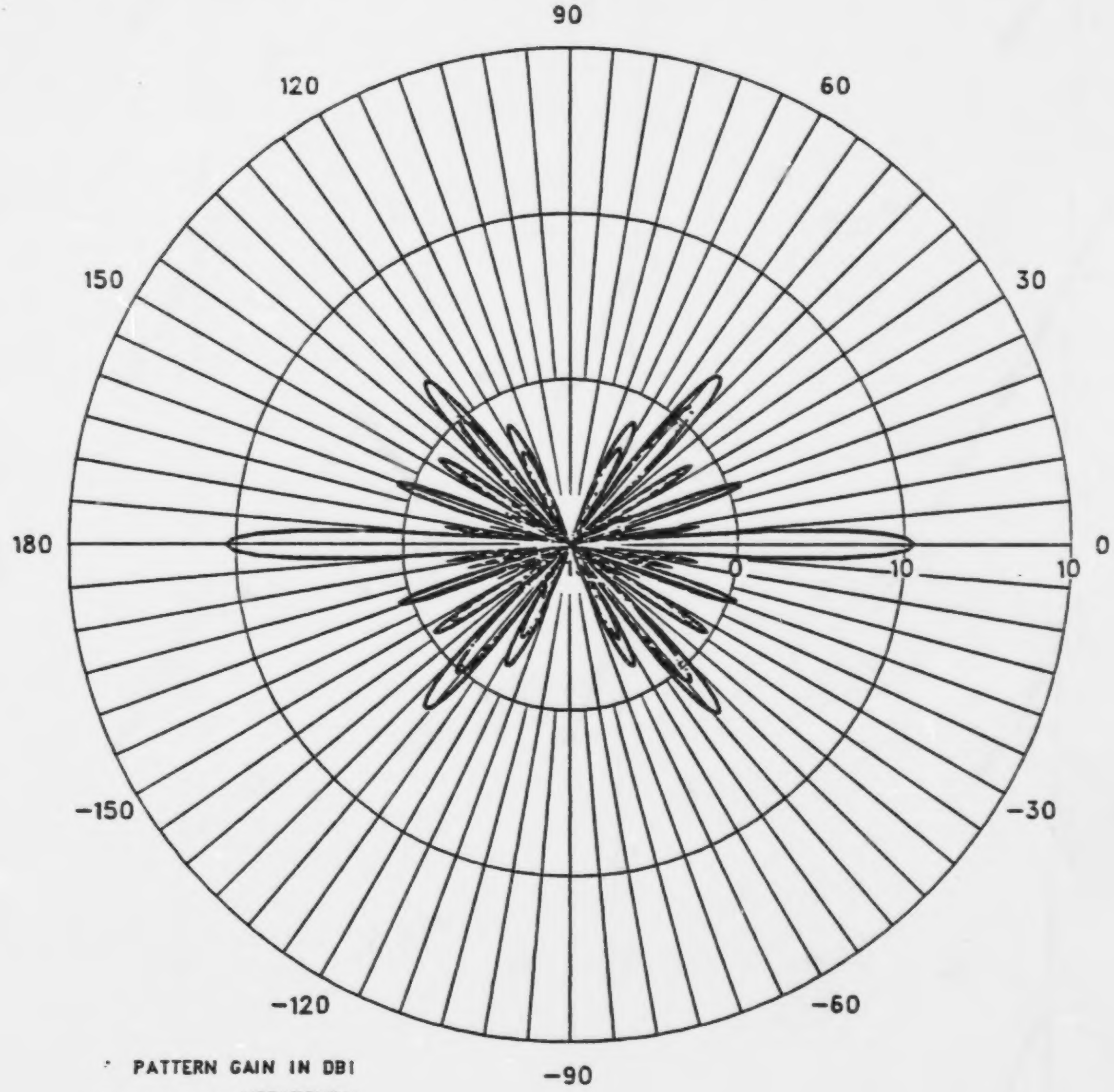

PATTERN GAIN IN DBI

--------- HORIZONTAL

——·—— VERTICAL

———— TOTAL

ELEVATION ANGLE

395<

FIGURE C 43

CETEC JAT TURNSTILE ANTENNA

4 X 4 BAYS -- 1.5 LAMBDA SPACING -- CHANNEL 10

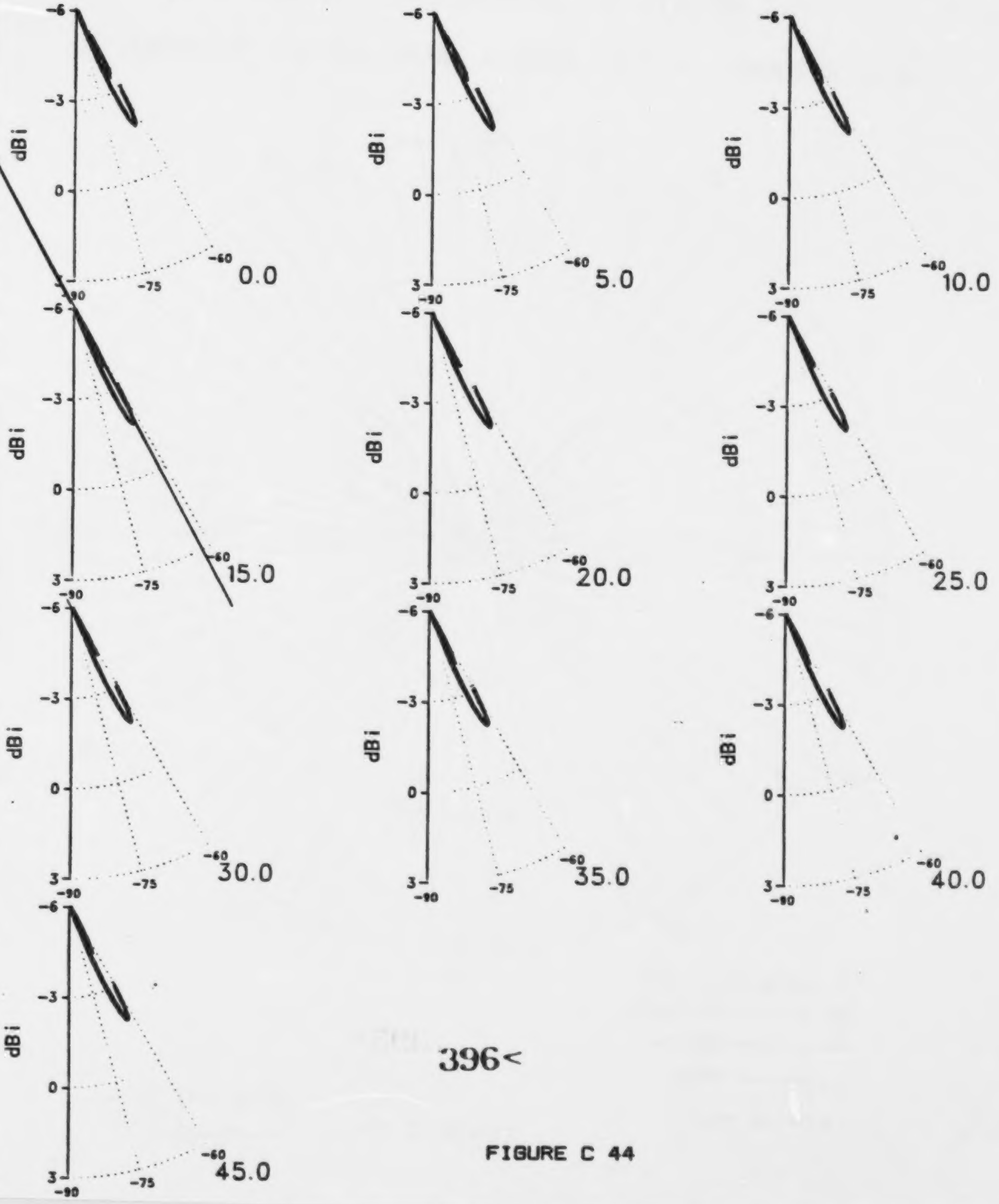

FIGURE C 44

CETEC JAT TURNSTILE ANTENNA 4 BAYS CHANNEL 2

SPACING OF .75 LAMBDA BETWEEN BAYS

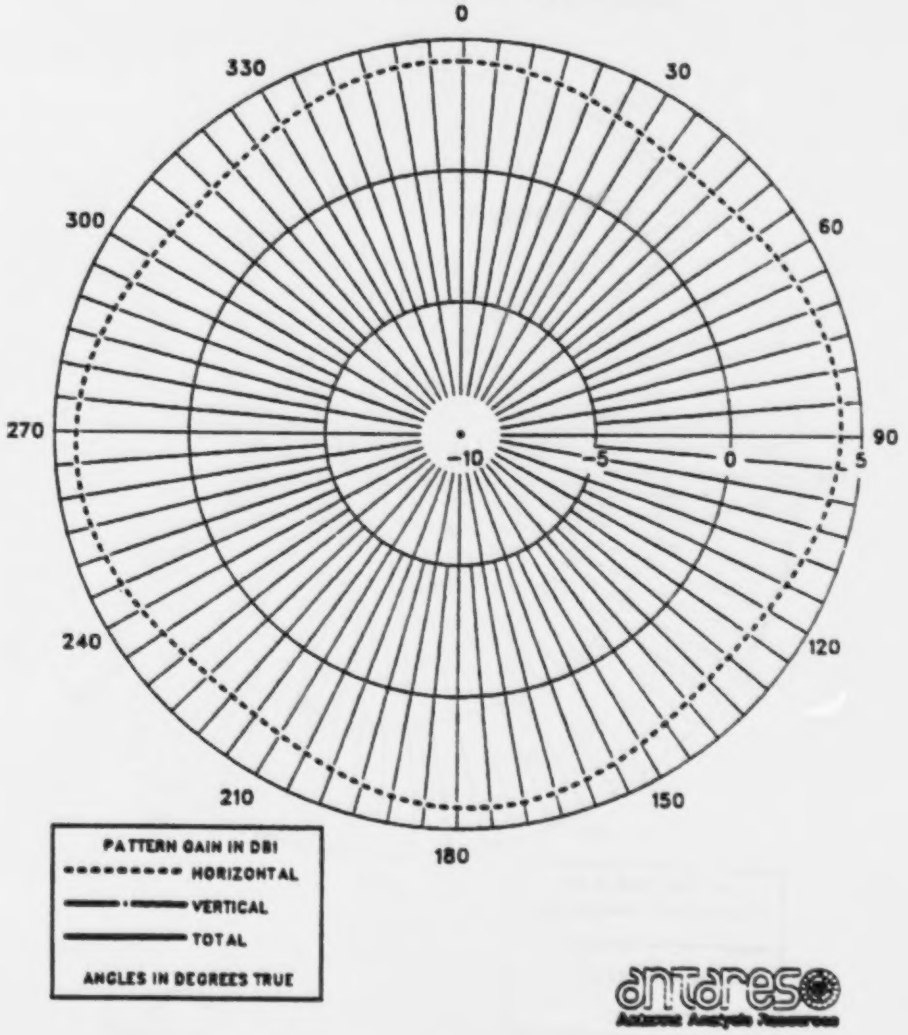

FIGURE C 45

CETEC JAT TURNSTILE ANTENNA 4 BAYS CHANNEL 2

SPACING OF .75 LAMBDA BETWEEN BAYS

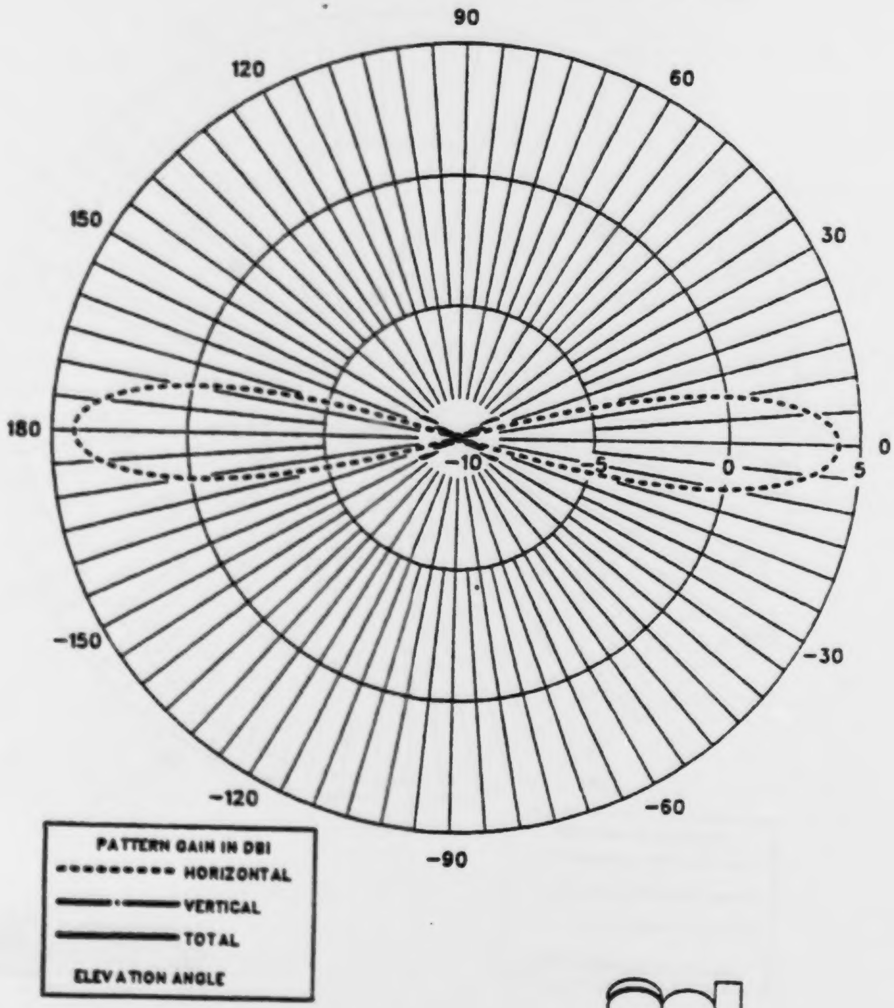

FIGURE C 46

CETEC JAT TURNSTILE ANTENNA 4 BAYS CHANNEL 2

SPACING OF .75 LAMBDA BETWEEN BAYS

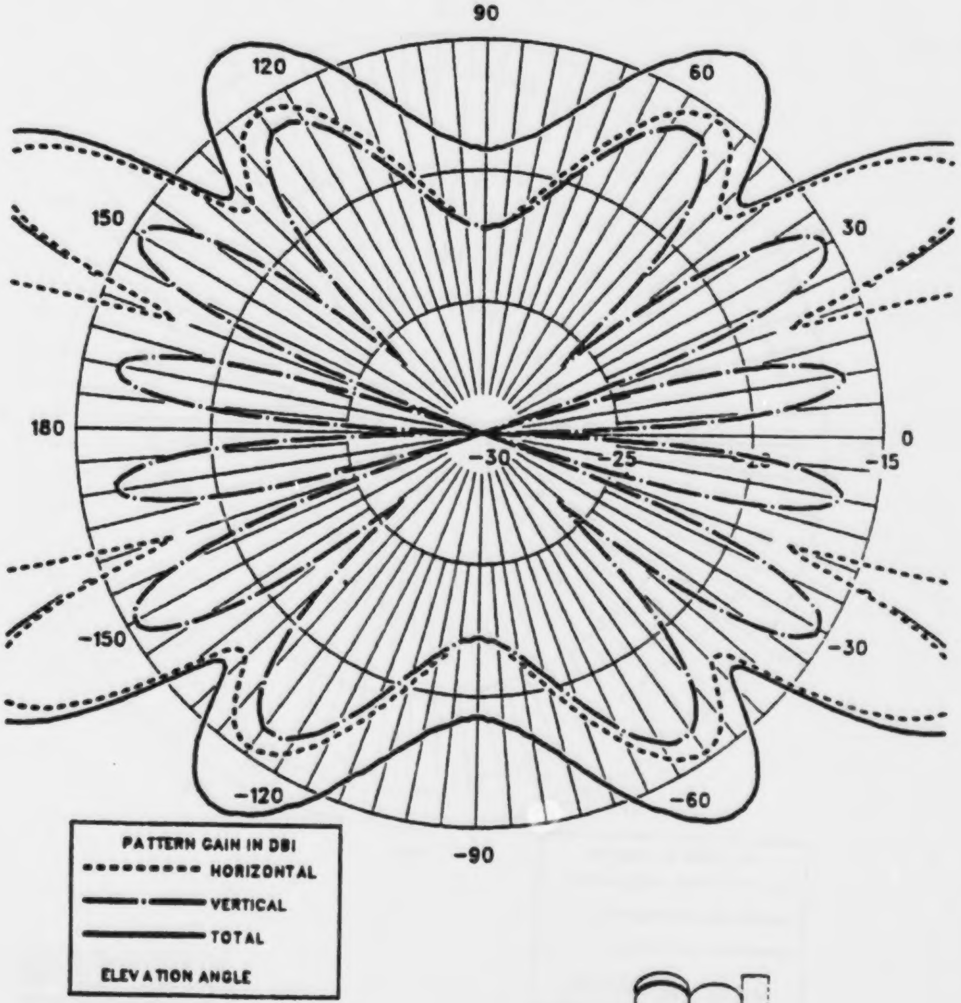

FIGURE C 47

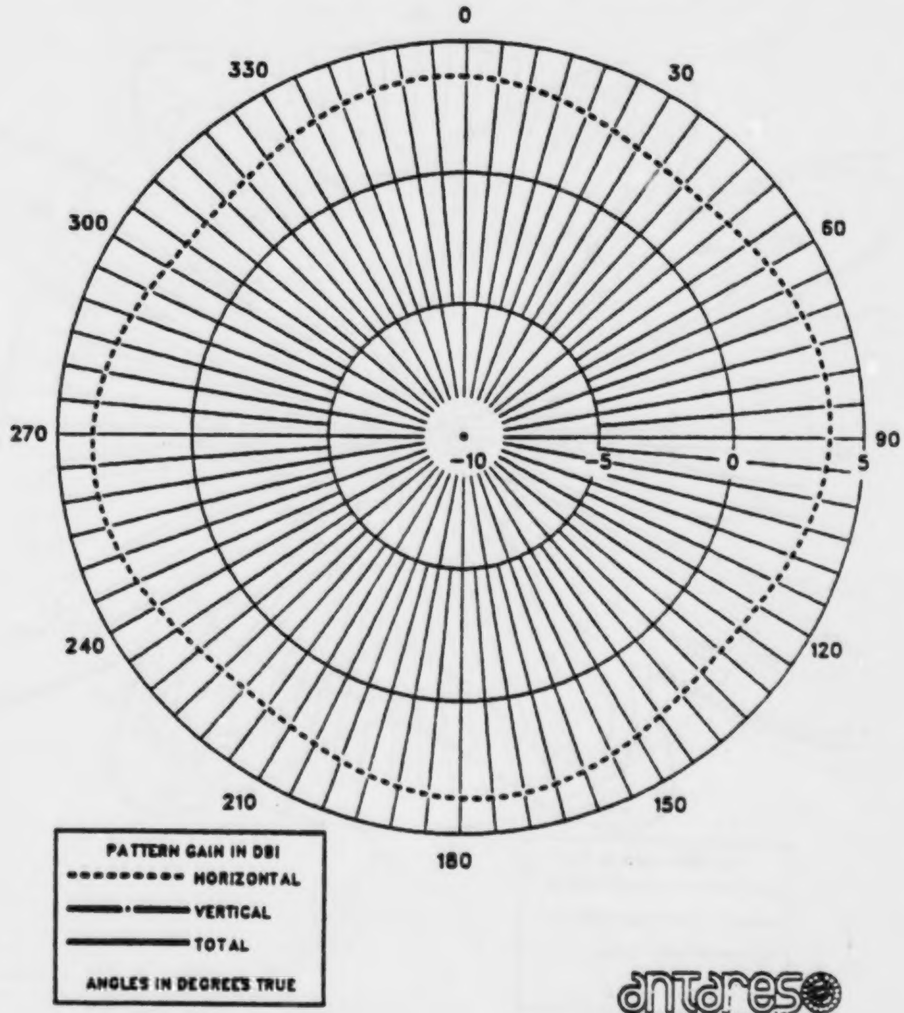

CETEC JAT TURNSTILE ANTENNA 4 BAYS CHANNEL 2

SPACING OF .875 LAMBDA BETWEEN BAYS

antares
Antares Analysis Resources

FIGURE C 48

CETEC JAT TURNSTILE ANTENNA 4 BAYS CHANNEL 2

SPACING OF .875 LAMBDA BETWEEN BAYS

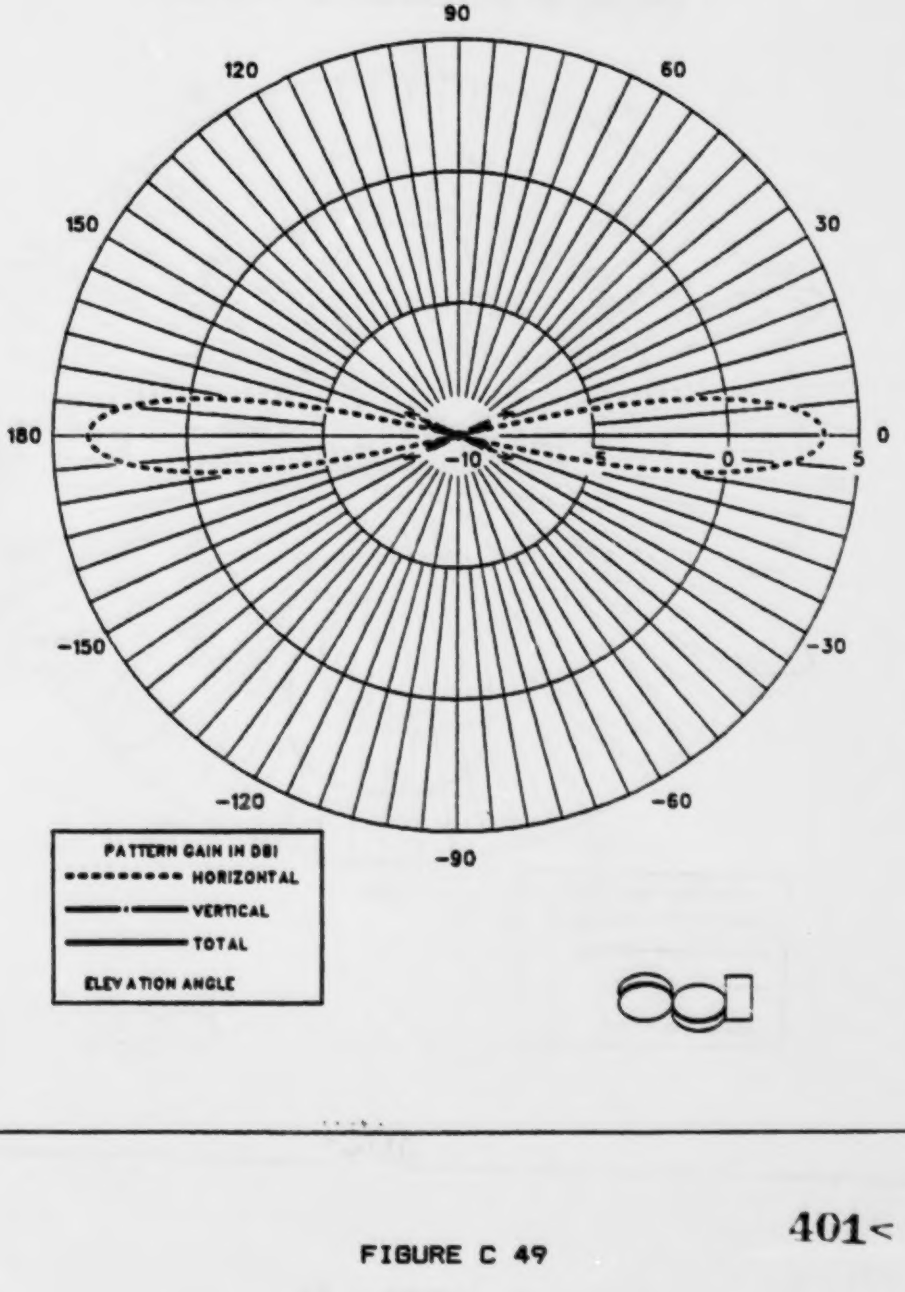

FIGURE C 49

CETEC JAT TURNSTILE ANTENNA 4 BAYS CHANNEL 2

SPACING OF .875 LAMBDA BETWEEN BAYS

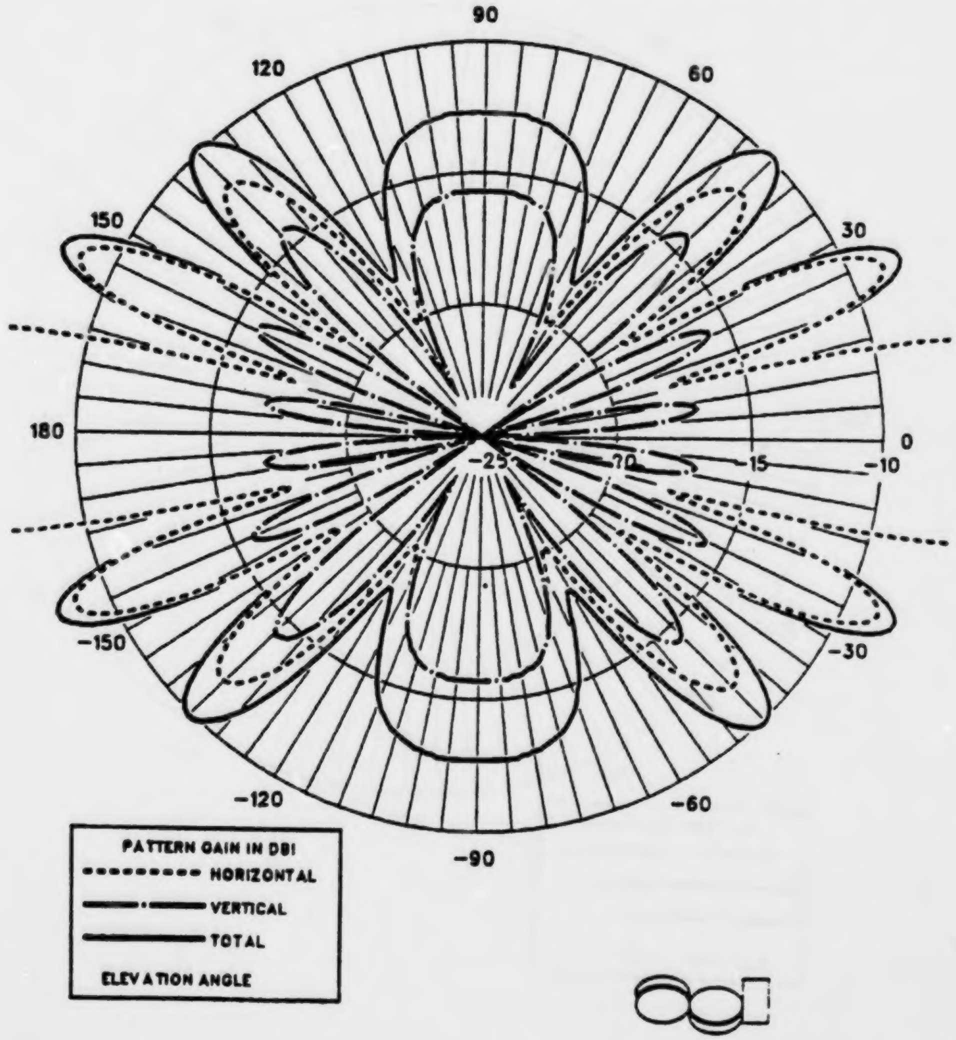

FIGURE C 50

CETEC JAT TURNSTILE ANTENNA 4 BAYS CHANNEL 2

SPACING OF 1.0 LAMBDA BETWEEN BAYS

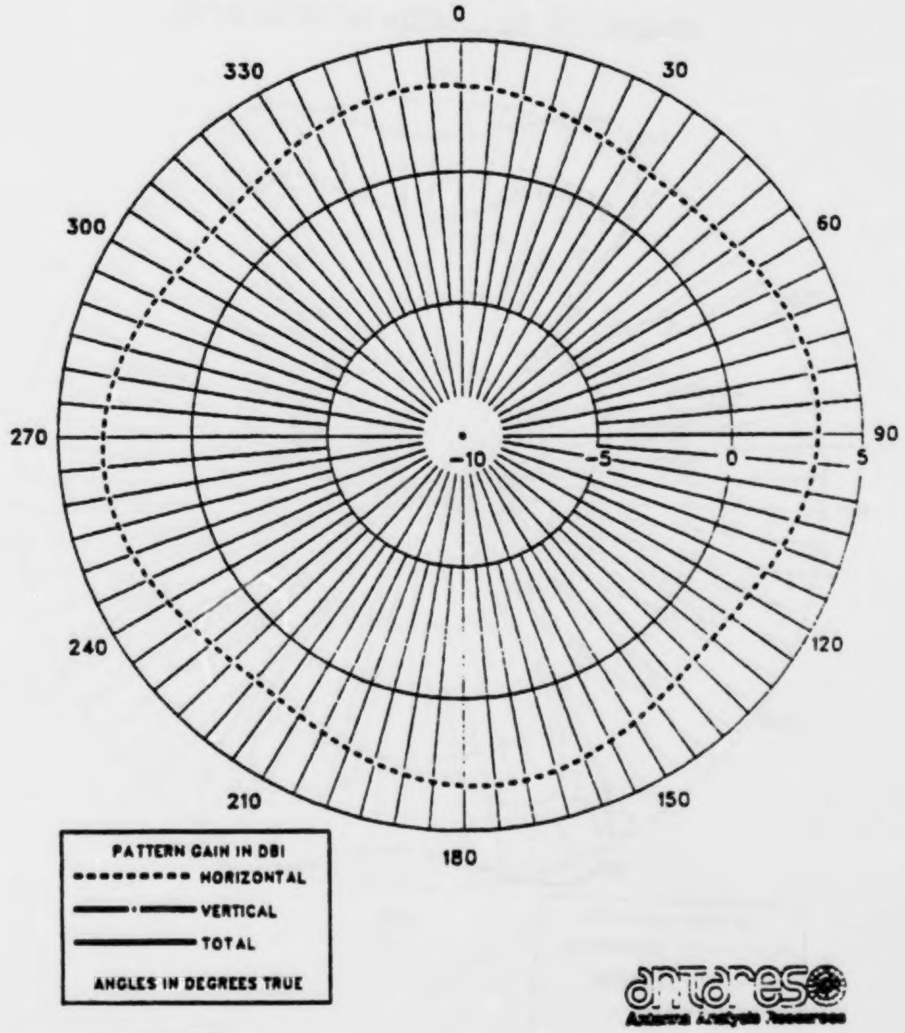

· FIGURE C 51

CETEC JAT TURNSTILE ANTENNA 4 BAYS CHANNEL 2

SPACING OF 1.0 LAMBDA BETWEEN BAYS

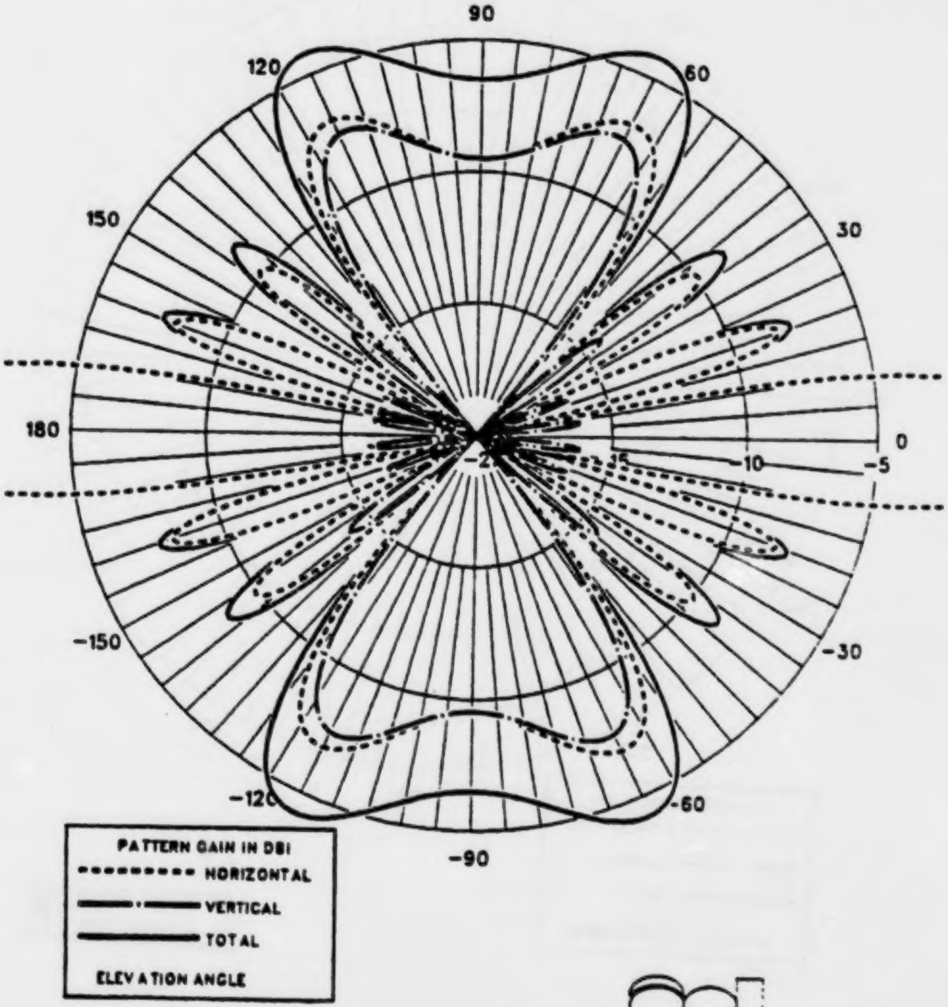

FIGURE C 52

CETEC JAT TURNSTILE ANTENNA 4 BAYS CHANNEL 2

SPACING OF 1.125 LAMBDA BETWEEN BAYS

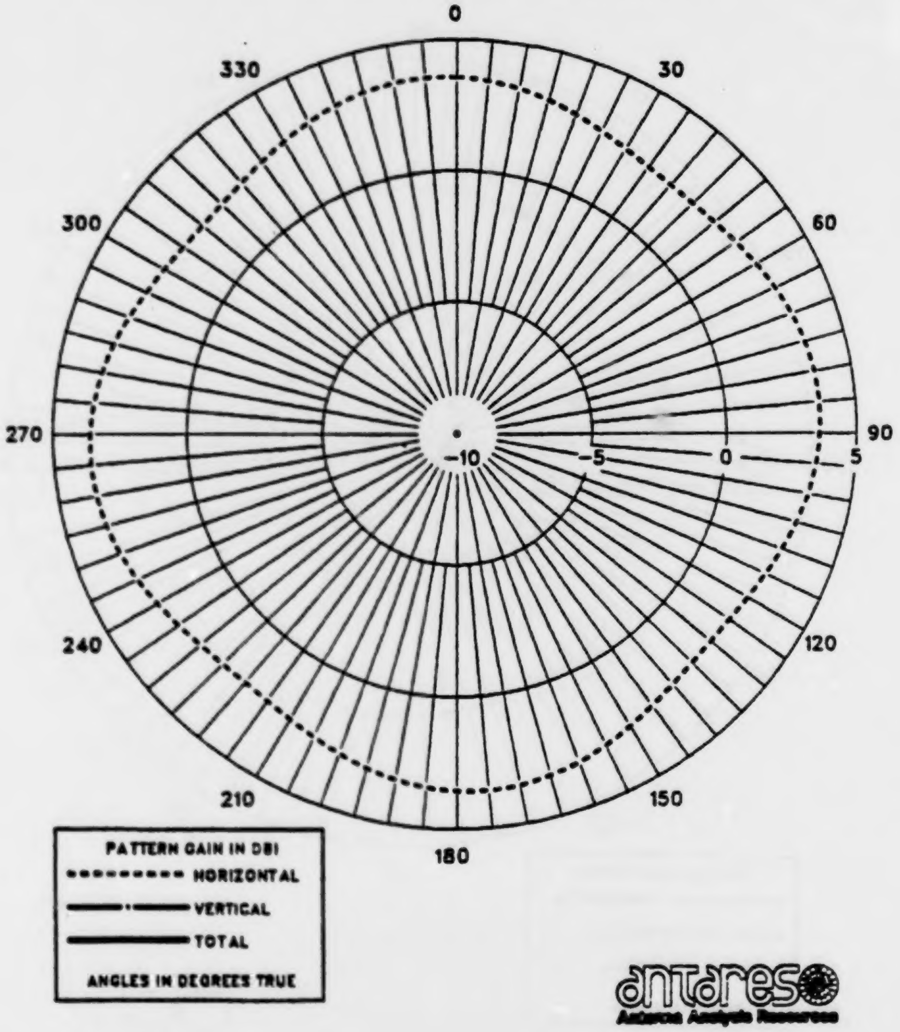

antares
Antares Analysis Resources

FIGURE C 53

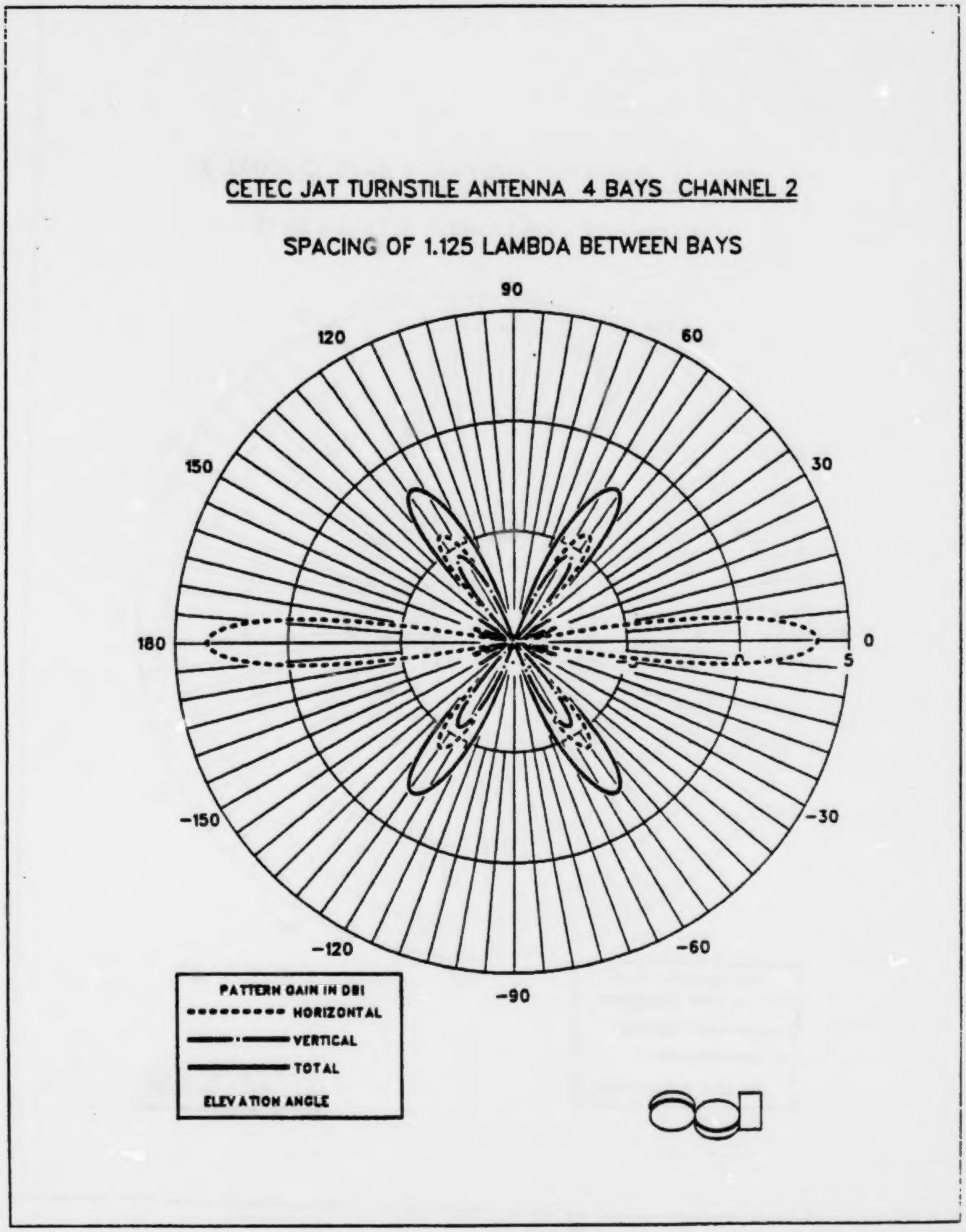
CETEC JAT TURNSTILE ANTENNA 4 BAYS CHANNEL 2
SPACING OF 1.125 LAMBDA BETWEEN BAYS
90
120
60
150
30
180
0
5
-150
-30
-120
-60
-90
PATTERN GAIN IN DBI
HORIZONTAL
VERTICAL
TOTAL
ELEVATION ANGLE

FIGURE C 54

CETEC JAT TURNSTILE ANTENNA 4 BAYS CHANNEL 2

SPACING OF 1.125 LAMBDA BETWEEN BAYS

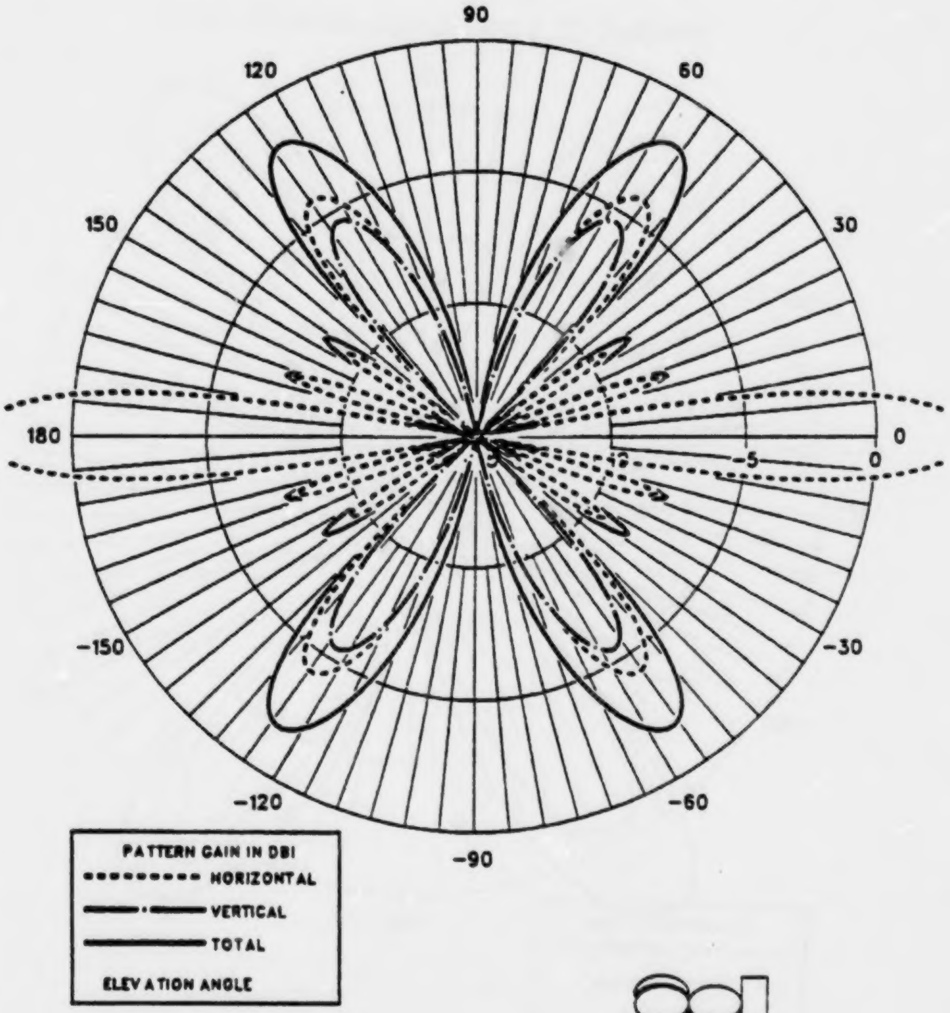

FIGURE C 55

CETEC JAT TURNSTILE ANTENNA 4 BAYS CHANNEL 2

SPACING OF 1.125 LAMBDA BETWEEN BAYS

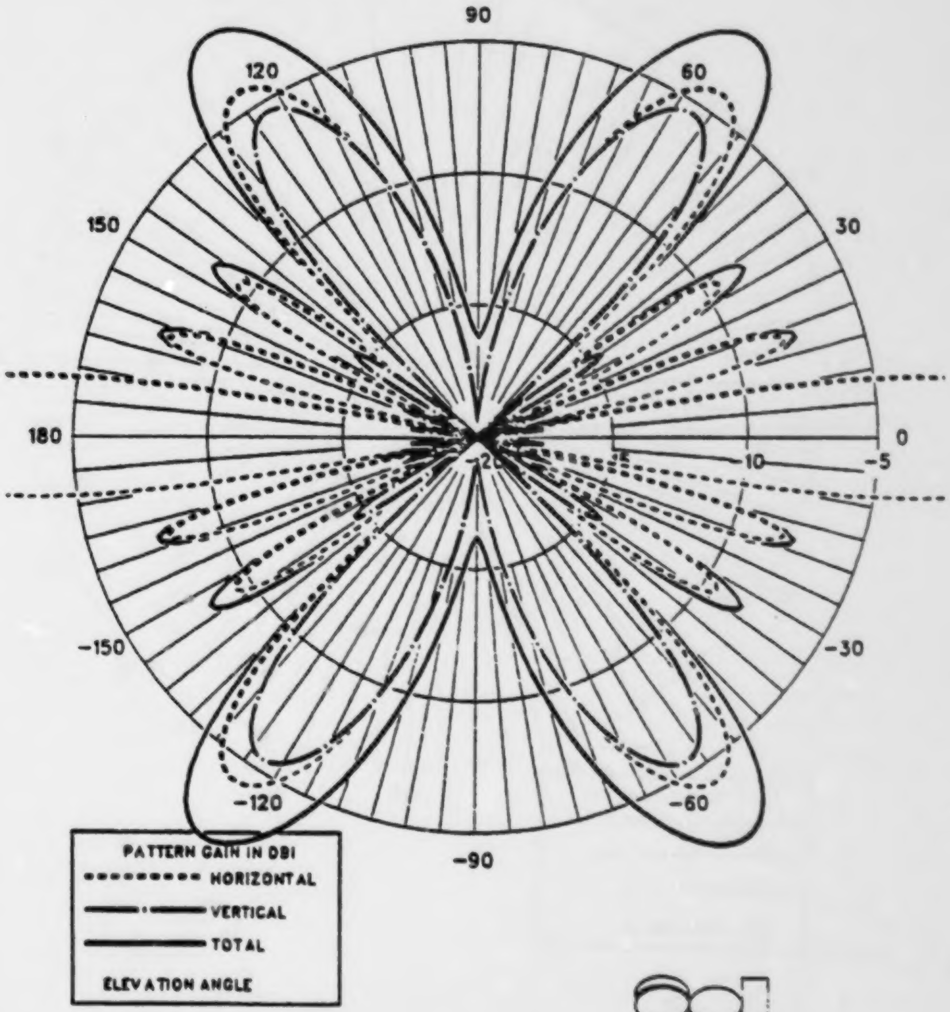

FIGURE C 56

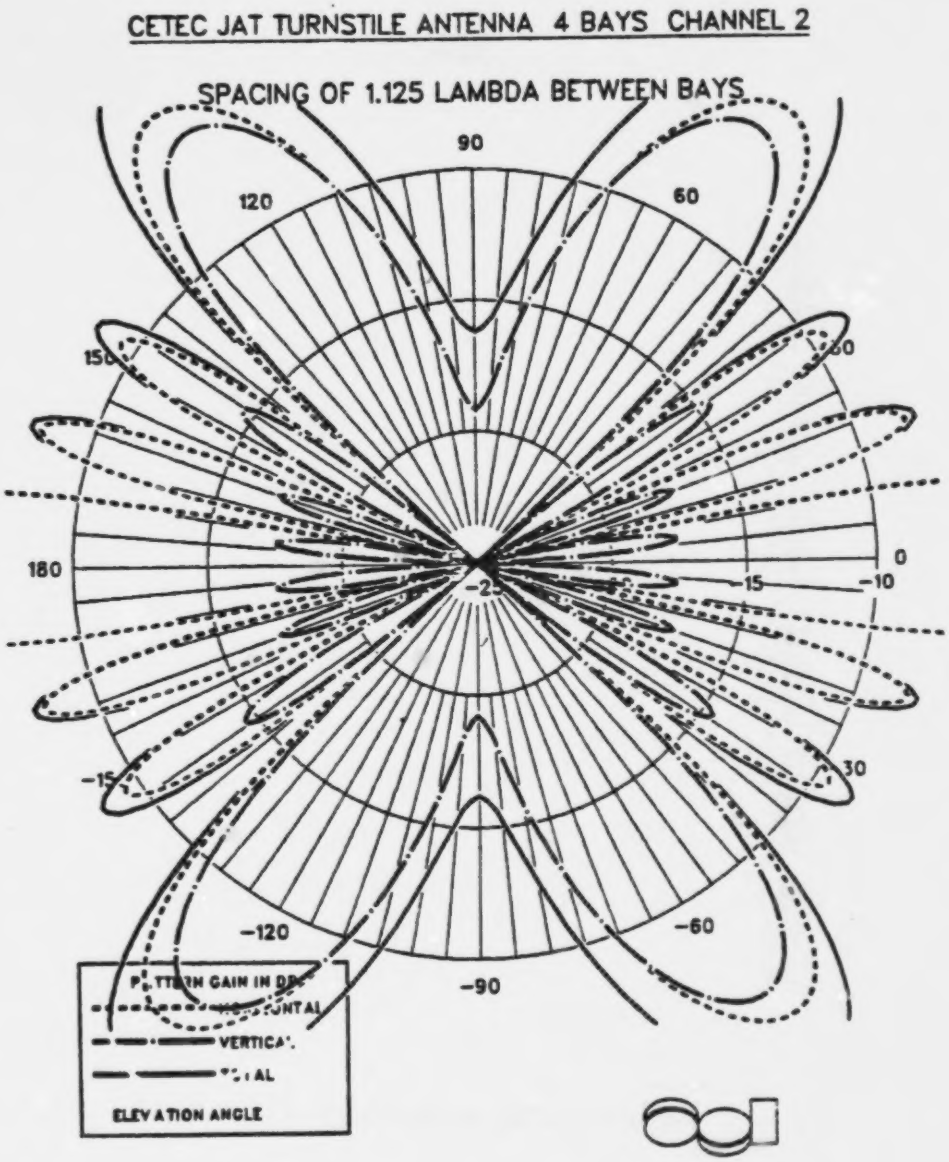
CETEC JAT TURNSTILE ANTENNA 4 BAYS CHANNEL 2

SPACING OF 1.125 LAMBDA BETWEEN BAYS

FIGURE C 57

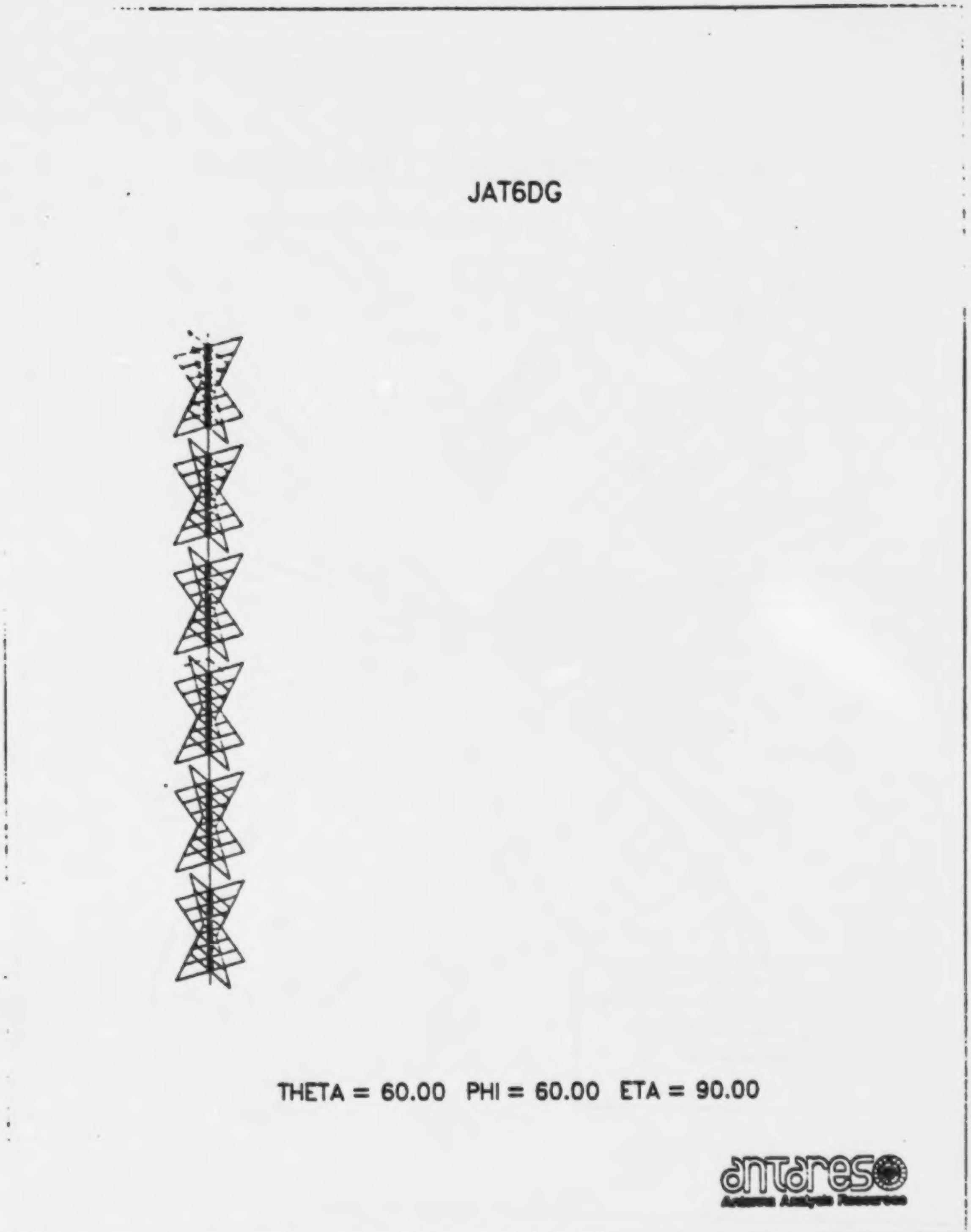
JAT6DG
THETA = 60.00 PHI = 60.00 ETA = 90.00
antares
Antenna Analysis Resources

FIGURE C 58

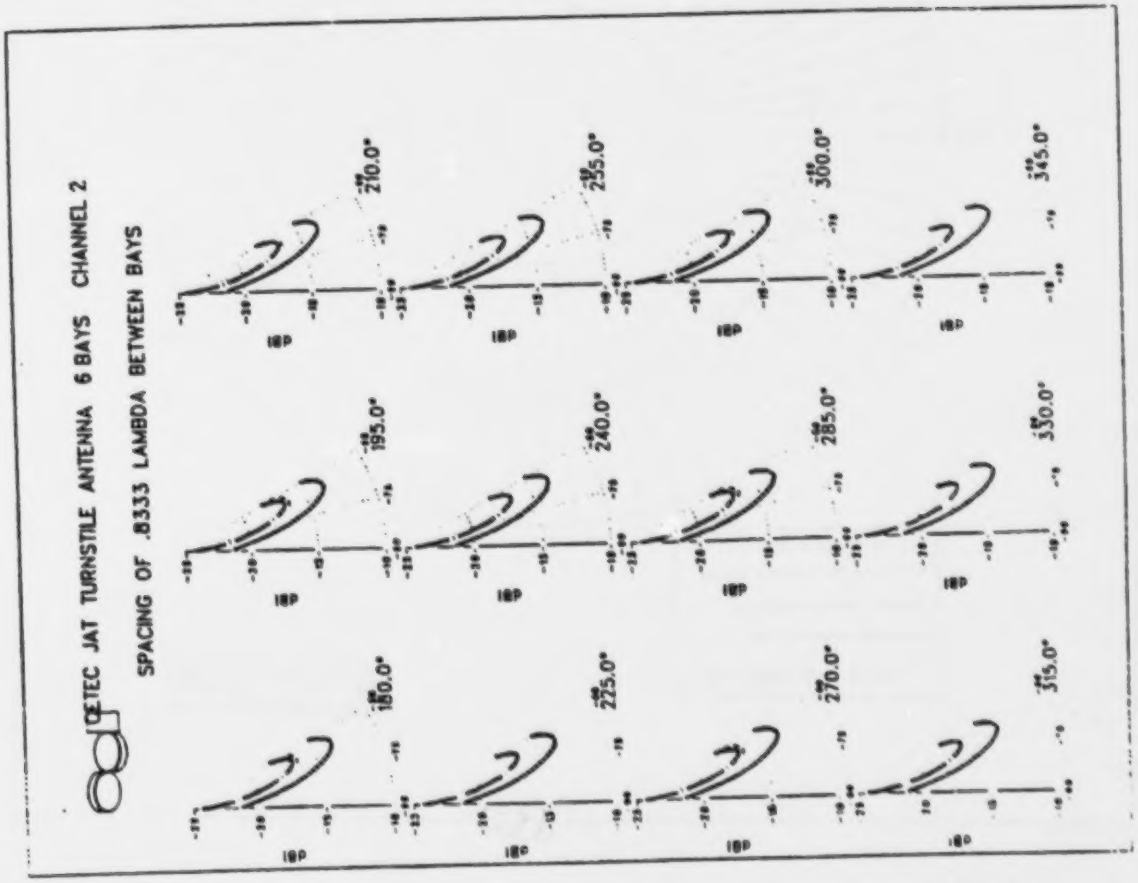
CETEC JAT TURNSTILE ANTENNA 6 BAYS CHANNEL 2
SPACING OF .8333 LAMBDA BETWEEN BAYS
180.0°
195.0°
210.0°
225.0°
240.0°
255.0°
270.0°
285.0°
300.0°
315.0°
330.0°
345.0°

FIGURE C 59

CETEC JAT TURNSTILE ANTENNA 6 BAYS CHANNEL 2

SPACING OF .8333 LAMBDA BETWEEN BAYS

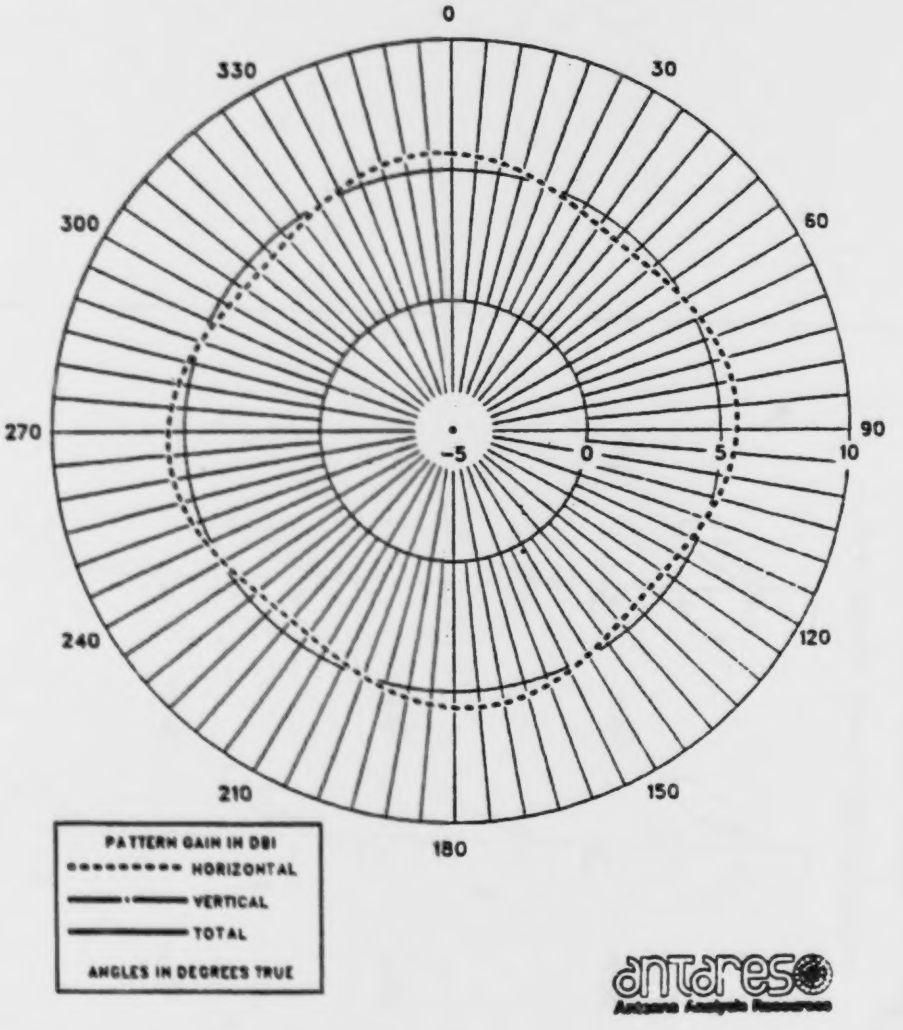

antares
Antenna Analysis Resources

FIBURE C 60

CETEC JAT TURNSTILE ANTENNA 6 BAYS CHANNEL 2

SPACING OF .8333 LAMBDA BETWEEN BAYS

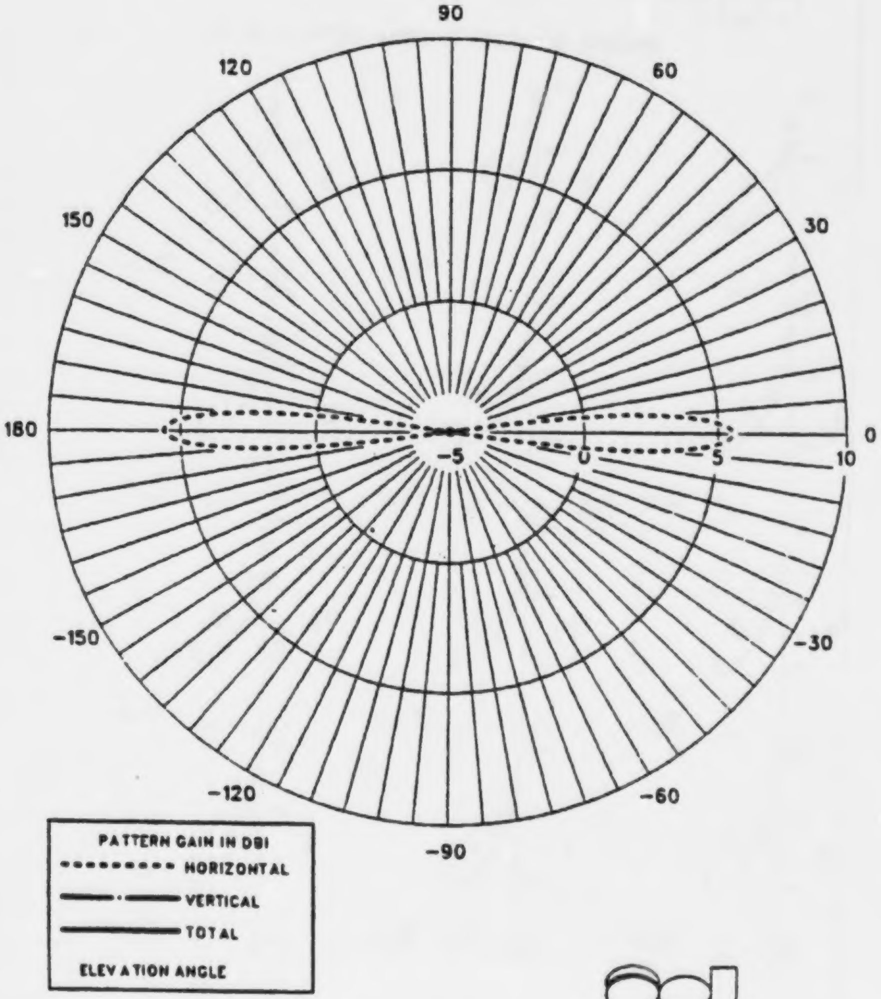

FIGURE C 61

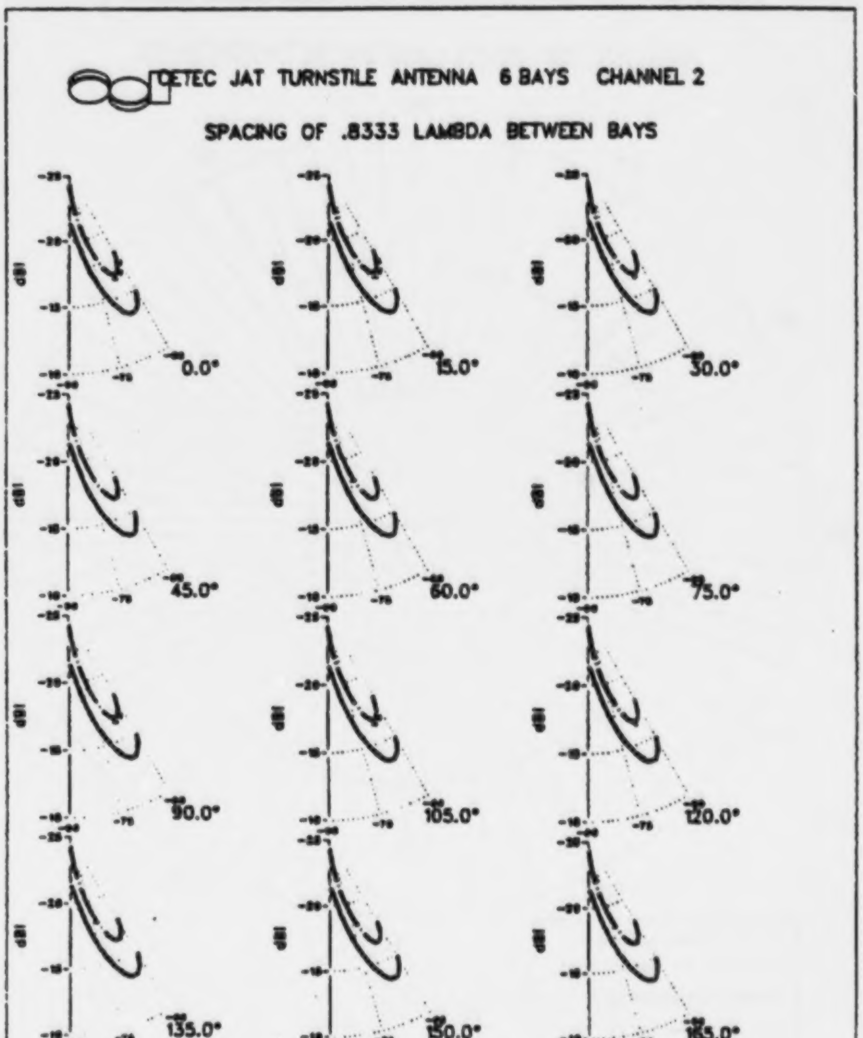

CETEC JAT TURNSTILE ANTENNA 6 BAYS CHANNEL 2

SPACING OF .8333 LAMBDA BETWEEN BAYS

FIGURE C 62

APPENDIX D

FM ARRAY GAIN/SPACING CURVES

RADIATION PATTERNS

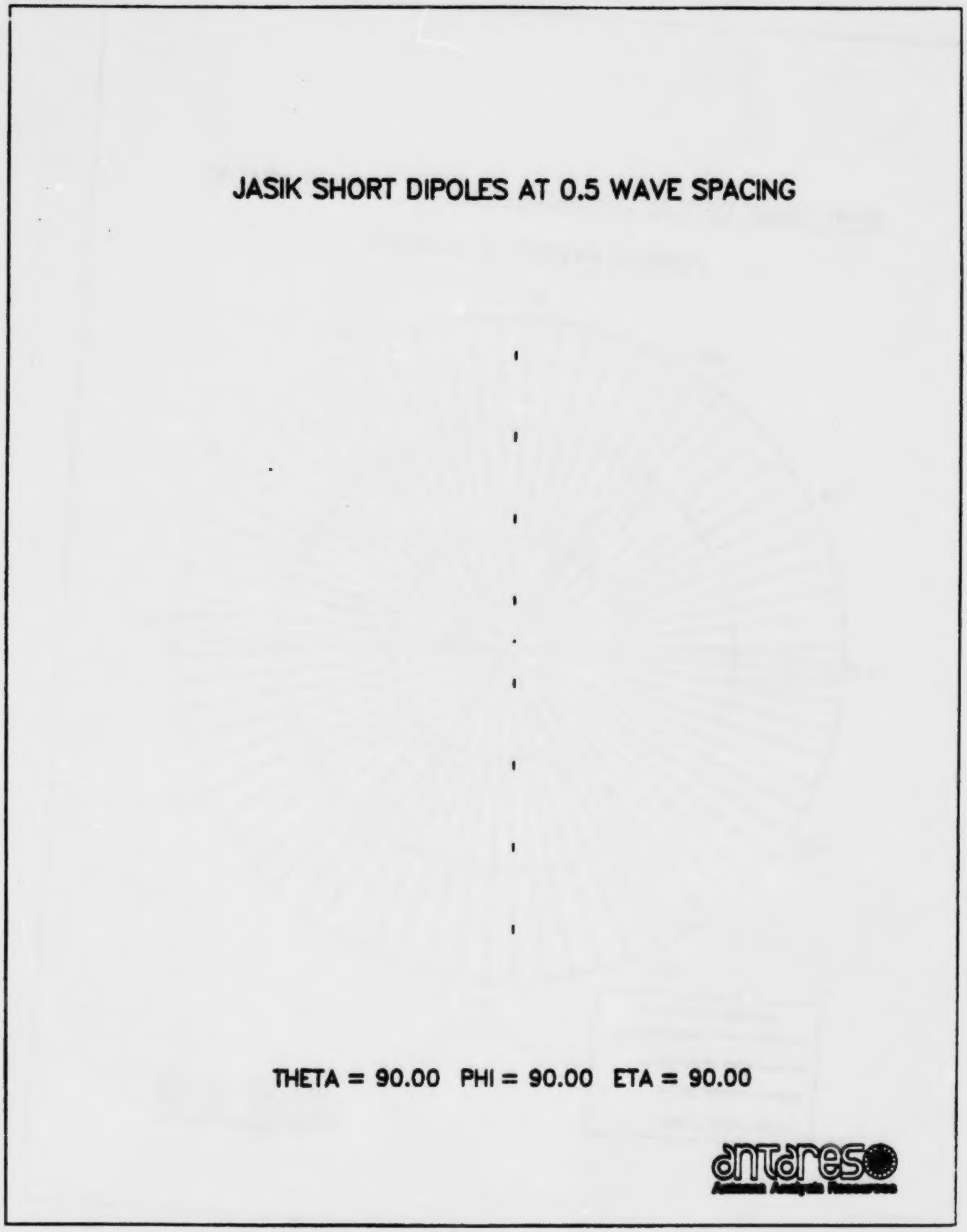
JASIK SHORT DIPOLES AT 0.5 WAVE SPACING
THETA = 90.00 PHI = 90.00 ETA = 90.00
antares
Antenna Analysis Resources

FIGURE D 1

EIGHT SHORT DIPOLES COAXIALLY ARRAYED 1.2 WAVE SPACING

VERTICAL PATTERN AT BORESITE

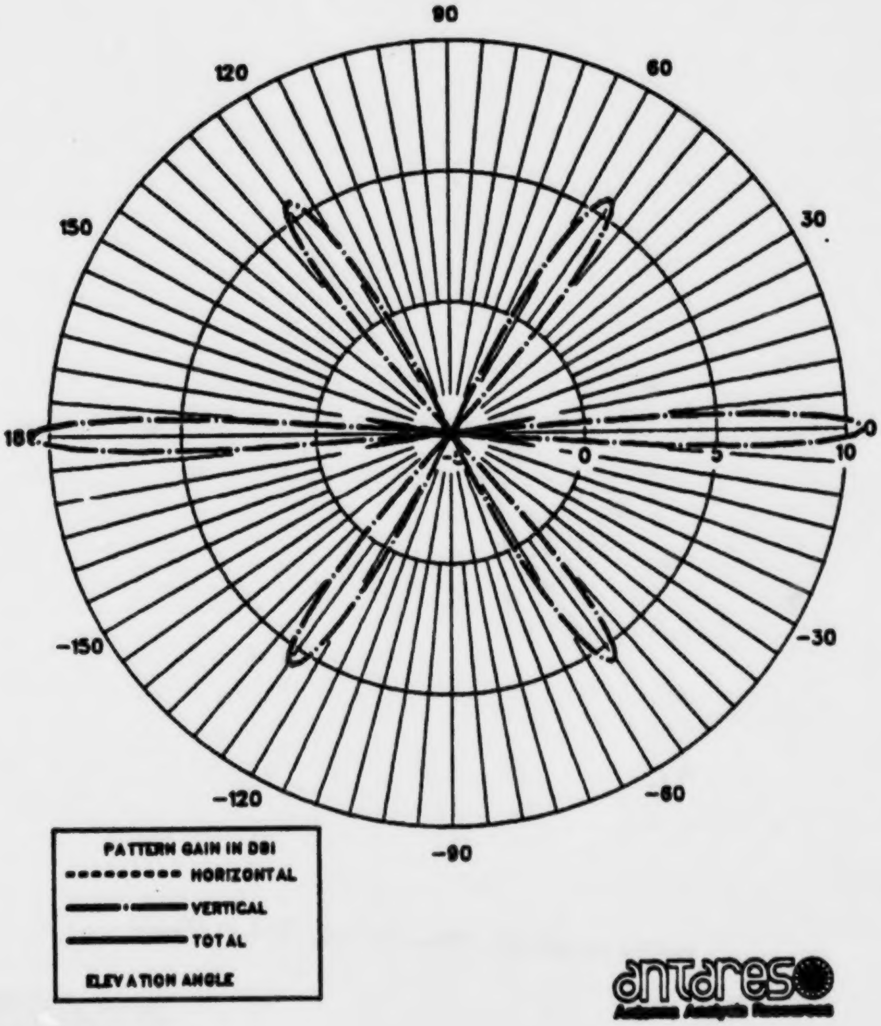

FIGURE D 2

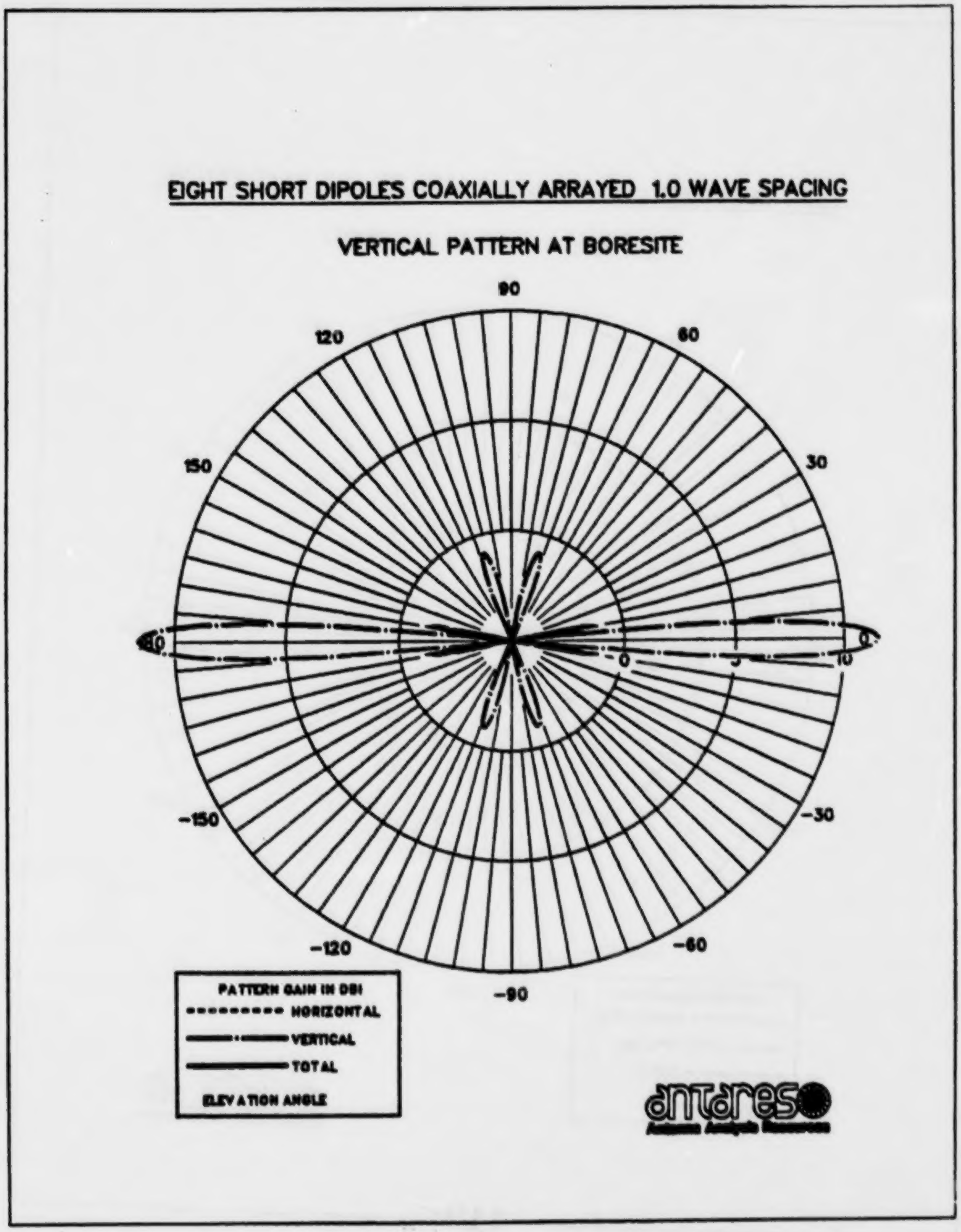

EIGHT SHORT DIPOLES COAXIALLY ARRAYED 1.0 WAVE SPACING

VERTICAL PATTERN AT BORESITE

FIGURE D 3

EIGHT SHORT DIPOLES COAXIALLY ARRAYED 0.7 WAVE SPACING

VERTICAL PATTERN AT BORESITE

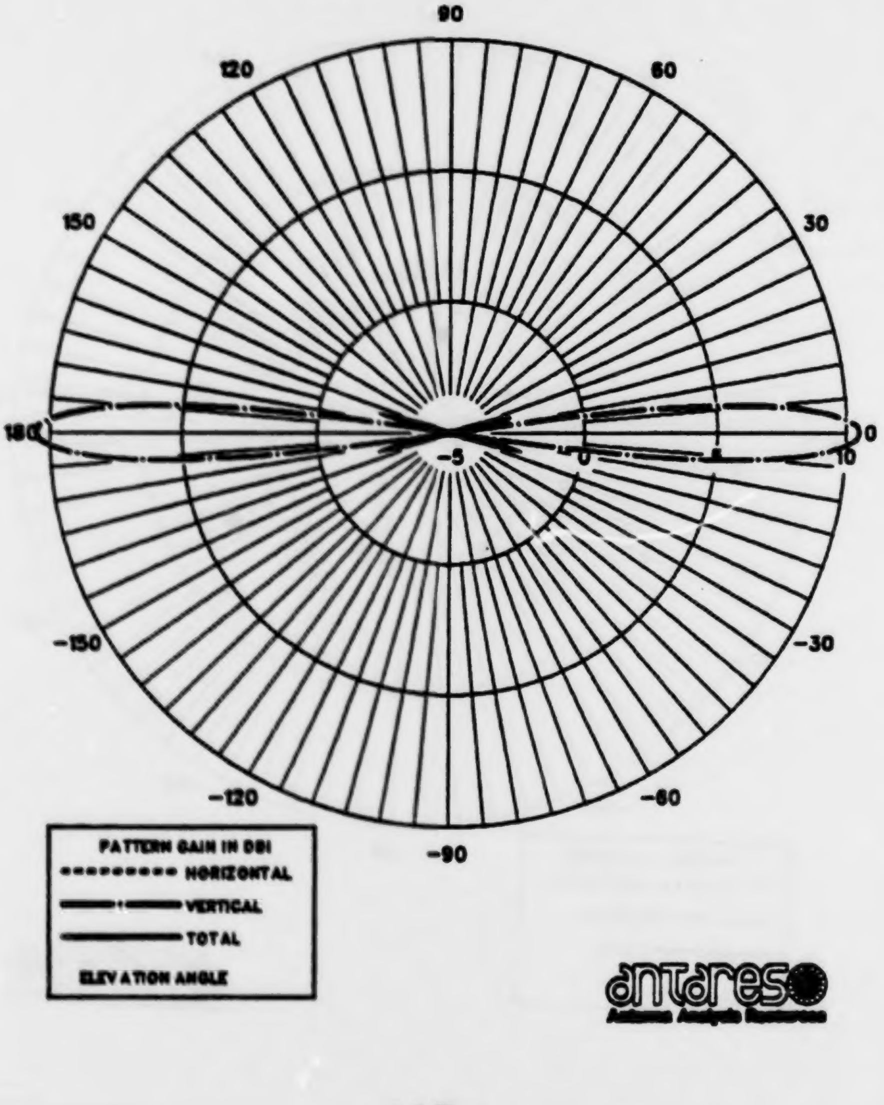

FIGURE D 4

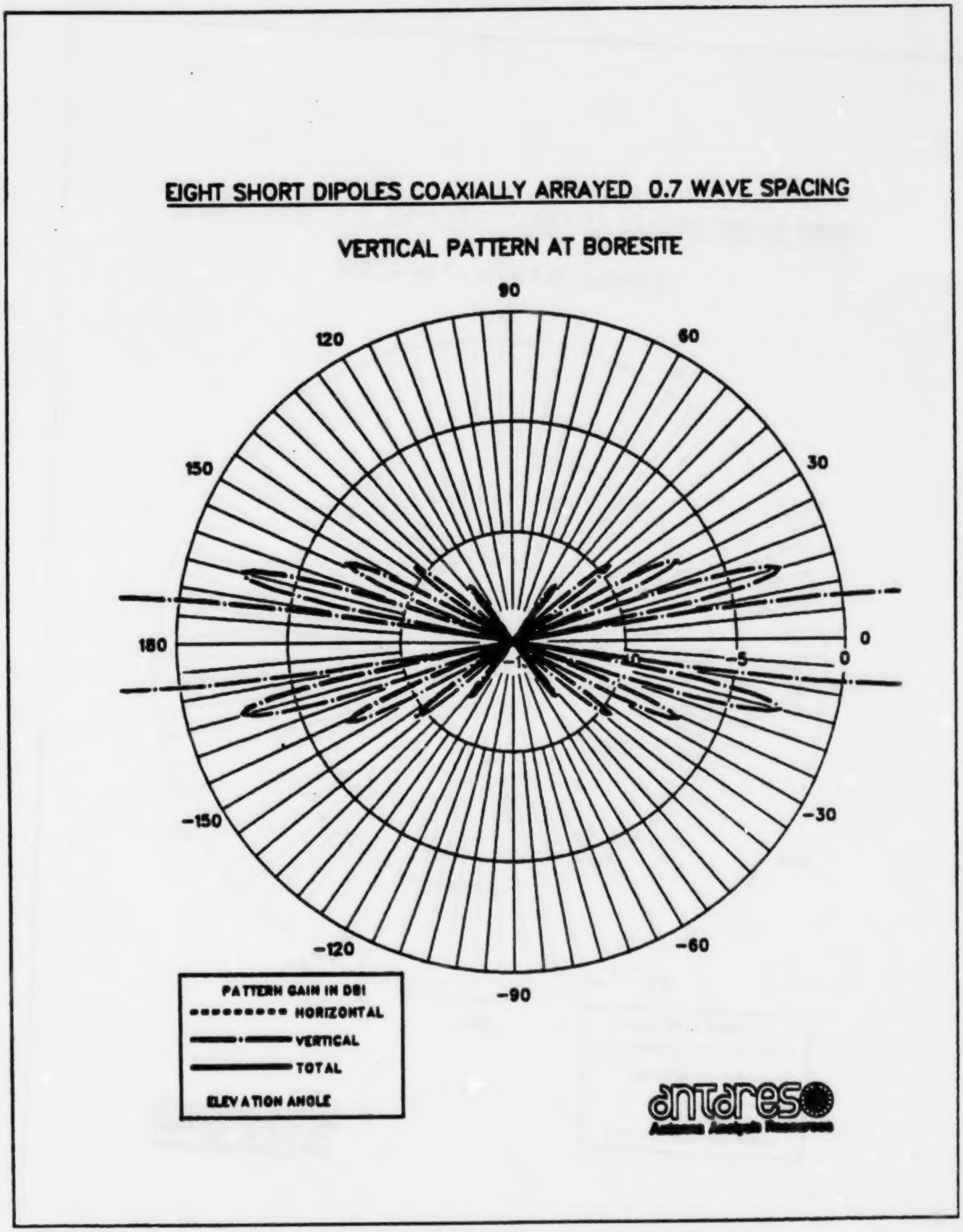
EIGHT SHORT DIPOLES COAXIALLY ARRAYED 0.7 WAVE SPACING

VERTICAL PATTERN AT BORESITE

FIGURE D 5

EIGHT SHORT DIPOLES COAXIALLY ARRAYED 0.5 WAVE SPACING

VERTICAL PATTERN AT BORESITE

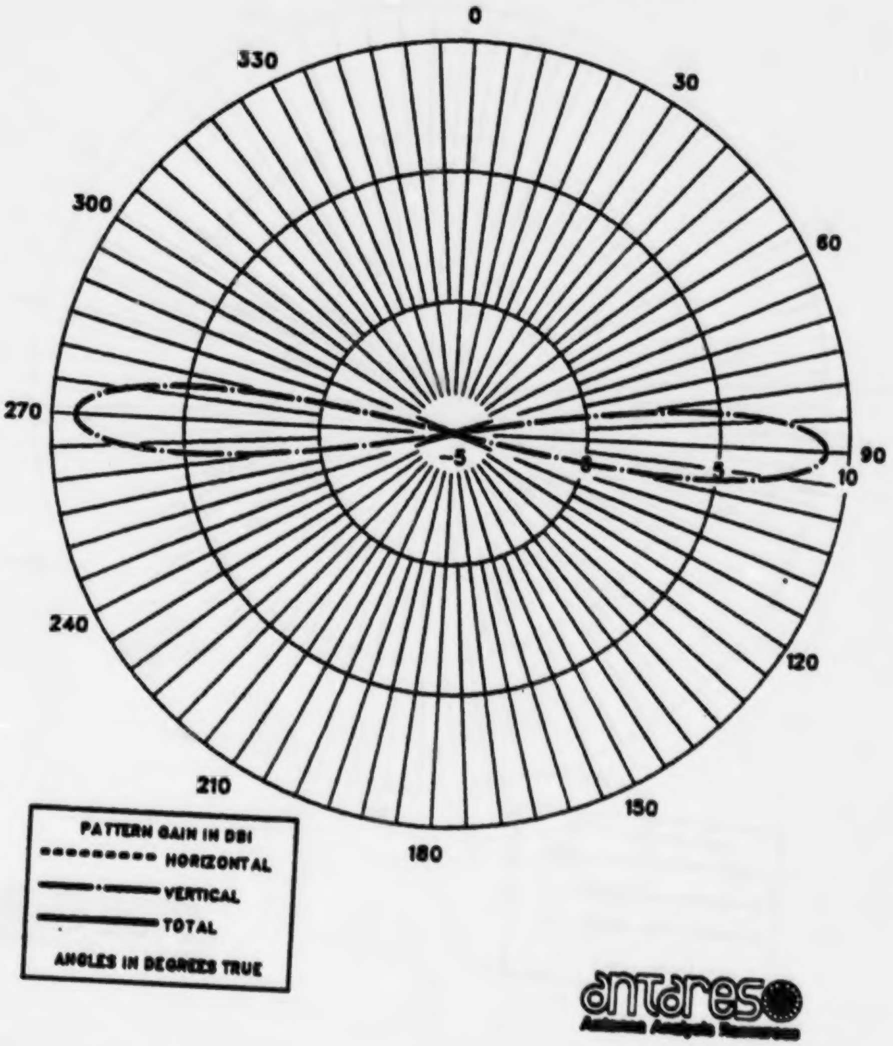

antares

FIGURE D 6

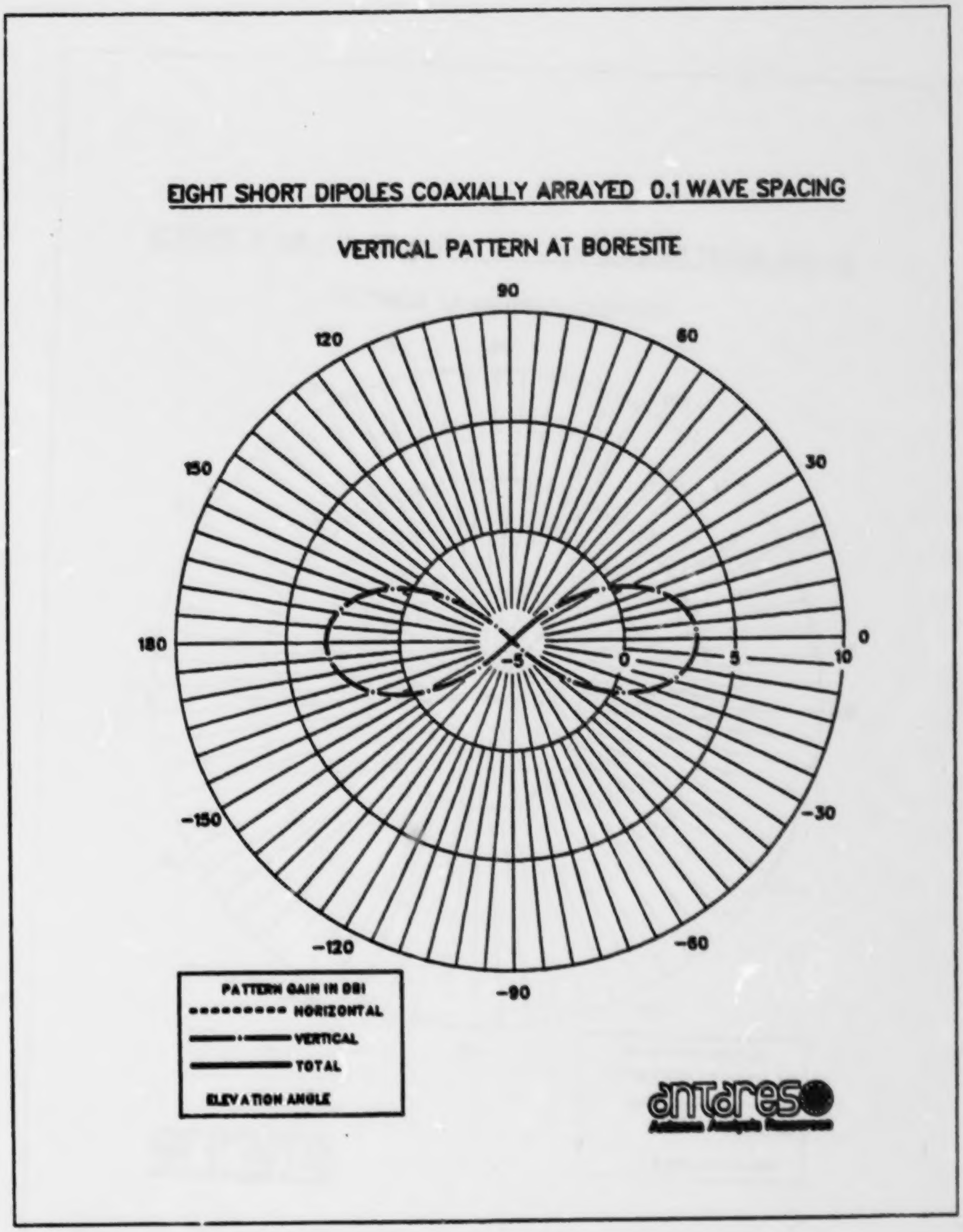
EIGHT SHORT DIPOLES COAXIALLY ARRAYED 0.1 WAVE SPACING

VERTICAL PATTERN AT BORESITE

FIGURE D 7

SIXTEEN SHORT DIPOLES COAXIALLY ARRAYED 0.5 WAVE SPACING

VERTICAL PATTERN AT BORESITE

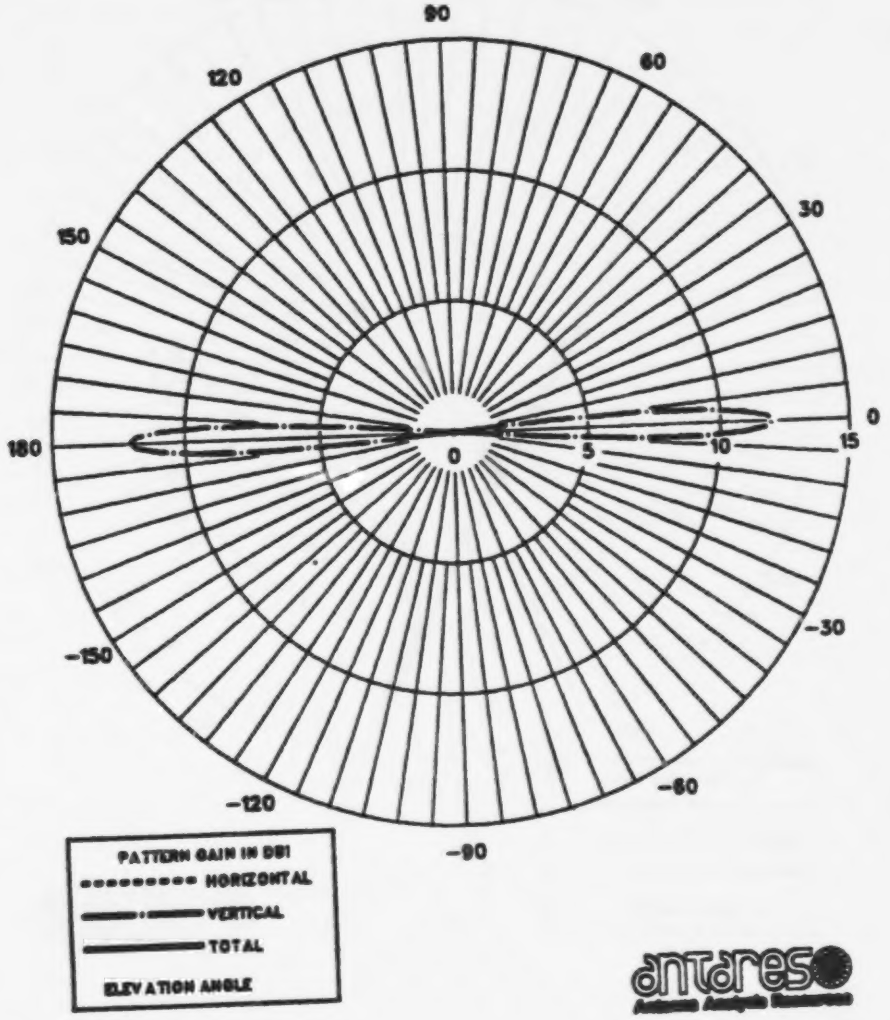

FIGURE D 8

JASIK SHORT DIPOLES AT 0.5 WAVE SPACING

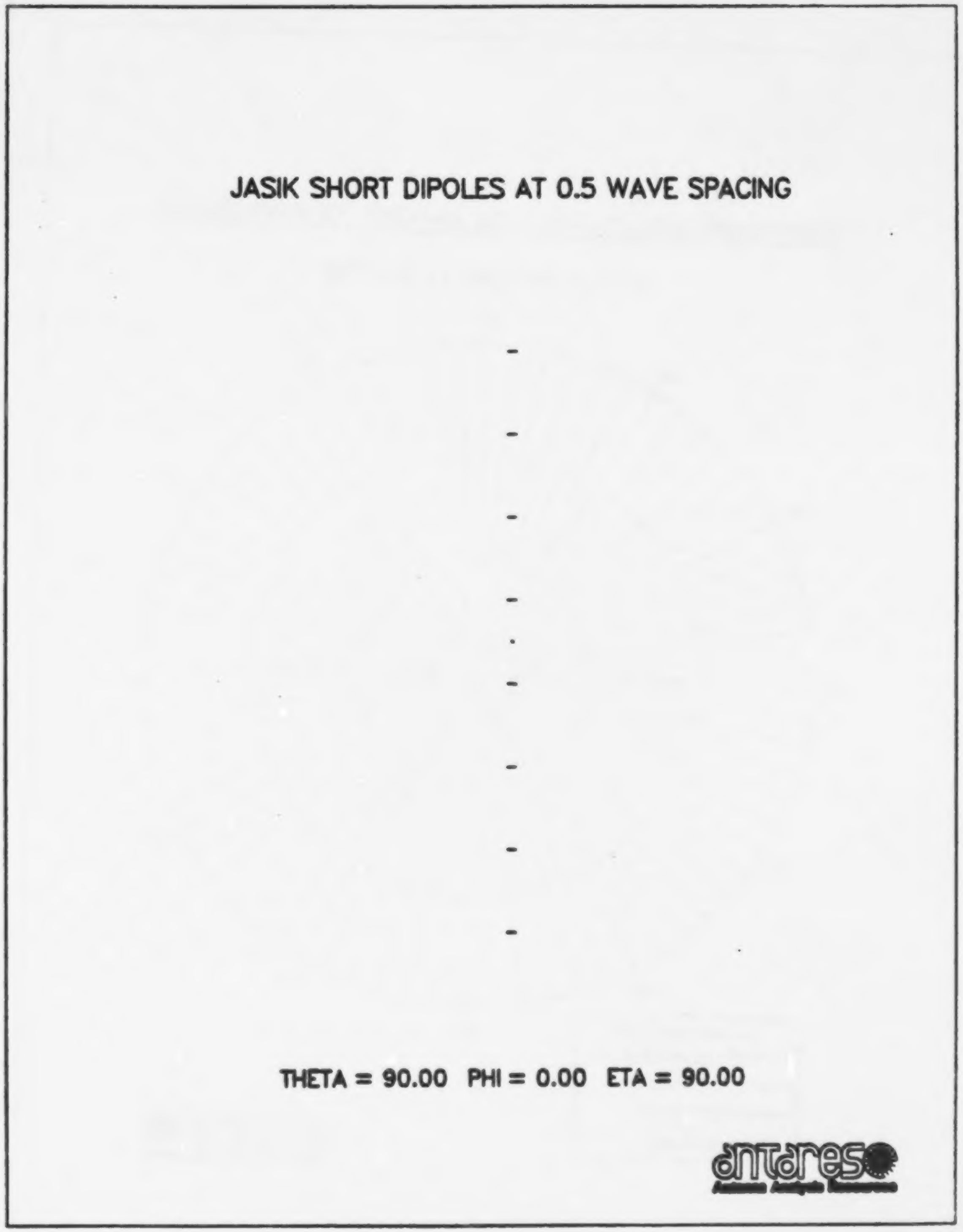

THETA = 90.00 PHI = 0.00 ETA = 90.00

FIGURE D 9

EIGHT SHORT DIPOLES BROADSIDE ARRAYED 1.2 WAVE SPACING

VERTICAL PATTERN AT BORESITE

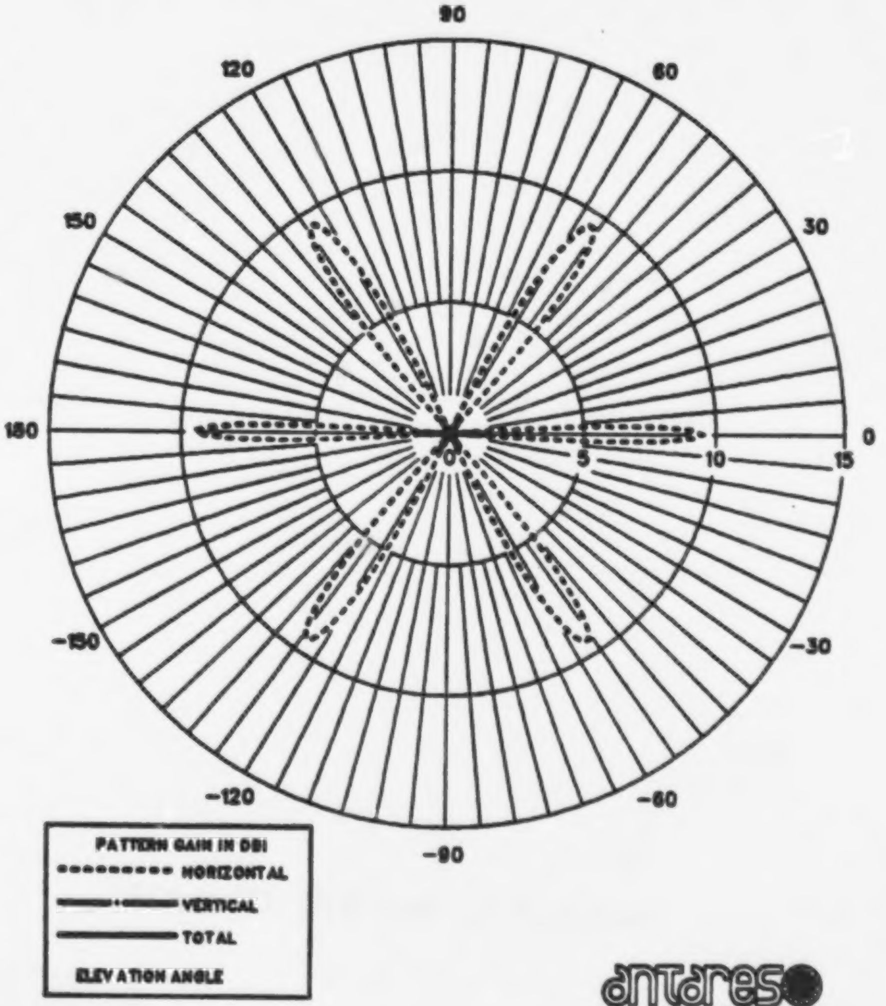

antares
Antenna Analysis Resources

FIGURE D 10

EIGHT SHORT DIPOLES BROADSIDE ARRAYED 1.0 WAVE SPACING

VERTICAL PATTERN AT BORESITE

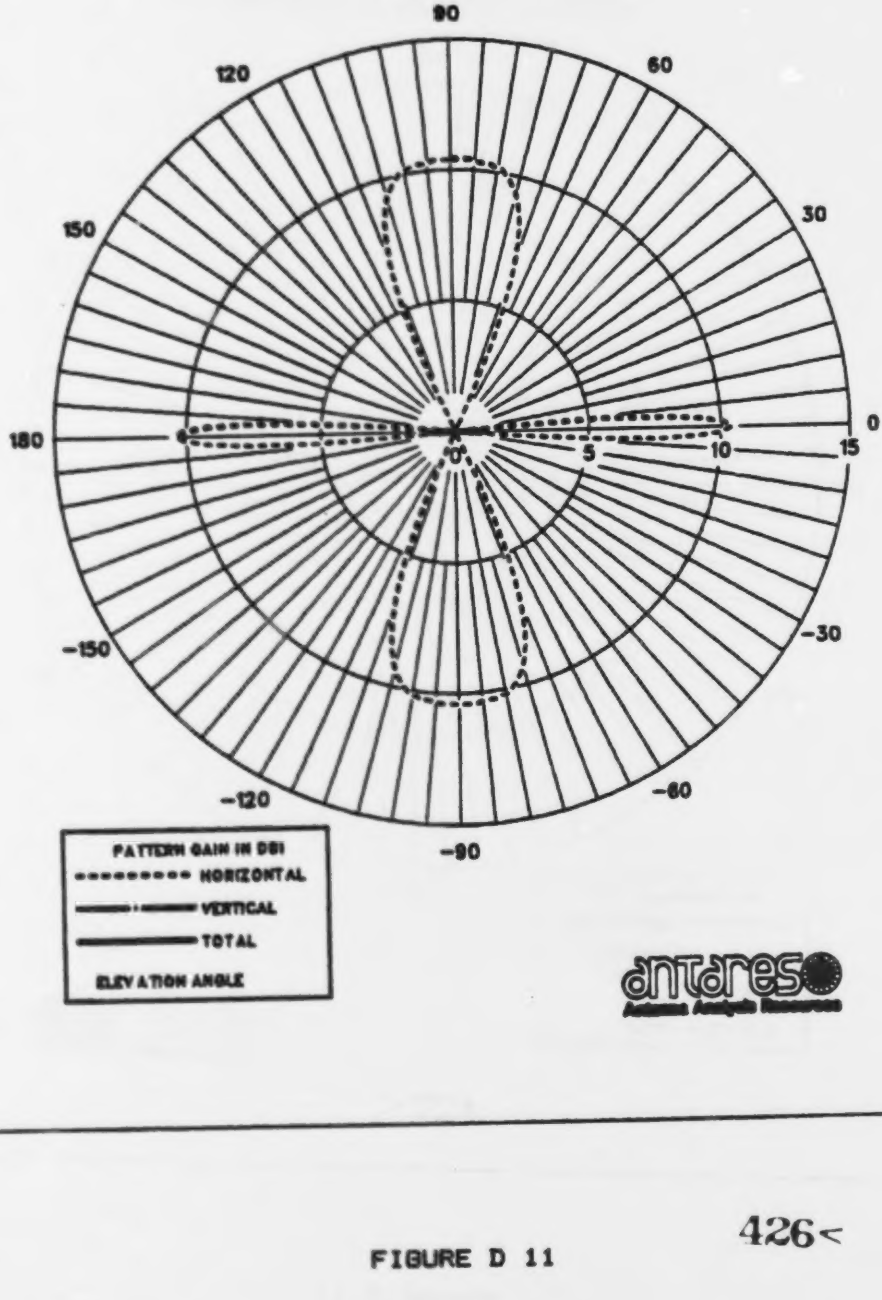

FIGURE D 11

EIGHT SHORT DIPOLES BROADSIDE ARRAYED 0.95 WAVE SPACING

VERTICAL PATTERN AT BORESITE

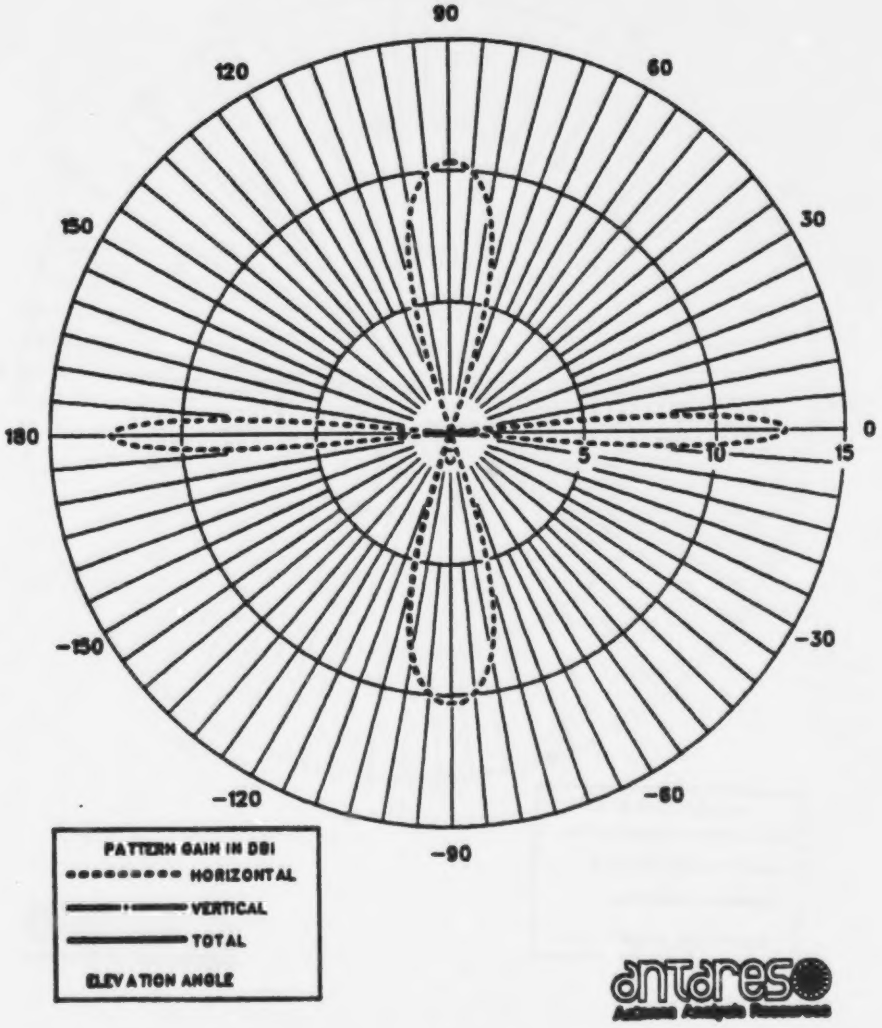

antares
Antenna Analysis Resources

427<

FIGURE D 12

EIGHT SHORT DIPOLES BROADSIDE ARRAYED 0.9 WAVE SPACING

VERTICAL PATTERN AT BORESITE

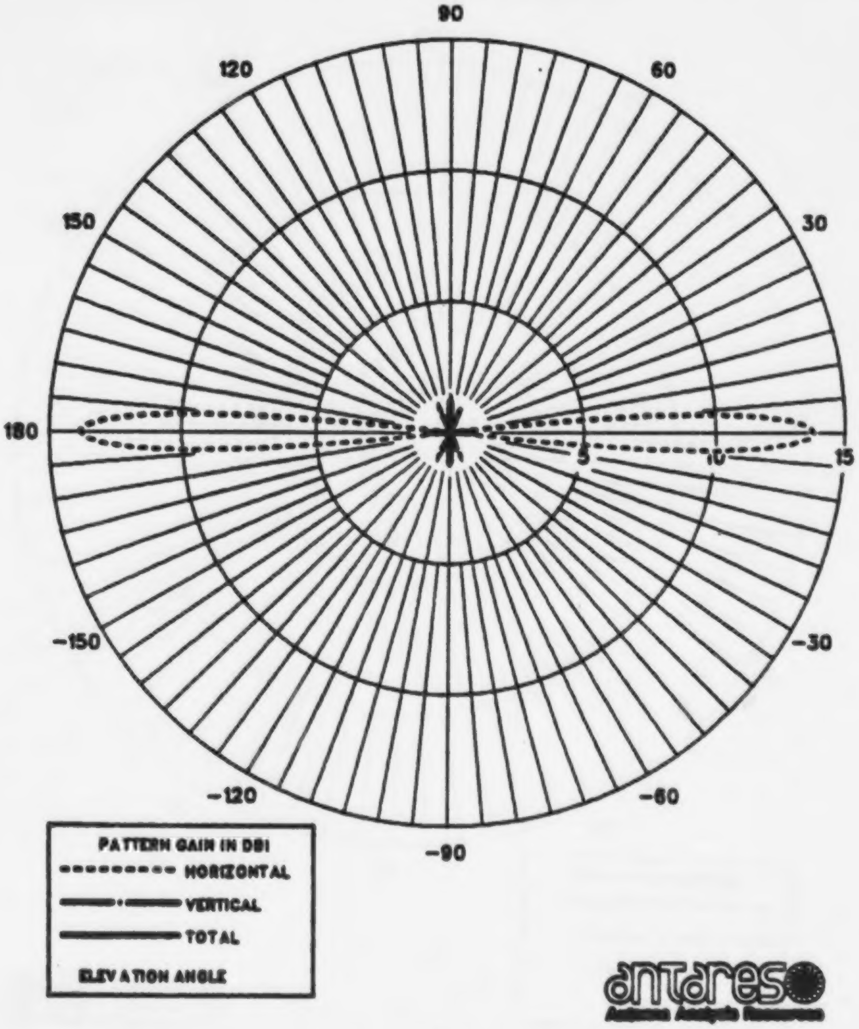

antares
Antenna Analysis Resources

FIGURE D 13

EIGHT SHORT DIPOLES BROADSIDE ARRAYED 0.7 WAVE SPACING

VERTICAL PATTERN AT BORESITE

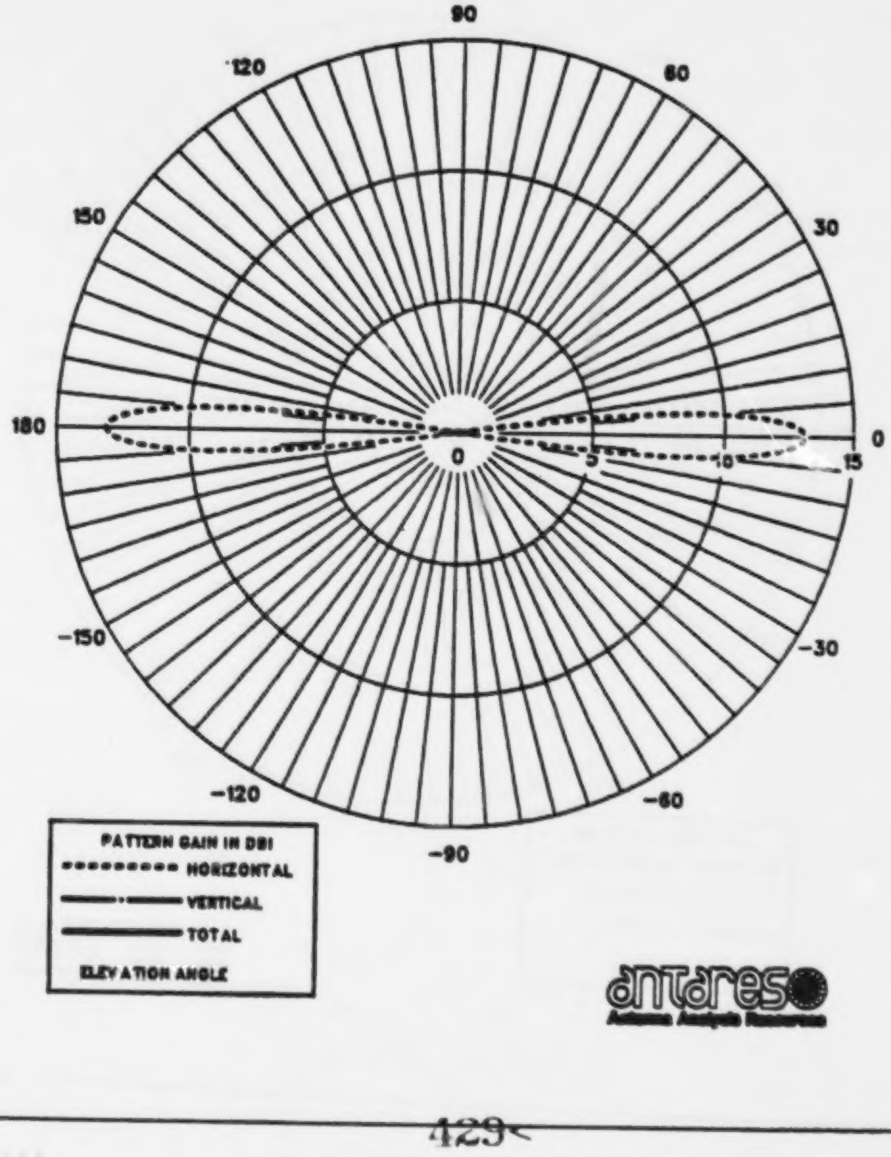

FIGURE D 14

EIGHT SHORT DIPOLES BROADSIDE ARRAYED 0.5 WAVE SPACING

VERTICAL PATTERN AT BORESITE

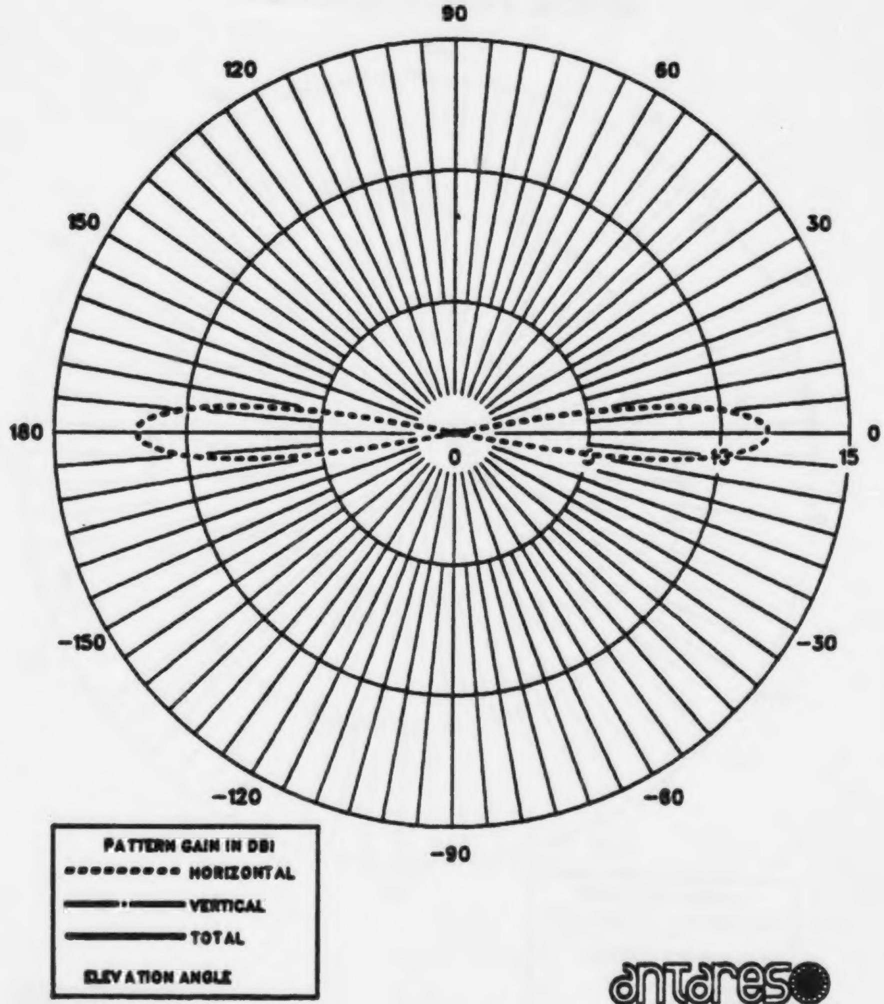

antares
Antenna Analysis Resources

430<

FIGURE D 15

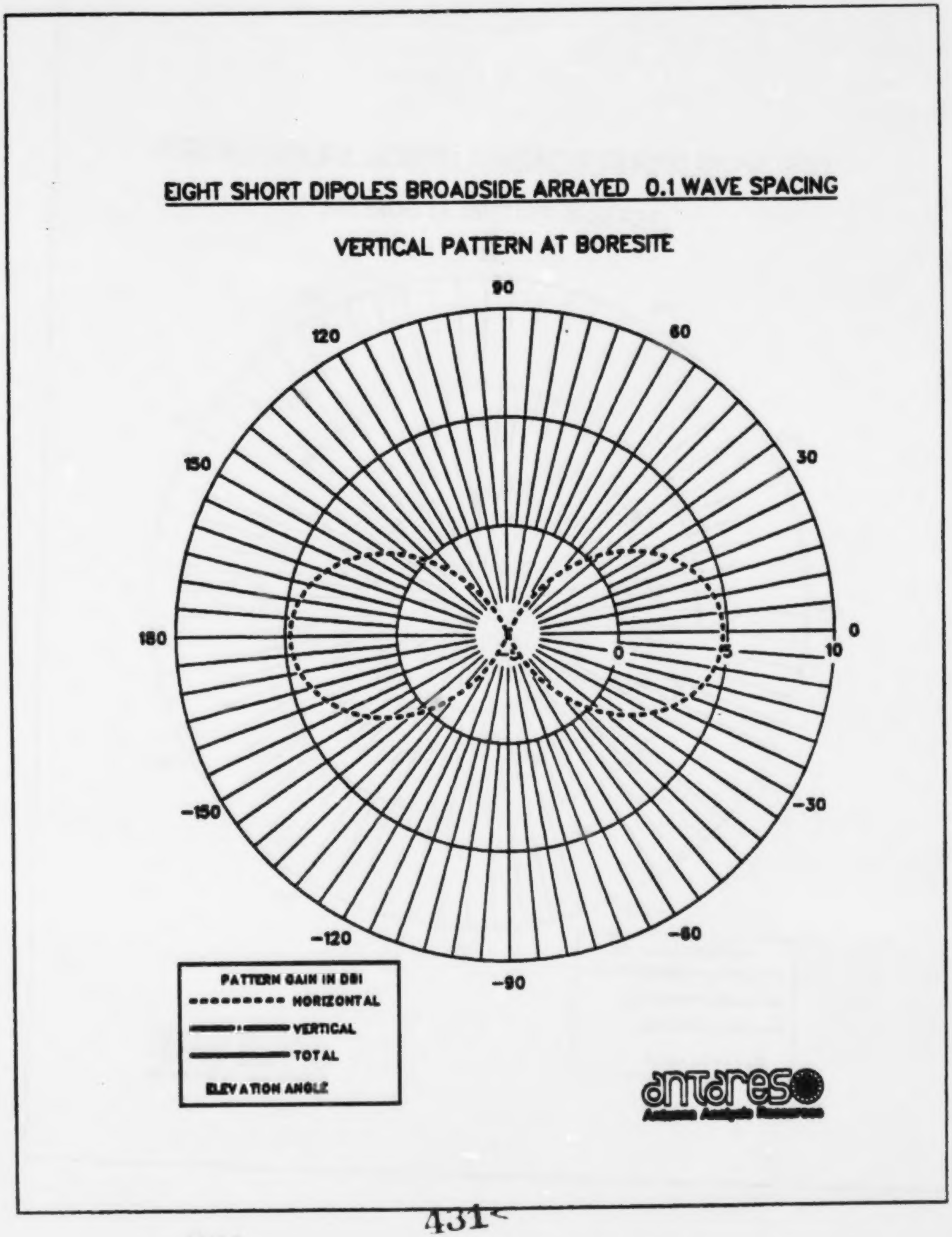
EIGHT SHORT DIPOLES BROADSIDE ARRAYED 0.1 WAVE SPACING
VERTICAL PATTERN AT BORESITE
90
120
60
150
30
180
0
-5
0
5
10
-150
-30
-120
-60
-90
PATTERN GAIN IN DBI
HORIZONTAL
VERTICAL
TOTAL
ELEVATION ANGLE
antares
Antenna Analysis Resources

FIGURE D 16

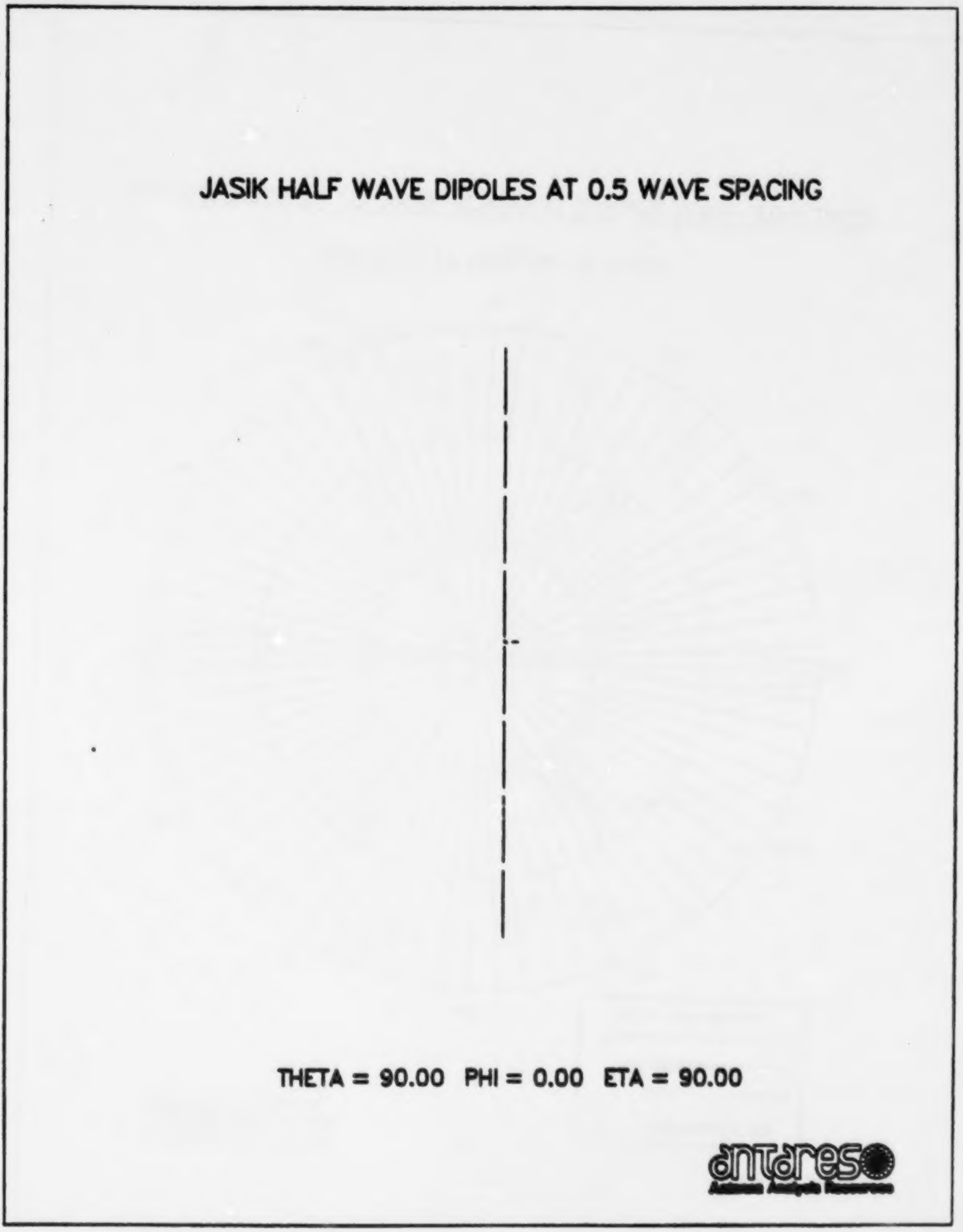
JASIK HALF WAVE DIPOLES AT 0.5 WAVE SPACING

THETA = 90.00 PHI = 0.00 ETA = 90.00

432<

FIGURE D 17

EIGHT HALF-WAVE DIPOLES COAXIALLY ARRAYED 1.2 WAVE SPACING

VERTICAL PATTERN AT BORESITE

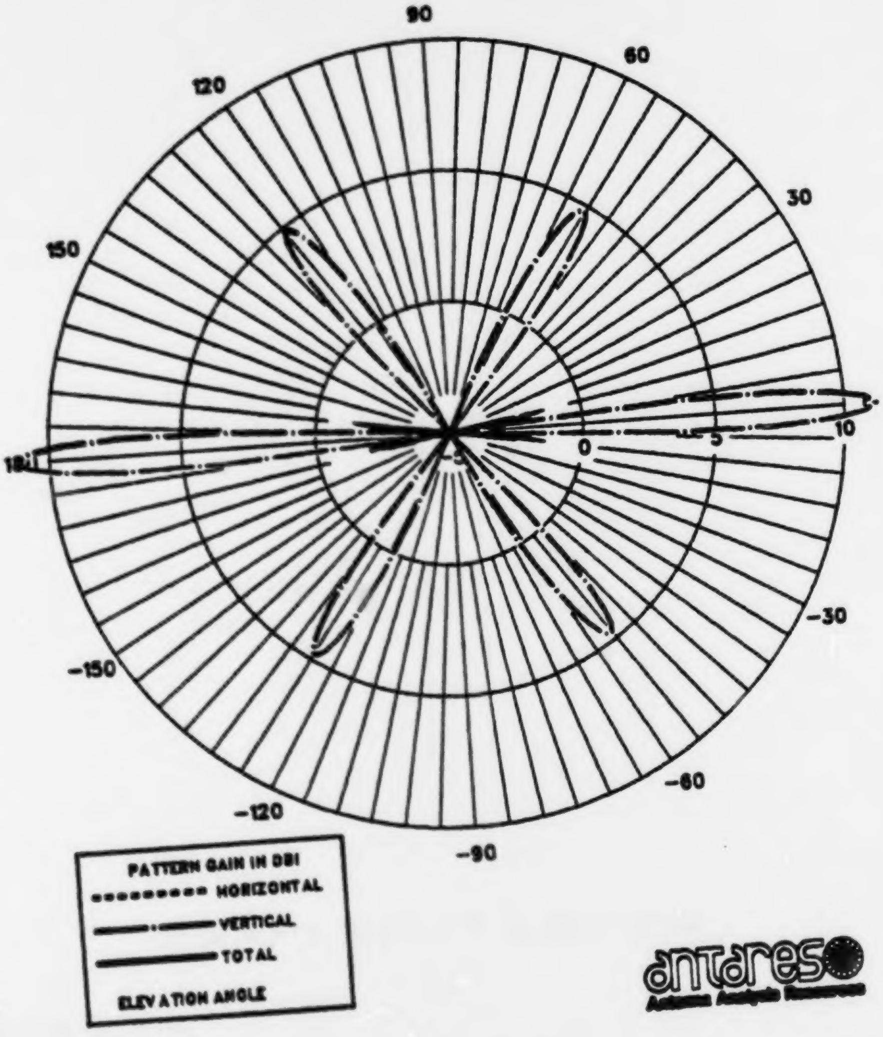

FIGURE D 18

EIGHT HALF-WAVE DIPOLES COAXIALLY ARRAYED 1.0 WAVE SPACING

VERTICAL PATTERN AT BORESITE

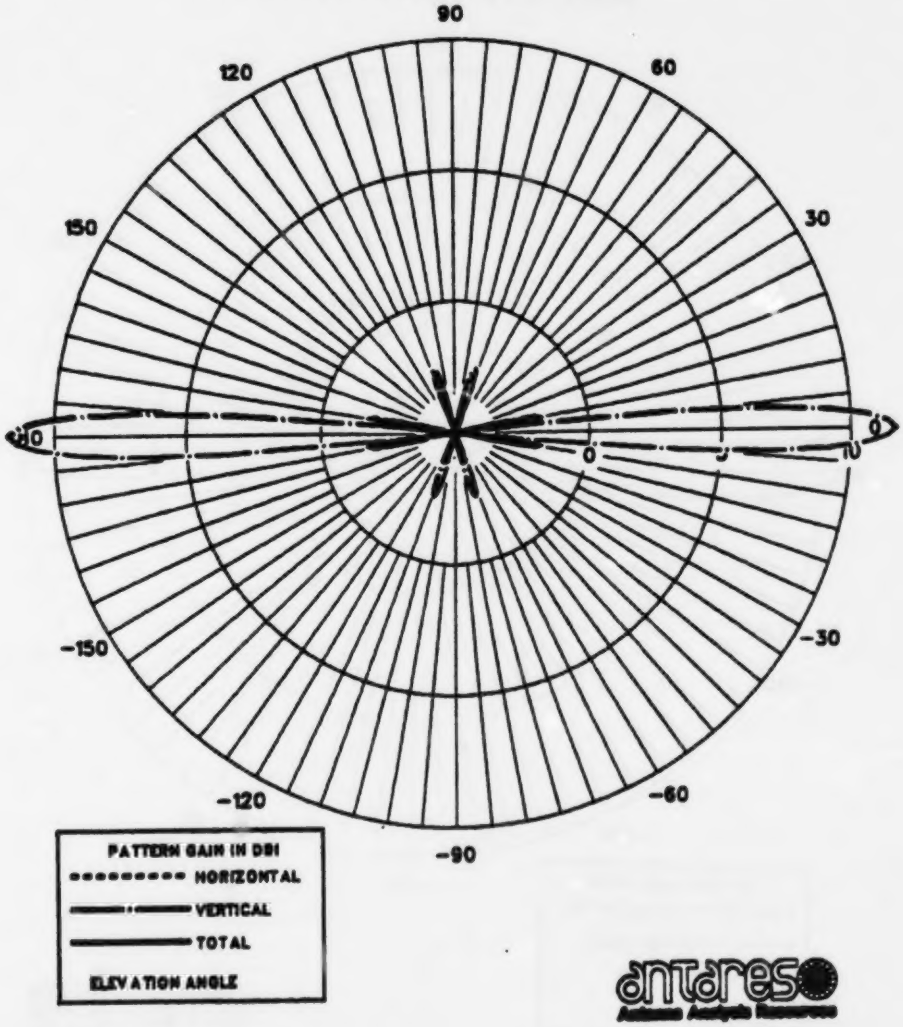

antares
Antenna Analysis Resources

434<

FIGURE D 19

EIGHT HALF-WAVE DIPOLES COAXIALLY ARRAYED 0.7 WAVE SPACING

VERTICAL PATTERN AT BORESITE

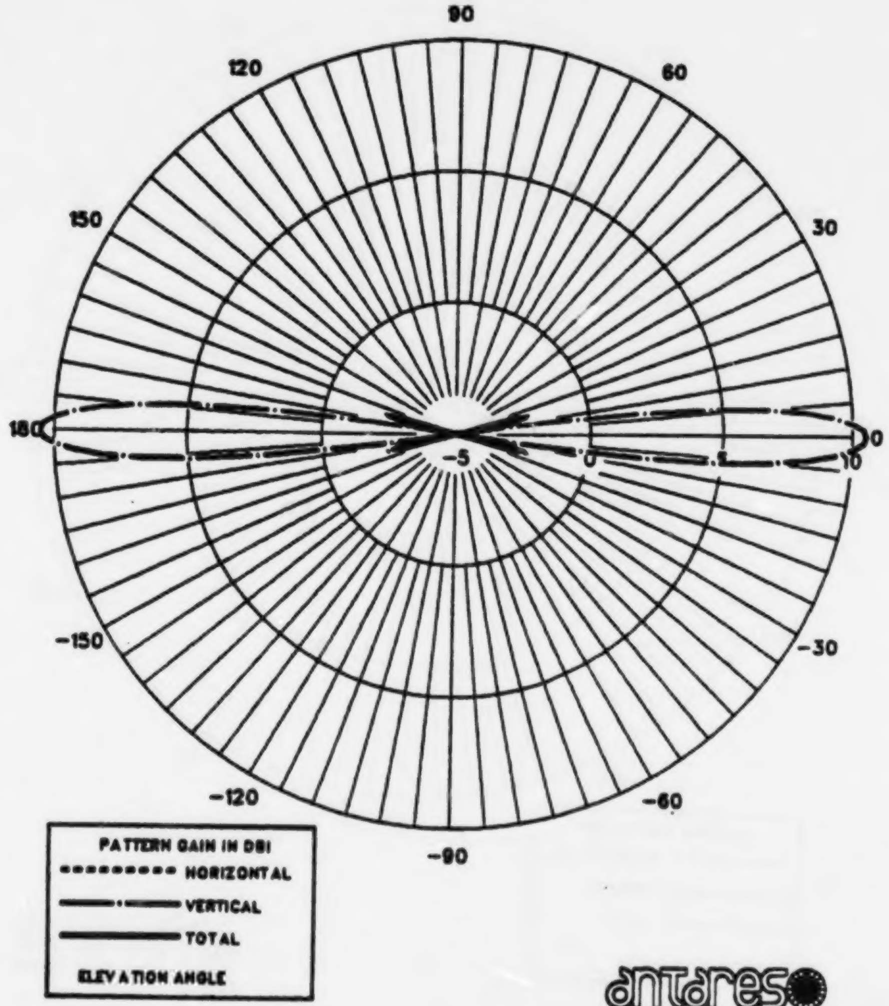

antares
Antenna Analysis Resources

FIGURE D 20

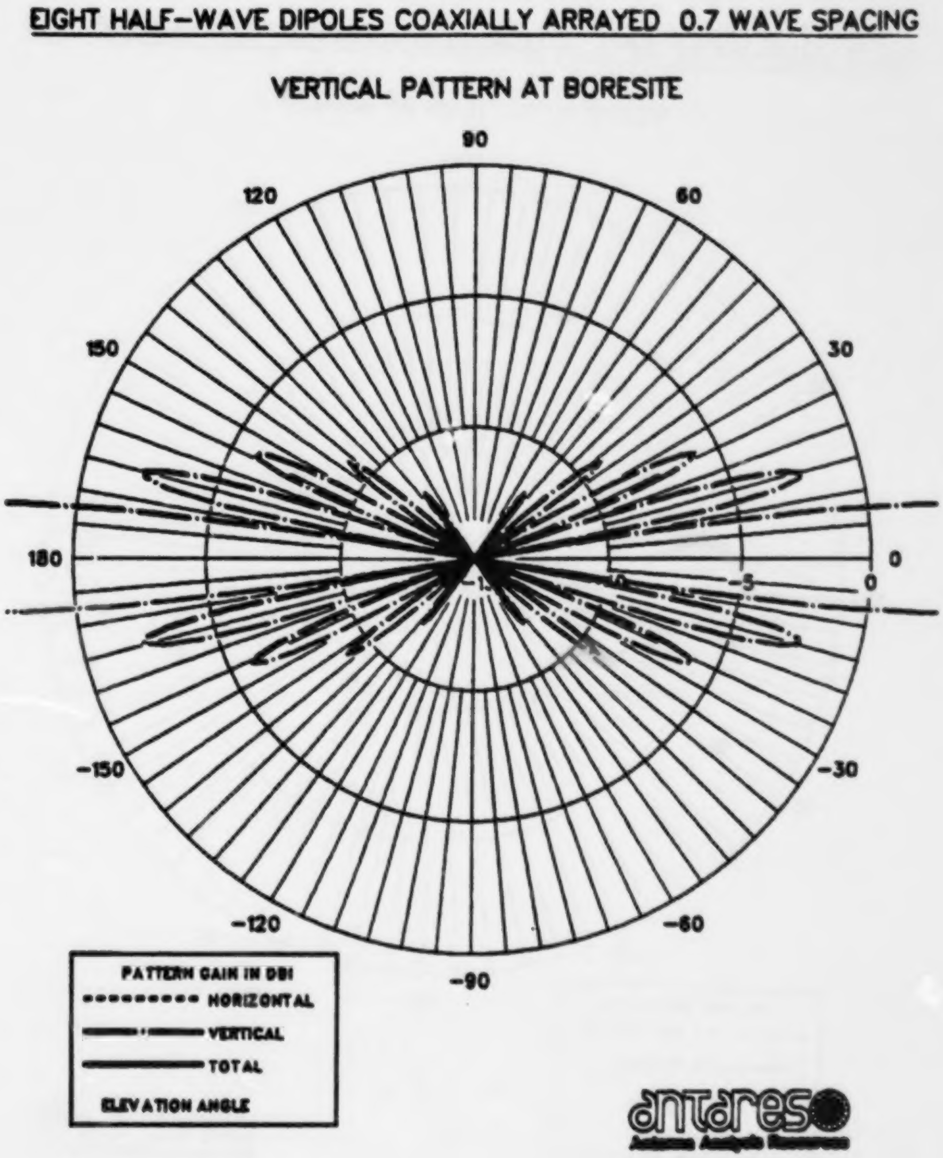
EIGHT HALF-WAVE DIPOLES COAXIALLY ARRAYED 0.7 WAVE SPACING

VERTICAL PATTERN AT BORESITE

antares
Antenna Analysis Resources

FIGURE D 21

EIGHT HALF-WAVE DIPOLES COAXIALLY ARRAYED 0.5 WAVE SPACING

VERTICAL PATTERN AT BORESITE

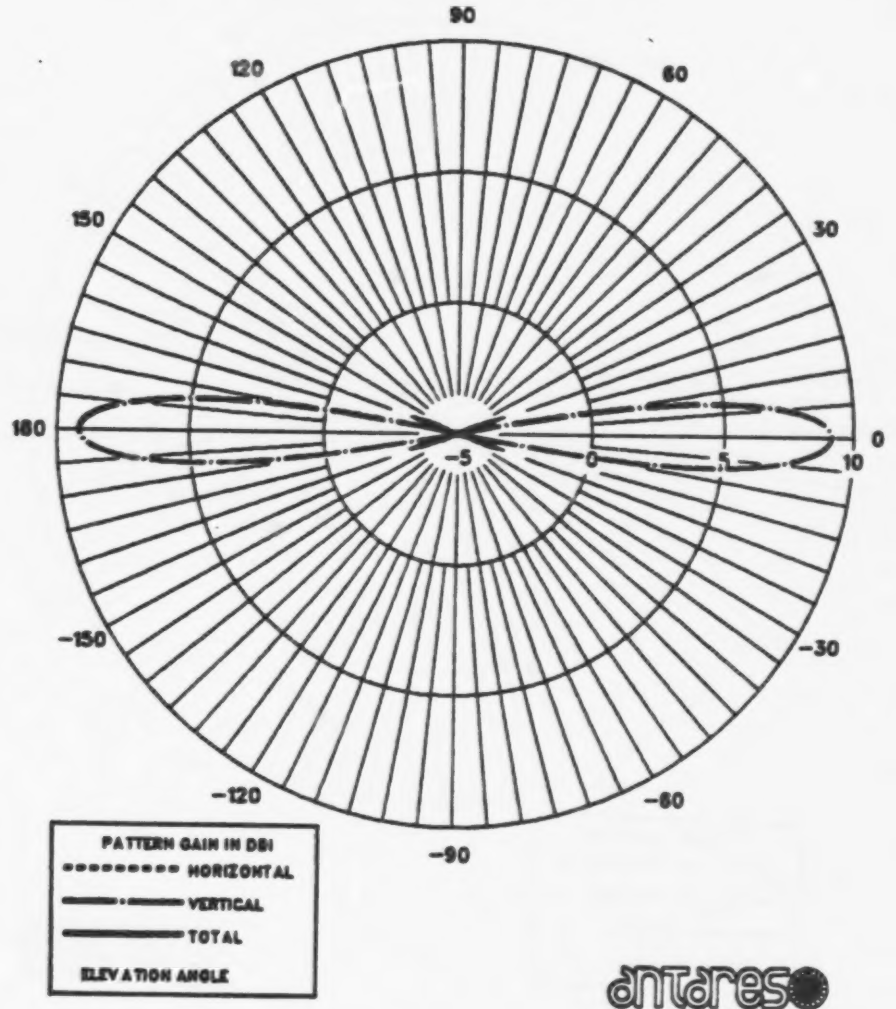

antares
Antenna Analysis Resources

FIGURE D 22

JASIK HALF WAVE DIPOLES AT 0.5 WAVE SPACING

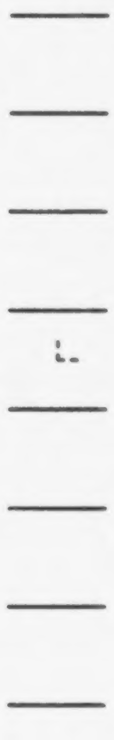

THETA = 90.00 PHI = 0.00 ETA = 90.00

FIGURE D 23

EIGHT HALF-WAVE DIPOLES BROADSIDE ARRAYED 1.2 WAVE SPACING

VERTICAL PATTERN AT BORESITE

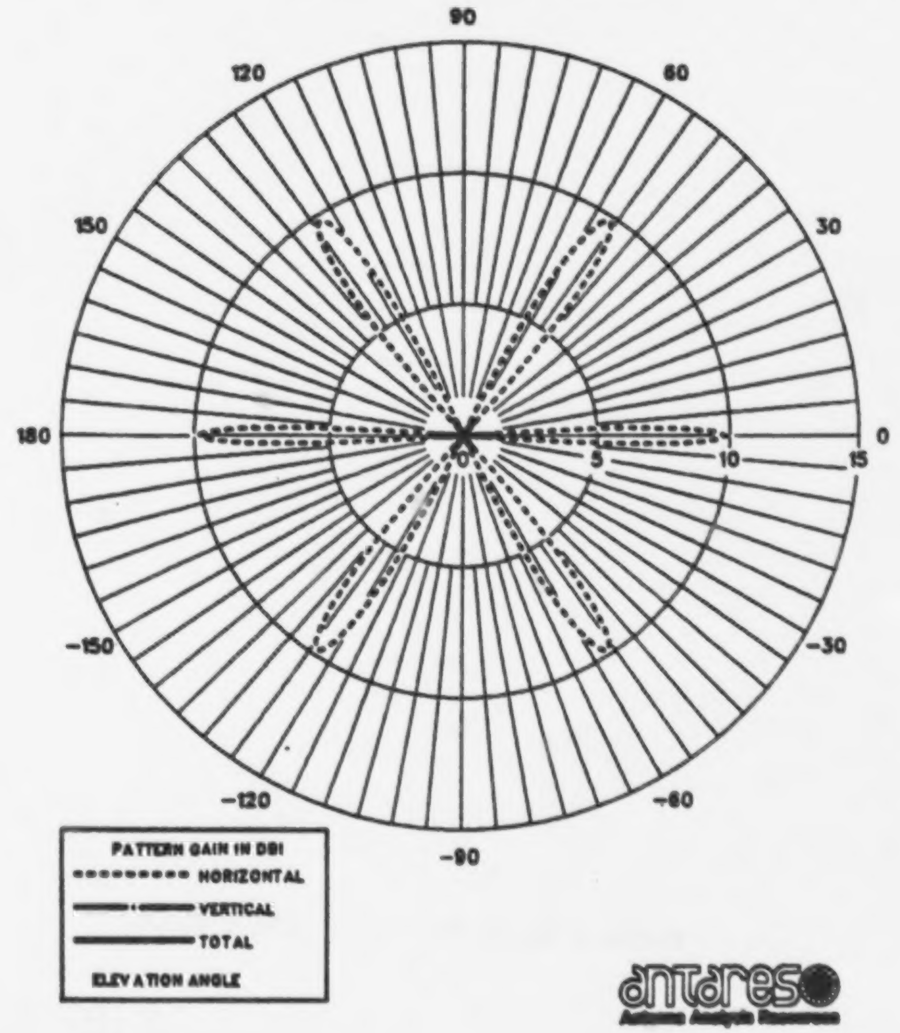

antares
Antenna Analysis Resources

FIGURE D 24

EIGHT HALF-WAVE DIPOLES BROADSIDE ARRAYED 1.0 WAVE SPACING

VERTICAL PATTERN AT BORESITE

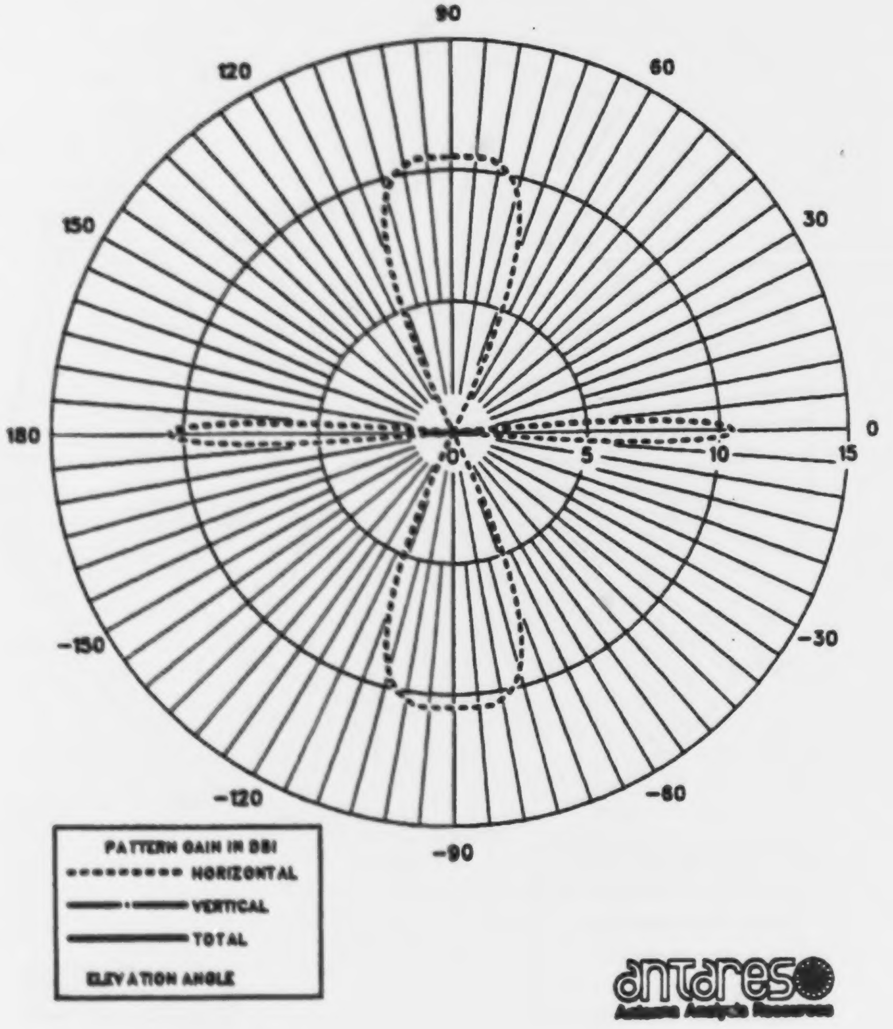

FIGURE D 25

EIGHT HALF-WAVE DIPOLES BROADSIDE ARRAYED 0.95 WAVE SPACING

VERTICAL PATTERN AT BORESITE

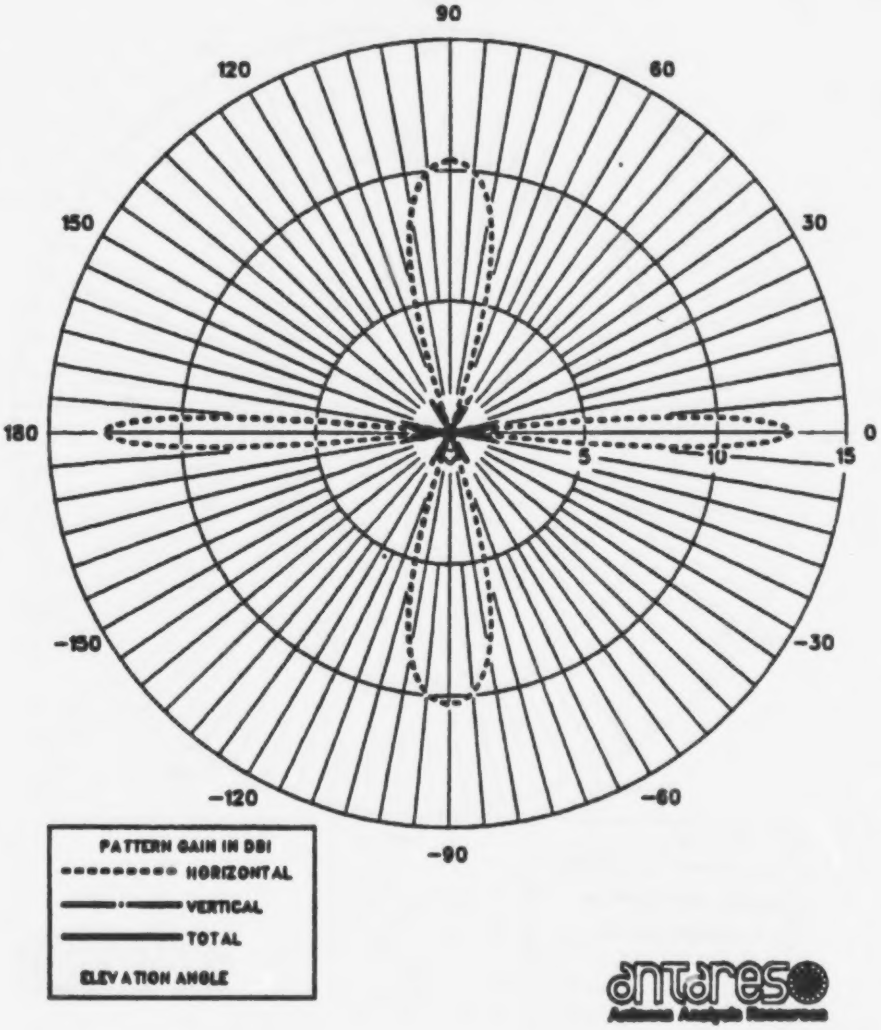

FIGURE D 26

EIGHT HALF-WAVE DIPOLES BROADSIDE ARRAYED 0.9 WAVE SPACING

VERTICAL PATTERN AT BORESITE

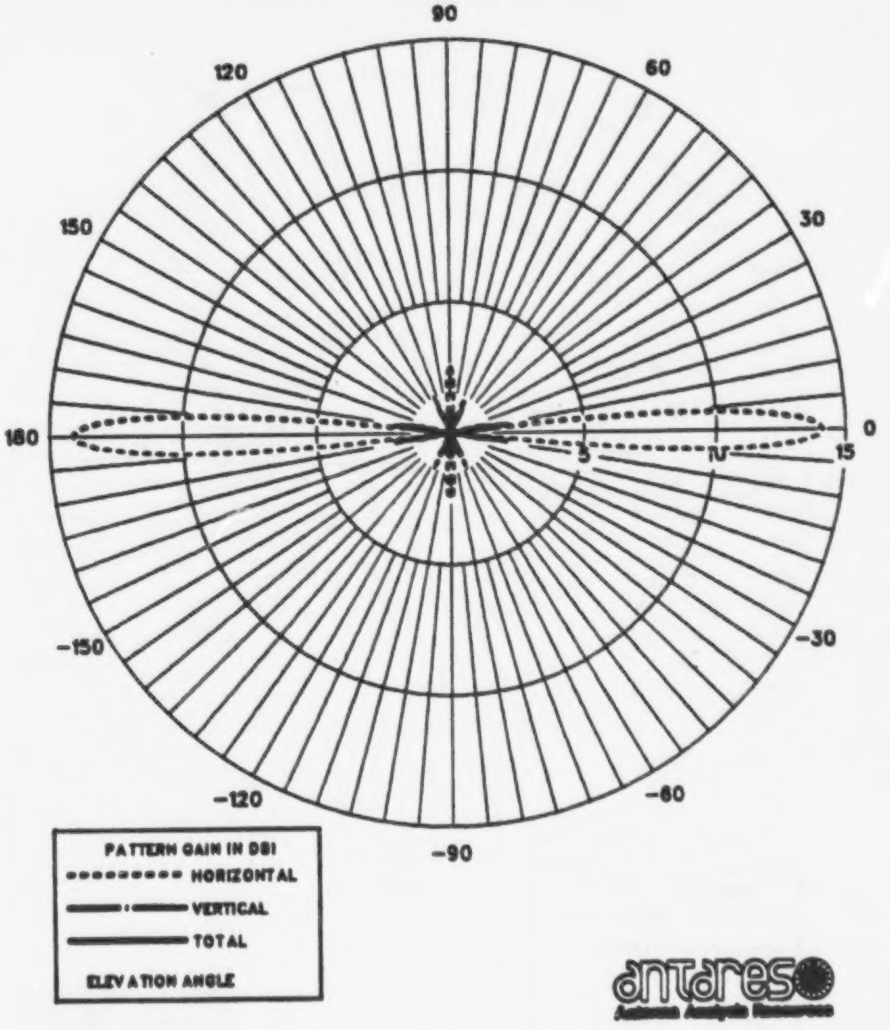

FIGURE D 27

EIGHT HALF-WAVE DIPOLES BROADSIDE ARRAYED 0.7 WAVE SPACING

VERTICAL PATTERN AT BORESITE

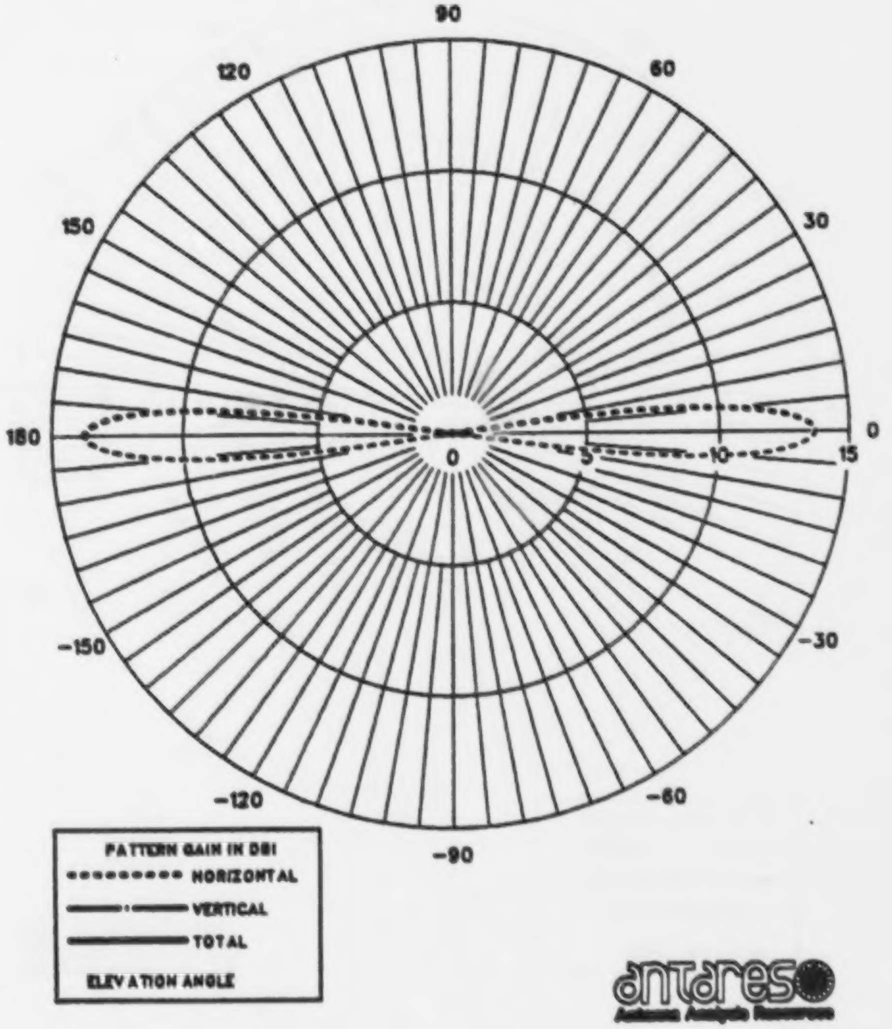

FIGURE D 28

EIGHT HALF-WAVE DIPOLES BROADSIDE ARRAYED 0.5 WAVE SPACING

VERTICAL PATTERN AT BORESITE

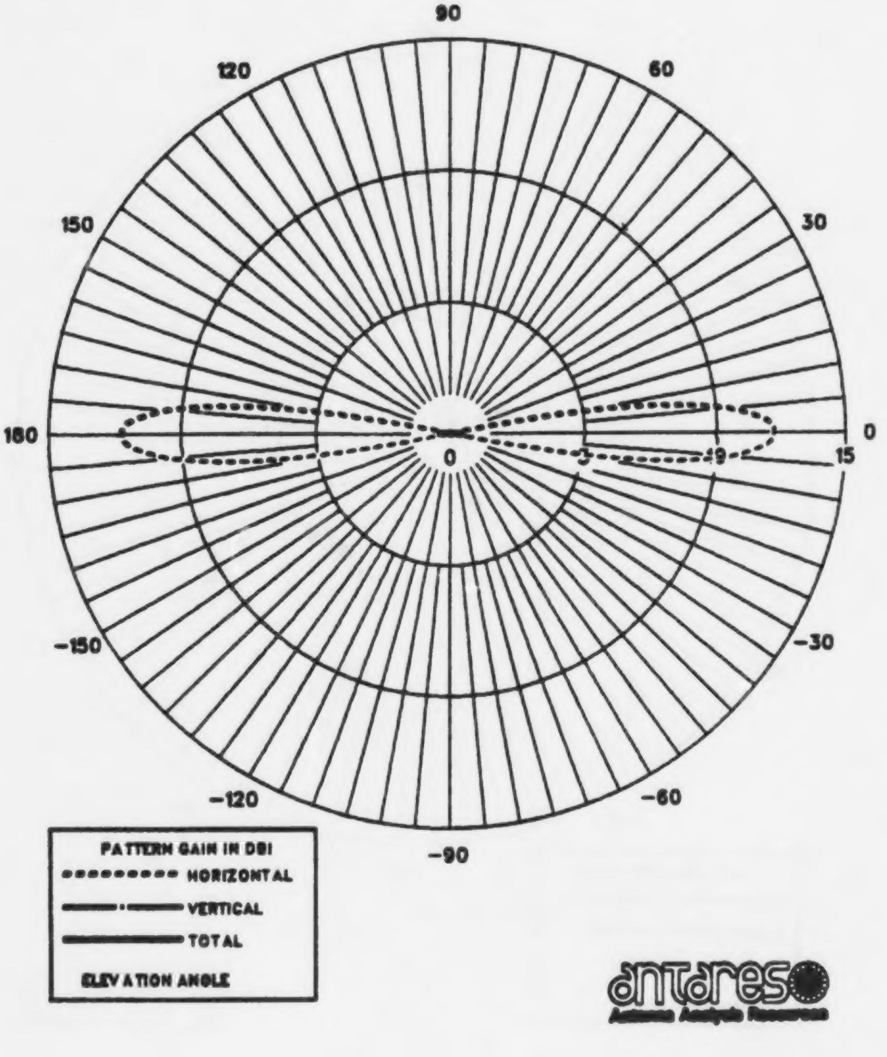

FIGURE D 29

EIGHT HALF-WAVE DIPOLES BROADSIDE ARRAYED 0.1 WAVE SPACING

VERTICAL PATTERN AT BORESITE

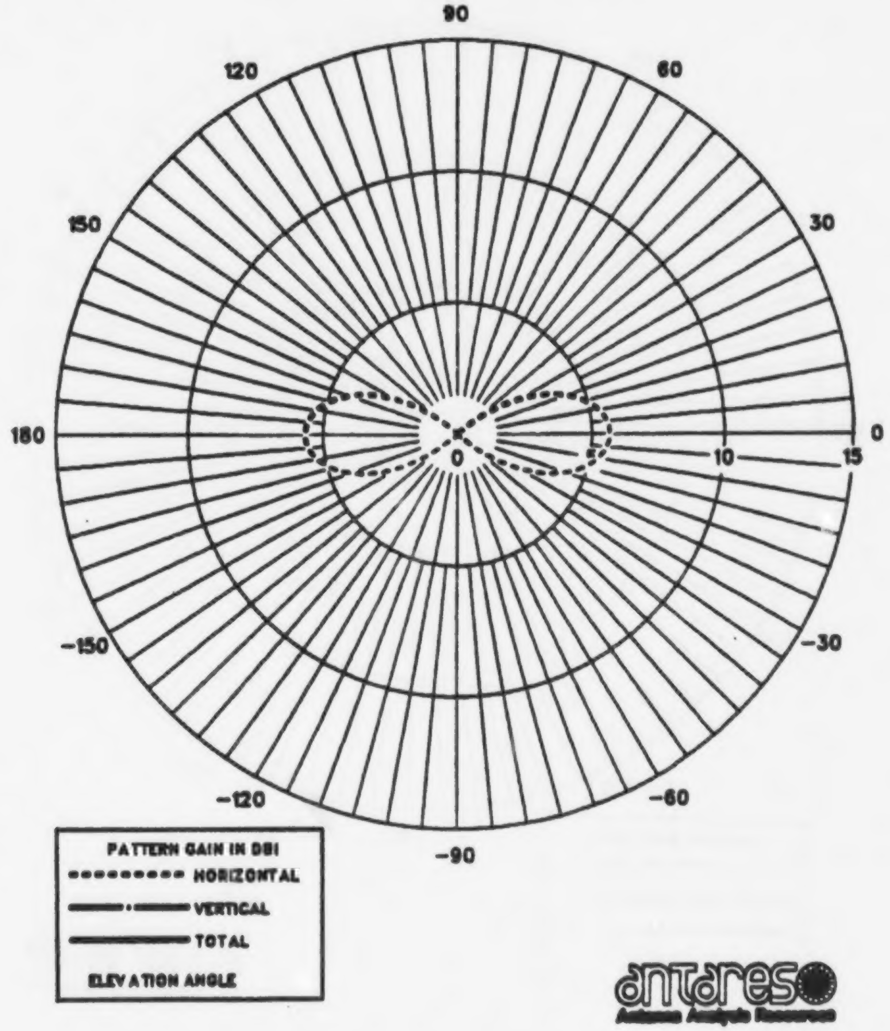

antares
Antenna Analysis Resources

FIGURE D 30

THE FMH ELEMENT

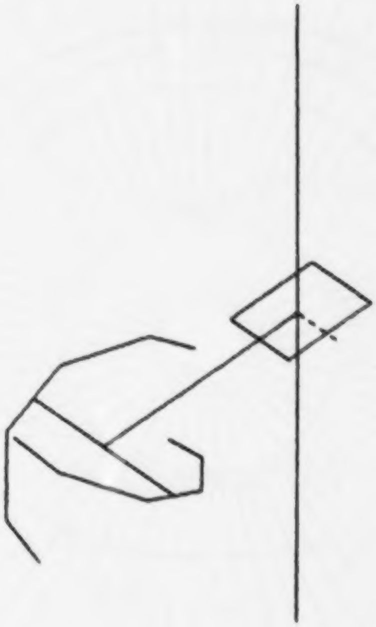

THETA = 45.00 PHI = 45.00 ETA = 90.00

FIGURE D 31

THE FMH ELEMENT

AZIMUTH PLANE PATTERN AT THE HORIZON

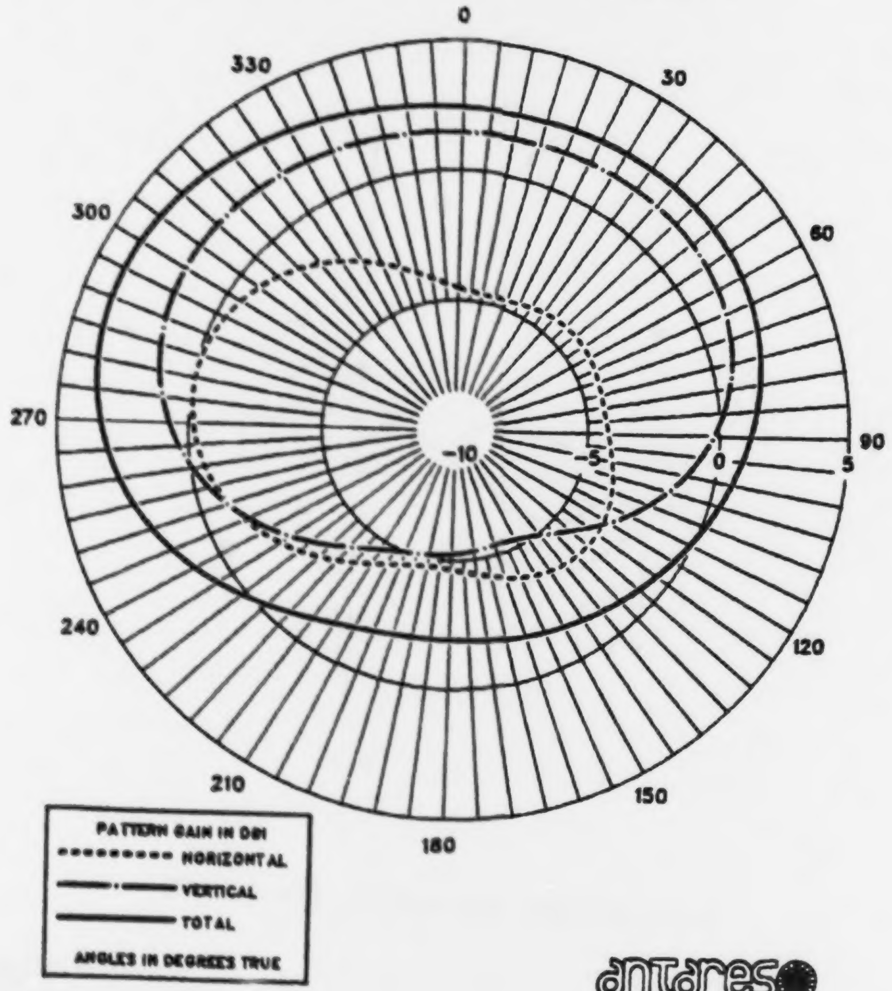

antares
Antenna Analysis Resources

FIGURE D 32

THE FMH ELEMENT

VERTICAL PLANE PATTERN AT "BORESIGHT"

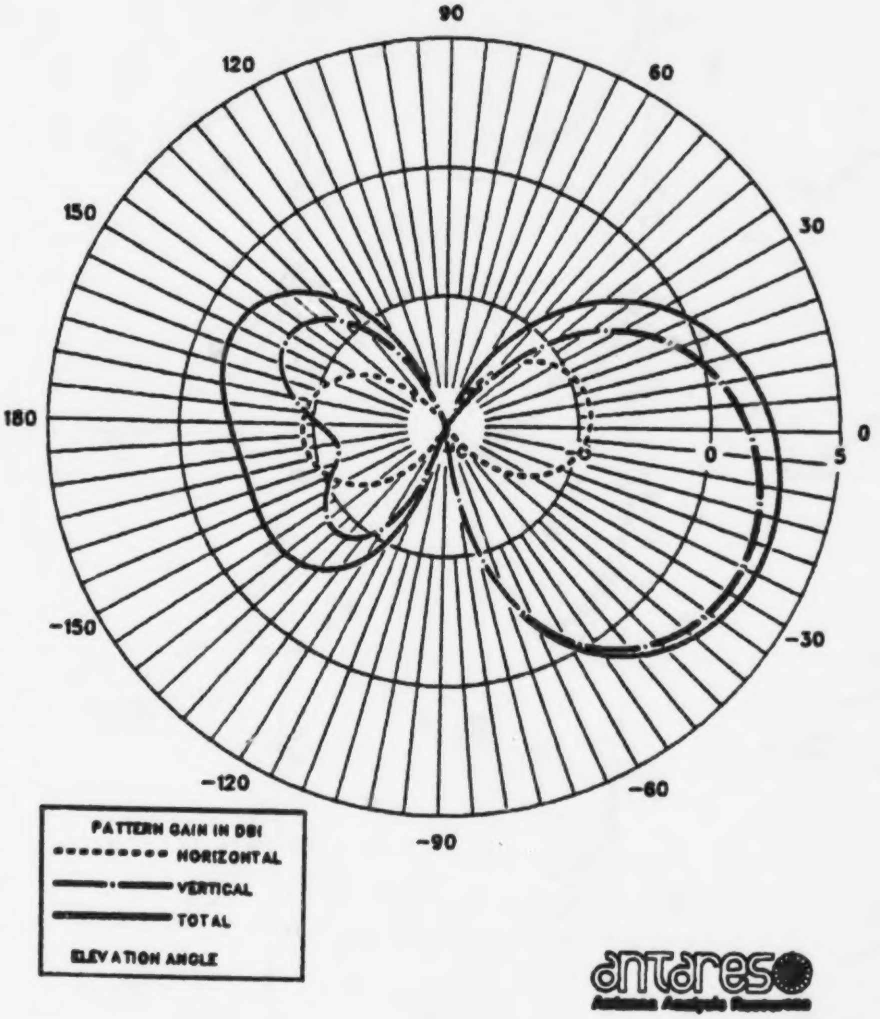

FIGURE D 33

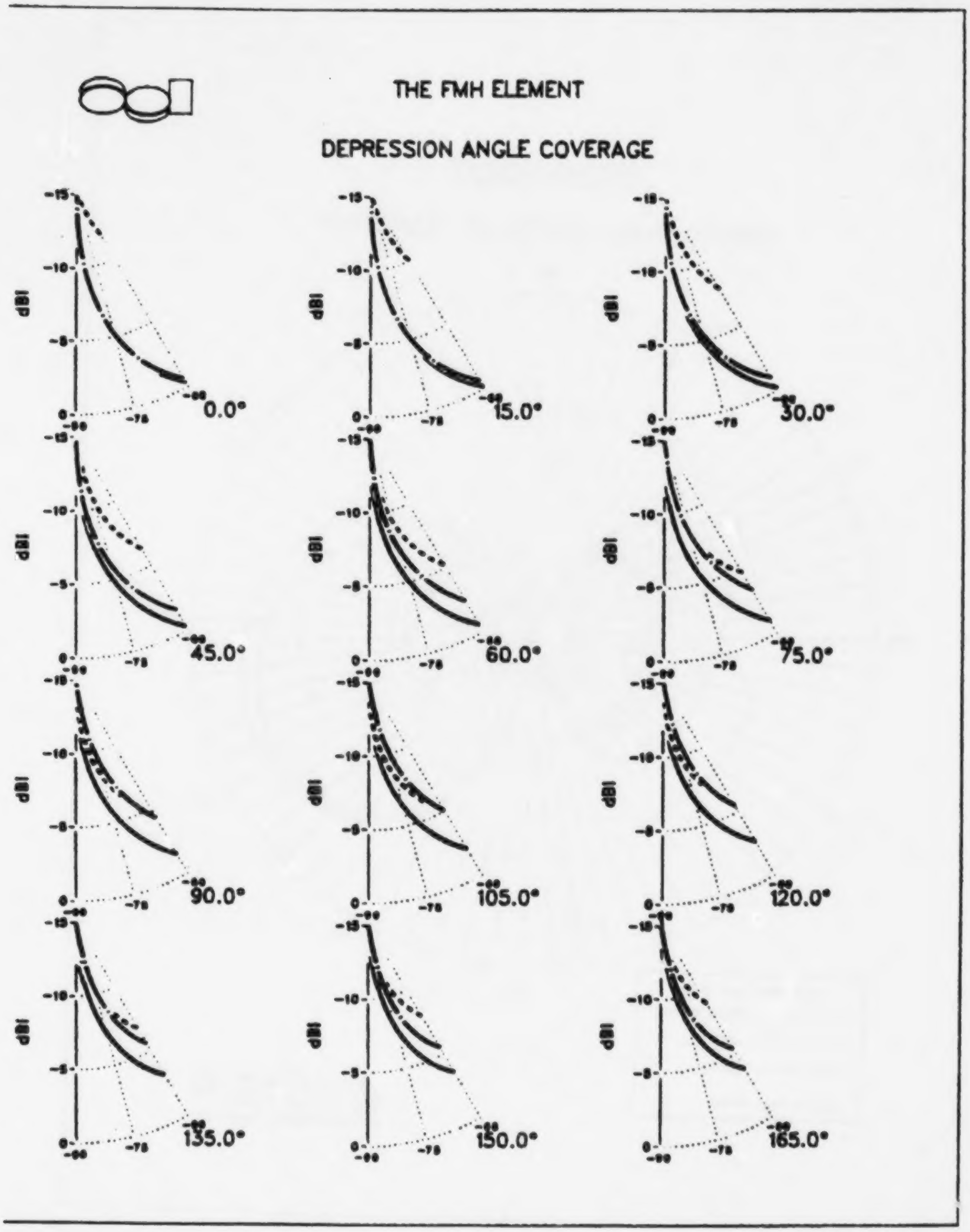
THE FMH ELEMENT
DEPRESSION ANGLE COVERAGE
dBi
-15
-10
-5
0
-90
-75
-60
0.0°
15.0°
30.0°
45.0°
60.0°
75.0°
90.0°
105.0°
120.0°
135.0°
150.0°
165.0°

FIGURE D 34

THE FMH ELEMENT

DEPRESSION ANGLE COVERAGE

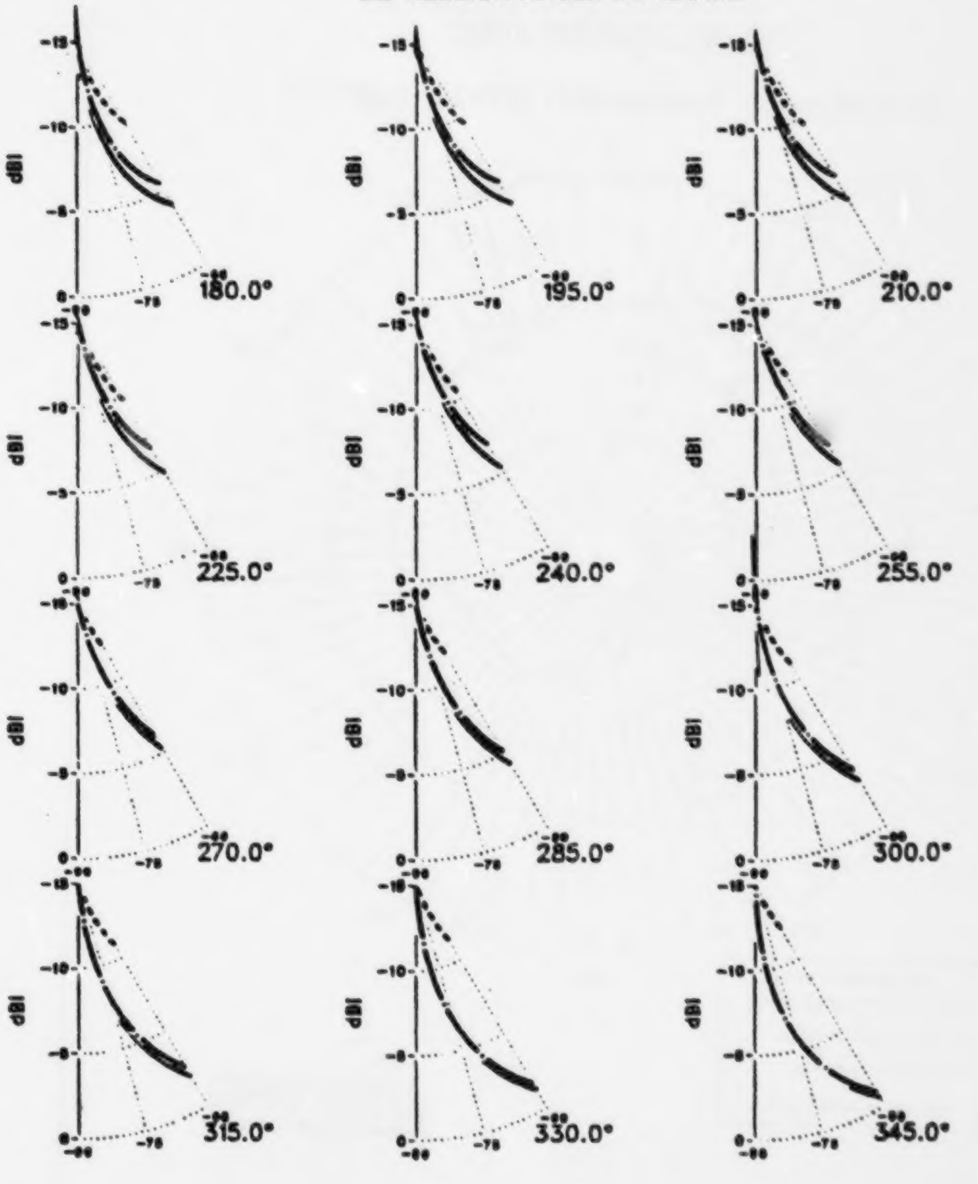

450<

FIGURE D 35

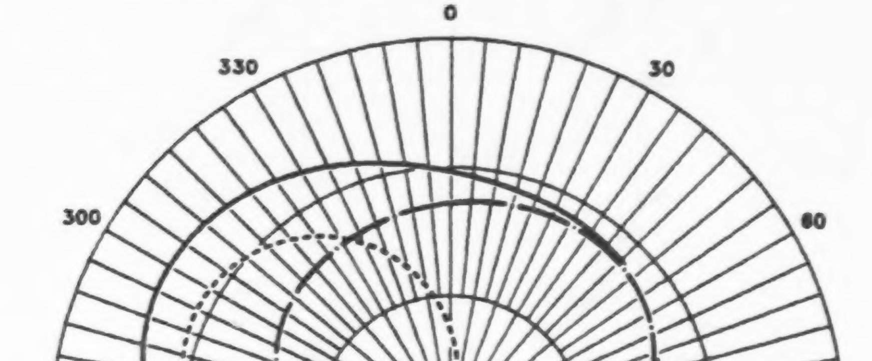

THE FMH 2 ELEMENT ARRAY

SPACING OF 0.2 WAVELENGTHS BETWEEN ELEMENTS

FIGURE D 36

THE FMH 2 ELEMENT ARRAY

SPACING OF 0.2 WAVELENGTHS BETWEEN ELEMENTS

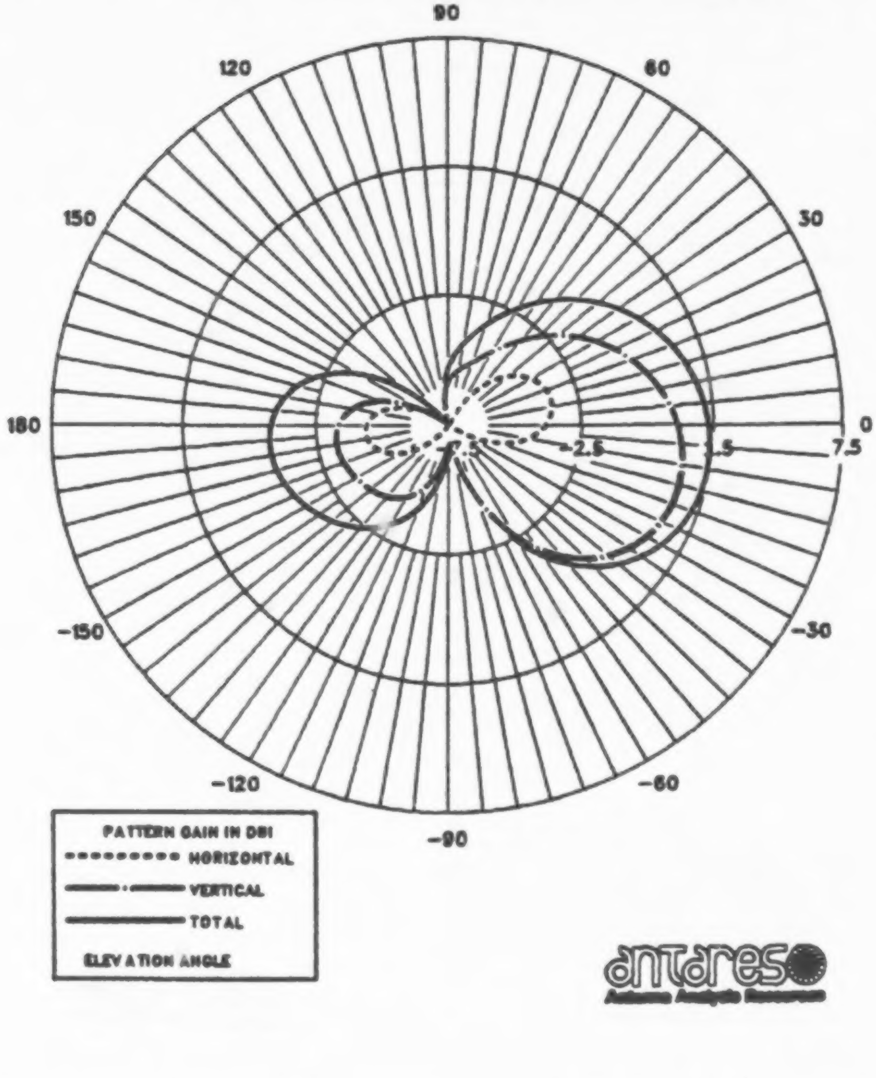

452<

FIGURE D 37

THE FMH 2 ELEMENT ARRAY

SPACING OF 0.4 WAVELENGTHS BETWEEN ELEMENTS

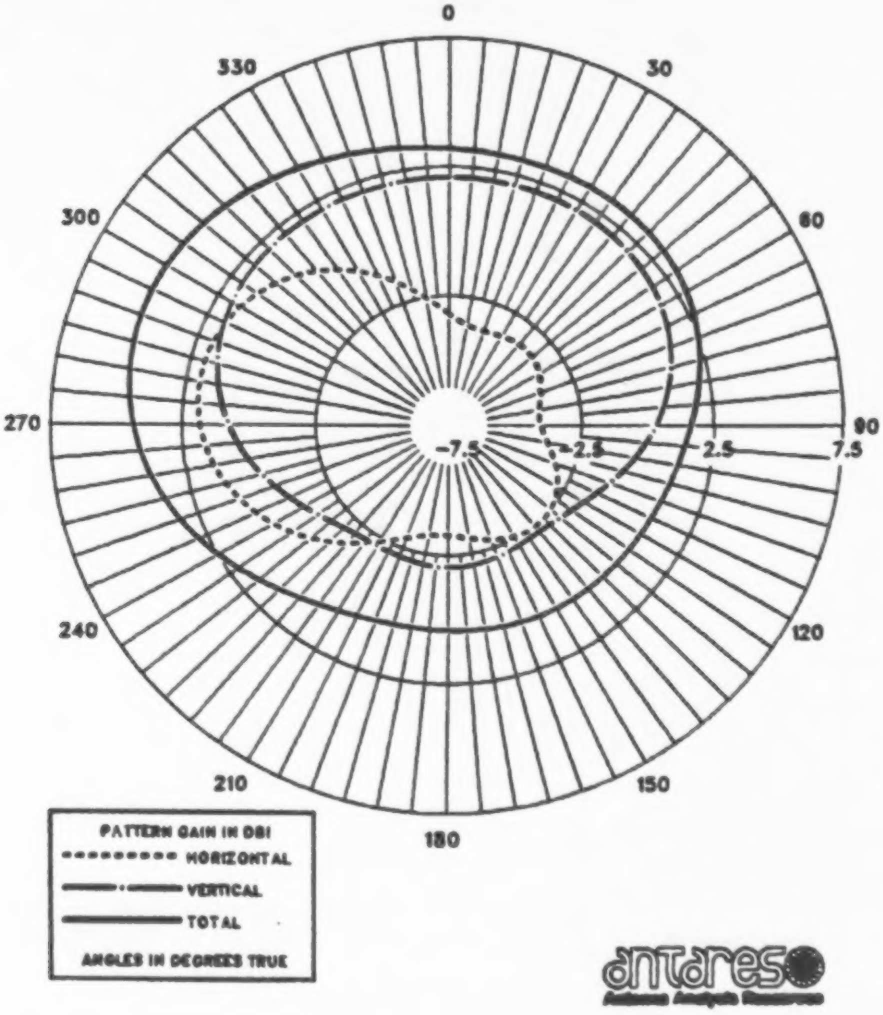

FIGURE D 38

THE FMH 2 ELEMENT ARRAY

SPACING OF 0.4 WAVELENGTHS BETWEEN ELEMENTS

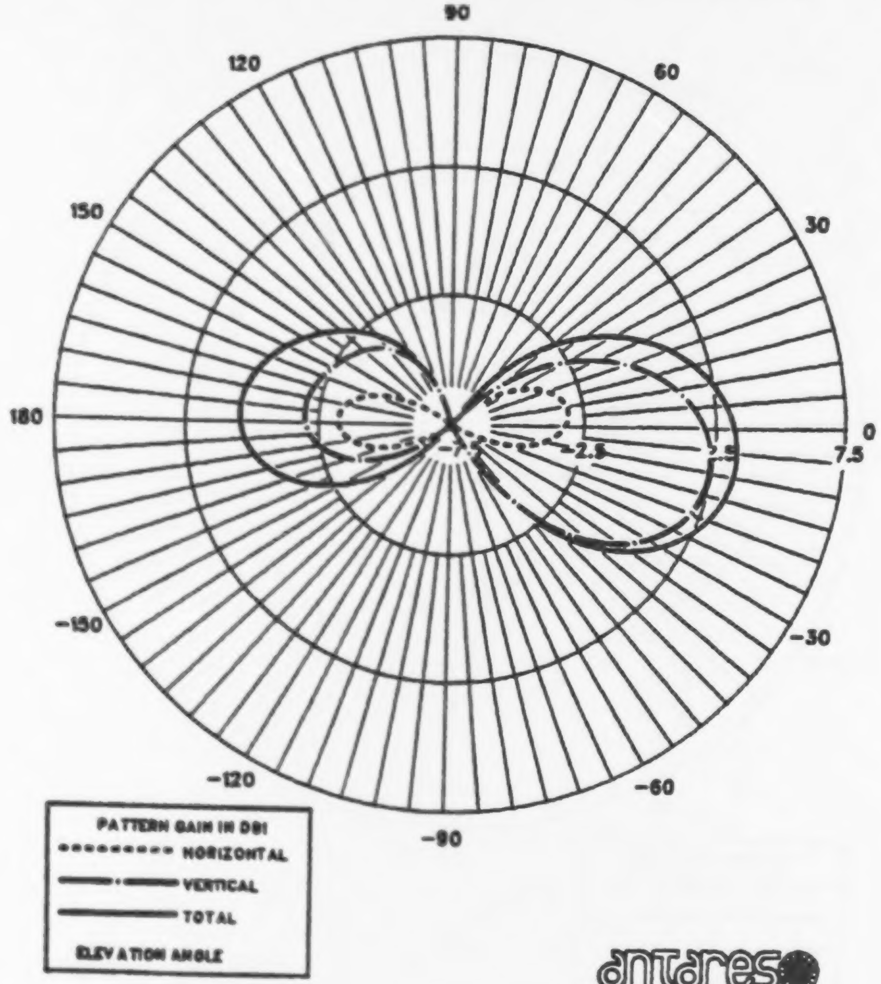

antares
Antenna Analysis Resources

FIGURE D 39

THE FMH 2 ELEMENT ARRAY

SPACING OF 0.5 WAVELENGTHS BETWEEN ELEMENTS

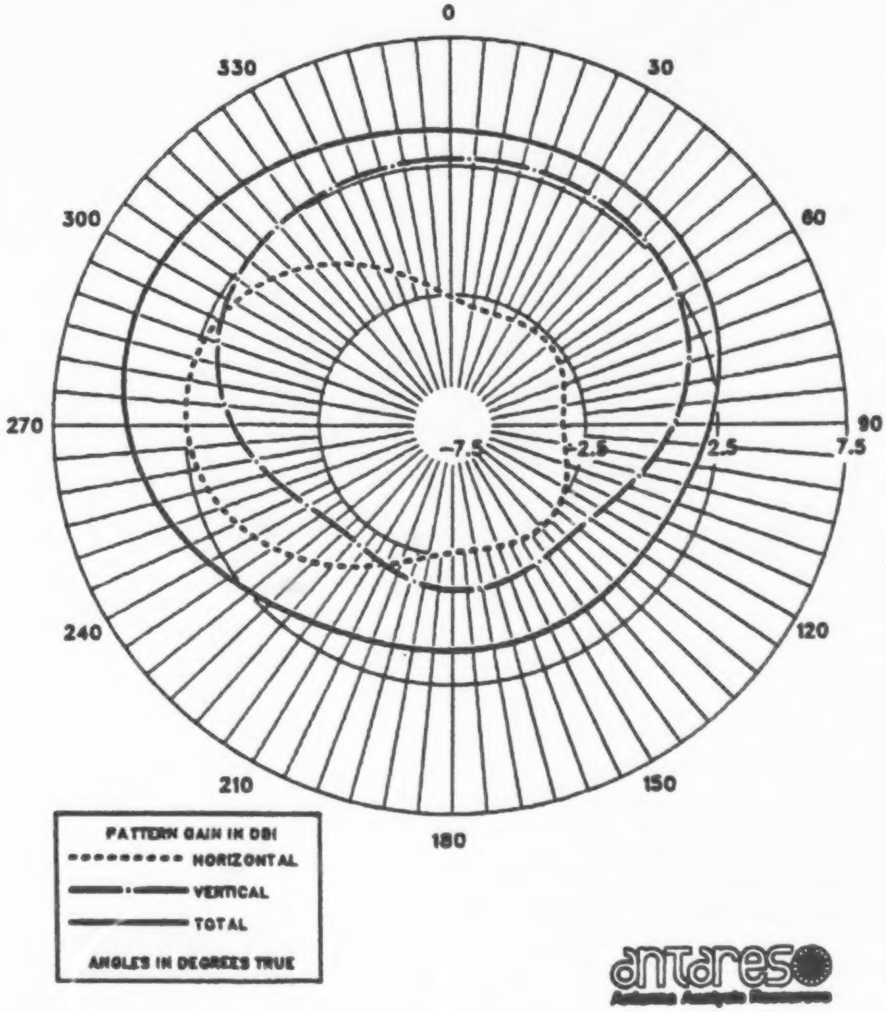

antares
Antenna Analysis Resources

FIGURE D 40

THE FMH 2 ELEMENT ARRAY

SPACING OF 0.5 WAVELENGTHS BETWEEN ELEMENTS

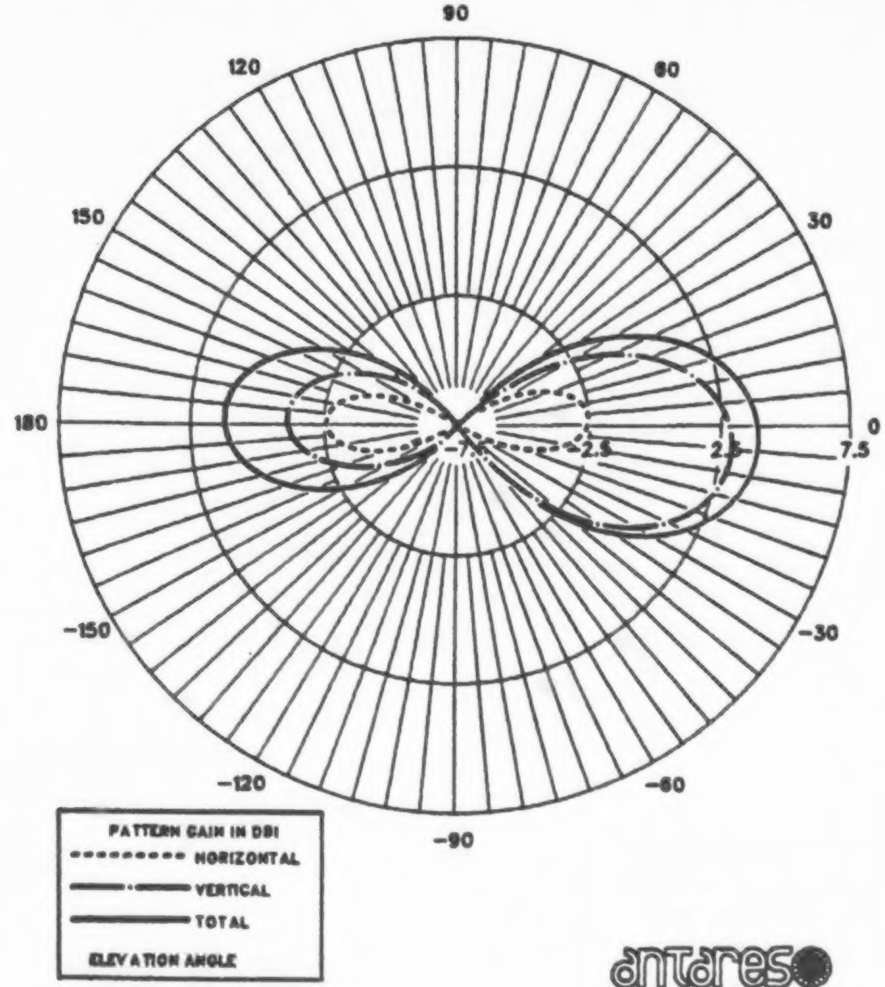

antares
Antenna Analysis Resources

FIGURE D 41

THE FMH 2 ELEMENT ARRAY

SPACING OF 0.7 WAVELENGTHS BETWEEN ELEMENTS

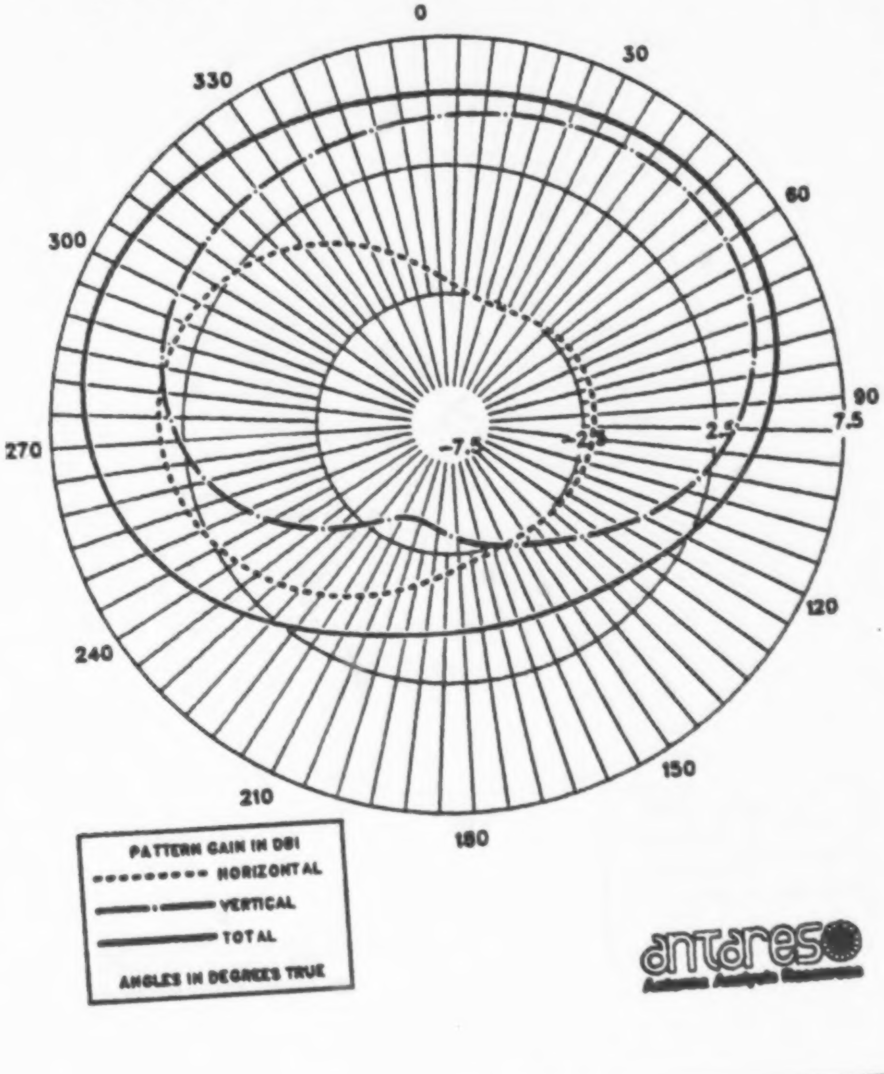

antares
Antenna Analysis Resources

FIGURE D 42

THE FMH 2 ELEMENT ARRAY

SPACING OF 0.7 WAVELENGTHS BETWEEN ELEMENTS

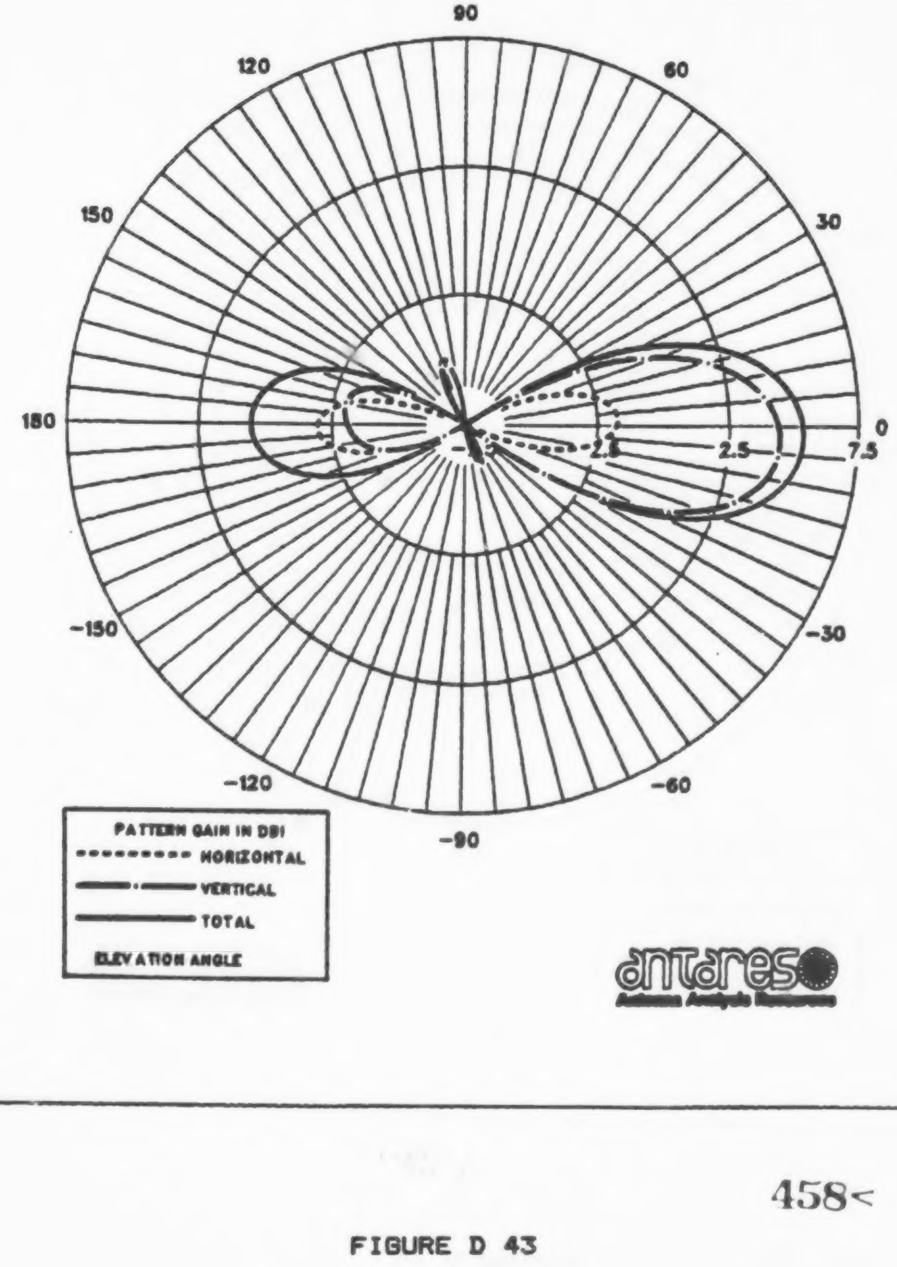

antares
Antenna Analysis Resources

FIGURE D 43

THE FMH 2 ELEMENT ARRAY

SPACING OF 0.9 WAVELENGTHS BETWEEN ELEMENTS

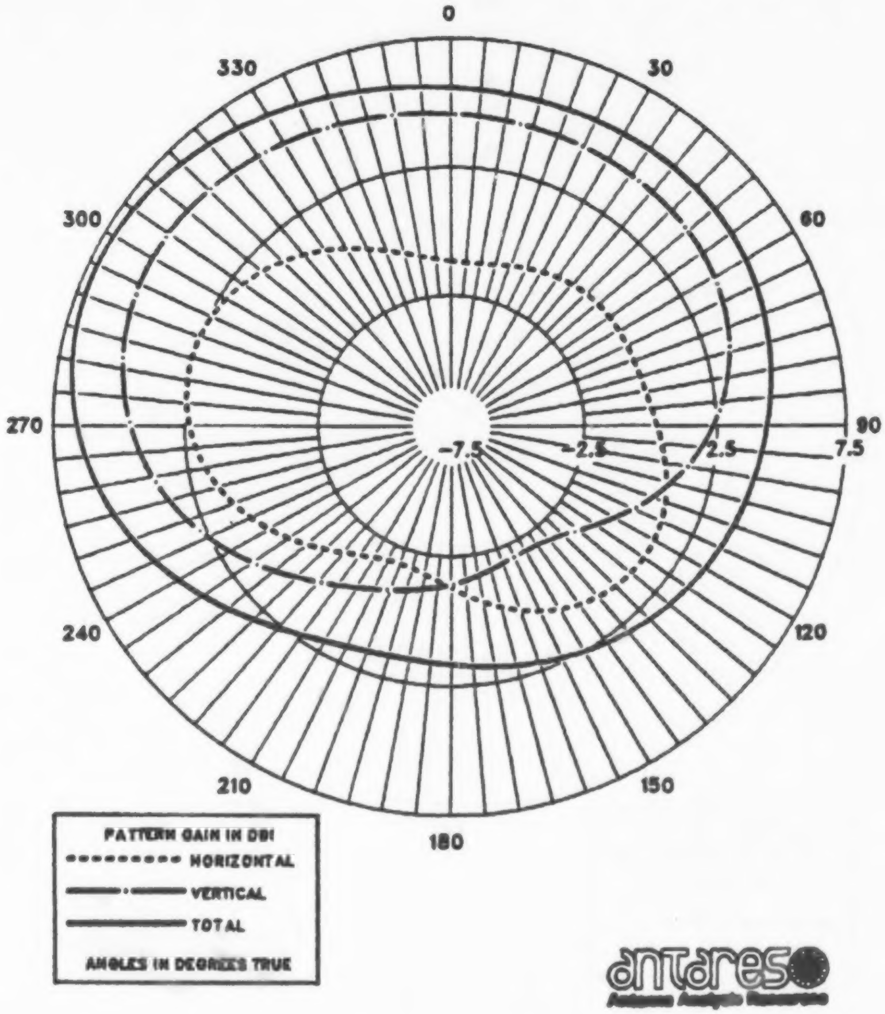

FIGURE D 44

THE FMH 2 ELEMENT ARRAY

SPACING OF 0.9 WAVELENGTHS BETWEEN ELEMENTS

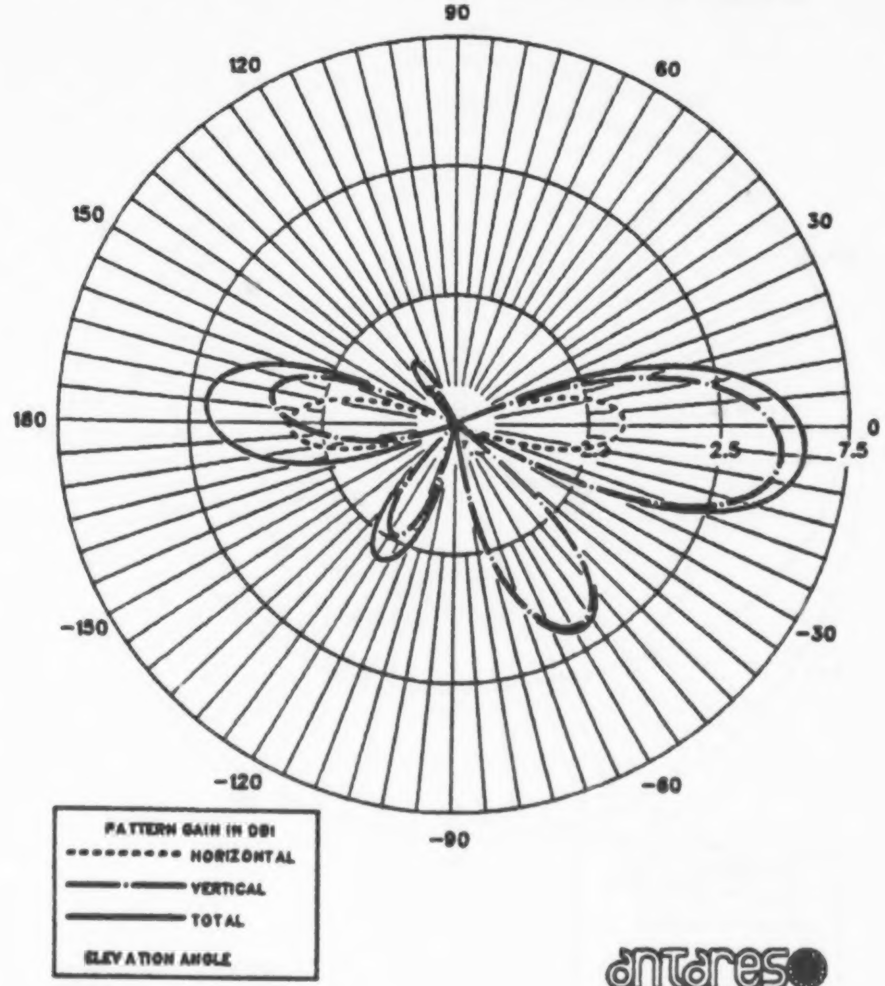

antares
Antenna Analysis Resources

FIGURE D 45

THE FMH 2 ELEMENT ARRAY

SPACING OF 1.0 WAVELENGTHS BETWEEN ELEMENTS

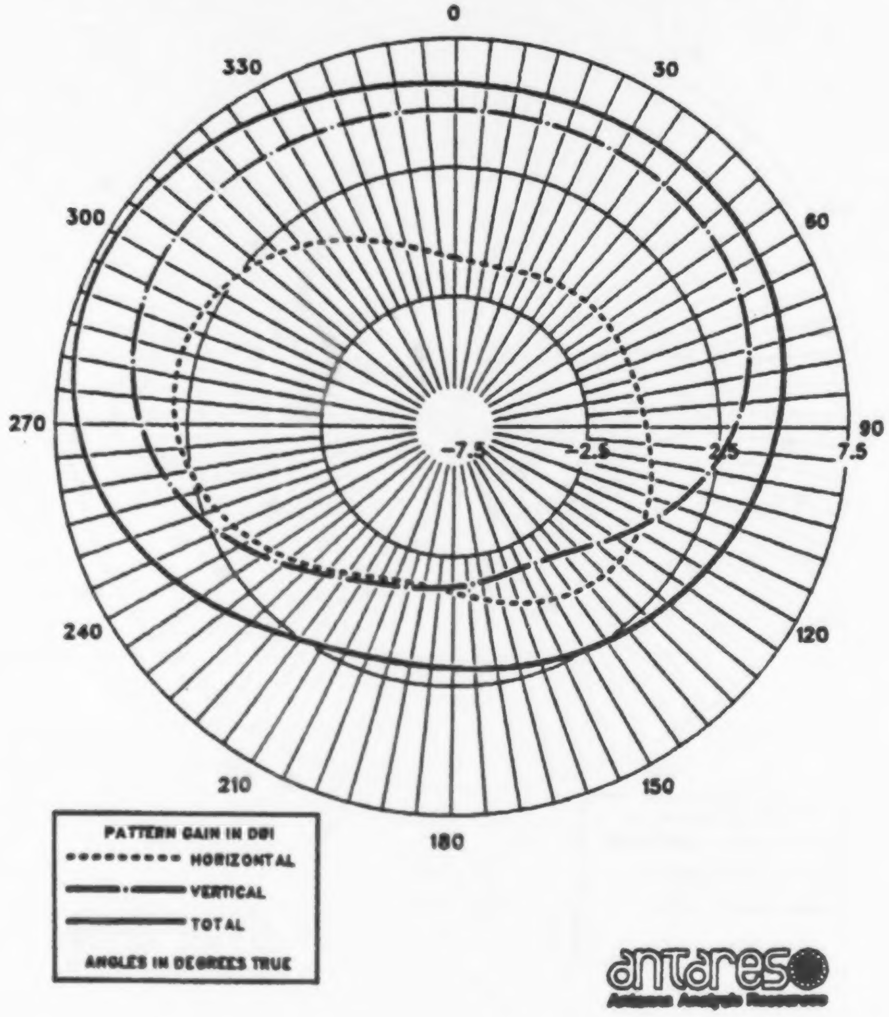

FIGURE D 46

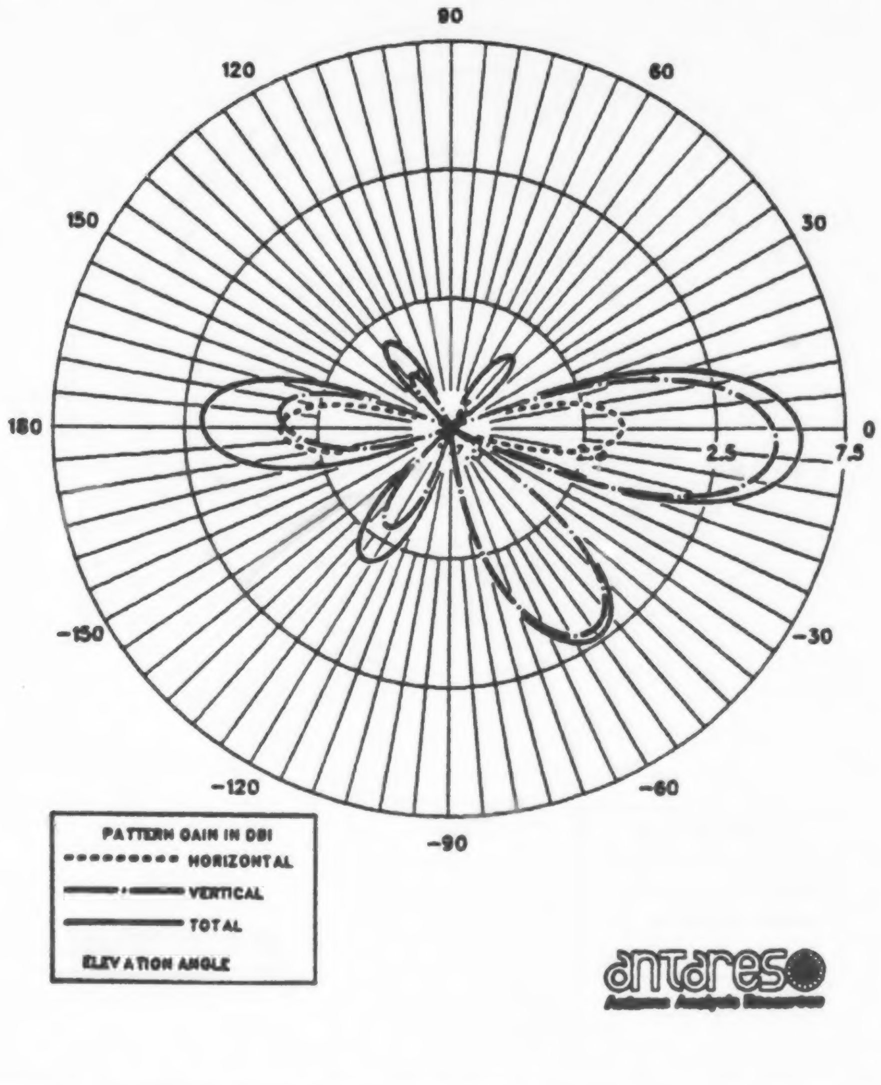

THE FMH 2 ELEMENT ARRAY

SPACING OF 1.0 WAVELENGTHS BETWEEN ELEMENTS

FIGURE D 47

THE FMH 2 ELEMENT ARRAY

SPACING OF 1.1 WAVELENGTHS BETWEEN ELEMENTS

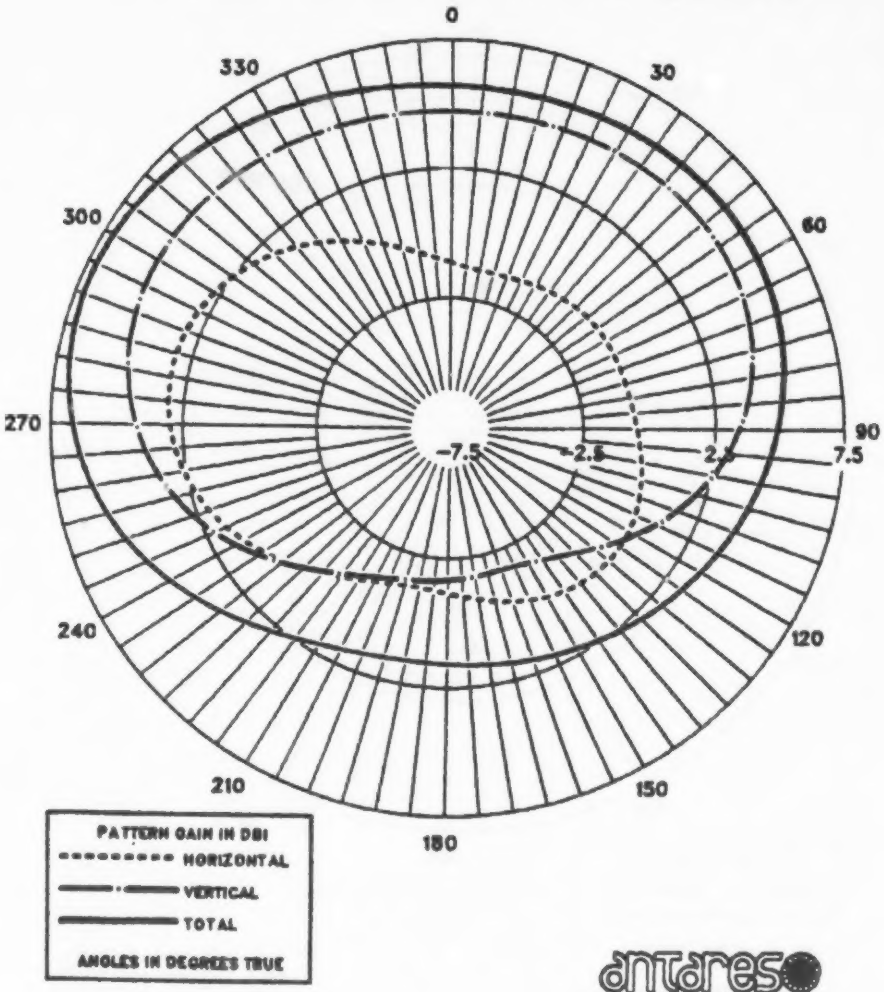

FIGURE D 48

THE FMH 2 ELEMENT ARRAY

SPACING OF 1.1 WAVELENGTHS BETWEEN ELEMENTS

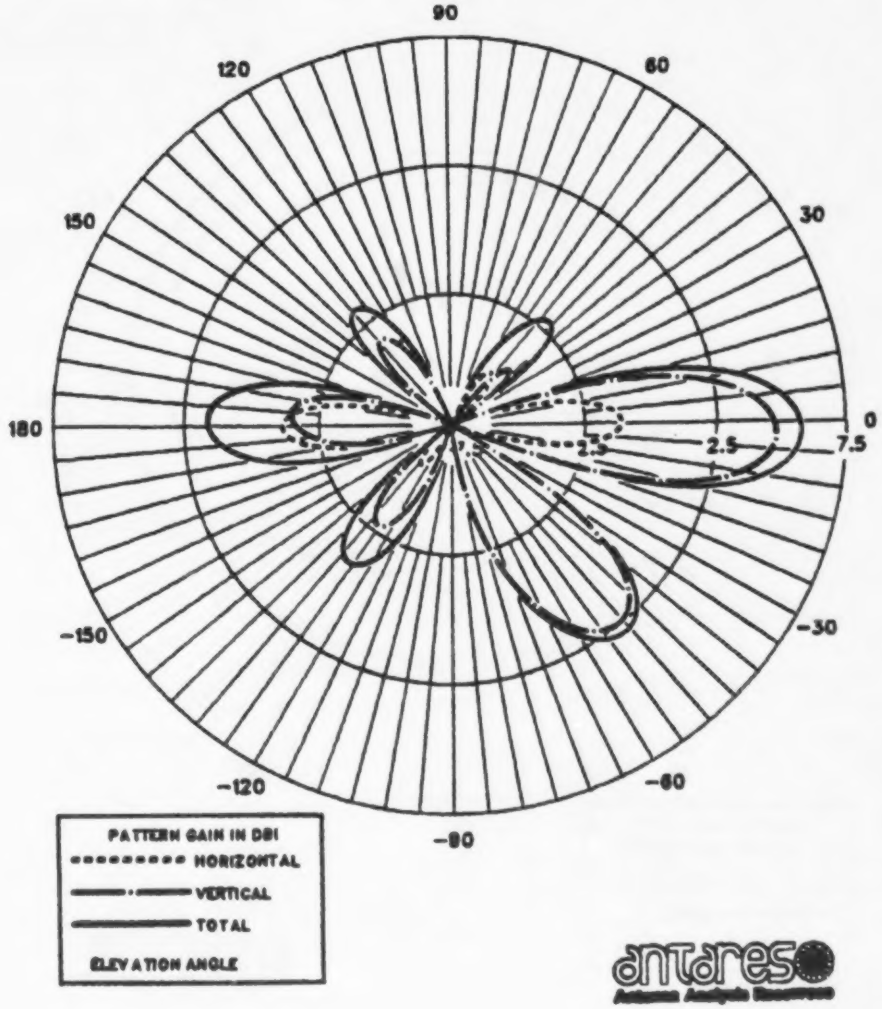

FIGURE D 49

THE FMH 2 ELEMENT ARRAY

SPACING OF 1.2 WAVELENGTHS BETWEEN ELEMENTS

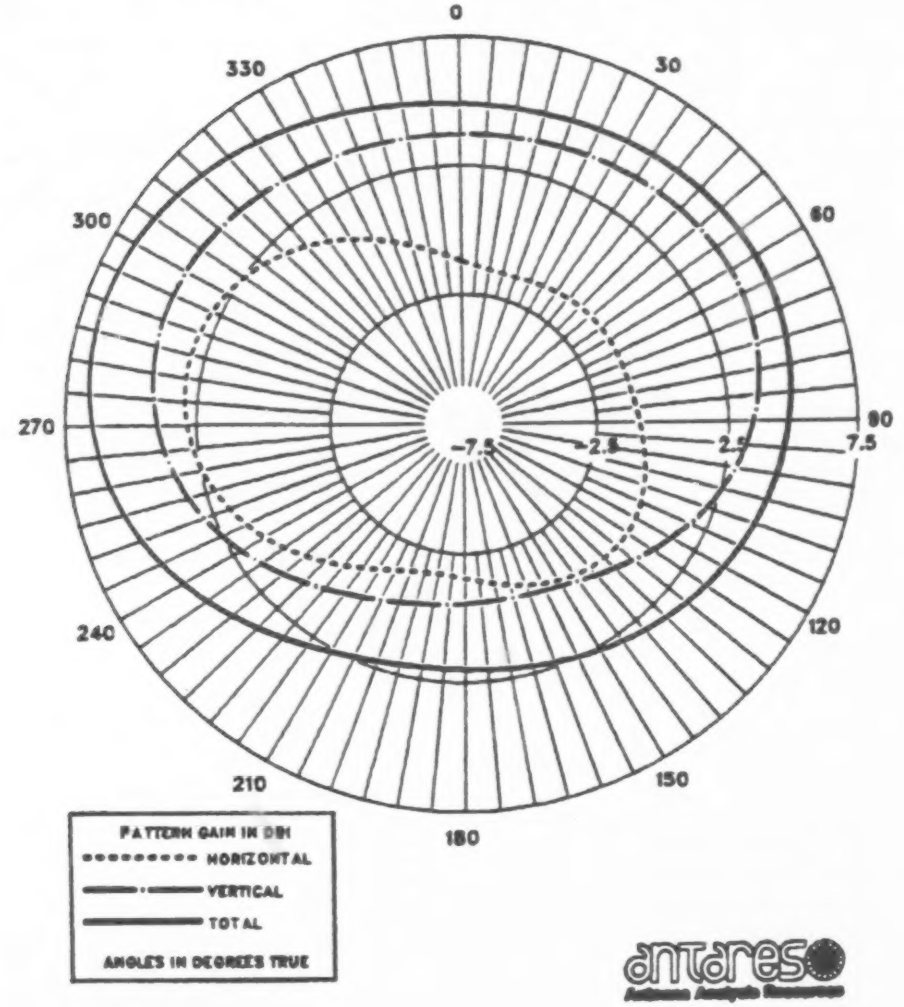

FIGURE D 50

THE FMH 2 ELEMENT ARRAY

SPACING OF 1.2 WAVELENGTHS BETWEEN ELEMENTS

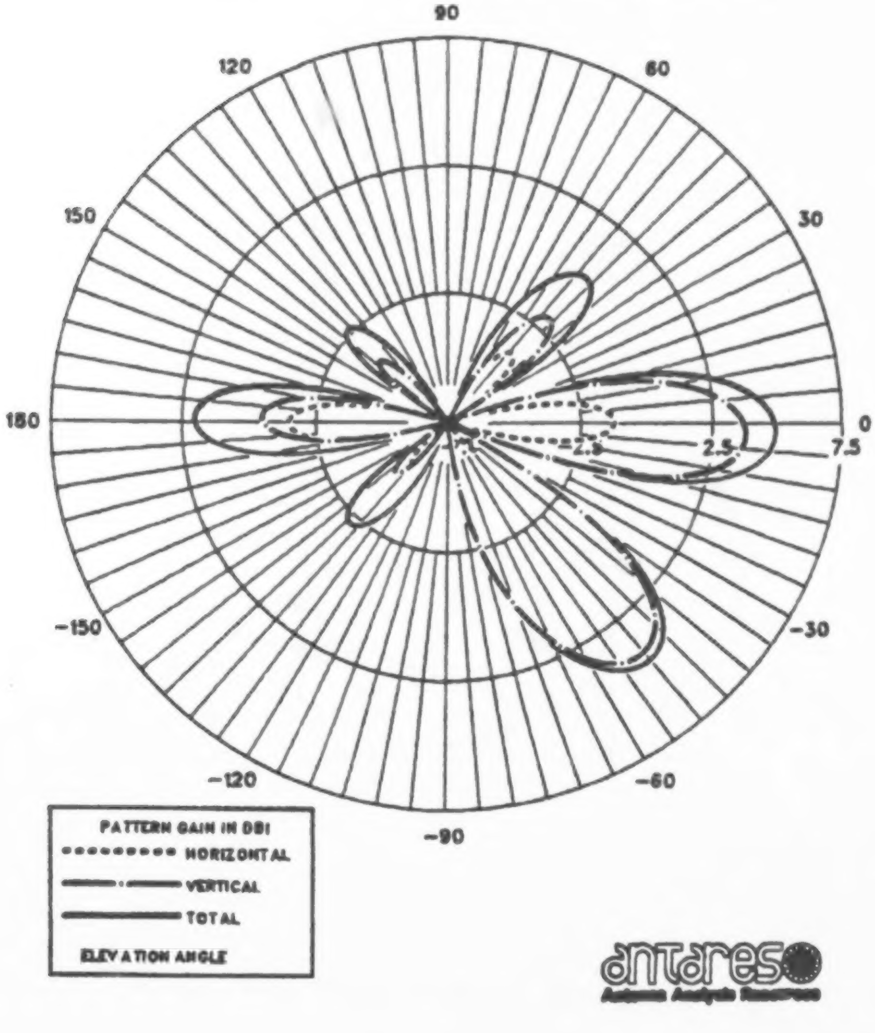

FIGURE D 51

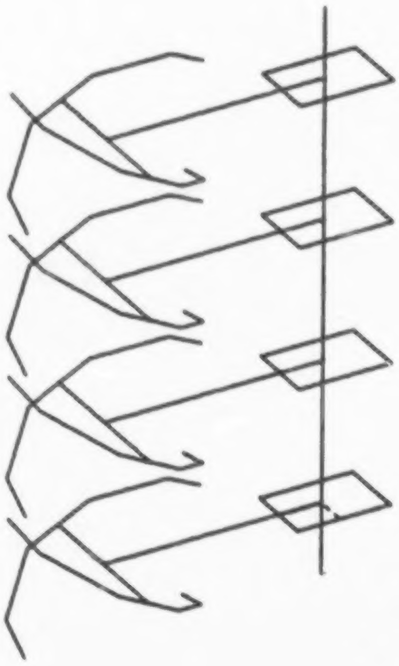

antares
Antenna Analysis Resources

FIGURE D 52

THE FMH 4 ELEMENT ARRAY

SPACING OF 0.2 WAVELENGTHS BETWEEN ELEMENTS

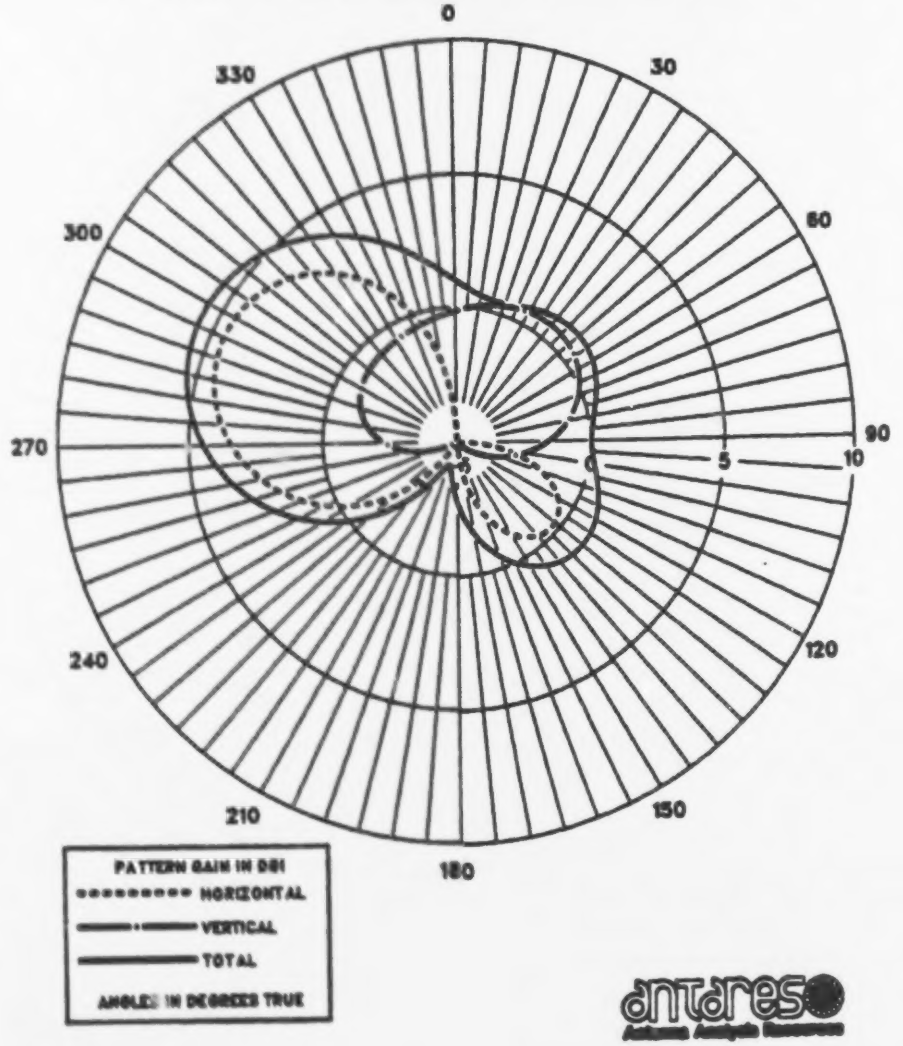

FIGURE D 53

THE FMH 4 ELEMENT ARRAY

SPACING OF 0.2 WAVELENGTHS BETWEEN ELEMENTS

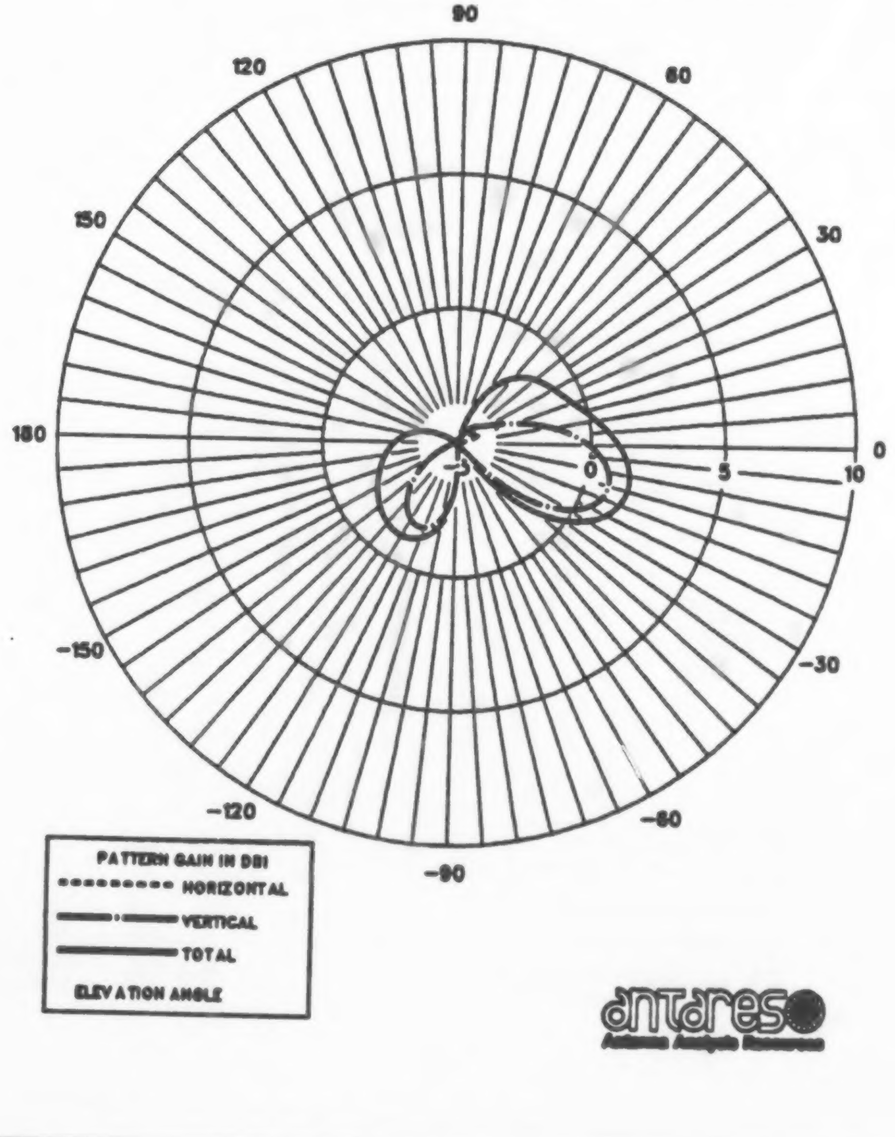

FIGURE D 54

FMH4P4

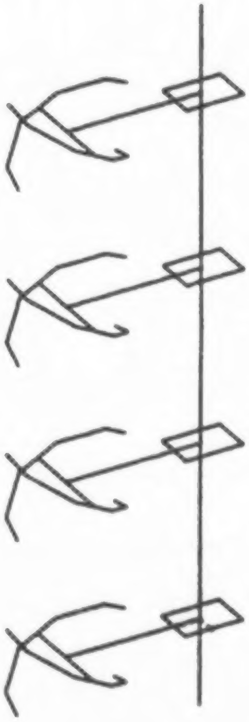

THETA = 60.00 PHI = 60.00 ETA = 90.00

antares

FIGURE D 55

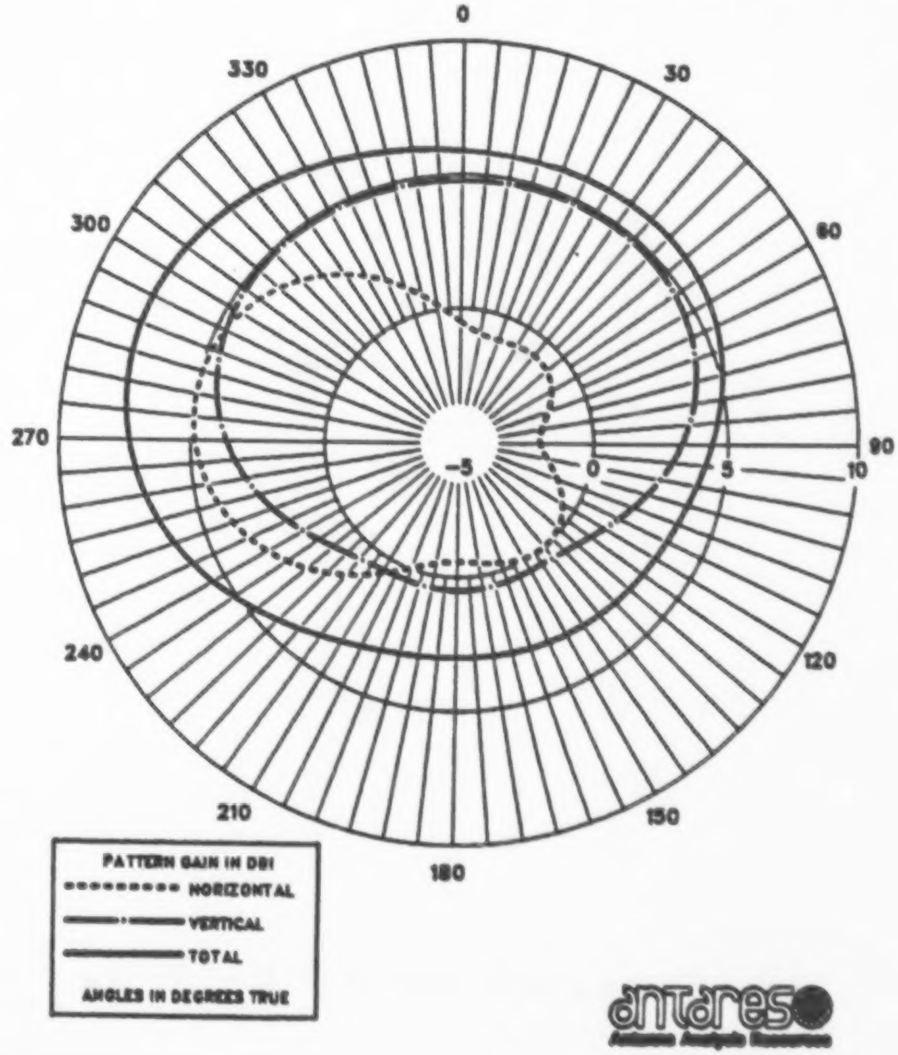

THE FMH 4 ELEMENT ARRAY

SPACING OF 0.4 WAVELENGTHS BETWEEN ELEMENTS

FIGURE D 56

THE FMH 4 ELEMENT ARRAY

SPACING OF 0.4 WAVELENGTHS BETWEEN ELEMENTS

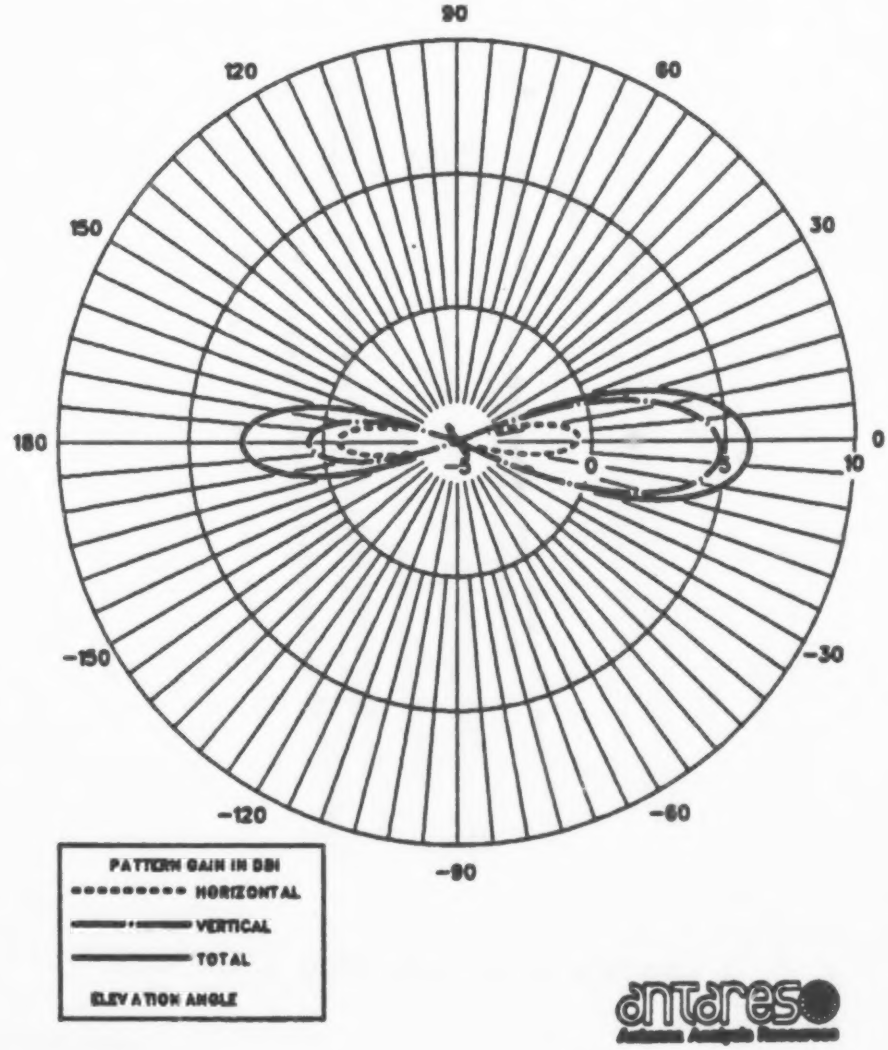

antares
Antenna Analysis Resources

FIGURE D 57

FMH4P5

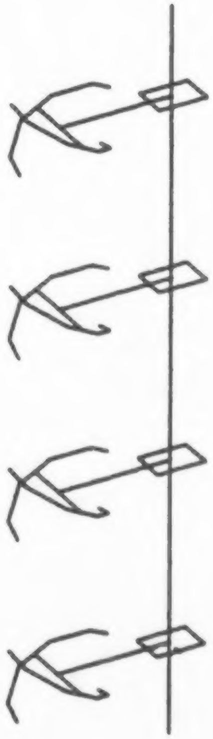

THETA = 60.00 PHI = 60.00 ETA = 90.00

antares

FIGURE D 58

THE FMH 4 ELEMENT ARRAY

SPACING OF 0.5 WAVELENGTHS BETWEEN ELEMENTS

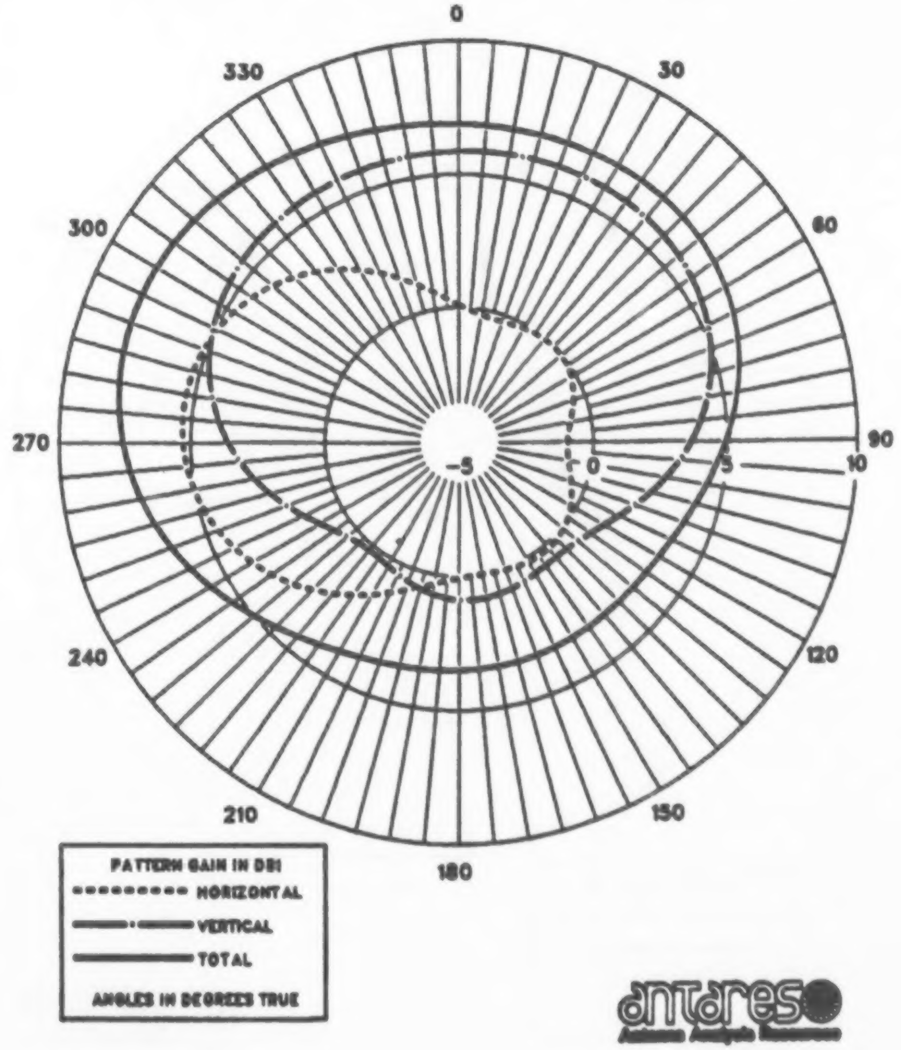

antares
Antenna Analysis Resources

FIGURE D 59

THE FMH 4 ELEMENT ARRAY

SPACING OF 0.5 WAVELENGTHS BETWEEN ELEMENTS

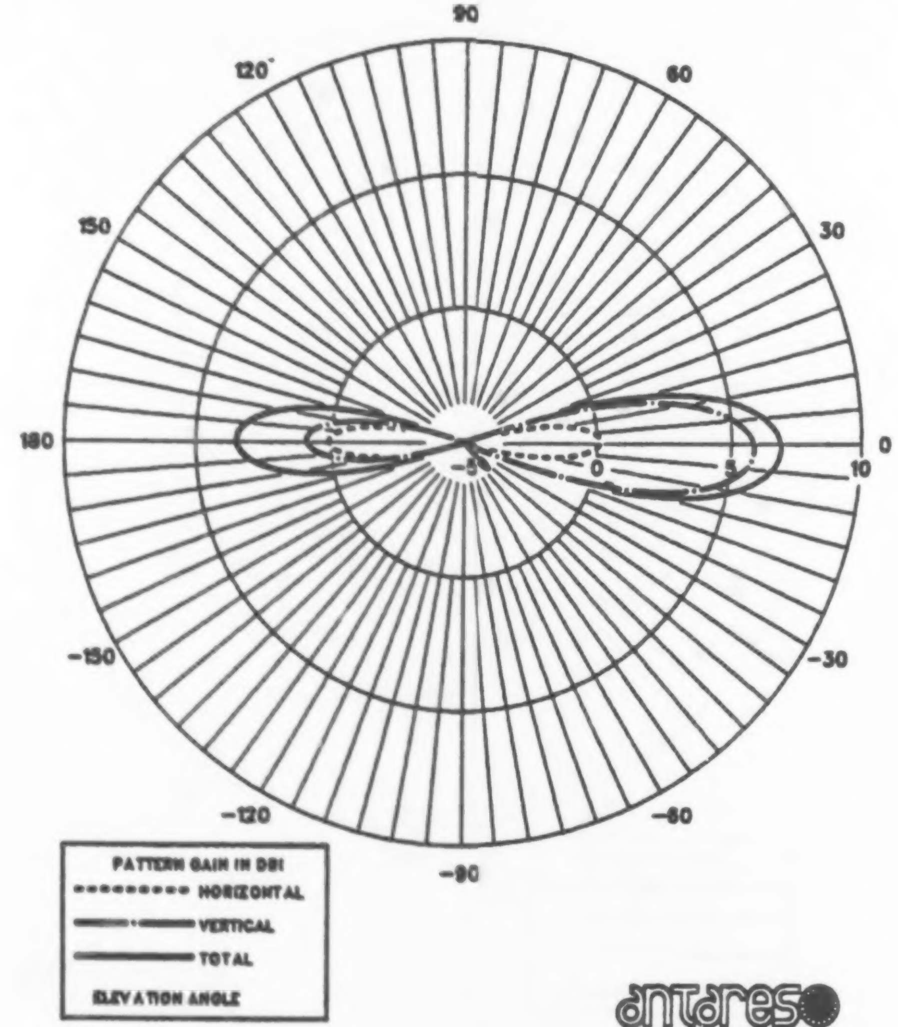

FIGURE D 60

FMH4P7

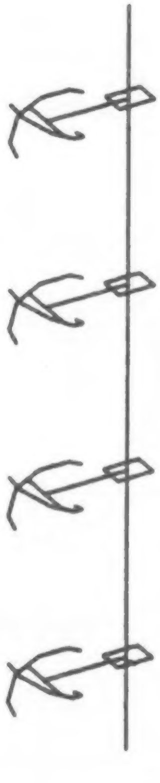

THETA = 60.00 PHI = 60.00 ETA = 90.00

476<

FIGURE D 61

THE FMH 4 ELEMENT ARRAY

SPACING OF 0.7 WAVELENGTHS BETWEEN ELEMENTS

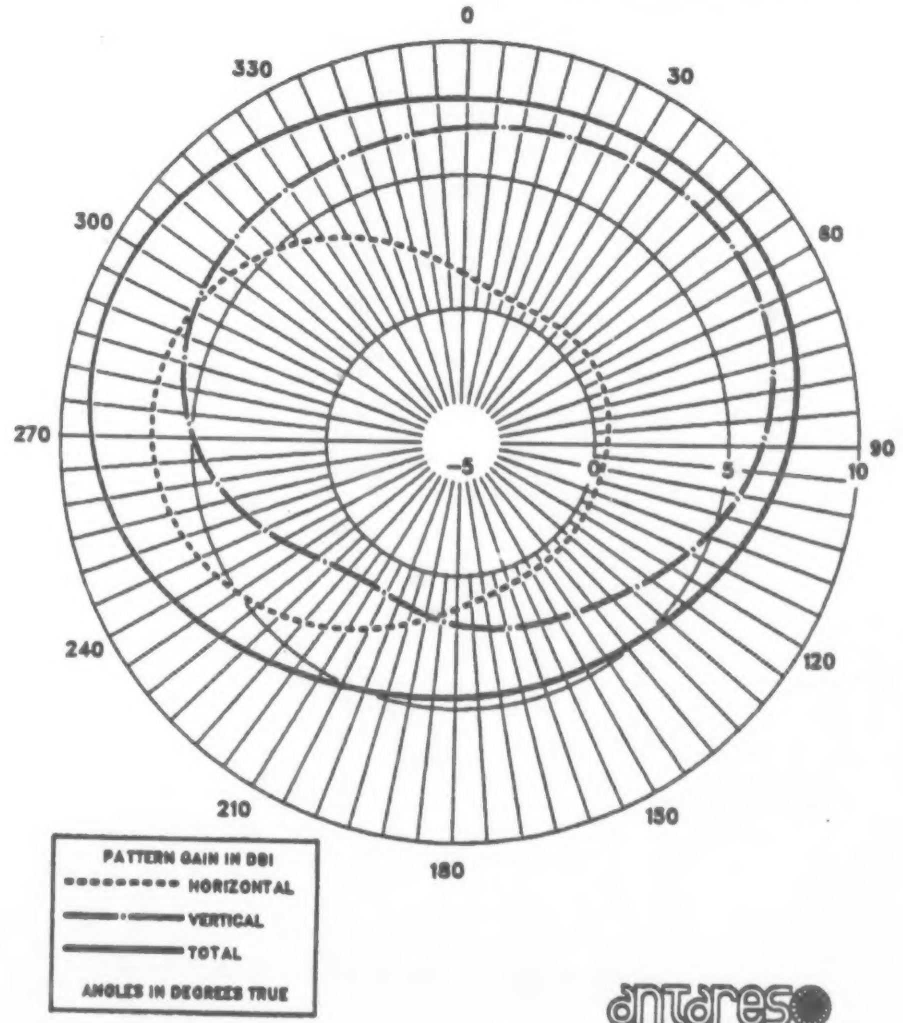

antares
Antenna Analysis Resources

FIGURE D 62

THE FMH 4 ELEMENT ARRAY

SPACING OF 0.7 WAVELENGTHS BETWEEN ELEMENTS

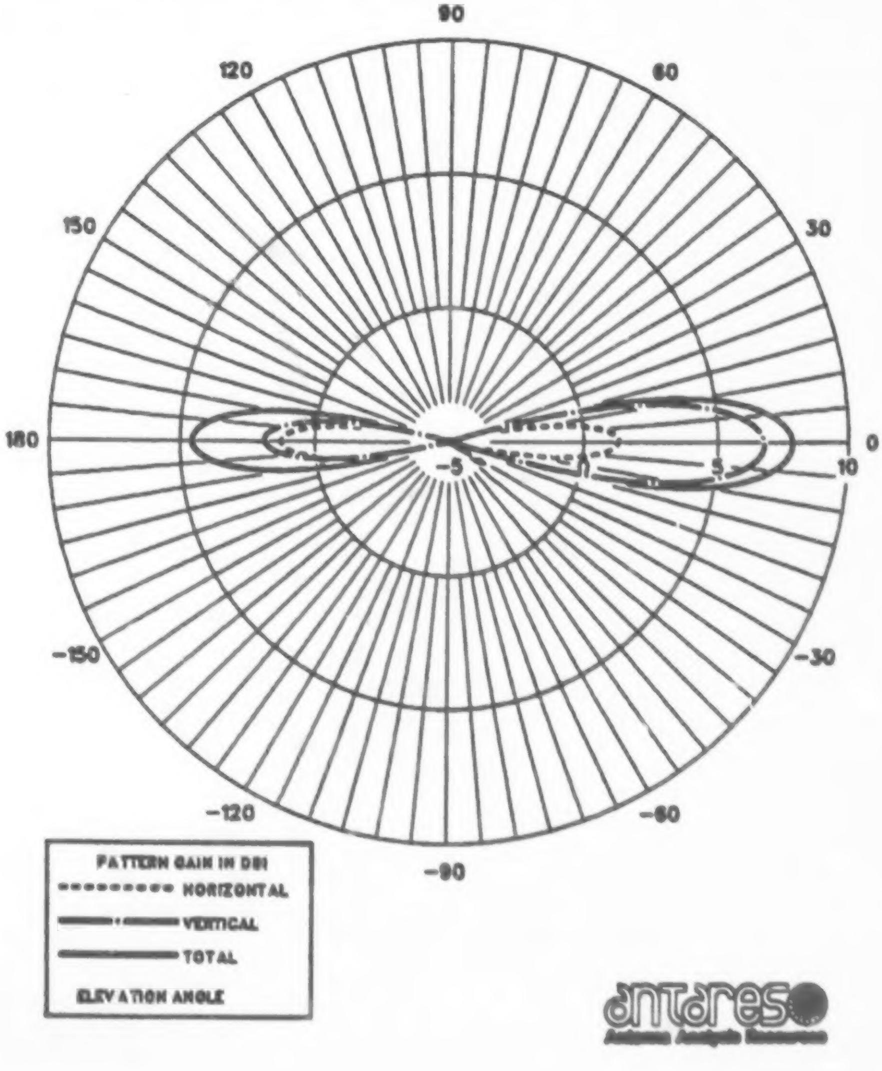

FIGURE D 63

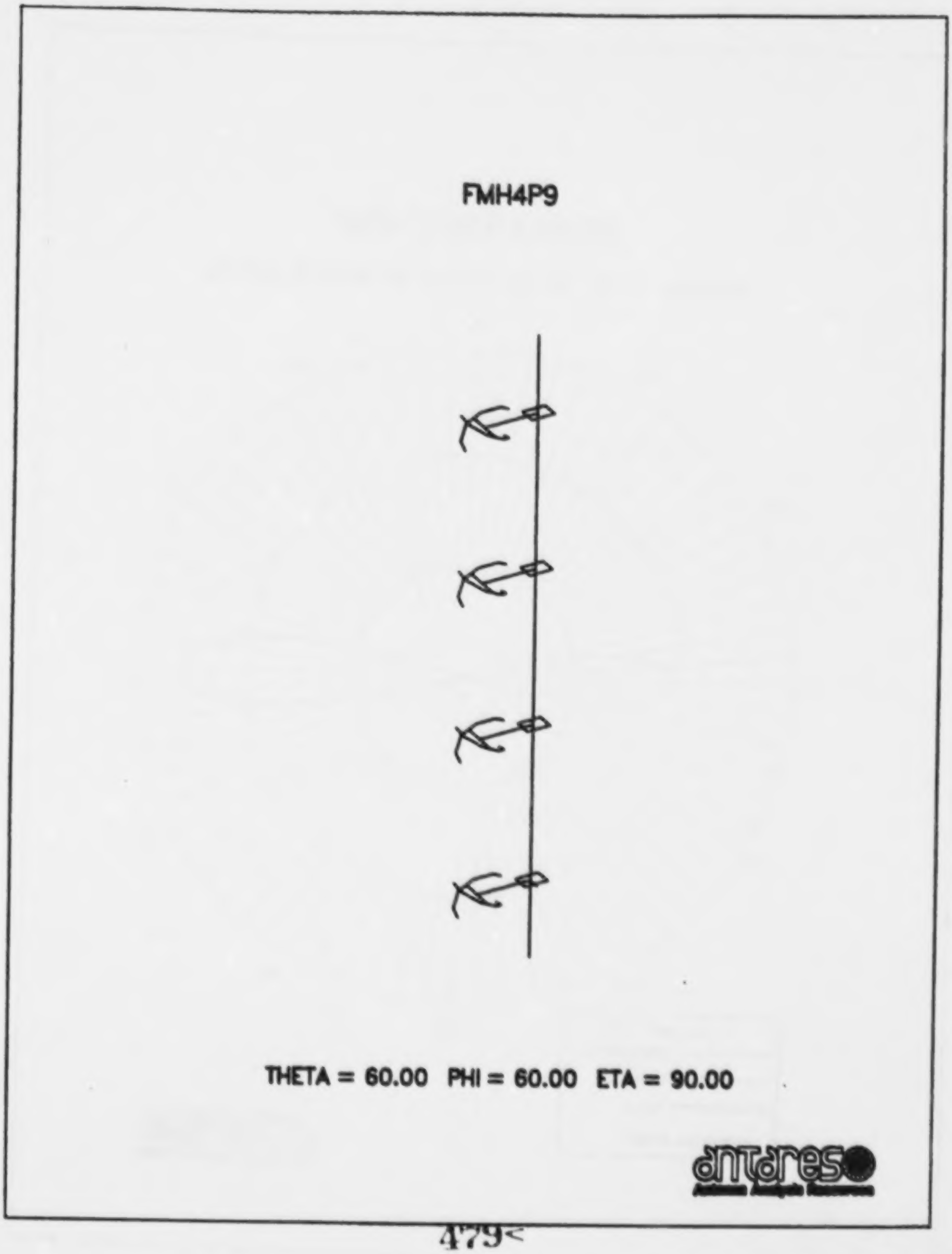
FMH4P9
THETA = 60.00 PHI = 60.00 ETA = 90.00
antares
Antenna Analysis Resources

FIGURE D 64

THE FMH 4 ELEMENT ARRAY

SPACING OF 0.9 WAVELENGTHS BETWEEN ELEMENTS

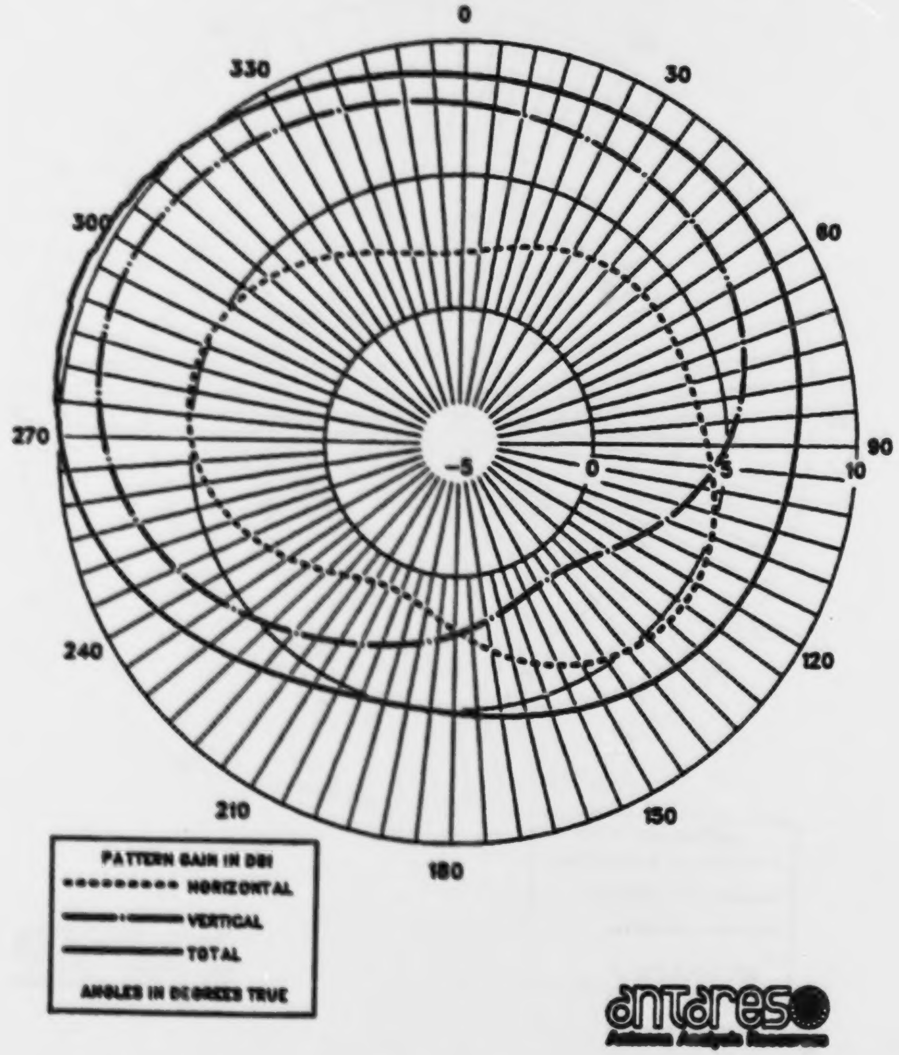

antares
Antenna Analysis Resources

FIGURE D 65

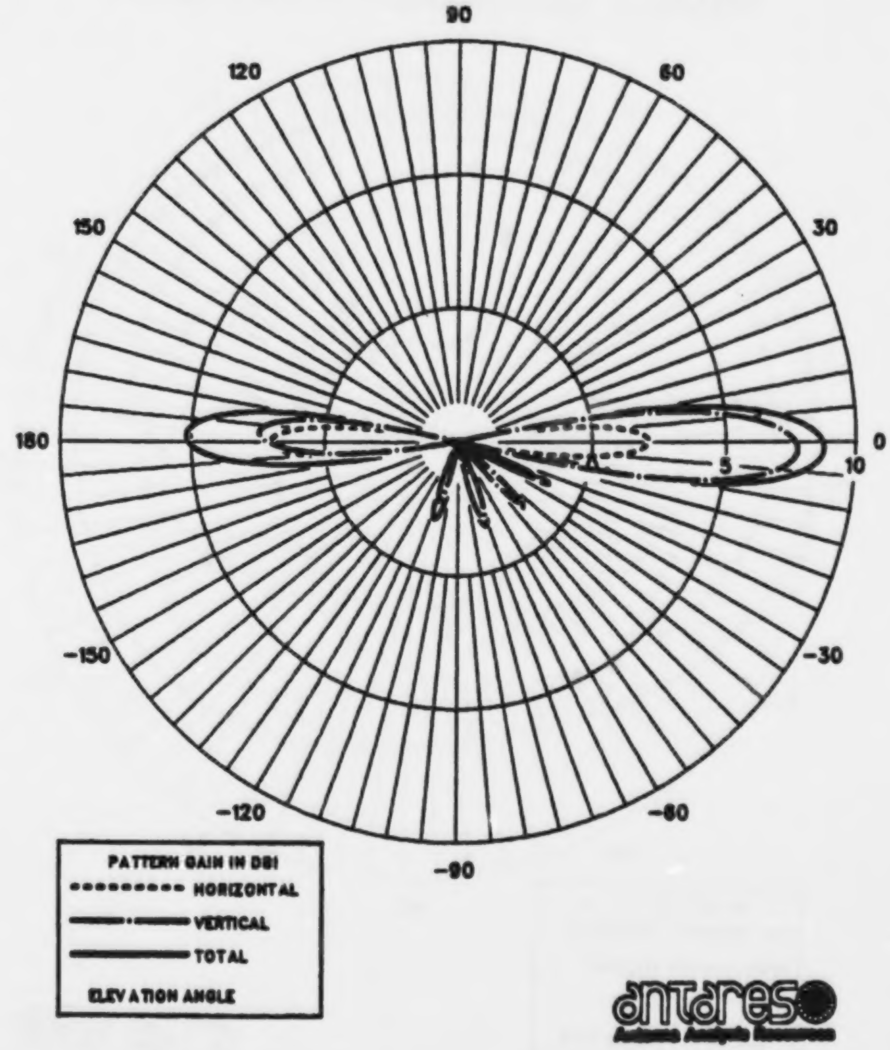

THE FMH 4 ELEMENT ARRAY

SPACING OF 0.9 WAVELENGTHS BETWEEN ELEMENTS

antares
Antenna Analysis Resources

FIGURE D 66

FMH41PO

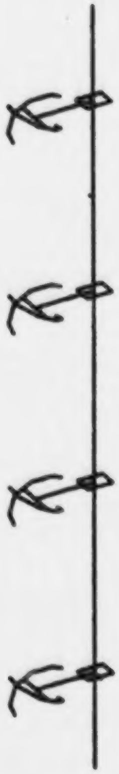

THETA = 60.00 PHI = 60.00 ETA = 90.00

antares
Antenna Analysis Resources

482<

FIGURE D 67

THE FMH 4 ELEMENT ARRAY

SPACING OF 1.0 WAVELENGTHS BETWEEN ELEMENTS

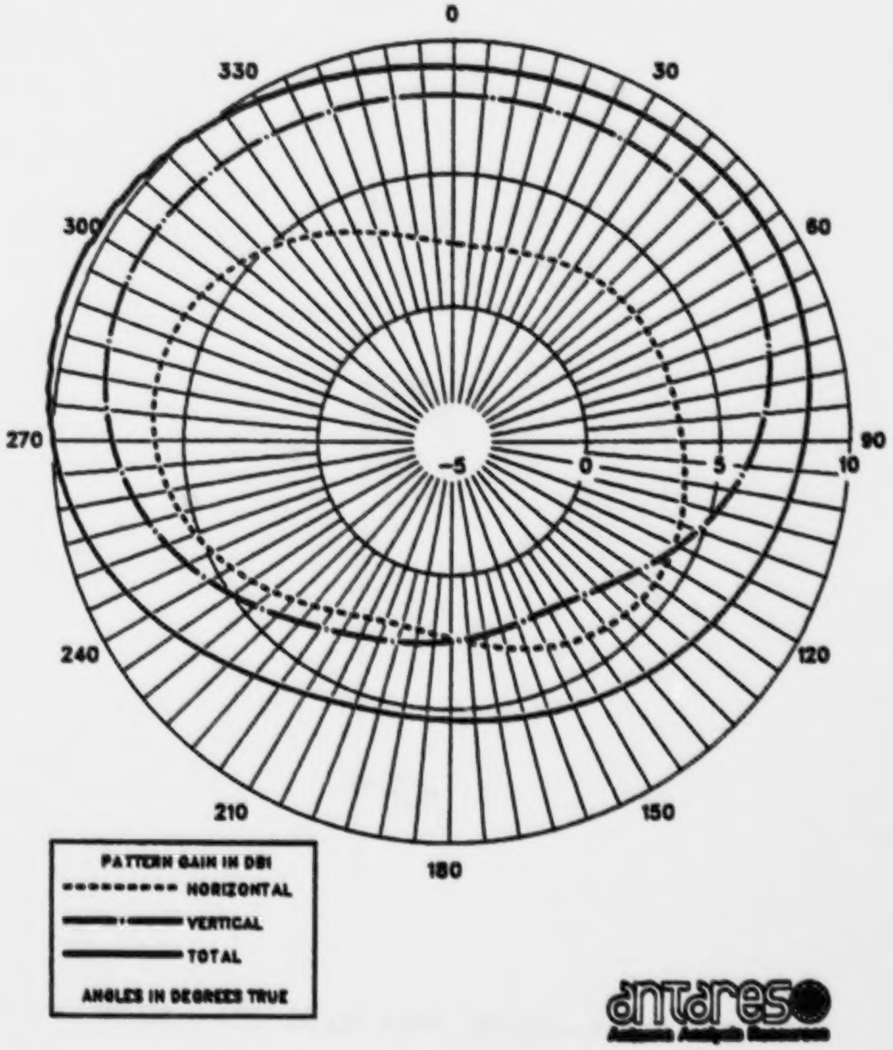

antares

FIGURE D 68

THE FMH 4 ELEMENT ARRAY

SPACING OF 1.0 WAVELENGTHS BETWEEN ELEMENTS

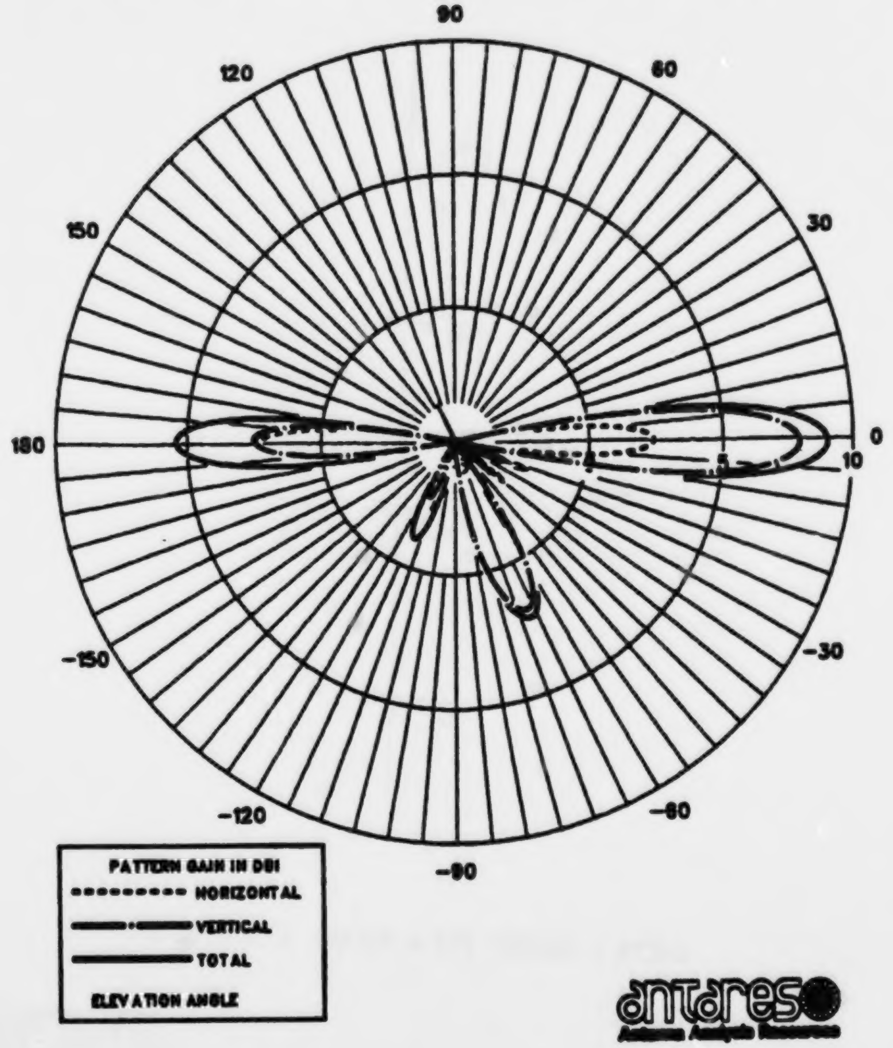

antares
Antenna Analysis Resources

FIGURE D 69

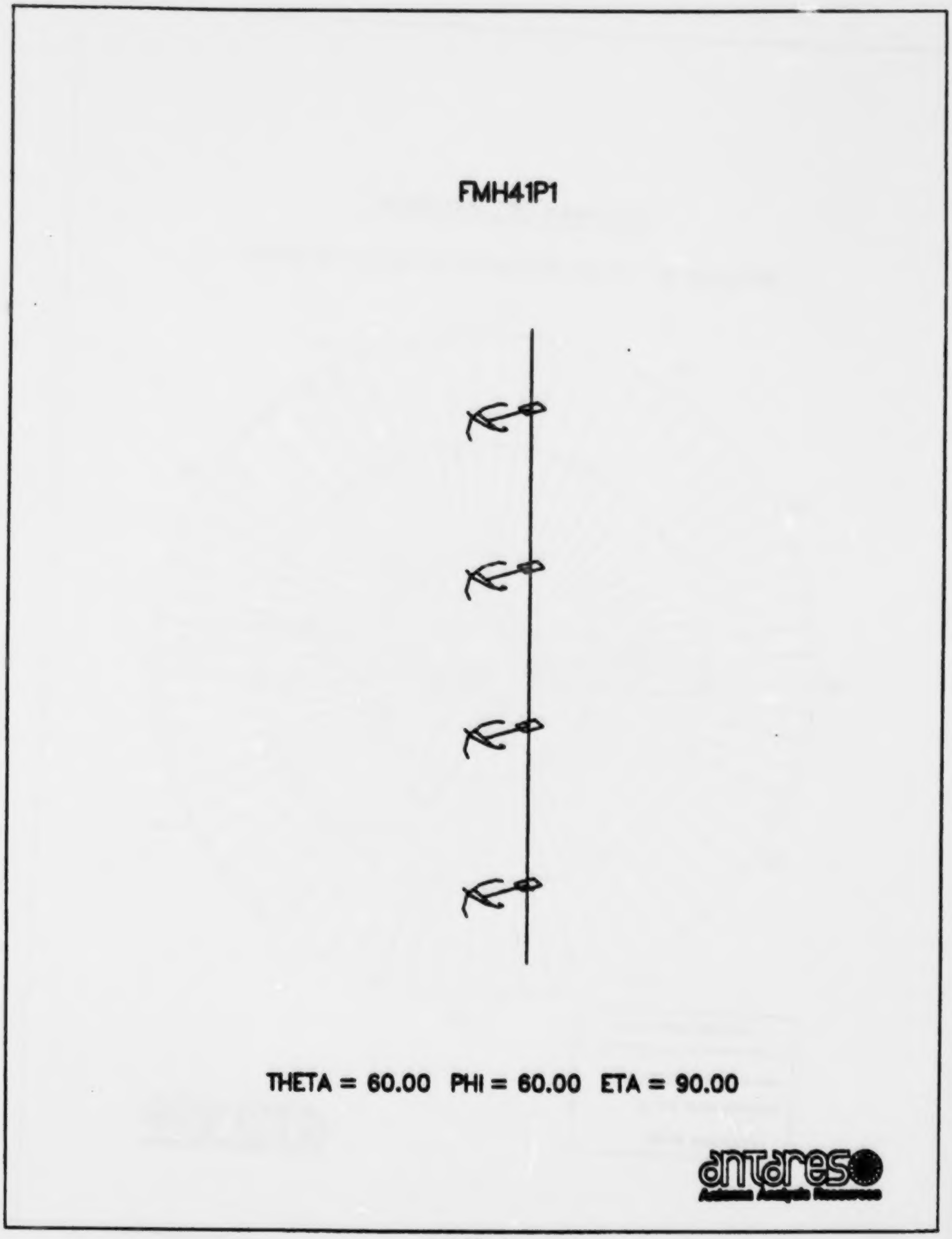
FMH41P1
THETA = 60.00 PHI = 60.00 ETA = 90.00
antares
Antenna Analysis Resources

FIGURE D 70

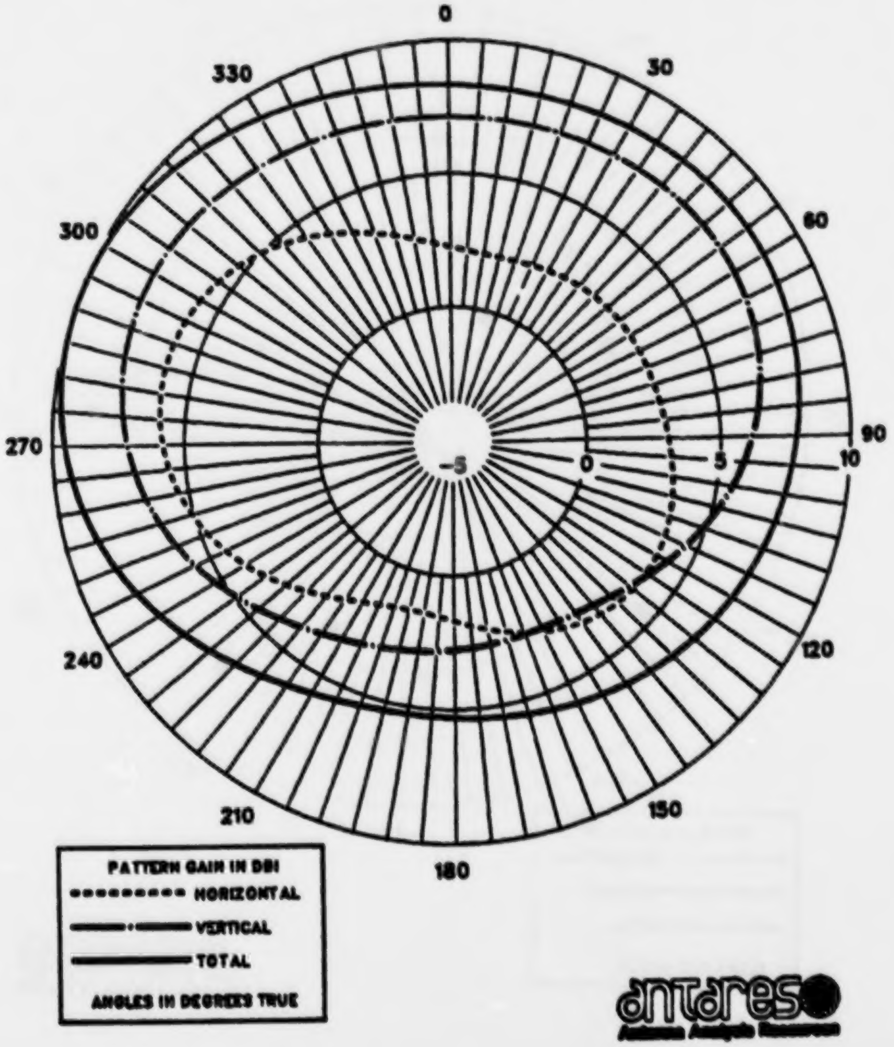

THE FMH 4 ELEMENT ARRAY

SPACING OF 1.1 WAVELENGTHS BETWEEN ELEMENTS

antares
Antenna Analysis Resources

FIGURE D 71

THE FMH 4 ELEMENT ARRAY

SPACING OF 1.1 WAVELENGTHS BETWEEN ELEMENTS

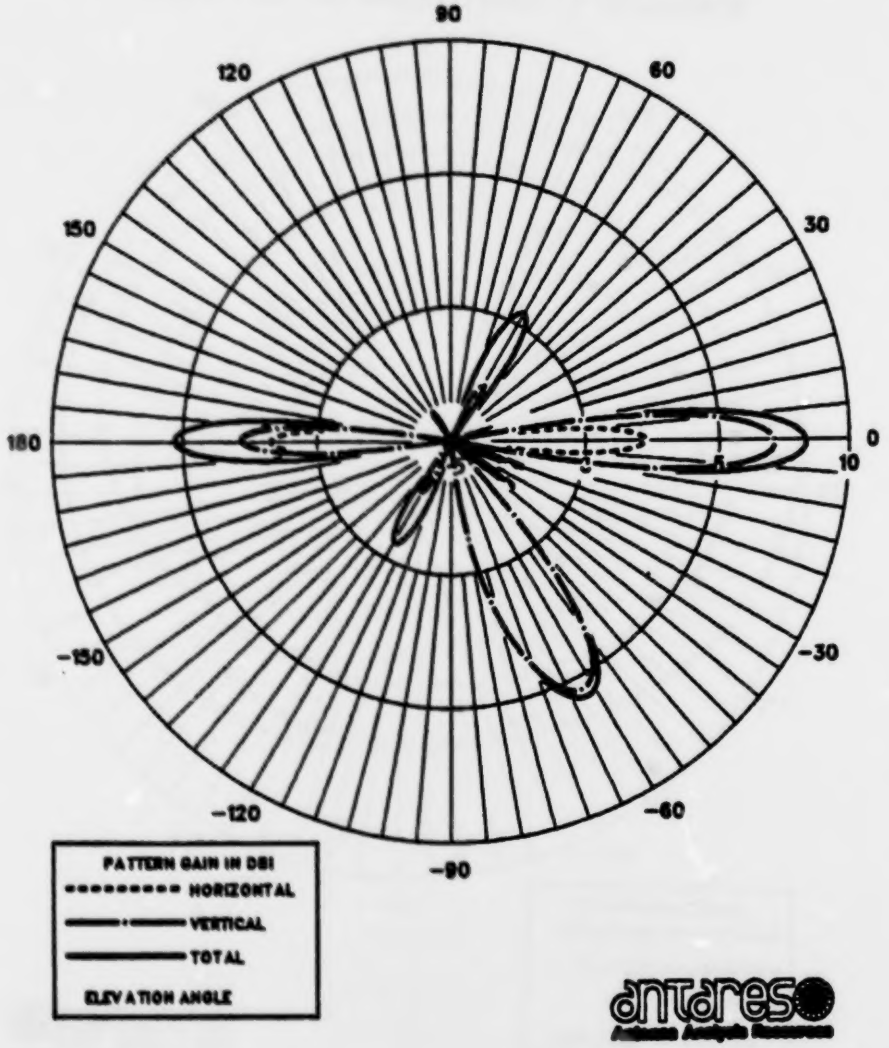

antares
Antenna Analysis Resources

FIGURE D 72

FMH41P2

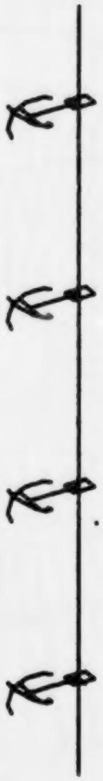

THETA = 60.00 PHI = 60.00 ETA = 90.00

488<

FIGURE D 73

THE FMH 4 ELEMENT ARRAY

SPACING OF 1.2 WAVELENGTHS BETWEEN ELEMENTS

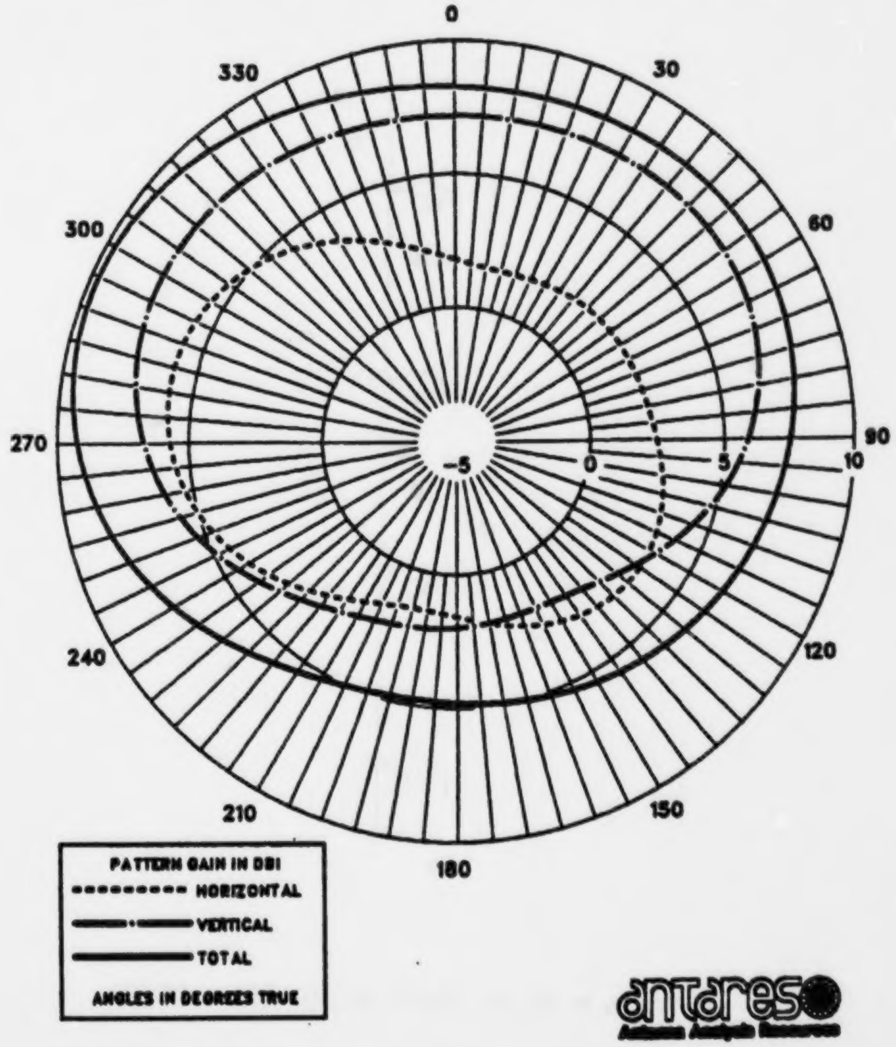

antares
Antenna Analysis Resources

FIGURE D 74

THE FMH 4 ELEMENT ARRAY

SPACING OF 1.2 WAVELENGTHS BETWEEN ELEMENTS

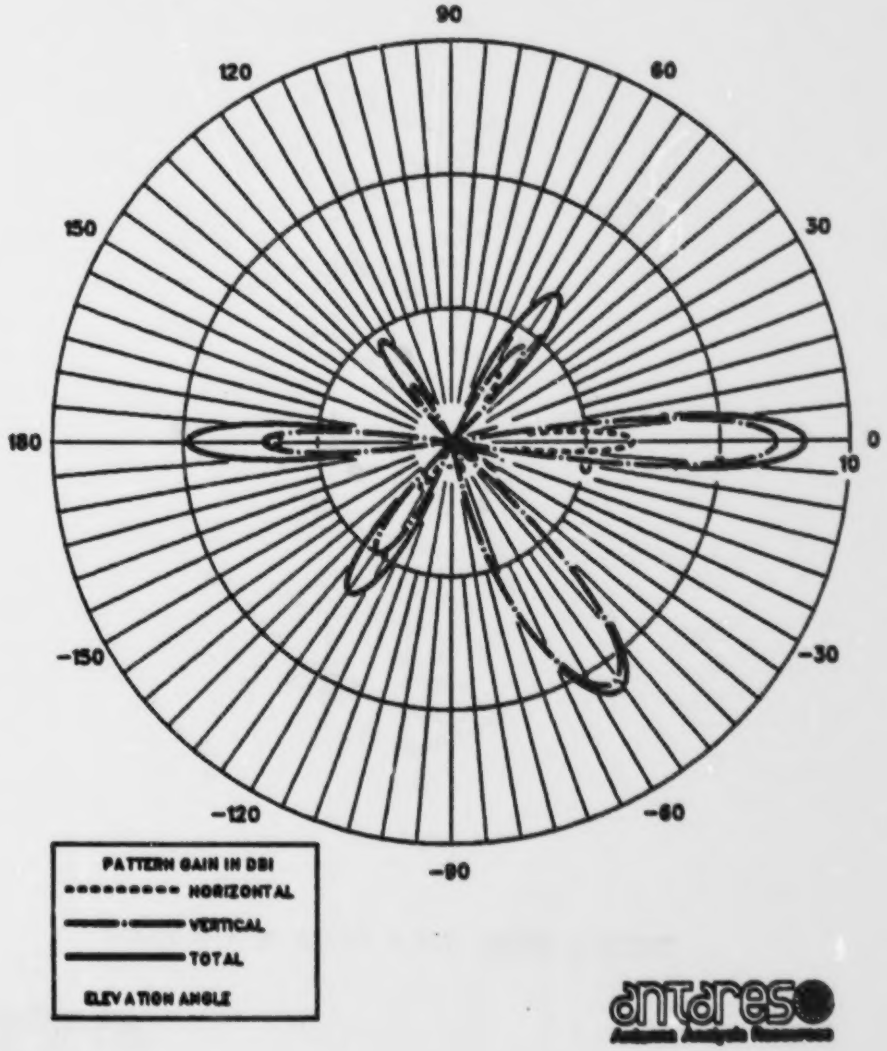

antares
Antenna Analysis Resources

FIGURE D 75

FMH8P2

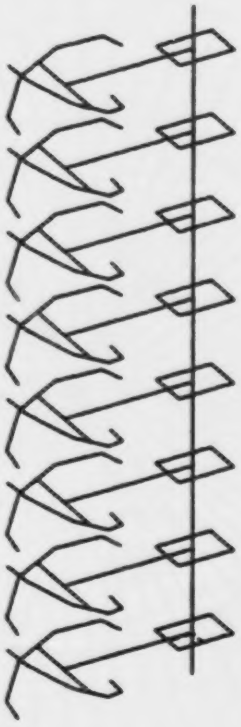

THETA = 60.00   PHI = 60.00   ETA = 90.00

antares
Antenna Analysis Resources

491<

FIGURE D 76

THE FMH 8 ELEMENT ARRAY

SPACING OF 0.2 WAVELENGTHS BETWEEN ELEMENTS

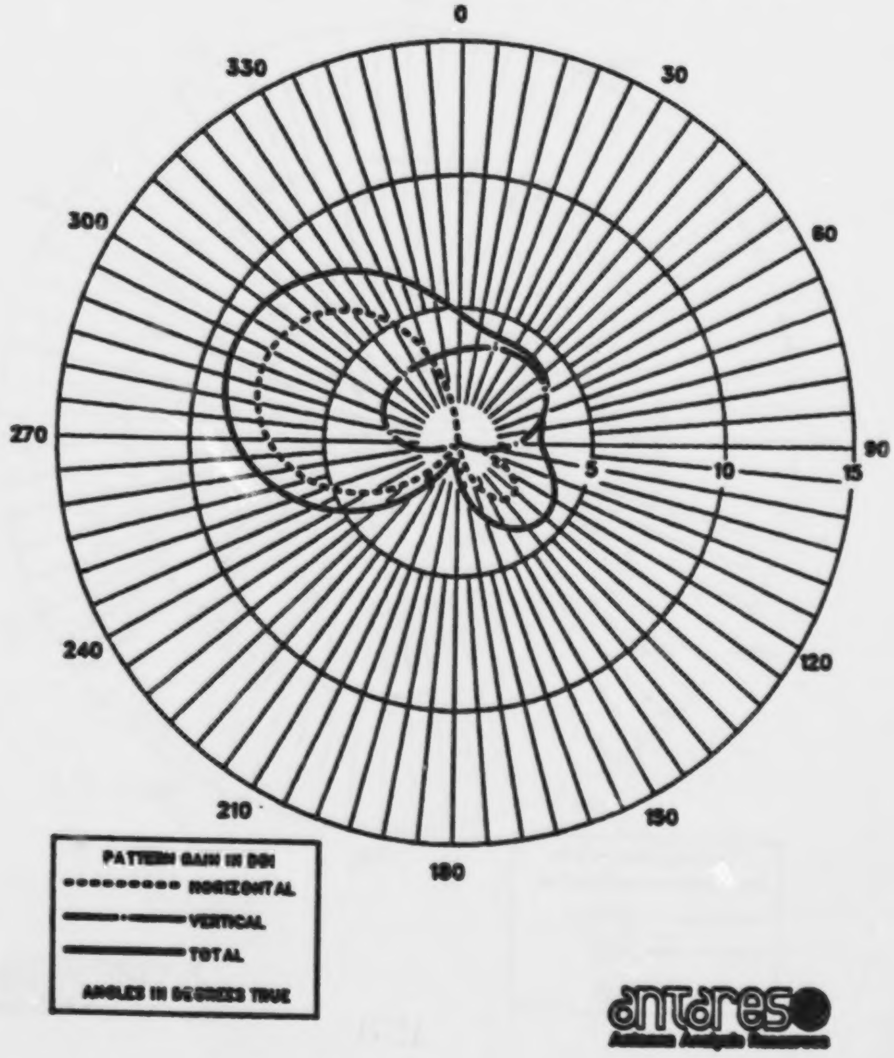

FIGURE D 77

THE FMH 8 ELEMENT ARRAY

SPACING OF 0.2 WAVELENGTHS BETWEEN ELEMENTS

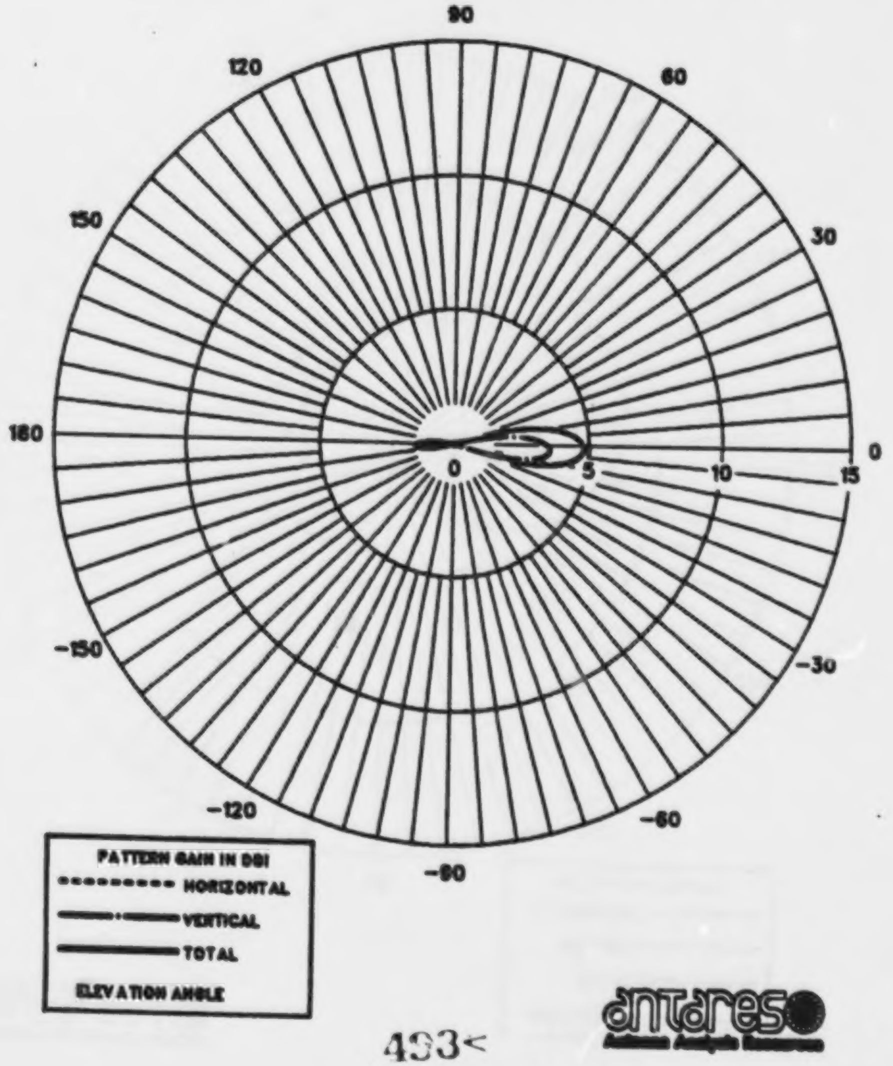

antares
Antenna Analysis Resources

493<

FIGURE D 78

FMH8P4

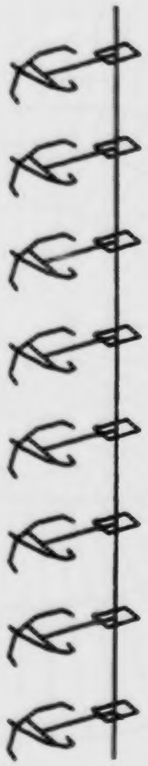

THETA = 60.00 PHI = 60.00 ETA = 90.00

FIGURE D 79

THE FMH 8 ELEMENT ARRAY

SPACING OF 0.4 WAVELENGTHS BETWEEN ELEMENTS

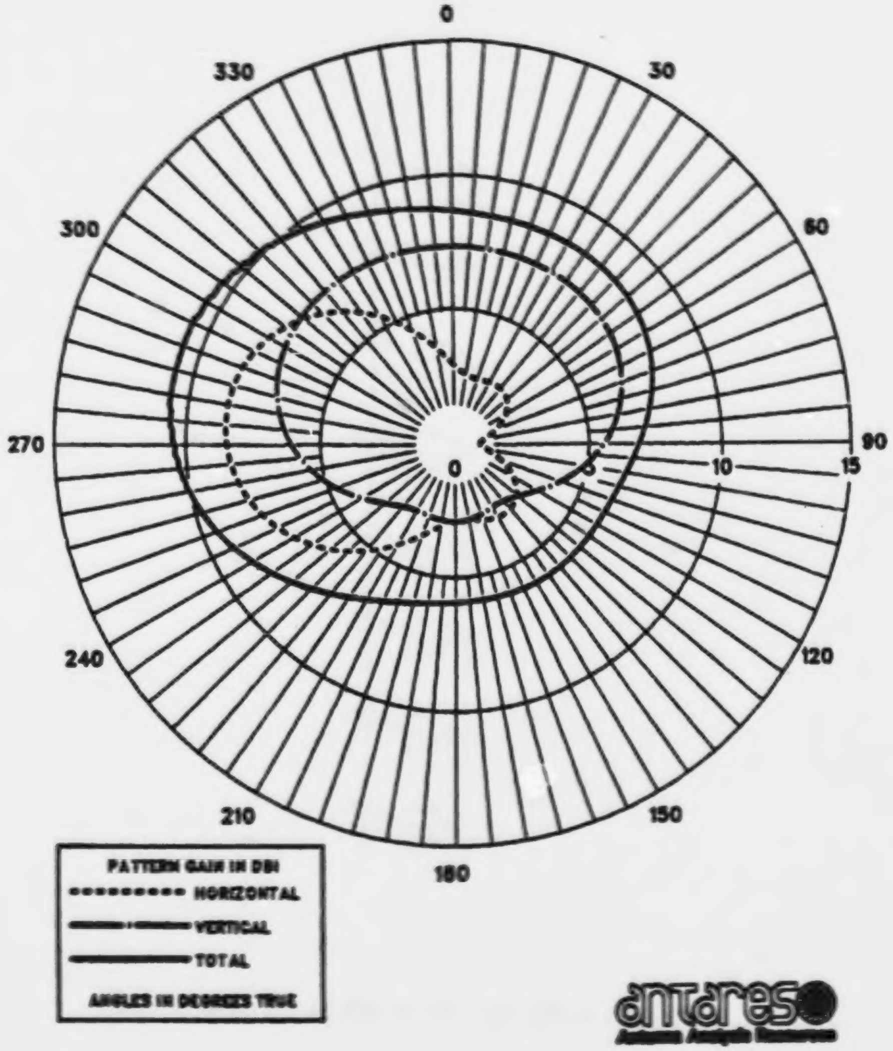

FIGURE D 80

THE FMH 8 ELEMENT ARRAY

SPACING OF 0.4 WAVELENGTHS BETWEEN ELEMENTS

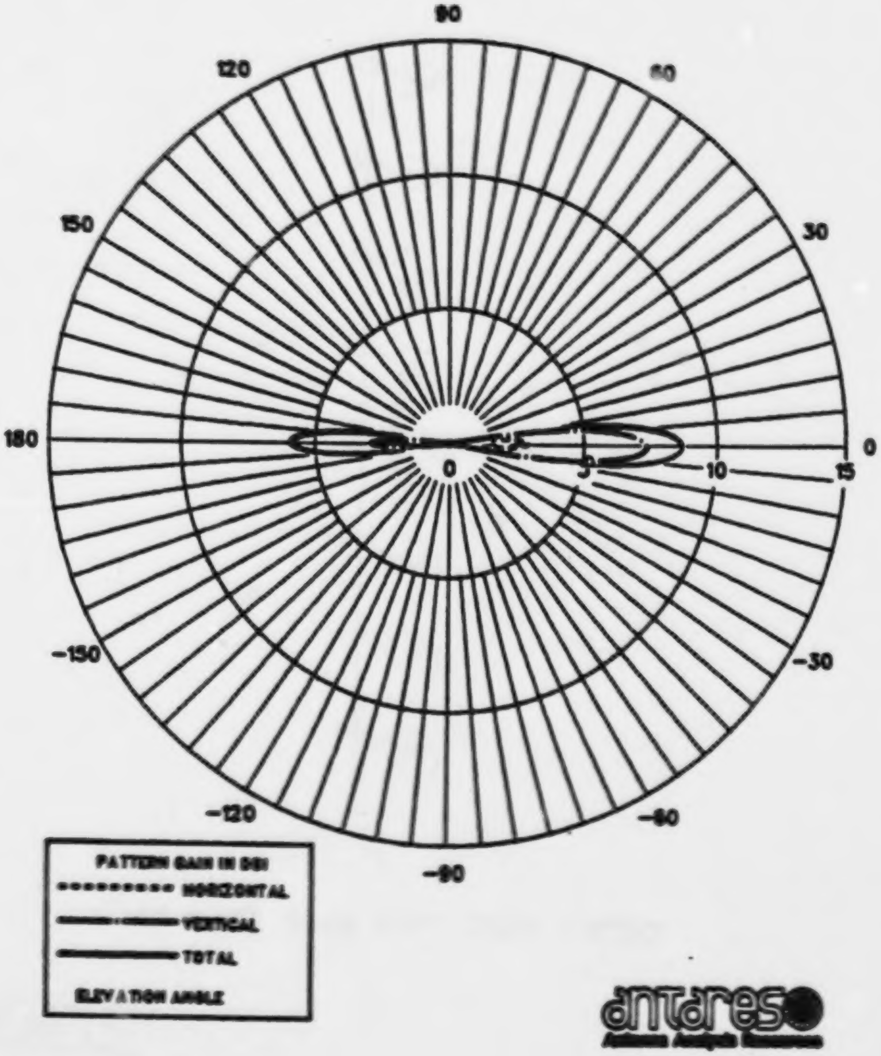

antares
Antenna Analysis Resources

FIGURE D 81

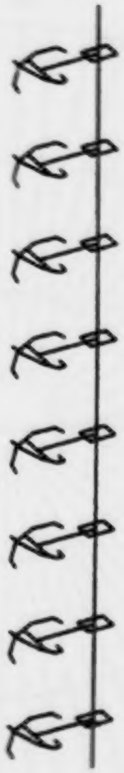

FMH8P5

THETA = 60.00 PHI = 60.00 ETA = 90.00

antares

FIGURE D 82

THE FMH 8 ELEMENT ARRAY

SPACING OF 0.5 WAVELENGTHS BETWEEN ELEMENTS

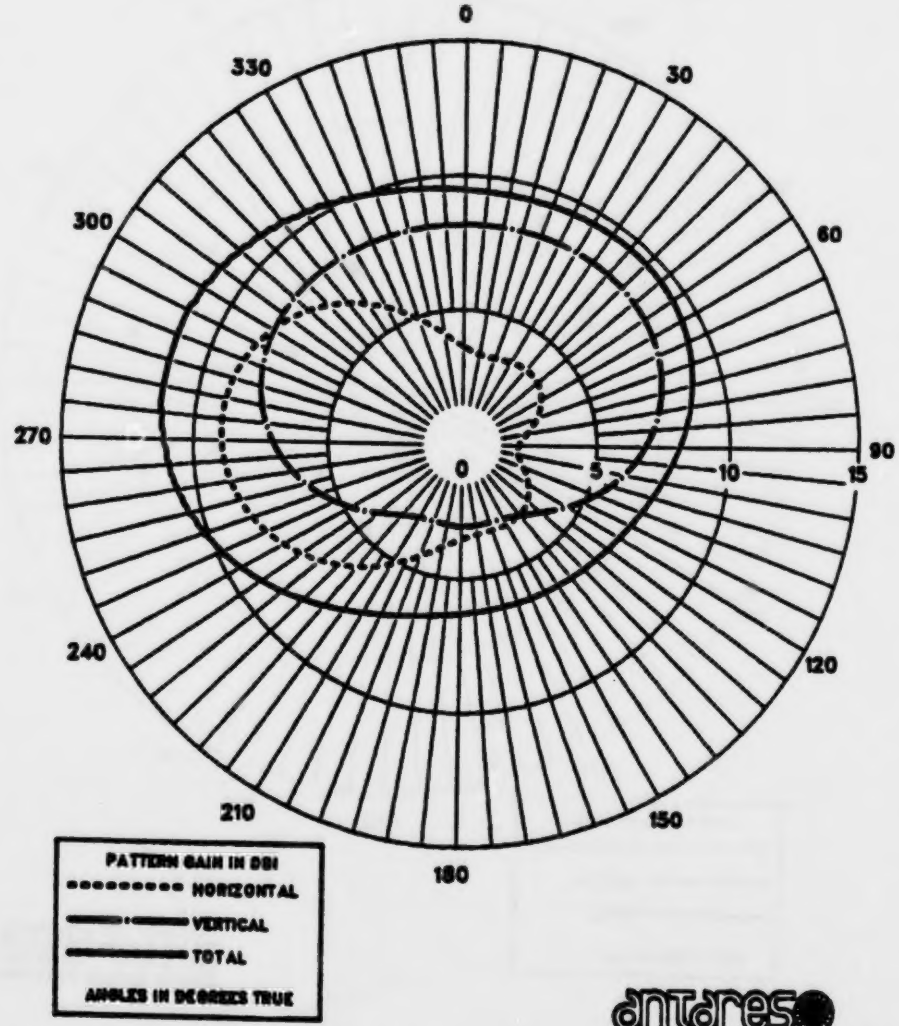

antares
Antenna Analysis Resources

FIGURE D 83

THE FMH 8 ELEMENT ARRAY

SPACING OF 0.5 WAVELENGTHS BETWEEN ELEMENTS

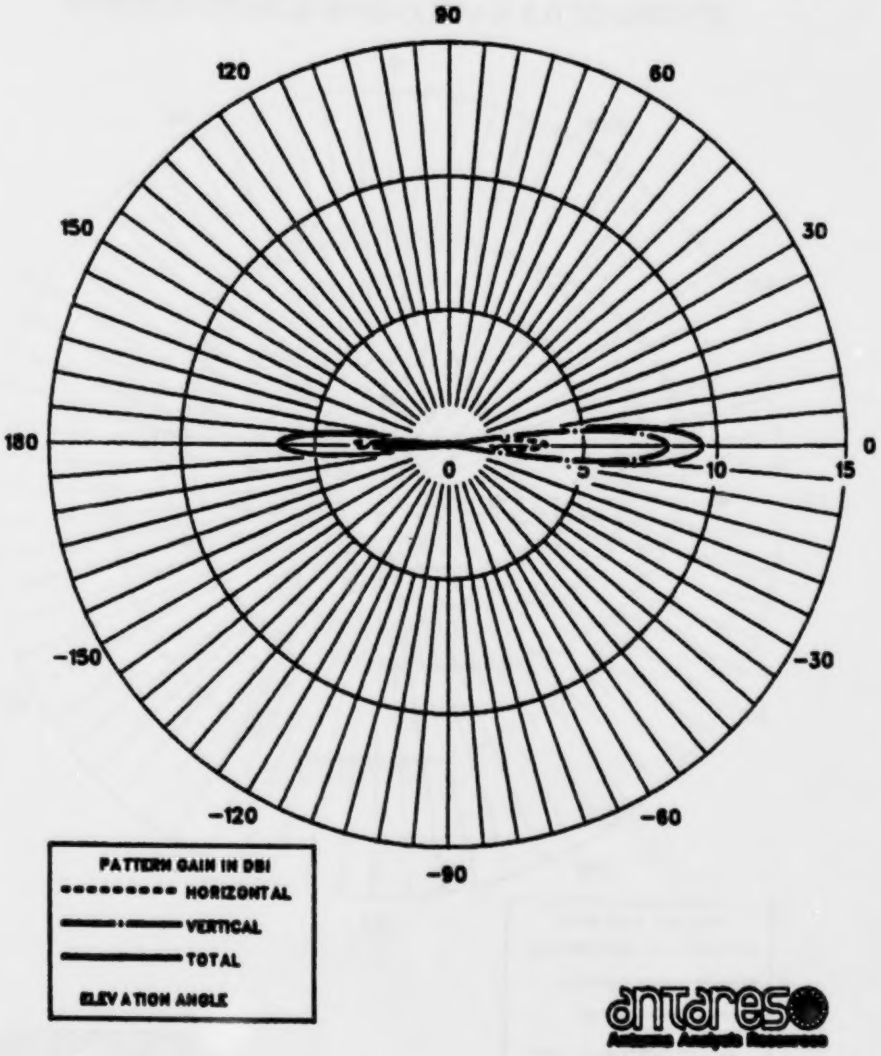

FIGURE D 84

FMH8P7

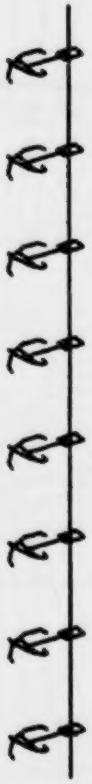

THETA = 60.00 PHI = 60.00 ETA = 90.00

FIGURE D 85

500<

THE FMH 8 ELEMENT ARRAY

SPACING OF 0.7 WAVELENGTHS BETWEEN ELEMENTS

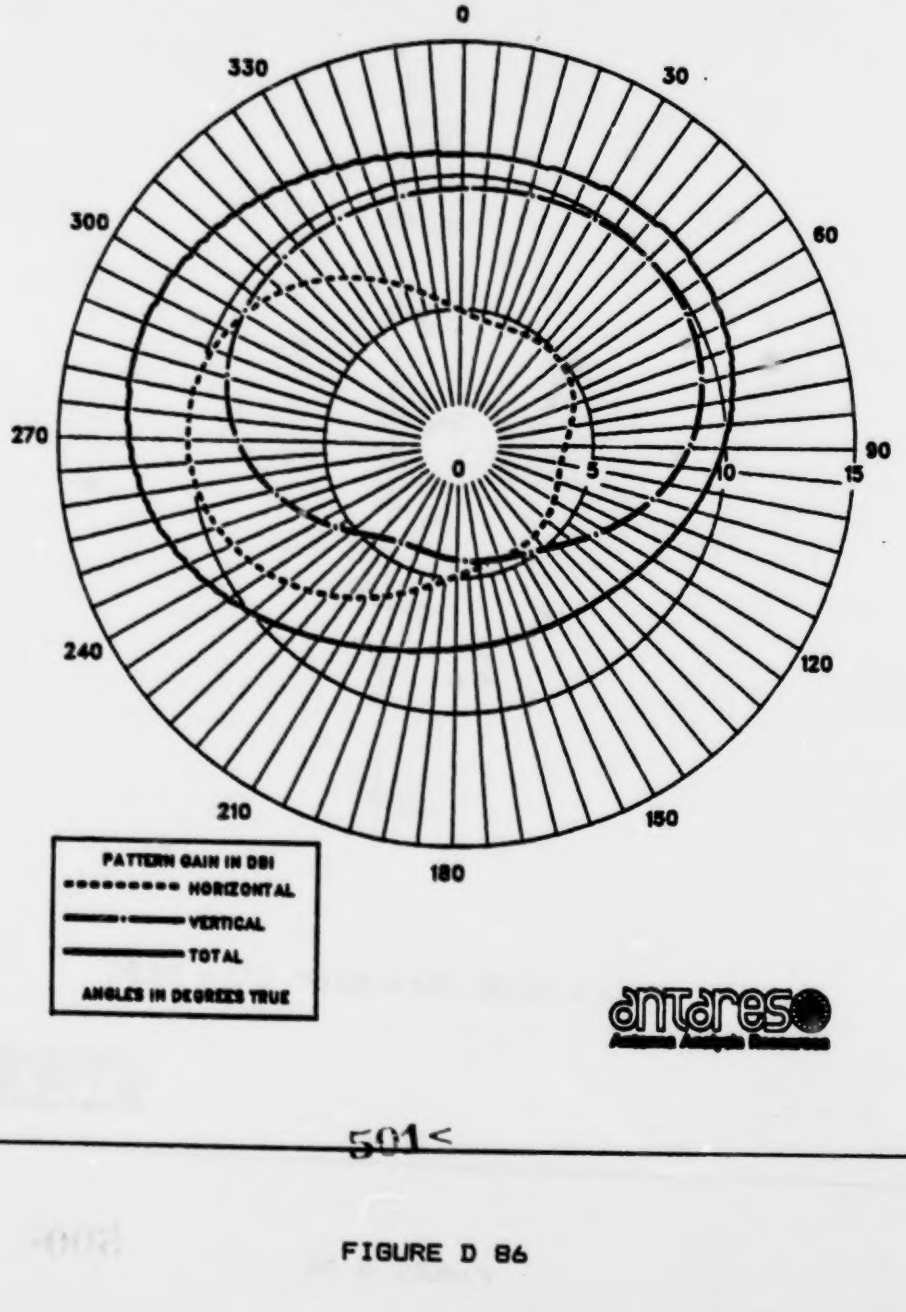

antares
Antenna Analysis Resources

FIGURE D 86

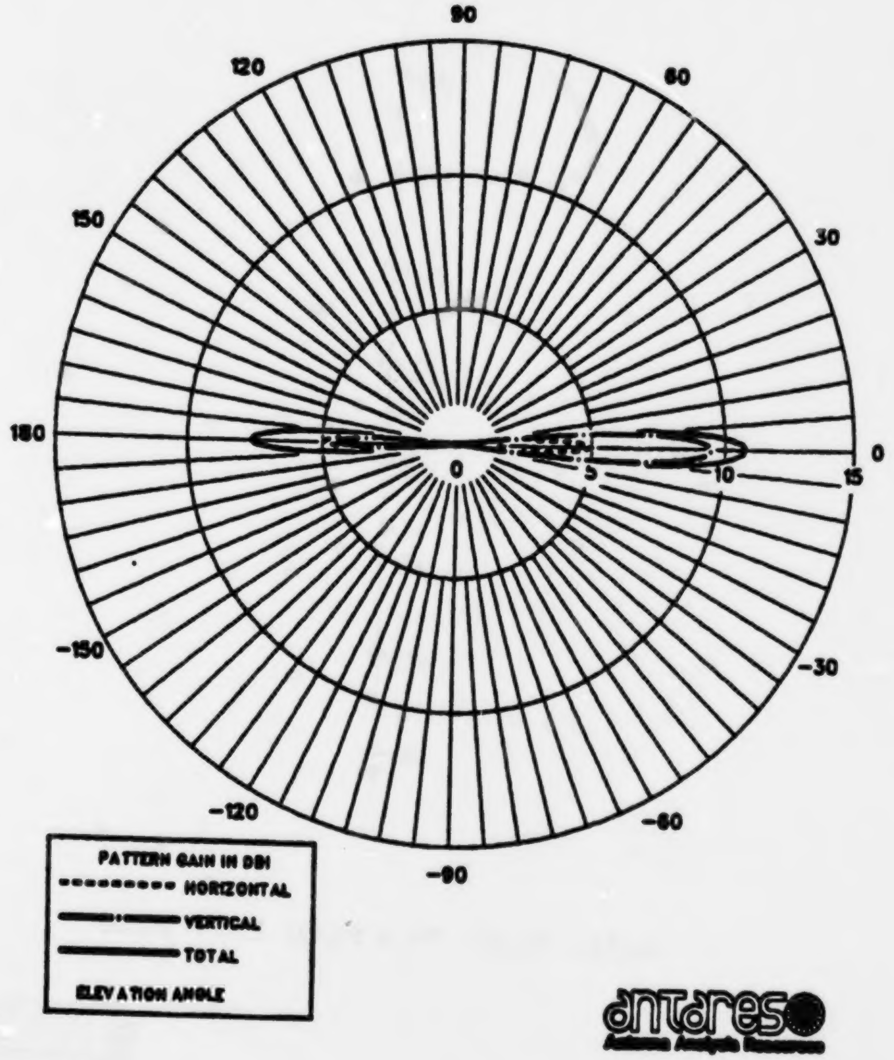

THE FMH 8 ELEMENT ARRAY

SPACING OF 0.7 WAVELENGTHS BETWEEN ELEMENTS

Antenna Analysis Resources

FIGURE D 87

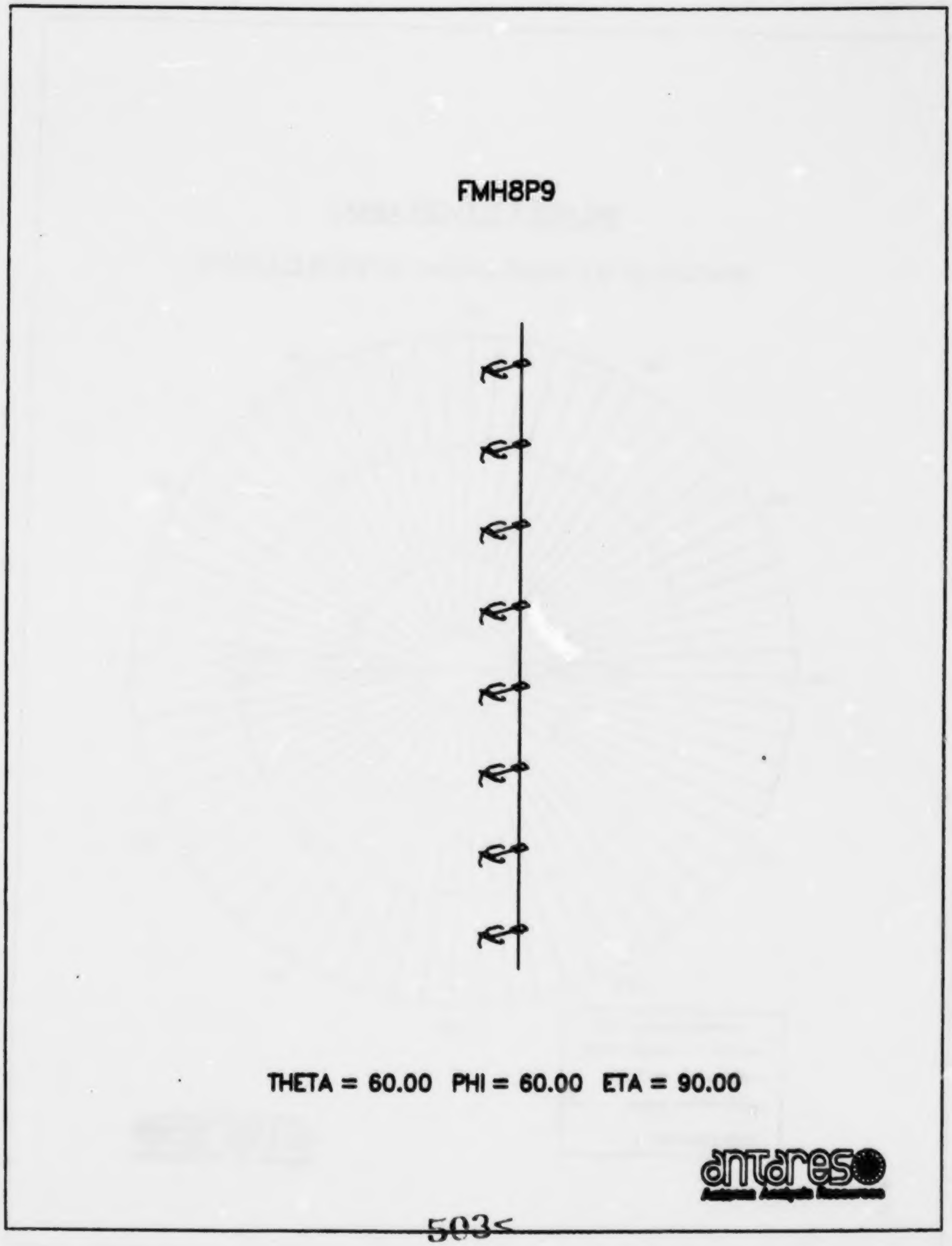
FMH8P9
THETA = 60.00 PHI = 60.00 ETA = 90.00
antares
Antenna Analysis Resources

FIGURE D 88

THE FMH 8 ELEMENT ARRAY

SPACING OF 0.9 WAVELENGTHS BETWEEN ELEMENTS

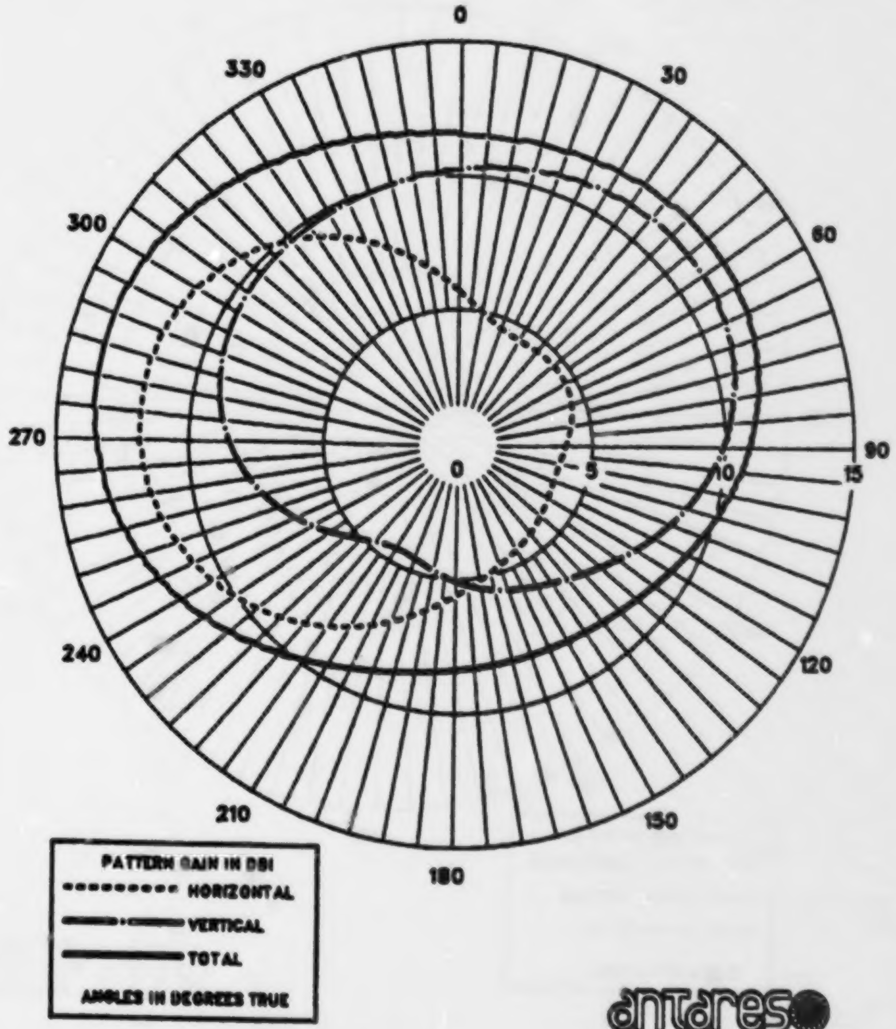

antares
Antenna Analysis Resources

FIGURE D 89

THE FMH 8 ELEMENT ARRAY

SPACING OF 0.9 WAVELENGTHS BETWEEN ELEMENTS

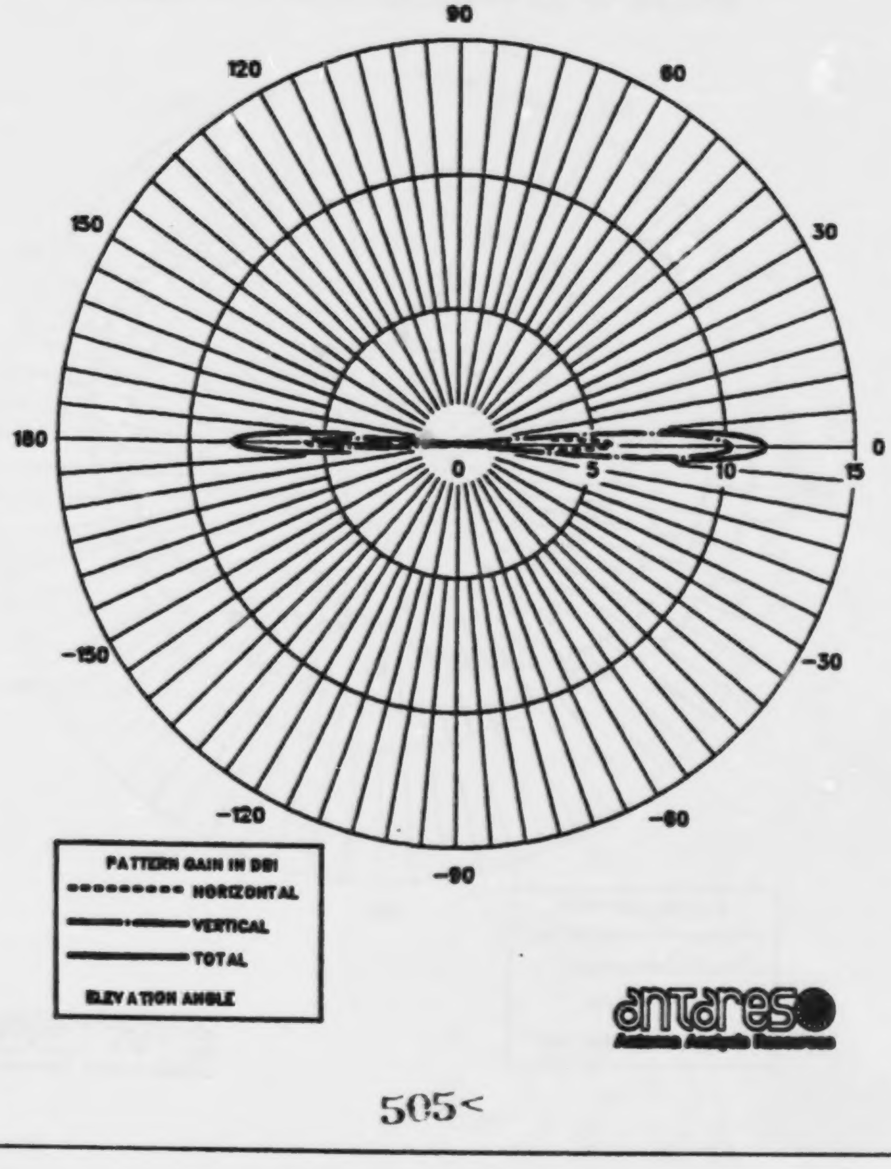

antares
Antenna Analysis Resources

FIGURE D 90

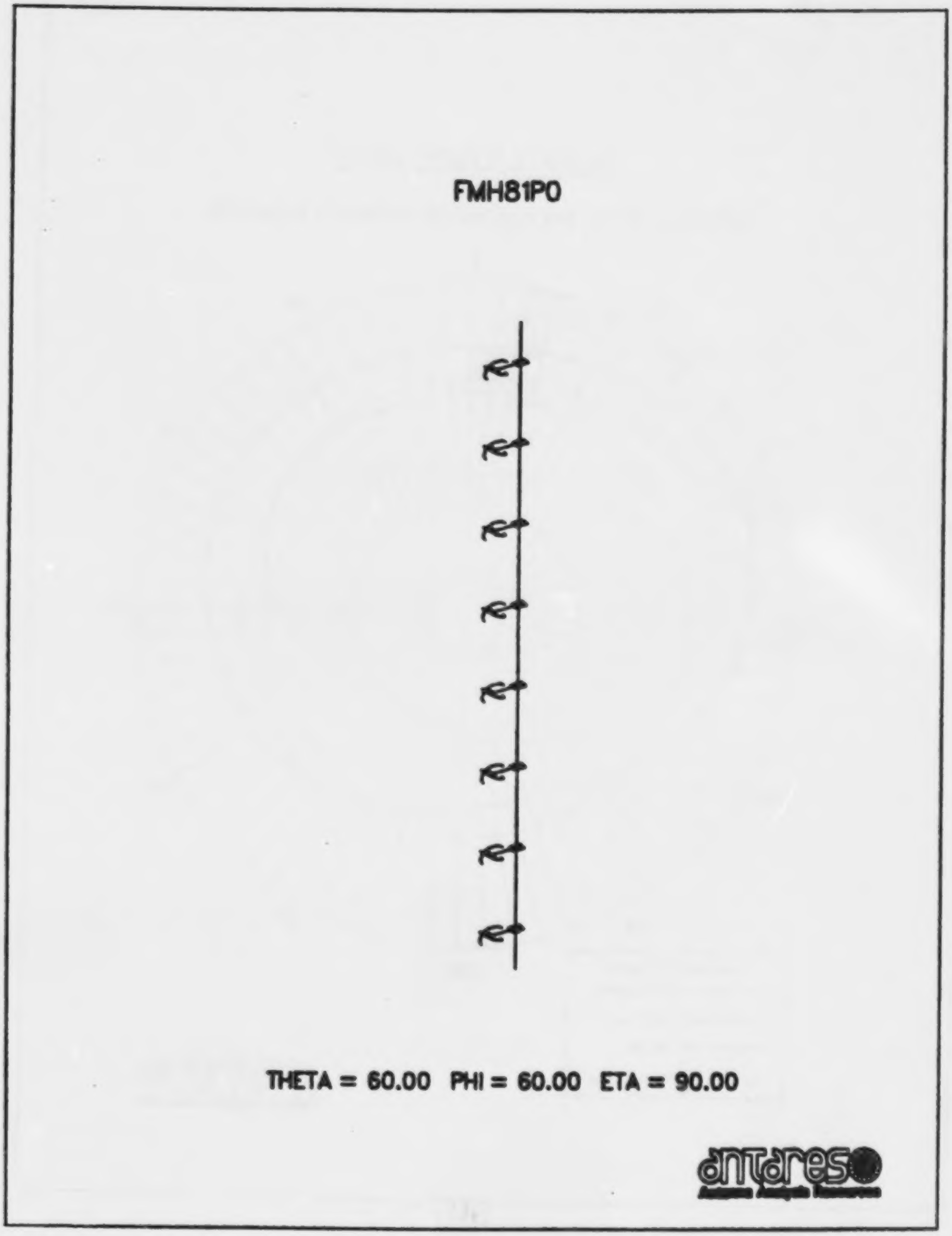
FMH81PO
THETA = 60.00 PHI = 60.00 ETA = 90.00
antares
Antares Analysis Resources

FIBURE D 91

THE FMH 8 ELEMENT ARRAY

SPACING OF 1.0 WAVELENGTHS BETWEEN ELEMENTS

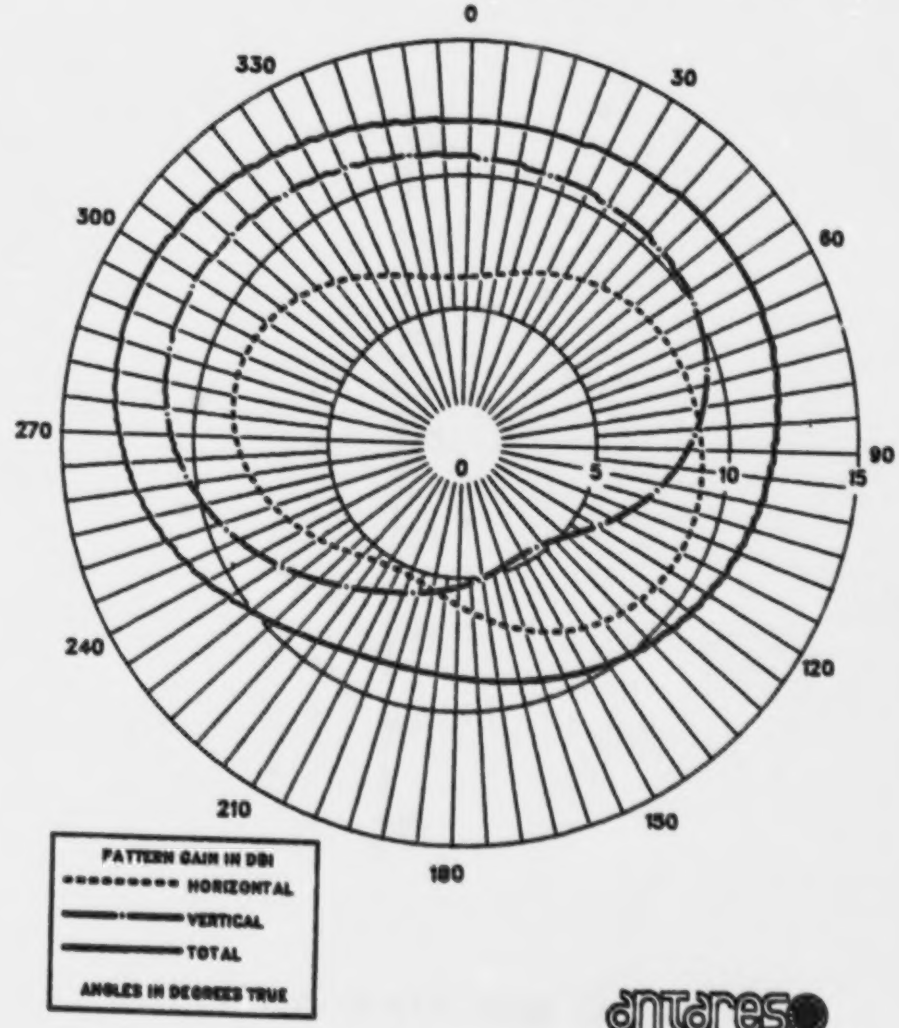

antares
Antenna Analysis Resources

FIGURE D 92

THE FMH 8 ELEMENT ARRAY

SPACING OF 1.0 WAVELENGTHS BETWEEN ELEMENTS

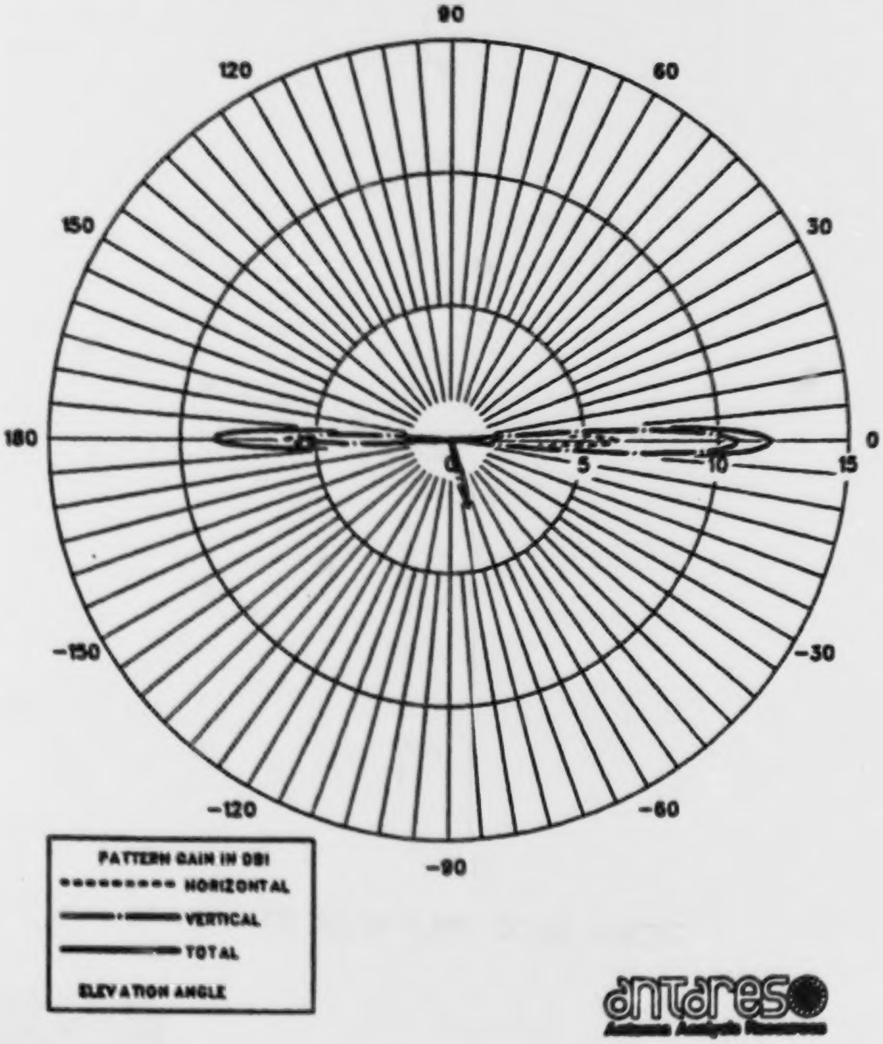

antares
Antenna Analysis Resources

FIGURE D 93

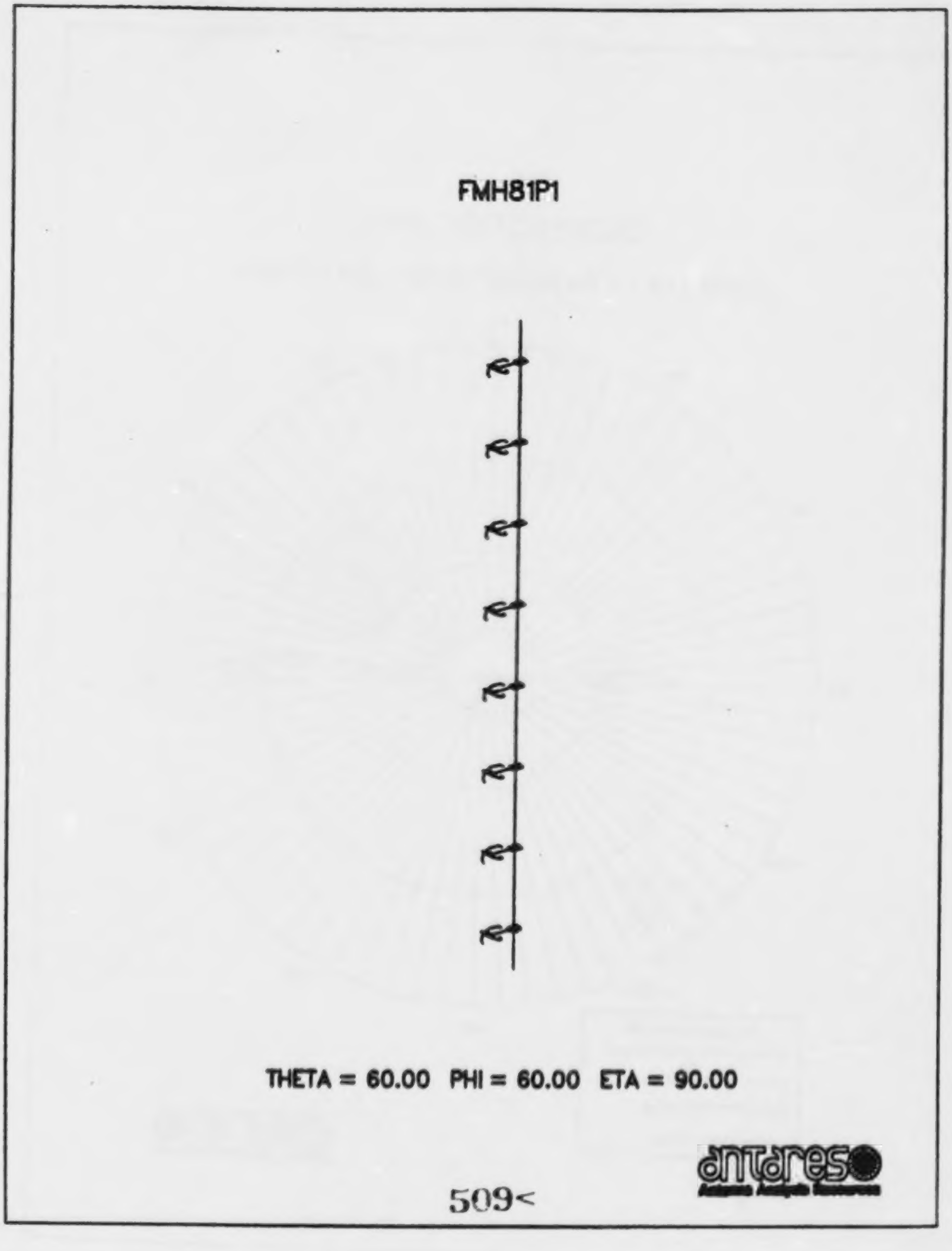

FIGURE D 94

THE FMH 8 ELEMENT ARRAY

SPACING OF 1.1 WAVELENGTHS BETWEEN ELEMENTS

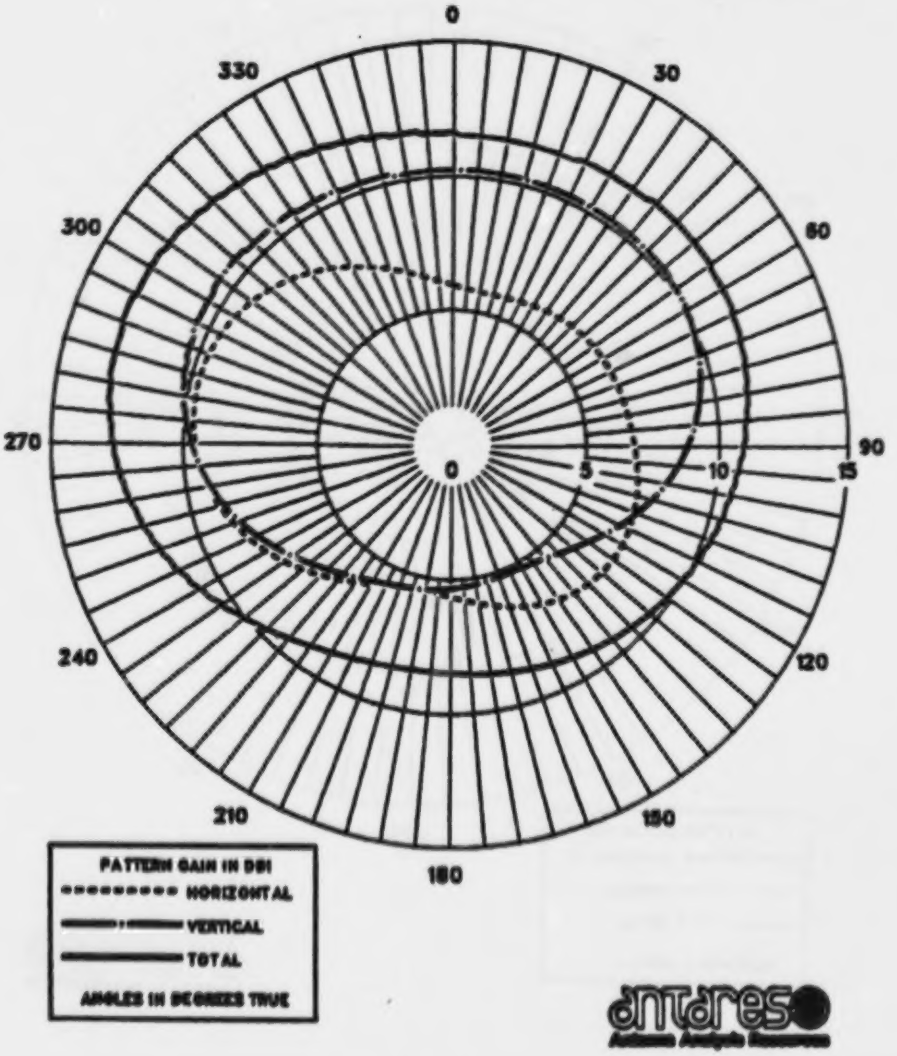

antares
Antenna Analysis Resources

FIGURE D 95

THE FMH 8 ELEMENT ARRAY

SPACING OF 1.1 WAVELENGTHS BETWEEN ELEMENTS

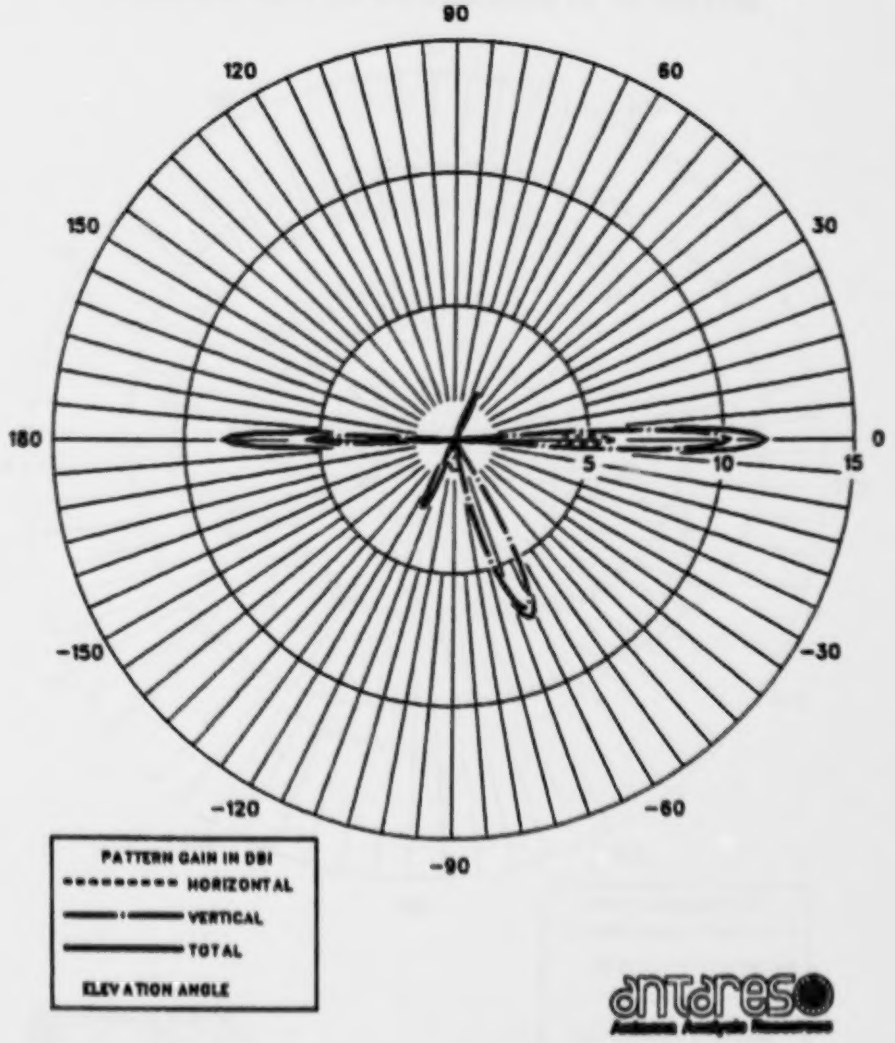

antares
Antenna Analysis Resources

FIGURE D 96

FHM81P2

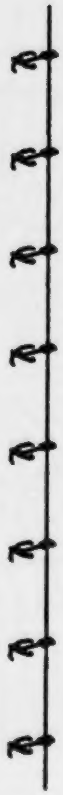

THETA = 60.00 PHI = 60.00 ETA = 90.00

antares
Antares Analysis Resources

FIGURE D 97

THE FMH 8 ELEMENT ARRAY

SPACING OF 1.2 WAVELENGTHS BETWEEN ELEMENTS

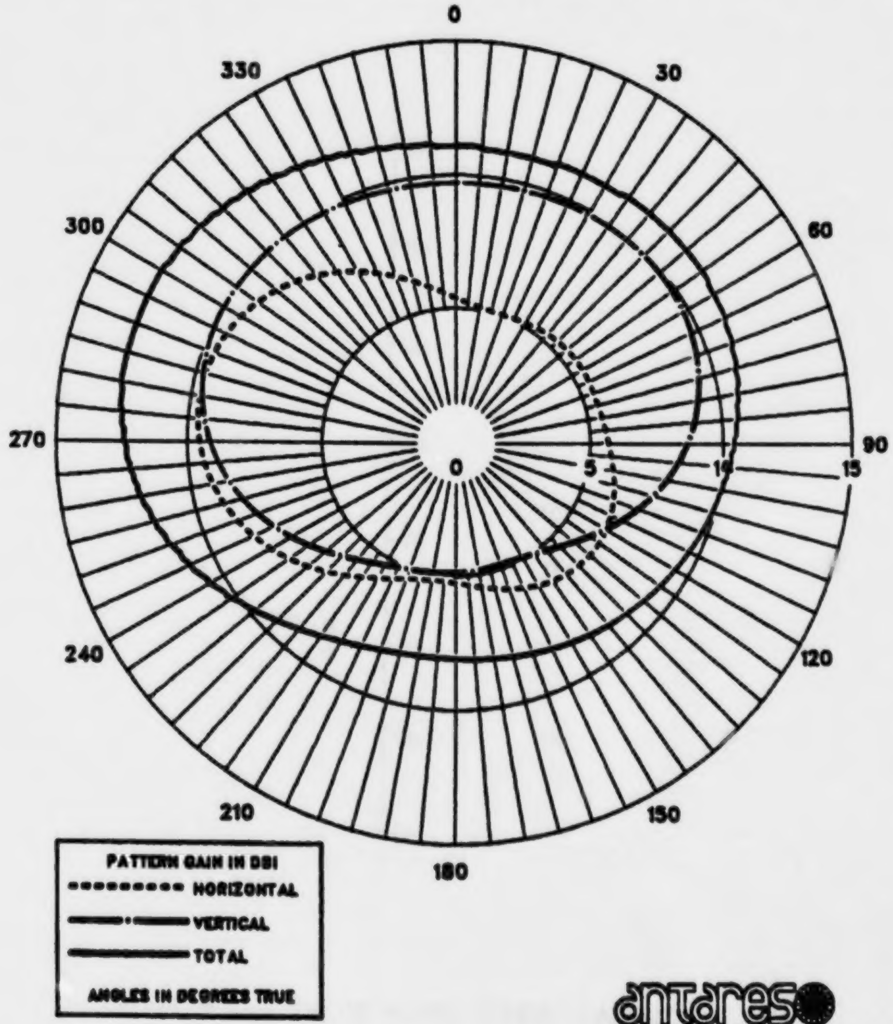

antares
Antenna Analysis Resources

FIGURE D 98

THE FMH 8 ELEMENT ARRAY

SPACING OF 1.2 WAVELENGTHS BETWEEN ELEMENTS

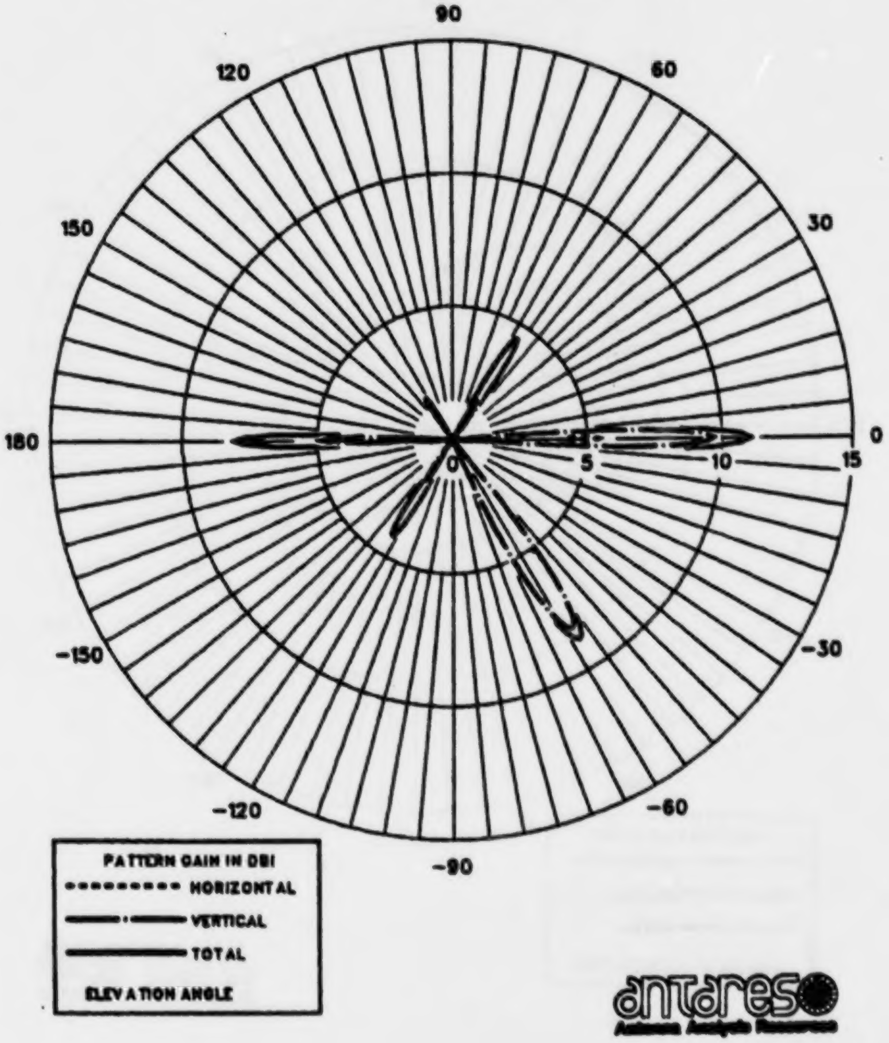

antares
Antenna Analysis Resources

FIGURE D 99

THE FMH 16 ELEMENT ARRAY

SPACING OF 0.2 WAVELENGTHS BETWEEN ELEMENTS

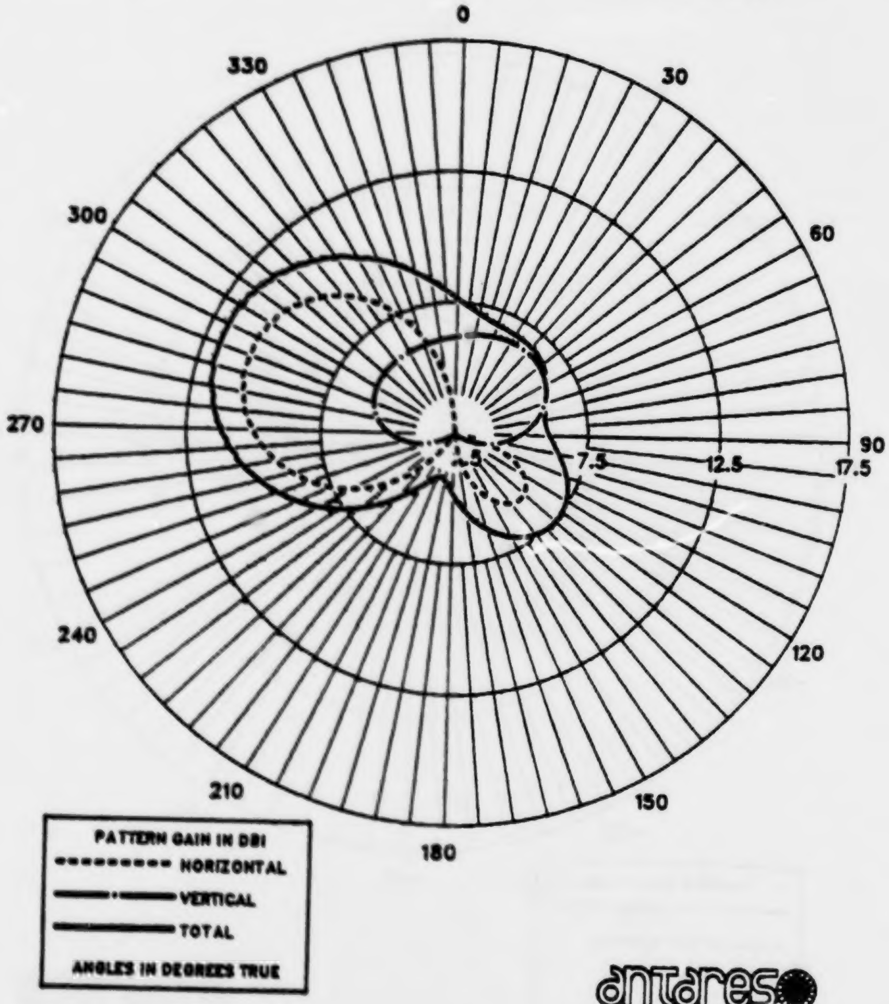

515<

FIGURE D 100

FMH16P2

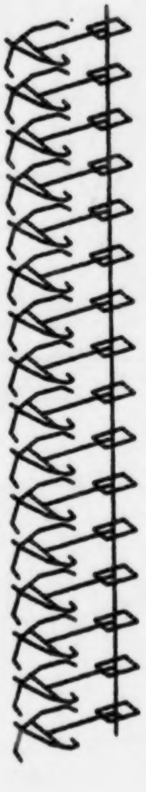

THETA = 60.00 PHI = 60.00 ETA = 90.00

antares
Antenna Analysis Resources

FIGURE D 101

THE FMH 16 ELEMENT ARRAY

SPACING OF 0.2 WAVELENGTHS BETWEEN ELEMENTS

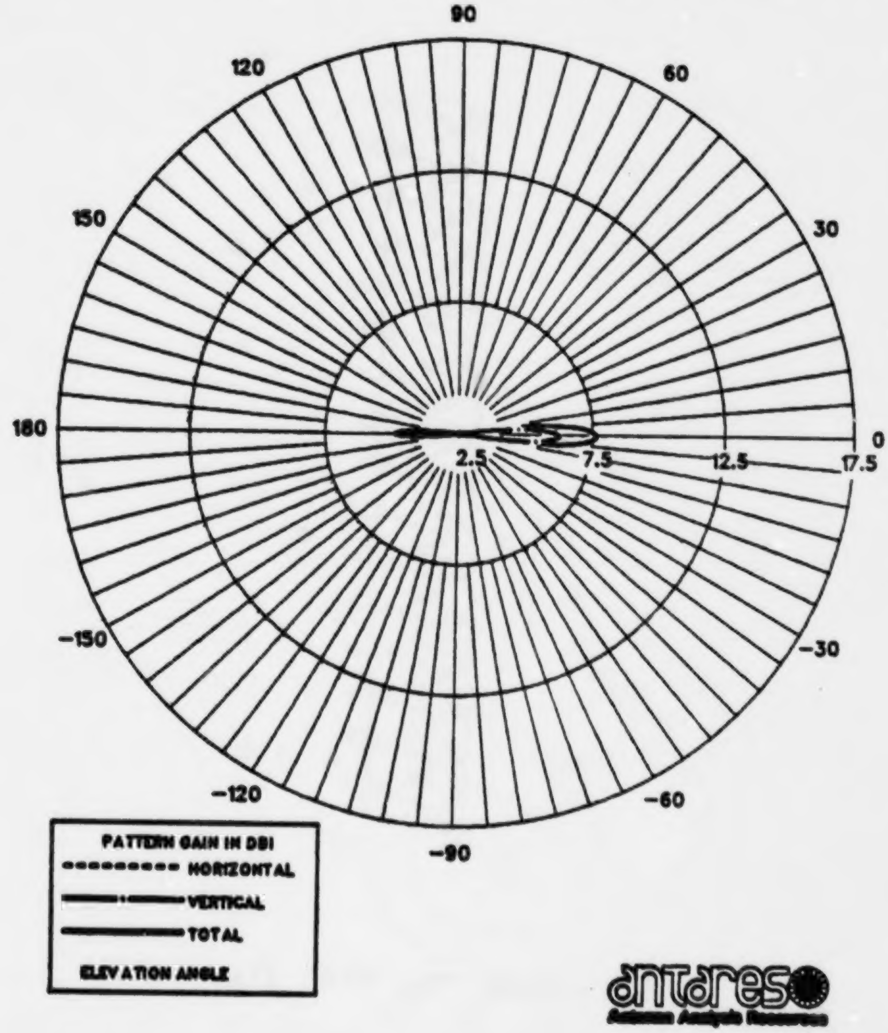

antares
Antenna Analysis Resources

517<

FIGURE D 102

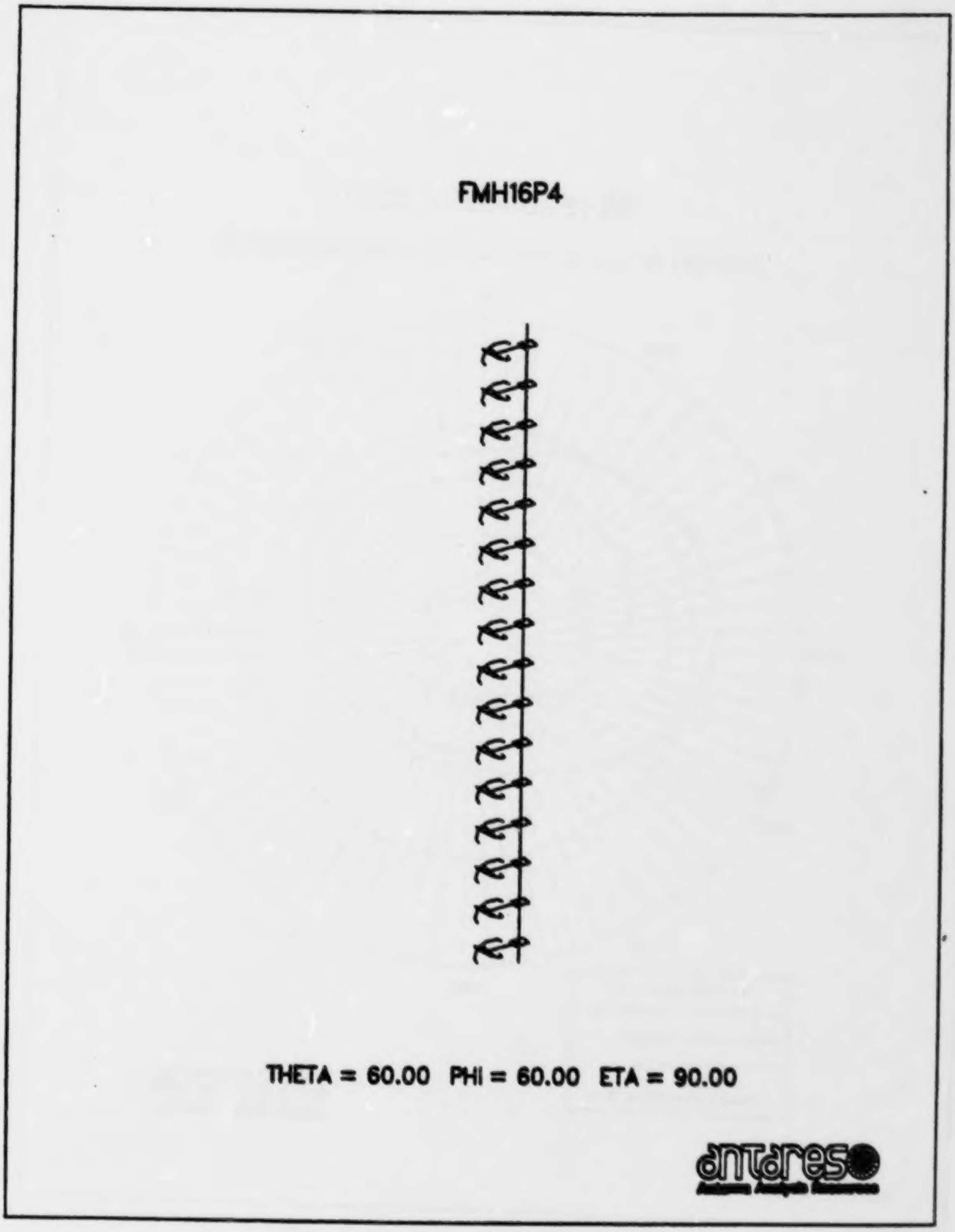
FMH16P4
THETA = 60.00 PHI = 60.00 ETA = 90.00
antares
Antenna Analysis Resources

FIGURE D 103

THE FMH 16 ELEMENT ARRAY

SPACING OF 0.4 WAVELENGTHS BETWEEN ELEMENTS

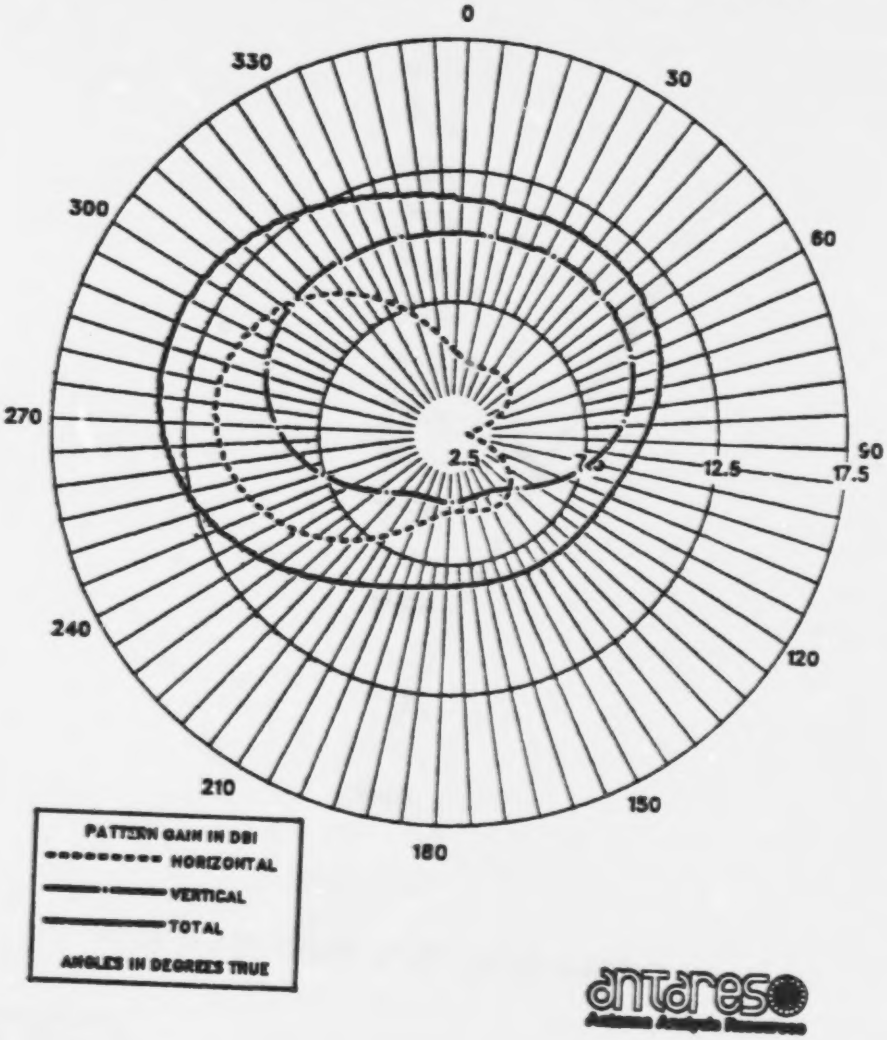

antares
Antenna Analysis Resources

FIGURE D 104

THE FMH 16 ELEMENT ARRAY

SPACING OF 0.4 WAVELENGTHS BETWEEN ELEMENTS

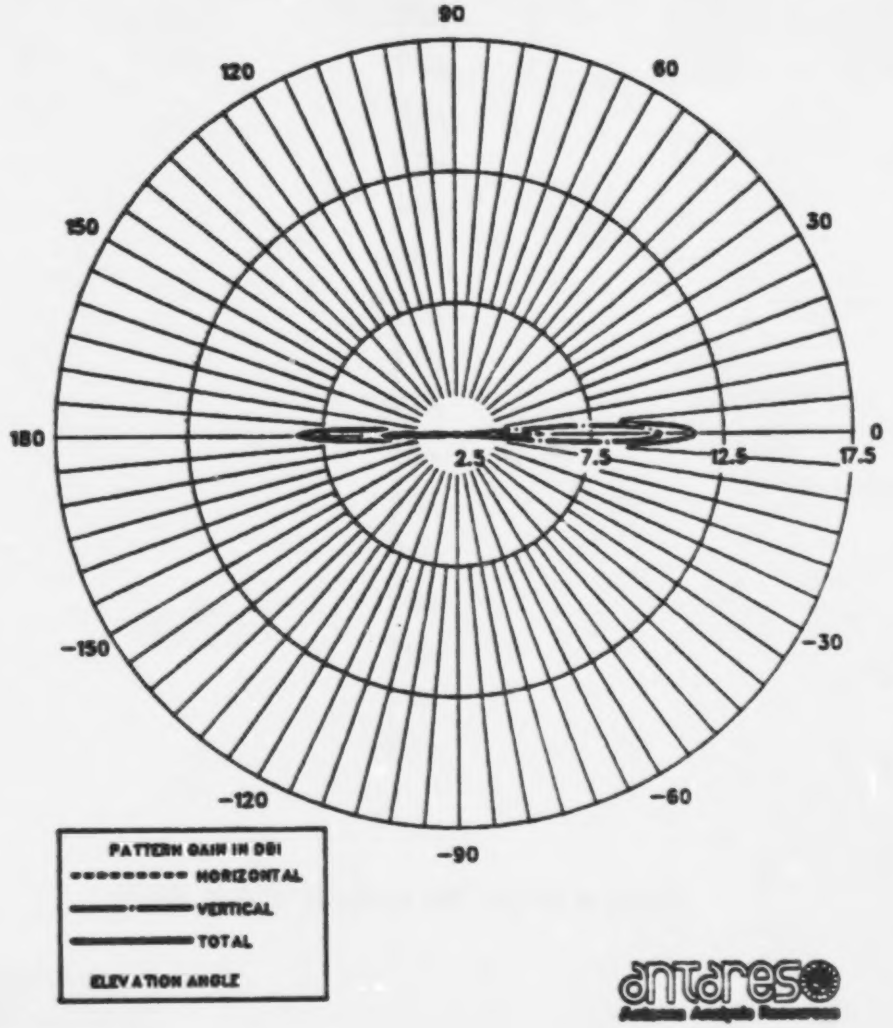

FIGURE D 105

FMH16P5

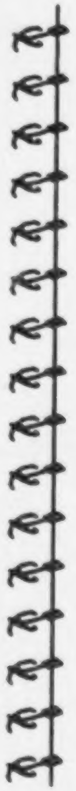

THETA = 60.00 PHI = 60.00 ETA = 90.00

antares Aerospace Analysis Resources

FIGURE D 106

THE FMH 16 ELEMENT ARRAY

SPACING OF 0.5 WAVELENGTHS BETWEEN ELEMENTS

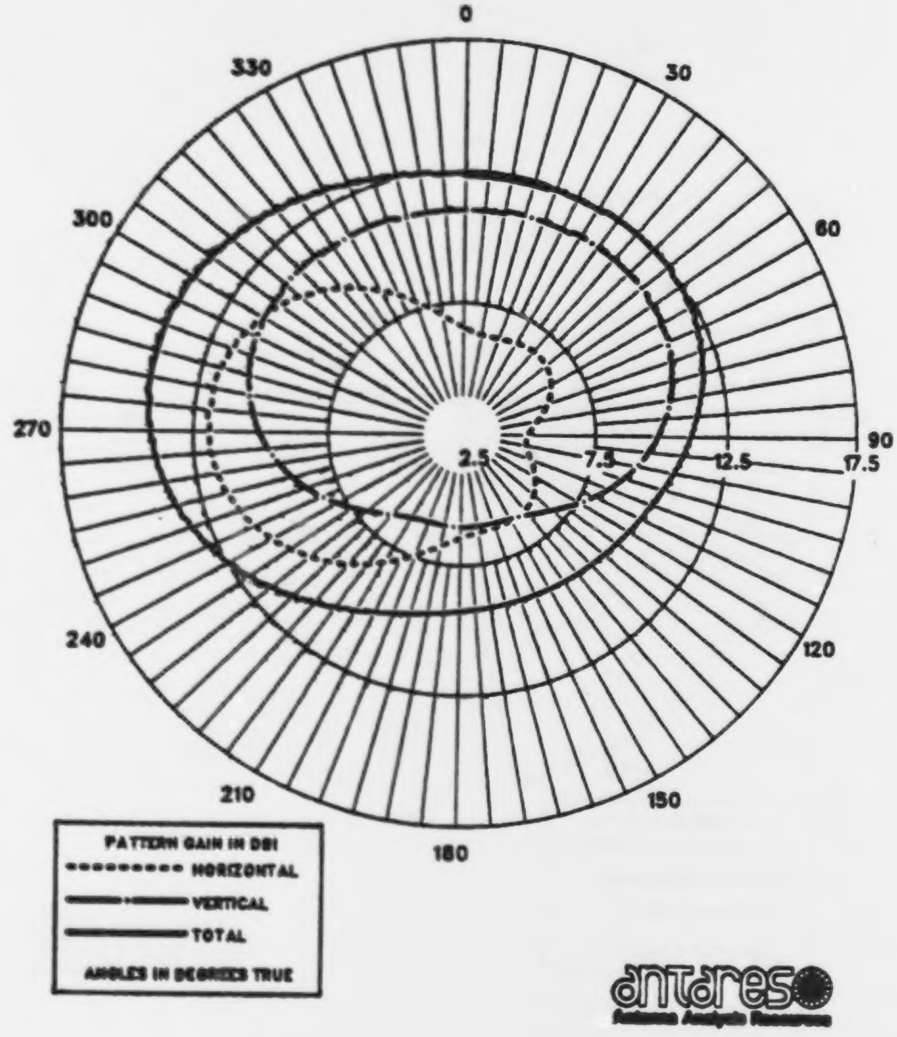

FIGURE D 107

THE FMH 16 ELEMENT ARRAY

SPACING OF 0.5 WAVELENGTHS BETWEEN ELEMENTS

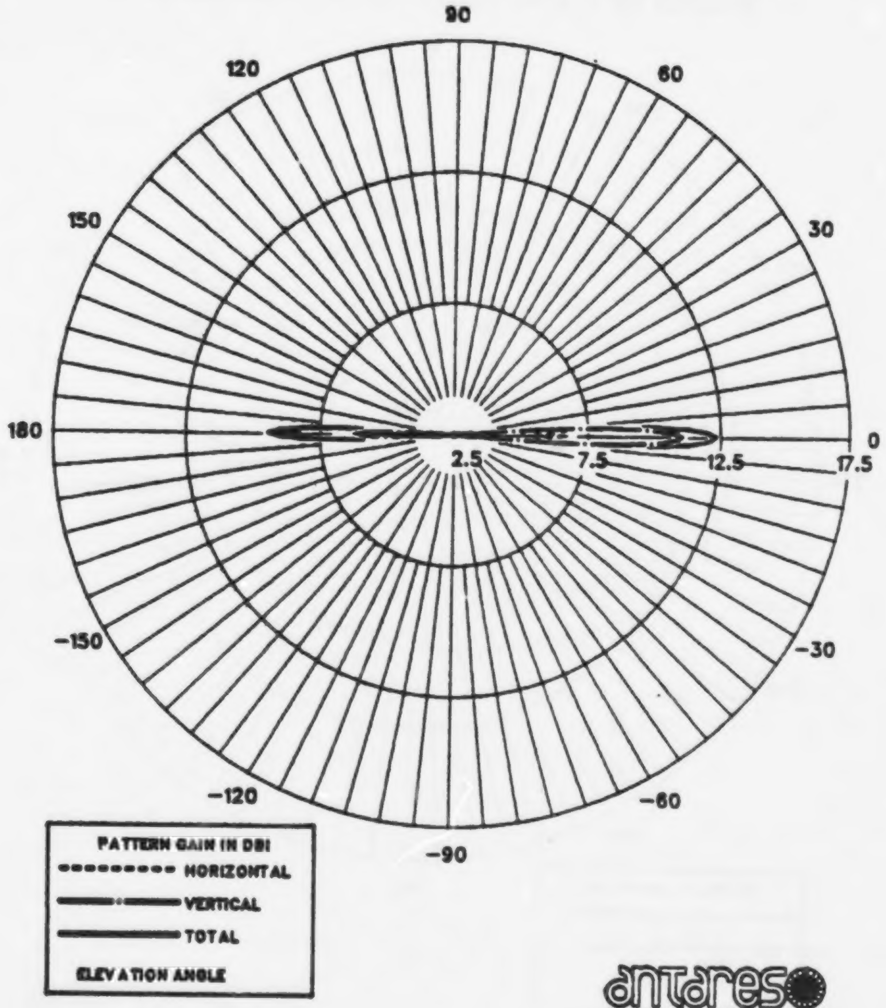

antares
Antenna Analysis Resources

523<

FIGURE D 108

FMH16P7

THETA = 60.00 PHI = 60.00 ETA = 90.00

FIGURE D 109

THE FMH 16 ELEMENT ARRAY

SPACING OF 0.7 WAVELENGTHS BETWEEN ELEMENTS

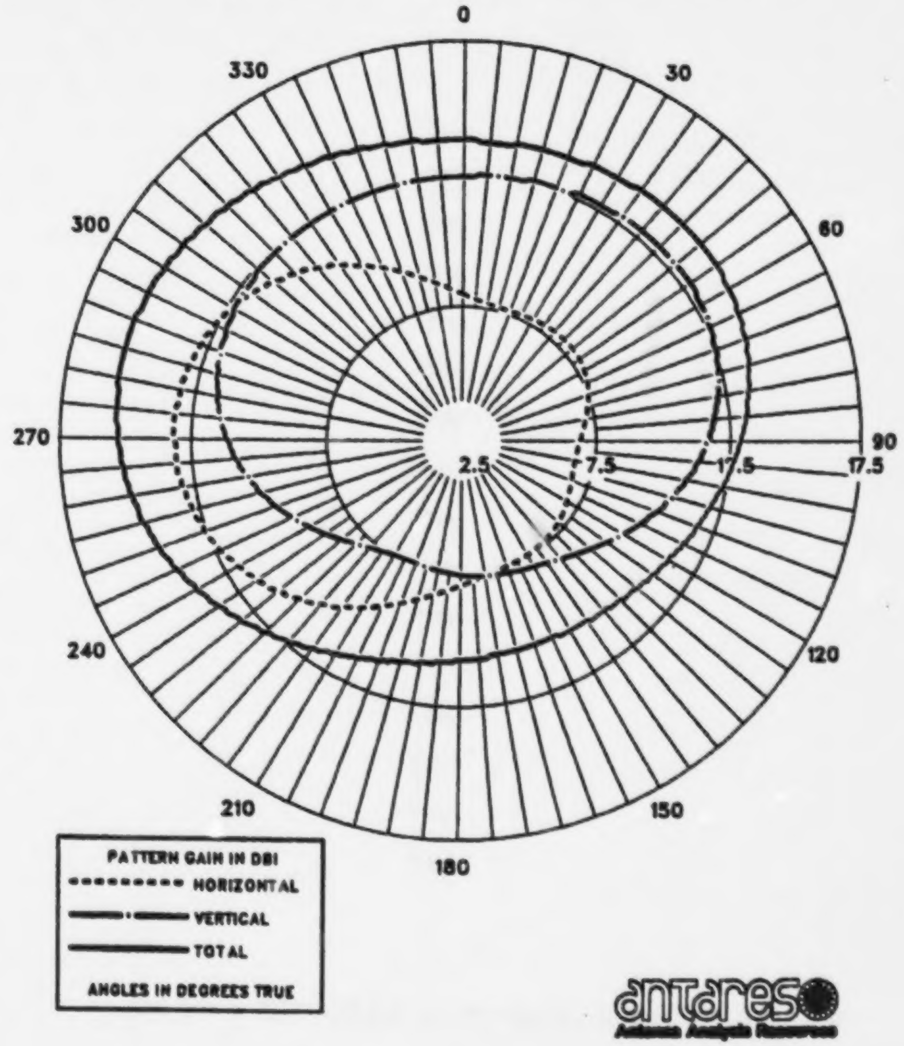

antares
Antenna Analysis Resources

FIGURE D 110

THE FMH 16 ELEMENT ARRAY

SPACING OF 0.7 WAVELENGTHS BETWEEN ELEMENTS

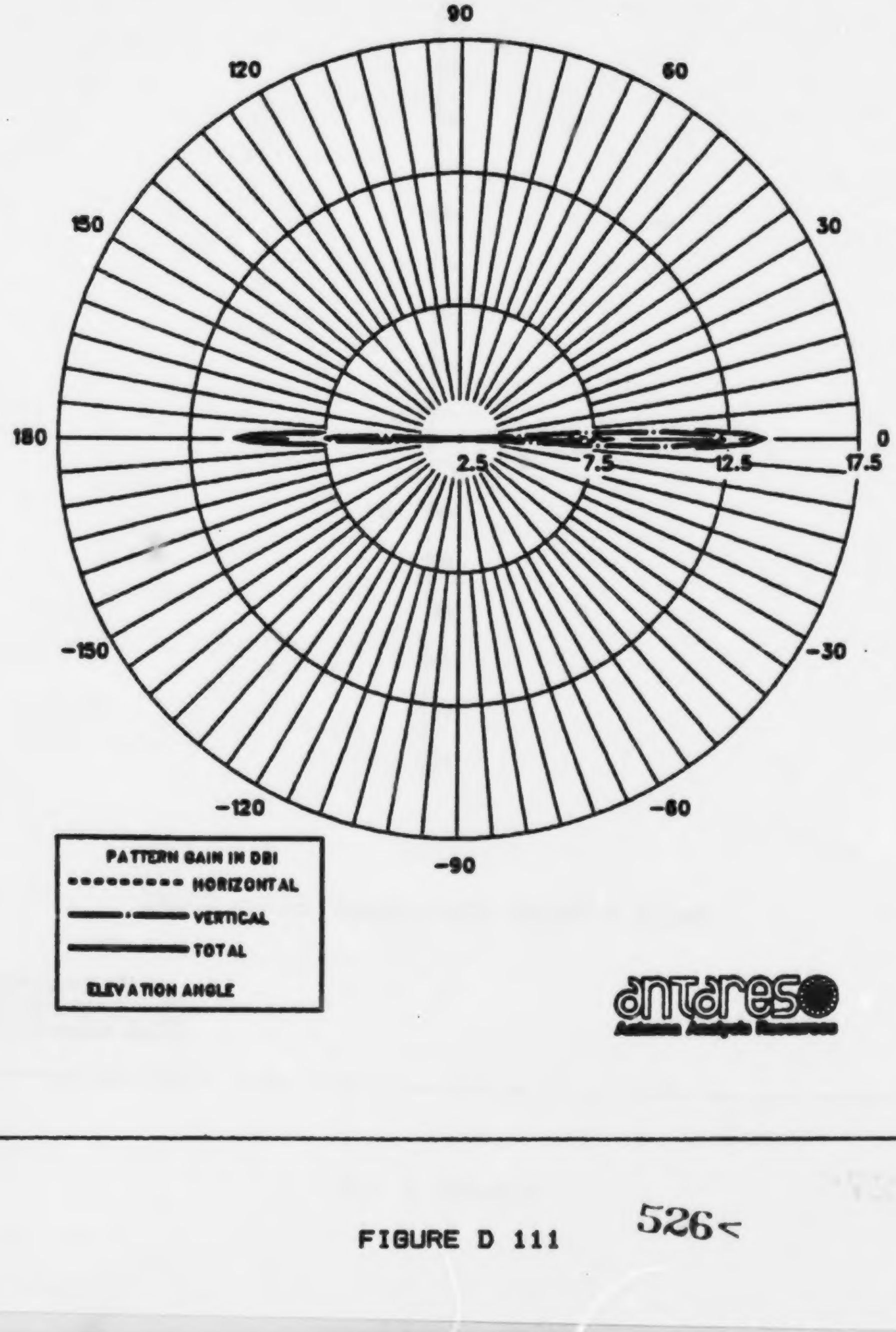

FIGURE D 111 526<

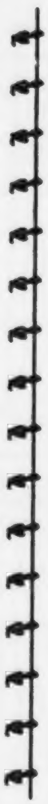

THETA = 60.00 PHI = 60.00 ETA = 90.00

antares
Antenna Analysis Resources

527<

FIGURE D 112

THE FMH 16 ELEMENT ARRAY

SPACING OF 0.9 WAVELENGTHS BETWEEN ELEMENTS

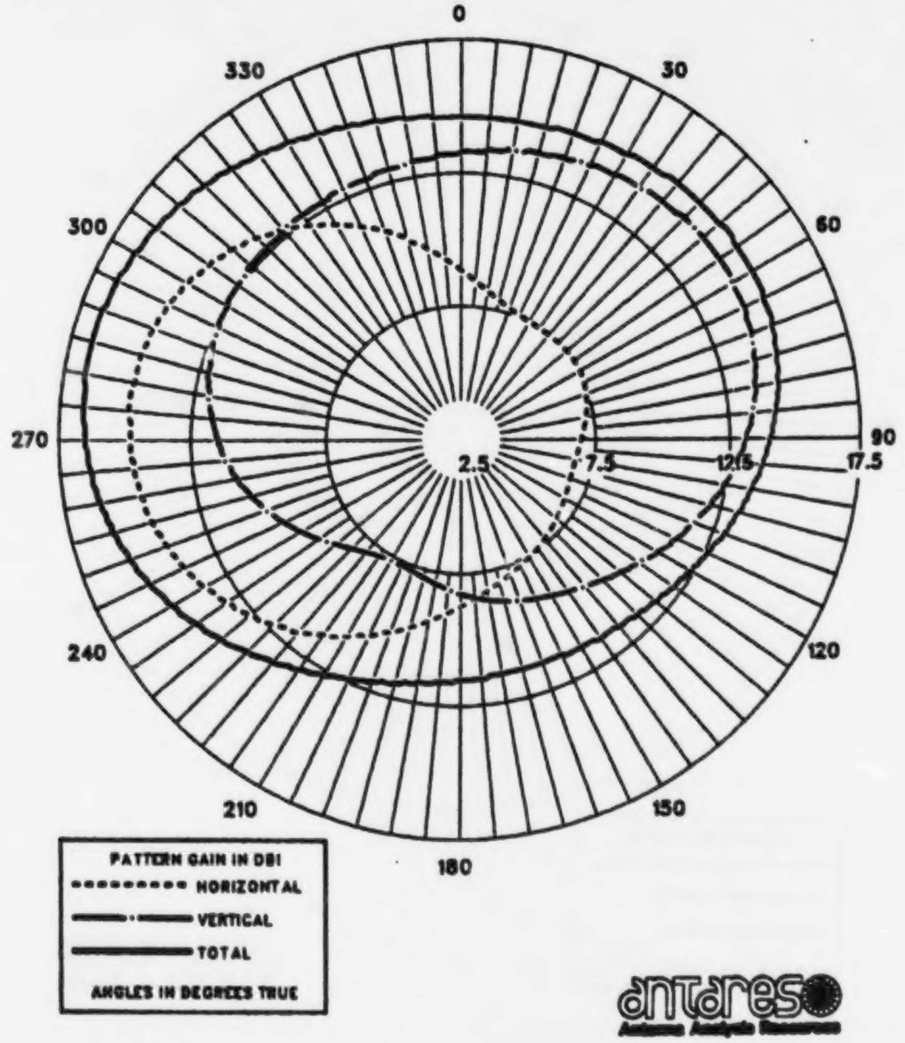

antares
Antenna Analysis Resources

FIGURE D 113

THE FMH 16 ELEMENT ARRAY

SPACING OF 0.9 WAVELENGTHS BETWEEN ELEMENTS

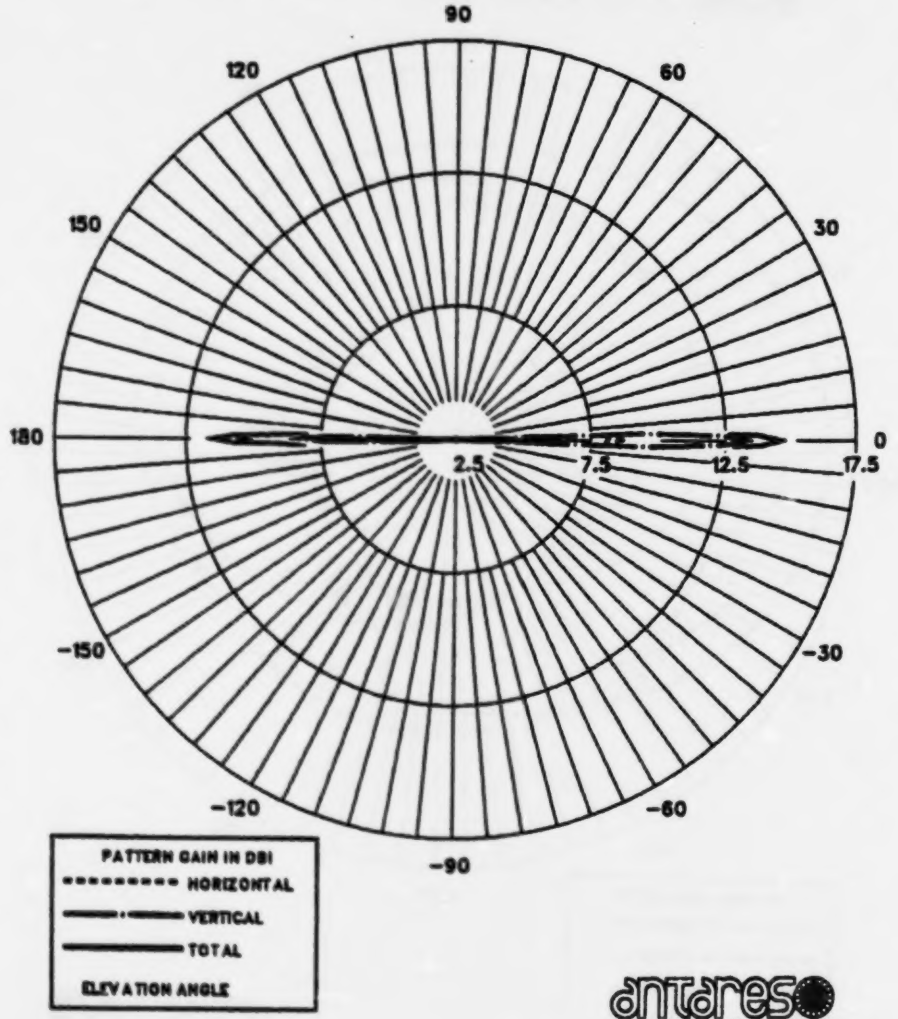

antares
Antenna Analysis Resources

FIGURE D 114

FMH16

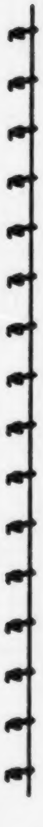

THETA = 60.00 PHI = 60.00 ETA = 90.00

FIGURE D 115

THE FMH 16 ELEMENT ARRAY

SPACING OF 1.0 WAVELENGTHS BETWEEN ELEMENTS

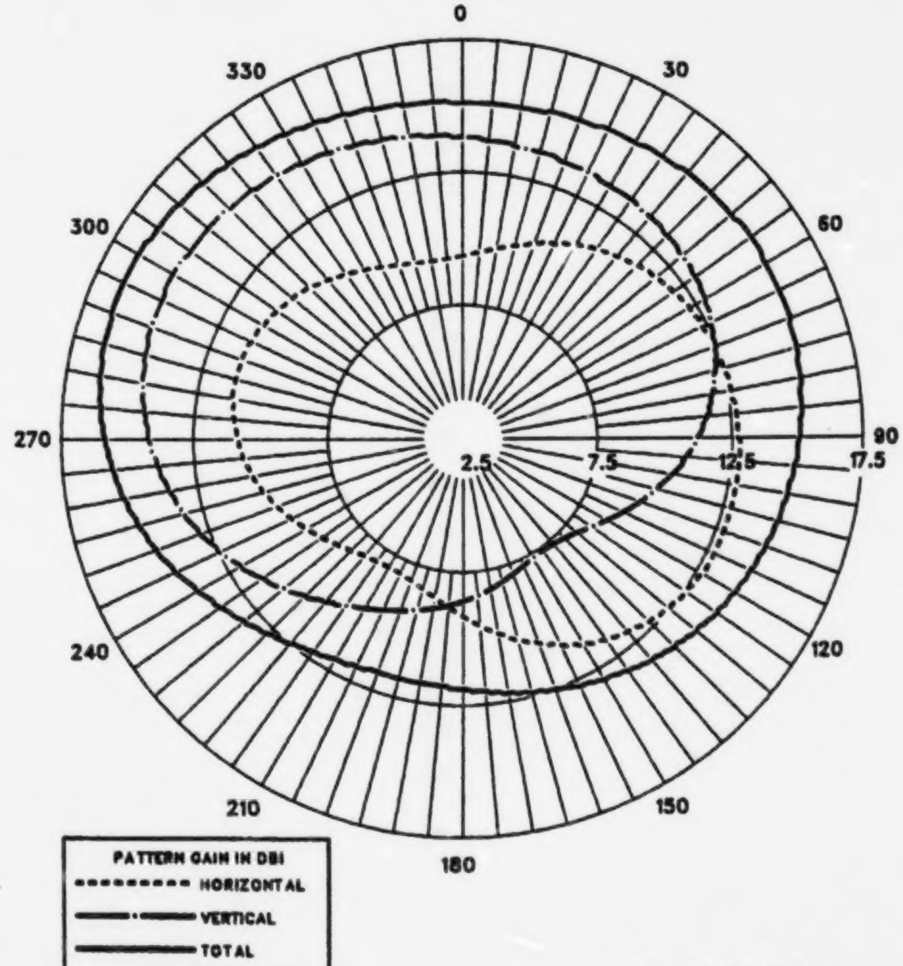

antares
Antenna Analysis Resources

FIGURE D 116

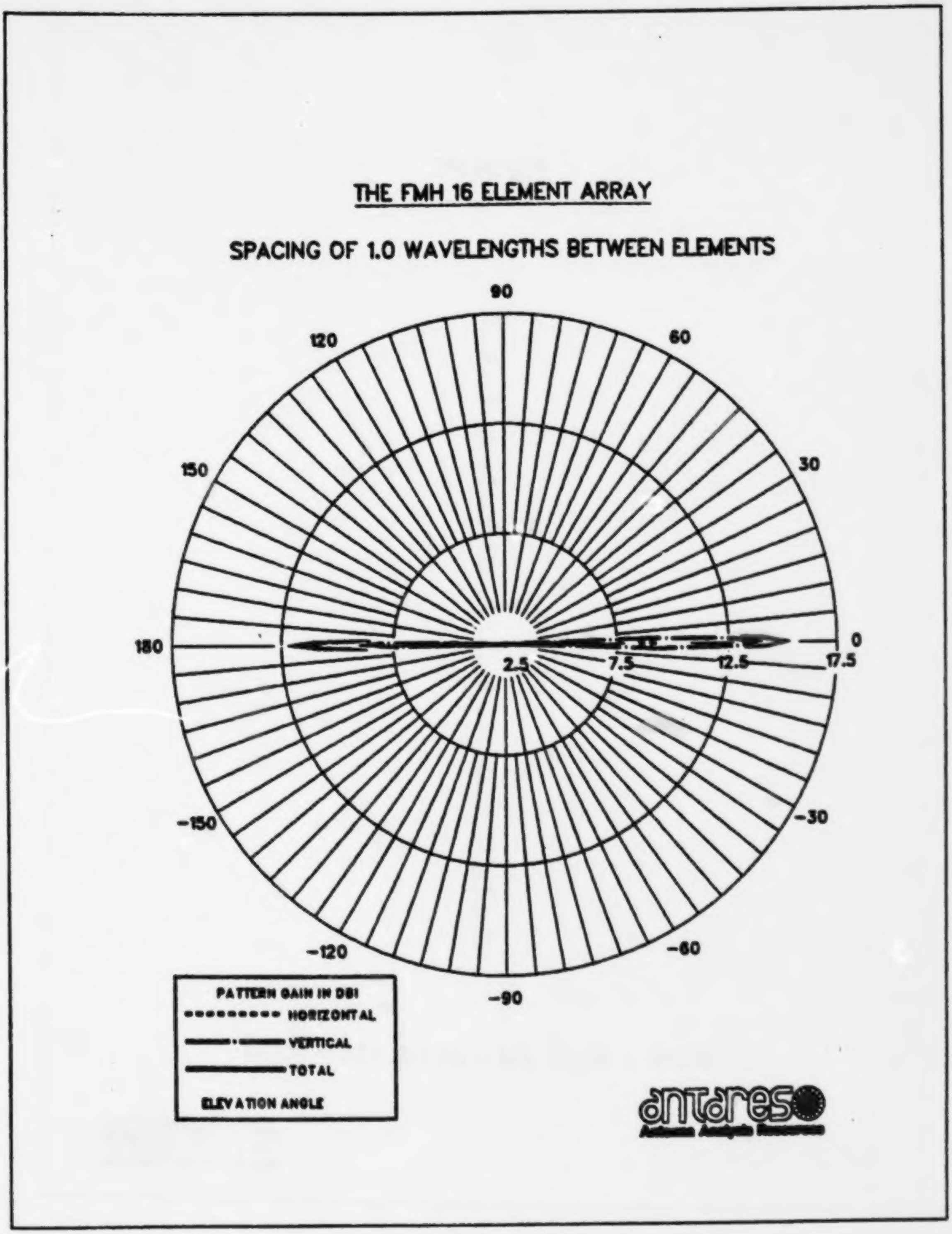
THE FMH 16 ELEMENT ARRAY

SPACING OF 1.0 WAVELENGTHS BETWEEN ELEMENTS

FIGURE D 117

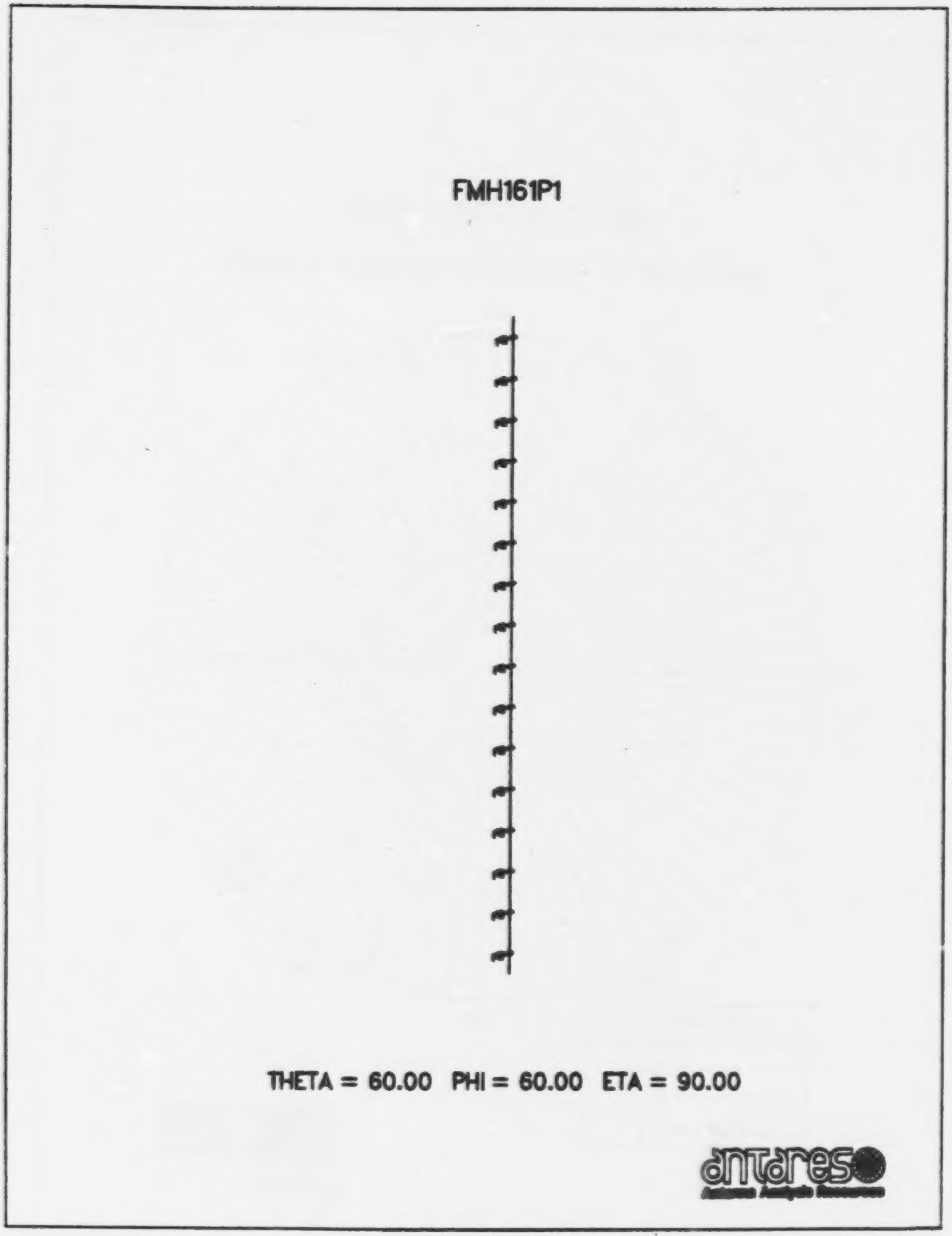

FIGURE D 118

THE FMH 16 ELEMENT ARRAY

SPACING OF 1.1 WAVELENGTHS BETWEEN ELEMENTS

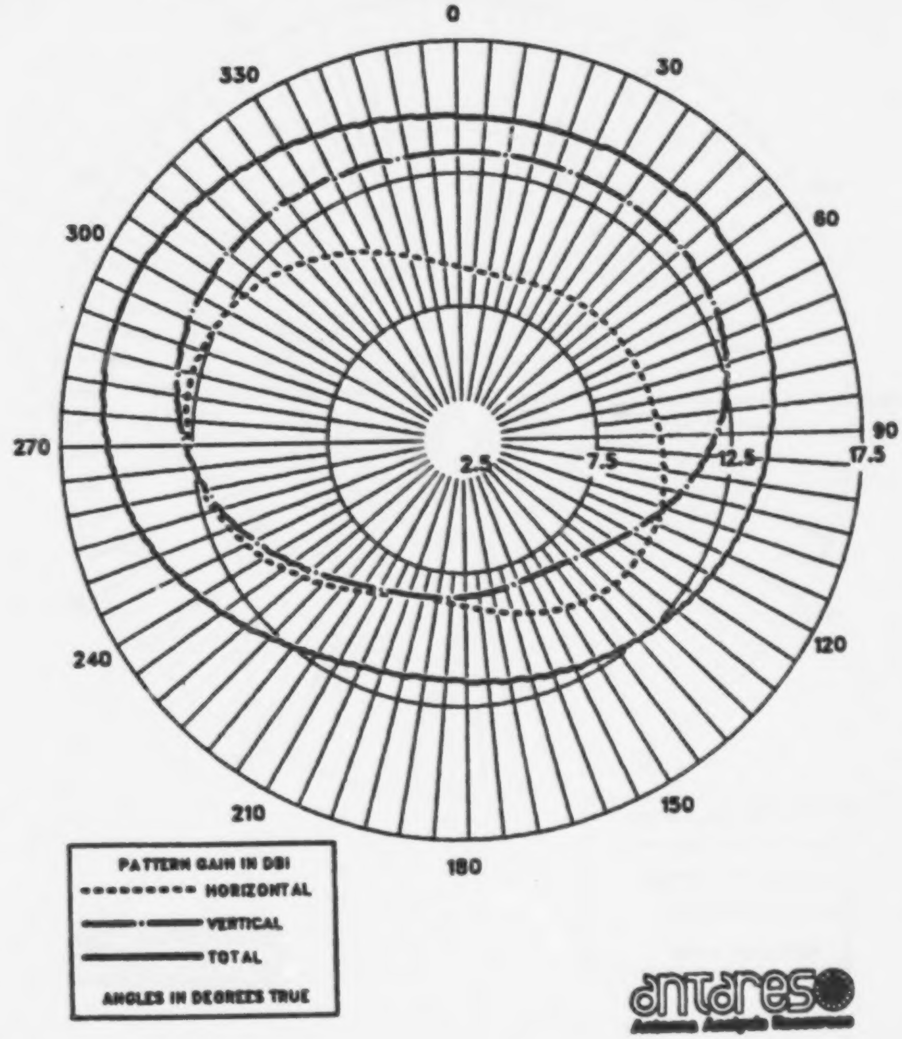

antares
Antenna Analysis Resources

FIGURE D 119

THE FMH 16 ELEMENT ARRAY

SPACING OF 1.1 WAVELENGTHS BETWEEN ELEMENTS

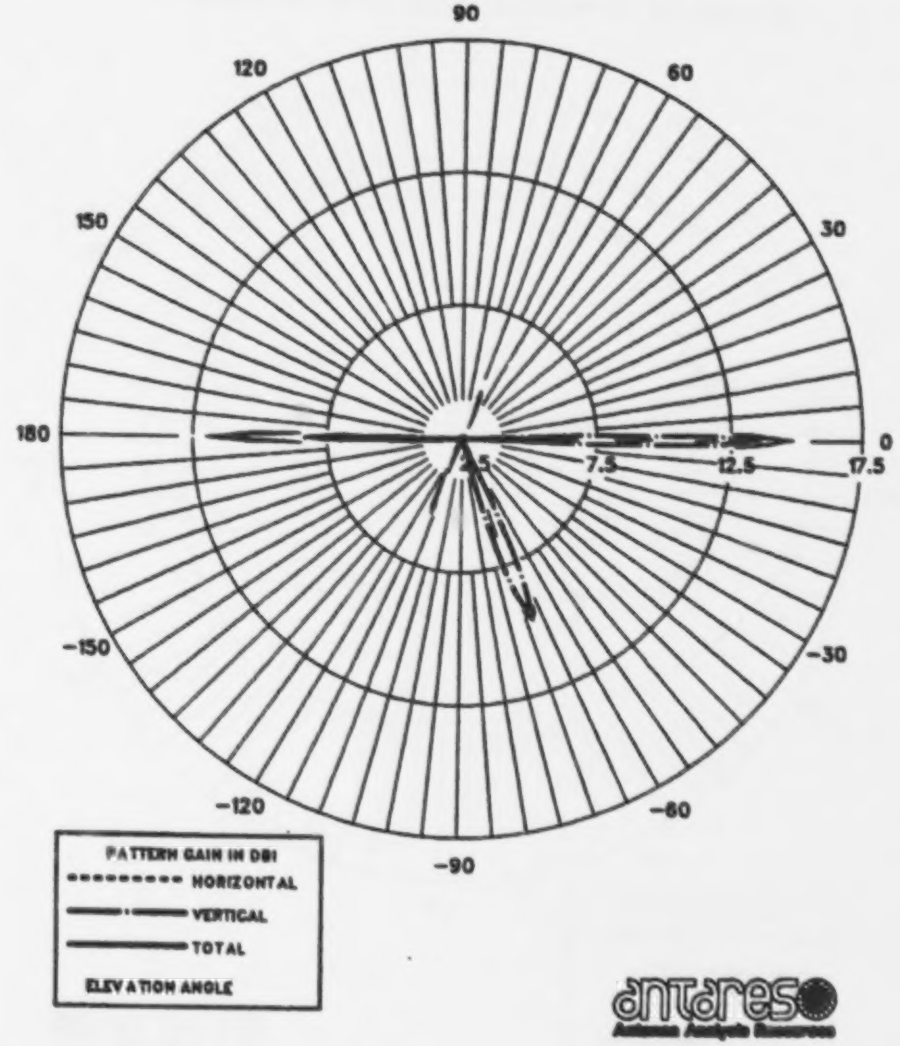

FIGURE D 120

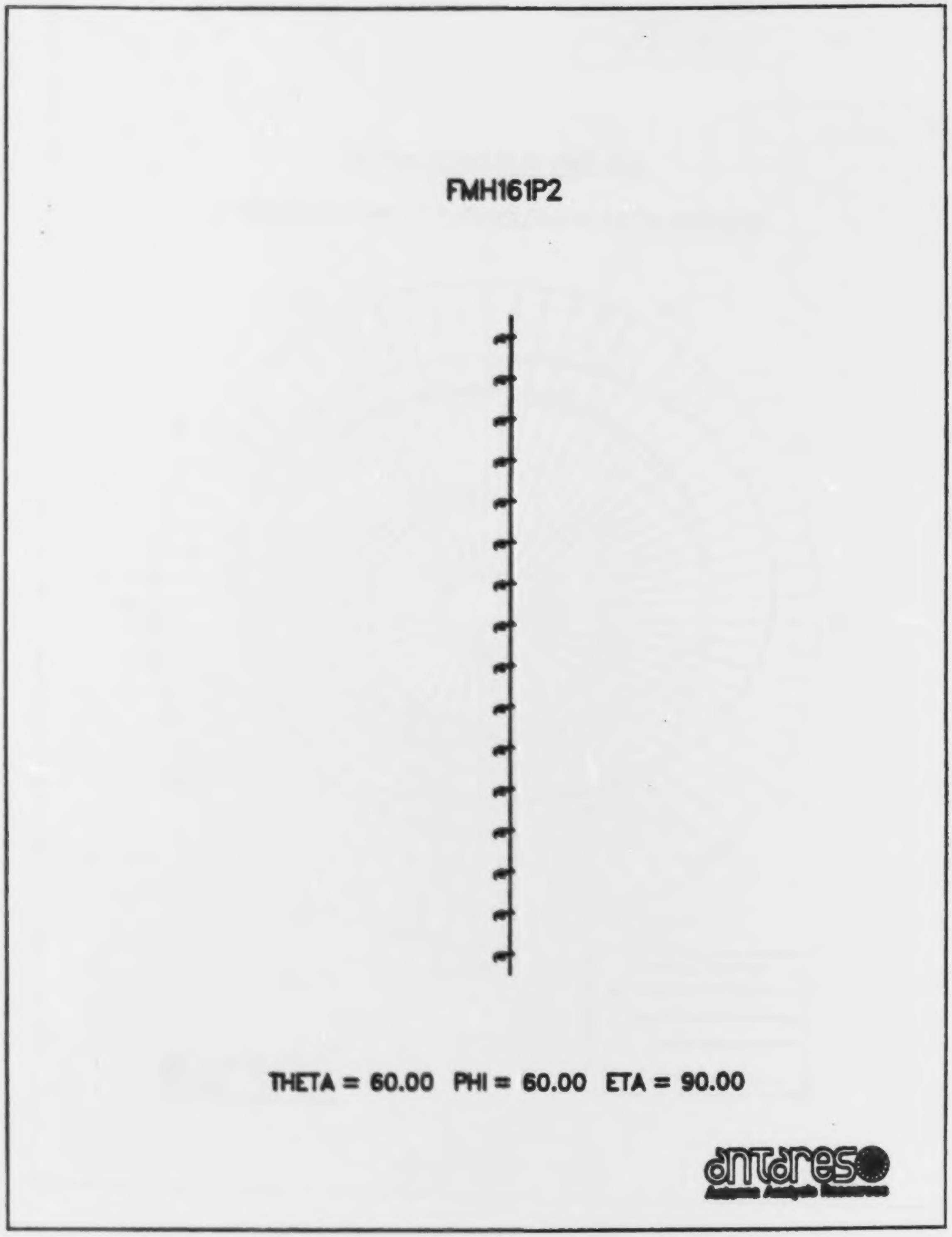
FMH161P2
THETA = 60.00 PHI = 60.00 ETA = 90.00
antares
Antenna Analysis Resources

FIGURE D 121

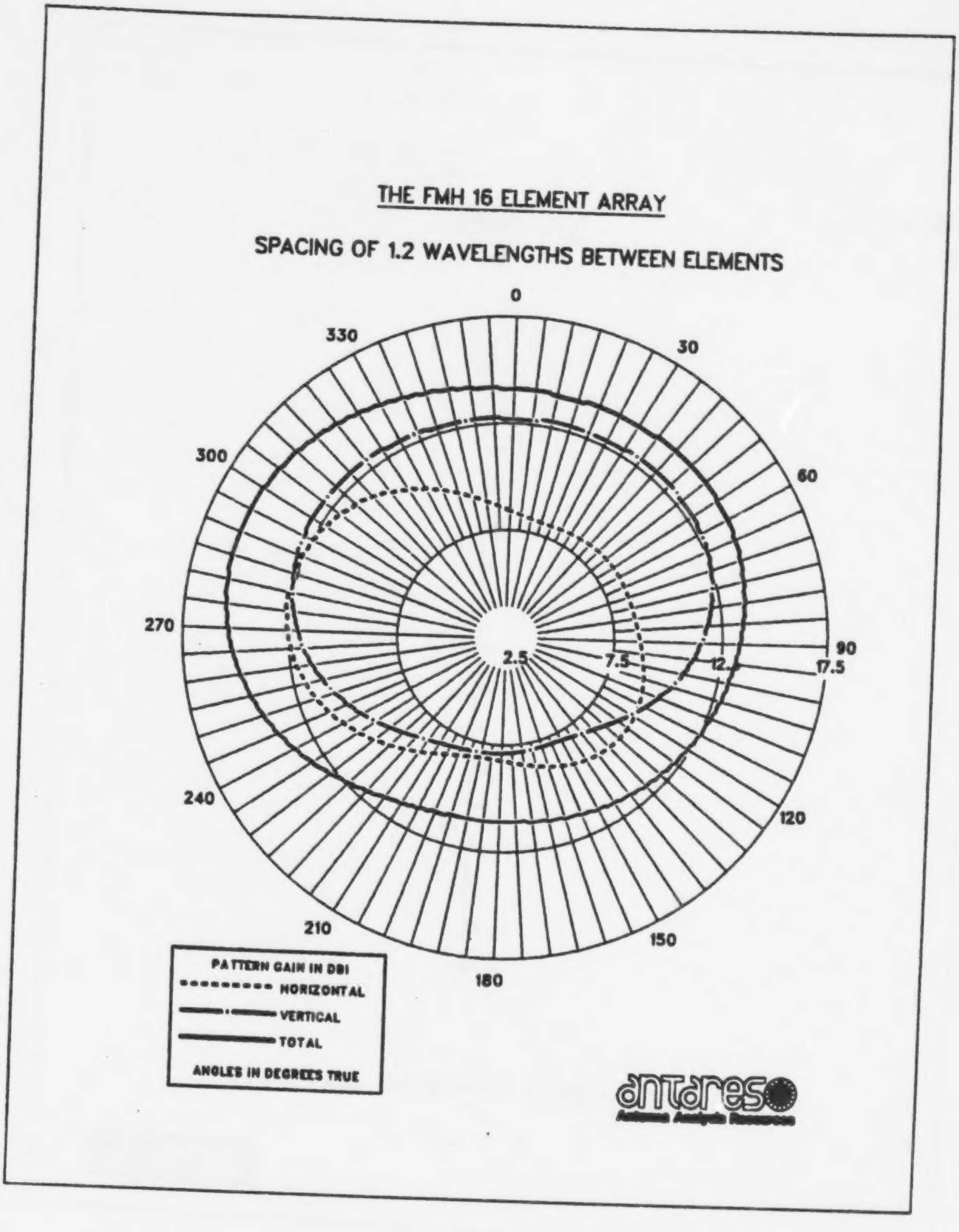
THE FMH 16 ELEMENT ARRAY
SPACING OF 1.2 WAVELENGTHS BETWEEN ELEMENTS
0
30
60
90
120
150
180
210
240
270
300
330
2.5
7.5
12.5
17.5
PATTERN GAIN IN DBI
HORIZONTAL
VERTICAL
TOTAL
ANGLES IN DEGREES TRUE
antares
Antenna Analysis Resources

FIGURE D 122

THE FMH 16 ELEMENT ARRAY

SPACING OF 1.2 WAVELENGTHS BETWEEN ELEMENTS

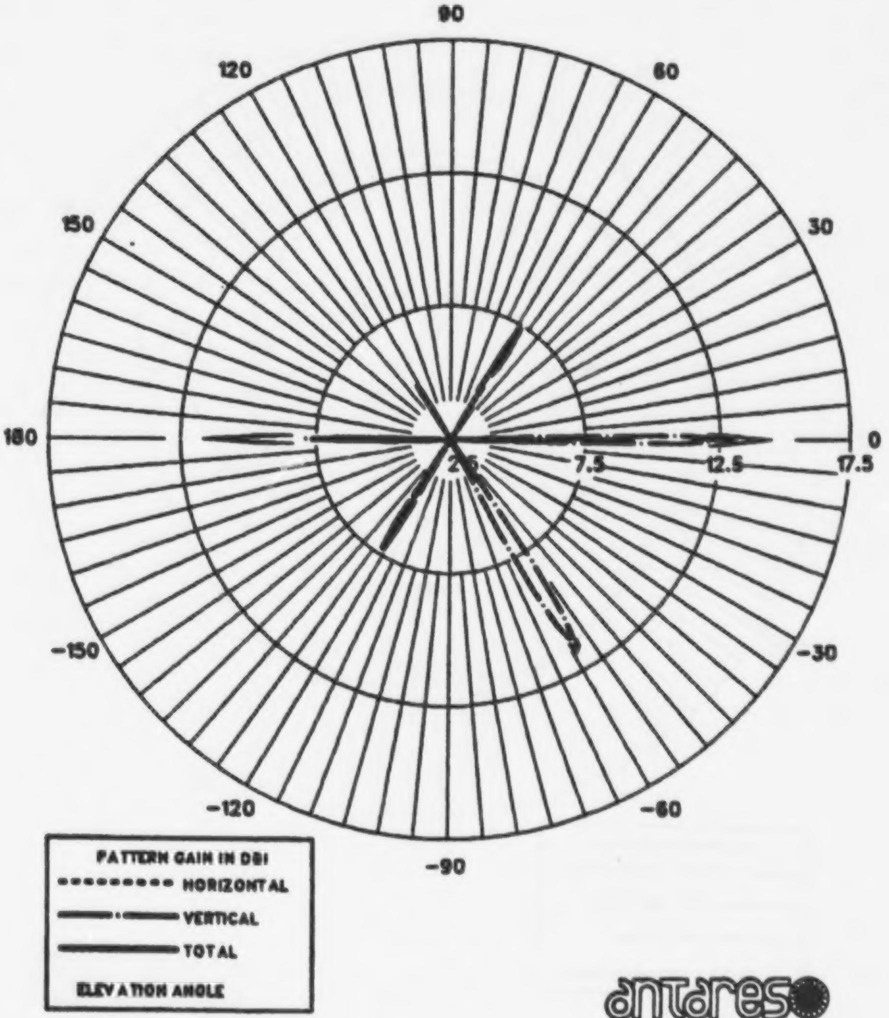

antares
Antenna Analysis Resources

FIGURE D 123

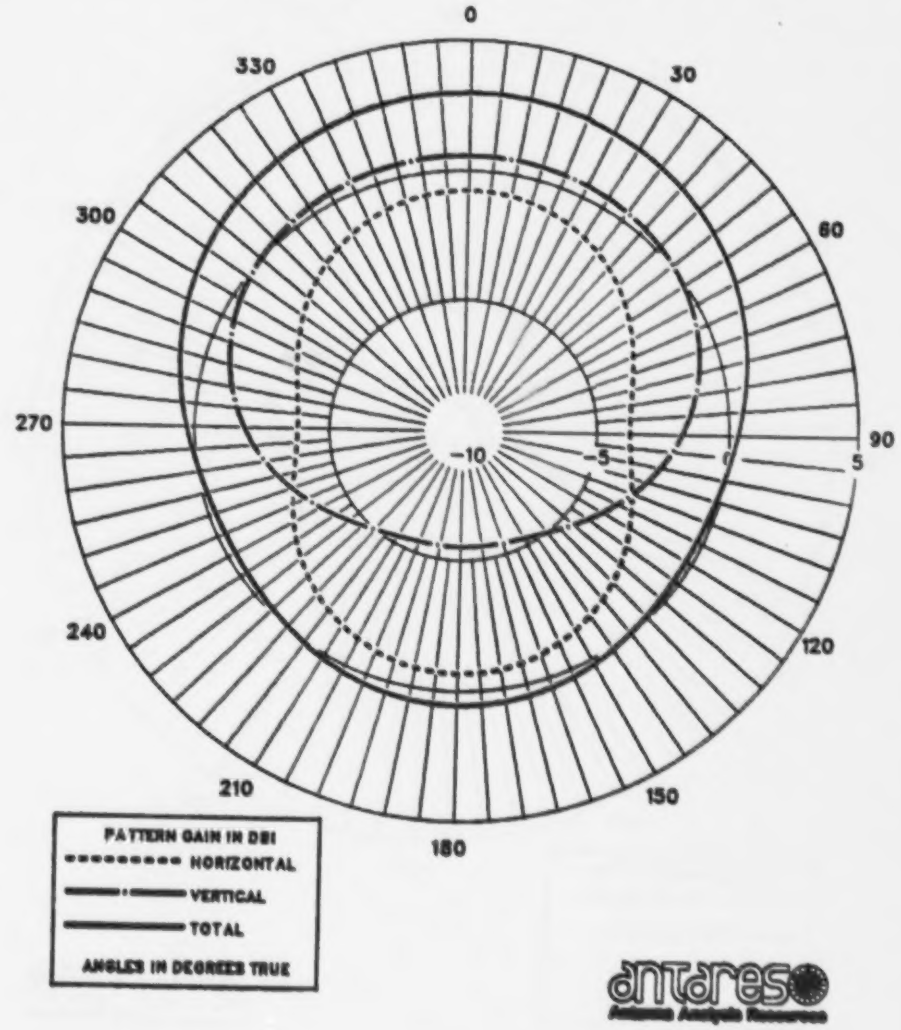

ONE CYCLOID ELEMENT W/ FEEDLINE

AZIMUTH PATTERN AT HORIZON

FIGURE D 124

ONE CYCLOID ELEMENT W/ FEEDLINE

VERTICAL PATTERN AT BORESITE

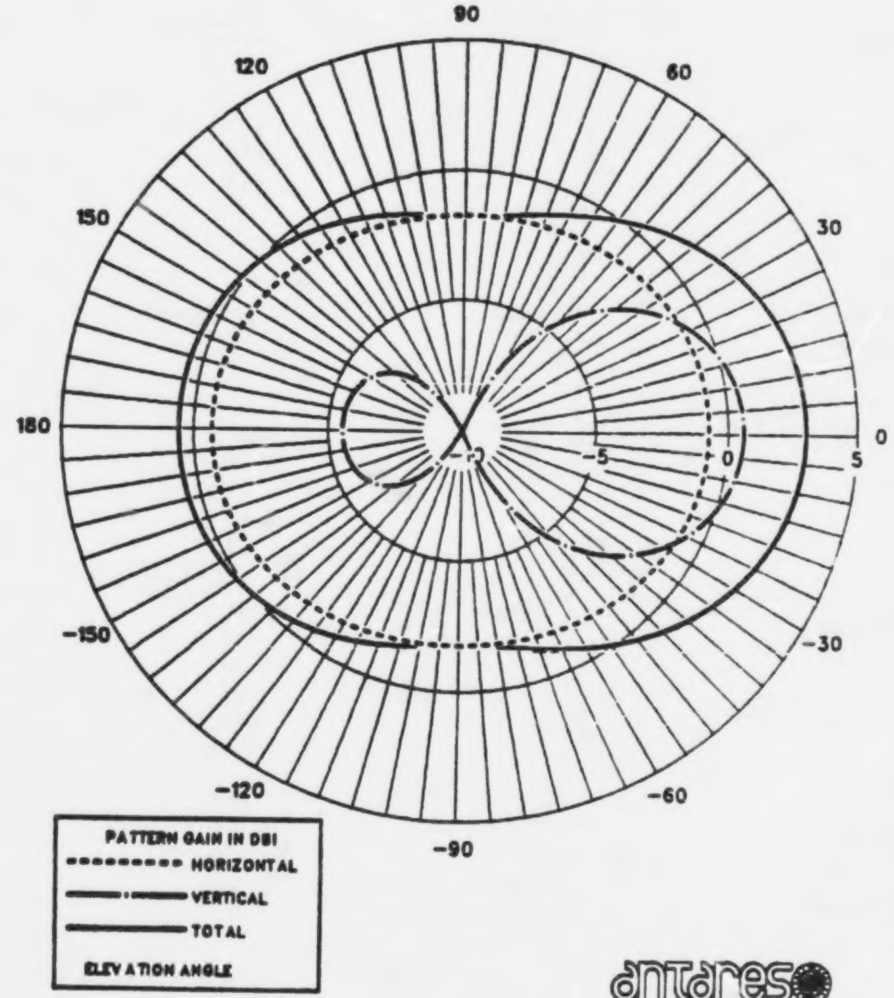

antares
Antenna Analysis Resources

FIGURE D 125

ONE CYCLOID ELEMENT W/ FEEDLINE

VERTICAL PATTERN AT BORESITE

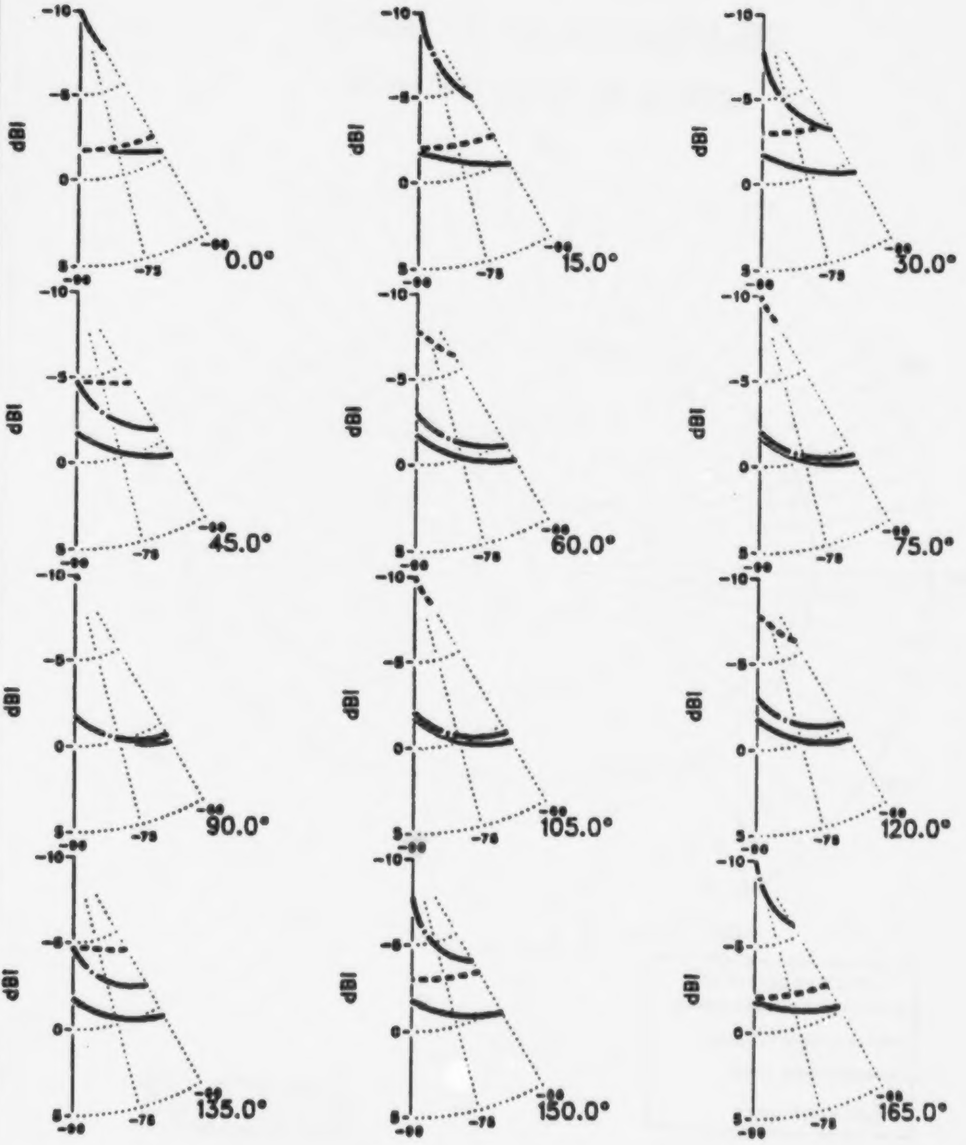

541<

FIGURE D 126

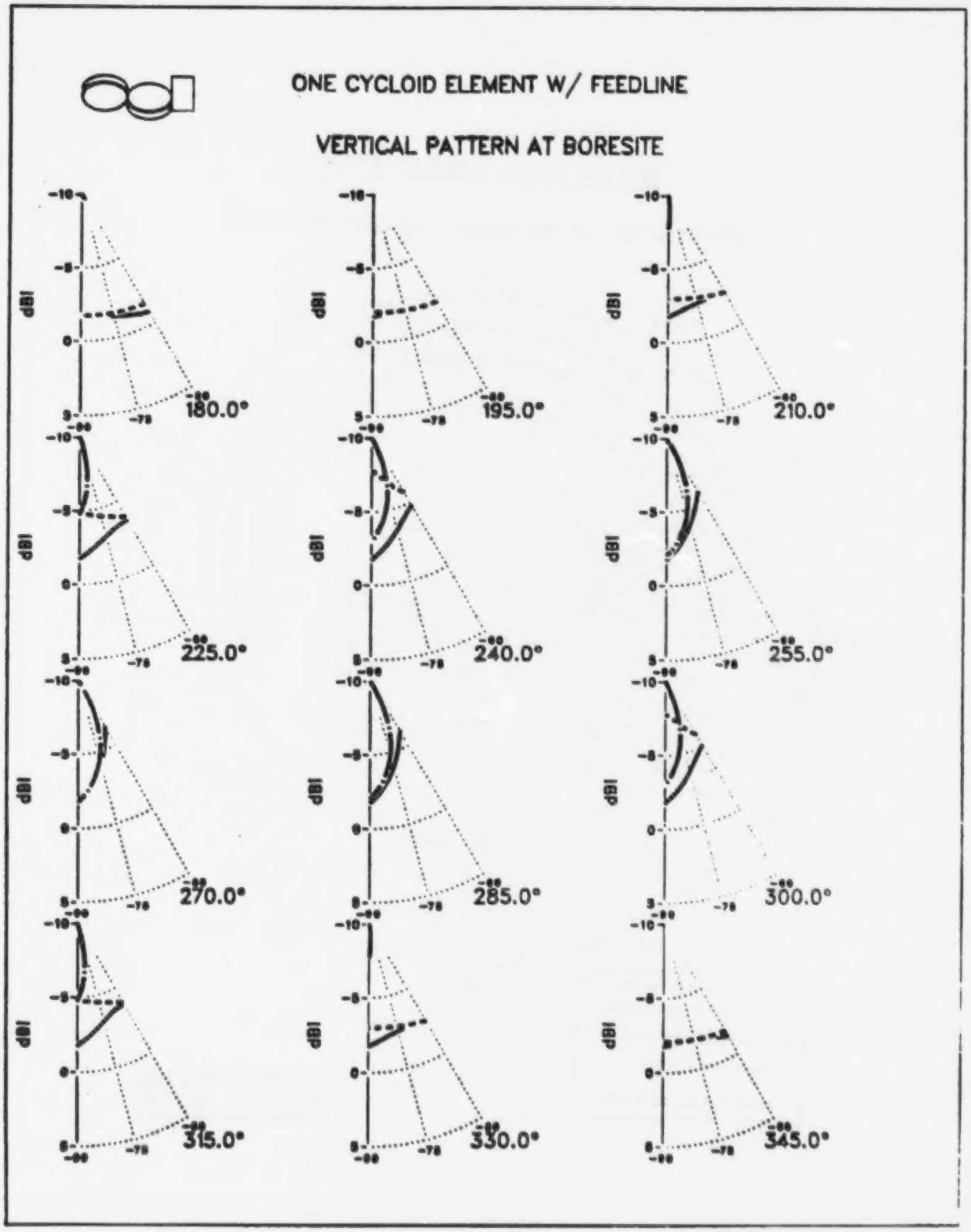
ONE CYCLOID ELEMENT W/ FEEDLINE

VERTICAL PATTERN AT BORESITE

FIGURE D 127

THE CYCLOID 2 ELEMENT ARRAY

SPACING OF 0.2 WAVELENGTHS BETWEEN BAYS

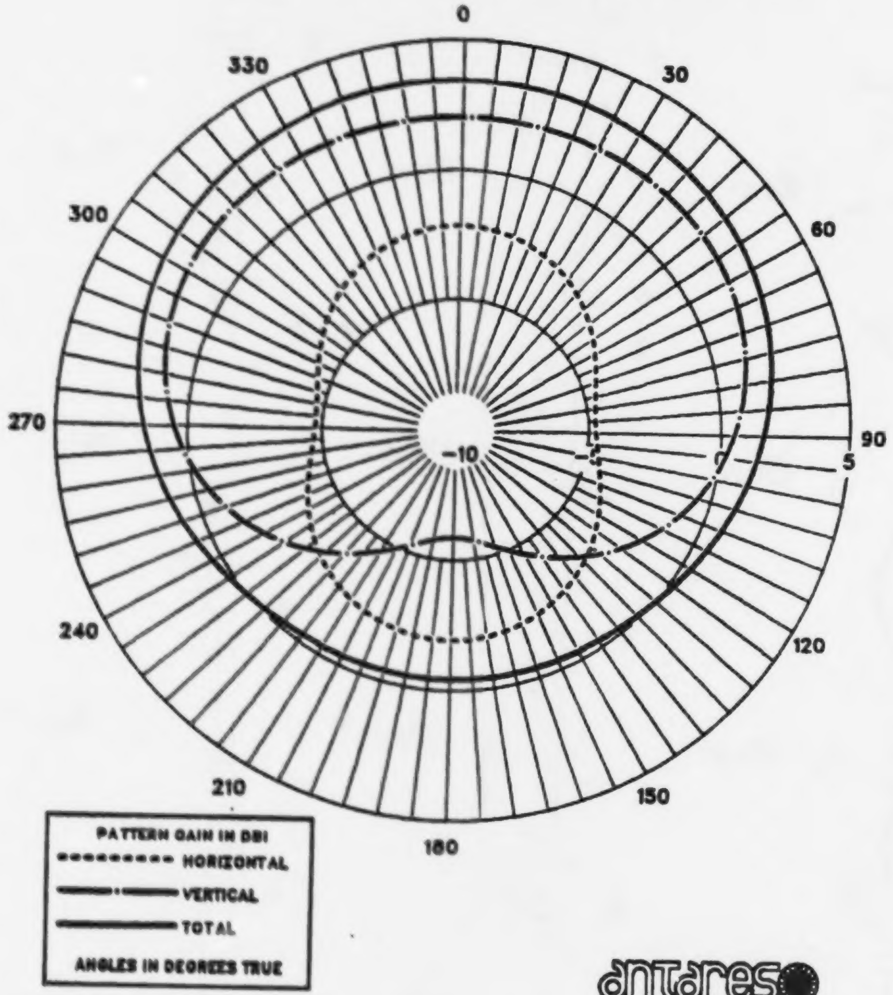

FIGURE D 128

THE CYCLOID 2 ELEMENT ARRAY

SPACING OF 0.2 WAVELENGTHS BETWEEN BAYS

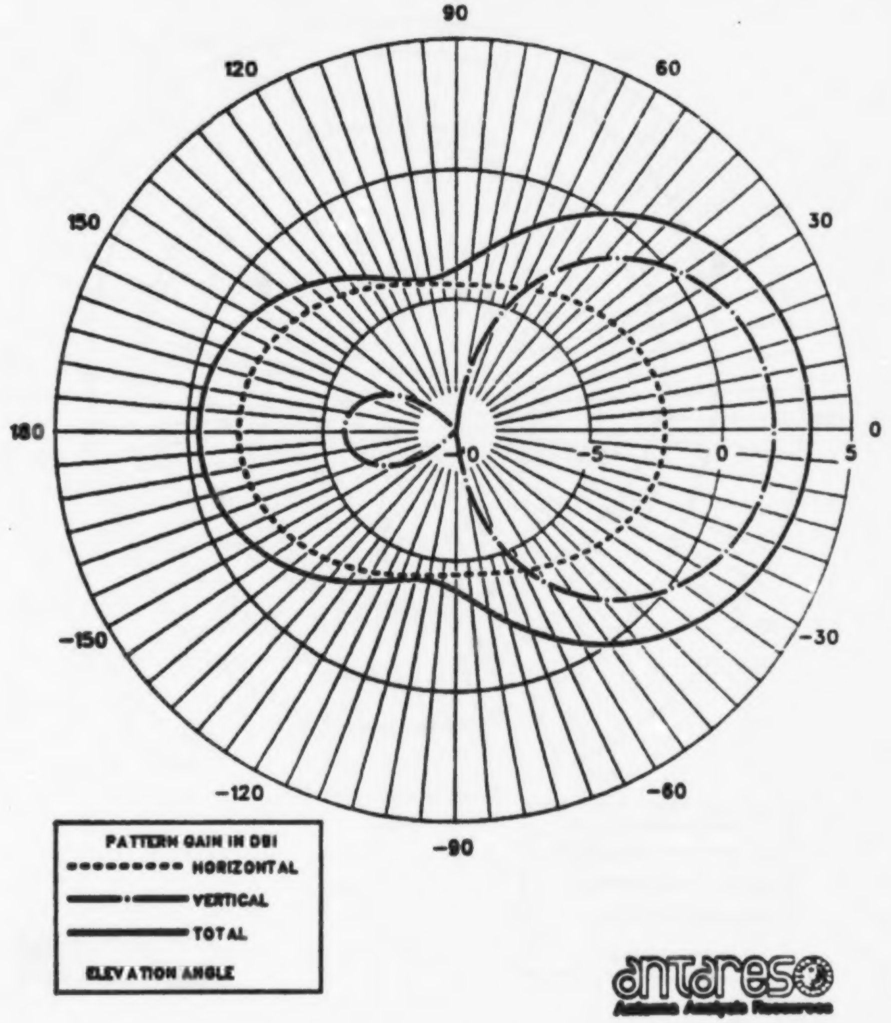

antares
Antenna Analysis Resources

FIGURE D 129

THE CYCLOID 2 ELEMENT ARRAY

SPACING OF 0.4 WAVELENGTHS BETWEEN BAYS

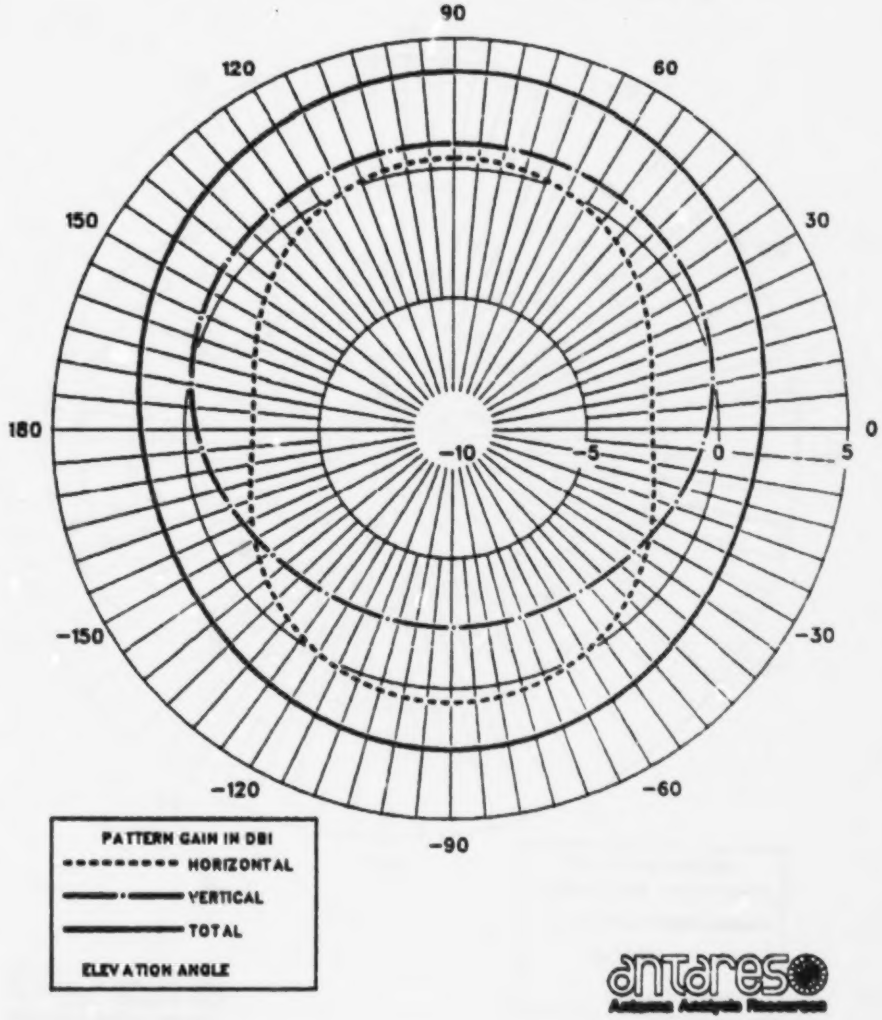

FIGURE D 130

THE CYCLOID 2 ELEMENT ARRAY

SPACING OF 0.4 WAVELENGTHS BETWEEN BAYS

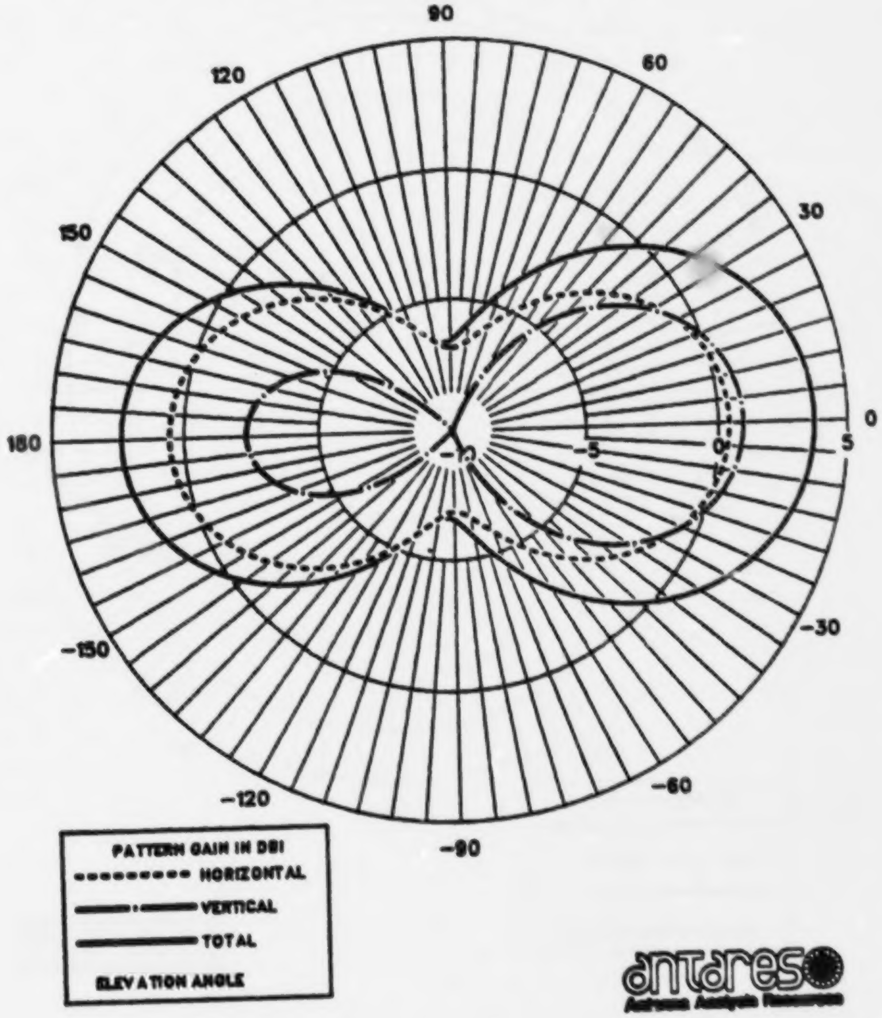

FIGURE D 131

THE CYCLOID 2 ELEMENT ARRAY

SPACING OF 0.5 WAVELENGTHS BETWEEN BAYS

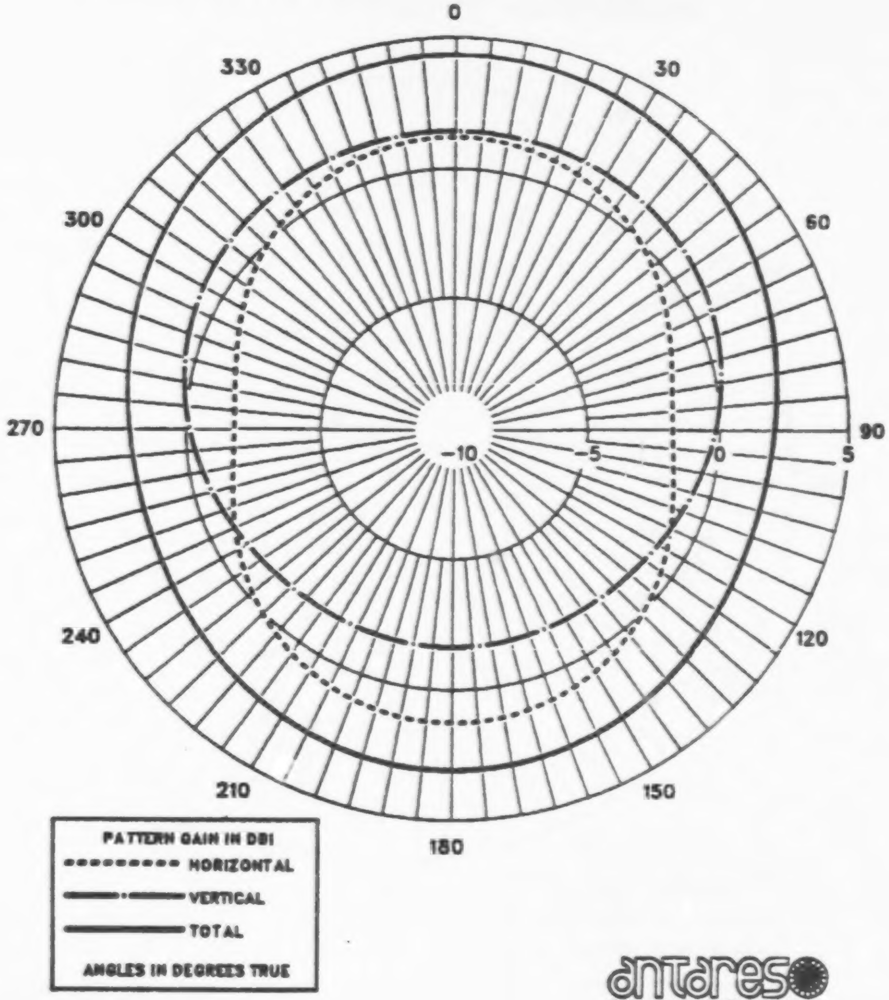

antares
Antenna Analysis Resources

FIGURE D 132

THE CYCLOID 2 ELEMENT ARRAY

SPACING OF 0.5 WAVELENGTHS BETWEEN BAYS

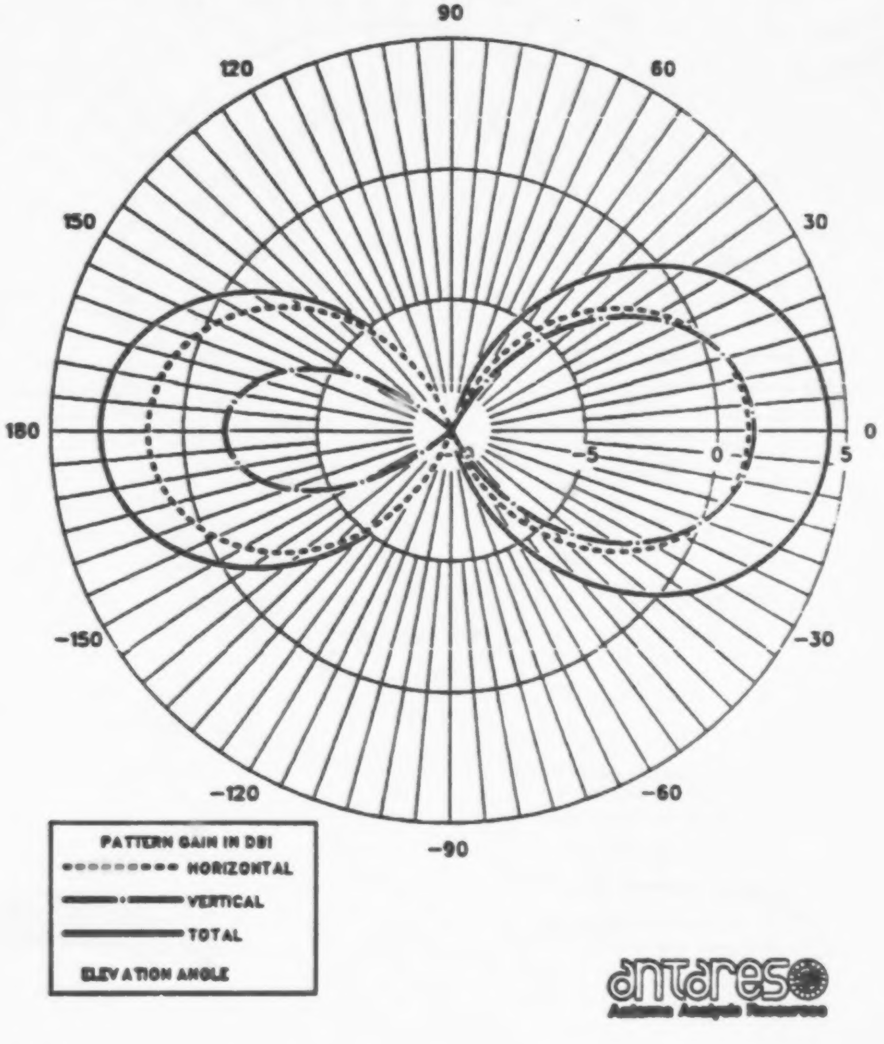

antares
Antenna Analysis Resources

FIGURE D 133

THE CYCLOID 2 ELEMENT ARRAY

SPACING OF 0.7 WAVELENGTHS BETWEEN BAYS

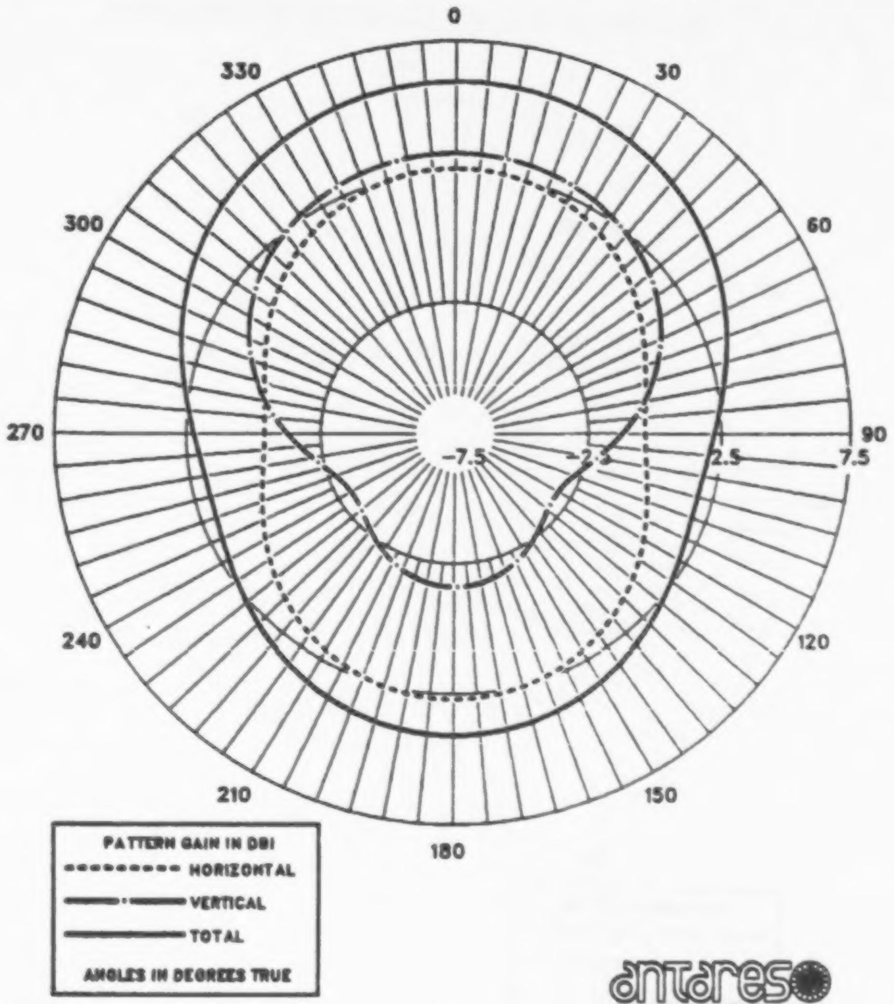

antares
Antenna Analysis Resources

FIGURE D 134

THE CYCLOID 2 ELEMENT ARRAY

SPACING OF 0.7 WAVELENGTHS BETWEEN BAYS

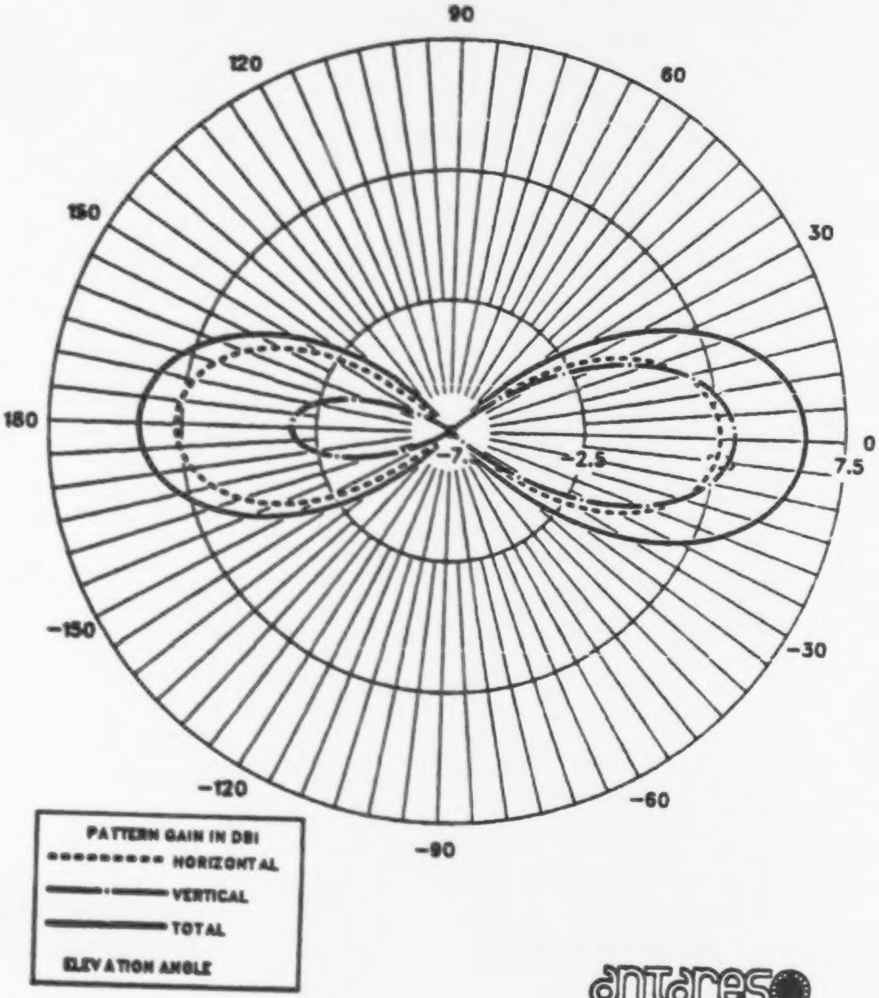

antares
Antenna Analysis Resources

FIGURE D 135

THE CYCLOID 2 ELEMENT ARRAY

SPACING OF 0.9 WAVELENGTHS BETWEEN BAYS

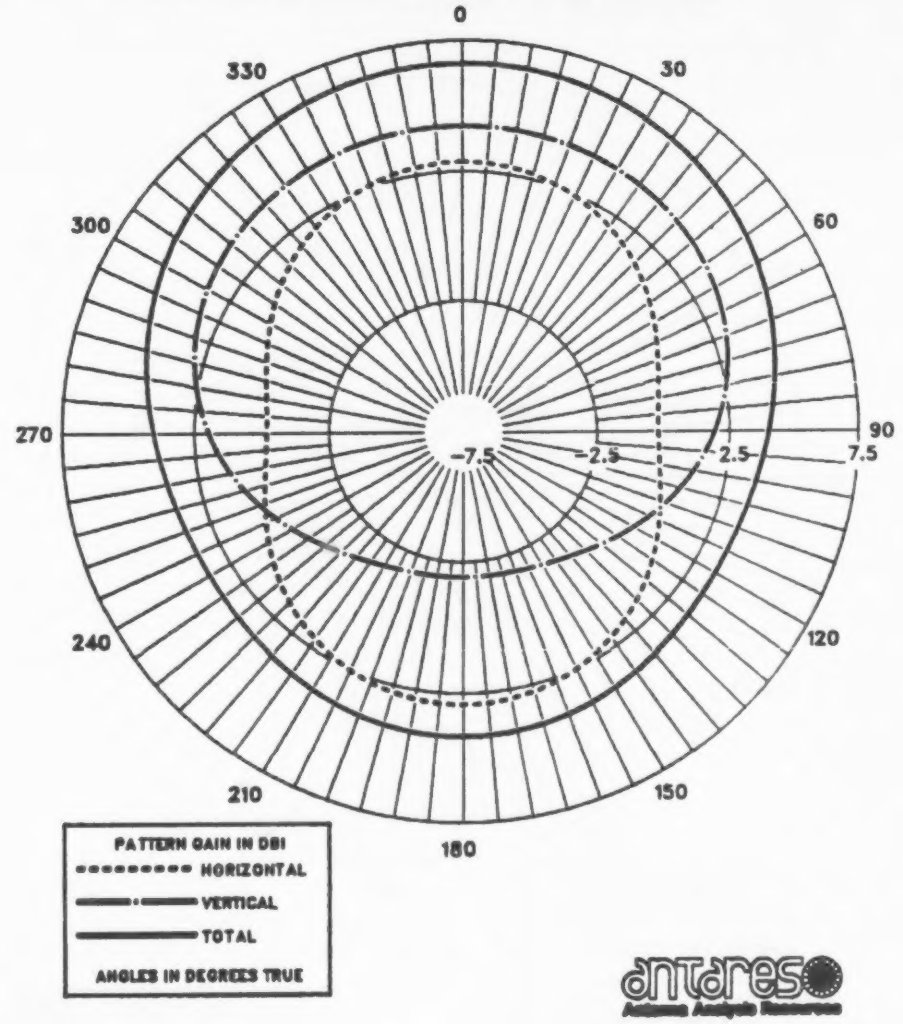

antares
Antenna Analysis Resources

FIGURE D 136

THE CYCLOID 2 ELEMENT ARRAY

SPACING OF 0.9 WAVELENGTHS BETWEEN BAYS

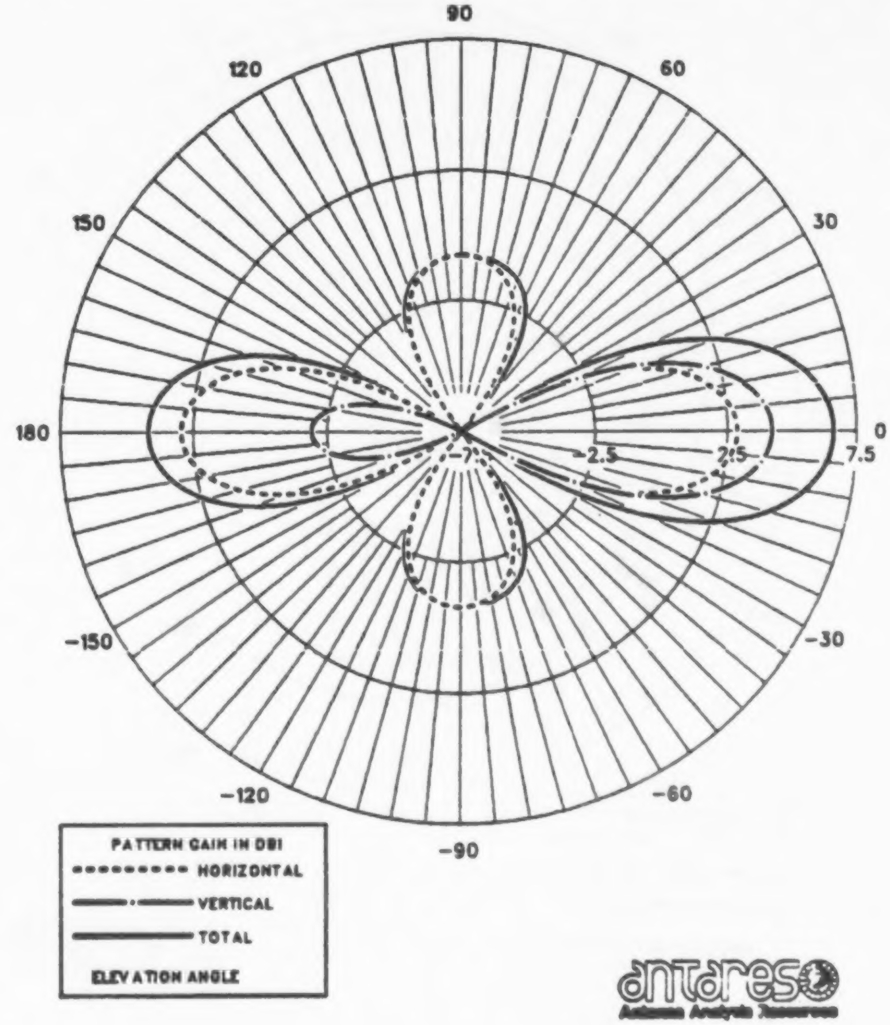

antares
Antenna Analysis Resources

FIGURE D 137

THE CYCLOID 2 ELEMENT ARRAY

SPACING OF 1.0 WAVELENGTHS BETWEEN BAYS

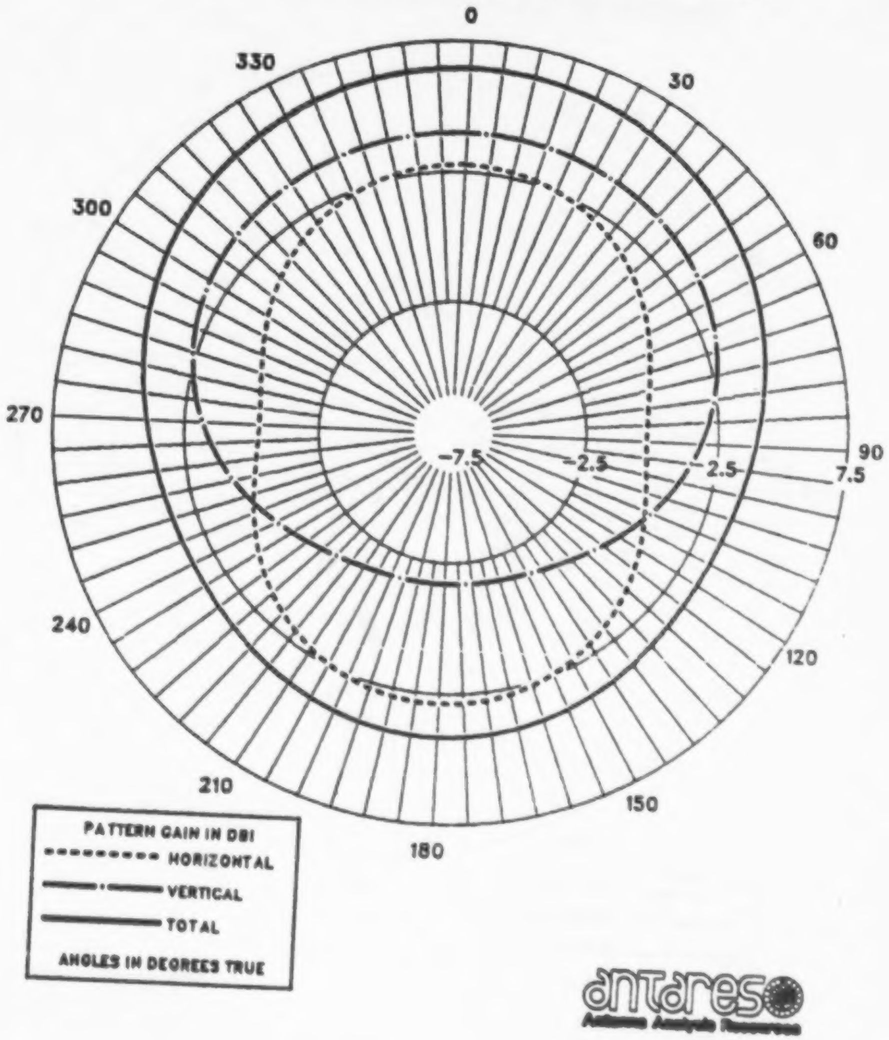

FIGURE D 138

THE CYCLOID 2 ELEMENT ARRAY

SPACING OF 1.0 WAVELENGTHS BETWEEN BAYS

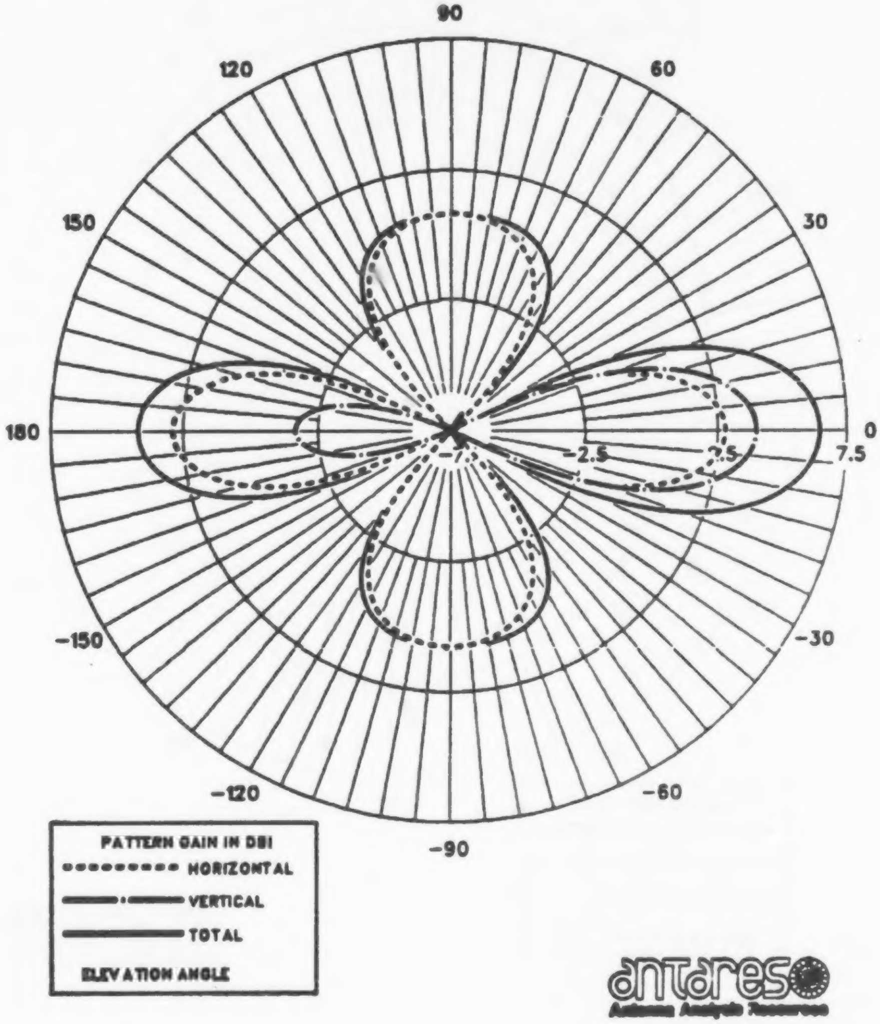

antares
Antenna Analysis Resources

FIGURE D 139

THE CYCLOID 2 ELEMENT ARRAY

SPACING OF 1.1 WAVELENGTHS BETWEEN BAYS

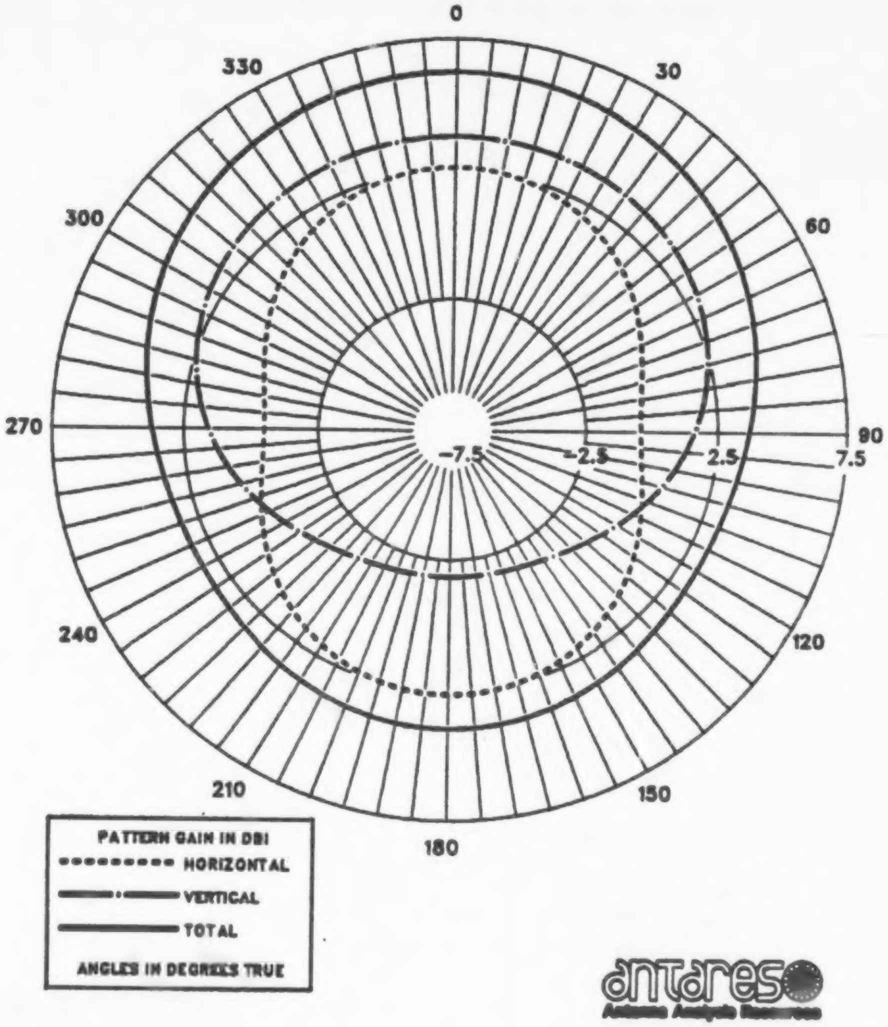

FIGURE D 140

THE CYCLOID 2 ELEMENT ARRAY

SPACING OF 1.1 WAVELENGTHS BETWEEN BAYS

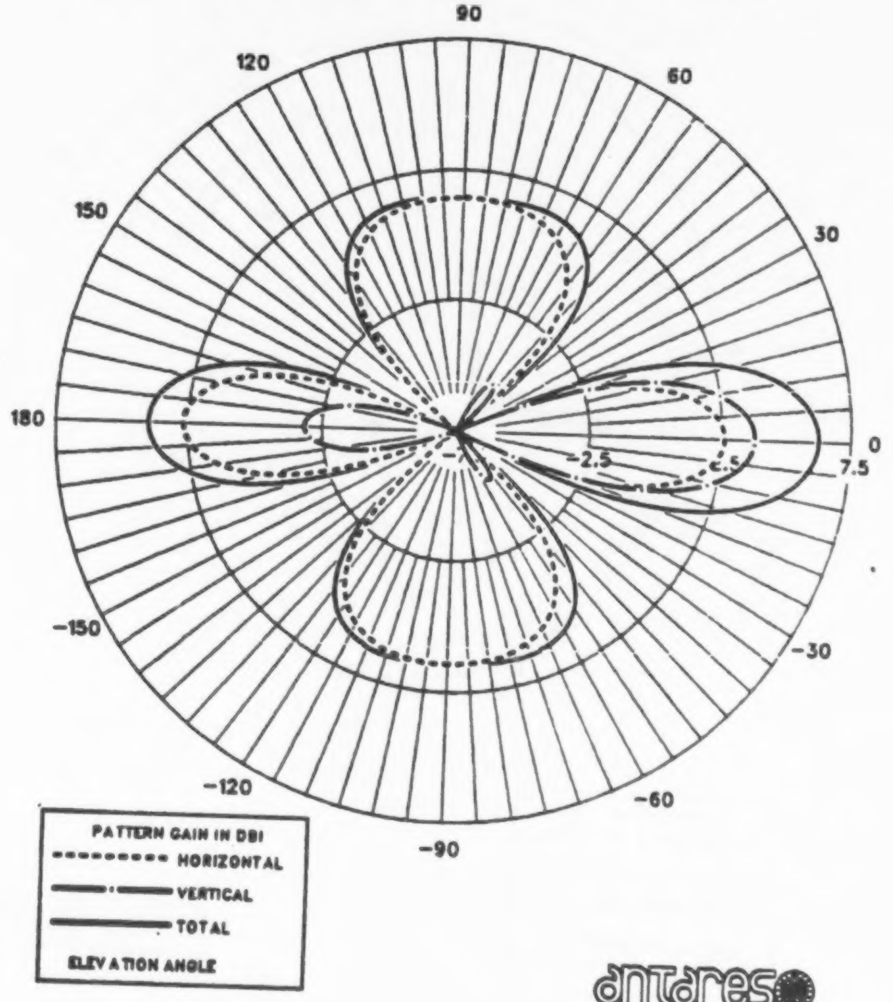

FIGURE D 141

THE CYCLOID 2 ELEMENT ARRAY

SPACING OF 1.2 WAVELENGTHS BETWEEN BAYS

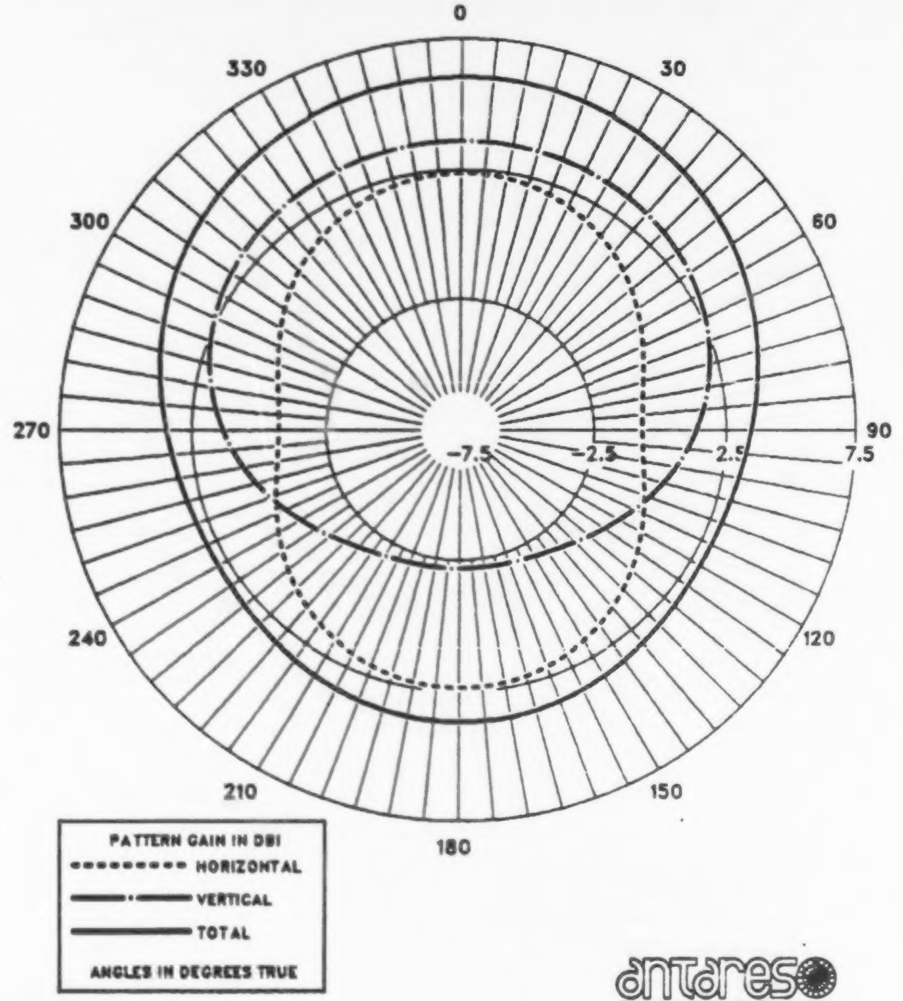

antares
Antenna Analysis Resources

FIGURE D 142

THE CYCLOID 2 ELEMENT ARRAY

SPACING OF 1.2 WAVELENGTHS BETWEEN BAYS

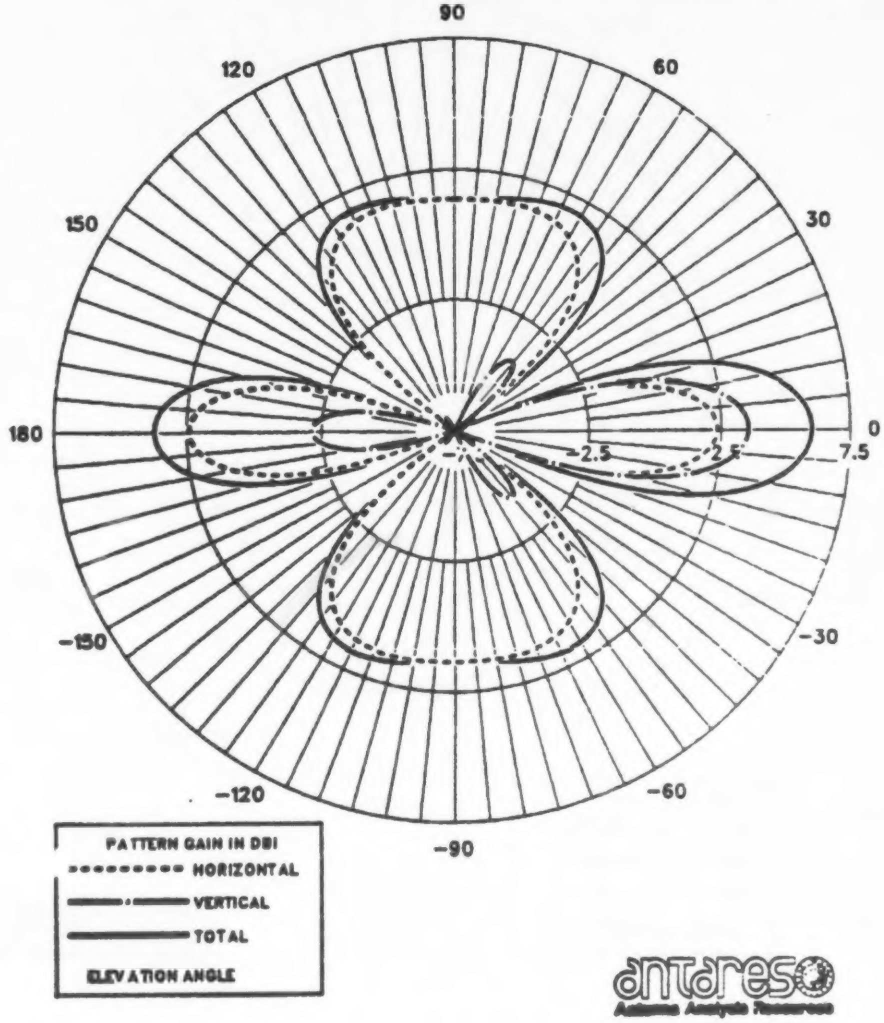

FIGURE D 143 558<

THE CYCLOID 4 ELEMENT ARRAY

SPACING OF 0.2 WAVELENGHTS BETWEEN BAYS

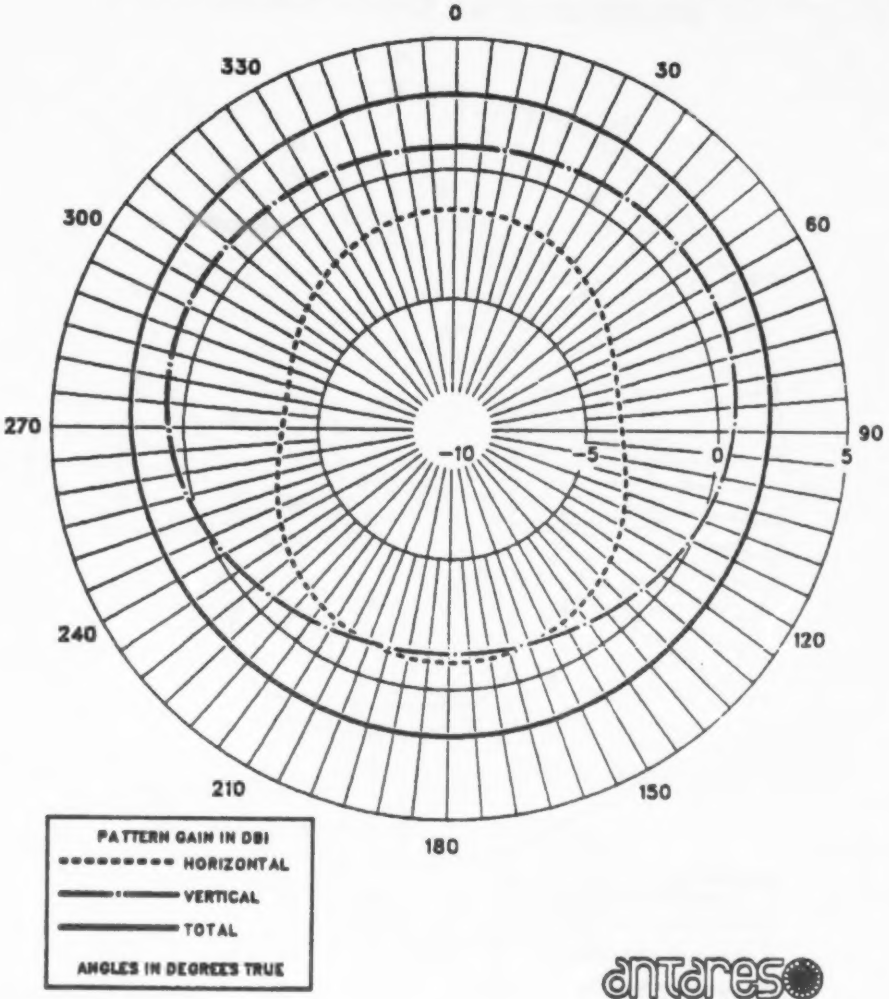

antares
Antenna Analysis Resources

FIGURE D 144

THE CYCLOID 4 ELEMENT ARRAY

SPACING OF 0.2 WAVELENGHTS BETWEEN BAYS

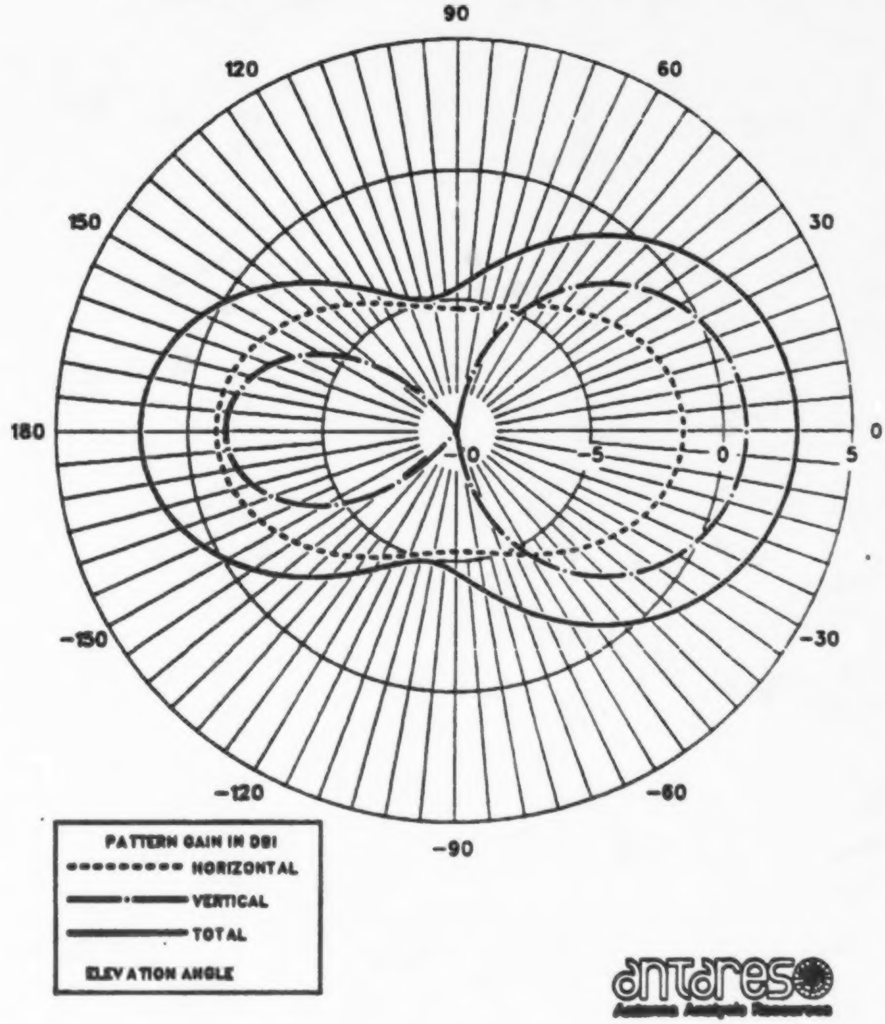

FIGURE D 145

THE CYCLOID 4 ELEMENT ARRAY

SPACING OF 0.2 WAVELENGHTS BETWEEN BAYS

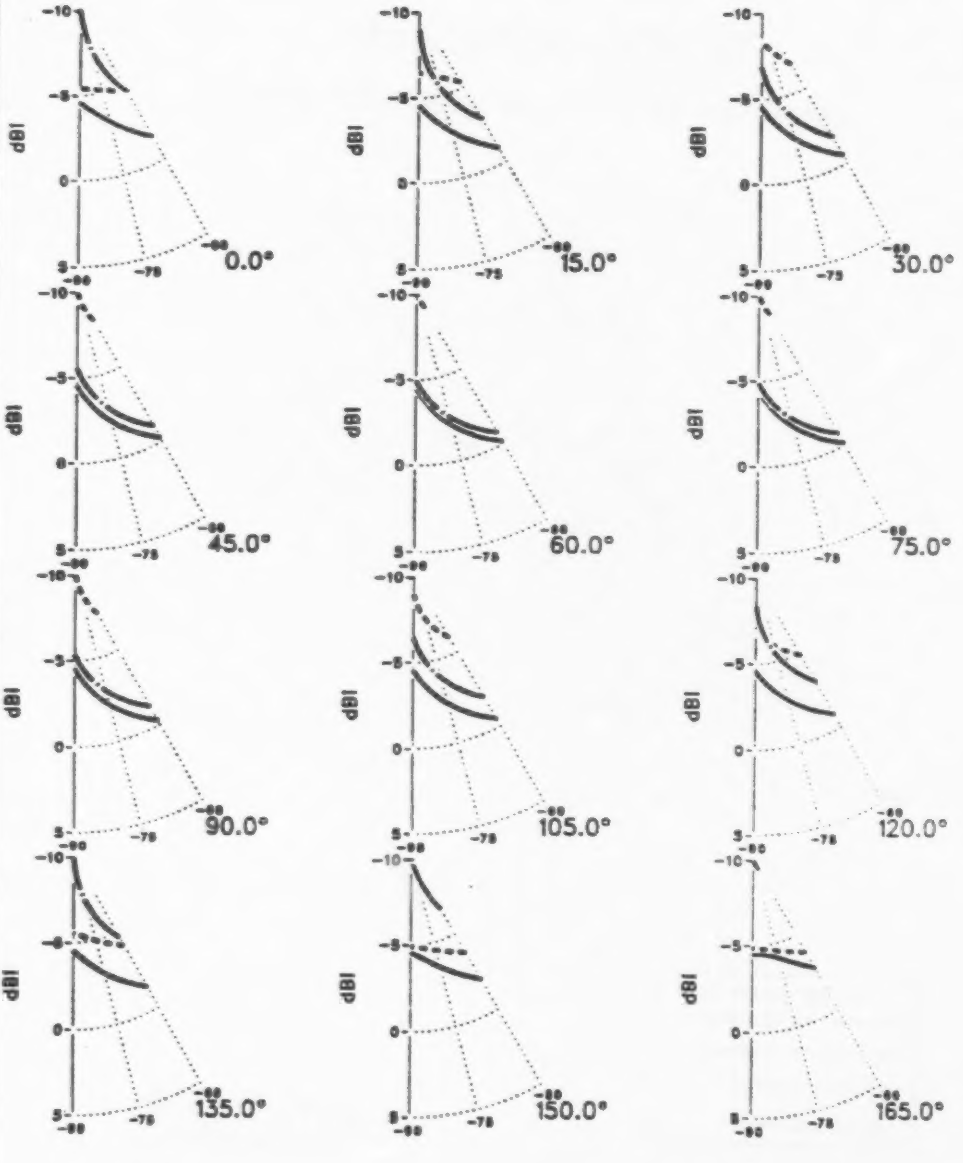

FIGURE D 146

THE CYCLOID 4 ELEMENT ARRAY

SPACING OF 0.2 WAVELENGHTS BETWEEN BAYS

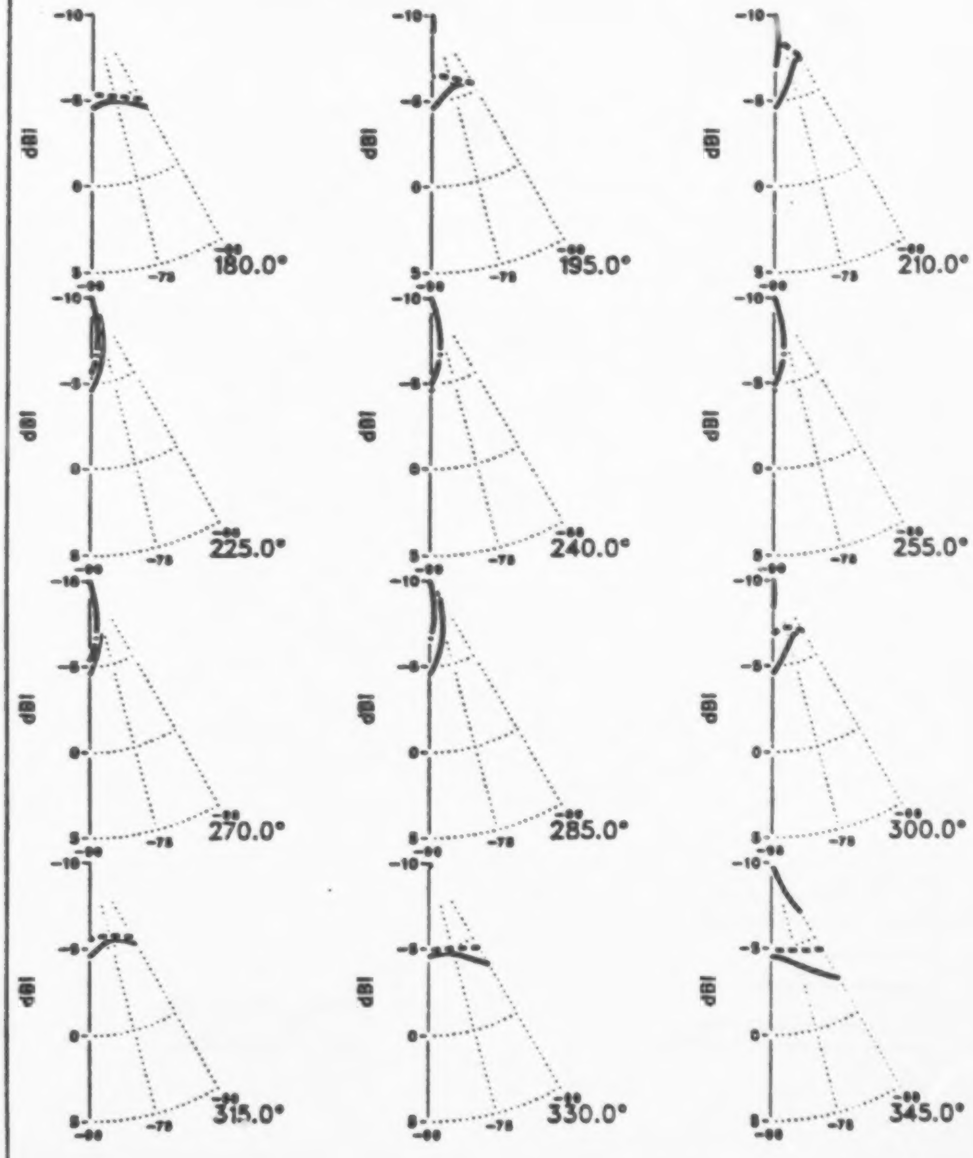

562<

FIGURE D 147

THE CYCLOID 4 ELEMENT ARRAY

SPACING OF 0.4 WAVELENGHTS BETWEEN BAYS

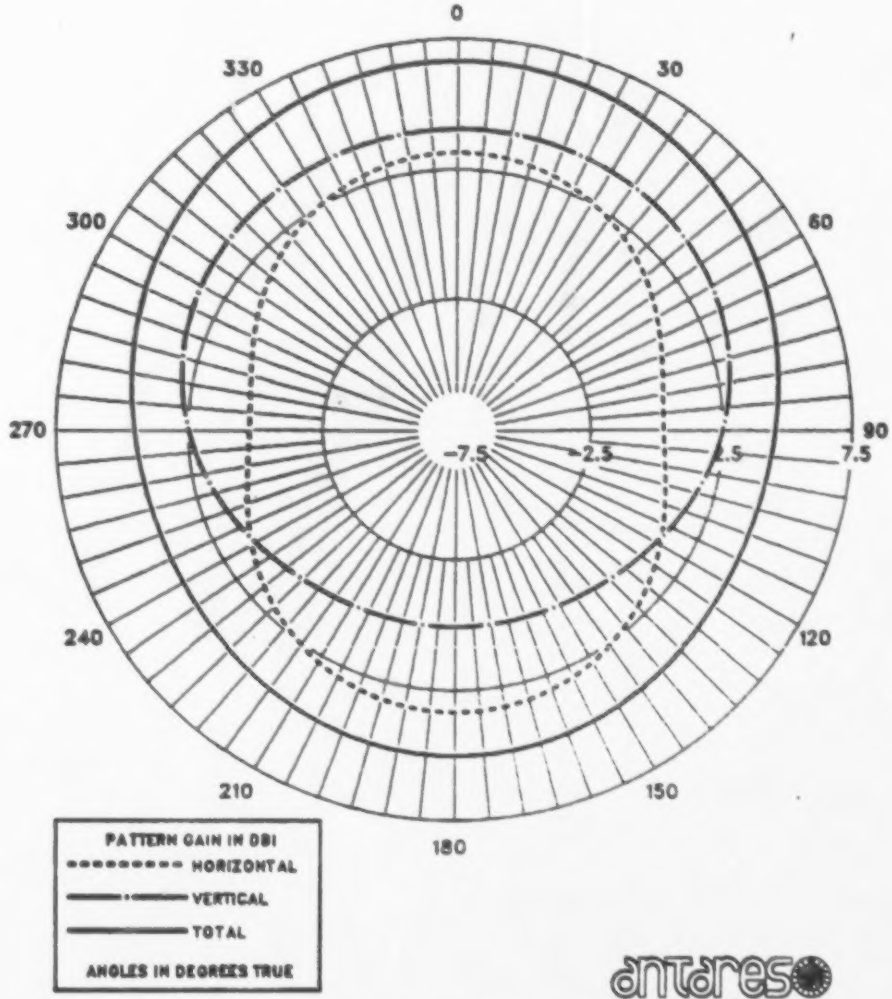

antares
Antenna Analysis Resources

FIGURE D 148

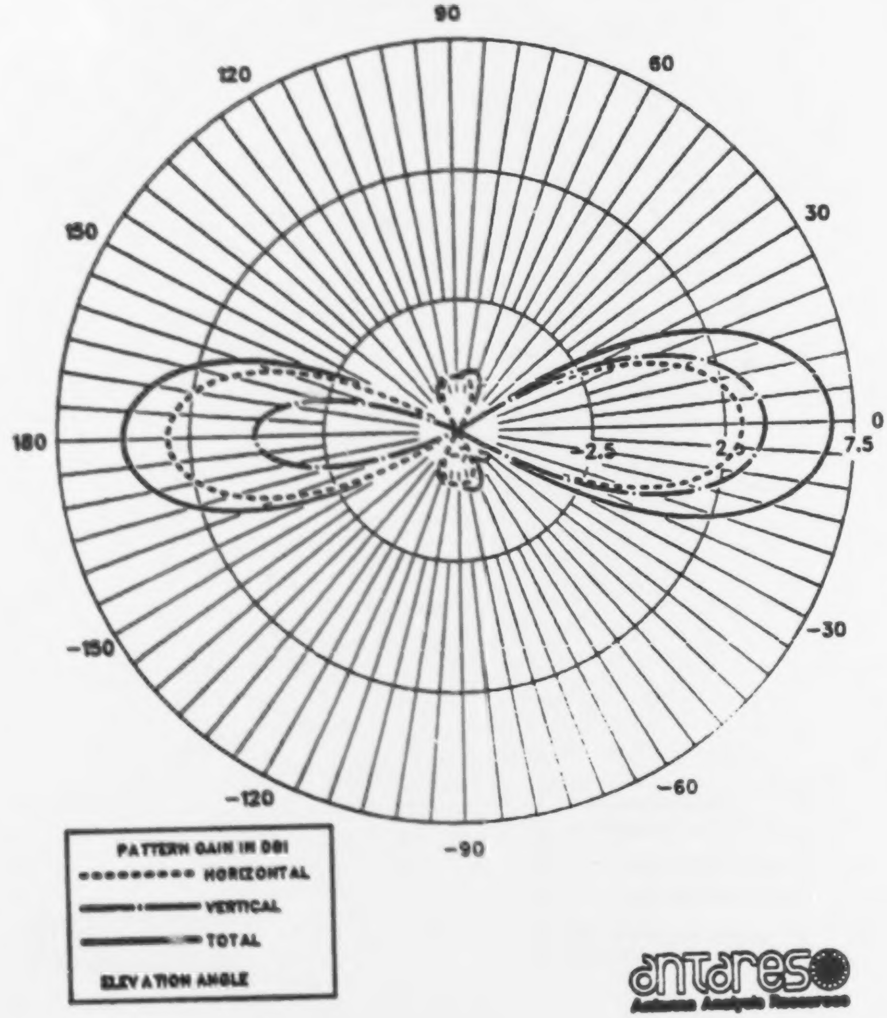

THE CYCLOID 4 ELEMENT ARRAY

SPACING OF 0.4 WAVELENGTHS BETWEEN BAYS

FIGURE D 149

THE CYCLOID 4 ELEMENT ARRAY

SPACING OF 0.5 WAVELENGTHS BETWEEN BAYS

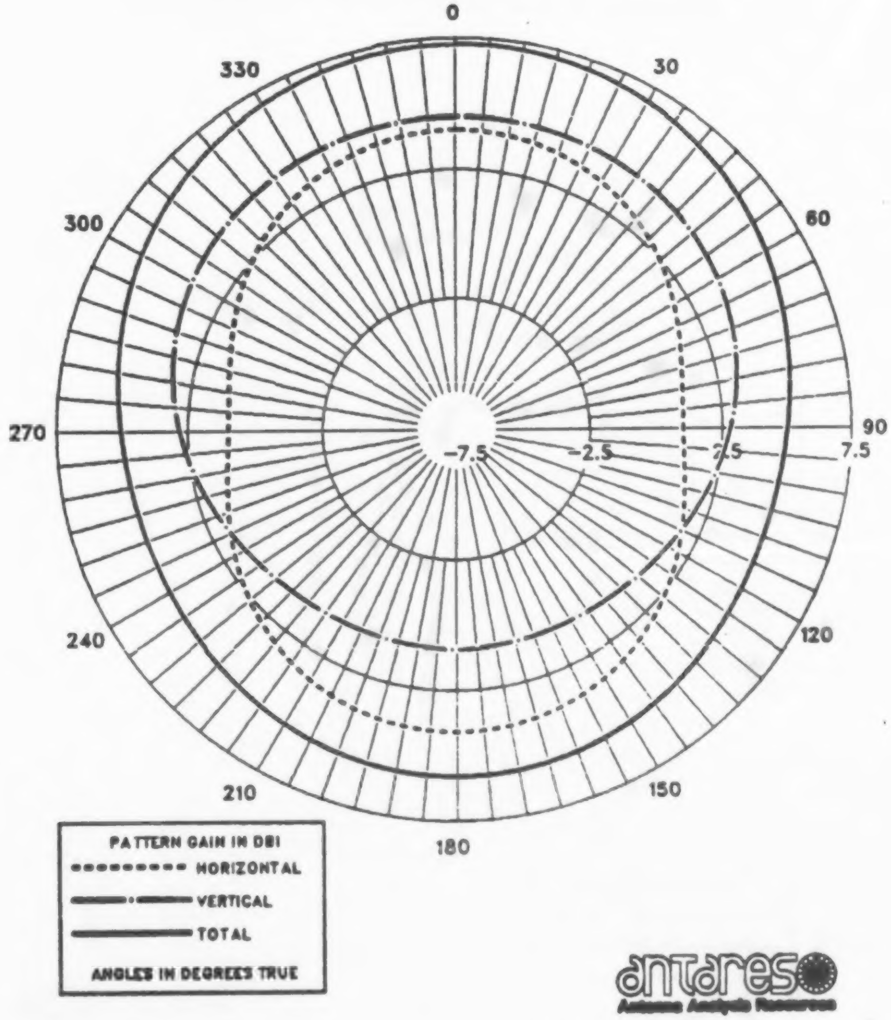

FIGURE D 150

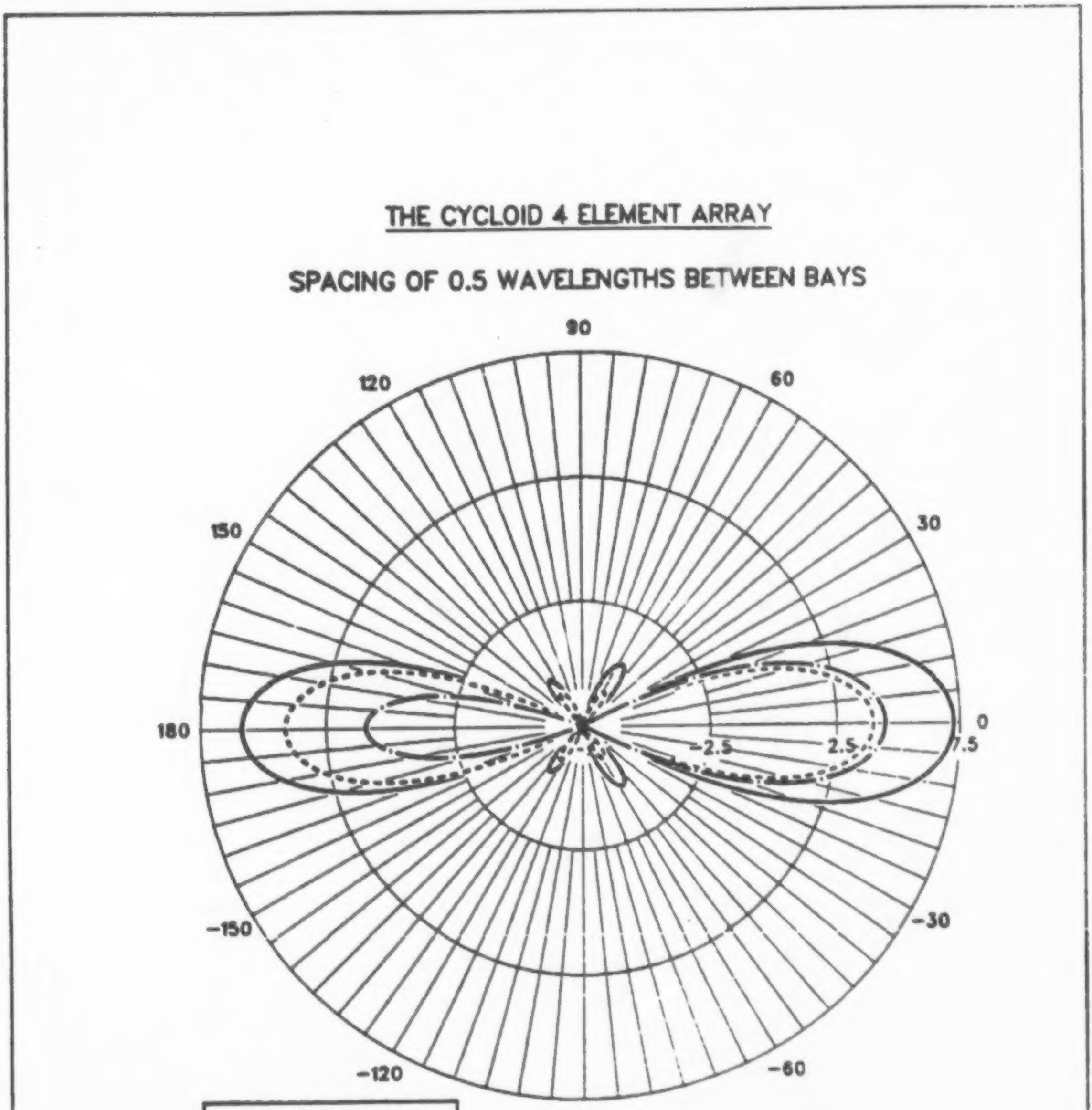

THE CYCLOID 4 ELEMENT ARRAY

SPACING OF 0.5 WAVELENGTHS BETWEEN BAYS

FIGURE D 151

THE 4 ELEMENT CYCLOID ARRAY

SPACING OF 0.7 WAVELENGTHS BETWEEN BAYS

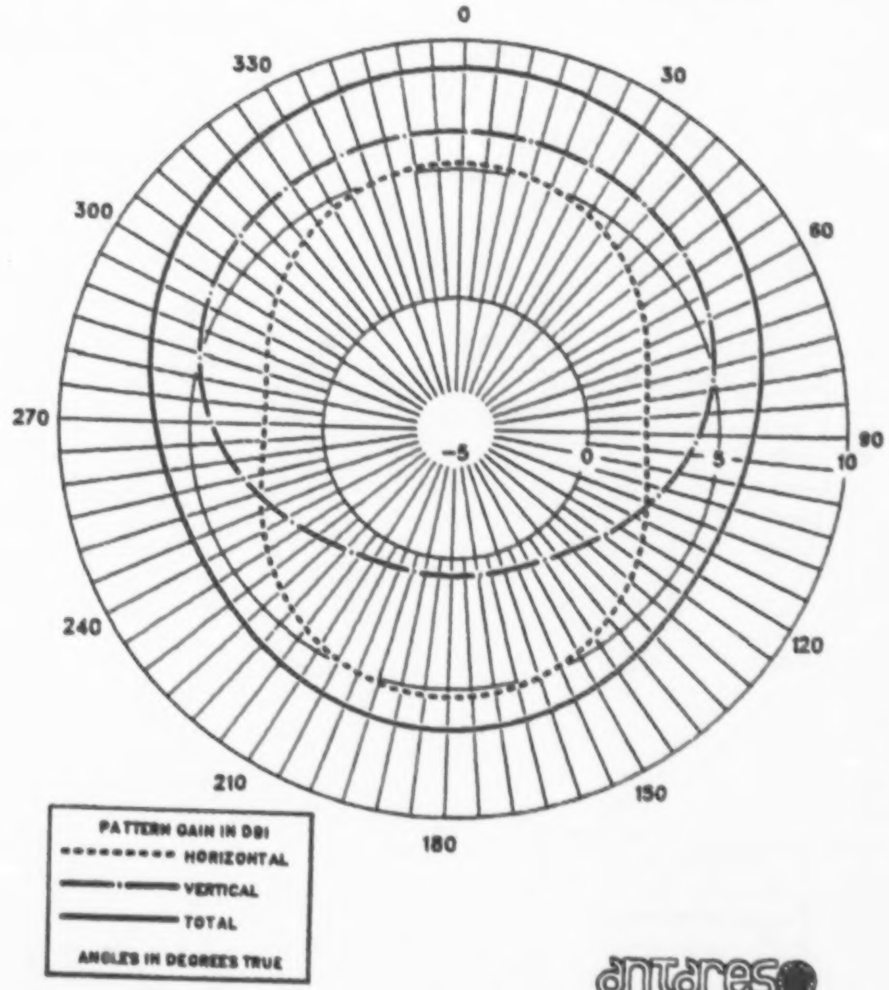

antares
Antenna Analysis Resources

FIGURE D 152

THE 4 ELEMENT CYCLOID ARRAY

SPACING OF 0.7 WAVELENGTHS BETWEEN BAYS

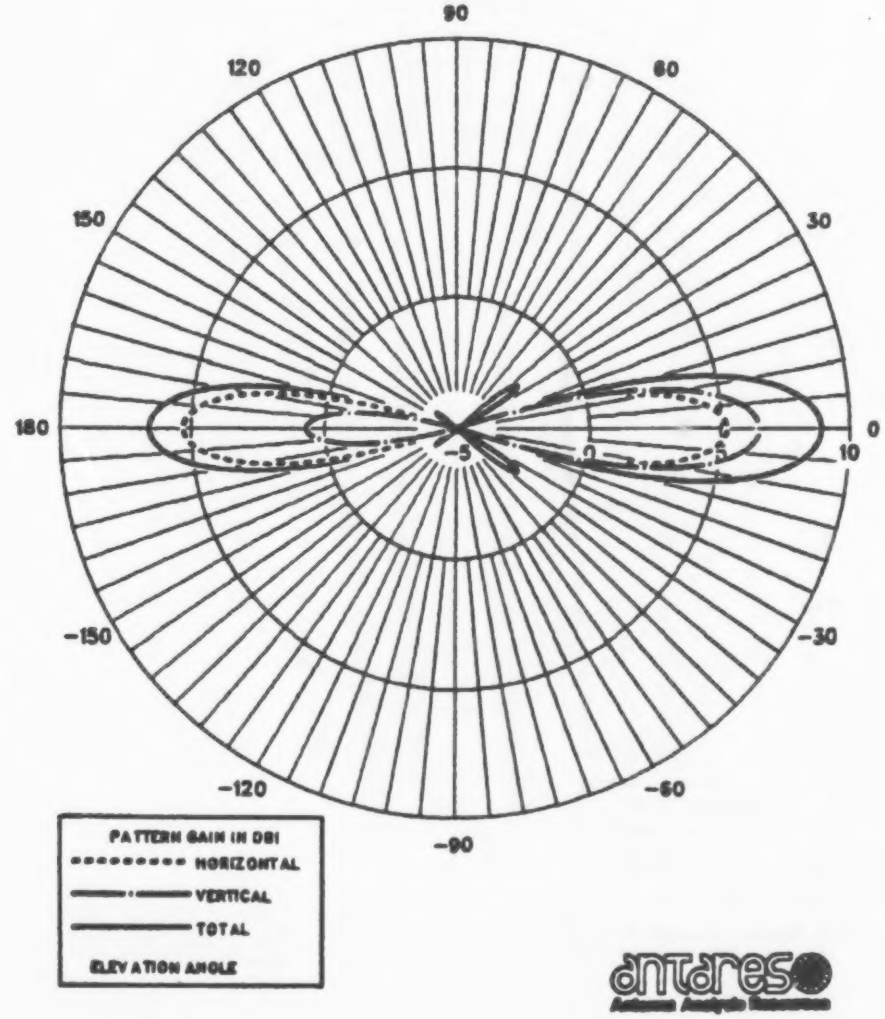

FIGURE D 153

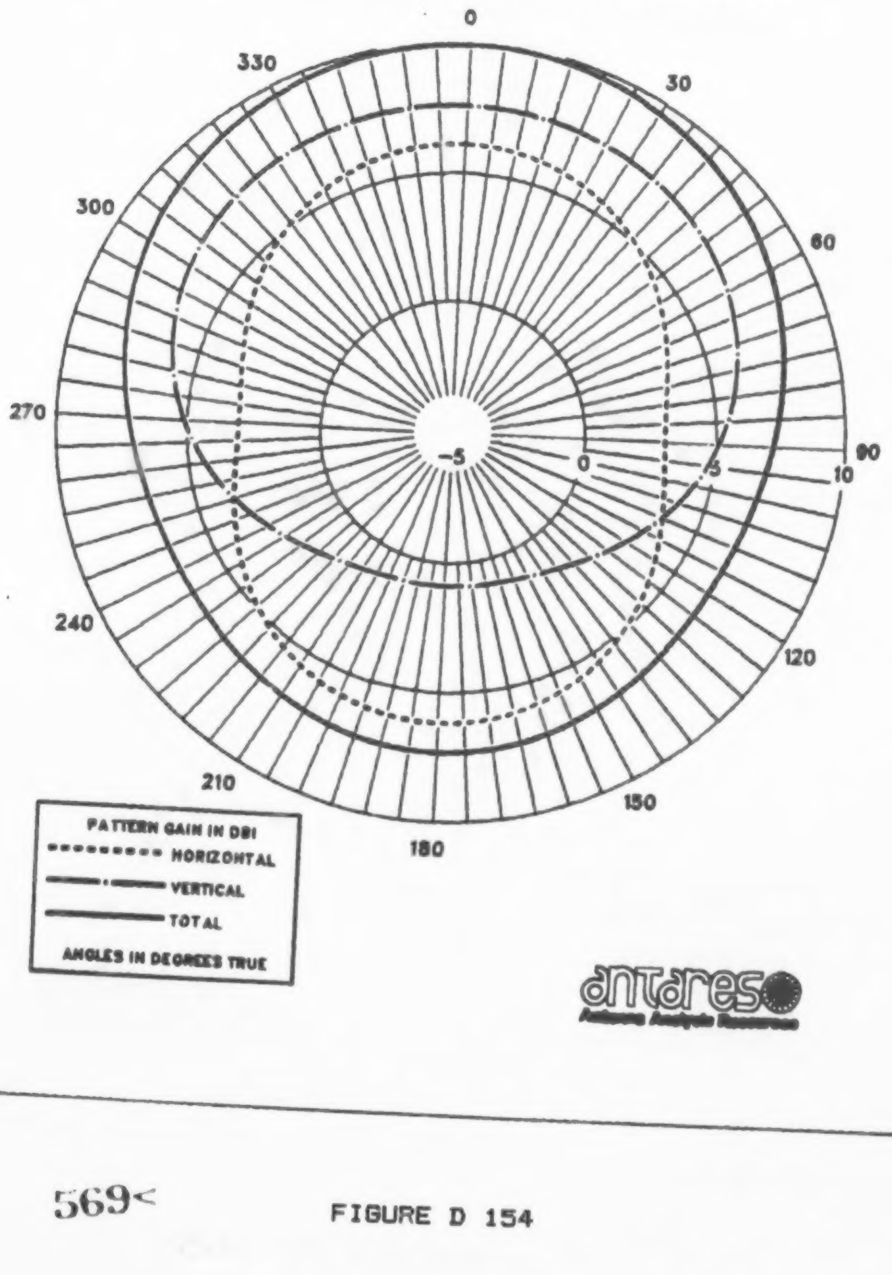

THE 4 ELEMENT CYCLOID ARRAY

SPACING OF 0.9 WAVELENGTHS BETWEEN BAYS

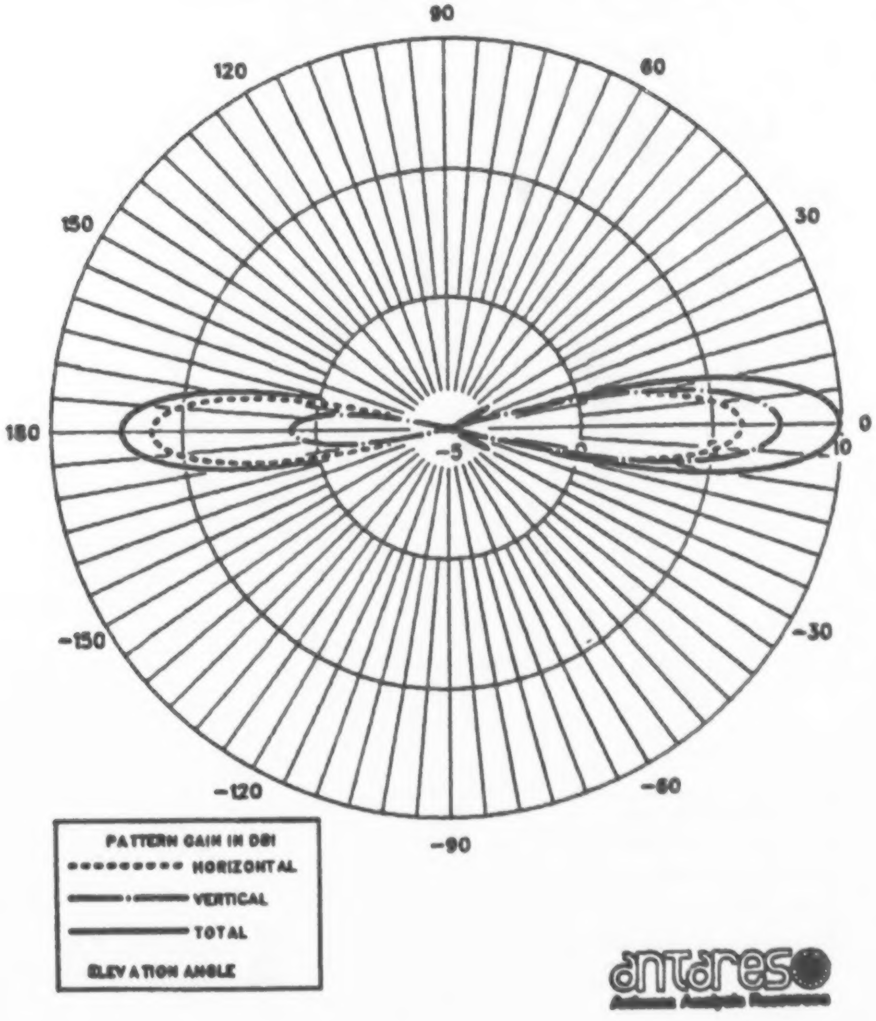

FIGURE D 155

THE 4 ELEMENT CYCLOID ARRAY

SPACING OF 1.0 WAVELENGTHS BETWEEN BAYS

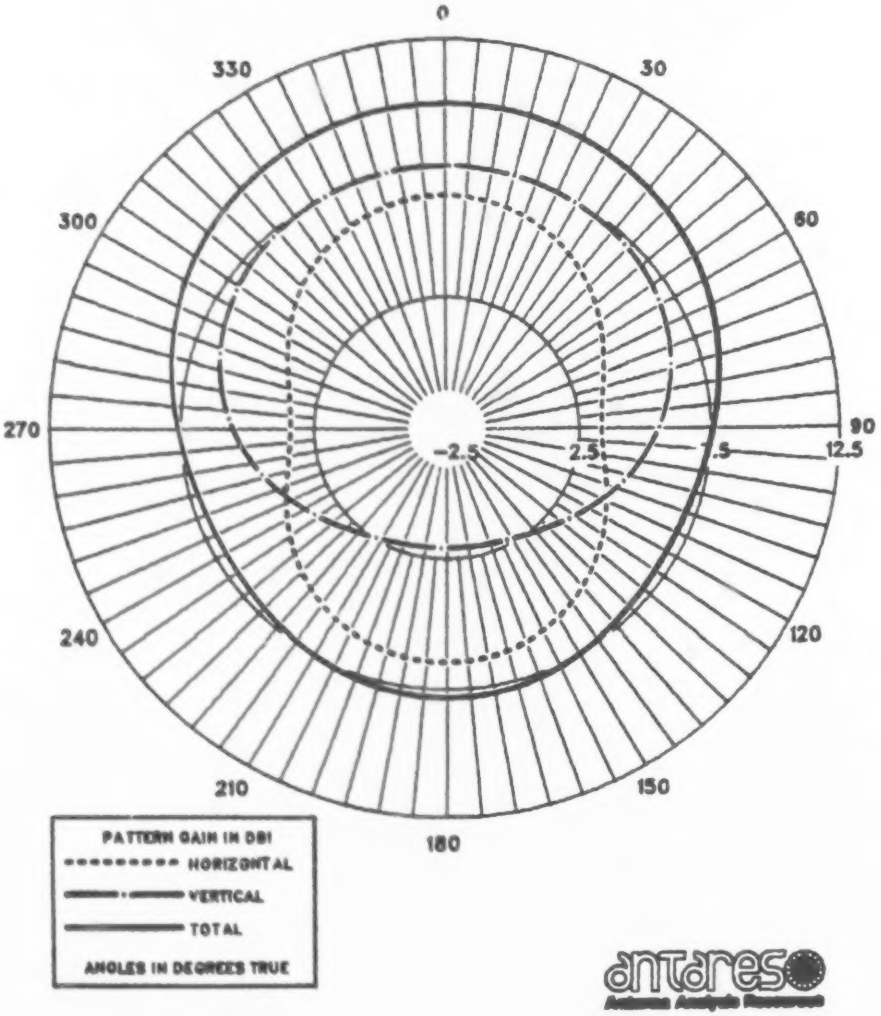

antares
Antenna Analysis Resources

571<

FIGURE D 156

THE 4 ELEMENT CYCLOID ARRAY

SPACING OF 1.0 WAVELENGTHS BETWEEN BAYS

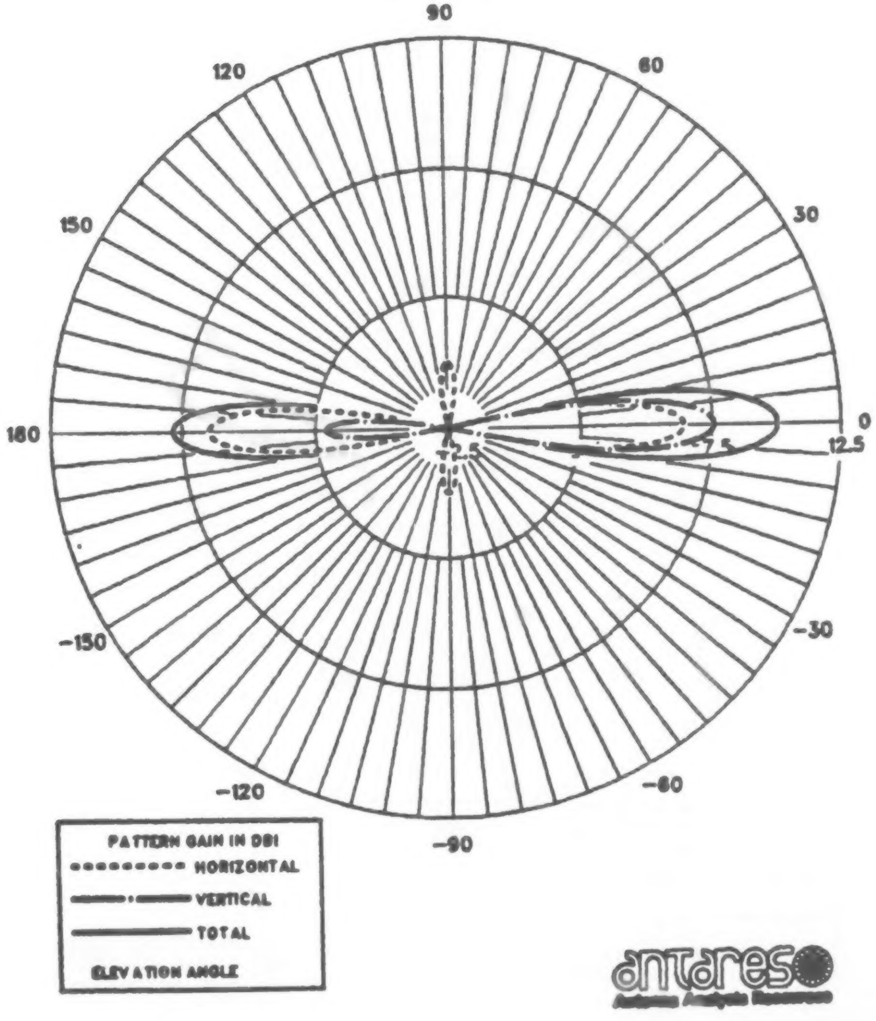

FIGURE D 157

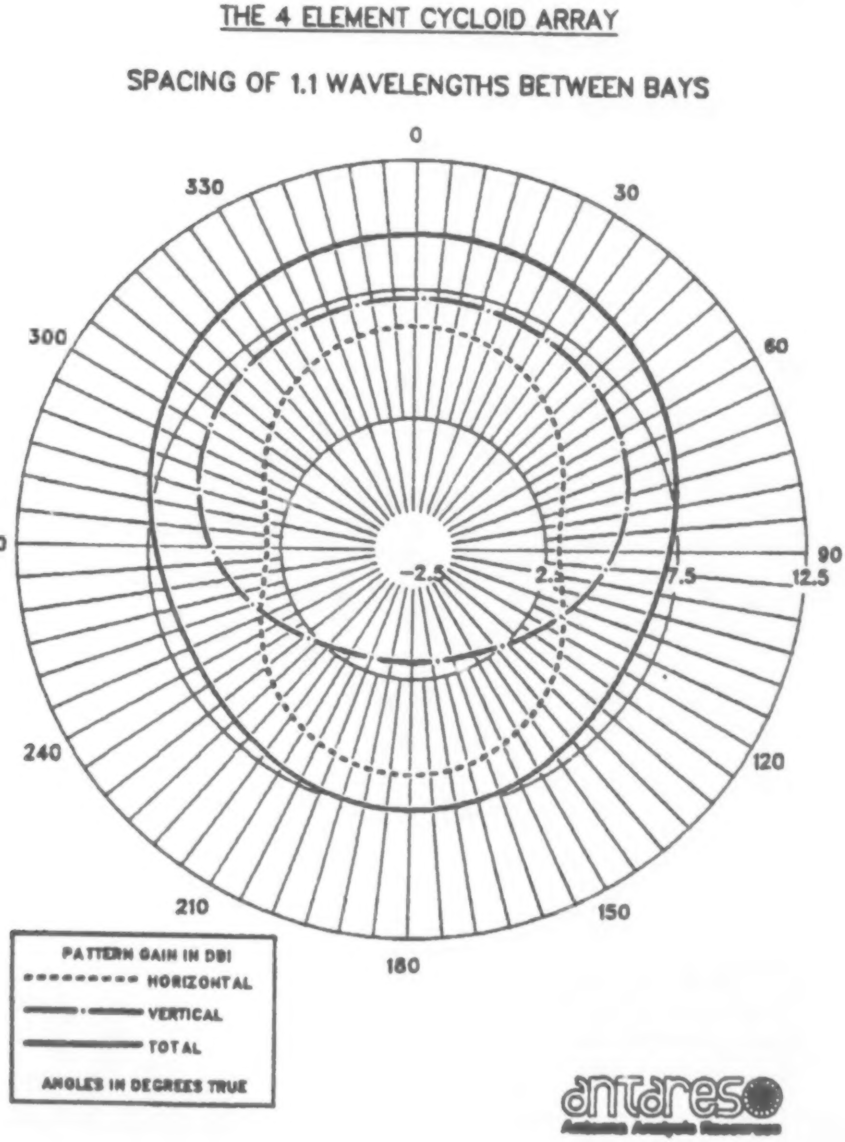

THE 4 ELEMENT CYCLOID ARRAY

SPACING OF 1.1 WAVELENGTHS BETWEEN BAYS

FIGURE D 158

THE 4 ELEMENT CYCLOID ARRAY

SPACING OF 1.1 WAVELENGTHS BETWEEN BAYS

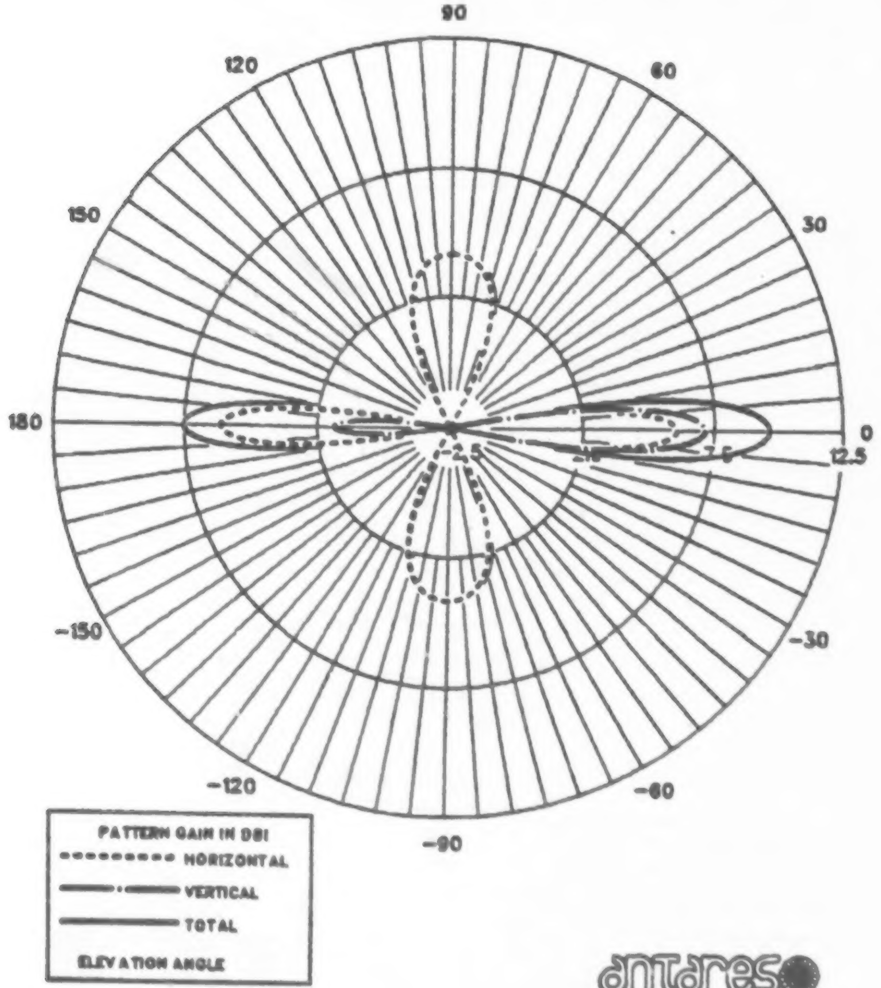

FIGURE D 159

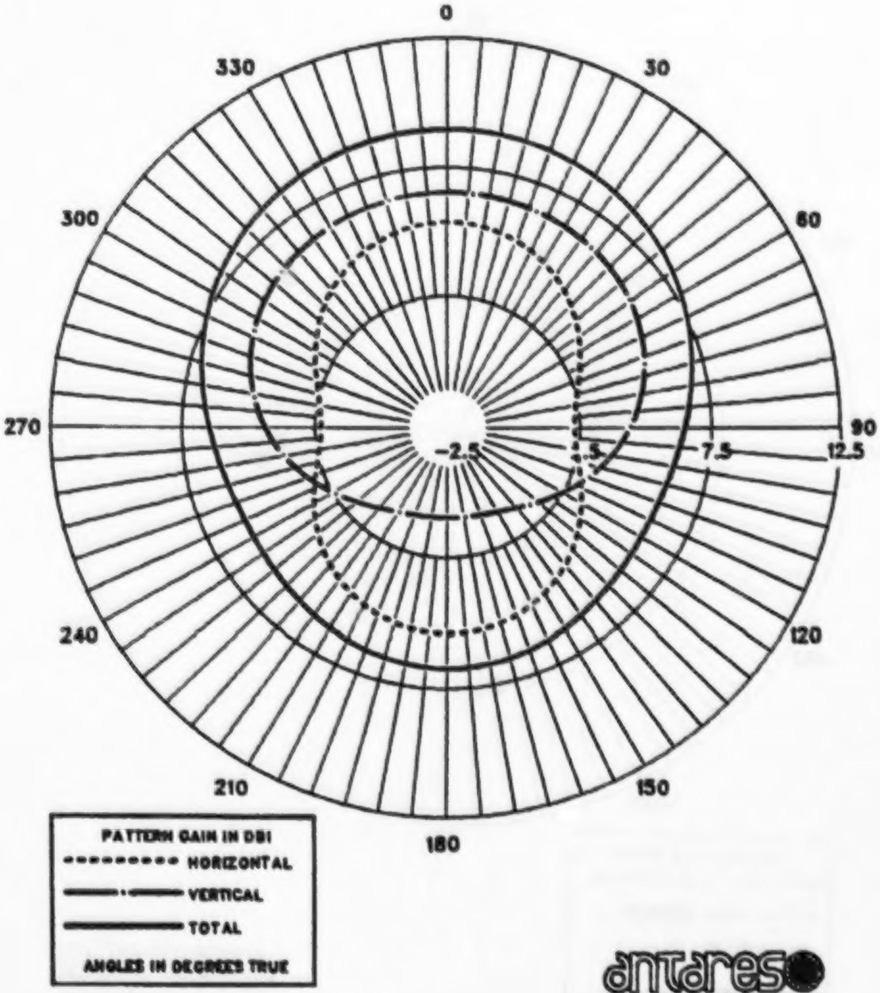

THE 4 ELEMENT CYCLOID ARRAY

SPACING OF 1.2 WAVELENGTHS BETWEEN BAYS

antares
Antenna Analysis Resources

FIGURE D 160

THE 4 ELEMENT CYCLOID ARRAY

SPACING OF 1.2 WAVELENGTHS BETWEEN BAYS

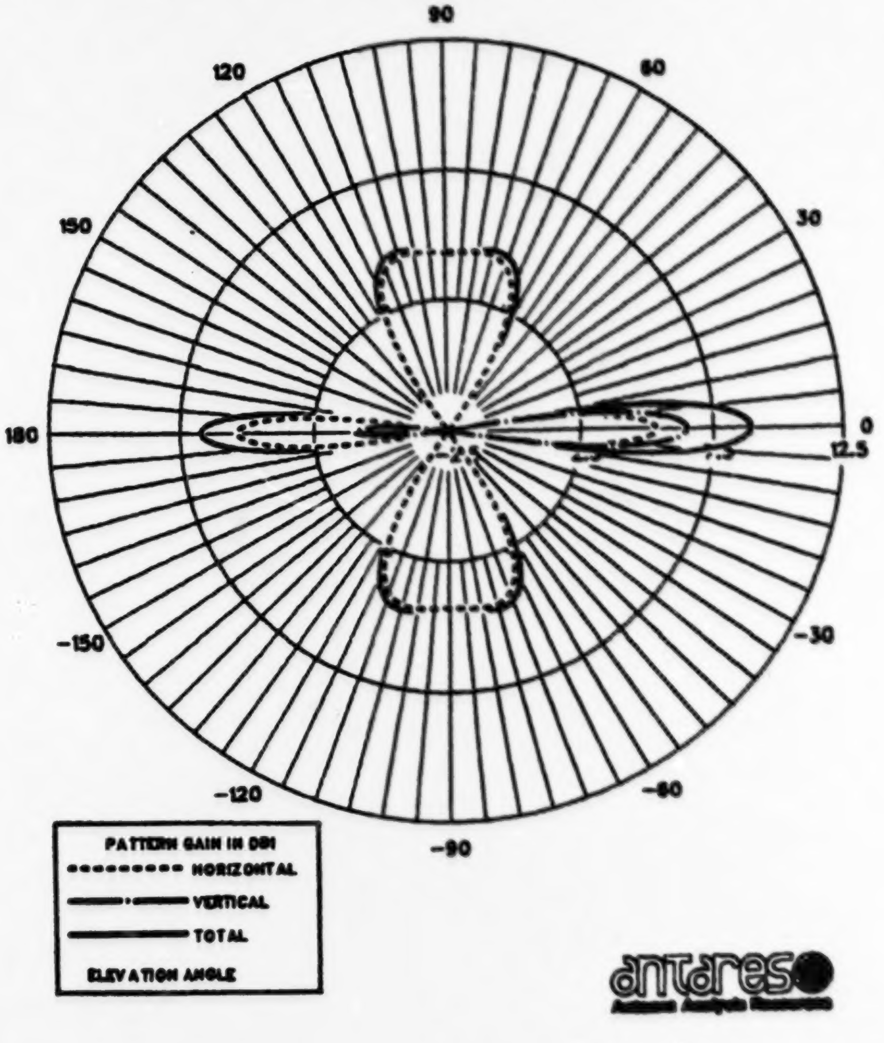

FIGURE D 161

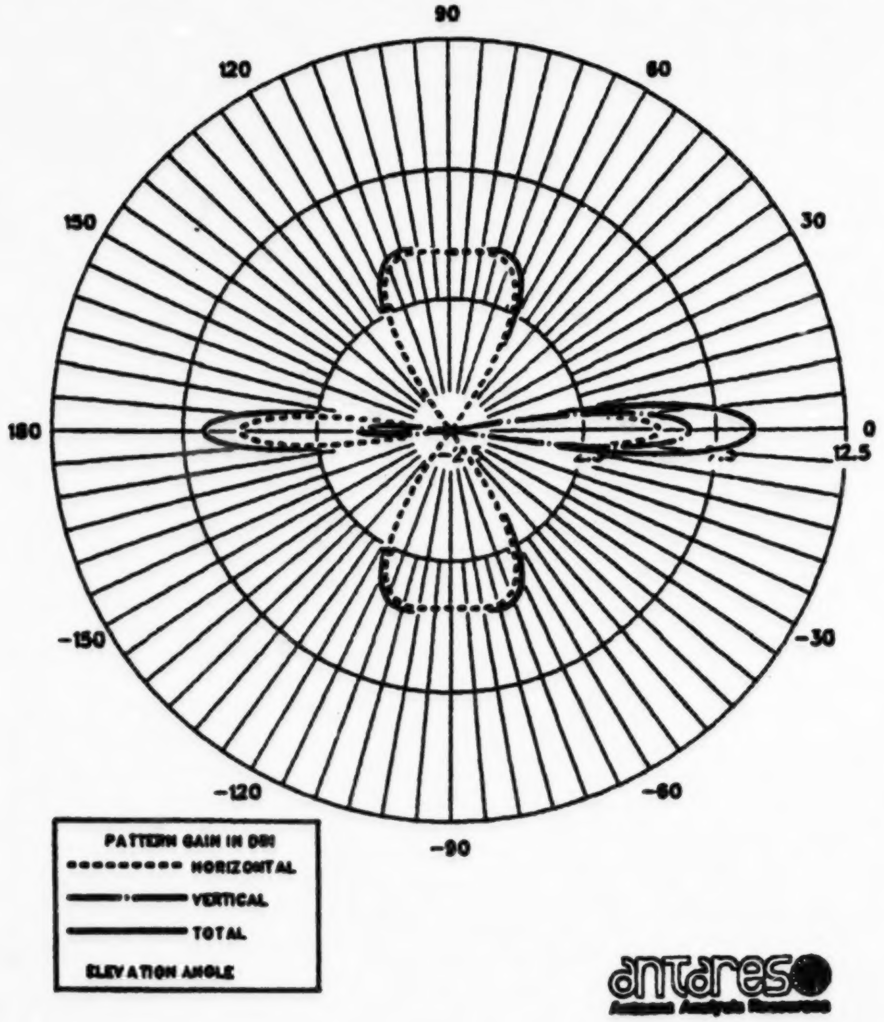

THE 4 ELEMENT CYCLOID ARRAY

SPACING OF 1.2 WAVELENGTHS BETWEEN BAYS

FIGURE D 161